APPENDIX G3 - Part 4 of 4

Comments Received that Do Not Require Response

This page intentionally left blank.

California's Oil Refineries

California's refineries are located in the San Francisco Bay area, Los Angeles area and the Central Valley. Each day approximately two million barrels (a barrel is equal to 42 U.S. gallons) of petroleum are processed into a variety of products, with gasoline representing about half of the total product volume. (A list of refineries, their location and capacity is shown in the table below.)

Refineries can be classified as topping, hydroskimming or complex. Topping refineries are the least sophisticated and contain only the atmospheric distillation tower and possibly a vacuum distillation tower. The topping refiner's ability to produce finished products depends on the quality of the petroleum being processed. A hydroskimming refinery has reforming and desulfurization process units in addition to basic topping units. This allows the refiner to increase the octane levels of motor gasoline and reduce the sulfur content of diesel fuel. Complex refineries are the most sophisticated refinery type and have additional process units to "crack" the heavy gas oils and distillate oils into lighter, more valuable products.

Using a variety of processes including distillation, reforming, hydrocracking, catalytic cracking, coking, alkylation and blending, the refinery produces many different products. The four basic groups are motor gasolines, aviation fuel, distillate fuel and residual fuel. On a statewide average, about 12 percent of the product from California's refineries is aviation fuel, 13 percent is distillate fuel and 9 percent is residual fuel.

Complex refineries have the highest utilization rate at approximately 95 percent. Utilization rate is the ratio of barrels input to the refinery to the operating capacity of the refinery. Complex refineries are able to produce a greater proportion of light products, such as gasoline, and operate near capacity because of California's large demand for gasoline. Permitting Issues. It is unlikely that new refineries will be built in California. In fact, from 1985 to 1995, 10 California refineries closed, resulting in a 20 percent reduction in refining capacity. Further refinery closures are expected for small refineries with capacities of less than 50,000 barrels per day. The cost of complying with environmental regulations and low product prices will continue to make it difficult to continue operating older, less efficient refineries.

To comply with federal and state regulations, California refiners invested approximately $5.8 billion to upgrade their facilities to produce cleaner fuels, including reformulated gasoline and low-sulfur diesel fuel. These upgrades received permits since low-sulfur diesel fuel regulations went into effect in 1993. Requirements to produce federal reformulated gasoline took effect at the beginning of 1995, and more stringent state requirements for CARB reformulated gasoline went into effect statewide on April 1, 1996. That requirement was removed by Governor Gray Davis when it was found that the oxygenate, methyl tertiary butyl-ether or MTBE, was leaking from some underground storage tanks and polluting water supplies. MTBE was phased out and removed as of December 31, 2003, and replaced by ethanol.

For information about oil production and imports to refineries, please see Petroleum Data, Facts, and Statistics.

Refineries Outside of California That Can Produce California Gasoline

Domestic sources include refineries located in Washington State and the US Gulf Coast. Foreign sources include Eastern Canada, Finland, Germany, US Virgin Islands, Middle East, and Asia.

California Refineries

California Oil Refinery Locations and Capacities

Refinery Name	Barrels Per Day	CARB Diesel	CARB Gasoline
Tesoro Refining & Marketing Company, Carson Refinery	257,300	Yes	Yes
Chevron U.S.A. Inc., El Segundo Refinery	269,000	Yes	Yes
Chevron U.S.A. Inc., Richmond Refinery	245,271	Yes	Yes
Tesoro Refining & Marketing Company, Golden Eagle Martinez Refinery	166,000	Yes	Yes
Shell Oil Products US, Martinez Refinery	156,400	Yes	Yes
ExxonMobil Refining & Supply Company, Torrance Refinery	149,500	Yes	Yes

Valero Energy, Benicia Refinery	145,000	Yes	Yes
Phillips 66, Wilmington Refinery	139,000	Yes	Yes
Tesoro Refining & Marketing Company, Wilmington Refinery	104,500	Yes	Yes
Valero Energy, Wilmington Refinery	85,000	Yes	Yes
Phillips 66, Rodeo San Francisco Refinery	78,000	Yes	Yes
ALON USA, Bakersfield Refinery	66,000	Yes	Yes
Paramount Petroleum Corporation, Paramount Refinery	84,500	No	Yes
Phillips 66, Santa Maria Refinery	41,800	No	No
Kern Oil & Refining Company, Bakersfield Refinery	26,000	Yes	Yes
San Joaquin Refining Company Inc., Bakersfield Refinery	15,000	Yes	No
Greka Energy, Santa Maria Refinery	9,500	No	No
Lunday Thagard, South Gate Refinery	8,500	No	No
Valero Wilmington Asphalt Refinery	6,300	No	No

Classification of refiners based on crude oil capacity in barrels per day - Information as of February 2016

Note: Data on this table represents total crude oil capacity not gasoline, distillate production, diesel fuel production or production of other products. Production potential varies depending on time of year and status of the refinery. A rule of thumb is that **roughly** 50 percent of total capacity is gasoline production (about 1.0 million barrels of gasoline - 42 million gallons - is produced per day).

Source: California Energy Commission Fuels Office Staff.

Terminal Facilities

California's nearly 100 terminals receive petroleum and petroleum products by tanker, barge, pipeline, rail or truck. Most of California's terminals are marine terminals. At these facilities petroleum or product is transferred from or to tankers or barges. Tankers loaded with Alaska North Slope petroleum, for example, enter marine terminals in northern and southern California, where the crude oil is then sent to refineries by pipeline for processing. An example of pipeline receipts of petroleum at a terminal is heavy California petroleum produced in the Bakersfield area that is sent by pipeline to a refinery at Martinez.

Terminals also serve as refiner's wholesale distribution points for products. Product, such as gasoline, is sold to distributors (jobbers) who then sell to consumers through the distributors' own retail stations. The distributor may also resell the gasoline to other station dealers. Gasoline can also be sold directly to station dealers from the terminal. The marketing structure differs depending on the type of product being sold.

A terminal can be linked with several refineries and storage facilities and be supplied by privately-owned pipelines or a common carrier line. Total capacity at a terminal can range from a few thousand barrels to a few million barrels. The most apparent equipment at a terminal are the tanks used for storage and separation of different product grades. The number of tanks can range from a few to more than 70. Other equipment found includes piping, pumps, valves, and meters needed for bulk receipts and for loading racks used for small deliveries to trucks. Marine terminals have vessel length and water depth limits that dictate the size of tankers that can off-load at the facility.

Permitting Issues. Some of the environmental and safety issues associated with permitting petroleum and petroleum product terminals include:

- Changes in visual quality
- Disturbances to vegetation and wildlife
- Emissions from floating roof tanks
- Potential water and soil contamination from earthquake-damaged tanks
- Increased tanker traffic and potential for spills at marine facilities

References

1. **U.S. Petroleum Refining, Meeting Requirements for Cleaner Fuels and Refineries, Volume I**, National Petroleum Council, August, 1993. This document is a comprehensive assessment of how environmental regulations impact the petroleum refining industry and U.S. consumers.
2. **Fuels Report**, California Energy Commission, December, 1995, Publication No. P300-95-017. The Fuels Report describes emerging trends and long range forecasts of the demand, supply and price of petroleum, petroleum products, natural gas, coal and synthetic and other fuels. It is the state's principal fuels policy document.
3. Petroleum Industry Information Reporting Act submittals from the petroleum industry to the California Energy Commission.
4. **Quarterly Oil Report**, Fourth Quarter 1993, April 1994, California Energy Commission, Publication No. P300-94-003. This report describes petroleum fuels market trends, price trends, refinery activity, oil production trends and petroleum company financial performance. It contains aggregated petroleum statistics for California based on industry submittals to the Commission including refinery utilization rates.
5. **1994 Annual Report**, Western States Petroleum Association.

Sources:

Refinery list - California Energy Commission staff, updated regularly.

Background information and discussion - Energy Aware Planning Guide II: Energy Facilities, California Energy Commission, Publication No. 700-96-006, December 1996, Appendices B-24 and B-25.in

Research | Children's Health

Air Pollution and Childhood Respiratory Allergies in the United States

Jennifer D. Parker,[1] Lara J. Akinbami,[1] and Tracey J. Woodruff[2]

[1]National Center for Health Statistics, Centers for Disease Control and Prevention, Hyattsville, Maryland, USA; [2]Program on Reproductive Health and the Environment, Department of Obstetrics, Gynecology, and Reproductive Sciences, University of California–San Francisco, San Francisco, California, USA

Background: Childhood respiratory allergies, which contribute to missed school days and other activity limitations, have increased in recent years, possibly due to environmental factors.

Objective: In this study we examined whether air pollutants are associated with childhood respiratory allergies in the United States.

Methods: For the approximately 70,000 children from the 1999–2005 National Health Interview Survey eligible for this study, we assigned between 40,000 and 60,000 ambient pollution monitoring data from the U.S. Environmental Protection Agency, depending on the pollutant. We used monitors within 20 miles of the child's residential block group. We used logistic regression models, fit with methods for complex surveys, to examine the associations between the reporting of respiratory allergy or hay fever and annual average exposure to particulate matter ≤ 2.5 μm in diameter ($PM_{2.5}$), PM ≤ 10 μm in diameter, sulfur dioxide, and nitrogen dioxide and summer exposure to ozone, controlling for demographic and geographic factors.

Results: Increased respiratory allergy/hay fever was associated with increased summer O_3 levels [adjusted odds ratio (AOR) per 10 ppb = 1.20; 95% confidence interval (CI), 1.15–1.26] and increased $PM_{2.5}$ (AOR per 10 μg/m^3 = 1.23; 95% CI, 1.10–1.38). These associations persisted after stratification by urban–rural status, inclusion of multiple pollutants, and definition of exposures by differing exposure radii. No associations between the other pollutants and the reporting respiratory allergy/hay fever were apparent.

Conclusions: These results provide evidence of adverse health for children living in areas with chronic exposure to higher levels of O_3 and $PM_{2.5}$ compared with children with lower exposures.

Key words: allergy, children, hay fever, ozone, particulate matter. *Environ Health Perspect* 117:140–147 (2009). doi:10.1289/ehp.11497 available via *http://dx.doi.org/* [Online 30 September 2008]

Children in the United States are generally healthy; > 80% are in excellent or very good health according to the 2006 National Health Interview Survey (NHIS) (Bloom and Cohen 2007). However, a significant proportion of children are affected by respiratory conditions, including allergies, which are associated with missed school days and activity limitations (Blaiss 2004). Parent responses to questions in the 2006 NHIS indicate that about 9% of children < 18 years of age had had hay fever in the preceding 12 months, and slightly more had had respiratory allergies (Bloom and Cohen 2007). These estimates are higher than comparable statistics from the 1982 NHIS, where 5.5% of children were reported to have had hay fever or allergic rhinitis in the previous 12 months [National Center for Health Statistics (NCHS) 1985]. Respiratory allergies manifest as a variety of symptoms of varying duration and severity. In a recent review, Blaiss (2004) concluded that childhood allergic rhinitis, or allergies, contributes to increased loss of school days, impaired school performance, and increased mental health disorders from the various allergic symptoms and resulting increased sleep disruptions. Recent data from the NHIS support this conclusion; in a simple cross-tabulation, children with respiratory allergies or hay fever were more likely to miss school than those without these conditions (Parker et al. 2007). A brief review by Simons (1996) describes the impacts of allergies, including effects of medications used to treat allergies, on learning impairment in children.

A possible factor affecting respiratory allergic symptoms is exposure to ambient air pollution, particularly traffic pollutants. Reviews of the effects of air pollution on allergies have concluded that pollutants likely exacerbate effects of allergens among those with existing susceptibility, rather than initiating allergies among people without existing allergies (e.g., Bartra et al. 2007; D'Amato et al. 2005; von Mutius 2000). D'Amato et al. (2005) list possible rationales for the associations among components of air pollution, allergens, and allergic response, including the effects of the pollutants on the potency of the allergens and the increased susceptibility of the subjects via an inflammatory effect on the airway, increased airway reactivity, or increased bronchial responsiveness. Experimental evidence, for example, has shown that exposure to diesel particles may increase allergic response (e.g., Knox et al. 1997; Riedl and Diaz-Sanchez 2005), and a recent review of experimental studies outlines possible pathways for these effects (Riedl 2008). Human experimental studies have shown increased allergic response among predisposed adult subjects directly exposed to ozone at high (Jörres et al. 1996) or moderate but repeated (Holz et al. 2002) levels.

No comprehensive studies have examined associations between allergic symptoms and air pollution among a nationwide sample of U.S. children. From Europe and Asia, increases in indices of air pollution have been found to exacerbate childhood allergic symptoms in some studies (Annesi-Maesano et al. 2007; Hajat et al. 2001; Hwang et al. 2006; Janssen et al. 2003; Krämer et al. 2000; Lee et al. 2003; Morgenstern et al. 2007, 2008; Pénard-Morand et al. 2005; Yu et al. 2005) but not all (Nicolai et al. 2003; Ramadour et al. 2000). Some variation in results can be attributed to differences in case definitions. Many studies examine asthma, upper and lower respiratory infection, or other allergic symptoms, such as food or skin allergies, in addition to allergic rhinitis. The specific pollution exposures studied as well as other place-specific factors, such as local flora, may contribute to the differences in findings; across the United States, for example, pollen varieties and seasonal impact vary (Blaiss 2004). An intriguing study by von Mutius et al. (1998) documented the change in the incidence of seasonal allergic rhinitis after the reunification of Germany. Before reunification, allergies and asthma were less common in East Germany, an area with more industrial pollution, than in West Germany, with more traffic pollution. After reunification, allergies, but not asthma, increased among children in East Germany as East Germany's living conditions became more westernized, including more traffic. In a recent review, Heinrich and Wichmann (2004) concluded that the evidence linking traffic-related air pollutants and allergic rhinitis is equivocal. As argued by Brunekreef and Sunyer (2003),

Address correspondence to J. Parker, Office of Analysis and Epidemiology, National Center for Health Statistics, Centers for Disease Control and Prevention, 3311 Toledo Rd., Room 6107, Hyattsville, MD 20782 USA. Telephone: (301) 458-4419. Fax: (301) 458-4038. E-mail: jdparker@cdc.gov

The findings and conclusions in this article are those of the authors and do not necessarily represent the views of the National Center for Health Statistics, Centers for Disease Control and Prevention.

Data files were created by N. Kravets, Nova Research, supported by interagency agreement 05-037 between the National Center for Health Statistics and the Office of the Assistant Secretary for Planning and Evaluation.

The authors declare they have no competing financial interests.

Received 20 March 2008; accepted 30 September 2008.

more studies on air pollution and allergic rhinitis are needed.

The objective of this study was to explore possible relationships between air pollution measures and respiratory allergies in a large nationwide sample of U.S. children. In this study, we used data from the 1999–2005 NHIS that had been geographically linked to annual air monitoring data for several pollutants [particulate matter (PM), O_3, sulfur dioxide, and nitrogen dioxide] from the U.S. Environmental Protection Agency (U.S. EPA 2008). With both air pollution and allergen levels expected to rise with global climate change (Confalonieri et al. 2007), understanding the potential consequences for children's well-being is important both now and in the future.

Materials and Methods

NHIS. The NHIS is a large nationally representative survey of the civilian noninstitutionalized U.S. population (NCHS 2008c). Very briefly, the NHIS is a cross-sectional household interview survey conducted continuously throughout the year. For survey years 1999–2005, after state-level stratification, the first stage of its multistage probability design consisted of a sample of 358 primary sampling units (PSUs) drawn from approximately 1,900 geographically defined PSUs. PSUs are counties or groups of counties, or a metropolitan statistical area. Within a PSU, second-stage units are drawn (segments), and within each segment, all occupied households are targeted for interview. Black and Hispanic populations were oversampled during survey years 1999–2005. The probabilities of selection, along with adjustments for nonresponse and poststratification, are reflected in the sample weights (Botman et al. 2000). For additional information, see NCHS (2008b).

In 1999–2005, about 35,000 households were sampled each year, yielding almost 100,000 total respondents each year. In addition to the core family questionnaire each family member answers, within each family with children, a sample child was selected for additional questions on health and health care (Bloom and Cohen 2007). Response rates were generally high. During these data years, information was provided for > 90% of children selected for the sample child questionnaire; multiplied by the sample family response rates of 85–90%, the unconditional response rate for the sample child is about 80%. Special NHIS files geocoded to U.S. Census block and block group have been created and are available only through the NCHS Research Data Center (NCHS 2008d).

A total of 73,198 children 3–17 years of age provided information for the sample child questions in the 1999–2005 NHIS. Of these, a small number are missing data for one or more of the NHIS variables described below, leaving 72,279 eligible for this study.

Ambient air monitoring data. The Air Quality System (AQS) database provides annual averages of air monitoring data—ambient concentrations of criteria and hazardous air pollutants at monitoring sites, primarily in cities and towns (U.S. EPA 2008). The AQS database is updated daily by the U.S. EPA, primarily by the staff of state and local environmental agencies that measure ambient concentrations of criteria air pollutants at several thousand monitoring sites throughout the United States. Each month, the U.S. EPA extracts a summary of the measurements recorded at each air monitoring station (e.g., the highest value in a year and the average) and updates its database.

As part of a larger project to create linked NHIS–AQS data files, we extracted monitor-specific annual averages for several pollutants, including O_3, fine PM (PM with aerodynamic diameter ≤ 2.5 μm; $PM_{2.5}$), respirable PM (PM with aerodynamic diameter ≤ 10 μm; PM_{10}), NO_2, and SO_2 from the AQS using the annual summary web pages (Parker et al. 2008a); in addition, we calculated exposure to O_3 during the summer (May through September) for these linked data files using daily measures. We calculated summer O_3 exposures separately to obtain more comparable measures throughout the United States than annual average O_3 exposures—although differing monitoring periods are used across geographic areas, summertime is the most frequently monitored period (U.S. EPA 2006).

Linkage of the NHIS to the U.S. EPA air monitoring data. We assigned pollution exposure values to individual NHIS records for each survey year by averaging the monitor-specific annual averages for each pollutant for that year from monitors within a specified distance, and within the same county, of the respondent. Although the individual observations for each monitor are available for these pollutants, we used the annual arithmetic averages calculated by the U.S. EPA, except for O_3, as described above. We considered obtaining the annual arithmetic averages from the U.S. EPA preferable to calculating these or other metrics directly from the raw data because they reflect U.S. EPA methodology, are readily obtained, and are more easily replicated (Parker et al. 2008a). We calculated distances between the NHIS participants and the air quality monitors using the latitude and longitude assigned to the block group (population-weighted centroid) of residence of NHIS participants and the latitude and longitude of the U.S. EPA monitors. Using these distances to identify nearby monitors, we calculated annual pollution estimates within specified distances of each NHIS respondent's block group (Parker et al. 2008a).

For this study, we examined air pollution exposures for $PM_{2.5}$, PM_{10}, summer O_3, SO_2, and NO_2 calculated from monitors within a 20-mile radius, averaged using inverse-distance weighting, as the primary exposure measures. We chose these metrics to maximize the number of available children in the analyses. We conducted additional analyses using exposures estimated over 5 miles and with the annual O_3 exposure available from the U.S. EPA. Although children interviewed at the beginning of the calendar year may be less accurately assigned exposure based on calendar-year estimates because interview questions ask about the previous 12 months, correlations of annual exposures for these pollutants, grouped by county, were nearly always > 0.80 and often > 0.90.

Variable definitions. We categorized outcomes using responses to the following questions: "During the past 12 months, has [child's name] had any of the following conditions? Hay fever? Any kind of respiratory allergy? Any kind of food or digestive allergy? Eczema or any kind of skin allergy?" Children whose parents reported either hay fever or respiratory allergy in the previous 12 months were combined into one group because both conditions result in symptoms of allergic rhinitis—watery, itchy eyes, congestion, allergic cough, sneezing, and runny nose. We included children ≥ 3 years of age: Seasonal allergies typically develop after 2 years of age because children must be repeatedly exposed to seasonal pollens before developing a specific immunologic response (Fireman 2000).

We considered several additional factors that could influence observed associations between air pollution and reporting of respiratory allergy/hay fever: survey year, child's age, family structure (two parents, single mother, other), usual source of care (yes, no), health insurance (insured, uninsured), family income relative to federal poverty level (< 100%, 100% to < 200%, 200% to < 400%, ≥ 400%), child's race/ethnicity (non-Hispanic black, Mexican or Mexican American, non-Hispanic white, other groups). We separated the Mexican or Mexican-American subgroup from the other Hispanic subgroups because of the heterogeneity among these subgroups (Hajat et al. 2001). For the approximately 30% of records without reported income, we used the NHIS imputed income files to assign family income level (NCHS 2008a). We coded health insurance as insured or uninsured using the definition used by NCHS (2007). These factors are related to the reporting of childhood allergies and may affect estimated associations between allergies and air pollution.

We also included county-level geographic level covariates: median income from the 2000 U.S. Census, an index of urban–rural status (Ingram and Franco 2006), and region, as used

by the U.S. EPA (2003). We included urban–rural status and region because components of air pollution may differ geographically. We included median county-level income as a potentially confounding factor, related to both health outcomes (including the reporting of childhood allergies and available health services) and air pollution exposures.

Asthma is an important childhood condition related to the reporting of allergies and air pollution exposures and, in the United States, related to many of the covariates listed above (Akinbami 2006; Johnson et al. 2002). To examine the influence of asthma on possible associations between allergies and air pollution, we defined children as having current asthma if their parent or guardian reported that they had ever been told the child had asthma and that the child had had an asthma attack in the previous 12 months.

Environmental tobacco smoke affects the respiratory health of children. Unfortunately, the NHIS does not collect smoking information from all adults, just from one sampled adult per family. As a result, our smoking information for a child's exposure can only be dichotomized as yes versus unknown. Data on the smoking status of children is not collected in the NHIS.

Analysis. We evaluated possible associations between air pollution and childhood respiratory allergy/hay fever using logistic regression models. We used statistical software for surveys (SUDAAN; RTI International 2006) because of the complex clustered sample design of the NHIS. We included the design information, including the strata, PSUs, and adjusted sampling weights, to ensure proper statistical inference.

We fitted unadjusted and adjusted models separately for each pollutant. We tested interaction terms to determine whether associations differed by characteristics described above. We fitted additional models to examine the impact, if any, of current asthma; because the relationship between allergies and asthma among children is complex (Weinmayr et al. 2007), we decided to examine the role of asthma as a potential confounder in this study. However, given that the role of asthma may be more direct, making its inclusion in the models inappropriate, these analyses are secondary to the main analyses. We also examined the effect of the presence of an adult smoker in the

Table 1. Characteristics of eligible study population, percentage of children with respiratory allergies/hay fever, and characteristics of children linked to air pollution.

Characteristic	All eligible children (% distribution) (n = 72,279)	Respiratory allergy/ hay fever (%)[a]	Characteristics of children by linkage to each pollutant (% distribution)				
			Summer O_3 (n = 58,147)	SO_2 (n = 42,791)	NO_2 (n = 42,467)	$PM_{2.5}$ (n = 57,273)	PM_{10} (n = 50,874)
All	100.0	19.2	100.0	100.0	100.0	100.0	100.0
Percent of poverty threshold							
< 100	17.3	15.4	16.6	16.9	17.5	16.9	17.4
100 to < 200	21.5	17.1	20.4	20.2	20.5	20.7	21.0
200 to < 400	32.5	19.7	31.9	31.5	30.4	31.7	31.3
≥ 400	28.7	22.5	31.1	31.4	31.6	30.7	30.3
Insurance coverage							
Yes	89.4	19.8	89.7	89.8	88.9	89.7	89.2
No	10.6	13.8	10.3	10.2	11.1	10.3	10.8
Usual source of care							
Yes	94.1	19.7	94.4	94.6	93.9	94.3	93.9
No	5.9	11.1	5.6	5.4	6.1	5.7	6.1
Race/ethnicity							
Non-Hispanic black	14.6	16.8	15.7	17.8	17.5	16.2	16.7
Mexican or Mexican American	11.7	12.6	12.5	11.7	15.3	12.1	14.3
Non-Hispanic white	62.4	21.4	59.0	56.6	51.8	59.0	55.3
All other groups	11.3	16.7	12.8	13.9	15.4	12.8	13.6
Highest level of education of adult in household							
Less than high school	11.3	11.8	11.6	12.0	13.1	11.6	12.5
High school graduate	23.5	16.3	22.2	22.1	21.4	22.1	21.6
Some college	33.1	21.0	32.2	31.6	31.2	32.3	32.2
College graduate	19.7	21.5	20.6	20.6	20.6	20.7	20.5
Postgraduate	12.4	23.0	13.4	13.8	13.7	13.4	12.2
Family structure							
Two parents	61.0	19.5	60.0	58.7	57.8	60.0	58.9
One parent	15.9	19.6	16.1	16.8	16.5	16.3	16.6
Other groups	23.1	18.0	23.8	24.5	25.7	23.7	24.5
Age (years)							
3–5	19.6	14.3	19.9	20.0	20.1	20.1	20.0
6–9	26.3	18.1	26.4	26.5	26.4	26.4	26.4
10–14	34.1	21.1	34.0	34.1	34.0	34.1	34.0
15–17	20.0	22.1	19.8	19.5	19.5	19.4	19.6
Level of urbanization							
Large central metro	28.1	16.6	35.2	42.5	47.6	34.5	40.6
Large fringe metro	25.1	20.4	29.5	31.7	32.4	28.2	27.8
Medium metro	20.1	20.3	23.3	18.8	16.4	22.9	21.1
Small metro and other areas	26.0	19.9	12.0	7.1	3.7	14.4	10.5
Region							
Northeast	21.4	18.8	24.9	30.1	27.9	23.2	21.7
Southeast	26.1	20.3	24.4	21.8	22.2	25.0	24.1
Industrial Midwest	21.5	19.3	21.1	22.4	16.6	20.6	19.0
Upper Midwest	6.9	18.5	4.9	5.0	3.9	5.3	4.9
Southwest	5.6	20.8	4.7	3.9	6.1	5.0	5.7
Northwest	10.9	21.5	10.6	7.1	10.2	11.9	13.8
Southern California	7.6	12.3	9.3	9.7	13.2	9.0	10.9

All percentages were weighted using NHIS survey weights.
[a]All $p < 0.05$ for associations between variables and respiratory allergy/hay fever.

family on any observed associations; because this information is not collected for every adult in the household, making the variable imprecise, we included these results in the secondary analyses. Because the subsets of children with each pollution exposure differ, we performed extensive sensitivity analyses, including models with multiple pollutants and with exposures measured over smaller areas.

Results

All characteristics shown in Table 1 were significantly associated with respiratory allergies/hay fever as demonstrated by chi-square statistics without consideration of multiple comparisons. Using the combined outcome, 19.2% of this cohort of children 3–17 years of age are reported to have had hay fever, respiratory allergy, or both within the previous 12 months (Table 1); of this group, 11.4% reported hay fever, 12.8% reported respiratory allergy, and 5% reported both conditions. These estimates are slightly higher than those reported above (Bloom and Cohen 2007) because of the slightly older study cohort.

The number of children linked to air monitoring data varies by pollutant (Table 1). Of the eligible 72,279 children, 32,137 had exposure data for each of these pollutants within 20 miles, and 47,989 had exposure data for both PM_{10} and $PM_{2.5}$, allowing an approximate estimate of the coarse PM exposure by the difference ($PM_{2.5–10}$ = PM_{10} levels – $PM_{2.5}$ levels). In all linkage groups, respiratory allergy/hay fever reporting was slightly lower than in the overall sample of children, ranging from 18.3% for children linked to NO_2 to 19.0% for children linked to $PM_{2.5}$. There are small demographic differences and larger geographic differences among the linkage subsets.

Table 2. Median (interquartile range) and correlations among pollution variables within a 20-mile radius of study subjects.[a]

	Pollutant					
Measure	Summer O_3 (ppb)	SO_2 (ppb)	NO_2 (ppb)	$PM_{2.5}$ (μg/m^3)	$PM_{2.5–10}$ (μg/m^3)	PM_{10} (μg/m^3)
Median (interquartile range)	31.5 (27.6–35.1)	3.90 (2.35–5.50)	17.8 (13.6–23.4)	13.1 (10.9–15.2)	11.2 (8.2–15.2)	24.1 (20.8–28.7)
Correlation						
Summer O_3	1.00	0.00	–0.07	0.10	0.16	0.26
SO_2		1.00	–0.26	0.21	–0.33	–0.19
NO_2			1.00	0.53	0.29	0.48
$PM_{2.5}$				1.00	0.02	0.51
$PM_{2.5–10}$					1.00	0.86
PM_{10}						1.00

[a]Number of children with pollutant exposure is given in Table 1. Number of children with data for two pollutants varies by combination.

Table 3. ORs (95% CIs) per approximate interquartile range[a] for associations between annual average air pollution exposures and reporting of respiratory allergy/hay fever among children.

		Single-pollutant models		
Pollutant	No. of children	Unadjusted	Adjusted[b]	Adjusted[c]
Summer O_3	58,147	1.18 (1.13–1.23)	1.15 (1.11–1.20)	1.20 (1.15–1.26)
SO_2	42,791	1.05 (1.01–1.09)	1.00 (0.96–1.04)	1.03 (0.97–1.08)
NO_2	42,467	0.83 (0.79–0.86)	0.87 (0.84–0.92)	0.95 (0.90–1.01)
$PM_{2.5}$	57,273	0.79 (0.74–0.84)	0.87 (0.80–0.93)	1.16 (1.04–1.30)
$PM_{2.5–10}$	47,867	0.92 (0.89–0.97)	1.02 (0.97–1.06)	1.01 (0.95–1.07)
PM_{10}	50,874	0.89 (0.86–0.92)	0.97 (0.94–1.01)	1.04 (0.99–1.09)

We averaged O_3 for May through September; all other pollutants represent annual averages.
[a]Summer O_3 per 10 ppb; SO_2 per 3 ppb; NO_2 per 10 ppb; PM per 10 μg/m^3. [b]Adjusted for year, poverty, race, family structure, insurance, usual source of care, age, and education of adult. [c]Additionally adjusted for urban status, region, and median income of county.

Table 4. AORs (95% CIs) per approximate interquartile range[a] for associations between annual average air pollution exposures and reporting of respiratory allergy/hay fever among children: single- and multiple-pollutant models (n = 32,080).

Pollutant	Single-pollutant model	Multiple-pollutant model
Summer O_3	1.24 (1.15–1.34)	1.18 (1.09–1.27)
SO_2	0.95 (0.88–1.02)	0.97 (0.90–1.04)
NO_2	0.98 (0.90–1.07)	0.99 (0.89–1.10)
$PM_{2.5}$	1.23 (1.04–1.46)	1.29 (1.07–1.56)
$PM_{2.5–10}$	1.13 (1.05–1.22)	1.16 (1.06–1.24)

We averaged O_3 for May through September; all other pollutants represent annual averages. Adjustments include year, poverty, race, family structure, insurance, usual source of care, age, education of adult, urban status, region, and median income of county. The multiple-pollutant model includes each pollutant; the single-pollutant models are separate models for each pollutant, using the same children as the multiple-pollutant model.
[a]Summer O_3 per 10 ppb; SO_2 per 3 ppb; NO_2 per 10 ppb; PM per 10 μg/m^3.

Table 2 shows correlations among the pollutants. Generally, correlations are low, with negative correlations between PM_{10} and SO_2 and between $PM_{2.5–10}$ and SO_2. Correlations between pollutants were, for the most part, similar whether we used the subset of 32,137 children linked to all pollutants for all calculations or used different subsets, depending on available data, for each calculation.

Associations between reporting of respiratory allergy/hay fever and air pollution varied among the pollutants (Table 3). After adjustment for demographic and geographic variables, increases in summer O_3 were associated with increased reporting of respiratory allergy/hay fever. $PM_{2.5}$ was associated with reporting of these conditions after including geographic indicators in the models. Other gaseous pollutants were not associated with increased respiratory allergy/hay fever and, in some cases, were negatively associated. After controlling for multiple pollutants (Table 4), associations between reporting of respiratory allergy/hay fever and air pollution persisted for summer O_3 and $PM_{2.5}$. The association between respiratory allergy/hay fever and $PM_{2.5–10}$ increased in the subset linked to multiple pollutants, both without and with adjustment for multiple pollutants, suggesting possible sample selection effects in this group.

Because including geographic variables had a large impact on the associations, we examined whether effects were similar by urban–rural status by including interaction terms in the regression models. In single-pollutant models, associations were significantly different by urban–rural status for summer O_3, PM_{10}, and $PM_{2.5–10}$, but not for $PM_{2.5}$ or the other gaseous pollutants. Summer O_3 had a slightly stronger effect on reporting of respiratory allergy/hay fever in the more urban areas compared with the small metropolitan and rural areas, whereas PM_{10} and $PM_{2.5–10}$ had slightly stronger associations in medium and fringe metropolitan areas (data not shown).

Given the differences in reporting respiratory allergy/hay fever by child's race, family poverty status, and child's age and sex, we examined interactions (products of these factors and the pollutants) to determine whether associations for summer O_3 and PM variables differed by these factors. Model results with interaction terms indicated that associations did not differ significantly (using $p < 0.05$ as criterion) by race/ethnicity, sex, or age category for either PM or summer O_3. Associations did not differ significantly by poverty status for PM variables, but the associations between summer O_3 exposure and respiratory allergy/hay fever for children in poverty categories > 200% of poverty were stronger than for those < 200% of poverty: < 100% poverty, adjusted odds ratio (AOR) = 1.05 [95% confidence interval (CI) =

0.95–1.16]; 100% to < 200%, 1.13 (1.01–1.27); 200% to < 400%, 1.28 (1.17–1.39); 400% or higher, 1.25 (1.15–1.35).

Because the 20-mile exposure radius may be inadequate for assigning exposure for the gaseous pollutants, we replicated the full models using the subsets of children within 5 miles of pollution monitors. Fewer than half of the children with 20-mile exposure variables were available for the 5-mile analyses, ranging from 14,034 for SO_2 to 26,898 for $PM_{2.5}$. Results for summer O_3 from a model adjusted for demographic and geographic variables remained statistically significant (OR = 1.16; 95% CI, 1.07–1.25), if slightly weaker than the OR shown in Table 3. With the smaller sample size, results for $PM_{2.5}$ were elevated but lower than those shown in Table 3, and no longer significant (OR = 1.09; 95% CI, 0.93–1.28). Associations between reporting of respiratory allergy/hay fever and the other pollutants were similar to those reported using the 20-mile exposures shown in Table 3. Correlations between the 20-mile and 5-mile pollution variables were high, especially for summer O_3 and $PM_{2.5}$ ($r > 0.95$); for the other pollutants, correlations between the 20-mile and 5-mile variable were at least 0.85. Although the 20-mile and 5-mile exposure variables, calculated from many of the same monitors, are not independent and hence statistical inferences from these correlations are inappropriate, the correlations give an indication of the similarity of the measures.

We fit models without controlling for survey year, with similar results (data not shown). Including survey year would be considered appropriate for the control of temporal changes that may have affected reporting of respiratory allergies, such as access to health care; on the other hand, year is also correlated with air pollution levels, and including year would be considered overcontrol if, for example, changes in reporting over time were attributed to the corresponding temporal changes in air pollution. Because we cannot distinguish the two scenarios, we examined results both ways.

We compared the results for the summer O_3 with those using the annual averages of the daily 8-hr running O_3 averages provided by the U.S. EPA. These averages were, by design, lower than the summer averages but highly correlated ($r = 0.80$) despite the differing O_3 reporting periods throughout the United States, the use of average daily measurement to calculate the summer-O_3 variable, and the use of daily 8-hr averages to calculate the annual O_3 variable. Corresponding to the high correlation, the association between annual O_3 exposure and respiratory allergy/hay fever adjusted for demographic and geographic factors (AOR = 1.16; 95% CI, 1.11–1.21) was similar to that reported for summer O_3 (Table 3).

In further tabulations of our study sample, of the children with respiratory allergy/hay fever, > 30% had been told at some time that they had asthma; in contrast, only 9% of children without allergies or hay fever had been told they had asthma. Adjustment for asthma in the logistic regression models did not change the findings for either summer O_3 or $PM_{2.5}$, although the independent effect of asthma on respiratory allergy/hay fever was large (data not shown).

Finally, we fit models that included adult smoking (yes vs. unknown). In the eligible sample, 20.3% of children lived in a family with a known smoker. Although adult smoking in the family had an independent effect on respiratory allergy/hay fever, its inclusion in the models did not affect associations between respiratory allergy/hay fever and either $PM_{2.5}$ or O_3 (data not shown).

Discussion

We found a persistent association between increased levels of summer O_3 and reporting of respiratory allergies and hay fever among U.S. children. These findings were stronger in urban than in less urban areas and persisted when controlling for family income, parental education, family structure, child's age, median county-level income, access to care, and current asthma status. The association between O_3 and respiratory allergy/hay fever was weaker among children living in the less metropolitan counties, which may suggest variation in types of allergens or other factors related to level of urbanization (climate, societal) that modify the effects of O_3 on respiratory allergies/hay fever. Furthermore, that the association became stronger as family income rose suggests one of two scenarios: *a*) Real differences exist and there is something about more privileged children that increases their susceptibility; or *b*), parents in lower-income groups are underreporting.

Although the findings for increased reporting of respiratory allergy/hay fever with increased O_3 exposure were most robust, we also found a strong association between $PM_{2.5}$ exposure and reporting of respiratory allergy/hay fever after controlling for geographic variables. Effects of $PM_{2.5–10}$ on the reporting of respiratory allergy/hay fever were weaker than the effects of $PM_{2.5}$ and varied somewhat geographically.

In contrast, we found no evidence with these data that annual average exposure to NO_2 or SO_2 when derived by spatial averages within 20 or within 5 miles of a child's residence was associated with reporting of childhood respiratory allergy/hay fever. Although these findings may indeed reflect no association, there is some evidence that metrics for these gaseous pollutants based on ambient monitoring are less representative of exposure than are similar metrics for O_3 or PM (Ito et al. 2005; Kim et al. 2006).

Our findings for O_3 are consistent with a recent study of > 6,000 children in France that showed increased allergic sensitivity and lifetime allergic rhinitis with increasing O_3 exposure (Pénard-Morand et al. 2005) and a time series study from England that showed physician visits for allergies increased with increasing O_3 exposure among children (Hajat et al. 2001); in addition, a study of Austrian school children (Frischer et al. 2001) showed increases in a biomarker related to airway inflammation (urinary eosinophil protein X) and respiratory response with increasing O_3 exposure. However, studies from France (Ramadour et al. 2000) and Taiwan (Hwang et al. 2006) showed no association between O_3 and measures of respiratory allergy. In the United States, earlier results from the Harvard Six Cities study showed an elevated, but not statistically significant, risk of hay fever in cities with higher O_3 levels (Dockery et al. 1989). A study of 170 German school children showed that the increased allergic responses associated with increased levels of O_3 were reduced with constant high levels of O_3, possibly indicating an adaptive response (Kopp et al. 1999). How this potentially adaptive response affects overall associations in a study area as large as the United States with widely varying underlying O_3 levels is unknown.

Fewer studies have specifically examined PM. Recent German studies of $PM_{2.5}$ found increased allergic symptoms (sneezing/runny nose) for very young children (Morgenstern et al. 2007) and allergic sensitization and hay fever for these children up to 6 years of age (Morgenstern et al. 2008) exposed to higher pollution levels. In a study in Paris, Nikasinovic et al. (2006) observed associations between markers of nasal inflammation and $PM_{2.5}$ exposure in children with mild-to-moderate allergic asthma but not in other children. Similarly, a separate study in France showed a relatively large effect of $PM_{2.5}$ on allergic asthma but not on allergic rhinitis (Annesi-Maesano et al. 2007). The studies by Pénard-Morand et al. (2005) and Hajat et al. (2001), mentioned above, also showed positive associations between high PM_{10} levels and lifetime allergies and doctor visits, respectively. On the other hand, a study of schoolchildren in Norway generally showed no associations between traffic-related pollutants, including $PM_{2.5}$, and allergen sensitization (Oftedal et al. 2007); the authors suggested that Oslo pollution levels are too low to detect associations. Similarly, in a prospective cohort study of children from the Netherlands, $PM_{2.5}$ was not associated with allergic sensitization, except for food allergies (Brauer et al. 2007).

Inferences for the effects of PM on allergies, for the most part, have been based on

traffic studies. Studies from Germany have arrived at different conclusions. One German study showed elevated but not significantly elevated prevalence of hay fever for children exposed to more traffic; in this study, traffic-related pollution was associated with allergic sensitization among children who were also exposed to tobacco smoke (Nicolai et al. 2003). Other German studies showed increased hay fever and other allergic symptoms with markers of traffic exposure (Duhme et al. 1996; Krämer et al. 2000; Weiland et al. 1994); however, another study from Germany showed no associations between traffic indices and allergic symptoms (Hirsch et al. 1999). A study of Dutch children related truck, but not automobile, traffic to increased respiratory symptoms and allergy sensitization (Janssen et al. 2003); an earlier Dutch study showed elevated but not significantly higher risks of allergies for children living on busy streets compared with those living on quieter streets (Oosterlee et al. 1996). From Asia, studies from Thailand (Pothikamjorn et al. 2002) and Taiwan (Lee et al. 2003) showed more allergic symptoms for children exposed to more traffic. Although differences among these studies can readily be attributed to differences in measures of traffic exposure and markers of allergy, the collection supports our finding that increases in PM exposure can increase the burden of allergies among children.

Prior summaries of the epidemiology of respiratory allergies and hay fever are often coupled with examinations of other respiratory symptoms, especially asthma (Brunekreef and Sunyer 2003; Johnson et al. 2002; Nicolai 2002). Most children with asthma also report respiratory allergies/hay fever; both diseases cover a spectrum of conditions and can be triggered by similar agents (e.g., pollen or cat). Although a detailed examination of air pollution effects on indicators of asthma was not part of this study, our results for effects of O_3 and $PM_{2.5}$ on reported allergy persisted after controlling for current asthma. More targeted analysis is required to understand the effects of air pollution on the co-reporting of respiratory allergies/hay fever and indices of asthma.

The strength of this study is its nationwide scope and its large number and diversity of children. The NHIS is carefully conducted, and survey weights are created to reflect all children in the United States. These data contain information on family characteristics, including family income and education of family members, to control for confounding. Using in-house geographic information, we could additionally consider geographic factors. Even with the reduced sample available to examine air pollution, the survey weights allow estimates to better reflect the population of children living near monitors throughout the United States.

A limitation of this study is its cross-sectional design, intended to provide prevalence estimates. From this design, we cannot establish the direction of the air pollution—hay fever/respiratory allergy association, and our results may be subject to length bias, where children with longer duration of hay fever/respiratory allergy will overrepresent cases compared with children with shorter duration (Rothman et al. 2008). Additionally, the definition of the primary outcome variable by parent self-report and the 12-month time span for the recall may lead to additional bias. With this case definition, we cannot, for example, examine the role of the timing of air pollution on the initiation of either atopic sensitization or the onset of symptoms. As expressed by Johnson et al. (2002), defining allergies is difficult—"the most significant and as yet unsolved methodological issue is one fundamental to the conduct of epidemiology: arriving at a definition of disease." Commonly used biomarkers for allergy—positive blood tests for allergen-specific serum immunoglobulin E and positive allergen-specific skin prick tests—are not always correlated with each other or with clinical allergic symptoms (Johnson et al. 2002). Allergies are also characterized by allergic sensitization measures, although correlates of respiratory allergic symptoms are not necessarily the same as those for sensitization. A generally used definition of childhood allergies is based on parental report of symptoms or report of a history of a provider diagnosis, similar to the case definition based on parental report in this study. As a consequence, making inferences from studies using different case definitions about allergy prevalence, onset, severity, or exacerbation is difficult.

We used a data set previously linked to annual exposure data (or summer-O_3 data), which may not cover the exact recall period for each respondent. These annual exposures, however, are correlated such that exposure for the calendar year is probably similar to exposure for the previous year; averaged over counties, the correlations between adjacent average exposures were high (e.g., for summer O_3, $r = 0.85$; for $PM_{2.5}$, $r = 0.80$). In addition, we have no information on local aeroallergen levels, which would have increased our understanding of the effects of air pollution on reported allergies.

Another limitation is the primary use of a 20-mile radius to define exposure from the NHIS respondent's residential block group. Ideally, more precise exposure measures would be available for each child, either from personal monitoring or finer spatial scales, which would lead to more precise effect estimates. With this survey, there is a substantial trade-off between criteria for proximity of monitors and the sample size and composition of the available data (Parker et al. 2008a, 2008b). In this case, the results using the substantially smaller samples within 5 miles of a pollution monitor were remarkably similar to the primary results presented. This similarity was apparent for both the PM exposures and the gaseous pollutant exposures. Indeed, this similarly suggests a robustness of the findings to both sample composition and exposure assignment. With the national data, spatial variation in exposure is relatively large; as evidenced by the correlations, rankings of the pollutant values are similar within the sample whether defined by 20 miles or 5 miles. Markedly few of these children lived within 1 mile of an O_3 (< 500) or $PM_{2.5}$ (< 3,000) monitor and were likely poorly distributed demographically and geographically across the United States.

A related issue is our impaired ability to compare within-area effects of local differences in exposure with between-area effects. The NHIS is not designed for local estimates; although it may be possible to define a local unit of analysis from which to frame the comparison, say, county or metropolitan statistical area, the clustered design does not lend itself to sufficiently varied exposures within most counties to adequately examine this question.

Children may be especially sensitive to effects of inhaled toxins and pollutants. Compared with adults, they have higher metabolic rates and minute ventilation rates (Bateson and Schwartz 2008). Most important, lung growth development continues through childhood and may be altered by environmental exposures. Studies of infant nonhuman primates exposed to O_3 for cyclical periods over 6 months demonstrated altered airway architecture with fewer and narrower small airways, disordered smooth muscle orientation, and hyperplastic bronchiolar epithelium (Fanucchi et al. 2006). In a prospective study of California children 10–18 years of age, living within 500 m of a freeway had an adverse effect on lung growth (Gauderman et al. 2007). In addition to lung development, sensitivity to allergens may also be affected by pollutant exposure over time. Exposing infant nonhuman primates to both O_3 and house dust mite allergen showed that O_3 had a synergistic effect on the effects of allergen exposure on atypical development of the basement membrane zone of the airway epithelium and alterations in immunoreactivity (Evans et al. 2003). Although the O_3 level in these studies (0.5 ppm) exceeded the average levels found in our study, these studies present evidence of permanently compromised lung structure and growth for early or chronic exposure to pollutants.

There have been several studies of children's respiratory health and air pollution from the United States. Although these studies focused more on allergies and other respiratory

symptoms, they highlight the importance of air pollution for children's health. For example, two multisite studies primarily related to asthma, the National Cooperative Inner-City Asthma Study (Mortimer et al. 2002) and a study of children in the Childhood Asthma Management Program (Schildcrout et al. 2006), reported increased asthma symptoms with increasing air pollutants. Poorer lung function was related to PM exposure among asthmatic children from Detroit, Michigan (Lewis et al. 2005). Similarly, Gent et al. (2003) reported exacerbation of respiratory systems with increasing levels of O_3 and $PM_{2.5}$ among asthmatic children in New England. The Children's Health Study from Southern California (Peters et al. 1999) has reported increased asthma medication use and wheezing (Millstein et al. 2004), school absenteeism (Gilliland et al. 2001), and poorer lung development (Gauderman et al. 2004) among children exposed to different air pollutants. Using data from East Bay Children's Respiratory Health Study, Kim et al. (2004) found that traffic-related pollution significantly increased respiratory symptoms among children in Northern California. Earlier studies of respiratory illness among children from the Harvard Six Cities Study (Dockery et al. 1989) and among 24 communities throughout the United States and Canada (Dockery et al. 1996) reported increases in some but not all symptoms and measures of PM.

Conclusion

The results of this study agree with the findings in the literature: exposures to O_3 and fine PM are associated with childhood respiratory allergies. The weight of the findings to date support detailed monitoring of air quality as high levels of exposure are increasingly being demonstrated as unsafe to public health and costly in terms of morbidity, lost school and work days, and lower quality of life.

References

Akinbami L. 2006. The State of Childhood Asthma in the United States 1980–2005. Advance Data from Vital and Health Statistics, No. 381. Hyattsville, MD:National Center for Health Statistics.

Annesi-Maesano I, Moreau D, Caillaud D, Lavaud F, Le Moullec Y, Taytard A, et al. 2007. Residential proximity fine particles related to allergic sensitization and asthma in primary school children. Resp Med 101:1721–1729.

Bartra J, Mullol J, del Cuvillo A, Dávila, Ferrer M, Jáuregui I, et al. 2007. Air pollution and allergens. J Invest Allergol Clin Immunol 17(suppl 2):2–8.

Bateson TF, Schwartz J. 2008. Children's response to air pollutants. J Toxicol Environ Health A 71:238–243.

Blaiss M. 2004. Current concepts and therapeutic strategies for allergic rhinitis in school-age children. Clin Ther 26:1876–1889.

Bloom B, Cohen R. 2007. Summary health statistics for U.S. children: National Health Interview Survey, 2006. National Center for Health Statistics. Vital Health Stat 10(234):1–79.

Botman SL, Moore TF, Moriarity CL, Parsons VL. 2000. Design and estimation for the National Health Interview Survey 1995–2004. National Center for Health Statistics. Vital Health Stat 2(130):1–31.

Brauer M, Hoek G, Smit HA, de Jongste JC, Gerritsen J, Postma DS, et al. 2007. Air pollution and development of asthma, allergy and infections in a birth cohort. Eur Respir J 29:879–888.

Brunekreef B, Sunyer J. 2003. Asthma, rhinitis and air pollution: is traffic to blame? Eur Respir J 21:913–915.

Confalonieri U, Menne B, Akhtar R, Ebi KL, Hauengue M, Kovats RS, et al. 2007. Human health. In: Climate Change 2007: Impacts, Adaptation and Vulnerability. Contributions of Working Group II to the Fourth Assessment Report of the Intergovernmental Panel on Climate Change (Perry ML, Canziani OF, Palutikof JP, van der Linden PH, Hansen CE, eds). Cambridge, UK:Cambridge University Press, 391–431.

D'Amato G, Liccardi G, D'Amato M, Holgate S. 2005. Environmental risk factors and allergic bronchial asthma. Clin Exp Allergy 35:1113–1124.

Dockery DW, Cunningham J, Damokosh AI, Neas LM, Spengler JD, Koutrakis P, et al. 1996. Health effects of acid aerosols on North American children: respiratory symptoms. Environ Health Perspect 104:500–505.

Dockery DW, Speizer FE, Stram DO, Ware JH, Spengler JD, Ferris BG. 1989. Effects of inhalable particles on respiratory health of children. Am Rev Respir Dis 139:587–594.

Duhme H, Weiland SK, Keil U, Kraemer B, Schmid M, Stender M, et al. 1996. The association between self-reported symptoms of asthma and allergic rhinitis and self-reported traffic density on street of residence in adolescents. Epidemiology 7:578–582.

Evans MJ, Fanucchi MV, Baker GL, Van Winkle LS, Pantle LM, Nishio SJ, et al. 2003. Atypical development of the tracheal basement membrane zone of infant rhesus monkeys exposed to ozone and allergen. Am J Physiol Lung Cell Mol Physiol 285:L931–L939.

Fanucchi MV, Plopper CG, Evans MJ, Hyde DM, Van Winkle LS, Gershwin LJ, et al. 2006. Cyclic exposure to ozone alters distal airway development in infant rhesus monkeys. Am J Physiol Lung Cell Mol Physiol 291:L644–L650.

Fireman P. 2000. Therapeutic approaches to allergic rhinitis: treating the child. J Allergy Clin Immunol 105 part 2:S616–S621.

Frischer T, Studnicka M, Halmerbauer G, Horak F Jr, Gartner C, Tauber E, et al. 2001. Ambient ozone exposure is associated with eosinophil activation in healthy children. Clin Exp Allergy 31:1213–1219.

Gauderman WJ, Avol E, Gilliland F, Vora H, Thomas D, Berhane K, et al. 2004. The effect of air pollution on lung development from 10 to 18 years of age. N Engl J Med 351:1057–1067.

Gauderman WJ, Vora H, McConnell R, Berhane K, Gilliland F, Thomas D, et al. 2007. Effect of exposure to traffic on lung development from 10 to 18 years of age: a cohort study. Lancet 369:571–577.

Gent JF, Triche EW, Holford TR, Belanger K, Bracken MB, Beckett WS, et al. 2003. Association of low-level ozone and fine particles with respiratory symptoms in children with asthma. JAMA 290:1859–1867.

Gilliland FD, Berhane K, Rappaport EB, Thomas DC, Avol E, Gauderman WJ, et al. 2001. The effects of ambient air pollution on school absenteeism due to respiratory illnesses. Epidemiology 12:43–54.

Hajat S, Haines A, Atkinson RW, Bremner SA, Anderson HR, Emberlin J. 2001. Association between air pollution and daily consultations with general practioners for allergic rhinitis in London, United Kingdom. Am J Epidemiol 153:704–714.

Heinrich J, Wichmann HE. 2004. Traffic related pollutants in Europe and their effect on allergic disease. Curr Opin Allergy Clin Immunol 4:341–348.

Hirsch T, Weiland SL, von Mutius E, Safeca AF, Gräfe H, Csaplovics E, et al. 1999. Inner city air pollution and respiratory health and atopy in children. Eur Respir J 14:669–677.

Holz O, Mucke M, Paasch K, Bohme S, Timm P, Richter K, et al. 2002. Repeated ozone exposures enhance bronchial allergen responses in subjects with rhinitis or asthma. Clin Exp Allergy 32:681–689.

Hwang BF, Jaakkola JJK, Lee YL, Lin YC, Leon Guo Y. 2006. Relation between air pollution and allergic rhinitis in Taiwanese schoolchildren. Resp Res 7:23.

Ingram DD, Franco S. 2006. 2006 NCHS Urban-Rural Classification Scheme for Counties. Available: http://www.cdc.gov/nchs/r&d/rdc_urbanrural.htm [accessed 5 December 2008].

Ito K, De Leon S, Thurston GD, Nádas A, Lippmann M. 2005. Monitor-to-monitor temporal correlation of air pollution in the contiguous US. J Expo Anal Environ Epidemiol 15:172–184.

Janssen NAH, Brunekreef B, van Vilet P, Aarts F, Meliefste K, Harssema H, et al. 2003. The relationship between air pollution from heavy traffic and allergic sensitization, bronchial hyperresponsiveness, and respiratory symptoms in Dutch schoolchildren. Environ Health Perspect 111:1512–1518.

Johnson CC, Ownby DR, Zoratti EM, Alford SH, Williams LK, Joseph CLM. 2002. Environmental epidemiology of pediatric asthma and allergy. Epidemiol Rev 24:154–175.

Jörres R, Nowak D, Magnussen H. 1996. The effect of ozone exposure on allergen responsiveness in subjects with asthma or rhinitis. Am J Respir Crit Care Med 153:56–64.

Kim D, Sass-Kortsak A, Purdham JT, Dales RE, Brook JR. 2006. Associations between personal exposures and fixed-site ambient measurements of fine particulate matter, nitrogen dioxide, and carbon monoxide in Toronto, Canada. J Expo Sci Environ Epidemiol 16:172–183.

Kim JJ, Smorodinsky S, Lipsett M, Singer BC, Hodgson AT, Ostro B. 2004. Traffic-related air pollution near busy roads. The East Bay Children's Respiratory Study. Am J Respir Crit Care Med 170:520–526.

Knox RB, Suphioglu C, Taylor P, Desai R, Watson HC, Peng JL, et al. 1997. Major grass pollen allergen Lol p 1 binds to diesel exhaust particles: implications for asthma and air pollution. Clin Exp Allergy 27:246–251.

Kopp MV, Ulmer C, Ihorst G, Seydewistz HH, Frischer T, Forster J, et al. 1999. Upper airway inflammation in children exposed to ambient ozone and potential signs of adaptation. Eur Respir J 14:854–861.

Krämer U, Koch T, Ranft U, Ring J, Behredt H. 2000. Traffic-related air pollution is associated with atopy in children living in urban areas. Epidemiology 11:64–70.

Lee YL, Shaw CK, Su HJ, Lai JS, Ko YC, Huang SL, et al. 2003. Climate, traffic-related air pollutants and allergic rhinitis prevalence in middle-school children in Taiwan. Eur Respir J 21:964–970.

Lewis TC, Robins TG, Dvonch JT, Keeler GJ, Yip FY, Mentz GB, et al. 2005. Air pollution-associated changes in lung function among asthmatic children in Detroit. Environ Health Perspect 113:1068–1075.

Millstein J, Gilliland F, Berhane K, Gaunderman WJ, McConnell R, Avol E, et al. 2004. Effects of ambient air pollutants on asthma medication use and wheezing among fourth-grade school children from 12 Southern California communities enrolled in the Children's Health Study. Arch Environ Health 59:505–514.

Morgenstern V, Zutavern A, Cyrys J, Brockow I, Gehring U, Koletzko S, et al. 2007. Respiratory health and individual estimated exposure to traffic-related air pollutants in a cohort of young children. Occup Environ Med 64:8–16.

Morgenstern V, Zutavern A, Cyrys J, Brockow I, Koletzko S, Krämer U, et al. 2008. Atopic diseases, allergic sensitization, and exposure to traffic-related air pollution in children. Am J Respir Crit Care Med 177:1331–1337.

Mortimer KM, Neas LM, Dockery DW, Redline S, Tager IB. 2002. The effect of air pollution on inner-city children with asthma. Eur Respir J 19:699–705.

NCHS (National Center for Health Statistics). 1985. Current estimates from the National Health Interview Survey, United States 1982. Vital Health Stat 10(150):1–200.

NCHS. 2007. Health, United States. Hyattsville, MD:National Center for Health Statistics.

NCHS (National Center for Health Statistics). 2008a. 2001 Imputed Family Income/Personal Earnings Files. Available: http://www.cdc.gov/nchs/about/major/nhis/2001imputedincome.htm [accessed 5 December 2008].

NCHS (National Center for Health Statistics). 2008b. 2005 National Health Interview Survey (NHIS): Public Use Data Release, NHIS Survey Description. Hyattsville, MD:Division of Health Interview Statistics, National Center for Health Statistics. Available: ftp://ftp.cdc.gov/pub/Health_Statistics/NCHS/Dataset_Documentation/NHIS/2005/srvydesc.pdf [accessed 27 August 2008].

NCHS (National Center for Health Statistics). 2008c. National Health Interview Survey (NHIS)—Celebrating the First 50 years: 1957–2007. Available: http://www.cdc.gov/nchs/nhis.htm [accessed 5 December 2008].

NCHS (National Center for Health Statistics). 2008d. Research Data Center (RDC). Available: http://www.cdc.gov/nchs/r&d/rdc.htm [accessed 5 December 2008].

Nicolai T. 2002. Pollution, environmental factors and childhood respiratory allergic disease. Toxicology 191–182:317–321.

Nicolai T, Carr D, Weiland SK, Duhme H, von Ehrenstein O, Wagner C, et al. 2003. Urban traffic and pollutant exposure

related to respiratory outcomes and atopy in a large sample of children. Eur Respir J 21:956–963.

Nikasinovic L, Just J, Sahraoui F, Seta N, Grimfeld A, Momas I. 2006. Nasal inflammation and personal exposure to fine particles $PM_{2.5}$ in asthmatic children. J Allergy Clin Immunol 17:1382–1388.

Oftedal B, Brunekreef B, Nystad W, Nafstad P. 2007. Residential outdoor air pollution and allergen sensitization in schoolchildren in Oslo Norway. Clin Exp Allergy 37:1632–1640.

Oosterlee A, Drijver M, Lebret K, Burnekreff B. 1996. Chronic respiratory symptoms in children and adults living along streets with high traffic density. Occup Env Med 53:241–247.

Parker JD, Akinbami L, Kravets N. 2007. Air pollution and childhood allergies in the United States [Abstract]. Epidemiology 18(suppl 5):S202.

Parker JD, Kravets N, Woodruff TJ. 2008a. Linkage of the National Health Interview Survey to air quality data. National Center for Health Statistics. Vital Health Stat(145):1–24.

Parker JD, Kravets N, Woodruff TJ, Akinbami L. 2008b. Linkage of the National Health Interview Survey to air monitoring data. Environ Res 106:384–392.

Pénard-Morand C, Charpin D, Raherison C, Kopferschmitt C, Caillaud D, Lavaud F, et al. 2005. Long-term exposure to background air pollution related to respiratory and allergic health in schoolchildren. 2005. Clin Exp Allergy 35:1279–1287.

Peters JM, Avol E, Navidi W, London SJ, Gauderman WJ, Lurmann F, et al. 1999. A study of twelve Southern California communities with differing levels and types of air pollution. I. Prevalence of respiratory morbidity. Am J Respir Crit Care Med 159:760–767.

Pothikamjorn SL, Ruxrungtham K, Thampanitchawong P, Fuangthong R, Srasuebkul P, Sangahsapaviriyah A, et al. 2002. Impact of particulate air pollutants on allergic diseases, allergic skin reactivity and lung function. Asian Pac J Allergy Immunol 20:77–83.

Ramadour M, Burrel C, Lanteaume A, Vervloet D, Charpin D, Brisse F, et al. 2000. Prevalence of asthma and rhinitis in relation to long-term exposure to gaseous air pollutants. Allergy 55:1163–1169.

Riedl MA. 2008. The effect of air pollution on asthma and allergy. Curr Allergy Asthma Rep 8:139–146.

Riedl MA, Diaz-Sanchez D. 2005. Biology of diesel exhaust effects on respiratory function. J Allergy Clin Immunol 115:221–228.

Rothman KJ, Greenland S, Lash TL. 2008. Modern Epidemiology. Philadelphia, PA:Lippincott Williams and Wilkins, 97.

RTI International. 2006. SUDAAN, version 9.01 [computer software]. Available: http://www.rti.org/sudaan/index.cfm [accessed 5 December 2008].

Schildcrout JS, Sheppard L, Lumley T, Slaughter JC, Koenig JQ, Shapiro GG. 2006. Ambient air pollution and asthma exacerbations in children: an eight-city analysis. Am J Epidemiol 164:505–517.

Simons FER. 1996. Learning impairment and allergic rhinitis. Allergy Asthma Proc 17:185–189.

U.S. EPA. 2003. National Air Quality and Emissions Trends Report. 2003 Special Studies Edition. Research Triangle Park, NC:U.S. Environmental Protection Agency. Available: http://www.epa.gov/air/airtrends/aqtrnd03/ [accessed 5 December 2008].

U.S. EPA. 2006. Air Quality Criteria for Ozone and Related Photochemical Oxidants (Final). EPA/600/R-05/004aF-cF, Vol 2, Table AX3-1. Washington, DC:U.S. Environmental Protection Agency.

U.S. EPA. 2008. AirData: Query AQS Data. U.S. Environmental Protection Agency. Available: http://www.epa.gov/aqspubl1/ [accessed 27 August 2008].

von Mutius E. 2000. The environmental predictors of allergic disease. J Allergy Clin Immunol 105:9–19.

von Mutius E, Weiland SK, Fritzsch C, Duhme H, Keil U. 1998. Increasing prevalence of hay fever and atopy among children in Leipzig, East Germany. Lancet 351:862–866.

Weiland SK, Mundt KA, Ruckmann A, Keil U. 1994. Self-reported wheezing and allergic rhinitis in children and traffic density on street of residence. Ann Epidemiol 4:243–247.

Weinmayr G, Weiland SK, Björkstén B, Brunekreef B, Büchele G, Cookson WO, et al. 2007. Atopic sensitization and the international variation of asthma symptom prevalence in children. Am J Respir Crit Care Med 176:565–574.

Yu JH, Lue KH, Lu KH, Sun HL, Lin YH, Chou MC. 2005. The relationship of air pollution to the prevalence of allergic diseases in Taichung and Chu-Shan in 2002. J Microbiol Immunol Infect 38:123–126.

ENVIRONMENTAL RESEARCH **72,** 24–31 (1997)
ARTICLE NO. ER963685

Association between Ozone and Hospitalization for Respiratory Diseases in 16 Canadian Cities[1]

RICHARD T. BURNETT,*,[2] JEFFREY R. BROOK,† WESLEY T. YUNG,‡ ROBERT E. DALES,§ AND DANIEL KREWSKI§

*Health Protection Branch, Health Canada, 203 Environmental Health Center, Tunney's Pasture, Ottawa, Ontario K1A 0L9, Canada; †Environment Canada, 4905 Dufferin Avenue, Downsview, Ontario M3H 5T4, Canada; ‡Statistics Canada, RH Coats Boulevard, Tunney's Pasture, Ottawa, Ontario K1A 0T6, Canada; and §Environmental Health Center, Health Canada, Tunney's Pasture, Ottawa, Ontario K1A 0L2, Canada

Received January 26, 1996

The effects of tropospheric ozone on lung function and respiratory symptoms have been well documented at relatively high concentrations. However, previous investigations have failed to establish a clear association between tropospheric ozone and respiratory diseases severe enough to require hospitalization after controlling for climate, and with gaseous and particulate air pollution at the lower concentrations typically observed in Canada today. To determine if low levels of tropospheric ozone contribute to hospitalization for respiratory disease, air pollution data were compared to hospital admissions for 16 cities across Canada representing 12.6 million people. During the 3927-day period from April 1, 1981, to December 31, 1991, there were 720,519 admissions for which the principle diagnosis was a respiratory disease. After controlling for sulfur dioxide, nitrogen dioxide, carbon monoxide, soiling index, and dew point temperature, the daily high hour concentration of ozone recorded 1 day previous to the date of admission was positively associated with respiratory admissions in the April to December period but not in the winter months. The relative risk for a 30 ppb increase in ozone varied from 1.043 ($P < 0.0001$) to 1.024 ($P = 0.0258$) depending on the selection of covariates in the regression model and subset of cities examined. The association between ozone and respiratory hospitalizations varied among cities, with relative risks ranging from 1.000 to 1.088 after simultaneous covariate adjustment. Particulate matter and carbon monoxide were also positively associated with respiratory hospitalizations. These results suggest that ambient air pollution at the relatively low concentrations observed in this study, including tropospheric ozone, is associated with excess admissions to hospital for respiratory diseases in populations experiencing diverse climates and air pollution profiles.

INTRODUCTION

Although several attempts have been made to link tropospheric ozone to respiratory diseases severe enough to require hospitalization (Thurston, 1995), convincing evidence for an independent association with ozone has been limited by ready access to computerized data on hospital admissions and lack of statistical control for the potential confounding effects of gaseous and particular air pollution, and climatic factors.

Canadians enjoy access to a publicly administered and funded health care system characterized by its universality, comprehensiveness, portability, and accessibility. There are no user fees and coverage is available to all residents (Scherer *et al.,* 1994). All hospital discharges in the country are recorded in a computerized format and aggregated at the national level, in part to allow for public accountability of the health care delivery system. A number of gaseous, particulate, and climatic air quality indicators are also monitored on an ongoing basis in a number of locations in the country and the results compiled into a national database (Environment Canada, 1994; Fuentes and Dann, 1993).

The purpose of the present study is to examine the association between ozone and hospitalizations for respiratory diseases in a number of locations simultaneously with diverse climatic, demographic, and environmental profiles, using consistent methods of

[1] Funding for this work was provided by Health Canada. Animals were not used in this study, nor was any personal information collected on humans.

[2] To whom correspondence should be addressed. Fax: (613) 941-4546. E-mail: rick–burnett@isdtcp3.hwc.ca.

0013-9351/97 $25.00

statistical analysis to control for measures of gaseous and particulate ambient air pollution, and climatic factors. To that end, daily environmental and hospitalization data were linked in 16 of Canada's largest cities, representing approximately half the country's population for the period 1981 to 1991, and spanning the breadth of the country.

METHODS

Information on discharges from all hospitals in Canada have been kept in a central registry at Statistics Canada since April 1, 1981. The latest date on record at the time of the commencement of the study was December 31, 1991. For this 3927-day period, the number of admissions to each hospital in selected cities for which the principle diagnosis was a respiratory disease were abstracted (International Classification of Disease Codes, Ninth Revision (ICD9): 466, 480–486, 490–494, and 496). A group of admissions not thought to be related to ambient air pollution were also abstracted (ICD9 codes 280–281.9 (blood system), 345–347, 350–356, 358–359.5 (nervous system), 530–534, 540–543, 560–569, 571, 572, 574–578 (digestive system), and 594 and 600 (genitourinary system)).

We selected Canadian cities with a population of over 100,000 based on the 1986 census, for which daily ozone measurements were available during the period of interest. This procedure yielded 16 cities spanning the breadth of the country from the west coast (Victoria, British Columbia) to the east coast (Halifax, Nova Scotia).

Estimates of daily population exposure to ozone and other air pollutants (sulfur dioxide, nitrogen dioxide, carbon monoxide, and soiling index) were obtained by averaging the available data on an hour by hour basis, from all monitoring stations within each city. Daily measures of particulate matter for all 16 cities were not available for the time period of interest. Instead, hourly levels of the soiling index (COH), which is correlated with airborne particles, were obtained for 11 cities (not including Halifax, Saint John, Quebec City, Regina, and Saskatoon). Dew point temperature was obtained from readings at the airport in each city.

Daily measures of the environmental variables were related to the daily number of respiratory admissions in each hospital using the random effects relative risk regression model: $E(y_{j(k)t}) = S_{jt}D_{jt}H_{j(k)}\exp(\beta_j x_{jt})$, where $E(y_{j(k)t})$ is the expected number of admissions for respiratory diseases in the kth hospital within the jth city on the tth day of sampling, S_{jt} is a 19-day linear filter (Burnett *et al.,* 1994a) of the average number of daily admissions in the jth city on the tth day of sampling, D_{jt} is a time series consisting of a repetition of seven unique values representing the average admission rate for each day of the week for the jth city, $H_{j(k)}$ is the average number of admissions to the kth hospital within the jth city, and β_j is a vector of unknown regression parameters, specific to the jth city, relating the environmental variables x_{jt}, which are common to all hospitals within a city, to the expected frequency of respiratory hospitalizations.

Since the admission data are low-frequency counts, the residual variation is assumed to be proportional to the expected response. In the regression model, S_{jt} adjusts for city-specific temporal fluctuations in admissions due to seasonal effects and subseasonal variations (due in part to infection rates in the population), D_{jt} removes differences in admission rates among day of the week, and $H_{j(k)}$ removes variation in admission rates among hospitals within each city (due to hospital size and its unique role in the health care delivery system), from the hospital-specific admission time series prior to an examination of the environmental factors.

Methods to estimate the log-relative risks β_j for the jth city and its standard error have been described previously (Burnett *et al.,* 1994a). A common estimate of the relative risk and its heterogeneity among cities was also determined. The approach used (Laird and Mosteller, 1990) is robust against mispecification of the within city error structure, including serial correlation. City-specific estimates of risk were calculated based on the entire sample using a random effects modeling approach (Hui and Berger, 1983). Summary risks were determined by combining season-specific effects among seasons. All significance levels (P values) reported are based on two-sided tests.

RESULTS

The locations of the 16 cities are given in Fig. 1, with community characteristics presented in Table 1. A total of 720,519 respiratory admissions, averaging 183 admissions per day, occurred during this period. Daily respiratory admissions per hospital averaged 1.37 for the 134 hospitals examined. Daily respiratory hospitalization rates varied among the cities examined, with the Saskatchewan communities of Saskatoon and Regina having the highest rates, and Calgary experiencing the lowest rate. The daily high hour ozone concentrations tended to be highest in the southwestern Ontario cities of Toronto, Hamilton, London, and Windsor.

Several ozone metrics were considered: daily av-

FIG. 1. Locations of study communities.

erage, average concentration from 8 AM to 8 PM, maximum 8-hr running average concentration, and daily high hour level. The daily high hour concentration displayed the greatest statistical significance compared to the other metrics for each lag time examined: 0 (day of admission), 1 (1 day prior to admission), or 2 (2 days prior to admission). Ozone levels measured on the day previous to admission were more strongly related to respiratory hospitalization rates than the day of admission or 2 days prior to admission. Concentrations averaged over lags 0 and 1, 0, 1 and 2, and 1 and 2 were not as strongly associated with admissions as concentrations at lag 1. Thus, the high hour concentration recorded 1 day previous to admission was used to further assess the relationship between ambient ozone and respiratory hospital admission frequencies.

The relative risk of a 30 ppb increase in ozone levels (approximately equal to difference between the 95th percentile and mean concentrations) on respiratory hospitalization rates is presented in Table 2 by season. Ozone tends to be highest in the summer and lowest in the winter, with an opposite pattern for respiratory admissions. Recall that seasonal trends in respiratory admissions have been removed from the hospital-specific daily admission series prior to an examination of the effects of ozone.

Little evidence exists for an ozone effect in the winter ($P = 0.6528$). However, positive associations are observed in the spring ($P = 0.0064$), summer ($P < 0.0001$), and fall ($P = 0.0750$). Further examination of the ozone effect was restricted to the spring, summer, and fall seasons where positive associations were detected.

There was no evidence of an association between the daily high hour ozone concentration recorded 1 day previous to a hospital admission for a control group of diseases which a priori were not thought to be related to air pollution in the April to December period (RR = 0.931; 95% CI: 0.860 to 1.009; based on a 30 ppb increase). The association between ozone

TABLE 1
Population and Ozone Characteristics by City, 1981–1991

City	Population[a] (×10^5)	Daily admissions (per 10^5 population)	% Missing ozone data	Ozone mean/95th percentile (ppb)[b]
Halifax	3.1	1.96	12.6	27/48
Saint John	1.4	2.04	5.4	37/65
Quebec City	5.7	1.61	3.4	28/50
Montreal	24.6	1.20	0.0	29/59
Ottawa	8.0	1.42	4.3	26/50
Toronto	31.4	1.43	0.0	31/66
Hamilton	4.2	1.34	4.2	34/73
London	3.3	1.43	8.7	38/77
Windsor	3.2	1.94	11.6	38/84
Winnipeg	5.9	1.65	7.2	31/54
Regina	1.8	3.04	13.6	34/59
Saskatoon	1.2	3.22	34.2[c]	29/47
Edmonton	7.2	1.82	0.1	31/53
Calgary	8.1	0.71	0.1	33/54
Vancouver	14.0	1.47	0.3	26/47
Victoria	2.6	1.82	47.7[d]	28/45
All cities	125.7	1.46	9.6	31/60

[a] Based on 1986 census.
[b] Mean and 95th percentile based on daily high hour ozone concentration.
[c] Ozone monitoring commenced in 1984.
[d] No ozone data for 1989 and 1990, with a large number of missing values for 1983, 1985, 1988, and 1991.

and respiratory hospitalizations was similar for those patients greater than 65 years of age (relative risk of 1.040 for a 30 ppb increase; $P = 0.0096$; 95% confidence interval of 1.010 to 1.072) representing one-third of admissions, and those patients less than 65 years old (relative risk of 1.045 for a 30 ppb increase; $P = 0.0001$; 95% confidence interval of 1.021 to 1.068).

The daily high hour concentrations of five additional covariates were considered as potential confounders to the ozone-hospitalization association: sulfur dioxide (SO_2; ppb), nitrogen dioxide (NO_2; ppb), carbon monoxide (CO; ppm), soiling index (Coefficient of Haze Units, COH; 1000 linear feet), and dew point temperature (DP; °C). Summary statistics for these variables are given in Table 3. Ozone was uncorrelated with carbon monoxide, sulfur dioxide, and the coefficient of haze, and modestly correlated with nitrogen dioxide and dew point temperature (Table 3). The Pearson correlation between ozone concentrations and covariate readings varied among communities and seasons (Table 3).

The association between each of the five covariates and hospitalization rates was examined separately for lags of 0, 1, and 2 days. Since the most statistically significant association for each covariate was based on the value recorded on the day of admission, a lag of 0 days was used to further examine the influence of these covariates on the ozone–admissions association. The associations between daily high and low hour temperature recorded on the day of admission and hospitalization rates for respiratory diseases were also examined. The ratios of the log-relative risks to their standard errors were less than that for dew point temperature. Since the three temperature measures are highly correlated, we selected dew point temperature for further consideration as a potential confounder in the ozone hospitalization association.

Cubic polynomials were fit for each of the six environmental factors separately in order to assess the appropriateness of the log-linear model. None of the cubic terms were statistically significant ($P > 0.1$). Quadratic polynomials in the five covariates were then fit separately to the hospitalization time series. The quadratic terms for four of the five variables were not statistically significant ($P > 0.1$); however, the quadratic term for carbon monoxide displayed a negative association with hospitalization rates ($P = 0.005$). It appears that a linear term for ozone, soiling index, nitrogen dioxide, sulfur dioxide, and dew point temperature was adequate to represent the respective associations with respiratory admissions. However, a quadratic term was required to model the association for carbon monoxide in addition to the linear term. The negative sign on the regression coefficient for the quadratic term, with a corresponding positive coefficient for the linear term, implies that incremental increases in carbon monoxide yield larger relative risks for low concentrations as compared to higher readings.

The six environmental factors were examined jointly in a multivariate random effects regression model, including a quadratic term for CO. There exists little evidence of an association between nitrogen dioxide ($P = 0.772$) or sulfur dioxide ($P = 0.134$) and respiratory hospitalizations after simultaneous adjustment for ozone, carbon monoxide, and dew point temperature. A 10 ppb increase in nitrogen dioxide or sulfur dioxide is associated with a relative risk (RR) of 0.999 (95% Confidence Interval (CI) 0.9922–1.0059) and 1.0055 (95% CI 0.9982–1.0128), respectively. Since other environmental factors appear to explain the association between nitrogen dioxide or sulfur dioxide and respiratory hospitalization rates, NO_2 and SO_2 were not considered in additional analyses.

City-specific relative risks corresponding to a 30 ppb increase in the daily high hour ozone concentration recorded 1 day prior to admission are given in Table 4 for selected covariate adjustment models. Here, city- and season-specific ozone log-relative

TABLE 2

Relative Risk Associated with a 30 ppb Increase in the Daily High Hour Ozone Concentration Recorded 1 Day Previous to Admission to Hospital for Respiratory Diseases by Season, 1981–1991

Statistic	Season			
	Winter (Jan–Mar)	Spring (Apr–Jun)	Summer (Jul–Sep)	Fall (Oct–Dec)
Ozone mean (ppb)	26	40	38	21
95th Percentile (ppb)	42	67	73	38
Daily admissions (per 10^6 population)	17.1	14.3	11.1	16.3
Relative Risk	0.994	1.042	1.050	1.028
95% Confidence interval	0.964–1.025	1.012–1.073	1.026–1.074	0.998–1.059

risks were determined and averaged over the spring, summer, and fall seasons for each city separately.

Simultaneous adjustment for carbon monoxide has little influence on the ozone relative risk (RR = 1.043; $P = 0.0001$). However, additional adjustment for dew point temperature attenuates the ozone relative risk considerably (RR = 1.031; $P = 0.0024$). Simultaneous adjustment for dew point temperature eliminates any association between ozone and respiratory hospitalizations in Montreal (RR = 1.000) and Vancouver (RR = 1.003). The ozone relative risk is 1.043 ($P < 0.0001$) after removal of these two cities and simultaneous adjustment for carbon monoxide and dew point temperature.

Daily particulate measures (soiling index) were available for only 11 of the 16 cities examined. The ozone relative risk based on these 11 cities simultaneously adjusting for dew point temperature, carbon monoxide, and soiling index is 1.024 ($P = 0.0258$). Again, little association between ozone and respiratory hospitalizations was observed for Montreal (RR = 0.998) and Vancouver (RR = 1.002). The ozone relative risk based on the 9 cities with soiling index readings but excluding Montreal and Vancouver is 1.038 ($P = 0.0014$) after simultaneously adjusting for carbon monoxide, soiling index, and dew point temperature.

The log-relative risk (standard error) of a unit change in the daily high hour soiling index reading is 0.0612 (0.0144) with simultaneous adjustment for ozone, dew point temperature, and carbon monoxide. The linear and quadratic terms for carbon monoxide in the same model are 0.0199 (0.0098) and –0.0018 (0.0009), respectively.

DISCUSSION

Positive associations between tropospheric ozone and admission to hospital for respiratory diseases were observed in all 16 communities examined in Canada in the April to December period. However, no such association was found in the winter months,

TABLE 3

Summary Statistics for Environmental Factors for April to December, 1981–1991

Environmental factor (units)	Percent missing	Correlation[a] (range)	Mean	Standard deviation	Percentile				
					25	50	75	95	99
O_3 (ppb)	9.1	1 (1,1)	32.9	16.7	21	30	41	64	87
CO (ppm)	17.5	–0.05 (–0.40,0.24)	2.2	1.7	1.0	1.9	2.9	5.4	9.0
SO_2 (ppb)	8.0	0.04 (–0.19,0.30)	14.4	22.2	3	10	19	45	97
NO_2 (ppb)	14.6	0.20 (–0.19,0.54)	35.5	16.5	25	33	43	62	87
COH (1000 in ft)	7.2[b]	0.04 (–0.36,0.60)	0.64	0.44	0.3	0.5	0.8	1.5	2.1
DP (°C)	1	0.23 (–0.17,0.54)	7.3	8.9	1.9	8.6	13.7	19.4	22.0

[a] Average Pearson correlation between environmental factor and high hour ozone among cities and seasons (minimum correlation, maximum correlation).

[b] Based on 11 cities (not including Halifax, Saint John, Quebec City, Regina, or Saskatoon).

TABLE 4

City-Specific Relative Risk Attributable to a 30 ppb Increase in the Daily High Hour Ozone Concentration Adjusting for Selected Covariates and Season, April to December, 1981–1991

City	Model specification			
	O_3	O_3, CO	O_3, CO, DP	O_3, CO, DP
Halifax	1.032	1.045	1.031	1.035
Saint John	1.035	1.034	1.024	1.033
Quebec City	1.057	1.042	1.031	1.037
Montreal	1.024	1.029	1.000	—
Ottawa	1.028	1.028	1.017	1.029
Toronto	1.050	1.055	1.037	1.038
Hamilton	1.034	1.039	1.038	1.045
London	1.049	1.042	1.043	1.048
Windsor	1.048	1.061	1.056	1.063
Winnipeg	1.050	1.047	1.022	1.026
Regina	1.035	1.064	1.069	1.088
Saskatoon	1.045	1.045	1.036	1.046
Edmonton	1.056	1.049	1.040	1.042
Calgary	1.032	1.031	1.021	1.030
Vancouver	1.023	1.021	1.003	—
Victoria	1.042	1.051	1.040	1.052
All cities	1.042	1.043	1.031	1.043
(t value)[a]	(5.12)	(4.45)	(3.04)	(4.00)

[a] Ratio of log-relative risk to its standard error for all cities combined.

a period of low personal exposure (Liu *et al.,* 1995). City- and season-specific control of gaseous (nitrogen dioxide, sulfur dioxide, and carbon monoxide) and particulate (soiling index) air pollution and weather (dew point temperature) reduced but did not eliminate the ozone association with respiratory hospital admission rates.

No association was observed between ambient ozone concentrations and admissions to hospital for a group of diseases not thought to be related to air pollution. This negative result suggests that the ozone association was not due to factors influencing admission to hospital in general.

There was considerable variation in the ozone relative risks among cities. Simultaneous adjustment for other environmental factors could not reduce the variation in relative risks among cities. In fact, adjustment for dew point temperature eliminated the ozone association with respiratory hospitalizations in the second (Montreal) and third (Vancouver) largest Canadian cities. Delfino *et al.* (1994) also found that the ozone association with respiratory hospitalizations could be eliminated after adjusting for temperature. Bates *et al.* (1992) did not find a statistically significant association between ozone and visits to emergency rooms for respiratory diseases in the greater Vancouver region. The unadjusted ozone relative risks are the lowest of the 16 cities examined for Montreal (RR = 1.024) and Vancouver (RR = 1.023). The Pearson correlations between ozone and dew point temperature for Montreal averaged 0.29 and for Vancouver 0.24 over the three seasons considered, values similar to the study mean (0.23). Thus the relatively weak association between ozone and respiratory hospitalizations in these two cities, and not the correlation with temperature, may be the reason for the sensitivity of the ozone effect to temperature adjustment. The reasons for such a weak ozone effect, however, remain unclear.

The adequacy of the fixed-site monitoring stations to represent ozone exposure among the population may have varied among cities due to differences in geography, the mix of air pollutants, and weather patterns among communities. Such misclassification among multivariate risk factors can bias the estimate of the ozone effect in either direction, and may differ by city.

Ozone may be acting, in part, as a surrogate for other environment factors that vary temporally. Adjustment for more complex weather model specifications (Kalkstein, 1993), or other air pollutants such as fine particulate matter and acid aerosols, may have reduced the heterogeneity of effects. However, data on these pollutants were not available for analysis. The nature, size, and characteristics of susceptible subgroups also may have varied among cities.

The strongest statistical evidence of an association between ozone and respiratory hospitalizations was for the daily high hour ozone concentration recorded on the day previous to admission. The daily average ozone concentration should a priori be a weaker predictor compared to measures taken in the daytime, since ozone exposures at night are very low (Liu *et al.,* 1995). The daytime measures are all highly correlated and yield similar levels of statistical significance. Due to the nature of the ozone profile throughout the day (low at night, gradually rising through the day, peaking in late afternoon, and then falling off in the evening), it is difficult, if not impossible, to separate the effects of these measures in this type of study. Associations were also observed with lags of 0, 1, and 2 days. Additional lag times were also examined, with a decline in the magnitude of the effect as the days lagged increased for all ozone metrics considered, suggesting that ozone is acting in a rapid manner to either trigger new respiratory symptoms or exacerbate existing conditions.

Positive associations for carbon monoxide and

particulate matter as measured by the soiling index were observed. Nitrogen dioxide and sulfur dioxide were also statistically significant predictors on their own, although formal statistical significance was lost when NO_2 and SO_2 were coregressed with the other environmental factors. Particulate matter has been linked to respiratory hospitalizations in a number of studies (Burnett *et al.,* 1994b; Schwartz, 1994a,b,c, 1995; Lipfert and Hammerstrom, 1992; Bates and Sitzo, 1987; Targonski *et al.,* 1995; Thurston *et al.,* 1992, 1994; Delfino *et al.,* 1994) and carbon monoxide with hospitalization for asthma in Helsinki (Ponka, 1991) and Chicago (Targonski *et al.,* 1995).

The literature has been unclear as to whether ozone is associated with respiratory symptoms severe enough to require hospitalization. Several investigators have found positive associations with ozone and respiratory hospitalizations. However, these associations have been reduced to the point of losing formal statistical significance after controlling for weather and/or other air pollutants ($P > 0.05$) (Ponka and Virtanen, 1994; Bates and Sitzo, 1987; Thurston *et al.,* 1994; Schwartz, 1994b,c; Delfino *et al.,* 1994). Two studies (Ponka, 1991; Thurston *et al.,* 1992) found statistically significant associations with ozone controlling for temperature but did not consider multivariate adjustments for other air pollutants. Positive associations between hospital admissions for asthma in 5- to 34-year-olds were observed in Chicago (Targonski *et al.,* 1995) even after controlling for temperature and gaseous pollutants. However, particulate matter was not considered. Summertime respiratory admissions were related to ozone in 168 hospitals in Ontario, Canada (Burnett *et al.,* 1994b). A relative risk of 1.032 was calculated after adjusting for both particulate sulfate and daily high hour temperature, for a 30 ppb increase in the daily high hour ozone concentration, a value similar to that obtained from the present study. An investigation of hospitalization for the elderly (>65 years of age) in Detroit (Schwartz, 1994a) yielded relative risks of 1.057 (95% CI 1.029–1.086) for pneumonia and 1.060 (95% CI 1.016–1.107) for chronic obstructive pulmonary disease, values similar to those estimated in a separate analysis of this database restricted to the geographically adjacent region of southern Ontario (Toronto, Hamilton, London, and Windsor) after simultaneous adjustment for carbon monoxide, soiling index, and dew point temperature (RR = 1.048; 95% CI 1.027–1.068) for all ages and respiratory diseases. Ozone was associated with respiratory hospitalizations in the elderly in Tacoma, Washington, but not in New Haven, Connecticut, after controlling for temperature and particulate matter or sulfur dioxide (Schwartz, 1995). Differences in the ozone risk between these two cities which span the breadth of the United States are similar to the variation in risk observed in the present study.

CONCLUSIONS

The present investigation demonstrates a statistically significant association between tropospheric ozone and respiratory diseases severe enough to require hospitalization in several locations simultaneously, even after controlling for temporal trends in hospitalization rates, hospital, city, day-of-week, and seasonal effects, gaseous and particulate air pollution, and climatic factors. Significant associations with several other air pollutants were also detected in multiple pollutant models. These associations are apparent at the relatively low ambient concentrations observed in this study.

REFERENCES

Bates, D. V., and Sitzo, R. (1987). Air pollution and hospital admissions in Southern Ontario: The acid summer haze effect. *Environ. Res.* **43,** 317–331.

Bates, D. V., Baker-Anderson, M., and Sitzo, R. (1992). Asthma attack periodicity: A study of hospital emergency visits in Vancouver. *Environ. Res.* **51,** 51–70.

Burnett, R., Bartlett, S., Krewski, D., Roberts, G., and Raad-Young, M. (1994a). Air pollution effects on hospital admissions: A statistical analysis of parallel time series. *Environ. Ecol. Stat.* **1,** 325–332.

Burnett, R. T., Dales, R. E. Raizenne, M. E., Krewski, D., Summers, P. W., Roberts, G. R., Raad-Young, M., Dann, T., and Brook, J. (1994b). Effects of low ambient levels of ozone and sulfates on the frequency of respiratory admissions to Ontario hospitals. *Environ. Res.* **65,** 172–193.

Burnett, R., and Krewski, D. (1994). Air pollution effects on hospital admission rates: A random effects modeling approach. *Can. J. Stat.* **22,** 441–458.

Delfino, R. J., Becklake, M. R., and Hanley, J. A. (1994). The relationship of urgent hospital admissions for respiratory illnesses to photochemical air pollution levels in Montreal. *Environ. Res.* **67,** 1–19.

Environment Canada. (1994). "National Air Pollution Surveillance (NAPS)." EPA 7/AP/25, Minister of Supply and Services Canada, ISBN 0-662-61263-9, National Printers, Ottawa, Canada.

Fuentes, J. D., and Dann, T. F. (1993). "Ground-Level Ozone in Canada During 1980 to 1991." Atmospheric Environment Service, Report ARD-93-010.

Hui, S. L., and Berger, J. O. (1983). Empirical Bayes estimation of rates in longitudinal studies. *J. Am. Stat. Assoc.* **78,** 753–760.

Kalkstein, L. S. (1993). Direct impacts in cities. *Lancet* **342,** 1397–1399.

Laird, N. M., and Mosteller, F. (1990). Some statistical methods for combining experimental results. *Int. J. Tech. Assess. Health Care* **6,** 5–30.

Lipfert, F. W., and Hammerstrom, T. (1992). Temporal patterns in air pollution and hospital admissions. *Environ. Res.* **59,** 374–399.

Liu, S., Kourtrakis, P., Broder, I., and Leech, J. (1995). Assessment of ozone exposures in the Greater Metropolitan Toronto area. *J. Air Waste Manage.* **45,** 223–234.

Ponka, A. P. (1991). Asthma and low level air pollution in Helsinki. *Arch. Environ. Health* **46,** 262–270.

Ponka, A., and Virtanen, M. (1994). Chronic bronchitis, emphysema, and low-level air pollution in Helsinki, 1987–1989. *Environ. Res.* **65,** 207–217.

Scherer, K., Kraut, A., Yassi, A., Wajda, A., Wajda, A., and Bebchuk, J. (1994). Using administrative health data to monitor potential adverse health effects of environmental studies. *Environ. Res.* **66,** 143–151.

Schwartz, J. (1994a). Air pollution and hospital admissions for the elderly in Detroit, Michigan. *Am. J. Respir. Care Med.* **150,** 648–655.

Schwartz, J. (1994b). PM_{10}, ozone, and hospital admissions for the elderly in Minneapolis-St. Paul. *Arch. Environ. Health* **49,** 366–374.

Schwartz, J. (1994c). Air pollution and hospital admissions for the elderly in Birmingham, Alabama. *Am. J. Epidemiol.* **139,** 589–598.

Schwartz, J. (1995). Short term fluctuations in air pollution and hospital admissions of the elderly for respiratory disease. *Thorax* **50,** 531–538.

Targonski, P. V., Scheff, P. A., Stokes, H., Ramakrishnan, V., Hryhorczuk, D., and Persky, V. W. (1995). The association of environmental ozone with hospitalization for asthma among 5–35 year olds in Chicago, 1987–1989. *In* "Proceedings of the Air & Waste Management Association 88th Annual Meeting & Exhibition, San Antonio, Texas, June 18–23, 1995." Manuscript 95-MP19.02.

Thurston, G. D., Ito, K., Kinney, P. L., and Lippmann, M. (1992). A multi-year study of air pollution and respiratory hospital admissions in three New York state metropolitan areas: Results for 1988 and 1989. *J. Expos. Anal. Environ. Epidemiol.* **2,** 429–450.

Thurston, G. D., Ito, K., Hayes, C. G., Bates, D. V., and Lippmann, M. (1994). Respiratory hospital admissions and summertime haze air pollution in Toronto, Ontario: Consideration of the role of acid aerosols. *Environ. Res.* **65,** 271–290.

Thurston, G. D. (1995). Associations of acute ambient ozone exposures with hospital admissions for respiratory causes. *In* "Proceedings of the Air & Waste Management Association 88th Annual Meeting & Exhibition, San Antonio, Texas, June 18–23, 1995." Manuscript 95-MP19.04.

Int J Biometeorol (2011) 55:187–202
DOI 10.1007/s00484-010-0324-2

ORIGINAL PAPER

Long-range ozone transport and its impact on respiratory and cardiovascular health in the north of Portugal

Jezabel M. Azevedo · Fabio L. T. Gonçalves · Maria de Fátima Andrade

Received: 16 April 2009 / Revised: 4 December 2009 / Accepted: 26 April 2010 / Published online: 1 July 2010

Abstract Ozone dynamics depend on meteorological characteristics such as wind, radiation, sunshine, air temperature and precipitation. The aim of this study was to determine ozone trajectories along the northern coast of Portugal during the summer months of 2005, when there was a spate of forest fires in the region, evaluating their impact on respiratory and cardiovascular health in the greater metropolitan area of Porto. We investigated the following diseases, as coded in the ninth revision of the International Classification of Diseases: hypertensive disease (codes 401–405); ischemic heart disease (codes 410–414); other cardiac diseases, including heart failure (codes 426–428); chronic obstructive pulmonary disease and allied conditions, including bronchitis and asthma (codes 490–496); and pneumoconiosis and other lung diseases due to external agents (codes 500–507). We evaluated ozone data from air quality monitoring stations in the study area, together with data collected through HYbrid Single-Particle Lagrangian Integrated Trajectory (HYSPLIT) model analysis of air mass circulation and synoptic-scale zonal wind from National Centers for Environmental Prediction data. High ozone levels in rural areas were attributed to the dispersion of pollutants induced by local circulation, as well as by mesoscale and synoptic scale processes. The fires of 2005 increased the levels of pollutants resulting from the direct emission of gases and particles into the atmosphere, especially when there were incoming frontal systems. For the meteorological case studies analyzed, peaks in ozone concentration were positively associated with higher rates of hospital admissions for cardiovascular diseases, although there were no significant associations between ozone peaks and admissions for respiratory diseases.

Keywords Ozone · Respiratory disease · Cardiovascular disease · Meteorological conditions · Fire

J. M. Azevedo (✉) · F. L. T. Gonçalves · M. de Fátima Andrade
Department of Atmospheric Sciences, Institute of Astronomy, Geophysics and Atmospheric Sciences, University of São Paulo, Sala 301, Butantã, Rua do Matão 1226, Cidade Universitária, 05508-900 São Paulo, SP, Brazil
e-mail: jezabelmiriam@model.iag.usp.br

Introduction

Long-range transport of air pollution was first studied in detail in the context of acid rain in Scandinavia and North America (Calvert 1983). In this work, the influence of long-range transport on ozone concentrations in Portugal was evaluated.

Natural ozone levels vary by region, altitude, and time of year. The 8-h cycle observed for ozone levels has been related to traffic patterns, confirming its dependence on anthropogenic activities (Alvim-Ferraz et al. 2006). The highest levels of tropospheric ozone generated by photochemical reactions, which have biogenic and anthropogenic precursors, typically occur far from the sources of pollution. According to the United States Environmental Protection Agency, the estimated range of annual average ozone levels in the US is 40–70 $\mu g/m^3$; in clean nonurban areas, the range of daily maximal 1-h level is 60–100 $\mu g/m^3$, although summertime maximal 1-h averages can be as high as 120–200 $\mu g/m^3$ (World Health Organization 2000).

Daily ozone levels vary by location and depend on factors such as formation, transport, and destruction. In the morning, ozone levels are low, peaking in the afternoon as the result of photochemical processes, as described by Schneider et al. (1989). The same authors reported that, during the night, ozone is removed by processes that include wind transport and vertical mixing. The broad

range of summer maximal ozone levels is explained by increased summer radiation in the presence of nitrogen oxides (NO_x), leading to an increase in photochemical ozone production associated with anthropogenic activities (Alvim-Ferraz et al. 2006).

In order to characterize the dynamics of pollutants in the Mediterranean and to understand the involvement of atmospheric circulation, the European Commission developed the following projects: (1) *Mesometeorological cycles of air pollution in the Iberian Peninsula*, designed to register the atmospheric circulation on the Iberian Peninsula in particular (Millán et al. 1992); (2) *Photooxidant dynamics in the Mediterranean basin in summer*, which characterizes the regional cycles of air pollution from the Atlantic coast of Portugal to Italy in the 1990–1991 period (Millán et al. 1997); and (3) *On the long-range transport of air pollutants form Europe to Africa*, which describes the cycles of air pollution in the South of Europe from 1992 to 1995 (Millán et al. 1997). These projects were concerned with the storage of pollutants and reactions for 2–3 days in a layer 300 km wide and at a depth of 2–3 km off the Mediterranean coast of Spain, with the most recently deposited pollutants near the top and the older ones near the sea. This layer acts as a reservoir for older pollutants to be deposited on land the next day. Tracer experiments have shown that turnover times range from 2 to 3 days. During the night, part of this system moves along the coast. Strong insolation promotes circulation, whereby a considerable portion of the NO_x and other precursors is converted into acid compounds, aerosols, and ozone (Millán 2003; Gangoiti et al. 2001; Millán et al. 1998, 2000).

Penkett et al. (2004) conducted seven experimental flights over large parts of the North Atlantic Ocean and presented evidence that the ozone concentration from the surface to an altitude of 8 km was associated with continental pollutants.

In the western Mediterranean, high ozone levels are often associated with synoptic-scale high pressure systems, whereas low pressure systems induce convergence over the Iberian Peninsula, forcing sea breezes to flow inland (Castell et al. 2006). Evtyugina et al. (2007) studied ozone formation along the west coast of Portugal during the summer months and found that the recirculation of sea breeze air masses to the coastal area at higher altitudes and the consequent contamination of air masses at the coastal entrance over the subsequent days was the main factor contributing to the observed ozone pollution episodes.

The atmosphere over Portugal is influenced by the Azores high pressure cell during the summer. In the city of the Porto, pollution levels are determined by the orography of the region, by meteorological conditions, and by the quantity of ozone precursors in the atmosphere. Air quality is one of the greatest challenges in the greater metropolitan area of Porto (GMAP; Maporto 2008), due to its large population (1,400,000 inhabitants in the 2001 census) and heavily traveled roadways. However, elevated ozone levels have been registered in remote areas where there are no anthropogenic sources of ozone and ozone precursors are not present.

The most significant effects of exposure to high ozone levels on human health are respiratory and ocular damage. For example, respiratory diseases constitute one of the leading causes of illness among children in New York State, where hospital admissions for respiratory complaints were found to correlate positively with ambient ozone concentrations during the preceding 48 h (Lin et al. 2008). Similarly, various studies conducted in the state of São Paulo, Brazil have shown correlations between air quality and human health (Gonçalves et al. 2005; Santos et al. 2005). Densely populated areas situated near large urban conglomerates, industrial centers, or other sources of pollution, such as sugar cane field burn-offs, have received special attention from the São Paulo State Environmental Protection Agency (CETESB 2005, 2006).

According to Alvim-Ferraz et al. (2006), the increased concentrations of photochemically produced tropospheric ozone in the GMAP recorded since the nineteenth century, can be correlated with increased emissions of anthropogenic pollutants. Exposure to environmental air pollutants has been linked to asthma, a complex disease whose symptoms include dyspnea, wheezing, chest tightness and recurrent cough (Alvim-Ferraz et al. 2005).

The objective of this study was to understand the long-range circulation of tropospheric ozone in rural and remote areas of Portugal, where the air quality is poor, evaluating its effect on the health of the inhabitants of the GMAP. We investigated the following diseases: hypertension; ischemic heart disease; other cardiac diseases, including heart failure; chronic obstructive pulmonary disease and allied conditions, including bronchitis and asthma; and pneumoconiosis and other lung diseases due to external agents. To that end, we grouped air quality monitoring stations and attempted to identify meteorological parameters that affect the behavior of tropospheric ozone. We applied statistical tools in order to evaluate the impact that such patterns have on health.

Materials and methods

Study period and area

We evaluated the period from June through August of 2005, in terms of the hourly levels of ozone, for the northern coast of Portugal (from 40.5°N to 41°N and from 9°E to 7.5°E; Figs. 1, 2).

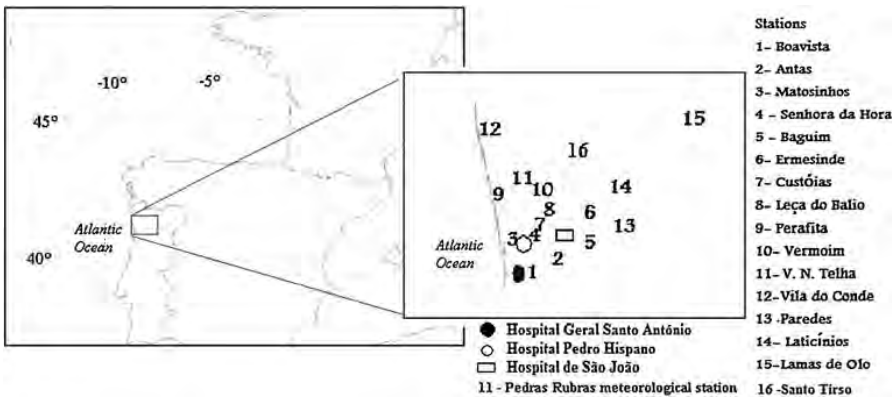

Fig. 1 Locations of the air quality monitoring stations operated by the Portuguese Environmental Agency and of the hospitals studied. Stations *1–14* are within the greater metropolitan area of Porto (GMAP; altitude, 30–150 m), and station *15* is in the countryside (altitude 1,086 m). All stations lie between latitudes 41°N and 41.35°N and between longitudes 8.75°E and 7.8°E. The location of the study hospitals is indicated. The Pedras Rubras meteorological station and the V.N. Telha air quality station are very close to one another and are therefore represented by the same number (*11*)

Meteorological data

We employed plot daily composites (averages) of the mean or anomalies (mean − total mean) of variables from the National Centers for Environmental Prediction (NCEP)/National Center for Atmospheric Research (NCAR) reanalysis (from the National Oceanic and Atmospheric Administration website), as well as other data sets. Total means are based on the 1968–1996 period. Data are available from January of 1948 onward (http://www.cdc.noaa.gov/data/composites/day/).

An analysis of the meteorological conditions during events of ozone levels above the public information threshold (180 μg/m^3) or above the secondary standard limit (public alert threshold, 240 μg/m^3) was performed using NCEP guidelines, which were also used in order to determine atmospheric pressure, wind direction and wind speed. In addition, trajectory analysis was performed using the HYbrid Single-Particle Lagrangian Integrated Trajectory (HYSPLIT) model (Draxler and Hess 2004) based on Reanalysis data, from the Air Resources Laboratory. The HYSPLIT model was used in the configuration "forward", in order to evaluate air parcel displacement from the point of emission, and "backward", in order to evaluate the arrival of the air parcel at its destination. The model counts backward in time, at different altitudes.

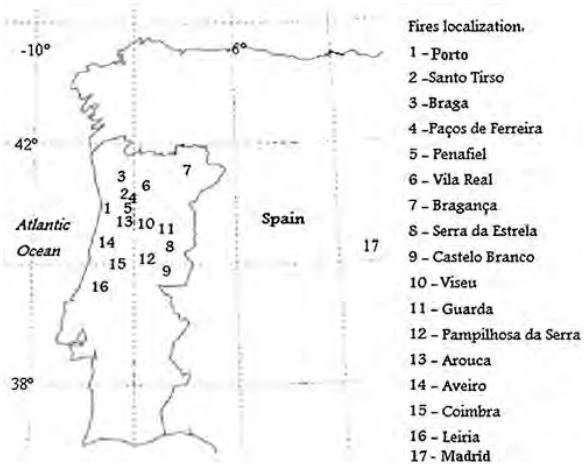

Fig. 2 Map of Portugal and part of Spain identifying cities in which there were fires in 2005. The numbers in Portugal represent forest fires, whereas the one number in Spain represents a fire that occurred at an electrical station

Health data

Three major public hospitals in the GMAP were selected: Santo António General Hospital, located in Porto City Center; Pedro Hispano Hospital, in the city of Matosinhos; and São João Hospital, located on the eastern outskirts of Porto (Fig. 1). The Urgency Service provides the data, which was the sum of the three hospitals.

We investigated the following diseases, as coded in the ninth revision of the International Classification of Diseases: hypertensive disease (codes 401–405); ischemic heart disease (codes 410–414); other cardiac diseases, including heart failure (codes 426–428); chronic obstructive pulmonary disease and allied conditions, including bronchitis and asthma (codes 490–496); and pneumoconiosis and other lung diseases due to external agents (codes 500–507). Data were collected during 2005.

Statistical tools

In the statistical analysis, we employed multiple regression analysis, which evaluates the quantitative relationship

between two or more variables, together with analysis of variance (ANOVA) and principal component analysis (PCA).

The regression analysis represents the information through an additive linear model, which includes systematic and random components:

$$Y = f(X) + \varepsilon$$

where Y is the answer or dependent variable, X is the independent or predictor variable, ε represents the random error, and f describes X in relation to Y. Values of $\alpha=0.05$ and $P<0.05$ were considered statistically significant, considering that P is the lowest α value at which the null hypothesis is rejected.

The ANOVA was based on weighted station values, considering Custóias as the geographically central station with the greatest weighted value (0.50).

PCA was used in this study in order to evaluate the ozone impact on respiratory and cardiovascular diseases, considering lag times [0–4 days; based on Gonçalves et al. (2005, 2007)]. In the PCA, values of $P<0.05$ were considered statistically significant.

The PCA method is a multivariate technique in which a number of correlated variables are transformed into a smaller set of uncorrelated variables. As described by Jackson (1991), PCA rewrites the original data matrix into a new set of principal components that are linearly independent and ordered by the degree of variance in the original data they explain. A correlation matrix is M_x, which yields eigenvalues (λ_j) of p (number of variables). Each eigenvalue is related to a corresponding eigenvector with p elements that represent a new base. Therefore, each principal component explains the variance according to the respective eigenvalue. In the present study, the number of factors retained in the PCA was three, and varimax rotated factor loading was used. Formally, varimax searches for a rotation (i.e., a linear combination) of the original factors such that the variance of the loadings is maximized. Many authors, such as Kalkstein (1991) and Smoyer et al. (2000), have used this technique in order to compare biological and meteorological variables.

Results and discussion

Ozone transport and synoptic events

During summertime, the area studied experiences mean temperatures in June, July, and August of approximately 20°C.

According to the Portuguese Meteorological Institute (Instituto de Meteorologia Português 2008), the prevailing wind was from the northwest for approximately 35% of the study period, from the east for approximately 20%, and from the west for approximately 17% (Fig. 3). In addition, during the early morning hours (01:00 UTC to 04:00 UTC), the prevailing wind was from the northeast.

According to the Portuguese Environmental Agency (Agência Portuguesa do Ambiente 2008), air quality monitoring stations in northern Portugal registered 42 days on which ozone levels were above the primary standard limit (180 μg/m^3, public information threshold) in 2005: 10 days in June; 13 days in July; and 19 days in August.

In the same year, 300 h during which ozone levels were above the public information threshold were registered at the Lamas d'Olo monitoring station, located at an altitude of approximately 1,086 m in Alvão Natural Park. On 22 June, for example, the ozone level was 361 μg/m^3. Since the park is a protected area, it is of interest to determine how and from where the high levels of ozone arrived there, as well as to characterize ozone transport in 2005 throughout the region, not only from highly populated areas to rural areas but also the inverse. Carvalho et al. (2006) performed a sensitivity analysis, the results of which indicated that topography is the principal mechanism driving the injection of air pollutants at the higher tropospheric levels along the upper west coast of the Iberian Peninsula.

According to the Portuguese Meteorological Institute (Instituto de Meteorologia Português 2008), the average temperature in 2005 was 15.6°C, which is 0.6°C above the average from the period 1961–1990. The year 2005 can

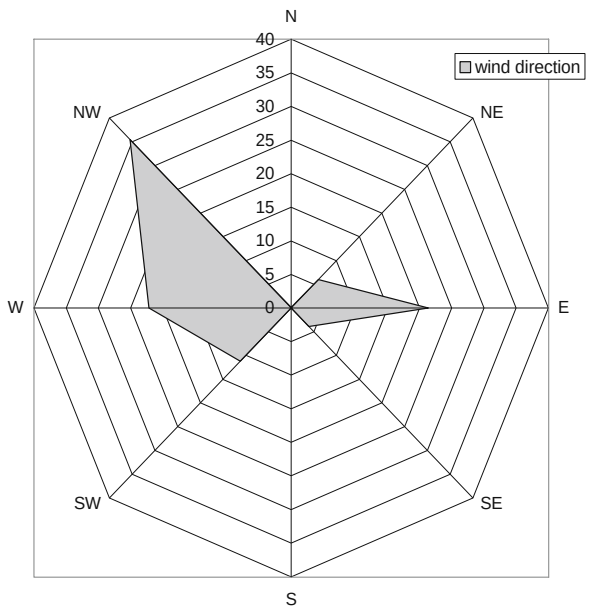

Fig. 3 Relative frequencies of wind directions observed during the study period (June–August of 2005)

also be classified as an extremely dry year, in which the total precipitation in 2005 was 1,265 mm, lower than the 1961–1990 average and the lowest registered annual precipitation since 1931.

The study area has a Mediterranean climate with maritime influence, resulting in hot, dry summers. Nevertheless, during 2005, there were two strong heat waves. On June 6 and 7, the Pedras Rubras station (located near the V. N. Telha air quality station) registered maximum temperatures that were 14.8°C above the average for this season. From 9–11 June, the stations registered gradually decreasing maximum temperatures. From 15–23 June, there was a second heat wave. The areas most affected were the southern and northern interior regions.

The air quality stations were chosen based on their proximity to the hospitals studied (preferably located within the sphere of influence of at least one of those hospitals), as well as on their characteristics in terms of the measurement of urban pollution. Each air quality monitoring station can register 1 or more hours, continuous or intercalated, during which the public information threshold for ozone levels is exceeded over the course of the same day. In June of 2005, there were at least two discernible periods in which the threshold was exceeded: from 8–10 June 8 (46 h above the threshold); and 22–23 June (78 h above the threshold, the highest level registered being 361 μg/m^3). There were two additional critical periods: 10–16 June (92 h above the threshold, the highest level registered being 359 μg/m^3); and 10–23 July (59 h above the threshold). Four such periods were observed during August in which ozone levels exceeded the public information threshold during a total of 129 hours (maximum, 320 μg/m^3), the strongest being 4–8 August.

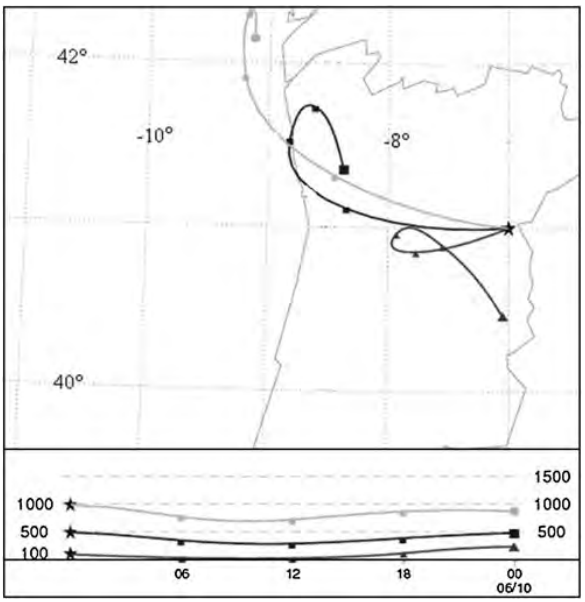

Fig. 5 Map showing 24-h wind trajectories at 100, 500, and 1,000 m of altitude from 00:00 UTC on 9 June 2005 until 00:00 UTC on 10 June 2005

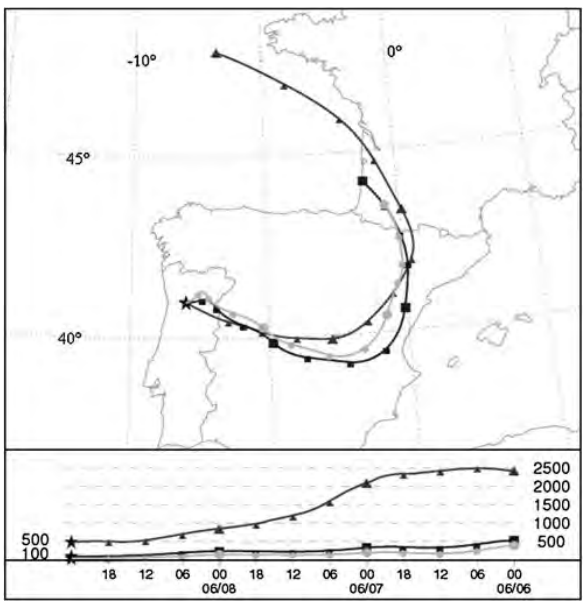

Fig. 4 Map showing 72-h wind trajectories at 20, 100, and 500 m altitude, delivering an air stream to northern Portugal at 00:00 UTC on 9 June 2005

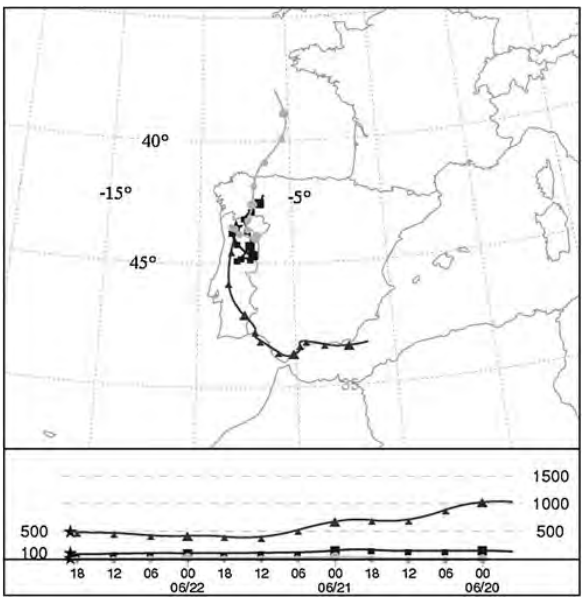

Fig. 6 Map showing 72-h wind trajectories at 20, 100, and 500 m altitude, delivering the air parcel to the Lamas d'Olo station at 19:00 UTC on 22 June 2005

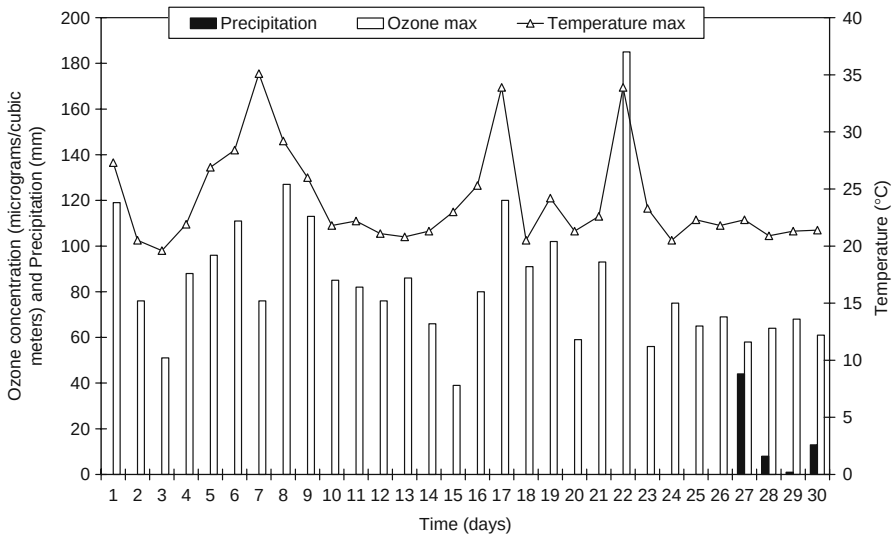

Fig. 7 Daily maximum ozone concentrations at the Antas station, and precipitation and temperature at Pedras Rubras station in June of 2005

June events

The public information threshold for ozone levels was most often exceeded during the period 8–10 June. National Oceanic and Atmospheric Administration Air Resources Laboratory data reveal that the air stream arrived in northern Portugal at 00:00 UTC on 9 June (Fig. 4). This air stream had begun its trajectory in southwest France approximately 72 h before. Wind transport appears to be one of the most important determining factors for ozone peaks occurring throughout the study area.

In the 9 June event, there was a period (15:00–23:00 UTC) during which ozone levels recorded at the Lamas d'Olo station exceeded the public information threshold on ten different occasions, the highest value (315 μg/m^3) being registered between 18:00 and 19:00 UTC.

Backward trajectory analysis showed that, 72 h before arriving at Lamas d'Olo, one air pocket traveled north to the western coast of France, passing through the center of the Pyrenees and entering the Iberian Peninsula in northern central Spain. On the same day at 12:00 UTC, the wind direction in the study area changed from easterly to westerly, which resulted in recirculation of the atmospheric gases (Fig. 5). Additionally, considering the NCEP/NCAR reanalysis data for the 7–9 June period, the wind speed decreased and the mean temperature increased gradually (from 23°C to 26°C). During this period, a low pressure system crossed the studied area, from South to North. On the regional scale, the

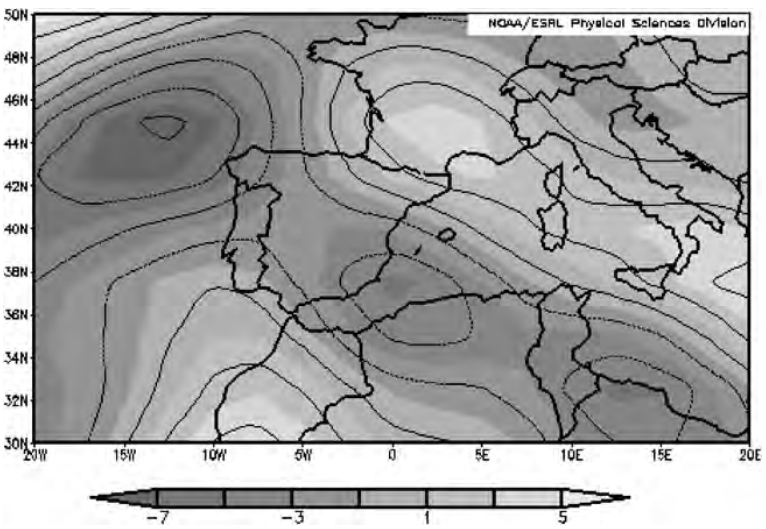

Fig. 8 Zonal wind (m/s) characteristics of the 9 July event. Negative numbers mean Eastward

HYSPLIT model showed recirculation (see also Fig. 5). Between 12:00 and 13:00 UTC, ozone levels peaked at the coastal stations (Boavista, 88 μg/m^3; Antas, 113 μg/m^3; Perafita 122 μg/m^3), decreasing gradually thereafter. These findings might be related to the 23:00 UTC peak registered at the Lamas d'Olo station (239 μg/m^3).

On 22 June, the wind speed on the Iberian Peninsula was low and the anomalous pressure was nearly zero. On the preceding days, the wind was from the North or Northeast. However, the zonal wind analysis indicated the approach of a prefrontal system, similar to the 9 June event, accompanied by an anticyclone system in the southwest of Portugal, moving to the north.

On 22 June, the highest ozone level registered at the Lamas d'Olo station was 361 μg/m^3 (between 19:00 and 20:00 UTC). High ozone levels were registered during certain hours of the day at the coastal stations (Ermesinde, 211 μg/m^3; Vila nova da Telha, 216 μg/m^3), and ozone levels exceeded the public information threshold during a total of 61 h in the study area as a whole. Over the course of the day, surface winds were weak (gusts from 0 to 6 m/s), varying in direction (easterly at 08:00 UTC; westerly at 17:00 UTC; southwesterly at 20:00 UTC; and southerly at 23:00 UTC). Those changes in wind direction caused recirculation at altitudes below 100 m (Fig. 6), where the maximum temperature was 33.1°C, which contributed to ozone formation.

Another air parcel, also beginning its trajectory 72 h prior to 22 June, at an altitude of less than 100 m, reached northern Portugal by way of northern Spain, moving into the Serra da Estrela region (Fig. 6), where there is a natural barrier (1,993 m in altitude). At approximately 12:00 UTC, the wind at an altitude of 100 m was from the west, blowing toward the interior of the country. However, during the early evening, the wind direction changed to northeasterly. The air parcel being transported at an altitude of 500 m came from Mediterranean Sea (Fig. 6) and moved from the southern Iberian Peninsula to the north, following the Peninsula shoreline and decreasing in altitude. In this case, the pollutants had been carried to lower levels, justifying the greater number of occasions on which ozone levels exceeded the public information threshold during the 22 June event.

Table 1 Fires in Portugal, June and July of 2005[a]

Date	Location
21 June	Electrical substation in Madrid
23 June	Mafra and Sintra
10 July	Castelo de Paiva
12 July	Mafra and Arouca
17 July	Saragoça, Zamora, and Cidade Real (Spain)
20July	Piódão and Seia
21 July	Seia
27 July	Viana do Castelo
29 July	Serra da Estrela, Chaves, Serra Arrábida, and Viseu

[a] http://sic.sapo.pt/online/jornalismo%20do%20cidadao/incendios?month=072005

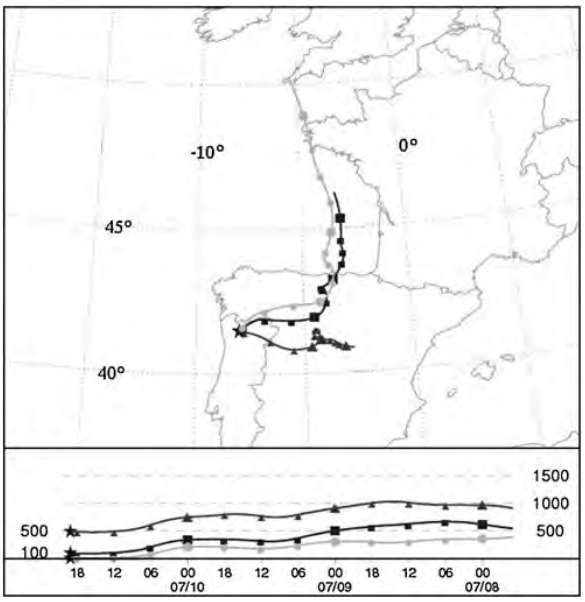

Fig. 9 Map showing 72-h wind trajectories at 20, 100, and 500 m of altitude, delivering an air stream to the Lamas d'Olo station at 19:00 UTC on 10 July 2005

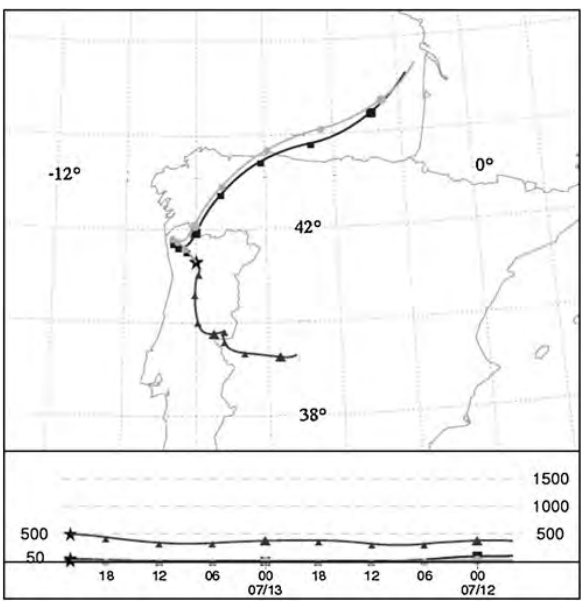

Fig. 10 Map showing 50-h wind trajectories at 20, 50, and 500 m of altitude, delivering the air parcel to the Lamas d'Olo station at 22:00 UTC on 13 July 2005

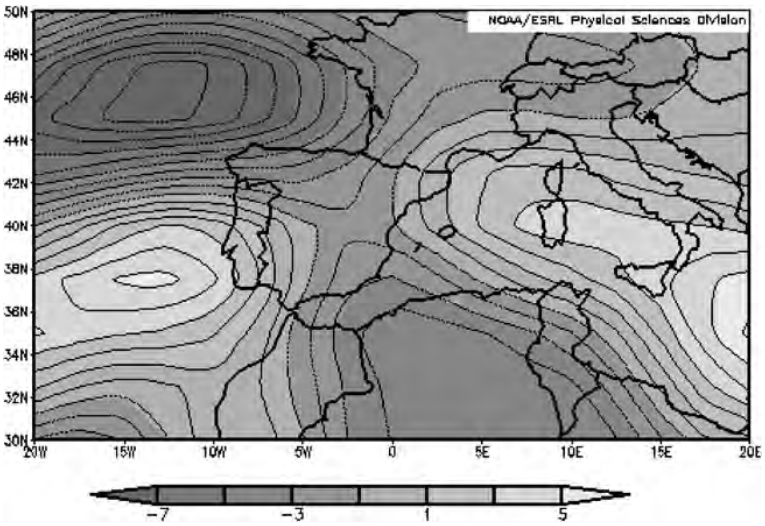

Fig. 11 Zonal wind (m/s) characteristics of 13 July event. Negative numbers mean Eastward

The ozone level variability during the beginning of June is clearly related to the arrival of a cold front that provoked a gradual decrease in maximum temperatures (from 27°C on 7 June o 23°C on 9 June). In the 27 June event, for example, the rainfall amount was 44 mm, compared with 8 mm in the 28 June event and 136 mm in the 30 June event (values obtained from the Pedras Rubras station). Precipitation typically decreases ozone levels by scavenging ozone precursors (Fig. 7).

July events

In July of 2005, there were two additional periods of significant pollution events. During the 7–9 July event, high ozone levels were observed in the early morning hours (00:00–04:00 UTC). These peaks might be related to the overnight transport (horizontal and vertical component) at the coastal stations in the greater Porto metropolitan area. The temperature decreased gradually from 24°C (maximum temperature on 6 July) to 12.4°C (minimum temperature on 7 July). The cooling during the night can force the ozone down, causing a relative maximum at dawn.

On a synoptic scale, the 7–9 July event and the 22 June event were quite similar. The advance of the frontal system decreased the anomalous pressure, thereby intensifying the cyclone over the northern portion of the Iberian Peninsula region, in opposition to the anticyclone, which was moving from south to north, as shown in Fig. 8.

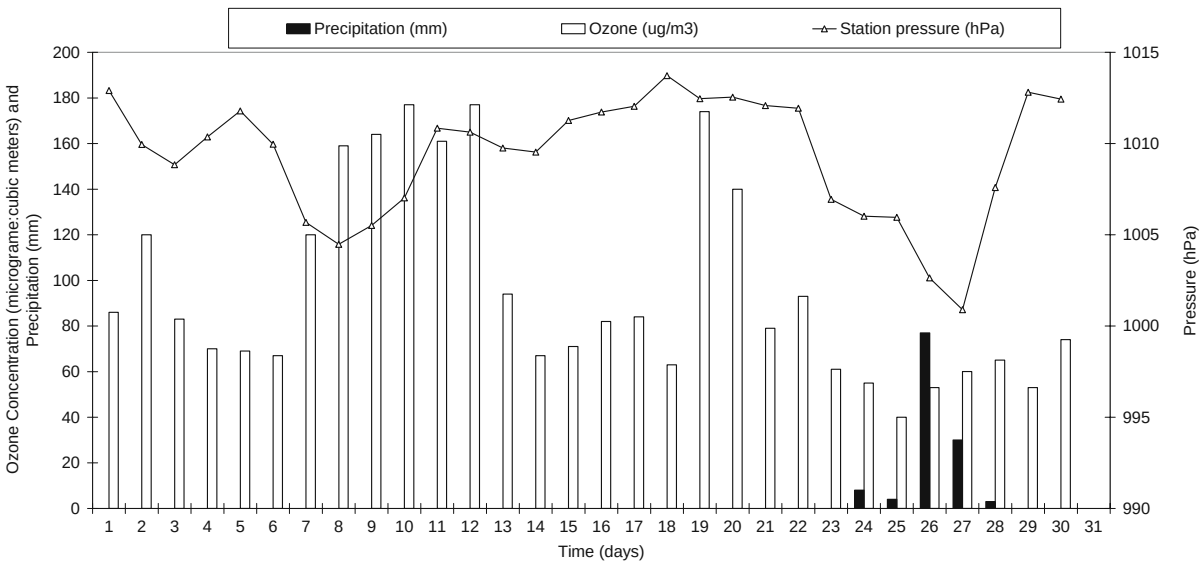

Fig. 12 Atmospheric pressure at the station level, precipitation, and ozone concentration for the month of July 2005

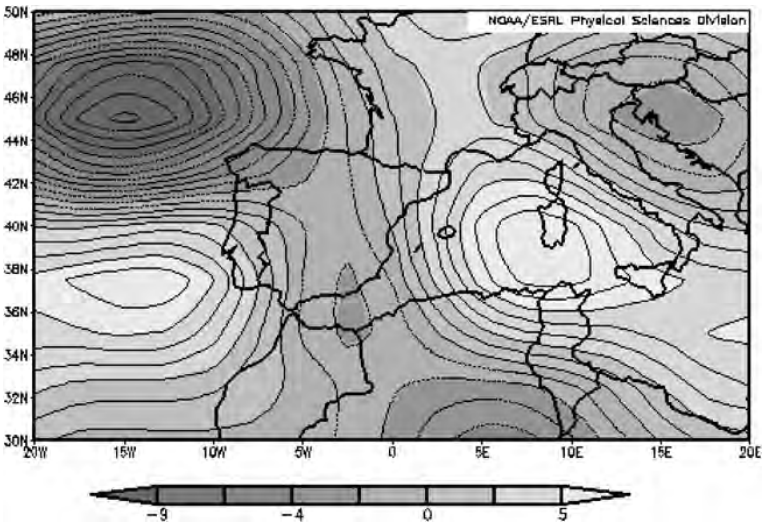

Fig. 13 Zonal wind (m/s) on 7 August. Negative numbers mean Eastward

At 00:00 UTC during the 9 July event, the prevailing winds were from the south, and the coastal stations registered low ozone levels. At 11:00 UTC, the wind changed to a westerly–northwesterly direction and again at 12:00 UTC. At the northwestern station of Matosinhos, an ozone level peak occurred when the wind began to blow from an easterly–southeasterly direction. The Antas station registered its maximum level (147 μg/m^3) at 14:00 UTC, followed by the Laticínios station (146 μg/m^3 at 16:00 UTC) and the Lamas d'Olo station (172 μg/m^3 at 19:00 UTC). During this period, the prevailing wind continued to come from the west. In the early morning hours of 9 July and 10 July, the Matosinhos station registered a relative maximum peak of 51 μg/m^3 at 01:00 UTC, whereas the Laticínios station registered 73 μg/m^3 at 03:00 UTC and the Lamas d'Olo station registered 129 μg/m^3 at 04:00 UTC.

The 10 July event is an example of how an easterly wind can increase coastal ozone levels during the night and early morning. On that day, a forest fire was active in the Castelo de Paiva area, approximately 40 km east of Porto (Table 1).

Table 2 Fires in Portugal, August 2005

Date	Location
2–6 August	Vale de Cambra[a]
3 August	Leiria, Aveiro and Penafiel[a]
4 August	Pombal (Coimbra), Coimbra, and Vila Real[a]
5 August	Leiria, Aveiro, Pombal (Coimbra)[b]
6 August	Majority of previously circumscribed fires[b]
7 August	Vila Real, Castelo Branco, Guarda, and Serra da Estrela Natural Park[b]
9 August	Arouca, Braga, Serra da Estrela, and Aveiro[b]
12 August	Vila Real, Viseu, Pampilhosa da Serra, and Penafiel[c]
14 August	Oporto, Sto Tirso, Braga, and Paços de Ferreira[d]
18 August	Bragança[d]
20 August	Ponte de Lima (Braga)[d]

[a] http://www.espigueiro.pt/noticias/c778a2d8bf30ef1d3c2d6bc5696defad.html

[b] http://sic.sapo.pt/online/jornalismo%20do%20cidadao/incendios?month=082005

[c] http://sic.sapo.pt/online/jornalismo%20do%20cidadao/incendios?month=082005

[d] http://pontelima.blogspot.com/2005_08_01_archive.html

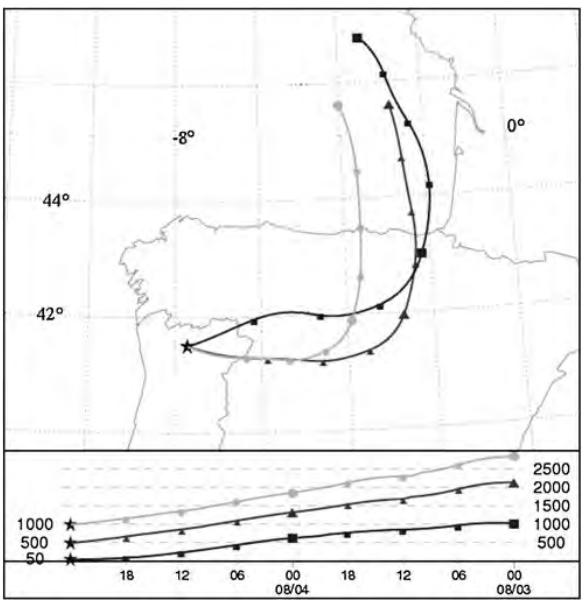

Fig. 14 Map showing 48-h wind trajectories at 50, 500, and 1,000 m of altitude, at 00:00 UTC on 5 August 2005

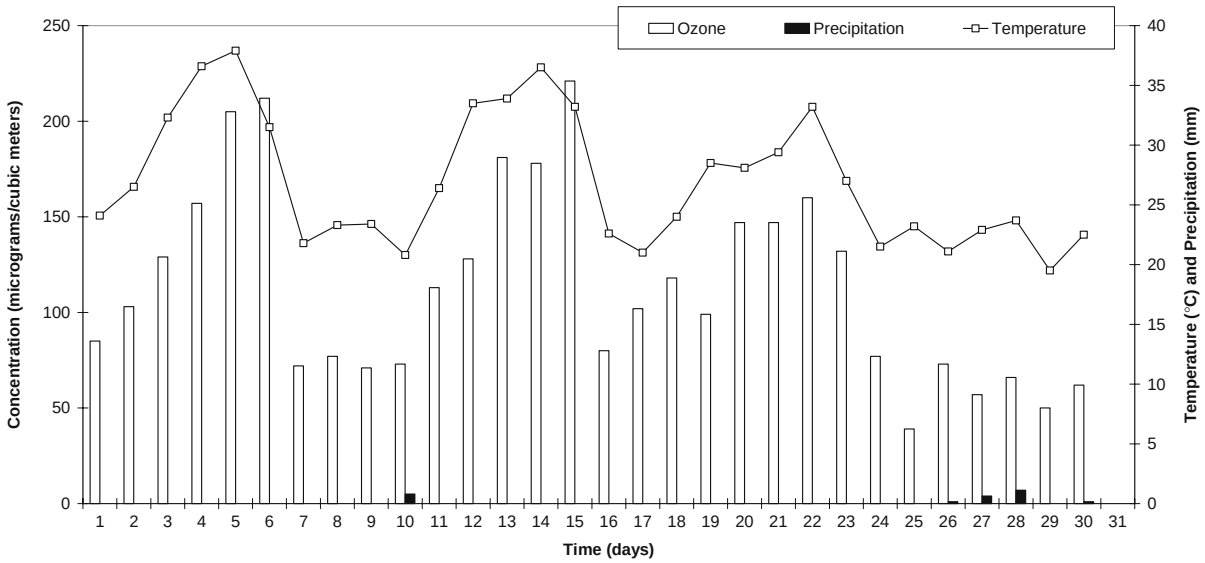

Fig. 15 Ozone concentrations, temperature, and precipitation during the month of August

According to the reanalysis, the surface winds (up to an altitude of approximately 500 m) were also from the east, as they had been on 9 July throughout the study area and in the adjacent areas of northern Spain (Fig. 9).

During the 13 July event, the prevailing winds at the Pedras Rubras station were from the western quadrant, varying from northwesterly to southwesterly, until 22:00 UTC. Atmospheric pressure also decreased, signaling the arrival of a cold front. Consequently, ozone levels at 00:00 UTC were below 50 μg/m^3 at the coastal stations of Antas, Baguim, Matosinhos, and Centro de Laticínios. However, at the Lamas d'Olo station, ozone levels remained above 160 μg/m^3 throughout the 13 July event, due to recirculation, as detected using the HYSPLIT model (Fig. 10). The recirculation continued for several hours along the northern coast.

In the 13 July event, the air parcel entered Portuguese territory at 00:00 UTC and moved southwest until 06:00 UTC, when it occupied the airspace over the area north of Vila do Conde. The wind direction then changed to southeasterly, promoting the surface dispersion of pollutants into the interior of the country. After 12:00 UTC, the coastal stations (Matosinhos, Antas, Ermesinde, Perafita, Baguim, and Espinho) registered ozone levels below 100 μg/m^3, and the Lamas d'Olo station registered an increase in ozone levels, which climbed above 180 μg/m^3 (maximum, 359 μg/m^3 at 16:00 UTC).

From 8 June to 10 June, an anticyclone system was moving from south to north. This anticyclone retained most of its original intensity until 19 June (Fig. 11). Mean zonal wind measurements taken on 19 June and 20 June showed that, although the anticyclone had decreased in intensity and was moving to the south, the ozone concentration was still high, perhaps due to transport and chemical reactions. A frontal system then arrived, accompanied by precipitation (8 mm rain on 24 July, and 122 mm rain on 29 July).

The system caused a reduction in the ozone level (Fig. 12), and the public information threshold was not exceeded again until the beginning of August.

Table 3 Varimax rotated factor loading with principal component extraction. Ozone time series from the Antas station; morbidity data set from the hospitals evaluated

Variable	Factor 1	Factor 2	Factor 3	Communalities
$O_{3\ MAXIMUM}$	0.48	0.73*	0.22	0.28
Hypertensive heart diseases	−0.77*	−0.05	−0.34	0.22
Ischemic heart diseases	−0.28	−0.19	0.23	0.04
Heart insufficiency	−0.58	0.53*	−0.34	0.20
Bronchitis/asthma	−0.41	−0.39	0.67*	0.15
Pneumoconiosis	0.46	−0.63	−0.49	0.25
Eigenvalues	1.62	1.41	1.01	
Proportion of explained variance	0.27	0.23	0.17	

*Significance or near significance

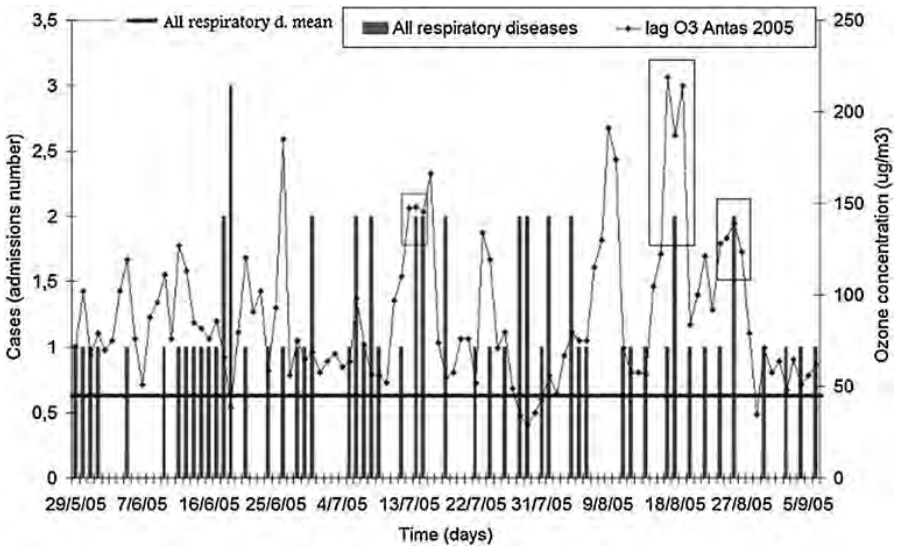

Fig. 16 Ozone concentration variation at the Antas station with a lag time of 4 days relative to the time series from all respiratory diseases considered in this study. The data points within frames represent the days on which maximum ozone levels coincided with maximum numbers of admissions

August events

On 4 and 5 August, a cyclonic system was registered on the Iberian Peninsula. The system was moving to the north ahead of an anticyclone. On 7 August, the synoptic-scale zonal wind analyses showed an area of intense low pressure over the study region (Fig. 13). An anticyclone in southwestern Portugal, followed by a cyclone in the north, favored a frontal system that developed and provoked precipitation on 10 August.

During the month of August, there were 240 h during which the public information threshold for ozone levels was exceeded in northern Portugal. From 4 August to 8 August, the following ozone levels were registered: 205 μg/m^3 on 5 August at the Ermesinde station; 320 μg/m^3 on 6 August at the Lamas d'Olo station; and 309 μg/m^3 on 7 August at the Lamas d'Olo station. These values are closely related not only to the meteorological conditions but also to the high pressure systems and the high number of fires that occurred in the northern region of the country. Numerous forest fires were active during the month of August (Table 2).

As can be seen in Fig. 11, the first events were related to a slight decrease in atmospheric pressure, from 1,022 hPa (on 3 August) to 1,009 hPa, which is characteristic of the arrival of a cold front.

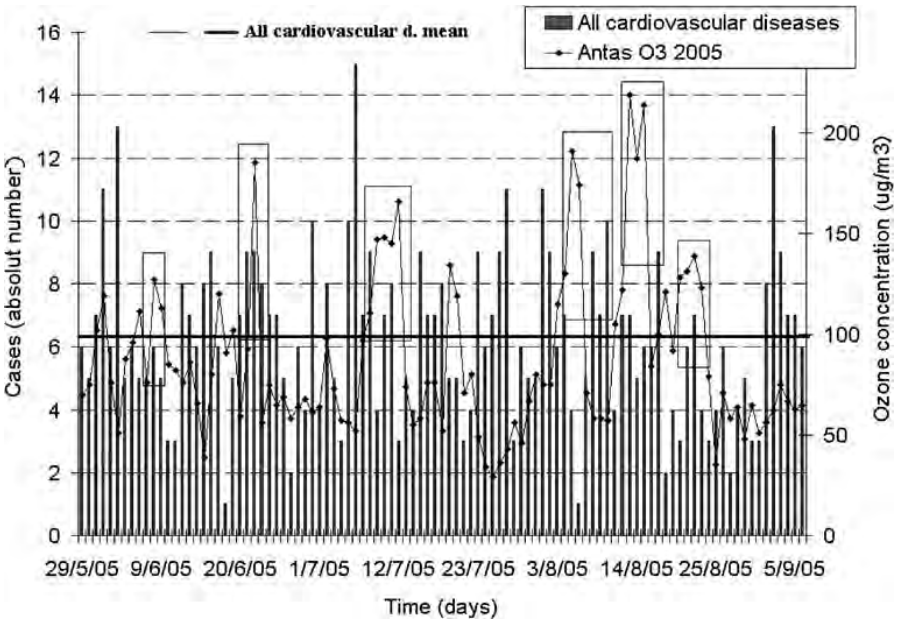

Fig. 17 Ozone concentration at the Antas station and the time series of all cardiac diseases considered in this study. Within the frames are the days on which maximum ozone levels coincided with maximum numbers of admissions. The mean daily number of admissions for cardiac diseases was 6.2

Table 4 Regression summary[a] for the dependent variable "ischemic heart diseases"

Ischemic heart diseases n=350	Beta	SE of Beta	B	SE of B	t n=342	P
Intercept			2.62*	0.41*	6.39*	0.00*
O_3	0.13*	0.05*	0.01*	0.00*	2.34*	0.02*
PM_{10}	−0.27*	0.13*	−0.02*	0.01*	−2.12*	0.03*
SO_2	−0.04	0.06	−0.02	0.02	−0.65	0.51
NO	0.12	0.10	0.02	0.01	1.17	0.24
CO	0.13	0.13	0.00	0.00	1.01	0.32
NO_2	0.13	0.12	0.02	0.02	1.09	0.28
$PM_{2.5}$ Vermoim	−0.12	0.13	−0.01	0.01	−0.92	0.36

*Significance or near significance

[a] R=0.28; R^2 =0.08; Adjusted R^2 =0.06; F(7.342)=4.07; P<0.0003; SE of estimate: 1.83

During the 10 August event, a cold front arrived, bringing precipitation to the area and effectively reducing ozone levels, from the maximum of 320 μg/m^3 registered at the Lamas d'Olo station on 6 August at 21:00 UTC to below the public information threshold. In the subsequent days, the levels of ozone increased gradually, indicating accumulation of pollutants in the atmosphere, until the next frontal system arrived.

According to the HYSPLIT model analysis, the air pockets at the surface (at 50 m in altitude) came from the Atlantic Ocean (Fig. 14). For the days on which the prevailing winds are from the east or northwest, the northernmost station in Portugal registered ozone levels that exceeded the public information threshold. The occurrence of such high levels registered from 3 August to 8 August appears to be associated with the continental wind. As presented in Fig. 14, 48 h before arriving in northern Portugal, air parcels traveling at altitudes that can vary from 50 m to 2,500 m move toward the south in the direction of the Iberian Peninsula. When the air streams arrive in the north of Spain, they begin to move west (Fig. 14). Such air streams typically enter Portuguese territory from the east, near the surface (at an altitude of approximately 50 m).

The period from 12–24 August was characterized by systems of low pressure (980–1,000 hPa), moving in from the east with prevailing north winds. Conditions were identical to those described for the 4–8 August period, with continental wind and high ozone levels (Fig. 15). Surface air streams coming from the British Isles entered the Iberian Peninsula from the northeast.

The events of 20 and 21 August 20 were characterized by northerly winds blowing from the inlands of the North Atlantic toward northern Spain and Portugal. On both of those days, there were fewer occurrences of ozone levels exceeding the public information threshold. Synoptically speaking, the main characteristic of this period was the low pressure system over the north of Portugal.

During the month of August, ozone levels recorded at the Lamas d'Olo station were never below 50 μg/m^3. This was attributed to higher insolation, synoptic conditions and pollutant transport.

Health impacts

2005

The PCA of the entire 2005 time series is presented in Table 3. In Factor 2, there was a clear positive association between cardiac diseases and ozone levels (0.53 and 0.73), which explained 23% of the total variance.

Case Studies

Considering the three summer months of 2005 (June–August), certain case studies were selected based on health

Table 5 Regression summary[a] for the dependent variable "other cardiac diseases, including heart failure"

Non-ischemic cardiac diseases n=350	Beta	SE of Beta	B	SE of B	t n=342	P
Intercept			2.64*	0.46*	5.75*	0.00*
O_3	0.10*	0.05*	0.01*	0.00*	1.88*	0.06*
PM_{10}	−0.01	0.13	0.00	0.01	−0.08	0.94
SO_2	0.02	0.06	0.01	0.03	0.25	0.80
NO	0.15	0.10	0.02	0.02	1.48	0.14
CO	0.15	0.13	0.00	0.00	1.19	0.24
NO_2	0.06	0.12	0.01	0.02	0.54	0.59
$PM_{2.5}$ Vermoim	−0.20	0.13	−0.02	0.01	−1.46	0.14

*Significance or near significance

[a] R=0.25; R^2 =0.06; Adjusted R^2 =0.043; F(7.342)=3.23; P<0.0025; SE of estimate: 2.05

Table 6 Regression summary[a] for the dependent variable "chronic obstructive pulmonary disease and allied conditions, including bronchitis and asthma"

Bronchitis/asthma n=350	Beta	SE of Beta	B	SE of B	t n=342	P
Intercept			0.46*	0.22*	2.09*	0.04*
O_3	0.09	0.05	0.00	0.00	1.59	0.11
PM_{10}	−0.11	0.13	0.00	0.00	−0.88	0.38
SO_2	0.06	0.06	0.01	0.01	0.91	0.36
NO	0.24*	0.10*	0.02*	0.01*	2.46*	0.01*
CO	0.26*	0.13*	0.00*	0.00*	2.04*	0.04*
NO_2	−0.16	0.12	−0.01	0.01	−1.39	0.16
$PM_{2.5}$ Vermoim	−0.09	0.13	0.00	0.01	−0.65	0.52

*Significance or near significance

[a] R=0.29; R^2 =0.087; Adjusted R^2 =0.068; $F(7.342)$=4.66; P < 0.00005; SE of estimate: 0.99

variability and the synoptic conditions previously described. For this analysis, we used the Antas station ozone level data set. The Antas station is located at a central position in relation to the three hospitals evaluated.

Figure 16 shows a time series of ozone and respiratory diseases for the summer months of 2005. Ozone levels are displayed with a lag time of 4 days relative to the respiratory disease data. The data points within frames represent the days on which maximum ozone levels coincided with maximum numbers of admissions. The mean daily number of hospital admissions for respiratory complaints was 0.66. Certain maximum ozone values were associated with high respiratory morbidity. Three cases studies were selected: one in July and two in August. It is of note that there were fewer hospital admissions for respiratory complaints during the summer months than during the remainder of the year (Nastos 2008), which accounts for the fact that there was only a weak association between such admissions and ozone concentrations. During the event of 7–12 July, ozone levels did not exceed the air quality standard at any time. However, on 14 and 15 July, a concentration of 148±41.1 μg/m^3, higher than on previous days, was found to be associated with an increase in respiratory morbidity (total, 4±0.76 admissions). August events were divided into two period/day pairs: 13–15 August (maximum ozone concentration, 219 μg/m^3), associated with a maximum morbidity event (two admissions) on 18 August (maximum ozone concentration, 139 μg/m^3); and 20–23 August, associated with a maximum morbidity event (two admissions) on 26 August.

Figure 17 shows the time series of all the cardiovascular diseases studied and the ozone concentrations. Six case studies were selected, the number of admissions and the mean ozone concentrations being as follows: on 8 June, 6 admissions and 127 μg/m^3; on 22 June, 9 admissions and 185 μg/m^3; between 8 July and 12 July, 31 admissions and 110–166 μg/m^3; on 5 August, 5 admissions and 191 μg/m^3; on 13 August, 7 admissions and 219 μg/m^3; on 15 August, 6 admissions and 214 μg/m^3; and on 22 August, 7 admissions and 139 μg/m^3.

On 8 and 22 June, ozone concentrations surpassed 180 μg/m^3 at many stations, as described in the previous section. These cases were clearly associated with cardiovascular morbidity, as was the ozone peak occurring during the 8–12 July event.

The August events seemed to exhibit a lag time. The high ozone concentration event of 5–6 August was potentially associated with the cardiovascular morbidity peaks of 8–10 August, a scenario that was apparently repeated for the 13–15 August case study. For the event of 20–22 August, both maximums are coincident. It must be stated that, during the first two events, there were fire spots near the GMAP (Table 2). Nevertheless, clear associations between ozone levels and cardiovascular disease have previously been demonstrated (Hong et al. 2002; Szyszkowicz 2007).

In addition to ozone, other pollutants and meteorological variables considered in this study presented health impacts related to both groups of diseases (Tables 4, 5, 6, 7, 8, 9 and 10).

Table 7 Analysis of variance for the dependent variable "ischemic heart diseases"

Effect of PM_{10}	Sums of squares	df	Mean squares	F	P
Regression	27.211*	1.00*	27.211*	7.747*	0.0056*
Residual	1264.405	360.00	3.512		
Total	1291.616				

*Significance or near significance

Table 8 Analysis of variance for the dependent variable "ischemic heart diseases"

Effect of $PM_{2.5}$	Sums of squares	df	Mean squares	F	P
Regression	18.225*	1.00*	18.225*	5.142*	0.024*
Residual	1251.240	353.00	3.545		
Total	1269.465				

*Significance or near significance

Table 9 Analysis of variance for the dependent variable "chronic obstructive pulmonary disease and allied conditions, including bronchitis and asthma"

Effect of CO	Sums of squares	df	Mean squares	F	*P*
Regression	11.848*	1.00*	11.848*	11.857*	0.0006*
Residual	359.732	360.00	0.999		
Total	371.580				

*Significance or near significance

Multiple regression results

These results show the standardized regression coefficients (Beta) and the raw regression coefficients (B). The magnitude of these Beta coefficients allows comparison of the relative contribution of each independent variable in the prediction of the dependent variable. As is evident in Tables 4–10, certain pollutants are major predictors of a number of respiratory and cardiovascular diseases. The regression coefficient for ozone was positive (Table 4), higher ozone levels translating to higher numbers of hospital admissions. Nevertheless, although cardiac diseases (codes 426–428) presented no significant correlation with ozone levels, we considered the relationship significant in the context of the significant correlations with the majority of the variables, and due the significance at the intercept (Table 5).

Table 6 shows that chronic obstructive pulmonary disease and allied conditions, including bronchitis and asthma, correlated significantly with NO and CO.

ANOVA results

The objective of performing the ANOVA was to test for significant differences among the means. Applying the ANOVA to all air pollutants measured and hospital admissions for the diseases studied, we found significant associations (Tables 7–10). The sums of squares were separated into two square sums (SQR, regression and SQE, error) and their cumulative degrees of freedom. The results showed that the ischemic heart diseases was related to PM_{10} (Table 7) and $PM_{2.5}$ (Table 8). In the regression model, chronic obstructive pulmonary disease and allied conditions, including bronchitis and asthma, were associated with CO and NO.

Table 7 shows that the F was 7.747, with the statistical distribution of 1.360, and the probability of observing a value greater than or equal to 7.747 was less than 0.0056, showing that β_1 was not equal to zero. The term r^2 is equal to 2.1%, indicating that 2.1% of the variability is explained by PM_{10}.

For the same set of diseases, the variability explained by $PM_{2.5}$ was 1.4%, and the difference was statistically significant (Table 8).

Chronic obstructive pulmonary disease and allied conditions, including bronchitis and asthma, presented a significant correlation with CO ($P<0.0006$, and the r^2 indicated that CO explains 3.2% of the variability (Table 9). For the same group of diseases, the probability of F (18.158) was significant ($P<0.000026$). There is strong evidence that β_1 is not equal to zero. For NO, the r^2 was equal to 4.7% and had a lower residual value than in the previous analysis (Table 10). Therefore, this was the case in which the variance was best explained by the model.

Table 10 Analysis of variance for the dependent variable "chronic obstructive pulmonary disease and allied conditions, including bronchitis and asthma"

Effect of NO	Sums of squares	df	Mean squares	F	*P*
Regression	17.778*	1.00*	17.778*	18.158*	0.000026*
Residual	355.390	363.00	0.979		
Total	373.167				

*Significance or near significance

Study limitations

One important limitation of the present study is that few of the air quality monitoring stations were in close proximity to the regional hospitals, which are located outside the larger urban centers. This might have resulted in an observation bias. The use of chemical analysis procedures could facilitate the quantification of ozone precursors, as well as the identification of events in which ozone levels exceed standard limits, in rural areas.

Conclusions

Peaks in ozone levels are typically registered at air quality monitoring stations situated along a line corresponding with the direction of wind transport. In the present study, lower ozone levels were associated with days of precipitation (arrival of frontal systems), as occurred on 27 July, 28 July, 9 August, and 26 August. High levels of ozone were found to be associated with wind transport, since ozone levels exceeded the public information threshold only when the wind was from the northeast and not when it was from the west. Ozone peaks occurring in the late morning/mid-afternoon and during the night were associated with changes in wind direction. On certain days, intense nocturnal cooling caused the ozone to descend closer to the surface, resulting in ozone peaks during the early

morning hours. Although the arrival of cold fronts, which bring precipitation, clearly led to reductions in ozone levels, we identified increased numbers of hospital admissions for respiratory diseases. This calls for further, more in-depth, research, preferably related to other processes of infection within the respiratory tract.

The results of this study are in accordance with those of other studies of the Iberian Peninsula, in which the synoptic conditions created by the Mediterranean climate, together with the geo-morphological characteristics of the region, have been implicated in the higher ozone levels observed during the summer months (Alvim-Ferraz et al. 2006; Pereira et al. 2005; Monteiro 1997).

In general, ozone exceedance events are related to elevated air temperatures resulted from specific synoptic conditions associated with prefrontal or frontal systems spawned by an anticyclone moving to the north accompanied by the cyclone over northwest Portugal.

According to Massambani and Andrade (1994), the nocturnal ozone peak can be caused by ozone precursors that are emitted by vehicular traffic. The authors postulated that, since vehicles begin to emit pollutant gases before sunrise, the NO emitted reacts with oxygen, producing NO_2 but, without insolation, the ozone is not depleted. Liu et al. (1990) and Samson (1978), among others, without examining the behavior of precursor gases, attributed nocturnal ozone peaks to local atmospheric circulation. However, Reitebuch et al. (2000) showed that two different types of this phenomenon are associated with a nocturnal low-level jet and the passage of a front. In both cases, the nocturnal increase in ozone level was accompanied by a significant increase in the standard deviation of the vertical wind speed across the lower stable boundary layer, indicating enhanced vertical mixing. According to Pretto et al. (2001), pollutants such as ozone have been advected by long-distance transport in the residual layer and can be transported downward into the surface layer, having a negative impact on air quality in the surface layer.

In this analysis of the health impacts of ozone concentration on the elderly population of the GMAP, two important findings should be considered. The first is that the PCA of the dataset for the entire year of 2005 identified a significant association between the sum of cardiovascular diseases and ozone peaks above 100 $\mu g/m^3$, although no clear association with respiratory disease was found, perhaps due to the generally fair weather during summers in the GMAP. The second is that the analysis of the specific case studies (8–12 July, 13–15 August and 20–22 August) revealed a clear increase in the number of hospital admissions for respiratory and cardiovascular diseases following these special events (total admissions, 65 and 11, respectively).

The results of our study further our understanding of pollutant circulation along the northern coast of Portugal and have implications for the assessment of air quality and its impact on respiratory and cardiovascular diseases. Increases in ozone concentrations were observed even in the nocturnal boundary layer in interior regions. In addition, our findings represent a call to address atmospheric pollution problems and their impact on human health in southern Europe.

Acknowledgments This paper was supported by the *Conselho Nacional de Desenvolvimento Científico e Tecnológico* (CNPq, National Council for Scientific and Technological Development). We are especially grateful to Dr. Maciel Barbosa, ARS-president, who provided access to the hospital data. We also thank Jeff Boyles and Miguel Lopes for their significant contributions.

References

Agencia Portuguesa do Ambiente (2008) Qualar [updated 19 June 2008; cited 19 June 2008]. Available from: http://www.qualar.org/

Alvim-Ferraz MCM, Pereira MC, Ferraz JM, Almeida e Mello AMC, Martins F (2005) European Directives for air quality: analysis of the new limits in comparison with asthmatic symptoms in children living in the Oporto metropolitan area, Portugal. Hum Ecol Risk Assess 11:607–616

Alvim-Ferraz MCM, Sousa SIV, Pereira MC, Martins FG (2006) Contribution of anthropogenic pollutants to the increase of tropospheric ozone levels in the Oporto Metropolitan Area, Portugal since the 19th century. Environ Pollut 140:516–524

Calvert JG (1983) Acid deposition: atmospheric processes in Eastern North America. National Academy Press, Washington, DC

Carvalho AC, Carvalho A, Gelpi I, Barreiro M, Borrego C, Miranda AI, Pérez-Muñuzur V (2006) Influence of topography and land use on pollutants dispersion in the Atlantic coast of Iberian Peninsula. Atmos Environ 40(21):3969–3982

Castell N, Mantilla E, Millán M (2006) Analysis of tropospheric ozone concentration on Western Mediterranean site: Castellon (Spain). Environ Monit Assess 136:3–11

CETESB (2005) Relatório da Qualidade do Ar no Estado de São Paulo 2004, Companhia de Tecnologia de Saneamento Ambiental http://www.cetesb.sp.gov.br/

CETESB (2006) Relatório da Qualidade do Ar no Estado de São Paulo 2005, Companhia de Tecnologia de Saneamento Ambiental http://www.cetesb.sp.gov.br/

Draxler RR, Hess GD (2004) Description of the HYSPLIT_4 Modeling System, NOAA Technical Memorandum ERL ARL-224. Air Resources Laboratory, Silver Spring, MD

Evtyugina MG, Pio C, Nunes T, Pinho PG, Costa CS (2007) Photochemical ozone formation at Portugal West Coast under sea breeze conditions as assessed by master chemical mechanism model. Atmos Environ 41(10):2171–2182

Gangoiti G, Millán M, Salvador R, Mantilla E (2001) Long-range transport and re-circulation of pollutants in the Western Mediterranean during the project regional cycles of air pollution in the West-central Mediterranean area. Atmos Environ 10:6267–6276

Gonçalves FLT, Carvalho LM, Conde F, Latorre MR, Dias O, Saldiva PHN, Braga ALF (2005) The effects of air pollution and meteorological parameters on respiratory morbidity during the summer in São Paulo City. Environ Int 31(3):343–349

Gonçalves FLT, Braun S, Silva Dias PL, Sharovsky R (2007) Influences of the weather and air pollutants on cardiovascular disease in the metropolitan area of Sao Paulo. Environ Res 104:275–281, ISSN: 0013-9351

Hong YC, Lee JT, Kim H, Kwon HJ (2002) Air pollution: a new risk factor in ischemic stroke mortality. Stroke 33:2165–2169

Instituto de Meteorologia Português (2008). Lisbon: The Institute [updated 19 June 2008; cited 19 June 2008]. Variabilidade climática. Available from: http://www.meteo.pt/pt/clima/clima_varclim.html

Jackson JE (1991) A user's guide to principal components. Wiley, New York, pp 1–79

Kalkstein LS (1991) A new approach to evaluate the impact of climate upon human mortality. Environ Health Perspect 96:145–50

Liu C, Liu S, Shen S (1990) A study of Taipei ozone problem. Atmos Environ 24:1461–1472

Lin S, Bell EM, Liu W, Walker RJ, Kim NK, Hwang S-A (2008) Ambient ozone concentration and hospital admissions due to childhood respiratory diseases in New York State, 1991–2001. Environ Res 108(1):42–47

Maporto (2008). Maporto: Área metropolitana do Porto; [cited 19 June 2008]. Available from: http://www.map.pt

Massambani O, Andrade MF (1994) Seasonal behavior of tropospheric ozone in the São Paulo (Brazil) metropolitan area. Atmos Environ 28(19):3165–3169

Millán M (2003) Ozone pollution in the Mediterranean. EXPORT-E2 Final Report, Ch20, pp 121–125

Millán M, Artiñano B, Alonso L, Castro M, Fernandez-Patier R, Goberna J (1992) Mesometeorological cycles of air pollution in the Iberian Peninsula (MECAPIP). Air Pollution Research Report. European Commission, 44, EUR 14834

Millán M, Salvador R, Mantilla E, Kallos G (1997) Photooxidant dynamics in the Mediterranean basin in summer: results from European research projects. J Geophys Res 102(D7):8811–8823

Millán M, Estrela MJ, Badenas C (1998) Meteorological processes relevant to forest fire dynamics on the Spanish Mediterranean Coast. J Appl Meteorol 37:83–100

Millán M, Mantilla E, Carratala R, Sanz MJ (2000) Ozone cycles in the Mediterranean basin: interpretation of monitoring data in complex coastal terrain. J Appl Meteorol 39:487–508

Monteiro A (1997) O Clima Urbano do Porto: Contribuição para a definição das estratégias de planeamento e ordenamento do território. Fundação Calouste Gulbenkian, Lisbon

Nastos PT (2008) Weather, ambient air pollution and bronchial asthma in Athens, Greece. In: Thomson MC, Garcia-Herrera R, Beniston M (eds), Seasonal forecasts, climatic change and human health. Advances in global change research series, Springer, Berlin, pp 173–188

Penkett AS, Evans MJ, Reeves CE, Law KS, Monks PS, Bauguitte SJB, Pyle JA, Green TJ, Bandy BJ, Mills G, Cardenas LM, Barjat H, Kley D, Schmitgen S, Kent JM, Dewey K, Methven J (2004) Long-range transport of ozone and related pollutants over the North Atlantic in spring and summer. Atmos Chem Phys Discuss 4:4407–4454

Pereira MC, Alvim-Ferraz MCM, Santos RC (2005) Relevant aspects of air quality in Oporto (Portugal): PM_{10} and O_3. Environ Monit Assess 101:203e221

Pretto A, Gatti LV, Rogero JR, Yamazaki A, Freitas ED, Dias PL Silva (2001) Nocturnal maximum ozone concentrations in Sao Paulo City. Available from: http://ies.jrc.cec.eu.int/Units/cc/events/torino2001/UP5.pdf

Reitebuch O, Strassburger A, Emeis S, Kuttler W (2000) Nocturnal secondary ozone concentration maxima analysed by sonar observations and surface measurements. Atmos Environ 34 (25):4315–4329

Samson PJ (1978) Nocturnal ozone maxima. Atmos Environ 12:951–955

Santos UdP, Braga ALF, Giorgi DMA, Pereira LAA, Grupi CJ, Lin CA, Bussacos MA, Zanetta DMT, Saldiva PHN, Terra Filho M (2005) Effects of air pollution on blood pressure and heart rate variability: a panel study of vehicular traffic controllers in the city of São Paulo, Brazil. Eur Heart J 26:193–200

Schneider T, Lee SD, Wolters GJR, Grant LD (eds) (1989) Studies in environmental science, no 35, Elsevier, Amsterdam, pp 523–532

Smoyer KE, Kalkstein LS, Greene JS, Ye H (2000) The impacts of weather and pollution on human mortality in Birmingham, Alabama and Philadelphia, Pennsylvania . Int J Climatol 20:881–897

Szyszkowicz M (2007) Air pollution and emergency department visits for depression in Edmonton, Canada. Int J Occup Med Environ Health 20:241–245

World Health Organization (2000) Regional Office for Europe [homepage on the Internet]. Copenhagen: The Office; c2000 [cited 19 June 2008]. Chapter 7.2: Ozone and other photochemical oxidants; Available from: http://www.euro.who.int/document/aiq/7_2ozone.pdf

Research | Children's Health

Birth Outcomes and Prenatal Exposure to Ozone, Carbon Monoxide, and Particulate Matter: Results from the Children's Health Study

Muhammad T. Salam,[1] Joshua Millstein,[1] Yu-Fen Li,[1] Frederick W. Lurmann,[2] Helene G. Margolis,[3] and Frank D. Gilliland[1]

[1]Department of Preventive Medicine, University of Southern California, Keck School of Medicine, Los Angeles, California, USA; [2]Sonoma Technology Inc., Petaluma, California, USA; [3]Air Resources Board, State of California, Sacramento, California, USA

Exposures to ambient air pollutants have been associated with adverse birth outcomes. We investigated the effects of air pollutants on birth weight mediated by reduced fetal growth among term infants who were born in California during 1975–1987 and who participated in the Children's Health Study. Birth certificates provided maternal reproductive history and residence location at birth. Sociodemographic factors and maternal smoking during pregnancy were collected by questionnaire. Monthly average air pollutant levels were interpolated from monitors to the ZIP code of maternal residence at childbirth. Results from linear mixed-effects regression models showed that a 12-ppb increase in 24-hr ozone averaged over the entire pregnancy was associated with 47.2 g lower birth weight [95% confidence interval (CI), 27.4–67.0 g], and this association was most robust for exposures during the second and third trimesters. A 1.4-ppm difference in first-trimester carbon monoxide exposure was associated with 21.7 g lower birth weight (95% CI, 1.1–42.3 g) and 20% increased risk of intrauterine growth retardation (95% CI, 1.0–1.4). First-trimester CO and third-trimester O_3 exposures were associated with 20% increased risk of intrauterine growth retardation. A 20-μg/m^3 difference in levels of particulate matter ≤ 10 μm in aerodynamic diameter (PM_{10}) during the third trimester was associated with a 21.7-g lower birth weight (95% CI, 1.1–42.2 g), but this association was reduced and not significant after adjusting for O_3. In summary, O_3 exposure during the second and third trimesters and CO exposure during the first trimester were associated with reduced birth weight. *Key words:* **air pollution, birth weight, carbon monoxide, intrauterine growth retardation, maternal exposure, nitrogen dioxide, ozone, particulate matter.** *Environ Health Perspect* **113:1638–1644 (2005). doi:10.1289/ehp.8111 available via** *http://dx.doi.org/* **[Online 18 July 2005]**

A growing body of evidence indicates that maternal exposures to air pollutants, including ozone, carbon monoxide, particulate matter with an aerodynamic diameter of ≤ 10 μm or ≤ 2.5 μm (PM_{10} and $PM_{2.5}$, respectively), nitrogen dioxide, and sulfur dioxide, are associated with adverse pregnancy outcomes. A major research focus has been to investigate the effects of air pollution on birth weight, low birth weight (LBW; < 2,500 g), and intrauterine growth retardation (IUGR).

Williams et al. (1977) first reported an inverse association between air pollution (based on the ambient levels of CO, NO_2, and O_3) and birth weight in Los Angeles, California, in the 1970s. Subsequently, several studies examining the effects of air pollution on fetal growth have been conducted in the United States (Chen et al. 2002; Maisonet et al. 2001; Parker et al. 2005; Ritz and Yu 1999), Canada (Liu et al. 2003), the United Kingdom (Bobak et al. 2001), the Czech Republic (Bobak 2000; Bobak and Leon 1999), China (Wang et al. 1997), South Korea (Ha et al. 2001; Lee et al. 2003), Taiwan (Lin et al. 2004; Yang et al. 2003), and Brazil (Gouveia et al. 2004).

Data from studies that were conducted in term infants showed significant associations between CO, PM_{10}, and $PM_{2.5}$ and reduced birth weight (Chen et al. 2002; Gouveia et al. 2004; Ha et al. 2001; Lee et al. 2003; Maisonet et al. 2001; Parker et al. 2005; Ritz and Yu 1999; Yang et al. 2003) and IUGR (Dejmek et al. 1999; Ha et al. 2001; Maisonet et al. 2001; Parker et al. 2005; Ritz and Yu 1999). However, the trimester-specific findings from these studies are inconsistent because they showed different windows of increased risk of reduced birth weight and IUGR for each pollutant. The explanations for the variations in results remain unclear. Although studies suggest that O_3 and NO_2 may be associated with birth weight, these pollutants have received less attention in epidemiologic studies.

To further investigate the effects of O_3, CO, PM_{10}, and NO_2 on reduced birth weight mediated by IUGR, we conducted a study among children who were born in southern California, a region with widely varying air pollution levels. We examined the associations between birth weight, LBW, and IUGR in term newborns and air pollution data in participants of the Children's Health Study (CHS), a population-based study of children residing in 12 southern California communities.

Materials and Methods

Study population. The elements of the CHS have been described previously (Peters et al. 1999a, 1999b). The population for this study was a subset of 6,259 participants in the CHS who were born in California between 1975 and 1987 and were recruited in four cohorts from public school classrooms from grades 4, 7, and 10 in 12 southern California communities in 1993–1996. At CHS entry, parents or guardians of each participating student provided written informed consent and completed a self-administered questionnaire, which included detailed demographic information as well as information regarding the mother's and child's respiratory health and exposure to different environmental factors that might contribute to the risk of reduced birth weight or could influence air pollution exposures. Race/ethnicity of the child was grouped as non-Hispanic white, Hispanic white, African American or black, Asian and Pacific Islander, and "other." Maternal smoking during pregnancy was assigned using self-report of any smoking during pregnancy. Socioeconomic status (SES) was determined from questionnaire items related to parent's educational level and annual family income at study entry (Table 1).

Birth information. Birth weight, gestational age, and other reproductive data were obtained from California birth certificates. Birth certificate information for California-born children who participated in the CHS was obtained by computerized linkage of participants with the California Department of Health Services Birth Statistical Master Files and Birth Cohort Files. Of the 6,259 cohort participants, 5,013 were born in California

Address correspondence to F.D. Gilliland, Department of Preventive Medicine, USC Keck School of Medicine, 1540 Alcazar St., CHP 236, Los Angeles, CA 90033 USA. Telephone: (323) 442-1096. Fax: (323) 442-3272. E-mail: gillilan@usc.edu

Supplemental material is available online at http://ehp.niehs.nih.gov/members/2005/8111/supplemental.pdf

We thank S.H. Alcorn for technical assistance in estimating air pollution levels.

This research was funded by the National Institute of Environmental Health Sciences (grants 5P01 ES009581, 5P01 ES011627, and 5P30 ES07048); the U.S. Environmental Protection Agency (grants R826708-01 and RD831861-01); the National Heart, Lung, and Blood Institute (grant 5R01HL61768); the California Air Resources Board (contract 94-331); and the Hastings Foundation.

The authors declare they have no competing financial interests.

Received 9 March 2005; accepted 18 July 2005.

according to parental report, and 4,842 were matched to a birth certificate record. Because preterm birth is associated with adverse birth outcomes and our analyses were focused on the effects of air pollutants on birth weight mediated by reduced fetal growth as opposed to reduced gestational age, we restricted our analyses in children who were born at term with gestational ages between 37 and 44 weeks, consistent with the methods used by earlier researchers. This criterion resulted in the exclusion of 941 children who were born before the 37th week of gestation, and our final sample consisted of 3,901 children. Data obtained from California birth certificates included birth weight, gestational age, maternal age at birth, maternal residence ZIP code at birth, parity, months since last live birth, gestational diabetes, and marital status. The estimated date of conception was assigned using the birth date and gestational age, corrected for the average 2-week difference between the last menstrual period and conception. First trimester was defined as gestational age < 13 weeks, second trimester was 13–27 weeks, and third trimester was 28 weeks to birth. We defined LBW as birth weight < 2,500 g in term infants and defined IUGR by less than the 15th percentile of predicted birth weight based on gestational age and sex in term infants.

Air pollution exposure assessment. Air pollution estimates were assigned using the ZIP code of the maternal residence at birth and monthly average air pollution estimates for each ZIP code interpolated from monitoring data obtained from the U.S. Environmental Protection Agency's (EPA) Aerometric Information Retrieval System through written request in 1999. Currently the 1999 data are available under the Air Quality System database of the U.S. EPA (U.S. EPA 2005). Temperature data were acquired from National Weather Service surface observations, the South Coast Air Quality Management District, the Bay Area Air Quality Management District, and CHS air pollution monitoring stations. Elevations above sea level were derived from 1-km horizontal resolution geophysical data from the U.S. Geological Survey's Earth Resources Observation Systems Data Center (U.S. Geological Survey 2005). Elevations were assigned to the ZIP code centroid of the maternal birth residence. Exposure estimates were calculated for monthly average of 24-hr O_3 ($O_{3[24hr]}$), 1000 hr to 1800 hr O_3 ($O_{3[10–6]}$), NO_2, CO, PM_{10}, and temperature by spatially interpolated monthly average levels to the geometric centroid coordinates of the ZIP code boundaries for the ZIP code region of the maternal birth residences.

The interpolation used inverse-distance-squared weighting based on data from up to the three nearest monitoring stations located within 50 km of the ZIP code centroid (100 km for O_3). Because the spatial gradients in monthly average data are smaller than hourly or daily data, the method was relative insensitive to the number of stations included in the interpolation and maximum interpolation radius. Three stations and a 50-km radius were selected because they preserved local gradients slightly better than did larger numbers of stations and greater distances. In cases where air monitoring data were available from a station located within 5 km of a ZIP code centroid, the assignments were based on the nearest station's data rather than interpolation. For this cohort, 29% of the NO_2 assignments and approximately 40% of the O_3, PM_{10}, and CO assignments were based on the nearest station's data. Each mother's exposures to O_3, NO_2, PM_{10}, and CO during each trimester were estimated using weighted averages of the calendar month averages. Although other studies included SO_2 exposures, it was not included in this study because ambient SO_2 concentrations are generally low in California and are measured at too few monitoring stations to make reliable exposure assignments.

Statistical analyses. The effect of each air pollutant on birth weight and 95% confidence intervals (CIs) were computed by fitting linear mixed-effects models using the SAS procedure GENMOD (SAS version 8.2; SAS Institute Inc., Cary, NC). Because of the nonlinearity in the relationship of birth weight with gestational age, a cubic polynomial in gestational age was necessary to adequately capture the nonlinearity. We therefore included linear, quadratic, and cubic terms for gestational age in all final models. The models also included maternal age, months since last live birth, parity, maternal smoking during pregnancy, SES, marital status at childbirth, gestational diabetes, and child's sex, race/ethnicity, and school grades (4th, 7th, and 10th) of the CHS cohort as fixed effects, and CHS study community as a random effect. To account for confounding by seasonal determinants of birth weight, the adjusted analyses included six terms for the basis matrix of a b-spline on Julian day of birth, with knots at days 91, 183, and 274 (De Boor 2001), because this has been suggested to be a more rigorous method of adjusting for temporal variations than adjusting for month or season of birth. We used missing indicators for missing data on maternal smoking during pregnancy, parity, SES, and race/ethnicity.

We considered the effects of pollutant exposures during the entire pregnancy and during each trimester. To illustrate the magnitude of the birth weight differences by air pollutant level, we presented the estimates scaled to the approximate interquartile ranges (IQRs) of average exposure for each pollutant. We also computed odds ratios (ORs) and 95% CIs for the association between pollutant levels and LBW and IUGR using appropriate logistic regression models that included the same adjustment variables as in the mixed-effects models. For pollutants that showed significant associations with birth weight in trimester-specific analysis, we fitted models that included average levels of those specific pollutants during specific trimesters. We fitted an additional model for O_3 that included three terms for average levels during each of the three trimesters.

For pollutants that were correlated with temperature and altitude, we conducted sensitivity analyses adding linear terms for elevation above sea level, temperature, and season of birth to the multivariate models. We also fitted a model with indicator variables for the

Table 1. Characteristics of study subjects (n = 3,901)[a] born at term in California between 1975 and 1987.

Characteristic	No. (%)
Gestational age (days)[b]	281.7 ± 10.3
Birth weight (g)[b]	3,486.7 ± 489.0
Sex (male)	1,888 (48.4)
LBW (< 2,500 g)	72 (1.8)
Term infants with IUGR	585 (15.0)
Maternal smoking during pregnancy	717 (18.8)
Unmarried at childbirth	632 (16.2)
Maternal gestational diabetes	18 (0.5)
Race/ethnicity	
Non-Hispanic white	2,315 (59.7)
Hispanic white	1,096 (28.3)
African American/black	183 (4.7)
Asian/Pacific Islander	100 (2.6)
Other	184 (4.7)
Maternal age at childbirth (years)	
< 20	356 (9.1)
20–22	607 (15.6)
23–29	1,917 (49.1)
30–32	550 (14.1)
33–35	298 (7.6)
≥ 36	173 (4.4)
Parity	
1	1,630 (41.9)
2	1,299 (33.4)
3	603 (15.5)
4	225 (5.8)
5	68 (1.8)
6–9	64 (1.6)
Months since last live birth	
0 (plural births)	25 (1.3)
10–25	537 (27.4)
26–36	464 (23.7)
36–57	446 (22.8)
≥ 58	485 (24.8)
SES based on parent's/guardian's education and annual household income	
Less than high school education or annual income < $15,000	838 (22.0)
Completed high school with annual income ≥ $15,000	655 (17.2)
Some college education with annual income ≥ $15,000	1,421 (37.2)
Completed 4-year college with annual income ≥ $15,000	310 (8.1)
Graduate-level education or annual family income ≥ $100,000	593 (15.5)

[a]Data are presented as n (%) unless otherwise specified. Subjects with missing data were not used to calculate the percentages. [b]Data presented as mean ± SD.

deciles of $O_{3[24hr]}$ exposure averaged over the entire pregnancy and presented the difference in birth weight associated with each decile of $O_{3[24hr]}$ exposure relative to the lowest decile. We assessed departure from linear relationships between birth weight and pollutants by examining appropriate residual plots and by comparing nested models with linear terms and categorical terms for each pollutant using partial *F*-tests. All significance tests were two sided at the 0.05 level.

Results

The sample included almost equal proportions of males and females (Table 1). About 60% of subjects were non-Hispanic, and 28% were Hispanic whites. Average birth weight was 3,487 g, with 72 infants (1.8%) with LBW and 585 infants (15%) with IUGR. Approximately 18% of mothers smoked during pregnancy. Few mothers had gestational diabetes ($n = 18$) or gave twin births ($n = 25$).

Table 2 shows the means ± SDs of the air pollutants, temperature, elevation, and their correlations with one another. For the trimester-specific averages, we observed strong positive correlation between $O_{3[24hr]}$ and $O_{3[10–6]}$ with correlation coefficient (r) > 0.9, and moderate positive correlation between O_3 and temperature with r approximately 0.6. Daily $O_{3[24hr]}$ was also positively correlated with PM_{10} ($r \sim 0.5$) but negatively correlated with NO_2 ($r \sim –0.1$) and CO ($r \sim –0.3$). Elevation was positively correlated with O_3 ($r \sim 0.3–0.4$) but negatively with CO ($r \sim –0.3$) and NO_2 ($r \sim –0.15$). O_3 levels in the first and second trimesters and the second and third trimesters were positively correlated ($r = 0.31$ in both instances), but levels in the first and third trimesters were negatively correlated ($r = –0.25$; data not shown).

Maternal exposure to O_3 averaged over the entire pregnancy was associated with reduced birth weight for both the $O_{3[24hr]}$ and the $O_{3[10–6]}$ average metrics (Table 3). For $O_{3[24hr]}$ levels during the entire pregnancy, mean birth weight was lower by 47.2 g (95% CI, 27.4–67.0 g) across the IQR of 12 ppb. Exposures to PM_{10}, NO_2, and CO when averaged over the entire pregnancy were not significantly associated with birth weight.

The inverse association between ambient O_3 levels and birth weight was stronger for exposure occurring during the second and third trimester for both the $O_{3[24hr]}$ and $O_{3[10–6]}$ average metrics (Table 3). With each IQR increase (i.e., 16 ppb and 17 ppb in the second and the third trimesters, respectively) in average $O_{3[24hr]}$ during the second and the third trimesters, birth weights were lower by 32.3 g (95% CI, 13.7–50.9 g) and 35.3 g (95% CI, 15.9–54.7 g), respectively. Trimester-specific analyses showed a statistically significant inverse association between CO concentrations in the first trimester and birth weight. Over an IQR in CO of 1.4 ppm, mean birth weight was lower by 21.7 g (95% CI, 1.1–42.3 g). The effects of PM_{10} were largest for the third trimester, and with each IQR increase in PM_{10} (i.e., 20 μg/m^3), birth weight was lower by 21.7 g (95% CI, 1.1–42.2 g).

In sensitivity analyses where further adjustments were made for temperature, elevation, and season of birth, the effect estimates were somewhat reduced for the average O_3 exposure over the entire pregnancy [Table S1 of the supplemental material (http://ehp.niehs.nih.gov/members/2005/8111/supplemental.pdf)]. However, greater birth weight deficits were observed for the second-trimester O_3 exposures after such adjustment compared with the estimates presented in Table 3. Greater influence

Table 2. Correlations for average exposures within each trimester of pregnancy.

		Correlations						
Exposure	Mean ± SD	$O_{3[10–6]}$	$O_{3[24hr]}$	PM_{10}	NO_2	CO	Temperature	Elevation
Entire pregnancy								
$O_{3[10–6]}$ (ppb)	50.6 ± 17.5	1	0.85	0.54	0.26	0.00	0.41	0.43
$O_{3[24hr]}$ (ppb)	27.3 ± 8.7		1	0.20	–0.10	–0.27	0.17	0.60
PM_{10} (μg/m^3)	45.8 ± 12.9			1	0.55	0.41	0.49	–0.02
NO_2 (ppb)	36.1 ± 15.4				1	0.69	0.54	–0.16
CO (ppm)	1.8 ± 0.9					1	0.32	–0.35
Temperature (°F)	61.2 ± 4.2						1	–0.19
Elevation (m)	219.1 ± 263.5							1
First trimester								
$O_{3[10–6]}$ (ppb)	51.0 ± 28.2	1	0.92	0.54	0.12	–0.17	0.69	0.28
$O_{3[24hr]}$ (ppb)	27.5 ± 14.1		1	0.34	–0.11	–0.32	0.60	0.38
PM_{10} (μg/m^3)	46.6 ± 15.9			1	0.48	0.29	0.47	0.00
NO_2 (ppb)	36.6 ± 16.9				1	0.68	0.20	–0.13
CO (ppm)	1.8 ± 1.1					1	–0.07	–0.29
Temperature (°F)	61.9 ± 7.3						1	–0.12
Second trimester								
$O_{3[10–6]}$ (ppb)	49.9 ± 25.5	1	0.91	0.50	0.10	–0.20	0.67	0.27
$O_{3[24hr]}$ (ppb)	27.0 ± 12.8		1	0.27	–0.15	–0.37	0.57	0.38
PM_{10} (μg/m^3)	45.4 ± 14.8			1	0.53	0.35	0.48	–0.04
NO_2 (ppb)	36.2 ± 16.9				1	0.72	0.21	–0.15
CO (ppm)	1.8 ± 1.1					1	–0.04	–0.30
Temperature (°F)	61.5 ± 6.8						1	–0.14
Third trimester								
$O_{3[10–6]}$ (ppb)	51.1 ± 27.1	1	0.91	0.52	0.11	–0.22	0.72	0.29
$O_{3[24hr]}$ (ppb)	27.5 ± 13.3		1	0.31	–0.14	–0.40	0.63	0.40
PM_{10} (μg/m^3)	45.4 ± 15.5			1	0.52	0.37	0.48	–0.01
NO_2 (ppb)	35.5 ± 16.6				1	0.71	0.18	–0.15
CO (ppm)	1.8 ± 1.1					1	–0.05	–0.30
Temperature (°F)	61.7 ± 7.1						1	–0.08

Table 3. Effects of air pollutants on birth weight from single-pollutant models.[a]

	IQR	Birth weight [g (95% CI)][b]	*p*-Value
Entire pregnancy			
$O_{3[10–6]}$	26 ppb	–49.9 (–72.0 to –27.8)	< 0.001
$O_{3[24hr]}$	12 ppb	–47.2 (–67.0 to –27.4)	< 0.001
PM_{10}	18 μg/m^3	–19.9 (–43.6 to 3.8)	0.10
NO_2	25 ppb	–7.2 (–34.7 to 20.4)	0.61
CO	1.2 ppm	2.2 (–20.1 to 24.4)	0.85
First trimester			
$O_{3[10–6]}$	33 ppb	–5.7 (–23.2 to 11.8)	0.52
$O_{3[24hr]}$	17 ppb	–10.4 (–28.6 to 7.7)	0.26
PM_{10}	20 μg/m^3	–3.0 (–22.7 to 16.7)	0.76
NO_2	25 ppb	–15.3 (–39.7 to 9.2)	0.22
CO	1.4 ppm	–21.7 (–42.3 to –1.1)	0.04
Second trimester			
$O_{3[10–6]}$	29 ppb	–25.7 (–42.7 to –8.7)	0.003
$O_{3[24hr]}$	16 ppb	–32.1 (–50.7 to –13.4)	< 0.001
PM_{10}	19 μg/m^3	–15.7 (–36.1 to 4.7)	0.13
NO_2	25 ppb	1.9 (–23.1 to 26.9)	0.88
CO	1.4 ppm	11.3 (–9.7 to 32.3)	0.29
Third trimester			
$O_{3[10–6]}$	33 ppb	–36.7 (–54.9 to –18.5)	< 0.001
$O_{3[24hr]}$	17 ppb	–35.2 (–54.6 to –15.8)	< 0.001
PM_{10}	20 μg/m^3	–21.7 (–42.2 to –1.1)	0.04
NO_2	25 ppb	–6.1 (–31.0 to 18.9)	0.63
CO	1.3 ppm	11.8 (–8.4 to 32.1)	0.25

[a]For detailed modeling information, see "Materials and Methods." [b]Minus sign denotes reduction in mean birth weight.

of these adjustment variables was observed on the CO effects on birth weight. The direction of association between CO exposures over the entire pregnancy and during the second and third trimesters changed from a positive to a negative one, and the negative association between first-trimester CO exposure and birth weight was attenuated. For PM_{10}, the effect estimate for the third trimester was reduced and was no longer statistically significant. However, the second-trimester PM_{10} results became stronger and achieved borderline significance.

In two-pollutant models that examined the joint effects of air pollutants that showed significant associations in trimester-specific analyses, CO effects were stronger in a two-pollutant model that included $O_{3[24hr]}$ and CO, and birth weight was lower by 28.6 g (95% CI, 6.9–50.4 g) per 1.4-ppm increase in ambient CO levels (Table 4). In contrast, in a two-pollutant model that included $O_{3[24hr]}$ and PM_{10}, the inverse association between PM_{10} and birth weight during the third trimester was attenuated and no longer was statistically significant. Including the three trimester-specific averages for O_3 in one model attenuated the effect estimates for the second trimester but did not change the estimates for the third trimester.

Maternal O_3 exposures averaged over the entire pregnancy and during the third trimester and CO exposure during the first trimester were significantly associated with increased risk of IUGR (Table 5). A 17-ppb difference in maternal $O_{3[24hr]}$ exposure during the third trimester increased the risk of IUGR by 20% (95% CI, 1.0–1.3). Over an IQR in CO of 1.4 ppm during the first trimester, the risk of IUGR increased by 20% (95% CI, 1.0–1.4). A 17-ppb difference in the third-trimester O_3 exposures was associated with 40% increased risk of LBW (95% CI, 1.0–1.9); however, the estimates had substantial uncertainty due to the small number of LBW newborns.

We also observed a dose–response relationship of birth weight with average $O_{3[24hr]}$ that was clearest above 30-ppb exposure levels (Figure 1). Relative to the lowest decile of average $O_{3[24hr]}$ estimates for the next five lowest deciles were approximately –40 g to –50 g, with no clear trend and with 95% confidence bounds that included zero. The highest four deciles of O_3 exposure showed an approximately linear decrease in birth weight, and all four 95% CIs excluded zero [estimates of birth weight deficits (grams) for the four uppermost deciles of exposure, in ranked order by decile median of exposure: –73.7 (95% CI, –139.0 to –7.4); –91.6 (95% CI, –157.9 to –25.3); –103.5 (95% CI, –170.3 to –36.7); –148.3 (95% CI, –214.7 to –81.9)]. There were no consistent dose–response relationships between birth weight and CO and PM_{10} from exposure during pregnancy or by trimester (data not shown).

The crude effect estimates without any adjustment for maternal (i.e., maternal age, race, smoking status) or fetal (i.e., gestational age, sex) factors were similar to the adjusted estimates. The directions and magnitude of the effect estimates did not change in sensitivity analyses after we excluded the plural births, infants born to mothers with gestational diabetes, and subjects with missing covariate information on maternal race/ethnicity, smoking during pregnancy, parity, and SES.

Table 4. Effects of air pollutants on birth weight estimated from multipollutant models.[a]

	IQR	Birth weight [g (95% CI)][b]	*p*-Value
Model 1: first trimester			
$O_{3[24hr]}$	17 ppb	–17.8 (–37.3 to 1.6)	0.07
CO	1.4 ppm	–28.6 (–50.4 to –6.9)	0.01
Model 2: third trimester			
$O_{3[24hr]}$	17 ppb	–31.6 (–52.2 to –11.0)	0.003
PM_{10}	20 μg/m^3	–10.8 (–31.8 to 10.2)	0.31
Model 3: all trimesters			
$O_{3[24hr]}$ (first trimester)	17 ppb	–18.6 (–39.0 to 1.7)	0.07
$O_{3[24hr]}$ (second trimester)	16 ppb	–17.5 (–38.6 to 3.7)	0.11
$O_{3[24hr]}$ (third trimester)	17 ppb	–36.9 (–58.9 to –15.0)	< 0.001

[a]For detailed modeling information, see "Materials and Methods." [b]Minus sign denotes reduction in mean birth weight.

Table 5. Effects of air pollutants on LBW and IUGR from single-pollutant models.

		IUGR		LBW	
	IQR	OR (95% CI)[a]	*p*-Value	OR (95% CI)[a]	*p*-Value
Entire pregnancy					
$O_{3[10–6]}$	26 ppb	1.2 (1.0 to 1.5)	0.02	1.5 (0.9 to 2.3)	0.10
$O_{3[24hr]}$	12 ppb	1.2 (1.0 to 1.4)	0.01	1.3 (0.9 to 1.8)	0.18
PM_{10}	18 μg/m^3	1.1 (0.9 to 1.3)	0.49	1.3 (0.8 to 2.2)	0.22
NO_2	25 ppb	1.1 (0.9 to 1.3)	0.51	0.8 (0.4 to 1.4)	0.44
CO	1.2 ppm	1.0 (0.9 to 1.2)	0.62	0.8 (0.6 to 1.3)	0.41
First trimester					
$O_{3[10–6]}$	33 ppb	1.0 (0.9 to 1.1)	0.92	1.0 (0.7 to 1.3)	0.92
$O_{3[24hr]}$	17 ppb	1.0 (0.9 to 1.2)	0.72	1.0 (0.7 to 1.3)	0.87
PM_{10}	20 μg/m^3	1.0 (0.9 to 1.2)	0.94	1.0 (0.7 to 1.5)	0.85
NO_2	25 ppb	1.2 (1.0 to 1.4)	0.07	0.9 (0.5 to 1.5)	0.67
CO	1.4 ppm	1.2 (1.0 to 1.4)	0.01	1.0 (0.7 to 1.5)	0.90
Second trimester					
$O_{3[10–6]}$	29 ppb	1.1 (1.0 to 1.2)	0.18	1.1 (0.8 to 1.5)	0.47
$O_{3[24hr]}$	16 ppb	1.1 (1.0 to 1.2)	0.10	1.1 (0.8 to 1.5)	0.65
PM_{10}	19 μg/m^3	1.0 (0.9 to 1.2)	0.74	1.2 (0.8 to 1.7)	0.34
NO_2	25 ppb	1.0 (0.8 to 1.2)	0.94	1.0 (0.6 to 1.6)	0.90
CO	1.4 ppm	1.0 (0.9 to 1.1)	0.72	0.9 (0.6 to 1.3)	0.66
Third trimester					
$O_{3[10–6]}$	33 ppb	1.2 (1.0 to 1.3)	0.01	1.4 (1.1 to 1.9)	0.02
$O_{3[24hr]}$	17 ppb	1.2 (1.0 to 1.3)	0.02	1.4 (1.0 to 1.9)	0.03
PM_{10}	20 μg/m^3	1.1 (0.9 to 1.3)	0.29	1.3 (0.9 to 1.9)	0.13
NO_2	25 ppb	1.0 (0.8 to 1.2)	0.93	0.6 (0.4 to 1.1)	0.11
CO	1.3 ppm	1.0 (0.8 to 1.1)	0.51	0.7 (0.5 to 1.1)	0.09

[a]For detailed modeling information, see "Materials and Methods."

Discussion

We observed that ambient CO levels in the first trimester and O_3 levels in the second and the third trimesters were independently associated with lower birth weight and IUGR in term infants through the mechanism of reduced fetal growth. Although PM_{10} exposure in the third trimester was associated with reduced birth weight, the PM_{10} effect was not statistically significant in a two-pollutant model that included PM_{10} and O_3. A clear pattern of increasing deficits in birth weight with increasing levels of O_3 was observed for

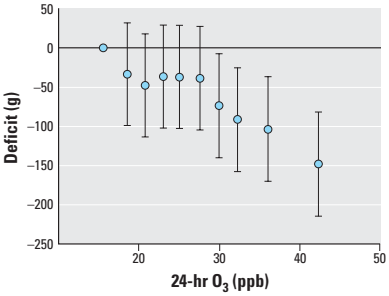

Figure 1. Birth weight deficit by decile of $O_{3[24hr]}$ exposure averaged over the entire pregnancy compared with the decile group with the lowest O_3 exposure. Deficits are plotted against the decile-group–specific median O_3 exposure. Error bars represent 95% CIs. Indicator variables for each decile of $O_{3[24hr]}$ exposure (except the least-exposed group) were included in a mixed model. For detailed modeling information, see "Materials and Methods."

24-hr average O_3 levels above 30 ppb, but no such trend was apparent for CO and PM_{10}. NO_2 levels were not associated with birth weight in this study. Although the differences in birth weight were small on average, those in the highest O_3 exposure group had deficits of a magnitude equivalent (~ 150 g) to those observed after exposure to cigarette smoke.

Our finding of an inverse association between maternal CO exposure during the first trimester and birth weight and IUGR is consistent with earlier reports (Gouveia et al. 2004; Ha et al. 2001; Lee et al. 2003). Although others have observed a significant negative effect of first-trimester CO exposure on birth weight (Maisonet et al. 2001; Ritz and Yu 1999), in a study of term infants born in California in 2000, Parker et al. (2005) did not observe a significant association between CO and birth weight. This lack of a strong association between CO and birth weight in a recent California birth cohort could be due to > 3-fold reduction in average third-trimester CO exposure levels from 1989–1993 to 2000 (2.5 and 0.8 ppm, respectively) (Parker et al. 2005; Ritz and Yu 1999).

Several lines of evidence support the plausibility of a negative effect of CO exposure on birth weight. CO reduces oxygen-carrying capacity of maternal hemoglobin, which could adversely affect O_2 delivery to fetal circulation. Because CO crosses the placental barrier (Sangalli et al. 2003) and fetal hemoglobin has greater affinity for binding CO than does adult hemoglobin, O_2 delivery to fetal tissues is further compromised (Di Cera et al. 1989). The resultant tissue hypoxia has the potential to reduce fetal growth.

The robust inverse association of O_3 concentrations with reduced birth weight is consistent with the early study of Williams et al. (1977) conducted in Los Angeles, California, in the 1970s. The present study found smaller deficits in birth weight across the range of O_3 concentrations than those observed in the study conducted by Williams et al., likely because they included children who were born preterm, and the levels of O_3 and other pollutants in the 1970s were much higher than levels during our study period. The 150-g deficit we observed in the highest decile of exposure in our study is of the same order of magnitude as the 314-g weight reduction in babies from areas with high O_3 levels compared with those living in the least-polluted areas, as was observed by Williams et al. (1977).

Of the more recent published reports that assessed the role of different ambient air pollutants on birth weight, a limited number assessed the effects of O_3 levels. Data from these studies suggested an inverse association between current ambient O_3 levels and birth weight (Chen et al. 2002; Gouveia et al. 2004; Ha et al. 2001). Chen et al. (2002) observed a borderline significant inverse association between ambient O_3 levels and birth weight in term infants born in Washoe County, Nevada, between 1991 and 1999. Mean 8-hr O_3 levels in Washoe County were substantially lower compared with the levels observed in this study (27.8 vs. 50.6 ppb). In Seoul, South Korea, with a median O_3 level of 22.4 ppb, Ha et al. (2001) also observed a significant association between levels of O_3 in the third trimester and LBW. Our results are consistent with the findings from these studies. In the study of term infants in Los Angeles, conducted by Ritz and Yu (1999), CO effects were the focus of the research, and associations of O_3 with birth weight were not reported. In addition, in this study, we observed significant reductions in birth weight with $O_{3[24hr]}$ concentrations ≥ 30 ppb. This may provide an explanation for not observing any association between O_3 and birth weight in areas with lower ambient O_3 levels. However, interpreting this observation as evidence for a threshold is not justified without further investigation.

In addition to epidemiologic reports, experimental studies in animal models also support a role of O_3 in reduced birth weight and suggest that the effect could be mediated through modulation of maternal inflammatory processes. In rats, neutrophilic inflammation was proportional to O_3 dose, and pregnant rats were more susceptible to acute pulmonary inflammation from O_3 than were virgin rats (Gunnison and Hatch 1999). The increased susceptibility during pregnancy arises from higher O_3 doses to the respiratory epithelial lining fluid (RELF) due to higher alveolar ventilation produced by increased tidal volumes and decreased ascorbic acid levels in the RELF. Kavlock et al. (1979) reported that mid and late gestational exposure to O_3 increased embryo toxicity in rats with evidence for a reduction in weight gain 6 days after birth. Bignami et al. (1994) observed reduced postnatal weight gain in mice whose mothers were exposed to 1.2 ppm O_3 over days 7–17 of gestation. Because pregnancy duration in mice is about 3 weeks (Thibodeaux et al. 2003), 7–17 days of gestation would correspond to the second and the third trimesters in mice. In a second study by this group, mice exposed prenatally to 0.6 ppm O_3 showed a long-lasting reduction in body weight (Dell'Omo et al. 1995).

Similar experimental studies of exposures cannot be conducted in pregnant women; however, in healthy human volunteers, effects of O_3 exposures on biomarkers have been observed, including increased peripheral neutrophil and lower ascorbic acid levels 6 hr after 0.2 ppm O_3 exposure for 2 hr (Mudway et al. 1999). Because pregnant women have higher alveolar ventilation than do nonpregnant women (Barclay 1997), the level of exposures during pregnancy is likely to be greater, and similar inflammatory responses could be more pronounced in pregnant women. Furthermore, inflammation due to O_3 results in the release of lipid peroxidation products and inflammatory cytokines into circulation (Hemmingsen et al. 1999; Larini and Bocci 2005). This could adversely affect placental circulation and function and can affect fetal growth. Further research is needed to define the mechanisms of O_3 on the maternal–fetal unit.

Our estimates of about a 22-g decrease in birth weight per 20-μg/m^3 increase in PM_{10} during the third trimester was comparable with the 11-g decrease in birth weight for a 10-μg/m^3 increase in PM_{10} levels, as observed by Chen et al. (2002). However, after adjustment for O_3, the estimate was reduced by about 50% and was not statistically significant. Further investigation of the relationship of PM_{10} and birth outcomes is needed, especially in the context of exposures to ambient levels of O_3 and PM_{10}.

Although a South Korean research group observed a significant negative effect of first-trimester NO_2 exposure on birth weight in two studies (Ha et al. 2001; Lee et al. 2003) where the study population of the first study was part of the second study, other researchers did not observe any significant association between NO_2 and birth weight (Gouveia et al. 2004; Lin et al. 2004; Liu et al. 2003). Moreover, there was a high correlation between NO_2, CO, and total suspended particles or PM_{10} in the studies conducted in South Korea, and it is not clear whether NO_2 had an independent negative effect in these studies.

Although third-trimester O_3 exposure was positively associated with LBW, we did not observe any significant association between any of the measured pollutants and LBW in our sample for exposures averaged over the entire pregnancy or for exposures during the first and second trimesters. One reason for observing significant associations between air pollutants and birth weight on a continuous scale but not on a categorical scale could be due to the low prevalence (i.e., < 2%) of LBW. Because a set cut-point of 2,500 g is used to define LBW, and the prevalence of LBW in term infants in developed countries is low, the use of LBW may not be ideal for assessing the impact of air pollution on birth weight in developed countries.

In contrast with earlier studies, the present study had information on maternal smoking and SES to adjust for potential confounding by these factors. Because maternal smoking during pregnancy may affect the associations between air pollutants and birth weight, and we did not have enough power to detect any significant effect modification, we restricted our analysis to mothers who did not smoke during their pregnancy with the index

child and observed similar results (data not shown).

The findings from this study must be interpreted in light of the methods used to assign exposure during the period of pregnancy. Air pollution exposures were assigned based on the centroid of the ZIP code of maternal residence at childbirth and may not reflect the actual exposure levels for the duration of the entire pregnancy. Studies have shown that about 20–25% of pregnant women change their residences during pregnancy (Khoury et al. 1988; Shaw and Malcoe 1992). However, pregnant women most often move to a different house in the same locality (Fell et al. 2004), probably because of the proximity to their workplaces, health care providers, and schools for those with older children. Residential address from birth certificates most often reflects maternal location during the last trimester (Schulman et al. 1993). This may have minimized the measurement error in exposure assessment during the third trimester, and as such, the third-trimester–specific results are likely to have less error than do the other trimester-specific results. We also lacked information on maternal employment location and commuting patterns. Because the resultant misclassification in exposure assignment is not likely to be differential, it may have attenuated the risk estimates. Exposure misclassification may explain the null findings for NO_2, but this would not account for the deficits in birth weight that we observed from exposures to the other pollutants. Because we did not have direct measures of maternal exposures to indoor and occupational pollutants during pregnancy, we could not address the effects of these exposures on the birth outcomes.

Another source for error in the air pollution estimates may be the distance between maternal residence and the air monitoring stations used to assign exposure. The proportion of data on O_3, PM_{10}, NO_2, and CO interpolated from monitoring stations < 5 km from the maternal birth residence ranged from 29.2 to 41.1%, whereas 51.2–61.3% were between 5 and 25 km, and the remaining 2.8–9.6% were interpolated from stations between 25 and 50 km for PM_{10}, NO_2, and CO and between 25 and 100 km for O_3 [Table S2 of the supplemental material (http://ehp.niehs.nih.gov/members/2005/8111/supplemental.pdf)]. We conducted sensitivity analyses to assess the influence of distance of the monitoring stations on the associations between air pollutants and birth outcomes excluding women living farther from these monitors, and the results showed little change (data not shown). Furthermore, a recent study in California showed high correlation ($r \sim 0.9$) of air pollutant levels between monitors located within 5 miles (i.e., ~ 8 km) from the maternal residence and those located at the county level (Basu et al. 2004), suggesting that the ZIP-code–based air pollution data could be a good proxy for exposure levels at the residences and in the region surrounding residences where subjects spend most of their time.

Although measurement errors of pollutants in single-pollutant models are likely to attenuate the magnitude of birth weight deficits associated with air pollutants, the findings from two-pollutant models as well as those adjusted for temperature and elevation should be evaluated with some caution given the correlation structure between these environmental factors. In two-pollutant models where levels of pollutants are correlated and the measurement error in one pollutant is larger than the other, Zeger et al. (2000) showed that the effects of the relatively poorly measured pollutant are decreased and could introduce positive bias in the effect of the better measured pollutant in the presence of strong negative correlation between the measurement errors of the two pollutants. We would expect attenuation in the CO effect estimate in the first trimester in a two-pollutant model that included O_3, because the measurement error in CO was possibly larger than O_3 and the pollutants were negatively correlated ($r \sim 0.3$). However, the CO effect estimates remained robust in a two-pollutant model, suggesting an independent CO effect on birth weight in the first trimester. PM_{10} and O_3, on the other hand, were positively correlated in the third trimester ($r \sim 0.5$), and the effect of PM_{10} was reduced about 2-fold in the two-pollutant model. Because a strong negative correlation between the measurement errors in PM_{10} and O_3 seems unlikely, the independent PM_{10} effects may be smaller.

Measures of maternal nutrition (i.e., prepregnancy weight-for-height, gestational weight gain, and intake of nutrients) were not available to assess the potential effects of these factors on the associations observed in this study. Although maternal nutrition may be a determinant of birth weight in the developing world, Kramer (1987) did not observe any significant role of maternal nutrition in LBW in developed countries. Also, earlier literature has shown that maternal race/ethnicity (Cohen et al. 2001), maternal education (Kramer et al. 2000), and maternal age (Haiek and Lederman 1989) are associated with maternal nutrition. Because we adjusted for race, maternal education, and maternal age and found little evidence for confounding in our analyses, we may have indirectly adjusted for the nutritional differences during pregnancy. Therefore, maternal nutrition is unlikely to confound the associations of air pollutants with birth weight in this study.

We also considered the possibility of bias from the potential effects of air pollutants on preterm births. In California, birth certificate data for birth weight have been found to be valid and reliable (Von Behren and Reynolds 2003). However, the data on gestational age based on maternal recall of last menstrual period may be less accurate. We may have included some preterm births in our analysis, but because our outcome of interest was reduction in mean birth weight, our results are not likely to be biased by the effects of air pollutants on gestational age at birth.

In conclusion, we observed an association between lower birth weight and IUGR with O_3 concentrations. The second- and third-trimester O_3 levels were most strongly associated with deficits in birth weight. In addition, CO levels in the first trimester were associated with about a 22-g reduction in birth weight over an IQR of 1.4 ppm. These findings suggest that ambient CO in the first trimester and O_3 in the second and third trimesters are determinants of birth weight and IUGR. Because exposures to the levels of ambient air pollutants observed in this study are common, and fetal growth is an important determinant for childhood and adult morbidity and mortality, our findings are likely to have important public health and regulatory implications.

REFERENCES

Barclay ML. 1997. Critical physiologic alterations in pregnancy. In: Emergency Care of the Woman (Pearlman MD, Tintinalli JE, eds). New York:McGraw Hill, 303–312.

Basu R, Woodruff TJ, Parker JD, Saulnier L, Schoendorf KC. 2004. Comparing exposure metrics in the relationship between $PM_{2.5}$ and birth weight in California. J Expo Anal Environ Epidemiol 14(5):391–396.

Bignami G, Musi B, Dell'Omo G, Laviola G, Alleva E. 1994. Limited effects of ozone exposure during pregnancy on physical and neurobehavioral development of CD-1 mice. Toxicol Appl Pharmacol 129(2):264–271.

Bobak M. 2000. Outdoor air pollution, low birth weight, and prematurity. Environ Health Perspect 108:173–176.

Bobak M, Leon DA. 1999. Pregnancy outcomes and outdoor air pollution: an ecological study in districts of the Czech Republic 1986–8. Occup Environ Med 56(8):539–543.

Bobak M, Richards M, Wadsworth M. 2001. Air pollution and birth weight in Britain in 1946. Epidemiology 12(3):358–359.

Chen L, Yang W, Jennison BL, Goodrich A, Omaye ST. 2002. Air pollution and birth weight in northern Nevada, 1991–1999. Inhal Toxicol 14(2):141–157.

Cohen GR, Curet LB, Levine RJ, Ewell MG, Morris CD, Catalano PM, et al. 2001. Ethnicity, nutrition, and birth outcomes in nulliparous women. Am J Obstet Gynecol 185(3):660–667.

De Boor C. 2001. A Practical Guide to Splines. New York:Springer-Verlag.

Dejmek J, Selevan SG, Benes I, Solansky I, Šrám RJ. 1999. Fetal growth and maternal exposure to particulate matter during pregnancy. Environ Health Perspect 107:475–480.

Dell'Omo G, Fiore M, Petruzzi S, Alleva E, Bignami G. 1995. Neurobehavioral development of CD-1 mice after combined gestational and postnatal exposure to ozone. Arch Toxicol 69(9):608–616.

Di Cera E, Doyle ML, Morgan MS, De Cristofaro R, Landolfi R, Bizzi B, et al. 1989. Carbon monoxide and oxygen binding to human hemoglobin F0. Biochemistry 28(6):2631–2638.

Fell DB, Dodds L, King WD. 2004. Residential mobility during pregnancy. Paediatr Perinat Epidemiol 18(6):408–414.

Gouveia N, Bremner SA, Novaes HM. 2004. Association between ambient air pollution and birth weight in São Paulo, Brazil. J Epidemiol Community Health 58(1):11–17.

Gunnison AF, Hatch GE. 1999. O3-induced inflammation in prepregnant, pregnant, and lactating rats correlates with O3 dose estimated by 18O. Am J Physiol 276(2 pt 1): L332–L340.

Ha EH, Hong YC, Lee BE, Woo BH, Schwartz J, Christiani DC.

2001. Is air pollution a risk factor for low birth weight in Seoul? Epidemiology 12(6):643–648.

Haiek L, Lederman SA. 1989. The relationship between maternal weight for height and term birth weight in teens and adult women. J Adolesc Health Care 10(1):16–22.

Hemmingsen A, Allen JT, Zhang S, Mortensen J, Spiteri MA. 1999. Early detection of ozone-induced hydroperoxides in epithelial cells by a novel infrared spectroscopic method. Free Radic Res 31(5):437–448.

Kavlock R, Daston G, Grabowski CT. 1979. Studies on the developmental toxicity of ozone. I. Prenatal effects. Toxicol Appl Pharmacol 48(1 pt 1):19–28.

Khoury MJ, Stewart W, Weinstein A, Panny S, Lindsay P, Eisenberg M. 1988. Residential mobility during pregnancy: implications for environmental teratogenesis. J Clin Epidemiol 41(1):15–20.

Kramer MS. 1987. Determinants of low birth weight: methodological assessment and meta-analysis. Bull WHO 65(5):663–737.

Kramer MS, Seguin L, Lydon J, Goulet L. 2000. Socio-economic disparities in pregnancy outcome: why do the poor fare so poorly? Paediatr Perinat Epidemiol 14(3):194–210.

Larini A, Bocci V. 2005. Effects of ozone on isolated peripheral blood mononuclear cells. Toxicol In Vitro 19(1):55–61.

Lee BE, Ha EH, Park HS, Kim YJ, Hong YC, Kim H, et al. 2003. Exposure to air pollution during different gestational phases contributes to risks of low birth weight. Hum Reprod 18(3):638–643.

Lin CM, Li CY, Yang GY, Mao IF. 2004. Association between maternal exposure to elevated ambient sulfur dioxide during pregnancy and term low birth weight. Environ Res 96(1):41–50.

Liu S, Krewski D, Shi Y, Chen Y, Burnett RT. 2003. Association between gaseous ambient air pollutants and adverse pregnancy outcomes in Vancouver, Canada. Environ Health Perspect 111:1773–1778.

Maisonet M, Bush TJ, Correa A, Jaakkola JJ. 2001. Relation between ambient air pollution and low birth weight in the northeastern United States. Environ Health Perspect 109(suppl 3):351–356.

Mudway IS, Krishna MT, Frew AJ, MacLeod D, Sandstrom T, Holgate ST, et al. 1999. Compromised concentrations of ascorbate in fluid lining the respiratory tract in human subjects after exposure to ozone. Occup Environ Med 56(7):473–481.

Parker JD, Woodruff TJ, Basu R, Schoendorf KC. 2005. Air pollution and birth weight among term infants in California. Pediatrics 115(1):121–128.

Peters JM, Avol E, Gauderman WJ, Linn WS, Navidi W, London SJ, et al. 1999a. A study of twelve southern California communities with differing levels and types of air pollution. II. Effects on pulmonary function. Am J Respir Crit Care Med 159(3):768–775.

Peters JM, Avol E, Navidi W, London SJ, Gauderman WJ, Lurmann F, et al. 1999b. A study of twelve southern California communities with differing levels and types of air pollution. I. Prevalence of respiratory morbidity. Am J Respir Crit Care Med 159(3):760–767.

Ritz B, Yu F. 1999. The effect of ambient carbon monoxide on low birth weight among children born in southern California between 1989 and 1993. Environ Health Perspect 107:17–25.

Sangalli MR, McLean AJ, Peek MJ, Rivory LP, Le Couteur DG. 2003. Carbon monoxide disposition and permeability-surface area product in the foetal circulation of the perfused term human placenta. Placenta 24(1):8–11.

Schulman J, Selvin S, Shaw GM, Malcoe LH. 1993. Exposure misclassification due to residential mobility during pregnancy in epidemiologic investigations of congenital malformations. Arch Environ Health 48(2):114–119.

Shaw GM, Malcoe LH. 1992. Residential mobility during pregnancy for mothers of infants with or without congenital cardiac anomalies: a reprint. Arch Environ Health 47(3):236–238.

Thibodeaux JR, Hanson RG, Rogers JM, Grey BE, Barbee BD, Richards JH, et al. 2003. Exposure to perfluorooctane sulfonate during pregnancy in rat and mouse. I: maternal and prenatal evaluations. Toxicol Sci 74(2):369–381.

U.S. EPA (U.S. Environmental Protection Agency). 2005. Technology Transfer Network Air Quality System (AQS). Available: http://www.epa.gov/ttn/airs/airsaqs/detaildata/downloadaqsdata.htm [accessed 5 October 2005].

U.S. Geological Survey. 2005. Earth Resources Observation Systems Data Center. Available: http://edc.usgs.gov/products/elevation/gtopo30.html [accessed 5 October 2005].

Von Behren J, Reynolds P. 2003. Birth characteristics and brain cancers in young children. Int J Epidemiol 32(2):248–256.

Wang X, Ding H, Ryan L, Xu X. 1997. Association between air pollution and low birth weight: a community-based study. Environ Health Perspect 105:514–520.

Williams L, Spence A, Tideman SC. 1977. Implications of the observed effects of air pollution on birth weight. Soc Biol 24(1):1–9.

Yang CY, Tseng YT, Chang CC. 2003. Effects of air pollution on birth weight among children born between 1995 and 1997 in Kaohsiung, Taiwan. J Toxicol Environ Health A 66(9):807–816.

Zeger SL, Thomas D, Dominici F, Samet JM, Schwartz J, Dockery D, et al. 2000. Exposure measurement error in time-series studies of air pollution: concepts and consequences. Environ Health Perspect 108:419–426.

American Journal of Epidemiology
Vol. 163, No. 6
DOI: 10.1093/aje/kwj078
Advance Access publication January 27, 2006

Original Contribution

The Effect of Ozone and PM_{10} on Hospital Admissions for Pneumonia and Chronic Obstructive Pulmonary Disease: A National Multicity Study

Mercedes Medina-Ramón[1], Antonella Zanobetti[1], and Joel Schwartz[1,2]

[1] Department of Environmental Health, Harvard School of Public Health, Boston, MA.
[2] Channing Laboratory, Brigham and Women's Hospital, Department of Medicine, Harvard Medical School, Boston, MA.

Received for publication August 18, 2005; accepted for publication October 27, 2005.

A case-crossover study was conducted in 36 US cities to evaluate the effect of ozone and particulate matter with an aerodynamic diameter of $\leq$10 μm (PM_{10}) on respiratory hospital admissions and to identify which city characteristics may explain the heterogeneity in risk estimates. Respiratory hospital admissions and air pollution data were obtained for 1986–1999. In a meta-analysis based on the city-specific regression models, several city characteristics were evaluated as effect modifiers. During the warm season, the 2-day cumulative effect of a 5-ppb increase in ozone was a 0.27% (95% confidence interval (CI): 0.08, 0.47) increase in chronic obstructive pulmonary disease admissions and a 0.41% (95% CI: 0.26, 0.57) increase in pneumonia admissions. Similarly, a 10-$\mu g/m^3$ increase in PM_{10} during the warm season resulted in a 1.47% (95% CI: 0.93, 2.01) increase in chronic obstructive pulmonary disease at lag 1 and a 0.84% (95% CI: 0.50, 1.19) increase in pneumonia at lag 0. Percentage of households with central air conditioning reduced the effect of air pollution, and variability of summer apparent temperature reduced the effect of ozone on chronic obstructive pulmonary disease. The study confirmed, in a large sample of cities, that exposure to ozone and PM_{10} is associated with respiratory hospital admissions and provided evidence that the effect of air pollution is modified by certain city characteristics.

air pollution; effect modifiers (epidemiology); ozone; pneumonia; pulmonary disease, chronic obstructive

Abbreviations: CI, confidence interval; COPD, chronic obstructive pulmonary disease; PM_{10}, particulate matter with an aerodynamic diameter of $\leq$10 μm; $PM_{2.5}$, particulate matter with an aerodynamic diameter of $\leq$2.5 μm.

Air pollution has been associated with hospital admissions for respiratory disease in cities all over the world (1–7). The most common and consistent associations have been found with particulate matter and tropospheric ozone (4). The magnitude of the effect of these pollutants, however, has differed substantially across locations. Moreover, many studies have examined all respiratory admissions, possibly combining outcomes with different sensitivities to air pollution and different lags between exposure and hospitalization. In addition, the number of cities examined in individual studies of respiratory admissions has generally been modest, particularly for ozone, and a large national sample would avoid selection bias, especially in light of evidence for heterogeneity in results across individual cities.

Because of limited numbers of locations, few studies have addressed the issue of whether the observed variability in exposure-effect relations can be explained by differences in meteorology, pollution sources, or socioeconomic characteristics of the cities. A study conducted in 14 US cities did not find evidence of modification by sociodemographic characteristics of the association between particulate matter with an aerodynamic diameter of $\leq$10 μm (PM_{10}) and hospital admissions (8). A subsequent analysis using the same data found that the proportion of traffic-related particles in PM_{10} modified the effect of PM_{10} on

Correspondence to Dr. Mercedes Medina-Ramón, Department of Environmental Health, Harvard School of Public Health, 401 Park Drive, Landmark Center, Suite 415 West, Boston, MA 02215 (e-mail: mmedinar@hsph.harvard.edu).

hospital admissions for cardiovascular disease, but results were inconclusive for respiratory admissions (9). This study also found a stronger effect of PM_{10} on chronic obstructive pulmonary disease (COPD) admissions with decreasing proportion of central air conditioning, and similar results, although only marginally significant, were found for pneumonia admissions.

These studies had limited statistical power because they included a relatively small number of cities. In addition, they did not address modifiers of the association between ozone exposure and respiratory hospital admissions. We therefore conducted a large, multicity study in 36 US cities to evaluate the effect of daily PM_{10} and ozone concentrations on hospital admissions for COPD and for pneumonia and to assess whether the heterogeneity in the effect estimates across cities may be explained by differences in city characteristics such as meteorology, pollution sources, or socioeconomic factors.

MATERIALS AND METHODS

Study design

We conducted a case-crossover analysis using hospital admissions and air pollution data from 36 US cities during the period 1986–1999. We first selected cities that monitored PM_{10} daily and subsequently expanded the sample to include other large cities covering all regions of the United States. The cities selected were Albuquerque, New Mexico; Atlanta, Georgia; Baltimore, Maryland; Birmingham, Alabama; Boston, Massachusetts; Boulder, Colorado; Canton, Ohio; Chicago, Illinois; Cincinnati, Ohio; Cleveland, Ohio; Colorado Springs, Colorado; Columbus, Ohio; Denver, Colorado; Detroit, Michigan; Honolulu, Hawaii; Houston, Texas; Jersey City, New Jersey; Los Angeles, California; Minneapolis, Minnesota; Nashville, Tennessee; New Haven, Connecticut; New York City, New York; Palm Beach, Florida; Philadelphia, Pennsylvania; Pittsburgh, Pennsylvania; Provo, Utah; Sacramento, California; Salt Lake City, Utah; San Diego, California; San Francisco, California; Seattle, Washington; Steubenville, Ohio; St. Louis, Missouri; Spokane, Washington; Washington, DC; and Youngstown, Ohio.

The case-crossover design is a variant of the matched case-control design in which a case subject becomes a control subject on days when no event (hospital admission) occurs (10). By using control days close in time to the event day, there is no confounding by slowly varying personal characteristics since each subject is the perfect match for himself or herself. Bateson and Schwartz (11, 12) demonstrated that, by using such a matching scheme, even very strong seasonal confounding of exposure can be removed. If, in addition, as suggested by Levy et al. (13), we apply a time-stratified approach to choose the control days, a subtle selection bias can be avoided. A simulation study has shown that such an approach gives both unbiased estimates of effects and unbiased coverage probabilities (14). We followed this approach in our study by choosing control days only within the same month of the same year when the admission occurred (refer to the Statistical Analyses section of the text for more details on the specific selection criteria for days within that month).

Hospital admissions data

We extracted data on hospital admissions from the US Health Care Financing Administration (Medicare) billing records for the period 1986–1999. The Medicare system provides hospital coverage for all US citizens aged 65 years or older. The system includes data on type of admission, primary and secondary causes of admission, and other personal characteristics. Using this information, we selected for analyses those persons who had been admitted to the hospital on an emergency or urgent basis with a primary diagnosis of COPD (*International Classification of Diseases*, Ninth Revision: codes 490–496, except code 493) or pneumonia (*International Classification of Diseases*, Ninth Revision: codes 480–487).

Environmental data

We obtained air pollution data from the US Environmental Protection Agency's Aerometric Retrieval System (15). We estimated daily mean concentrations of ozone (8-hour) and PM_{10} (24-hour) for each city by using an algorithm that averaged levels reported by multiple monitoring locations (16). All cities except Minneapolis had daily measurements for ozone during the warm season (May–September), but only 16 had complete ozone measurements during the cold season (October–April). For all cities, PM_{10} levels were available throughout the year, although frequency of measurements varied across cities and within a city, with measurements typically made every 2, 3, or 6 days.

For each city, we obtained daily mean temperature and relative humidity from the nearest National Weather Service surface station (EarthInfo Inc., Boulder, Colorado). We used this information to calculate the apparent temperature, a composite index of perceived air temperature at a given humidity, previously used to control for weather in air pollution studies (17–20).

City characteristics

For each city, we calculated the mean and variance of the daily summer (June–August) apparent temperature by using the data described above. We calculated the percentage of people aged 65 years or older living in poverty by using data from the 1990 US Census. We calculated the percentage of households with central air conditioning by using data from the American Housing Survey of the US Census Bureau (21) for the period 1994–2002. We calculated the average annual mortality rate for emphysema among people aged 65 years or older by using data from the National Center for Health Statistics during 1989–2000. We took the latter as an indication of the smoking history of the population. Finally, we calculated the percentage of ambient PM_{10} from traffic (highway vehicles) by using data from the National Emission Trends 1996 (NET96) of the Environmental Protection Agency (22).

Statistical analyses

In the first stage of the analyses, we analyzed the association between exposure to air pollution and hospital admissions (for COPD and for pneumonia) by using city-specific conditional logistic regression models (the PROC PHREG procedure in SAS version 8.2 software, 2001; SAS Institute, Inc., Cary, North Carolina). We fitted separate models for ozone and PM_{10} exposure. For each hospitalization, we selected control days within the same month of the same year, leaving at least 2 days between each control day to minimize serial correlation. In all analyses, we controlled for day of the week and weather—the latter by using one cubic regression spline for the same day's apparent temperature and another for the previous day's apparent temperature.

For the ozone analysis, we examined the effect of exposure on the same day (lag 0) and on the day before (lag 1) admission. For each city, we first fitted a model including lag 0 and lag 1, then calculated the cumulative risk estimate for ozone exposure by summing the estimates from lag 0 and lag 1. We computed the overall standard error (SE) of the cumulative estimate as $SE = \text{sqrt}[\text{var}(\text{lag } 0) + \text{var}(\text{lag } 1) + 2 \times \text{cov}(\text{lag } 0, \text{lag } 1)]$.

Because PM_{10} was predominantly measured during nonconsecutive days, we assessed the effect of exposure to PM_{10} at lag 0 and lag 1 in separate models. We repeated the analyses of ozone and PM_{10} by examining separate effects for exposure in the warm season and in the cold season.

As a sensitivity analysis, we tested the use of an alternative matching scheme by selecting control days within the same month of the same year of the event and matching on apparent temperature (same rounded degrees Centigrade). In this analysis, we included in all models a cubic spline for the previous day's apparent temperature and indicator variables for day of the week. These models, by matching on temperature and month, control for potentially nonlinear temperature effects and for any interaction between temperature and month of the year (18). To study the effect of ozone exposure, we additionally tested a matching scheme that selected control days within the same month of the same year of the event and matched on day of the week. In this instance, models included a cubic spline for apparent temperature on the same day and another cubic spline for the previous day's apparent temperature. Because of the irregular sampling scheme for PM_{10}, we could not follow this approach for PM_{10}.

In the second stage of the analyses, we combined the city-specific results in a meta-analysis by using restricted maximum likelihood random-effects models (REML in Stata version 8 software; Stata Corporation, College Station, Texas) (23). After estimating the overall effect of ozone and PM_{10} on hospital admissions, we assessed the potential for effect modification of several city characteristics by including them (one at a time) as covariates in the meta-regression models. Then, we used the estimated model coefficients to predict the effect of air pollution on hospital admissions at the 25th and the 75th percentiles of the distribution of each city characteristic. A significant difference between these two predicted values indicates that the city characteristic modifies the effect of air pollution on hospital admissions, that is, the existence of an interaction between air pollution and the city characteristic.

RESULTS

Our analyses included 578,006 COPD admissions and 1,384,813 pneumonia admissions. Table 1 shows the counts of hospital admissions and describes the main environmental variables for each city. Ozone levels were higher in the warm season (average across all cities, 45.8 ppb (standard deviation, 9.2)) than in the cold season (27.6 ppb (standard deviation, 6.3)). PM_{10} levels were similar during both seasons, with an average concentration across all cities of 30.4 $\mu g/m^3$ (standard deviation, 5.1). Los Angeles had the highest average levels of both ozone and PM_{10}.

Table 2 shows the results of the meta-analysis across all cities based on the city-specific models in which the baseline matching scheme was used. Overall, during the warm season, there was an increase in hospital admissions associated with ozone exposure, specifically with such exposure on the day before. The 2-day cumulative effect of a 5-ppb increase in 8-hour ozone levels was a 0.27 percent (95 percent confidence interval (CI): 0.08, 0.47) increase in COPD admissions and a 0.41 percent (95 percent CI: 0.26, 0.57) increase in pneumonia admissions. The distribution of the city-specific estimates for the warm season is shown in figure 1, with the extreme values corresponding to those estimates with larger standard errors. Results from the meta-analysis showed that hospital admissions during the cold season decreased with increasing ozone concentrations, which resulted in a weak positive association for the full-year period. Results were very similar when other matching schemes were used. The increases in COPD and pneumonia admissions during the warm season, for instance, were 0.26 percent (95 percent CI: −0.05, 0.57) and 0.32 percent (95 percent CI: 0.12, 0.52), respectively, when additionally matching on temperature, and 0.30 percent (95 percent CI: 0.10, 0.51) and 0.48 percent (95 percent CI: 0.30, 0.67), respectively, when matching on day of the week. After we restricted the analysis to those days for which PM_{10} measurements were available, adjustment for PM_{10} did not substantially modify the results (not shown).

As shown in table 2, there was also an overall increase in respiratory hospital admissions associated with PM_{10} concentrations throughout the year, with a more marked effect during the warm season. The between-city variability in the estimates for that season is presented in figure 1. Results from the meta-analysis showed that, for COPD, the larger increase during the warm season (1.47 percent for every 10-$\mu g/m^3$ increase in PM_{10}) was associated with PM_{10} exposure on the day before (lag 1); for pneumonia, the main increase (0.84 percent) occurred on the same day of exposure (lag 0). Repeating the analyses for the warm season matching also for apparent temperature led to similar results, with an increase of 1.30 percent (95 percent CI: 0.58, 2.02) in COPD admissions associated with PM_{10} at lag 1 and of 0.94 percent (95 percent CI: 0.41, 1.46) in pneumonia admissions associated with PM_{10} at lag 0. The associations remained unaltered when analyses were repeated adjusting for ozone (results not shown).

TABLE 1. Environmental variables and respiratory hospital admissions in 36 US cities during 1986–1999

City, state	Mean (SD*) ozone level (ppb)		Mean (SD) PM_{10}* level ($\mu g/m^3$)	Mean (SD) apparent temperature (°C)	Total population aged ≥65 years (no.)	COPD* admissions (no.)	Pneumonia admissions (no.)
	Warm season	Cold season					
Albuquerque, New Mexico	50.5 (9.3)	34.5 (10.2)	27.9 (16.5)	12.2 (8.9)	50,379	3,115	9,035
Atlanta, Georgia	55.9 (21.4)		33.0 (16.4)	17.1 (10.2)	155,955	15,503	36,488
Baltimore, Maryland	52.3 (20.2)	26.8 (13.0)	32.4 (17.1)	13.0 (11.1)	197,438	19,950	40,858
Birmingham, Alabama	49.7 (17.0)		36.1 (21.0)	17.4 (10.5)	119,809	13,134	33,011
Boston, Massachusetts	42.3 (17.8)	28.3 (11.3)	25.4 (11.7)	10.0 (10.3)	342,322	34,700	88,936
Boulder, Colorado	51.3 (14.2)		24.2 (15.5)	8.5 (9.7)	17,048	1,678	3,427
Canton, Ohio	52.6 (17.8)		26.1 (12.6)	9.3 (11.2)	53,216	7,534	12,965
Chicago, Illinois	40.0 (16.1)	22.7 (9.8)	33.6 (17.4)	9.5 (11.9)	631,826	49,581	142,576
Cincinnati, Ohio	50.0 (17.8)		32.2 (15.6)	11.9 (11.5)	115,000	10,797	33,323
Cleveland, Ohio	44.6 (17.6)		37.1 (19.1)	9.8 (11.3)	220,659	29,947	50,262
Colorado Springs, Colorado	45.5 (11.3)	30.4 (11.6)	23.3 (13.4)	7.8 (9.0)	31,674	2,497	5,729
Columbus, Ohio	49.8 (18.1)		30.5 (14.6)	11.1 (11.5)	92,485	12,571	21,900
Denver, Colorado	44.0 (14.0)	22.1 (12.7)	33.2 (18.8)	8.5 (9.7)	64,152	4,219	11,820
Detroit, Michigan	41.7 (17.2)		33.7 (19.7)	9.3 (11.5)	263,997	5,751	12,393
Honolulu, Hawaii	15.0 (8.4)		15.9 (6.2)	27.5 (2.9)	91,485	28,404	57,682
Houston, Texas	44.9 (22.1)	32.9 (17.1)	30.3 (16.0)	22.2 (10.1)	196,474	3,798	14,463
Jersey City, New Jersey	50.3 (23.4)		32.2 (17.0)	12.4 (11.1)	70,014	18,863	41,754
Los Angeles, California	63.0 (23.4)	31.4 (20.2)	44.0 (19.3)	16.5 (4.3)	855,666	9,211	12,645
Minneapolis, Minnesota			27.3 (14.6)	7.4 (12.5)	175,854	63,316	174,241
Nashville, Tennessee	44.9 (16.8)	23.9 (13.5)	32.2 (14.9)	15.5 (11.3)	59,235	9,805	26,923
New Haven, Connecticut	45.4 (19.5)		26.0 (16.1)	9.6 (10.8)	117,863	5,962	14,719
New York City, New York	41.0 (19.5)	19.7 (10.0)	28.9 (13.9)	12.5 (10.8)	952,731	8,082	22,954
Palm Beach, Florida	28.6 (12.7)	33.7 (12.0)	20.0 (8.1)	27.1 (6.3)	210,389	70,181	187,043
Philadelphia, Pennsylvania	47.8 (21.0)	23.0 (13.0)	32.1 (15.8)	12.9 (11.1)	241,206	10,626	22,170
Pittsburgh, Pennsylvania	48.4 (19.9)		30.3 (20.0)	10.3 (10.9)	232,505	26,604	47,126
Provo, Utah	54.6 (10.9)		35.1 (26.7)	9.6 (10.4)	18,429	33,408	52,148
Sacramento, California	55.6 (15.7)	32.7 (14.2)	31.1 (19.7)	14.4 (7.0)	109,674	718	4,081
Salt Lake City, Utah	54.0 (12.5)		35.7 (23.9)	9.6 (10.4)	61,079	8,680	21,840
San Diego, California	47.6 (12.1)	40.4 (15.2)	33.3 (13.1)	17.0 (4.4)	272,348	2,090	9,348
San Francisco, California	22.8 (8.1)	19.3 (10.2)	27.7 (16.8)	12.6 (3.8)	105,263	17,632	43,446
Seattle, Washington	35.0 (14.2)		28.8 (18.6)	9.5 (6.3)	167,328	4,711	18,139
Steubenville, Ohio	46.1 (17.3)		34.7 (19.9)	10.3 (10.9)	23,878	9,334	23,732
St. Louis, Missouri	48.4 (17.1)		27.7 (12.7)	13.7 (12.3)	214,492	4,039	9,412
Spokane, Washington	44.6 (10.4)		32.2 (28.3)	6.5 (9.0)	47,877	5,633	8,976
Washington, DC	48.4 (20.2)	20.1 (12.3)	27.7 (13.4)	14.2 (11.2)	77,672	17,665	54,386
Youngstown, Ohio	47.1 (20.3)		31.2 (15.6)	8.9 (11.0)	61,122	8,267	14,862

* SD, standard deviation; PM_{10}, particulate matter with an aerodynamic diameter of ≤10 μm; COPD, chronic obstructive pulmonary disease.

We further examined the potential for effect modification of the city characteristics presented in table 3. In general, all characteristics varied from city to city. The proportion of households with central air conditioning was especially variable, ranging from 6.2 percent in Seattle to 93.3 percent in Houston. Central air conditioning and poverty were more common in those cities with a higher summer apparent temperature (Spearman's $r = 0.74$ and $r = 0.52$, respectively) but were unrelated to the variance of summer apparent temperature ($r = 0.07$ and $r = 0.23$, respectively).

The association between hospital admissions and air pollution during the warm season was modified by some of the city characteristics (table 4). Overall, in cities with a large proportion of households with central air conditioning, the effect of air pollution on hospital admissions was milder, especially for pneumonia admissions. For instance, in a city

TABLE 2. Percentage change in respiratory hospital admissions associated with air pollution exposure across 36 US cities during 1986–1999*

	COPD†						Pneumonia					
	Lag 0		Lag 1		2-day cumulative estimates		Lag 0		Lag 1		2-day cumulative estimates	
	%	95% CI†	%	95% CI	%	95% CI	%	95% CI	%	95% CI	%	95% CI
Ozone‡	−0.32	−0.49, −0.15	0.33	0.19, 0.47	0.04	−0.13, 0.20	−0.23	−0.32, −0.13	0.21	0.11, 0.30	0.30	−0.12, 0.08
Warm season	−0.25	−0.46, −0.04	0.48	0.30, 0.66	0.27	0.08, 0.47	0.01	−0.12, 0.13	0.42	0.29, 0.55	0.41	0.26, 0.57
Cold season§	−0.48	−0.75, −0.21	0.14	−0.13, 0.42	−0.31	−0.61, −0.01	−0.61	−0.85, −0.36	−0.17	−0.34, −0.004	−0.83	−1.13, −0.53
PM_{10}¶	0.29	−0.01, 0.58	0.59	0.30, 0.88			0.45	0.27, 0.64	0.26	0.01, 0.52		
Warm season	0.81	0.22, 1.41	1.47	0.93, 2.01			0.84	0.50, 1.19	0.79	0.45, 1.13		
Cold season	0.06	−0.40, 0.51	0.10	−0.30, 0.49			0.30	0.07, 0.53	0.14	−0.17, 0.45		

* Estimates are presented as percentage increase in hospital admissions associated with a 5-ppb increase in ozone or a 10-μg/m^3 increase in particulate matter with an aerodynamic diameter of ≤10 μm (PM_{10}).
† COPD, chronic obstructive pulmonary disease; CI, confidence interval.
‡ Estimates for ozone exposure at lag 0 and lag 1 were obtained by including both variables in the same model.
§ Estimates for ozone exposure during the cold season are based on 16 cities.
¶ Estimates for PM_{10} exposure at lag 0 and lag 1 were obtained by using separate models for each lag.

with a low proportion of central air conditioning (in the 25th percentile of the distribution), the estimated percentage increase in pneumonia admissions for every 10-μg/m^3 increase in PM_{10} was 1.47 percent; whereas, in a city with a high proportion of central air conditioning (in the 75th percentile), the change in pneumonia admissions was negligible (−0.11 percent). The effect of air pollution was consistently lower for those cities with a higher summer apparent temperature, although the interaction was statistically significant for the association between PM_{10} and pneumonia admissions only and disappeared after adjusting for percentage of central air conditioning ($p = 0.96$, results not shown). Similarly, the milder effect of PM_{10} on cities with a large proportion of people living in poverty disappeared after adjusting for percentage of central air conditioning ($p = 0.38$, results not shown). The variability of summer apparent temperature modified the effect of ozone on COPD (about a fourfold decrease when the 25th percentile was compared with the 75th percentile) and remained the same after adjustment for other city characteristics. When we examined modification of the association between PM_{10} and hospital admissions for the entire year, we obtained results similar to the ones presented in table 4 but weaker associations (results not shown).

DISCUSSION

In a large, multicity study, we found effects of ozone and PM_{10} on hospital admissions for COPD and pneumonia and identified several city characteristics as effect modifiers. We found increased risks of COPD and pneumonia admissions associated with ambient ozone and PM_{10} levels, predominantly during the warm season. The proportion of households with central air conditioning was the most important effect modifier in that season. The variance of summer apparent temperature was associated with a milder effect of ozone on COPD.

Most of the literature about ozone effects on respiratory hospital admissions is based on data from single cities (6). One of the strengths of our study is that we included a large number of cities across the United States involving great diversity in weather, geography, and other characteristics that enabled us to analyze how these characteristics may modify the effect of air pollution. In addition, we analyzed more years of follow-up than previous multicity studies on the respiratory effects of ozone (3, 7, 24) and PM_{10} (25, 26). These two circumstances provided us with a larger sample size and more stable estimates than prior investigations offered.

In our study, we found that the risk of daily hospital admissions for COPD and for pneumonia increased with ozone concentration during the warm season but not during the cold season. Consistently, epidemiologic studies conducted in the United States and in other industrialized countries have also found an increased risk of both respiratory hospital admissions (3, 27) and total mortality (18, 28) associated with ozone exposure during the warm season only. Differences in the effect of ozone during these two seasons could be explained by the higher ozone concentrations and the larger amount of time spent outdoors during the warm

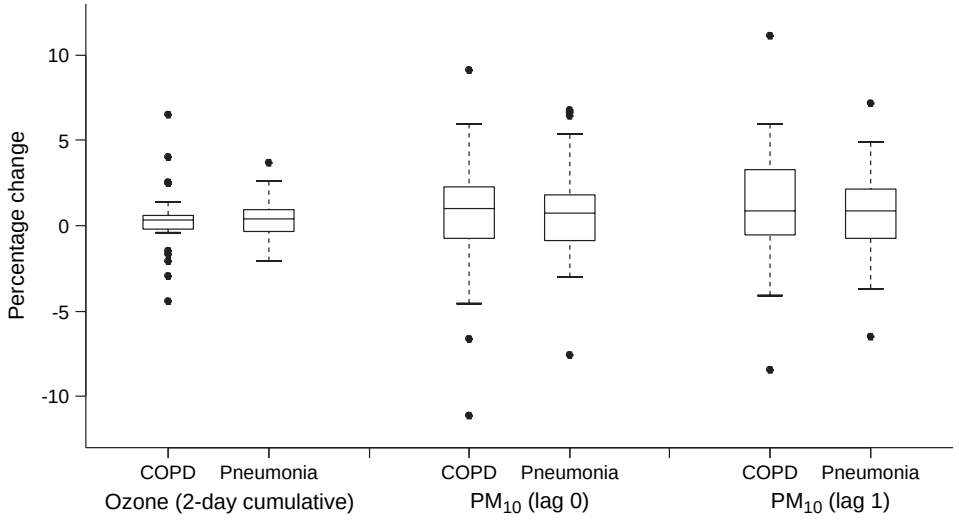

FIGURE 1. Distribution of the city-specific estimates of the percentage change in respiratory hospital admissions associated with air pollution during the warm season in 36 US cities during 1986–1999. Estimates are presented as the percentage increase in hospital admissions associated with a 5-ppb increase in ozone or a 10-μg/m^3 increase in particulate matter with an aerodynamic diameter of ≤10 μm (PM_{10}). COPD, chronic obstructive pulmonary disease.

season (29). In addition, ozone is a highly reactive gas whose indoor concentrations are extremely low in buildings with low ventilation (closed windows, etc.), which occurs more often in the winter. In the summer, open windows can result in some indoor exposure as well, and this exposure difference could also partially explain why positive effects are seen during the warm season only.

We also found an increased risk of COPD and pneumonia admissions associated with PM_{10} levels, which closely agrees with findings by Zanobetti et al. (2) using data from 10 US cities and also with results from the APHEA-2 study in eight European cities (26). The effect of PM_{10} on respiratory admissions was evident throughout the year but was stronger during the warm season. Because PM_{10} levels are usually similar during the warm and cold seasons, few studies have examined the effect of PM_{10} separately for these two seasons. A stronger effect during the warm season may be related to an increase in individual exposure (i.e., more time spent outdoors, higher ventilation rates, etc.) rather than to an overall increase in the outdoor ambient concentration. These results are consistent with those of Peng et al. (30), who recently reported that the effect of PM_{10} on mortality was higher in the summer. In our study, exposure to PM_{10} seemed to have an earlier effect on pneumonia admissions, occurring predominantly on the same day of exposure, than on COPD admissions, occurring predominantly 1 day after the exposure. An earlier effect of PM_{10} on pneumonia than on COPD was also observed in a mortality study of 20 US cities (31) and could be due to differences in the biologic mechanisms involved in the aggravation of these two respiratory disorders.

The effect of air pollution on respiratory hospital admissions was smaller in those cities with a larger proportion of central air conditioning. In a meta-analysis of 14 US cities, Janssen et al. (9) studied the role of air conditioning as an effect modifier of the relation between PM_{10} and hospital admissions and found a smaller effect for COPD, and possibly pneumonia, in cities with a larger proportion of central air conditioning. Several studies have shown that homes with air conditioning typically have lower exchange rates than homes that use open windows for ventilation (32, 33), suggesting a higher penetration of outdoor pollutants in homes without air conditioning. Therefore, those living in a home with central air conditioning are likely to be less exposed to outdoor air pollutants, resulting in attenuation of the association between ambient air pollution and health effects.

We observed a milder effect of ozone on COPD admissions during the warm season for those cities with a large variability in their summer temperature. Levels of ozone are generally related to temperature (18); thus, cities with a variable summer temperature are expected to also have more variable ozone levels. In our study, the variance of summer temperature was significantly correlated with the variance of ozone levels during the warm season (Spearman's $r = 0.41$). Therefore, a possible explanation for the observed effect modification would be that persons with COPD are more likely to be affected by high ozone concentrations when high levels have been sustained for several consecutive days. However, we did not find a statistically significant effect modification by ozone variability in our study ($p = 0.20$, results not shown), suggesting that there must also be

TABLE 3. City characteristics included in the analysis of effect modification, United States, 1986–1999

City, state	People aged ≥65 years		Daily summer apparent temperature (°C)		Percentage of households with central air conditioning	Percentage of PM_{10}* from traffic
	Percentage living in poverty	Emphysema mortality rate (deaths/100,000)	Mean	Variance		
Albuquerque, New Mexico	10.7	45.8	22.9	6.3		1.0
Atlanta, Georgia	13.7	58.7	29.0	10.5	82.6	2.8
Baltimore, Maryland	13.2	23.5	26.6	22.0	67.3	3.2
Birmingham, Alabama	18.3	29.5	29.5	10.9	70.2	1.5
Boston, Massachusetts	9.6	34.9	22.6	25.0	17.0	2.5
Boulder, Colorado	8.7	46.9	20.0	11.3	6.3	1.7
Canton, Ohio	8.7	49.5	22.6	23.1	29.9	2.3
Chicago, Illinois	11.2	34.3	23.7	29.6	43.2	5.0
Cincinnati, Ohio	11.2	29.3	25.4	20.7	66.2	3.5
Cleveland, Ohio	10.2	33.0	23.3	24.4	39.3	5.5
Colorado Springs, Colorado	8.1	65.5	18.2	10.6	13.4	1.6
Columbus, Ohio	10.3	61.0	24.7	22.7	63.7	3.4
Denver, Colorado	12.7	87.9	20.0	11.3	25.7	3.0
Detroit, Michigan	13.5	40.2	23.2	25.7	41.0	7.5
Honolulu, Hawaii	7.8	25.4	29.8	2.0		2.8
Houston, Texas	15.8	46.9	32.9	6.3	93.3	1.1
Jersey City, New Jersey	15.2	27.9	26.1	23.3	35.1	3.2
Los Angeles, California	9.2	28.4	20.7	6.2	32.1	11.7
Minneapolis, Minnesota	8.0	32.7	22.5	25.1	48.4	3.2
Nashville, Tennessee	14.5	63.9	28.7	14.7	72.2	2.5
New Haven, Connecticut	7.7	17.8	22.9	23.1	23.9	5.6
New York City, New York	16.5	17.2	25.6	22.1	11.1	2.4
Palm Beach, Florida	7.1	35.5	32.9	2.7		2.2
Philadelphia, Pennsylvania	16.3	19.9	26.6	23.5	38.8	3.5
Pittsburgh, Pennsylvania	10.1	34.9	23.2	21.3	33.4	5.0
Provo, Utah	6.7	38.4	22.2	17.4	26.9	2.2
Sacramento, California	6.8	46.3	22.2	13.1	71.7	5.6
Salt Lake City, Utah	7.8	42.0	22.2	17.4	39.7	2.8
San Diego, California	6.3	39.3	21.2	7.5	26.6	3.5
San Francisco, California	9.9	29.5	15.8	4.6	13.2	9.0
Seattle, Washington	7.3	34.7	16.7	12.1	6.2	3.0
Steubenville, Ohio	11.4		23.2	21.3	71.6	1.2
St. Louis, Missouri	10.7	37.5	28.2	24.0	76.5	1.7
Spokane, Washington	10.9	73.8	17.3	20.1	28.2	2.2
Washington DC	17.2	23.4	27.9	21.2	86.7	7.9
Youngstown, Ohio	11.3	43.6	21.8	23.7	22.8	3.0
Median (25th, 75th percentiles)	10.5 (8.0, 13.4)	35.5 (29.3, 46.9)	23.2 (21.9, 26.6)	20.4 (10.6, 23.3)	38.8 (24.8, 68.8)	3.0 (2.2, 4.6)

* PM_{10}, particulate matter with an aerodynamic diameter of ≤ 10 μm.

other explanations for the interaction between ozone and variance of summer temperature.

Our results suggest that the observed interaction between PM_{10} and both the percentage of poverty and the mean summer apparent temperature may be explained by the high correlation of these variables with the proportion of central air conditioning rather than effect modification by the variables themselves. Although air pollution may affect different sociodemographic groups in different ways, in a study conducted in 14 US cities, the association between PM_{10}

TABLE 4. Modification by city characteristics of the effect of air pollution on hospital admissions in 36 US cities during 1986–1999: comparison of the predicted percentage change in hospital admissions at the 25th and the 75th percentiles of the effect-modifier distribution†

	Ozone exposure in the warm season‡							
	Change in COPD§ admissions at the				Change in pneumonia admissions at the			
	25th percentile		75th percentile		25th percentile		75th percentile	
	%	95% CI§	%	95% CI	%	95% CI	%	95% CI
Percentage of people aged ≥65 years living in poverty	0.38	0.06, 0.70	0.24	0.04, 0.45	0.50	0.24, 0.76	0.38	0.21, 0.55
Emphysema mortality rate for people aged ≥65 years (deaths/100,000)	0.28	0.08, 0.49	0.20	−0.10, 0.49	0.47	0.33, 0.61	0.32	0.12, 0.53
Daily summer apparent temperature (°C)								
Mean	0.29	0.04, 0.54	0.26	0.05, 0.48	0.51	0.31, 0.72	0.36	0.19, 0.53
Variance	0.45*	0.20, 0.70	0.12*	−0.12, 0.36	0.42	0.21, 0.63	0.40	0.21, 0.59
Percentage of households with central air conditioning	0.29	0.04, 0.53	0.23	−0.05, 0.51	0.54*	0.38, 0.70	0.30*	0.10, 0.49
	PM_{10} exposure in the warm season¶							
	Change in COPD admissions at the				Change in pneumonia admissions at the			
	25th percentile		75th percentile		25th percentile		75th percentile	
	%	95% CI	%	95% CI	%	95% CI	%	95% CI
Percentage of people aged ≥65 years living in poverty	1.61	0.65, 2.58	1.40	0.69, 2.11	1.37*	0.77, 1.98	0.52*	0.06, 0.98
Emphysema mortality rate for people aged ≥65 years (deaths/100,000)	1.78**	1.10, 2.46	1.03**	0.30, 1.77	0.91	0.49, 1.32	0.85	0.39, 1.31
Daily summer apparent temperature (°C)								
Mean	1.56	0.91, 2.22	1.33	0.52, 2.13	1.13*	0.71, 1.54	0.37*	−0.15, 0.88
Variance	0.96	−0.27, 2.19	1.53	0.95, 2.12	1.07	0.33, 1.80	0.84	0.50, 1.19
Percentage of households with central air conditioning	1.74	0.92, 2.55	1.07	0.03, 2.12	1.47*	0.94, 2.00	−0.11*	−0.79, 0.57
Percentage of PM_{10} from traffic	1.37	0.53, 2.20	1.47	0.93, 2.00	0.53	−0.01, 1.06	0.83	0.49, 1.18

* Two-sided $p < 0.05$ in the meta-regression model; **two-sided $p < 0.1$ in the meta-regression model.

† Estimates are presented as percentage increase in hospital admissions associated with a 5-ppb increase in ozone or a 10-μg/m^3 increase in particulate matter with an aerodynamic diameter of ≤10 μm (PM_{10}).

‡ Modification of the association between ozone during the warm season and hospital admissions was examined by using the 2-day cumulative-effect models.

§ COPD, chronic obstructive pulmonary disease; CI, confidence interval.

¶ Modification of the association between PM_{10} during the warm season and hospital admissions was examined by using the lag 1 model for COPD admissions and the lag 0 model for pneumonia admissions.

and respiratory hospital admissions was not modified by the percentage of poverty or by the percentage of non-White population (8). However, both the latter study and our study used county-level data, which may be too ecologic to be meaningful given that variation in socioeconomic status may be larger within a county than between counties.

In this study, the percentage of PM_{10} from traffic did not modify the risk of respiratory admissions due to PM_{10}. Two different studies in the United States showed that PM_{10} from traffic (31) and particulate matter with an aerodynamic diameter of ≤2.5 μm ($PM_{2.5}$) from mobile sources (34) were associated with a higher mortality risk than particulate matter from other sources. However, one of these studies (34) looked at cause-specific mortality and found no adverse effects of $PM_{2.5}$ from mobile sources for deaths due to COPD or pneumonia. In a morbidity study in 14 US cities, a higher proportion of PM_{10} from traffic was marginally significantly associated with a stronger effect of PM_{10} on pneumonia admissions but not on COPD admissions (9).

The mechanisms behind the adverse respiratory effects of exposure to ozone and PM_{10} are unclear. Some authors have suggested that air pollution may act as an irritant and induce defensive responses in the airways, such as increased mucus secretion and increased bronchial hyperreactivity (35). Both ozone (36) and PM_{10} (37) are potent oxidants that have been shown to produce free radicals and oxidative stress on lung cells. Experimental chamber studies have shown

decrements in forced expiratory volume in 1 second (FEV_1) after exposure to ozone (38), but large interindividual differences have been observed in the responsiveness of both healthy subjects and those with COPD (27). Animal studies have shown an increased vulnerability to PM_{10} in animals with cardiopulmonary disease (39) and exacerbations of ongoing pneumococcal infection after exposure to concentrated ambient $PM_{2.5}$ (40). Exposure to concentrated air particles has also been shown in vivo to increase reactive oxygen species in the lung (41).

The results presented here are unlikely to be due to inadequate control for weather and temporal trends, given that the results from the sensitivity analysis using alternative matching schemes (including control days matched on temperature) showed very similar associations. Confounding by individual characteristics is also unlikely because case-crossover sampling matches perfectly on individual characteristics (10–12). In our study, we did not address confounding by other air pollutants because of previous evidence that the effect of PM_{10} (2) and ozone (3) on respiratory hospital admissions remains practically unaltered after adjusting for other gaseous pollutants. A limitation of our study is that we used ambient air pollution as a surrogate for personal exposure, which may have resulted in a measurement error. Nevertheless, a recent article suggested that this measurement error would generally tend to bias estimates downward (25). Because of the irregular sampling scheme for PM_{10}, we could not assess the cumulative effect of PM_{10} exposure, which may have led to either an overestimation or an underestimation of the risk estimates for each lag. Finally, although the emission estimates from the Environmental Protection Agency should be a reasonable indicator of the actual composition of ambient PM_{10} (9), they may have changed throughout the study period. The same is applicable to data on the percentage of central air conditioning, which was estimated by using data from a population sample during several different years.

In summary, our study confirmed, in a considerably larger sample of cities than, to our knowledge, has been previously examined, that short-term increases in PM_{10} and ozone ambient concentrations are related to hospital admissions for COPD and pneumonia, especially during the warm season. Our findings suggest that some city characteristics modify the effect of air pollution on respiratory hospital admissions. In particular, we found evidence that use of central air conditioning decreases the effect of air pollution and that variability of summer apparent temperature decreases the effect of ozone on COPD. On the other hand, we did not find evidence of a higher toxicity of PM_{10} from traffic as other studies observed for cardiovascular diseases (9, 34).

ACKNOWLEDGMENTS

This study was funded by Environmental Protection Agency grant R-82735301-7 and National Institute of Environmental Health Sciences grant EH-0002.

Conflict of interest: none declared.

REFERENCES

1. Pope CA 3rd, Dockery DW, Schwartz J. Review of epidemiological evidence of health effects of particulate air pollution. Inhal Toxicol 1995;7:1–18.
2. Zanobetti A, Schwartz J, Dockery DW. Airborne particles are a risk factor for hospital admissions for heart and lung disease. Environ Health Perspect 2000;108:1071–7.
3. Burnett RT, Brook JR, Yung WT, et al. Association between ozone and hospitalization for respiratory diseases in 16 Canadian cities. Environ Res 1997;72:24–31.
4. Brunekreef B, Holgate ST. Air pollution and health. Lancet 2002;360:1233–42.
5. Health effects of outdoor air pollution. Committee of the Environmental and Occupational Health Assembly of the American Thoracic Society. Am J Respir Crit Care Med 1996;153:3–50.
6. Roth HD, Hwang PM, Li Y. Assessment of recent ozone short-term epidemiologic studies. Inhal Toxicol 2001;13:1–24.
7. Spix C, Anderson HR, Schwartz J, et al. Short-term effects of air pollution on hospital admissions of respiratory diseases in Europe: a quantitative summary of APHEA study results. Air Pollution and Health: a European Approach. Arch Environ Health 1998;53:54–64.
8. Samet JM, Zeger SL, Dominici F, et al. The National Morbidity, Mortality, and Air Pollution Study. Part II: morbidity and mortality from air pollution in the United States. Res Rep Health Eff Inst 2000;94:5–47.
9. Janssen NA, Schwartz J, Zanobetti A, et al. Air conditioning and source-specific particles as modifiers of the effect of PM_{10} on hospital admissions for heart and lung disease. Environ Health Perspect 2002;110:43–9.
10. Maclure M. The case-crossover design: a method for studying transient effects on the risk of acute events. Am J Epidemiol 1991;133:144–53.
11. Bateson TF, Schwartz J. Control for seasonal variation and time trend in case-crossover studies of acute effects of environmental exposures. Epidemiology 1999;10:539–44.
12. Bateson TF, Schwartz J. Selection bias and confounding in case-crossover analyses of environmental time-series data. Epidemiology 2001;12:654–61.
13. Levy D, Lumley T, Sheppard L, et al. Referent selection in case-crossover analyses of acute health effects of air pollution. Epidemiology 2001;12:186–92.
14. Schwartz J, Zanobetti A, Bateson T. Morbidity and mortality among elderly residents of cities with daily PM measurements. In: Revised analyses of time-series studies of air pollution and health. Special report. Boston, MA: Health Effects Institute, 2003:25–58.
15. Nehls GJ Akland GG. Procedures for handling aerometric data. J Air Pollution Control Assoc 1973;23:180–4.
16. Schwartz J. Assessing confounding, effect modification, and thresholds in the association between ambient particles and daily deaths. Environ Health Perspect 2000;108:563–8.
17. Schwartz J. Is the association of airborne particles with daily deaths confounded by gaseous air pollutants? An approach to control by matching. Environ Health Perspect 2004;112:557–61.
18. Schwartz J. How sensitive is the association between ozone and daily deaths to control for temperature? Am J Respir Crit Care Med 2005;171:627–31.
19. Kalkstein LS, Valimont KM. An evaluation of summer discomfort in the United States using a relative climatological index. Bull Am Meteorol Soc 1986;67:842–8.

20. Steadman RG. The assessment of sultriness. Part II: effects of wind, extra radiation and barometric pressure on apparent temperature. J Appl Meteorol 1979;18:874–85.
21. US Census Bureau. The American Housing Survey. Washington, DC: Department of Housing and Urban Development, 1994–2002. (http://www.census.gov/hhes/www/housing/ahs/ahs.html).
22. US Environmental Protection Agency. Emissions and air quality data. County emission summary by source category, 1996 (EI T-3 NET96). (http://www.epa.gov/ttn/naaqs/ozone/areas/state/stindex.htm).
23. Thompson SG, Sharp SJ. Explaining heterogeneity in meta-analysis: a comparison of methods. Stat Med 1999;18:2693–708.
24. Thurston GD, Ito K, Kinney PL, et al. A multi-year study of air pollution and respiratory hospital admissions in three New York State metropolitan areas: results for 1988 and 1989 summers. J Expo Anal Environ Epidemiol 1992;2:429–50.
25. Samet JM, Dominici F, Zeger SL, et al. The National Morbidity, Mortality, and Air Pollution Study. Part I: methods and methodologic issues. Res Rep Health Eff Inst 2000:5–74.
26. Atkinson RW, Anderson HR, Sunyer J, et al. Acute effects of particulate air pollution on respiratory admissions: results from APHEA 2 project. Air Pollution and Health: a European Approach. Am J Respir Crit Care Med 2001;164:1860–6.
27. Anderson HR, Spix C, Medina S, et al. Air pollution and daily admissions for chronic obstructive pulmonary disease in 6 European cities: results from the APHEA project. Eur Respir J 1997;10:1064–71.
28. Samet JM, Dominici F, Curriero FC, et al. Fine particulate air pollution and mortality in 20 U.S. cities, 1987–1994. N Engl J Med 2000;343:1742–9.
29. Burnett RT, Dales RE, Raizenne ME, et al. Effects of low ambient levels of ozone and sulfates on the frequency of respiratory admissions to Ontario hospitals. Environ Res 1994;65:172–94.
30. Peng RD, Dominici F, Pastor-Barriuso R, et al. Seasonal analyses of air pollution and mortality in 100 US cities. Am J Epidemiol 2005;161:585–94.
31. Zeka A, Zanobetti A, Schwartz J. Short-term effects of particulate matter on cause specific mortality: effects of lags and modification by city characteristics. Occup Environ Med 2005;62:718–25.
32. Wallace L. Indoor particles: a review. J Air Waste Manag Assoc 1996;46:98–126.
33. Suh HH, Spengler JD, Koutrakis P. Personal exposures to acid aerosols and ammonia. Environ Sci Technol 1992;26:2507–17.
34. Laden F, Neas LM, Dockery DW, et al. Association of fine particulate matter from different sources with daily mortality in six U.S. cities. Environ Health Perspect 2000;108:941–7.
35. Anderson HR, Atkinson RW, Bremner SA, et al. Particulate air pollution and hospital admissions for cardiorespiratory diseases: are the elderly at greater risk? Eur Respir J Suppl 2003;40:39s–46s.
36. Corradi M, Alinovi R, Goldoni M, et al. Biomarkers of oxidative stress after controlled human exposure to ozone. Toxicol Lett 2002;134:219–25.
37. Gilmour PS, Rahman I, Donaldson K, et al. Histone acetylation regulates epithelial IL-8 release mediated by oxidative stress from environmental particles. Am J Physiol Lung Cell Mol Physiol 2003;284:L533–40.
38. McDonnell WF, Stewart PW, Andreoni S, et al. Prediction of ozone-induced FEV_1 changes. Effects of concentration, duration, and ventilation. Am J Respir Crit Care Med 1997;156:715–22.
39. Costa DL, Dreher KL. Bioavailable transition metals in particulate matter mediate cardiopulmonary injury in healthy and compromised animal models. Environ Health Perspect 1997;105(suppl 5):1053–60.
40. Zelikoff JT, Chen LC, Cohen MD, et al. Effects of inhaled ambient particulate matter on pulmonary antimicrobial immune defense. Inhal Toxicol 2003;15:131–50.
41. Gurgueira SA, Lawrence J, Coull B, et al. Rapid increases in the steady-state concentration of reactive oxygen species in the lungs and heart after particulate air pollution inhalation. Environ Health Perspect 2002;110:749–55.

Ozone, Oxidant Defense Genes, and Risk of Asthma during Adolescence

Talat Islam[1], Rob McConnell[1], W. James Gauderman[1], Ed Avol[1], John M. Peters[1], and Frank D. Gilliland[1]

[1]Department of Preventive Medicine, University of Southern California Keck School of Medicine, Los Angeles, California

Rationale: **Although oxidative stress is a cardinal feature of asthma, the roles of oxidant air pollutants and antioxidant genes heme oxygenase 1 (HMOX-1), catalase (CAT), and manganese superoxide dismutase (MNSOD) in asthma pathogenesis have yet to be determined.**
Objectives: **We hypothesized that the functional polymorphisms of HMOX-1 ($[GT]_n$ repeat), CAT (−262C>T −844C>T), and MNSOD (Ala-9Val) are associated with new-onset asthma, and the effects of these variants vary by exposure to ozone, a potent oxidant air pollutant.**
Methods: **We assessed this hypothesis in a population-based cohort of non-Hispanic (n = 1,125) and Hispanic white (n = 586) children who resided in 12 California communities and who were followed annually for 8 years to ascertain new-onset asthma.**
Measurements and Main Results: **Air pollutants were continuously measured in each of the study communities during the 8 years of study follow-up. HMOX-1 "short" alleles (<23 repeats) were associated with a reduced risk for new-onset asthma among non-Hispanic whites (hazard ratio [HR], 0.64; 95% confidence interval [CI], 0.41–0.99). This protective effect was largest in children residing in low-ozone communities (HR, 0.48; 95% CI, 0.25–0.91) (interaction *P* value = 0.003). Little evidence for an association with HMOX-1 was observed among Hispanic children. In contrast, Hispanic children with a variant of the CAT-262 "T" allele (CT or TT) had an increased risk for asthma (HR, 1.78; *P* value = 0.01). The effects of these polymorphisms were not modified by personal smoking or secondhand-smoke exposure.**
Conclusions: **Functional promoter variants in CAT and HMOX-1 showed ethnicity-specific associations with new-onset asthma. Oxidant gene protection was restricted to children living in low-ozone communities.**

Keywords: asthma; catalase; heme oxygenase-1; MnSOD; oxidative stress; ozone

AT A GLANCE COMMENTARY

Scientific Knowledge on the Subject

The selected genes HMOX-1, CAT, and MNSOD are key candidate genes in the oxidative stress pathway; the latter has been shown to play an important role in asthma development.

What This Study Adds to the Field

We observed differential effect of HMOX-1 and CAT on asthma by ethnicity. Shorter repeat lengths of the HMOX-1 gene is strongly protective for asthma among non-Hispanic whites. This reduced risk was restricted to children living in low-ozone communities.

Airway oxidative stress is a cardinal feature of asthma and is believed to play a central role in its pathogenesis (1, 2). The evidence for a role of oxidative stress in the development of asthma is growing and includes studies showing increased oxidative stress and reduced antioxidant activity among patients with (3) and studies showing that the risk of developing asthma is greater among people with decreased ability to detoxify reactive oxygen species (ROS) (4).

Cells and other structural elements of the airways are continuously exposed to oxidants produced by cellular metabolism and from exogenous sources, including ambient air pollutants such as ozone and tobacco smoke, that lead to ROS production (5). Excess ROS production may produce oxidative stress and can lead to lipid peroxidation and oxidation products that can result in further oxidative stress (6).

Defenses to prevent excess oxidative stress exist in the airways and include small-molecule antioxidants and antioxidant enzymes, such as heme oxygenase (HO), superoxide dismutases (SODs), and catalase (5). HO provides the first line of defense against oxidative stress because it rapidly responds to oxidants (Figure 1). HO-1 is the inducible form of HO and is present in many tissues, including the lung (7). The HO-1 gene (HMOX-1) expression is up-regulated by stressors that increase oxidant burden (7). SOD provides cytoprotection by catalyzing the reaction of super oxides that result from oxidative stress to hydrogen peroxide (H_2O_2) (Figure 1). Manganese SOD (MnSOD), an important mitochondrial SOD, appears to play a role in lung disease (8). ROS detoxification is completed when H_2O_2 is reduced to H_2O by a third enzyme, catalase (Figure 1).

Given the potential importance of oxidant defenses in asthma pathogenesis, genetic variants in these key oxidant defense genes that alter the activity of the encoded enzymes may modulate the risk for new-onset asthma. One common variant in HMOX-1, a $(GT)_n$ dinucleotide tandem repeat of the 5′ flanking region, has been identified, and functional studies have been reported. Functional studies have shown that inducibility of HMOX-1 is inversely related to the number of $(GT)_n$ repeats (9–11). On the basis of the distribution and classification by Chen and colleagues (10), we categorized alleles with 23 or fewer $(GT)_n$ repeats as "short" (S). MNSOD has a commonly studied polymorphism, a T to C substitution in codon 16, that changes the amino acid at −9 position in the signal peptide from valine (Val) to alanine (Ala). This polymorphism (Ala-9Val) has been proposed to affect the enzyme targeting and function (12, 13). Of the several polymorphisms of the catalase gene (CAT), two common polymorphisms in the promoter region have been studied in this study. One, located 262 bp upstream to the transcription site (CAT-262C>T), has been reported to be associated with catalase expression (14–16) and asthma risk (17). Another potentially functional polymorphism, located 844 bp upstream to

(*Received in original form June 13, 2007; accepted in final form November 29, 2007*)

Supported by the NIEHS (grants 5P01ES009581, 5P01ES011627, and 5P30ES007048), the U.S. Environmental Protection Agency (grants R826708-01 and RD831861-01), the National Heart, Lung, and Blood Institute (grants 5R01HL061768 and 5R01HL076647), and the Hastings Foundation.

Correspondence and requests for reprints should be addressed to Frank Gilliland, M.D. Ph.D., Department of Preventive Medicine, USC Keck School of Medicine, 1540 Alcazar Street, CHP 236, Los Angeles, CA 90033. E-mail: gillilan@usc.edu

This article has an online supplement, which is accessible from this issue's table of contents at www.atsjournals.org

Am J Respir Crit Care Med Vol 177. pp 388–395, 2008
Originally Published in Press as DOI: 10.1164/rccm.200706-863OC on November 29, 2007
Internet address: www.atsjournals.org

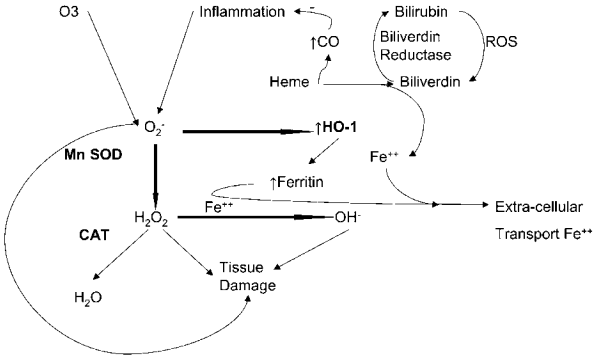

Figure 1. Cellular anti-oxidant defense. Reactive oxygen species (ROS), including O_2^-, are generated within cells in response to exogenous (i.e., O_3) and endogenous (i.e., inflammation) factors. O_2^-, which can directly cause tissue damage, is initially reduced to unstable H_2O_2 by manganese super oxide dismutase (MnSOD). This cytotoxic H_2O_2 is then reduced to H_2O by the action of catalase (CAT). O_2^- also induces heme oxygenase (HMOX-1), leading to catabolism of heme protein to biliverdin with the production of CO and Fe^{2+}. In the presence of biliverdin reductase, biliverdin is reduced to bilirubin, which, after taking up ROS, is then oxidized back to bilirubin. In the presence of biliverdin reductase and ROS, this process continues in a redox cycle, neutralizing cellular ROS.

the transcription site (CAT-844C>T), has been reported to be associated with essential hypertension (18).

On the basis of the role of oxidative stress in asthma and the function of the three genes in antioxidant defenses, we hypothesized that the aforementioned variants in HMOX-1, CAT, and MNSOD are associated with the risk of new-onset asthma during adolescence. Furthermore, we also hypothesized that these polymorphisms affect antioxidant responses to environmental ozone, a common environmental oxidant (Figure 1). To test these hypotheses, we examined health, genetic, and exposure data collected from 1,711 children of Hispanic and non-Hispanic white ethnicity who participated in the Children's Health Study (CHS), a longitudinal study of respiratory health among children in 12 Southern California communities (19, 20). Some of the results have been reported in abstract form (21).

METHODS

Subjects and Materials

Details concerning the design, methods, and characteristics of the CHS cohort have been presented in previous publications (19, 20). Briefly, fourth-, seventh-, and tenth-grade children were enrolled into the study from 12 communities of Southern California (selected primarily based on differential ambient pollution levels). All children were followed annually until high school graduation (*see* details in the online supplement).

Study Cohort

At baseline, parental questionnaire responses were used to classify subjects (n = 6,259) according to lifetime history of asthma and wheeze. Children with any history of asthma (n = 1,018), wheezing (n = 1,098), or missing information for wheeze or asthma history at baseline (n = 369) were excluded from this analysis. We further excluded another 776 children who had less than two follow-up visits, which were needed to assess new-onset asthma. Genetic data were available from 66.9% (n = 2,005) of the remaining eligible 2,998 children. Analyses were restricted to children of Hispanic (n = 576) or non-Hispanic white ethnicity (n = 1,125) due to insufficient representation of other races.

New-Onset Asthma

Children with no prior history of asthma at study entry who subsequently reported physician-diagnosed asthma at annual follow-up were classified as having new-onset asthma. The date of onset was assigned to be the midpoint of the interval between the interview date when asthma diagnosis was first reported and the previous interview date.

Air Pollution Data

Ambient levels of ozone (O_3), nitrogen dioxide (NO_2), particulate matter with an aerodynamic diameter of less than 10 μm (PM_{10}) and 2.5 μm ($PM_{2.5}$), acid vapor, and elemental and organic carbon in each of the 12 communities were measured at air-monitoring sites from 1994 onward. We calculated long-term mean pollutant levels (from 1994 through 2003) to assign exposure to children in each community for use in the statistical analysis. For the purposes of examining genetic susceptibility, communities were classified as "higher" or "lower" by numerically ranking the 12 communities for each ambient pollutant of interest and dividing the list in half. The ozone levels (10 A.M.–6 P.M.) ranged from 46.5 to 64.9 ppb in the higher ozone communities (mean = 55.2 ppb) and 28.6 to 45.5 ppb in the lower ozone communities (mean = 38.4 ppb) (for details *see* the online supplement).

Sociodemographic and Medical History Information

Personal information, such as ethnicity, birth weight, premature birth, maternal smoking during pregnancy, and allergy history, was collected at study entry. Family history of asthma was defined as asthma in any of the biological parents. Ethnicity was defined based on parental response to the baseline questionnaire. "Hispanicity" was based on parental response to the question, "Is your child of Hispanic or Spanish descent?" Parents who reported that their children were white and not of "Hispanic or Spanish" descent were considered non-Hispanic whites. Hispanic whites included children who were of "Hispanic or Spanish" descent and whites. We categorized body mass index (BMI) into age- and sex-specific percentiles based on the Centers for Disease Control and Prevention BMI growth charts using 1-month age intervals (22). Participants with BMI at or above the 85th percentile were classified as overweight/at risk of overweight. This personal information, household and indoor exposures (pets, pests, humidifier use, and household smoking), and air pollution were considered as potential effect modifiers as well as confounders in this analysis (for details *see* the online supplement).

Genotyping

Details of sample collection, processing, and genotyping have been provided earlier (23) and are included in the online supplement. In brief, genomic DNA was extracted from buccal mucosal cells using a Puregene DNA purification kit (Gentra Systems, Minneapolis, MN). Genotyping of MNSOD Ala-9Val (rs4880), CAT-262C>T (rs1001179), and CAT-844C>T (rs769214) was performed using the TaqMan Allelic Discrimination (AD) assay (Applied Biosystems, Foster City, CA). For HMOX-1, the size of $(GT)_n$ repeats in each fluorescence-labeled polymerase chain reaction product was determined with GeneScan Analysis software (Applied Biosystems). Five samples with known HMOX-1 $(GT)_n$ repeats were run in each experiment as positive controls. Genotypes of 12 homozygous samples were confirmed by an automatic sequencing (BigDye version 3.1, 377XL DNA sequencer; Applied Biosystems). In each run, 10% of the samples were randomly selected and used for quality control.

Statistical Methods

On the basis of the distribution and classification by Chen and coworkers (10), we categorized alleles with 23 or fewer $(GT)_n$ repeats as short (S). An association test between the tandem repeat polymorphism and asthma was performed by comparing children with at least one S-allele with those without any S-allele. We also calculated the biallelic average of $(GT)_n$ repeats for each individual as the mean of the number of tandem repeats at both alleles. Using the biallelic average number of repeats, asthma risk in children with the average at or below the 25th percentile value was compared with those greater than the 25th percentile. On the basis of a previous publication, CAT-262C>T and MNSOD Ala-9Val polymorphisms were treated

as dominant genetic models in this analysis (17). The best genetic model for CAT-844C>T and asthma association was selected based on the model with the lowest Aikaike information criterion (AIC) value (24).

We fitted Cox proportional hazard regression models with the time scale defined as the follow-up time to investigate the association between specific genotype and newly diagnosed asthma expressed as hazard ratio (HR) and 95% confidence interval (95% CI). All models were adjusted for community as a fixed effect, and race/ethnicity with sex-specific and age-specific (integer years) baseline hazard. Additional covariates identified *a priori* as potential confounders were considered for inclusion in the model based on whether their inclusion changed the HR by more than 10%. By comparing appropriate models with and without interaction terms using likelihood ratio tests, we assessed heterogeneity of associations among subgroups. Sensitivity analyses were conducted by limiting the case definition to those who reported inhaled medication use.

To assess the effect of ambient air pollution on the relationship between genetic polymorphisms and new-onset asthma, we accounted for the clustering effect of children in communities by fitting a hierarchical two-stage model to these time-dependent data (25) (details in the online supplement). In these models, the community-specific average air pollutant levels were fitted as continuous variables together with the appropriate interaction terms for genes and air pollutants. The communities were treated as random effects in these models. From our initial analysis, we noted that the choice of fixed or random effect of the communities does not substantially affect the estimates for the gene effects (data not shown). To compare the effect of genotype on the risk of new-onset asthma in communities with higher/lower levels of ambient pollutants, we also performed a stratified analysis using Cox proportional hazards models.

To assess whether the results could be replicated in independent groups of children, we performed a stratified analysis for the two independent fourth-grade cohorts of the current study population recruited in 1993 and 1996. These two cohorts have the same age structure, ethnic distributions, and air pollution exposure profiles because they represent the fourth-graders of the same study communities and schools recruited 3 years apart.

All analyses, except the hierarchical two-stage model, were conducted using SAS software version 9 (SAS Institute, Cary, NC). The hierarchical two-stage model was conducted in R-program using COXP procedure (26, 27). All hypothesis testing was conducted using a 0.05 significance level and a two-sided alternative hypothesis. Because the genes were selected based on specific hypotheses defined by biologically relevant antioxidative pathways (Figure 1) and only four functional polymorphisms were tested, the significance levels for the *a priori* hypothesis tests were not adjusted for multiple testing.

RESULTS

Participant Characteristics

Over the follow-up period, 160 new cases of asthma were diagnosed, for an overall crude incidence rate (IR) of 16.6 per 1,000 person-years. The IRs did not differ between non–Hispanic-white (IR = 16.7/1,000 person-years) and Hispanic (IR = 16.6/1,000 person-years) white children. A number of baseline characteristics varied between those with and without genetic data (Tables E3 and E4 of the online supplement); however, except for current maternal smoking and smokers at home, the magnitude of difference between the two groups was too small to affect the overall association. Furthermore, none of those factors were risk factors for newly diagnosed asthma in either of the populations (Tables 1 and 2).

Allele Frequencies

The number of $(GT)_n$ repeats of the HMOX-1 gene showed a bimodal distribution with the two peaks being 23 and 30 repeats in both ethnic groups (*see* Figure E1). Hispanics were more likely to have a higher number of repeats compared with non-Hispanic whites (P value < 0.001) (Table 3). The biallelic average number of repeats was also significantly less among non-Hispanic whites compared with Hispanics (P value < 0.01) (*see* Figure E2). Both polymorphisms of CAT and the Ala-9Val polymorphism of MNSOD were in Hardy-Weinberg equilibrium in both ethnic groups.

TABLE 1. SELECTED CHARACTERISTICS OF NON-HISPANIC WHITE CHILDREN AT STUDY ENTRY

	No Asthma (*n = 1,022*)	Newly Diagnosed Asthma (*n = 103*)	*P* Value*
Age group, yr			
7–9	520 (50.9)	65 (63.1)	0.003
10–11	217 (21.2)	24 (23.3)	
>11	285 (27.9)	14 (13.6)	
Boys	481 (47.1)	38 (36.9)	0.05
Overweight/at risk of overweight	97 (9.5)	16 (15.7)	0.06
Parental history of asthma	149 (15.2)	25 (25.2)	0.01
History of allergy	232 (23.3)	26 (26.0)	0.55
Humidifier use	297 (29.8)	33 (32.7)	0.54
Smokers at home	177 (17.5)	13 (12.7)	0.21
Maternal smoking during pregnancy	175 (17.5)	17 (16.7)	0.83
Maternal smoking at study entry	102 (10.1)	7 (6.9)	0.28
Pests of any kind	851 (86.7)	78 (76.5)	0.009
Pets at home	920 (90.0)	96 (93.2)	0.28
Health insurance	909 (90.3)	93 (90.3)	0.99
Income, $†			
⩽14,999	69 (7.8)	5 (5.1)	0.63
15,000–49,999	347 (39.1)	38 (39.2)	
⩾50,000	470 (53.0)	54 (55.6)	
Highest parental education level†			
Less than high school	56 (5.5)	2 (2.0)	0.21
College	776 (77.0)	85 (83.3)	
Graduate	177 (17.5)	15 (14.7)	
Community ozone status, higher	539 (52.7)	47 (45.6)	0.17
Community PM_{10} status, higher	468 (45.8)	42 (40.8)	0.33

Values indicate the number of children (%) available in the specific group.

* Chi-square P value determining the difference in distribution between children with and without newly diagnosed asthma during follow-up.

† The numbers do not add up to the total due to missing data.

Association between Candidate Genes and Asthma

Among non-Hispanic whites, children with at least one S-allele were at a reduced risk of asthma compared with those who had no S-allele (HR, 0.64; 95% CI, 0.41–0.99) (Table 4). A similar protective effect was observed for children with a biallelic average number of repeats in the lowest quartile (⩽26.5 repeats; HR, 0.56; 95% CI, 0.36–0.89) compared with those with a biallelic average number of repeats greater than 26.5. No statistically significant associations between this tandem repeat polymorphism of HMOX-1 and the risk of new-onset asthma were observed among Hispanic children.

In contrast to HMOX-1, we found that the CAT-262C>T variant was associated with asthma in Hispanic-white children but was not associated with asthma in non-Hispanic white children. Among Hispanic children, carriers of the variant T allele (CT or TT) of CAT-262C>T were at an increased risk of new-onset asthma compared with the children who were homozygous for the common allele (CC) (HR, 1.93; P value = 0.01). CAT-262C>T was not associated with asthma risk among non-Hispanic white children. No statistically significant association between asthma and the CAT-844C>T or Ala-9Val polymorphism of MNSOD was observed in either ethnic group.

In further analysis, these genetic associations were neither confounded nor modified by parental history of asthma, history of allergy, secondhand smoke (SHS), current SHS exposure, *in utero* exposure to maternal smoking, personal smoking, physical activity, socioeconomic status (SES), health insurance, or over-

TABLE 2. SELECTED CHARACTERISTICS OF HISPANIC WHITE CHILDREN AT STUDY ENTRY

	No Asthma (*n = 519*)	Newly Diagnosed Asthma (*n = 57*)	*P* Value*
Age group, yr			
7–9	296 (57.0)	38 (66.7)	0.08
10–11	107 (20.6)	13 (22.8)	
>11	116 (22.3)	6 (10.5)	
Boys	215 (41.4)	23 (40.3)	0.87
Overweight/at risk of overweight	94 (18.4)	13 (23.2)	0.38
Parental history of asthma	60 (12.3)	6 (11.1)	0.80
History of allergy	65 (13.0)	8 (14.3)	0.79
Humidifier use	74 (15.3)	14 (25.4)	0.07
Smokers at home	53 (10.5)	8 (14.5)	0.38
Maternal smoking during pregnancy	36 (7.1)	5 (9.3)	0.57
Maternal smoking at study entry	25 (4.9)	1 (1.8)	0.25
Pests of any kind	308 (69.5)	41 (77.4)	0.23
Pets at home	342 (65.9)	41 (71.9)	0.35
Health insurance	353 (69.3)	45 (80.4)	0.08
Income, $†			
⩽14,999	103 (24.7)	8 (16.7)	0.15
15,000–49,999	215 (51.8)	23 (47.9)	
⩾50,000	97 (23.5)	17 (35.4)	
Highest parental education level†			
Less than high school	158 (32.8)	10 (18.5)	0.09
College	293 (61.0)	39 (72.2)	
Graduate	30 (6.2)	5 (9.3)	
Community ozone status, higher	263 (50.1)	27 (47.4	0.63
Community PM_{10} status, higher	272 (52.4)	32 (56.1)	0.59

Values indicate the number of children (%) available in the specific group.

* Chi-square *P* value determining the difference in distribution between children with and without newly diagnosed asthma during follow-up.

† The numbers do not add up to the total due to missing data.

weight/at risk of overweight (Table E5, model 1). As a sensitivity analysis, we restricted the asthma definition to those new-onset asthma cases who also used an inhaler (n = 121). The use of this restricted case definition resulted in little change in the estimated genetic effects for all the loci examined. For example, in analyses using the restricted case definition, the HR associated with S-alleles among non-Hispanic whites and the CT or TT alleles of the CAT-262C>T polymorphism among Hispanics

TABLE 3. DISTRIBUTION OF HMOX-1, CATALASE, AND MNSOD GENOTYPE AMONG HISPANIC AND NON-HISPANIC WHITE CHILDREN

Genotype	Non-Hispanic White	Hispanic White
HMOX-1		
⩽23 (S)*	469 (22.3)	154 (14.7)
>23 (No-S)	1,631 (77.7)	892 (85.3)
At least one 'S'	421 (40.1)	148 (28.3)
CAT-262C>T		
CC	694 (62.4)	417 (73.2)
CT	381 (34.2)	135 (23.6)
TT	38 (3.4)	18 (3.2)
CAT-844C>T		
CC	494 (44.9)	162 (29.2)
CT	474 (43.2)	261 (47.1)
TT	131 (11.9)	131 (23.6)
MNSOD–Ala-9Val		
Ala/Ala (CC)	262 (24.2)	188 (34.0)
Ala/Val (CT)	531 (49.1)	281 (51.0)
Val/Val (TT)	289 (26.7)	83 (15.0)

Total number and percentages in parentheses are provided for the allele frequencies. The total number varies by genotype due to incomplete data for individual genotype. The distribution of the alleles between Hispanic and non-Hispanic whites varied significantly for all of the genes (*P* value < 0.01).

* Biallelic distribution of "S" or "no-S" allele.

TABLE 4. ASSOCIATION OF HMOX-1 (GT-REPEATS), CATALASE, AND MNSOD GENOTYPE WITH NEW-ONSET ASTHMA AMONG HISPANIC AND NON-HISPANIC WHITE CHILDREN

Model	Genes	Non-Hispanic HR (*95% CI*)	Hispanics HR (*95% CI*)
HMOX-1 (GT-repeats)			
Any S	No-S	1	1
	At least one S	0.64 (0.41–0.99)*	1.25 (0.64–2.47)
Biallelic average	>26.5	1	1
	⩽26.5	0.56 (0.36–0.89)*	1.31 (0.66–2.57)
CAT-262C-T (rs1001179)	CC	1	1
	CT or TT	0.90 (0.61–1.31)	1.93 (1.05–3.55)†
	Numbers of 'T' allele	0.77 (0.56–1.05)	0.92 (0.59–1.42)
CAT-844C-T (rs769214)			
MNSOD (rs4880)	Val/Val	1	1
	Ala/Val or Ala/Ala	1.26 (0.78–2.02)	0.90 (0.40–2.03)

Definition of abbreviations: CI = confidence interval; HR = hazard ratio.

The adjusted HR and 95% CI are reported from Cox's proportional hazard model controlling for communities with age- and sex-specific baseline hazard. We fitted the dominant model for CAT-262C-T and MNSOD, and the additive model for CAT-844C-T.

* *P* value < 0.01.

† *P* value < 0.05.

was 0.63 (95% CI, 0.38–1.04) and 2.13 (95% CI, 1.09–4.18), respectively (Table E5, model 2).

To investigate whether the associations could be replicated in an independent population, we performed a stratified analysis for the two fourth-grade cohorts of the current study population recruited in 1993 and 1996 (Table 5). The ethnicity-specific genetic-effect estimates for the genes in each of these cohorts were consistent in both cohorts of children.

Gene–Air Pollution Interaction

We found evidence that the effect of variation in the HMOX-1 gene on the risk of new-onset asthma differed by ambient ozone level (interaction *P* value = 0.003; Table 6). The largest protective effect of the $(GT)_n$ repeat polymorphism of HMOX-1 was observed for children who were S-allele carriers and resided in low-ozone communities (HR, 0.44; 95% CI, 0.23–0.83). The relative ratio of HR of S-allele carriers who resided in high-ozone communities (HR, 0.88) was twofold greater than in those who resided in the low-ozone communities (HR, 0.44).

TABLE 5. ASSOCIATION OF HMOX-1 (GT-REPEATS) AND CAT-262C-T (rs1001179) WITH NEW-ONSET ASTHMA AMONG HISPANIC AND NON-HISPANIC WHITE FOURTH-GRADERS, STRATIFIED BY YEAR OF RECRUITMENT

Model	Genes	Non-Hispanic HR (*95% CI*)	Hispanics HR (*95% CI*)
Recruited in 1993		n = 401	n = 167
Any S	LL/LM/MM	1	1
	SS/SM/SL	0.64 (0.3–1.2)*	1.87 (0.6–5.7)
CAT-262C-T (rs1001179)	CC	1	1
	CT or TT	0.75 (0.4–1.4)	1.76 (0.6–5.3)
Recruited in 1996		n = 382	n = 253
Any S	LL/LM/MM		
	SS/SM/SL	0.68 (0.3–1.4)*	1.59 (0.6–4.0)
CAT-262C-T (rs1001179)	CC	1	1
	CT or TT	1.11 (0.6–2.2)	2.33 (1.0–5.4)†

Definition of abbreviations: CI = confidence interval; HR = hazard ratio.

The adjusted HR and 95% CI are reported from Cox's proportional hazard model controlling for communities with age- and sex-specific baseline hazard.

* *P* value < 0.1.

† *P* value < 0.05.

TABLE 6. EFFECT OF HMOX-1 (GT-REPEATS) ON NEW-ONSET ASTHMA AMONG NON-HISPANIC WHITE CHILDREN IN HIGHER AND LOWER OZONE AND PM_{10} CHILDREN'S HEALTH STUDY COMMUNITIES

Community	No S-Allele HR (*95% CI*)	S-Allele HR (*95% CI*)	*P* Value*
Low ozone	1	0.44 (0.23–0.83)	0.003
High ozone	0.94 (0.36–2.43)	0.88 (0.33–2.34)	
Low PM_{10}	1	0.94 (0.54–1.62)	0.18
High PM_{10}	1.79 (0.69–4.61)	0.62 (0.20–1.87)	

Definition of abbreviations: CI = confidence interval; HR = hazard ratio; PM_{10} = particulate matter with an aerodynamic diameter of less than 10 μm.

* Interaction *P* value is reported from hierarchical two stage Cox's proportional hazard model fitting the community-specific ozone and PM_{10} levels (continuous) and controlling for random effect of the communities. The HRs are based on Cox's proportional hazard model with age- and sex-specific baseline hazard and adjusting for communities.

The observed pattern did not vary by children's participation in sports (data not shown) or time spent outdoors (*see* Table E6). Adjusting for individual level covariates, such as SES, parental education, health insurance, and SHS exposure, as well as community level PM_{10}, also did not change the modifying effect of ambient ozone (data not shown). No significant interaction was observed between nonozone pollutants, such as PM_{10}, and the HMOX-1 gene (Table 6). We found little evidence for interactions between any of the other polymorphisms and ambient pollutant levels.

DISCUSSION

Oxidative stress is believed to contribute to asthma pathogenesis (2, 4, 28). In this study, we show that for new-onset asthma during adolescence, variants in genes that encode antioxidant enzymes contribute to variations in asthma occurrence. Although these variants appear to modulate asthma risk, their associations depended on ethnicity and level of oxidant exposure. Shorter $(GT)_n$ repeats in the promoter region of the HMOX-1 gene appeared to be protective among non-Hispanic whites, and CAT-262C>T was a risk factor among Hispanics. Furthermore, the effect of the $(GT)_n$ repeat polymorphism of HMOX-1 also varied by the ambient ozone level.

The ethnicity-specific effect of HMOX-1 repeats and the CAT-262C>T polymorphism is consistent with some previous reports and emphasizes the importance of evaluating the ethnicity-specific effect of genetic polymorphisms in assessing gene–disease associations. An ethnicity-specific effect of the $(GT)_n$ repeat polymorphism has been observed in coronary artery disease, for which an association was observed among Asians (10) but not in whites (29). Similarly, the CAT-262C>T polymorphism has been shown to affect the catalase activity among whites but not among African Americans (16).

It is unlikely that population admixture can explain the observed ethnic differences because the incident rates of new-onset asthma did not vary substantially among the ethnic groups. The linkage disequilibrium (LD) pattern of HMOX-1 is very similar for Hispanic and non-Hispanic whites, although some variation was observed for the CAT gene between the two ethnic groups (*see* Figures E3–E6). Thus, a difference in the regional LD pattern is an unlikely explanation for the observed ethnic differences for HMOX-1, although it is a possibility for the ethnicity-specific effect of variants in the CAT gene. It is possible that the relevant genetic background varies in Hispanic and non-Hispanic whites and that the relative contributions of genes involved in maintaining the antioxidant balance differs among ethnic groups.

It is difficult to determine whether the observed differences in the allele frequencies and biological effects of the polymorphisms in Hispanic and non-Hispanic whites were due to direct effect of anti-/prooxidative environment exposures or due to some other indirect exposures. From an evolutionary biological perspective, it is possible that the S-allele of HMOX-1 (protective factor in asthma) is underselected in Hispanic whites compared with non-Hispanic whites (28.3 vs. 40.1%), whereas the CC genotype of CAT-262C>T plays a compensatory role in Hispanic whites compared with non-Hispanic whites (73.2 vs. 62.4%). It is likely that studies also need to consider genes in related pathways to understand the ethnic differences in gene associations. For example, biliverdin is synthesized by HO-1 and can contribute to antioxidative activity only in the presence of sufficient activity of biliverdin reductase (Figure 1). A differential activity of biliverdin reductase in Hispanic and non-Hispanic whites could contribute to the differential role of HMOX-1 by ethnicity. Furthermore, although we examined a number of common environmental exposures and found no evidence that exposures account for the ethnic differences in associations, we cannot rule out an influence of ethnic variation in diet or other unmeasured lifestyle factors and environmental exposures. On the basis of our previous and ongoing research, no ethnicity-specific difference was observed for genes involved in other parts of the oxidative pathway, such as GSTP1, GSTM1, and GSTT1 (23, 30, 31); however, an ethnicity-specific effect has been reported for other genes in relation to asthma (32).

Our findings for HMOX-1 in non-Hispanic whites are consistent with the known functionality of the enzyme and previous studies. Although multiple studies have shown that the presence of long ("long" has been defined by differing cutoffs in different studies) $(GT)_n$ repeat polymorphisms of HMOX-1 are associated with an increased risk of different oxidative stress–mediated respiratory (11, 33–35) and cardiovascular conditions (10), its role in asthma has not been reported. Emerging evidence indicates that HO-1 plays a significant protective role for oxidative stress and subsequent pulmonary inflammation (36). HO-1 degrades heme to biliverdin, which is readily converted to bilirubin, a potent antioxidant (37, 38). During this process, free iron and CO are produced, and HO-1 exerts a cytoprotective effect by regulating cellular iron (39). CO has been shown to act as a signaling molecule to activate guanyl cyclase (40), thus mediating several physiologic antioxidative processes (40) and smooth muscle relaxation (41). HO-1 has also been shown to inhibit airway smooth muscle proliferation in humans, a process that is central to asthma pathogenesis (42). This array of possible protective mechanisms of HO-1 against asthma supports a role for the GT repeat polymorphism of the HMOX-1 gene that up-regulates the enzymatic expression or activity of HO-1. The functional effect of $(GT)_n$ repeat sizes on the transcriptional activity of HMOX-1 promoter has been reported from studies using luciferase promoter constructs and transient transfection (10, 11). Both of these previous studies showed that $(GT)_n$ repeats fewer than 23 were associated with the greatest promoter activity. A novel study using lymphoblastoid cell lines established from persons of known $(GT)_n$ repeats showed that cell lines homozygous for $(GT)_n$ repeats of fewer than 27 were associated with 2.4- $\pm$ 0.6-fold increased HO-1 enzyme activity under oxidative stress, whereas the increase under similar conditions was 1 $\pm$ 0.2 for cells that were homozygous for $(GT)_n$ repeats of more than 32 (9). On the basis of the functional effect of the $(GT)_n$ repeat polymorphism on HMOX-1 expression and its association in different disease conditions, our finding is biologically plausible.

We defined the short allele as repeat numbers 23 or less based on the greatest promoter activity (10, 11) and the distribution in

our cohort (<2% had repeats < 23). Given the additive effect of the number of repeats in each allele in the antioxidative activity of the HMOX-1 as shown by Chen and colleagues (10), the biallelic average number of repeats categorized at the 25th percentile value (≤26.5) should also be associated with high HO-1 activity as shown by Hirai and coworkers (9). We observed a strong protective effect of the shorter length of the HMOX-1 polymorphism on asthma risk using both of these categorizations among non-Hispanic whites.

Catalase is involved in reducing H_2O_2 to H_2O (Figure 1) and plays a significant antioxidative role in human lungs, especially at the alveolar level (6). The presence of the minor allele (T) of the CAT-262C>T polymorphism has been shown to reduce the enzymatic activity of catalase in red blood cells (14–16). A single hospital-based case-control study has shown that the presence of the minor allele (CT or TT) is associated with asthma among Chinese patients with asthma. However, the presence of the T allele was associated with a protective effect against asthma despite reduced catalase activity (17), and no association was observed when cases and control subjects were stratified by atopic status. Our finding that the presence of the minor allele (CT or TT) of the CAT-262C>T polymorphism increases the risk of new-onset asthma is consistent with the observation that the presence of CT or TT decreases the antioxidative activity of catalase. This association was not modified by atopic status or family history of asthma.

Our finding that the Ala-9Val polymorphism of MNSOD is not associated with asthma is consistent with most of the previous reports of no association between this polymorphism and asthma (17, 43–45). However, Mak and colleagues (17) reported a protective effect of the C allele (Val/Ala or Ala/Ala) against asthma among atopic cases and control subjects who were never-smokers, yet they did not observe any overall association between this polymorphism and asthma. We cannot exclude the possibility that other polymorphisms in this gene region are associated with the risk for asthma.

Ozone, an ambient strong oxidant that induces inflammation, has been reported to be associated with asthma incidence and exacerbation (46, 47). Our research has previously shown that the protective effect of TNF-308 GG (a promoter variant of tumor necrosis factor) genotype against asthma was attenuated by ambient ozone levels (48). Similarly, in this study, we observed that the protective effect of short $(GT)_n$ repeats was observed in lower ozone communities but not in higher ozone communities. This effect did not vary by the time-activity pattern of the children (*see* Table E6). It appears that in environments of low ambient ozone, specific polymorphisms can increase the antioxidative activity in response to an increased oxidative stress when needed and thus can counter any temporary imbalance in an oxidant–antioxidant relationship. However, in the presence of high background ozone, those beneficial polymorphisms (S-allele in this analysis and TNF-308 GG in our earlier analysis) may already provide maximum activity, and variation in promoters no longer affects levels of expression. It is interesting to note that only ozone and not particulate matter modified the protective effect of HMOX-1; however, we note that differential effects of particulate matter and ozone on the respiratory health have been reported in the literature (49, 50). We speculate that ozone, being a stronger oxidant than particulates, has a different chemical mechanism and substrates that produce different toxic oxidation products and therefore has larger effects in genetically susceptible groups. In our CHS study, we have previously reported a differential role of ozone and particulate matters for lung function and asthma (51, 52). Further studies are required to characterize the gene expression patterns, oxidative stress levels, and acute and chronic responses in people with different HMOX-1 repeats exposed to different levels of background ozone and particulate matter, and to further replicate this finding in an independent study with adequate power and exposure contrast.

The structure of our study—a cohort study of school-age children with annual collection of their asthma diagnosis and air pollution exposure—was an effective foundation for the current study and has proved to be a strength. We had a substantial number of children with genetic data to perform ethnicity-specific analyses. Genetic data were available for 67% of the study population. There were some differences between those with and without available genetic data (Tables E3 and E4); however, except for factors associated with SHS status (current maternal smoking and numbers of smokers at home), the magnitude of difference between the two groups was too small to affect the overall association. These socioeconomic factors also varied between those who were lost to follow-up (n = 776) and the source population (n = 2,998) of this study (*see* Table E7). These factors are unlikely to produce a selection bias, as they are not dependent on the genotype of the children and are not independent risk factors of asthma. Exposure to SHS was higher among children of low SES in this cohort, and loss to follow-up and unavailability of genetic data were also more common among children of low SES because their parents were more likely to move for economic reasons (based on interviews). Furthermore, neither SHS nor other factors in the tables were confounders (Table E5, model 1) or effect modifiers (data not shown) for the observed associations; thus, the differences are not likely to substantially bias the findings of our study.

One potential limitation of our study could be the accuracy of the case definition for new-onset asthma because it was based on personal interview and questionnaire data. Excluding any child with a history of wheezing also minimized misclassification of asthma status at entry. A recent study noted that children as young as 7 years can provide information regarding their asthma with an acceptable level of validity and reliability (53). Furthermore, unless the diagnosis varied by genotype, error in determining asthma status would likely lead to a downward bias in genetic-effect estimates, and therefore would not explain the observed associations.

Access to care and differences in practice among physicians have the potential to influence asthma diagnoses (54). We found that adjustment for factors that mediate access to care, including family income, education, and medical insurance, did not explain our results, indicating that differential access to care did not substantially bias our results. To further investigate the potential for bias from variation in medical practices, we conducted analyses restricting cases to those who recently used inhaled medication and found little change in the risk estimates. Because the associations of the genotypes were apparent among the group of cases for which the diagnosis of asthma was most certain, our results are unlikely to be explained by misclassification of outcome.

One potential criticism of the interpretation of our finding is that we have not adjusted for multiple testing; however, we do not think it is justified to correct *P* values for multiple testing in this analysis because the selection of the genes was based on *a priori* hypotheses defined by a well-studied biological pathway (Figure 1) and reported genetic variant functionality (9–18). Adjusting for multiple testing in this analysis would have ignored the available prior knowledge. There were five hypothesis-driven tests for each ethnic group. Four tests were conducted in each ethnic group to identify the main effect of the single-nucleotide polymorphisms (SNPs). After identifying the main effects, based on our *a priori* hypothesis, we tested for possible effect modification by O_3 with HMOX-1 among non-Hispanic

whites and CAT-262C-T among Hispanic whites. Importantly, we showed a consistent pattern for the main effects in two similar populations by performing stratified analysis for the two fourth-grade cohorts of the current study population recruited in 1993 and 1996 (Table 5). The ethnicity-specific genetic-effect estimates for the genes in each of these cohorts were consistent with those in the main analysis. Because the methodology of this study (selection of genes and SNPs, selection of the genetic model, and tested interaction with ambient ozone) is based on previous findings and a defined oxidative pathway (Figure 1), the observed main effect of the genes and the modifying effect of ambient ozone are biologically plausible. Because the main effect was replicated in a cohort-specific analysis, we do not think that these findings can be explained by chance alone. Due to sample size issues, we could not test the modifying effect of ambient ozone in different cohorts, thus it needs to be confirmed in studies conducted by other investigators with similar age groups and environmental exposures.

In conclusion, promoter variants that affect expression of HMOX-1 and CAT are associated with the development of new-onset asthma in children. The ethnicity-specific association between the tandem repeats polymorphism of the promoter region of the HMOX-1 gene and the CAT-262C>T polymorphism with new-onset asthma suggests that, for some variants, it is necessary to consider the ethnicity in the study of the complex relationship between variants in antioxidant genes and asthma occurrence. The finding that beneficial polymorphisms fail to protect children from the injurious effect of ambient ozone when the levels are sufficiently elevated argues for regulations that account for the effects in genetically susceptible children.

Conflict of Interest Statement: None of the authors has a financial relationship with a commercial entity that has an interest in the subject of this manuscript.

References

1. Chung KF. Role of inflammation in the hyperreactivity of the airways in asthma. *Thorax* 1986;41:657–662.
2. Barnes PJ. New concepts in the pathogenesis of bronchial hyperresponsiveness and asthma. *J Allergy Clin Immunol* 1989;83:1013–1026.
3. Nadeem A, Chhabra SK, Masood A, Raj HG. Increased oxidative stress and altered levels of antioxidants in asthma. *J Allergy Clin Immunol* 2003;111:72–78.
4. Greene LS. Asthma and oxidant stress: nutritional, environmental, and genetic risk factors. *J Am Coll Nutr* 1995;14:317–324.
5. Rahman I, Adcock IM. Oxidative stress and redox regulation of lung inflammation in COPD. *Eur Respir J* 2006;28:219–242.
6. Rahman I, Biswas SK, Kode A. Oxidant and antioxidant balance in the airways and airway diseases. *Eur J Pharmacol* 2006;533:222–239.
7. Exner M, Minar E, Wagner O, Schillinger M. The role of heme oxygenase-1 promoter polymorphisms in human disease. *Free Radic Biol Med* 2004; 37:1097–1104.
8. Wang LI, Neuberg D, Christiani DC. Asbestos exposure, manganese superoxide dismutase (MnSOD) genotype, and lung cancer risk. *J Occup Environ Med* 2004;46:556–564.
9. Hirai H, Kubo H, Yamaya M, Nakayama K, Numasaki M, Kobayashi S, Suzuki S, Shibahara S, Sasaki H. Microsatellite polymorphism in heme oxygenase-1 gene promoter is associated with susceptibility to oxidant-induced apoptosis in lymphoblastoid cell lines. *Blood* 2003; 102:1619–1621.
10. Chen YH, Lin SJ, Lin MW, Tsai HL, Kuo SS, Chen JW, Charng MJ, Wu TC, Chen LC, Ding YA, *et al.* Microsatellite polymorphism in promoter of heme oxygenase-1 gene is associated with susceptibility to coronary artery disease in type 2 diabetic patients. *Hum Genet* 2002; 111:1–8.
11. Yamada N, Yamaya M, Okinaga S, Nakayama K, Sekizawa K, Shibahara S, Sasaki H. Microsatellite polymorphism in the heme oxygenase-1 gene promoter is associated with susceptibility to emphysema. *Am J Hum Genet* 2000;66:187–195.
12. Shimoda-Matsubayashi S, Matsumine H, Kobayashi T, Nakagawa-Hattori Y, Shimizu Y, Mizuno Y. Structural dimorphism in the mitochondrial targeting sequence in the human manganese superoxide dismutase gene: a predictive evidence for conformational change to influence mitochondrial transport and a study of allelic association in Parkinson's disease. *Biochem Biophys Res Commun* 1996;226:561–565.
13. Hiroi S, Harada H, Nishi H, Satoh M, Nagai R, Kimura A. Polymorphisms in the SOD2 and HLA-DRB1 genes are associated with nonfamilial idiopathic dilated cardiomyopathy in Japanese. *Biochem Biophys Res Commun* 1999;261:332–339.
14. Nadif R, Mintz M, Jedlicka A, Bertrand JP, Kleeberger SR, Kauffmann F. Association of CAT polymorphisms with catalase activity and exposure to environmental oxidative stimuli. *Free Radic Res* 2005;39: 1345–1350.
15. Nadif R, Kleeberger SR, Kauffmann F. Polymorphisms in manganese superoxide dismutase and catalase genes: functional study in Hong Kong Chinese asthma patients. *Clin Exp Allergy* 2006;36:1104–1105. [Author reply, 1105–1106.]
16. Ahn J, Nowell S, McCann SE, Yu J, Carter L, Lang NP, Kadlubar FF, Ratnasinghe LD, Ambrosone CB. Associations between catalase phenotype and genotype: modification by epidemiologic factors. *Cancer Epidemiol Biomarkers Prev* 2006;15:1217–1222.
17. Mak JC, Leung HC, Ho SP, Ko FW, Cheung AH, Ip MS, Chan-Yeung MM. Polymorphisms in manganese superoxide dismutase and catalase genes: functional study in Hong Kong Chinese asthma patients. *Clin Exp Allergy* 2006;36:440–447.
18. Jiang Z, Akey JM, Shi J, Xiong M, Wang Y, Shen Y, Xu X, Chen H, Wu H, Xiao J, *et al.* A polymorphism in the promoter region of catalase is associated with blood pressure levels. *Hum Genet* 2001;109:95–98.
19. Peters JM, Avol E, Gauderman WJ, Linn WS, Navidi W, London SJ, Lurmann F, Margolis H, Rappaport E, Vora H, *et al.* A study of 12 Southern California communities with differing levels and types of air pollution: II. Effects on Pulmonary Function. *Am J Respir Crit Care Med* 1999;159:768–775.
20. Peters JM, Avol E, Navidi W, London SJ, Gauderman WJ, Lurmann F, Linn WS, Margolis H, Rappaport E, Gong H, *et al.* A study of 12 Southern California communities with differing levels and types of air pollution: I. Prevalence of respiratory morbidity. *Am J Respir Crit Care Med* 1999;159:760–767.
21. Islam T, Gauderman W, McConnell R, Gilliland F. Heme oxygenase, ozone, and incident asthma [abstract]. *Proc Am Thorac Soc* 2007;175:A833.
22. A SAS program for the CDC growth charts [Internet]. Atlanta: Centers for Disease Control and Prevention; [updated 16 Dec 2005; accessed 10 Jan 2007] Available from: http://www.cdc.gov/nccdphp/dnpa/bmi
23. Gilliland FD, Gauderman WJ, Vora H, Rappaport E, Dubeau L. Effects of glutathione-S-transferase M1, T1, and P1 on childhood lung function growth. *Am J Respir Crit Care Med* 2002;166:710–716.
24. Akaike H. Information theory and an extension of the maximum likelihood principle. In: Petrov BN, Csaki F, editors. Second International Symposium on Information Theory. Budapest: Akademia Kiado; 1973. pp. 267–281.
25. Berhane K, Gauderman W, Stram D, Thomas D. Statistical issues in studies of the long term effects of air pollution: the Southern California Children Health Study. *Stat Sci* 2004;19:414–449.
26. Ma R, Krewski D, Burnett RT. Random effects Cox models: a Poisson modeling approach. *Biometrika* 2003;90:157–169.
27. Jerrett M, Burnett RT, Ma R, Pope CA, Krewski D, Newbold KB, Thurston G, Shi Y, Finkelstein N, Calle EE, *et al.* Spatial analysis of air pollution and mortality in Los Angeles. *Epidemiology* 2005;16: 727–736.
28. Barnes PJ. Reactive oxygen species and airway inflammation. *Free Radic Biol Med* 1990;9:235–243.
29. Endler G, Exner M, Schillinger M, Marculescu R, Sunder-Plassmann R, Raith M, Jordanova N, Wojta J, Mannhalter C, Wagner OF, *et al.* A microsatellite polymorphism in the heme oxygenase-1 gene promoter is associated with increased bilirubin and HDL levels but not with coronary artery disease. *Thromb Haemost* 2004;91:155–161.
30. Gilliland FD, Li YF, Dubeau L, Berhane K, Avol E, McConnell R, Gauderman WJ, Peters JM. Effects of glutathione S-transferase M1, maternal smoking during pregnancy, and environmental tobacco smoke on asthma and wheezing in children. *Am J Respir Crit Care Med* 2002; 166:457–463.
31. Gilliland FD, Rappaport EB, Berhane K, Islam T, Dubeau L, Gauderman WJ, McConnell R. Effects of glutathione S-transferase P1, M1, and T1 on acute respiratory illness in school children. *Am J Respir Crit Care Med* 2002;166:346–351.
32. Hersh CP, Raby BA, Soto-Quiros ME, Murphy AJ, Avila L, Lasky-Su J, Sylvia JS, Klanderman BJ, Lange C, Weiss ST, *et al.* Comprehensive

testing of positionally cloned asthma genes in two populations. *Am J Respir Crit Care Med* 2007;176:849–857.
33. Hersh CP, Demeo DL, Lange C, Litonjua AA, Reilly JJ, Kwiatkowski D, Laird N, Sylvia JS, Sparrow D, Speizer FE, *et al.* Attempted replication of reported chronic obstructive pulmonary disease candidate gene associations. *Am J Respir Cell Mol Biol* 2005;33:71–78.
34. Guenegou A, Leynaert B, Benessiano J, Pin I, Demoly P, Neukirch F, Boczkowski J, Aubier M. Association of lung function decline with the heme oxygenase-1 gene promoter microsatellite polymorphism in a general population sample: results from the European Community Respiratory Health Survey (ECRHS), France. *J Med Genet* 2006;43:e43.
35. Kikuchi A, Yamaya M, Suzuki S, Yasuda H, Kubo H, Nakayama K, Handa M, Sasaki T, Shibahara S, Sekizawa K, *et al.* Association of susceptibility to the development of lung adenocarcinoma with the heme oxygenase-1 gene promoter polymorphism. *Hum Genet* 2005; 116:354–360.
36. Almolki A, Taille C, Martin GF, Jose PJ, Zedda C, Conti M, Megret J, Henin D, Aubier M, Boczkowski J. Heme oxygenase attenuates allergen-induced airway inflammation and hyperreactivity in guinea pigs. *Am J Physiol Lung Cell Mol Physiol* 2004;287:L26–L34.
37. Stocker R, Ames BN. Potential role of conjugated bilirubin and copper in the metabolism of lipid peroxides in bile. *Proc Natl Acad Sci USA* 1987;84:8130–8134.
38. Stocker R, Yamamoto Y, McDonagh AF, Glazer AN, Ames BN. Bilirubin is an antioxidant of possible physiological importance. *Science* 1987;235:1043–1046.
39. Ferris CD, Jaffrey SR, Sawa A, Takahashi M, Brady SD, Barrow RK, Tysoe SA, Wolosker H, Baranano DE, Dore S, *et al.* Haem oxygenase-1 prevents cell death by regulating cellular iron. *Nat Cell Biol* 1999;1: 152–157.
40. Otterbein LE, Bach FH, Alam J, Soares M, Tao Lu H, Wysk M, Davis RJ, Flavell RA, Choi AM. Carbon monoxide has anti-inflammatory effects involving the mitogen-activated protein kinase pathway. *Nat Med* 2000;6:422–428.
41. Kinhult J, Uddman R, Cardell LO. The induction of carbon monoxide-mediated airway relaxation by PACAP 38 in isolated guinea pig airways. *Lung* 2001;179:1–8.
42. Taille C, Almolki A, Benhamed M, Zedda C, Megret J, Berger P, Leseche G, Fadel E, Yamaguchi T, Marthan R, *et al.* Heme oxygenase inhibits human airway smooth muscle proliferation via a bilirubin-dependent modulation of ERK1/2 phosphorylation. *J Biol Chem* 2003;278:27160–27168.
43. Gurel A, Tomac N, Yilmaz HR, Tekedereli I, Akyol O, Armutcu F, Yuce H, Akin H, Ozcelik N, Elyas H. The Ala-9Val polymorphism in the mitochondrial targeting sequence (MTS) of the manganese superoxide dismutase gene is not associated with juvenile-onset asthma. *Clin Biochem* 2004;37:1117–1120.
44. Holla LI, Kankova K, Vasku A. Functional polymorphism in the manganese superoxide dismutase (MnSOD) gene in patients with asthma. *Clin Biochem* 2006;39:299–302.
45. Kinnula VL, Lehtonen S, Koistinen P, Kakko S, Savolainen M, Kere J, Ollikainen V, Laitinen T. Two functional variants of the superoxide dismutase genes in Finnish families with asthma. *Thorax* 2004;59: 116–119.
46. Hiltermann JT, Lapperre TS, van Bree L, Steerenberg PA, Brahim JJ, Sont JK, Sterk PJ, Hiemstra PS, Stolk J. Ozone-induced inflammation assessed in sputum and bronchial lavage fluid from asthmatics: a new noninvasive tool in epidemiologic studies on air pollution and asthma. *Free Radic Biol Med* 1999;27:1448–1454.
47. McConnell R, Berhane K, Gilliland F, London SJ, Islam T, Gauderman WJ, Avol E, Margolis HG, Peters JM. Asthma in exercising children exposed to ozone: a cohort study. *Lancet* 2002;359:386–391.
48. Li YF, Gauderman WJ, Avol E, Dubeau L, Gilliland FD. Associations of tumor necrosis factor G-308A with childhood asthma and wheezing. *Am J Respir Crit Care Med* 2006;173:970–976.
49. Meng YY, Wilhelm M, Rull RP, English P, Ritz B. Traffic and outdoor air pollution levels near residences and poorly controlled asthma in adults. *Ann Allergy Asthma Immunol* 2007;98:455–463.
50. Lagorio S, Forastiere F, Pistelli R, Iavarone I, Michelozzi P, Fano V, Marconi A, Ziemacki G, Ostro BD. Air pollution and lung function among susceptible adult subjects: a panel study. *Environ Health* 2006; 5:11.
51. Gauderman WJ, Avol E, Gilliland F, Vora H, Thomas D, Berhane K, McConnell R, Kuenzli N, Lurmann F, Rappaport E, *et al.* The effect of air pollution on lung development from 10 to 18 years of age. *N Engl J Med* 2004;351:1057–1067.
52. Islam T, Gauderman WJ, Berhane K, McConnell R, Avol E, Peters JM, Gilliland FD. Relationship between air pollution, lung function and asthma in adolescents. *Thorax* 2007;62:957–963.
53. Olson LM, Radecki L, Frintner MP, Weiss KB, Korfmacher J, Siegel RM. At what age can children report dependably on their asthma health status? *Pediatrics* 2007;119:e93–e102.
54. Samet JM. Epidemiologic approaches for the identification of asthma. *Chest* 1987;91(6, Suppl):74S–78S.

The NEW ENGLAND JOURNAL of MEDICINE

ORIGINAL ARTICLE

Long-Term Ozone Exposure and Mortality

Michael Jerrett, Ph.D., Richard T. Burnett, Ph.D., C. Arden Pope III, Ph.D., Kazuhiko Ito, Ph.D., George Thurston, Sc.D., Daniel Krewski, Ph.D., Yuanli Shi, M.D., Eugenia Calle, Ph.D., and Michael Thun, M.D.

ABSTRACT

BACKGROUND

Although many studies have linked elevations in tropospheric ozone to adverse health outcomes, the effect of long-term exposure to ozone on air pollution–related mortality remains uncertain. We examined the potential contribution of exposure to ozone to the risk of death from cardiopulmonary causes and specifically to death from respiratory causes.

METHODS

Data from the study cohort of the American Cancer Society Cancer Prevention Study II were correlated with air-pollution data from 96 metropolitan statistical areas in the United States. Data were analyzed from 448,850 subjects, with 118,777 deaths in an 18-year follow-up period. Data on daily maximum ozone concentrations were obtained from April 1 to September 30 for the years 1977 through 2000. Data on concentrations of fine particulate matter (particles that are ≤2.5 μm in aerodynamic diameter [$PM_{2.5}$]) were obtained for the years 1999 and 2000. Associations between ozone concentrations and the risk of death were evaluated with the use of standard and multilevel Cox regression models.

RESULTS

In single-pollutant models, increased concentrations of either $PM_{2.5}$ or ozone were significantly associated with an increased risk of death from cardiopulmonary causes. In two-pollutant models, $PM_{2.5}$ was associated with the risk of death from cardiovascular causes, whereas ozone was associated with the risk of death from respiratory causes. The estimated relative risk of death from respiratory causes that was associated with an increment in ozone concentration of 10 ppb was 1.040 (95% confidence interval, 1.010 to 1.067). The association of ozone with the risk of death from respiratory causes was insensitive to adjustment for confounders and to the type of statistical model used.

CONCLUSIONS

In this large study, we were not able to detect an effect of ozone on the risk of death from cardiovascular causes when the concentration of $PM_{2.5}$ was taken into account. We did, however, demonstrate a significant increase in the risk of death from respiratory causes in association with an increase in ozone concentration.

From the University of California, Berkeley (M.J.); Health Canada, Ottawa (R.T.B.); Brigham Young University, Provo, UT (C.A.P.); New York University School of Medicine, New York (K.I., G.T.); the University of Ottawa, Ottawa (D.K., Y.S.); and the American Cancer Society, Atlanta (E.C., M.T.). Address reprint requests to Dr. Jerrett at the Division of Environmental Health Sciences, School of Public Health, University of California, 710 University Hall, Berkeley, CA 94720, or at jerrett@berkeley.edu.

N Engl J Med 2009;360:1085-95.

STUDIES CONDUCTED OVER THE PAST 15 years have provided substantial evidence that long-term exposure to air pollution is a risk factor for cardiopulmonary disease and death.[1-5] Recent reviews of this literature suggest that fine particulate matter (particles that are ≤2.5 μm in aerodynamic diameter [$PM_{2.5}$]) has a primary role in these adverse health effects.[6,7] The particulate-matter component of air pollution includes complex mixtures of metals, black carbon, sulfates, nitrates, and other direct and indirect byproducts of incomplete combustion and high-temperature industrial processes.

Ozone is a single, well-defined pollutant, yet the effect of exposure to ozone on air pollution–related mortality remains inconclusive. Several studies have evaluated this issue, but they have been short-term studies,[8-10] have failed to show a statistically significant effect,[1,3] or have been based on limited mortality data.[11] Recent reviews by the Environmental Protection Agency (EPA)[12] and the National Research Council[13] have questioned the overall consistency of the available data correlating exposure to ozone and mortality. Similar conclusions about the evidence base for the long-term effects of ozone on mortality were drawn by a panel of experts in the United Kingdom.[14]

Nonetheless, previous studies have suggested that a measurable effect of ozone may exist, particularly with respect to the risk of death from cardiopulmonary causes. In one of the larger studies, ozone was significantly associated with death from cardiopulmonary causes[15] but not with death from ischemic heart disease. However, the estimated effect of ozone on the risk of death from cardiopulmonary causes in this study was attenuated when $PM_{2.5}$ was added to the analysis in copollutant models. On the basis of suggested effects of ozone on the risk of death from cardiopulmonary causes (which includes death from respiratory causes) but an absence of evidence for effects of ozone on the risk of death from ischemic heart disease, we hypothesized that ozone might have a primary effect on the risk of death from respiratory causes.

METHODS

HEALTH, MORTALITY, AND CONFOUNDING DATA

Our study used data from the American Cancer Society Cancer Prevention Study II (CPS II) cohort.[16] The CPS II cohort consists of more than 1.2 million participants who were enrolled by American Cancer Society volunteers between September 1982 and February 1983 in all 50 states, the District of Columbia, and Puerto Rico. Enrollment was restricted to persons who were at least 30 years of age living in households with at least one person 45 years of age or older. After providing written informed consent, the participants completed a confidential questionnaire that included questions on demographic characteristics, smoking history, alcohol use, diet, and education.[17] Deaths were ascertained until August 1988 by personal inquiries of family members by the volunteers and thereafter by linkage with the National Death Index. Through 1995, death certificates were obtained and coded for cause of death. Beginning in 1996, codes for cause of death were provided by the National Death Index.[18]

The study population for our analysis included only those participants in CPS II who resided in U.S. metropolitan statistical areas within the 48 contiguous states or the District of Columbia (according to their address at the time of enrollment) and for whom data were available from at least one pollution monitor within their metropolitan area. The study was approved by the Ottawa Hospital Research Ethics Board, Canada.

Data on "ecologic" risk factors at the level of the metropolitan area representing social variables (educational level, percentage of homes with air conditioning, percentage of the population who were nonwhite), economic variables (household income, unemployment, income disparity), access to medical care (number of physicians and hospital beds per capita), and meteorologic variables were obtained from the 1980 U.S. Census and other secondary sources (see the Supplementary Appendix, available with the full text of this article at NEJM.org). These ecologic risk factors, as well as the individual risk factors collected in the CPS II questionnaire, were assessed as potential confounders of the effects of ozone.[3,5,19,20]

ESTIMATES OF EXPOSURE TO AIR POLLUTION

Ozone data were obtained from 1977 (5 years before the identification of the CPS II cohort) through 2000 for all air-pollution monitors in the study metropolitan areas from the EPA's Aerometric Information Retrieval System. Ozone data at each monitoring site were collected on an hourly basis, and the daily maximum value for the site was determined. All available daily maximum values for the monitoring site were averaged over

each quarter year. The quarterly average values were reported for each monitor only when at least 75% of daily observations for that quarter were available.

The averages of the second (April through June) and third (July through September) quarters were calculated for each monitor if both quarterly averages were available. The period from April through September was selected because ozone concentrations tend to be elevated during the warmer seasons and because fewer data were available for the cooler seasons.

The average of the second and third quarterly averages for each year was then computed for all the monitors within each metropolitan area to form a single annual time series of air-pollution measurements for each metropolitan area for the period from 1977 to 2000. In addition, a summary measure of long-term exposure to ambient warm-season ozone was defined as the average of annual time-series measurements during the entire period from 1977 to 2000. Individual measures of exposure to ozone were then defined by assigning the average for the metropolitan area to each cohort member residing in that area.

Data on exposure to $PM_{2.5}$ were also obtained from the Aerometric Information Retrieval System database for the 2-year period from 1999 to 2000 (data on $PM_{2.5}$ were not available before 1999 for most metropolitan areas).[5] The average concentrations of $PM_{2.5}$ were included in our analyses to distinguish the effect of particulates from that of ozone on outcomes.

STATISTICAL ANALYSIS

Standard and multilevel random-effects Cox proportional-hazard models were used to assess the risk of death in relation to exposures to pollution. The subjects were matched according to age (in years), sex, and race. A total of 20 variables with 44 terms were used to control for individual characteristics that might confound or modify the association between air pollution and death. These variables, which were considered to be of potential importance on the basis of previous studies, included individual risk factors for which data had been collected in the CPS II questionnaire. Seven ecologic covariates obtained from the 1980 U.S. Census (median household income, the proportion of persons living in households with an income below 125% of the poverty line, the percentage of persons over the age of 16 years who were unemployed, the percentage of adults with less than a high-school [12th-grade] education, the percentage of homes with air conditioning, the Gini coefficient of income inequality [ranging from 0 to 1, with 0 indicating an equal distribution of income and 1 indicating that one person has all the income and everyone else has no income[20]], and the percentage of persons who were white) were also included. These variables were included at two levels: as the average for the metropolitan statistical area and as the difference between the average for the ZIP Code of residence and the average for the metropolitan statistical area. Additional sensitivity analyses were undertaken for ecologic variables that were available for only a subgroup of the 96 metropolitan statistical areas (see the Supplementary Appendix). Models were estimated for either ozone or $PM_{2.5}$. In addition, models with both $PM_{2.5}$ and ozone were estimated.

In additional analyses, our basic Cox models were modified by incorporating an adjustment for community-level random effects, which allowed us to take into account residual variation in mortality among communities.[21] The baseline hazard function was modulated by a community-specific random variable representing the residual risk of death for subjects in that community after individual and ecologic risk factors had been controlled for (see the Supplementary Appendix).

A formal analysis was conducted to assess whether a threshold existed for the association between exposure to ozone and the risk of death (see the Supplementary Appendix). A standard threshold model was postulated in which there was no association between exposure to ozone and the risk of death below a specified threshold concentration and a linear association (on the logarithmic scale of the proportional-hazards model) above the threshold.

The question of whether specific time windows were associated with the health effects was investigated by subdividing the follow-up interval into four periods (1982 to 1988, 1989 to 1992, 1993 to 1996, and 1997 to 2000). Exposures were matched for each of these periods and also tested for a 10-year average on the basis of the 5-year follow-up period and the 5 years before the follow-up period (see the Supplementary Appendix).

RESULTS

The analytic cohort included 448,850 subjects residing in 96 metropolitan statistical areas (Fig. 1).

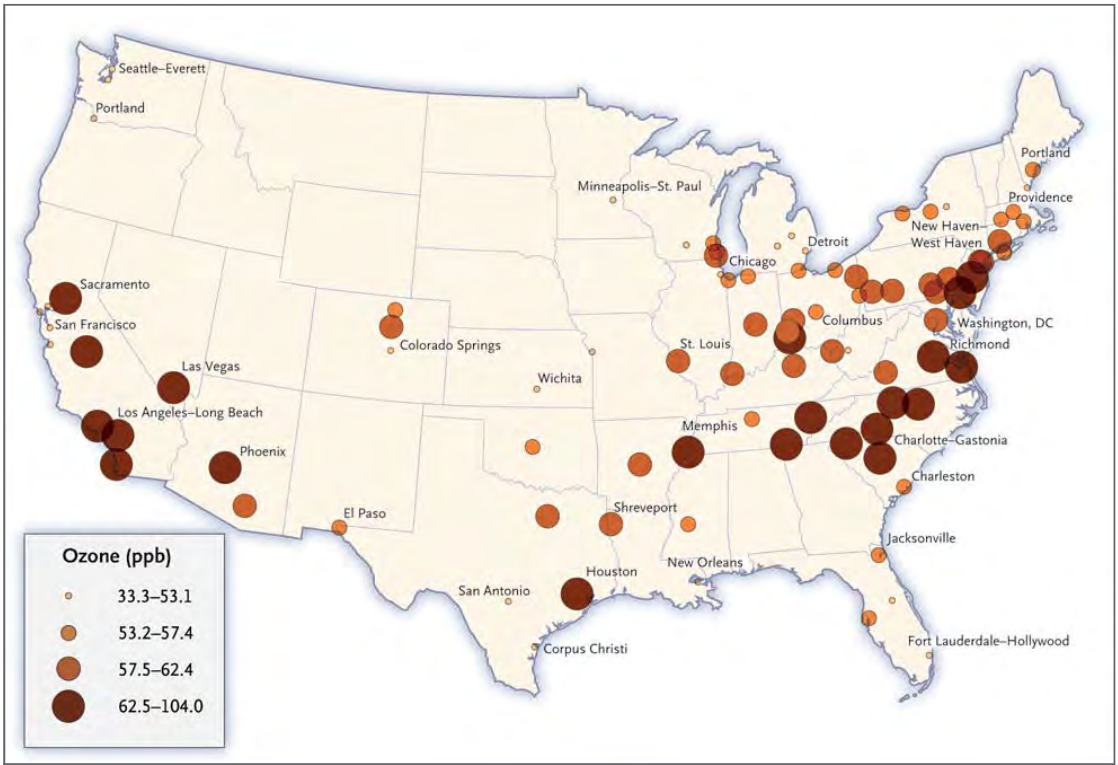

Figure 1. Ozone Concentrations in the 96 Metropolitan Statistical Areas in Which Members of the American Cancer Society Cohort Resided in 1982.

The average exposures were estimated from 1 to 57 monitoring sites within each metropolitan area from April 1 to September 30 for the years 1977 through 2000.

In 1980, the populations of these 96 areas ranged from 94,436 to 8,295,900. Data were available on the concentration of ambient ozone from all 96 areas and on the concentration of $PM_{2.5}$ from 86 areas. The average number of air-pollution monitors per metropolitan area was 11 (range, 1 to 57), and more than 80% of the areas had 6 or more monitors.

The average ozone concentration for each metropolitan area during the interval from 1977 to 2000 ranged from 33.3 ppb to 104.0 ppb (Fig. 1). The highest regional concentrations were in Southern California and the lowest in the Pacific Northwest and parts of the Great Plains. Moderately elevated concentrations were present in many areas of the East, Midwest, South, and Southwest.

The baseline characteristics of the study population, overall and as a function of exposure to ozone, are presented in Table 1. The mean age of the cohort was 56.6 years, 43.4% were men, 93.7% were white, 22.4% were current smokers, and 30.5% were former smokers. On the basis of estimates from 1980 Census data, 62.3% of homes had air conditioning at the time of initial data collection.

During the 18-year follow-up period (from initial CPS II data collection in 1982 through the end of follow-up in 2000), there were 118,777 deaths in the study cohort (Table 2). Of these, 58,775 were from cardiopulmonary causes, including 48,884 from cardiovascular causes (of which 27,642 were due to ischemic heart disease) and 9891 from respiratory causes.

In the single-pollutant models, exposure to ozone was not associated with the overall risk of death (relative risk, 1.001; 95% confidence interval [CI], 0.996 to 1.007) (Table 3). However, it was significantly correlated with an increase in the risk of death from cardiopulmonary causes. A

10-ppb increment in exposure to ozone elevated the relative risk of death from the following causes: cardiopulmonary causes (relative risk, 1.014; 95% CI, 1.007 to 1.022), cardiovascular causes (relative risk, 1.011; 95% CI, 1.003 to 1.023), ischemic heart disease (relative risk, 1.015; 95% CI, 1.003 to 1.026), and respiratory causes (relative risk, 1.029; 95% CI, 1.010 to 1.048).

Inclusion of the concentration of $PM_{2.5}$ measured in 1999 and 2000 as a copollutant (Table 3) attenuated the association with exposure to ozone for all the end points except death from respiratory causes, for which a significant correlation persisted (relative risk, 1.040; 95% CI, 1.013 to 1.067). The concentrations of ozone and $PM_{2.5}$ were positively correlated ($r=0.64$ at the subject level and $r=0.56$ at the metropolitan-area level), resulting in unstable risk estimates for both pollutants. The concentration of $PM_{2.5}$ remained significantly associated with death from cardio-

Table 1. Baseline Characteristics of the Study Population in the Entire Cohort and According to Exposure to Ozone.*

Variable	Entire Cohort (N=448,850)	Concentration of Ozone			
		33.3–53.1 ppb (N=126,206)	53.2–57.4 ppb (N=95,740)	57.5–62.4 ppb (N=106,545)	62.5–104.0 ppb (N=120,359)
No. of MSAs	96	24	24	24	24
No. of MSAs with data on $PM_{2.5}$	86	21	20	23	22
Concentration of $PM_{2.5}$ ($\mu g/m^3$)		11.9±2.5	13.1±2.9	14.7±2.1	15.4±3.2
Individual risk factors					
Age (yr)	56.6±10.5	56.7±10.4	56.4±10.7	56.3±10.4	56.9±10.5
Male sex (%)	43.4	43.5	43.1	43.5	43.2
White race (%)	93.7	94.3	95.1	93.9	91.8
Education (%)					
Less than high school	12.1	11.5	13.6	12.1	11.6
High school	30.6	30.2	33.6	32.1	27.4
Beyond high school	57.3	58.3	52.8	55.8	61.0
Smoking status					
Current smokers					
Percentage of subjects	22.4	22.0	23.5	22.2	21.9
No. of cigarettes/day	22.0±12.4	22.0±12.3	22.0±12.5	22.2±12.5	21.9±12.4
Duration of smoking (yr)	33.5±11.0	33.4±10.8	33.4±11.1	33.4±11.0	33.9±11.2
Started smoking <18 yr of age (%)	9.6	9.3	10.5	9.4	9.3
Started smoking ≥18 yr of age (%)	13.2	13.3	13.4	13.3	13.0
Former smokers					
Percentage of subjects	30.5	31.2	30.8	29.5	30.4
No. of cigarettes/day	21.6±14.7	21.6±14.6	22.2±15.1	21.6±14.6	21.3±14.6
Duration of smoking (yr)	22.2±12.6	22.1±12.5	22.6±12.6	22.0±12.5	22.4±12.7
Started smoking <18 yr of age (%)	11.9	11.8	12.7	11.5	11.8
Started smoking ≥18 yr of age (%)	18.5	19.3	17.9	17.9	18.5
Exposure to smoking (hr/day)	3.3±4.4	3.2±4.4	3.4±4.5	3.4±4.5	3.1±4.4
Pipe or cigar smoker only (%)	4.1	4.0	4.2	4.3	3.8
Marital status (%)					
Married	83.5	84.2	83.0	83.7	83.1
Single	3.6	3.4	4.0	3.8	3.2
Separated, divorced, or widowed	12.9	12.4	13.0	12.5	13.7

Table 1. (Continued.)

Variable	Entire Cohort (N=448,850)	Concentration of Ozone			
		33.3–53.1 ppb (N=126,206)	53.2–57.4 ppb (N=95,740)	57.5–62.4 ppb (N=106,545)	62.5–104.0 ppb (N=120,359)
Body-mass index†	25.1±4.1	25.1±4.1	25.3±4.2	25.1±4.1	24.8±4.0
Level of occupational exposure to particulate matter (%)‡					
0	50.7	50.9	50.0	50.8	51.0
1	13.3	13.4	13.1	13.3	13.3
2	11.4	11.5	10.8	11.4	11.9
3	4.6	4.7	4.8	4.6	4.5
4	6.1	6.2	6.2	6.1	6.0
5	4.2	4.2	4.3	4.1	4.1
6	1.1	1.0	9.5	1.4	8.4
Not able to ascertain	8.6	8.2	1.2	8.4	0.9
Self-reported exposure to dust or fumes (%)	19.5	19.5	19.8	19.7	19.1
Level of dietary-fat consumption (%)§					
0	14.5	13.7	14.9	14.1	15.3
1	15.9	15.8	16.5	15.6	15.9
2	17.4	17.6	17.7	17.2	17.1
3	21.2	21.8	21.1	21.3	20.8
4	30.9	31.1	29.8	31.9	30.9
Level of dietary-fiber consumption (%)¶					
0	16.6	16.0	17.5	16.7	16.6
1	19.9	19.4	20.5	20.1	19.7
2	18.8	18.6	19.2	19.1	18.5
3	22.8	23.0	22.4	22.8	22.7
4	21.9	23.0	20.4	21.3	22.5
Alcohol consumption (%)					
Beer					
Drinks beer	22.9	24.3	23.2	22.9	21.4
Does not drink beer	9.7	9.5	9.3	9.5	10.2
No data	67.4	66.2	67.5	67.6	68.4
Liquor					
Drinks liquor	28.0	30.4	27.9	25.4	27.9
Does not drink liquor	8.8	8.4	8.5	10.1	9.2
No data	63.2	61.2	63.6	65.5	62.9
Wine					
Drinks wine	23.5	25.4	22.5	21.1	24.3
Does not drink wine	8.9	8.7	8.8	9.3	9.1
No data	67.6	65.9	68.7	69.6	66.6

Table 1. (Continued.)

Variable	Entire Cohort (N=448,850)	Concentration of Ozone			
		33.3–53.1 ppb (N=126,206)	53.2–57.4 ppb (N=95,740)	57.5–62.4 ppb (N=106,545)	62.5–104.0 ppb (N=120,359)
Ecologic risk factors‖					
Nonwhite race (%)	11.6±16.8	10.5±16.4	9.3±15.5	10.2±16.0	15.9±18.3
Home with air conditioning (%)	62.3±27.0	55.4±31.2	59.4±24.0	65.3±24.8	69.1±24.3
High-school education or greater (%)	51.7±8.2	53.5±7.9	52.4±7.5	50.8±7.2	50.0±9.5
Unemployment rate (%)	11.7±3.1	12.1±3.4	11.3±2.6	11.3±2.9	11.8±3.4
Gini coefficient of income inequality**	0.37±0.04	0.37±0.05	0.37±0.04	0.37±0.04	0.38±0.04
Proportion of population with income <125% of poverty line	0.12±0.08	0.11±0.08	0.12±0.08	0.11±0.07	0.13±0.09
Annual household income (thousands of dollars)††	20.7±6.6	21.9±7.1	19.8±6.0	21.2±6.7	19.7±6.3

* MSA denotes metropolitan statistical area, and $PM_{2.5}$ fine particulate matter consisting of particles that are 2.5 μm or less in aerodynamic diameter. Plus–minus values are means ±SD. Because of rounding, percentages may not total 100. All baseline characteristics included in the survival model are listed (age, sex, and race were included as stratification factors). The model also includes squared terms for the number of cigarettes smoked per day and the number of years of smoking for both current and former smokers and a squared term for body-mass index.

† The body-mass index is the weight in kilograms divided by the square of the height in meters.

‡ Occupational exposure to particulate matter increases with increasing index number. The index was calculated by assigning a relative level of exposure to $PM_{2.5}$ associated with a cohort member's job and industry. These assignments were performed by industrial hygienists on the basis of their knowledge of typical exposure patterns for each occupation and specific job.[22]

§ Dietary-fat consumption increases with increasing index number. Dietary information from cohort members was used to define the level of fat consumption according to five ordered categories.[20]

¶ Dietary-fiber consumption increases with increasing index number. Dietary information from cohort members was used to define the level of fiber consumption according to five ordered categories.[23]

‖ For the ecologic variables, the model included terms for influences at the level of the average for the metropolitan statistical area and at the level of the difference between the value for the ZIP Code of residence and the average for the metropolitan statistical area to represent between- and within-metropolitan area confounding influence. Some values for ecologic variables and individual variables differ, although they appear to measure the same risk factor. For example, for the entire cohort, the percentage of whites as listed under individual variables is 93.7, whereas the percentage of nonwhites as listed under ecologic variables is 11.6±16.8. This apparent contradiction is explained by the fact that the former is an exact figure based on the individual reports of the study participants in the CPS II questionnaire, whereas the latter is a mean (±SD) for the population based on Census estimates for each metropolitan statistical area.

** The Gini coefficient is a statistical dispersion measure used to calculate income inequality. The coefficient ranges from 0 to 1, with 0 indicating an equal distribution of income and 1 indicating that one person has all the income and everyone else has no income.[20] A coefficient of 0.37 indicates that on average there is a measurable inequality in the distribution of income among the different income groups within the MSAs.

†† Average household incomes for the cohort and for each quartile of ozone concentration were calculated from the median household income for the metropolitan statistical area.

pulmonary causes, cardiovascular causes, and ischemic heart disease when ozone was included in the model. The association of ozone concentrations with death from respiratory causes remained significant after adjustment for $PM_{2.5}$.

Risk estimates for ozone-related death from respiratory causes were insensitive to the use of a random-effects survival model allowing for spatial clustering within the metropolitan area and state of residence (Table 1S in the Supplementary Appendix). The association between increased ozone concentrations and increased risk of death from respiratory causes was also insensitive to adjustment for several ecologic variables considered individually (Table 2S in the Supplementary Appendix).

Subgroup analyses showed that environmental temperature and region of the country, but not sex, age at enrollment, body-mass index, education, or concentration of $PM_{2.5}$, significantly modified the effects of ozone on the risk of death from respiratory causes (Table 4).

Figure 2 illustrates the shape of the relation between exposure to ozone and death from re-

Table 2. Number of Deaths in the Entire Cohort and According to Exposure to Ozone.

Cause of Death	Entire Cohort (N=448,850)	Concentration of Ozone			
		33.3–53.1 ppb (N=126,206)	53.2–57.4 ppb (N=95,740)	57.5–62.4 ppb (N=106,545)	62.5–104.0 ppb (N=120,359)
		number of deaths			
Any cause	118,777	32,957	25,642	27,782	32,396
Cardiopulmonary	58,775	16,328	12,621	13,544	16,282
Cardiovascular	48,884	13,605	10,657	11,280	13,342
Ischemic heart disease	27,642	7,714	6,384	6,276	7,268
Respiratory	9,891	2,723	1,964	2,264	2,940

Table 3. Relative Risk of Death Attributable to a 10-ppb Change in the Ambient Ozone Concentration.*

Cause of Death	Single-Pollutant Model†			Two-Pollutant Model‡	
	Ozone (96 MSAs)	Ozone (86 MSAs)	$PM_{2.5}$ (86 MSAs)	Ozone (86 MSAs)	$PM_{2.5}$ (86 MSAs)
			relative risk (95% CI)		
Any cause	1.001 (0.996–1.007)	1.001 (0.996–1.007)	1.048 (1.024–1.071)	0.989 (0.981–0.996)	1.080 (1.048–1.113)
Cardiopulmonary	1.014 (1.007–1.022)	1.016 (1.008–1.024)	1.129 (1.094–1.071)	0.992 (0.982–1.003)	1.153 (1.104–1.204)
Respiratory	1.029 (1.010–1.048)	1.027 (1.007–1.046)	1.031 (0.955–1.113)	1.040 (1.013–1.067)	0.927 (0.836–1.029)
Cardiovascular	1.011 (1.003–1.023)	1.014 (1.005–1.023)	1.150 (1.111–1.191)	0.983 (0.971–0.994)	1.206 (1.150–1.264)
Ischemic heart disease	1.015 (1.003–1.026)	1.017 (1.006–1.029)	1.211 (1.156–1.268)	0.973 (0.958–0.988)	1.306 (1.226–1.390)

* MSA denotes metropolitan statistical area, and $PM_{2.5}$ fine particulate matter consisting of particles that are 2.5 μm or less in aerodynamic diameter. Ozone concentrations were measured from April to September during the years from 1977 to 2000, with follow-up from 1982 to 2000; changes in the concentration of $PM_{2.5}$ of 10 μg per cubic meter were recorded for members of the cohort in 1999 and 2000. These models are adjusted for all the individual and ecologic risk factors listed in Table 1. For the ecologic variables, the model included terms for influences at the level of the average for the metropolitan statistical area and at the level of the difference between the value for the ZIP Code of residence and the average for the metropolitan statistical area to represent between- and within-metropolitan area confounding influence. The risk of death was stratified according to age (in years), sex, and race.

† The single-pollutant models were based on 96 metropolitan statistical areas for which information on ozone was available and 86 metropolitan statistical areas for which information on both ozone and fine particulate matter was available.

‡ The two-pollutant models were based on 86 metropolitan statistical areas for which information on both ozone and fine particulate matter was available.

spiratory causes. There was limited evidence that a threshold model specification improved model fit as compared with a nonthreshold linear model (P=0.06) (Table 3S in the Supplementary Appendix).

Because air-pollution data from 1977 to 2000 were averaged, exposure values for persons who died during this period are based partly on data that were obtained after death had occurred. Further investigation by dividing this interval into specific time windows of exposure revealed no significant difference between the effects of earlier and later time windows within the period of follow-up. Allowing for a 10-year period of exposure to ozone (5 years of follow-up and 5 years before the follow-up period) did not appreciably alter the risk estimates (Table 4S in the Supplementary Appendix). Thus, when exposure values were matched more closely to the follow-up period and when exposure values were based on data obtained before the deaths, there was little change in the results.

DISCUSSION

Our principal finding is that ozone and $PM_{2.5}$ contributed independently to increased annual mortality rates in this large, U.S. cohort study in analyses that controlled for many individual and ecologic risk factors. In two-pollutant models that

included ozone and $PM_{2.5}$, ozone was significantly associated only with death from respiratory causes.

For every 10-ppb increase in exposure to ozone, we observed an increase in the risk of death from respiratory causes of about 2.9% in single-pollutant models and 4% in two-pollutant models. Although this increase may appear moderate, the risk of dying from a respiratory cause is more than three times as great in the metropolitan areas with the highest ozone concentrations as in those with the lowest ozone concentrations. The effects of ozone on the risk of death from respiratory causes were insensitive to adjustment for individual, neighborhood, and metropolitan-area confounders or to differences in multilevel-model specifications.

There is biologic plausibility for a respiratory effect of ozone. In laboratory studies, ozone can increase airway inflammation[24] and can worsen pulmonary function and gas exchange.[25] In addition, exposure to elevated concentrations of tropospheric ozone has been associated with numerous adverse health effects, including the induction[26] and exacerbation[27,28] of asthma, pulmonary dysfunction,[29,30] and hospitalization for respiratory causes.[31]

Despite these observations, previous studies linking long-term exposure to ozone with death have been inconclusive. One cohort study conducted in the Midwest and eastern United States reported an inverse but nonsignificant association between ozone concentrations and mortality.[1] Subsequent reanalyses of this study replicated these findings but also suggested a positive association with exposure to ozone during warm seasons.[3] A study of approximately 6000 nonsmoking Seventh-Day Adventists living in Southern California showed elevated risks among men after long-term exposure to ozone,[11] but this finding was based on limited mortality data.

Previous studies using the CPS II cohort have also produced mixed results for ozone. An earlier examination based on a large sample of more than 500,000 people from 117 metropolitan areas and 8 years of follow-up indicated nonsignificant results for the relation between ozone and death from any cause and a significant inverse association between ozone and death from lung cancer. A positive association between death from cardiopulmonary causes and summertime exposure to ozone was observed in single-pollutant

Table 4. Relative Risk of Death from Respiratory Causes Attributable to a 10-ppb Change in the Ambient Ozone Concentration, Stratified According to Selected Risk Factors.*

Stratification Variable	% of Subjects in Stratum	Relative Risk (95% CI)	P Value of Effect Modification
Sex			0.11
Male	43	1.01 (0.99–1.04)	
Female	57	1.04 (1.03–1.07)	
Age at enrollment (yr)			0.74
<50	26	1.00 (0.90–1.11)	
50–65	54	1.03 (1.01–1.06)	
>65	20	1.02 (1.00–1.05)	
Education			0.48
High school or less	43	1.02 (1.00–1.05)	
Beyond high school	57	1.03 (1.01–1.06)	
Body-mass index†			0.96
<25.0	53	1.03 (1.01–1.06)	
25.0–29.9	36	1.03 (0.99–1.06)	
≥30.0	11	1.03 (0.96–1.10)	
$PM_{2.5}$ ($\mu g/m^3$)‡			0.38
<14.3	44	1.05 (1.01–1.09)	
>14.3	56	1.03 (1.00–1.05)	
Region§			0.05
Northeast	24.8	0.99 (0.92–1.07)	
Industrial Midwest	29.7	1.00 (0.91–1.09)	
Southeast	21.0	1.12 (1.05–1.19)	
Upper Midwest	5.2	1.14 (0.68–1.90)	
Northwest	7.7	1.06 (1.00–1.13)	
Southwest	3.9	1.21 (1.04–1.40)	
Southern California	7.8	1.01 (0.96–1.07)	
External temperature (°C)‡¶			0.01
<23.3	24	0.96 (0.90–1.01)	
>23.3 to <25.4	29	0.97 (0.87–1.08)	
>25.4 to <28.7	22	1.04 (0.92–1.16)	
>28.7	25	1.05 (1.03–1.08)	

* $PM_{2.5}$ denotes fine particulate matter consisting of particles that are 2.5 μm or less in aerodynamic diameter. Ozone exposures for the cohort were measured from April to September during the years from 1977 to 2000, with follow-up from 1982 to 2000, with adjustment for individual risk factors, and with baseline hazard function stratified according to age (single-year groupings), sex, and race. These analyses are based on the single-pollutant model for ozone shown in Table 3. Because of rounding, percentages may not total 100.
† The body-mass index is the weight in kilograms divided by the square of the height in meters.
‡ Stratum cutoff is based on the median of the distribution at the metropolitan-area level, not at the subject level.
§ Definitions of regions are those used by the Environmental Protection Agency.[3]
¶ External temperature is calculated as the average daily maximum temperature recorded between April and September from 1977 to 2000.

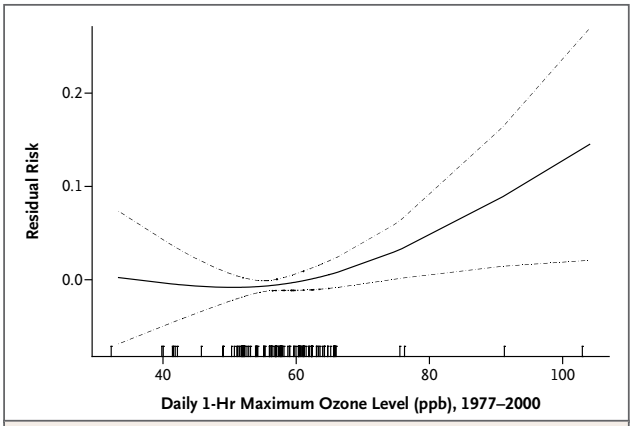

Figure 2. Exposure–Response Curve for the Relation between Exposure to Ozone and the Risk of Death from Respiratory Causes.

The curve is based on a natural spline with 2 df estimated from the residual relative risk of death within a metropolitan statistical area (MSA) according to a random-effects survival model. The dashed lines indicate the 95% confidence interval of fit, and the hash marks indicate the ozone levels of each of the 96 MSAs.

models, but the association with ozone was nonsignificant in two-pollutant models.[3] Further analyses based on 16 years of follow-up in 134 cities produced similarly elevated but nonsignificant associations that were suggestive of effects of summertime (July to September) exposure to ozone on death from cardiopulmonary causes.[5]

The increase in deaths from respiratory causes with increasing exposure to ozone may represent a combination of short-term effects of ozone on susceptible subjects who have influenza or pneumonia and long-term effects on the respiratory system caused by airway inflammation,[24] with subsequent loss of lung function in childhood,[32] young adulthood,[33,34] and possibly later life.[35] If exposure to ozone accelerates the natural loss of adult lung function with age, those exposed to higher concentrations of ozone would be at greater risk of dying from a respiratory-related syndrome.

In our two-pollutant models, the adjusted estimates of relative risk for the effect of ozone on the risk of death from cardiovascular causes were significantly less than 1.0, seemingly suggesting a protective effect. Such a beneficial influence of ozone, however, is unlikely from a biologic standpoint. The association of ozone with cardiovascular end points was sensitive to adjustment for exposure to $PM_{2.5}$, making it difficult to determine precisely the independent contributions of these copollutants to the risk of death. There was notable collinearity between the concentrations of ozone and $PM_{2.5}$.

Furthermore, measurement at central monitors probably represents population exposure to $PM_{2.5}$ more accurately than it represents exposure to ozone. Ozone concentration tends to vary spatially within cities more than does $PM_{2.5}$ concentration, because of scavenging of ozone by nitrogen oxide near roadways.[36] In the presence of a high density of local traffic, the measurement error is probably higher for exposure to ozone than for exposure to $PM_{2.5}$. The effects of ozone could therefore be confounded by the presence of $PM_{2.5}$ because of collinearity between the measurements of the two pollutants and the higher precision of measurements of $PM_{2.5}$.[37]

Measurements of $PM_{2.5}$ were available only for the end of the study follow-up period (1999 and 2000). Widespread collection of these data began only after the EPA adopted regulatory limits on such particulates in 1997. Since particulate air pollution has probably decreased in most metropolitan areas during the follow-up interval of our study, it is likely that we have underestimated the effect of $PM_{2.5}$ in our analysis.

A limitation of our study is that we were not able to account for the geographic mobility of the population during the follow-up period. We had information on home addresses for the CPS II cohort only at the time of initial enrollment in 1982 and 1983. Census data indicate that during the interval between 1982 and 2000, approximately 2 to 3% of the population moved from one state to another annually (with the highest rates in an age group younger than that of our study population).[38] However, any bias due to a failure to account for geographic mobility is likely to have attenuated, rather than exaggerated, the effects of ozone on mortality.

In summary, we investigated the effect of tropospheric ozone on the risk of death from any cause and cause-specific death in a large cohort, using data from 96 metropolitan statistical areas across the United States and controlling for the effect of particulate air pollutants. We were unable to detect a significant effect of exposure to ozone on the risk of death from cardiovascular causes when particulates were taken into account, but we did demonstrate a significant effect of exposure to ozone on the risk of death from respiratory causes.

Supported by the Health Effects Institute.

Dr. Krewski reports receiving grant support from the Natural Sciences and Engineering Research Council of Canada as holder of the Industrial Research Chair in Risk Science. This chair is funded by a peer-reviewed university–industry partnership program. No other potential conflict of interest relevant to this article was reported.

We thank the National Institute of Environmental Health Sciences for providing grant support (ES00260) to the New York University School of Medicine.

This article is dedicated to the memory of our coauthor and friend, Dr. Jeanne Calle, who died unexpectedly on February 17, 2009.

REFERENCES

1. Dockery DW, Pope AC, Xu X, et al. An association between air pollution and mortality in six U.S. cities. N Engl J Med 1993;329:1753-9.
2. Jerrett M, Burnett RT, Ma RJ, et al. Spatial analysis of air pollution and mortality in Los Angeles. Epidemiology 2005; 16:727-36.
3. Krewski D, Burnett RT, Goldberg MS, et al. Reanalysis of the Harvard Six Cities Study and the American Cancer Society Study of Particulate Air Pollution and Mortality: a special report of the institute's Particle Epidemiology Reanalysis Project. Part II. Sensitivity analyses. Cambridge, MA: Health Effects Institute, 2000.
4. Miller KA, Siscovick DS, Sheppard L, et al. Long-term exposure to air pollution and incidence of cardiovascular events in women. N Engl J Med 2007;356:447-58.
5. Pope CA III, Burnett RT, Thun MJ, et al. Lung cancer, cardiopulmonary mortality, and long-term exposure to fine particulate air pollution. JAMA 2002;287:1132-41.
6. Brook RD, Franklin B, Cascio W, et al. Air pollution and cardiovascular disease: a statement for healthcare professionals from the Expert Panel on Population and Prevention Science of the American Heart Association. Circulation 2004;109:2655-71.
7. Pope CA III, Dockery DW. Health effects of fine particulate air pollution: lines that connect. J Air Waste Manag Assoc 2006;56:709-42.
8. Bell ML, Dominici F, Samet JM. A meta-analysis of time-series studies of ozone and mortality with comparison to the National Morbidity, Mortality, and Air Pollution Study. Epidemiology 2005;16:436-45.
9. Ito K, De Leon SF, Lippmann M. Associations between ozone and daily mortality: analysis and meta-analysis. Epidemiology 2005;16:446-57.
10. Levy JI, Chemerynski SM, Sarnat JA. Ozone exposure and mortality: an empiric Bayes metaregression analysis. Epidemiology 2005;16:458-68.
11. Abbey DE, Nishino N, McDonnell WF, et al. Long-term inhalable particles and other air pollutants related to mortality in nonsmokers. Am J Respir Crit Care Med 1999;159:373-82.
12. Review of the national ambient air quality standards for ozone: policy assessment of scientific and technical information. Research Triangle Park, NC: Environmental Protection Agency, 2007. (Report no. EPA-452/R-07-007.)
13. Committee on Estimating Mortality Risk Reduction Benefits from Decreasing Tropospheric Ozone Exposure. Estimating mortality risk reduction and economic benefits from controlling ozone air pollution. Washington, DC: National Academies Press, 2008.
14. The Committee on the Medical Effects of Air Pollutants. The effects on health of long-term exposure to ozone. London: Department of Health, 2007. (Accessed February 17, 2009, at http://www.advisorybodies.doh.gov.uk/comeap/statementsreports/chptlongtermexpoozone.pdf.)
15. Krewski D, Jerrett M, Burnett RT, et al. Extended follow-up and spatial analysis of the American Cancer Society study linking particulate air pollution and mortality. Boston: Health Effects Institute (in press).
16. American Cancer Society. Cancer prevention study overviews. (Accessed February 17, 2009, at http://www.cancer.org/docroot/RES/content/RES_6_2_Study_Overviews.asp?)
17. Thun MJ, Calle EE, Namboodiri MM, et al. Risk factors for fatal colon cancer in a large prospective study. J Natl Cancer Inst 1992;84:1491-500.
18. Calle EE, Terrell DD. Utility of the National Death Index for ascertainment of mortality among Cancer Prevention Study II participants. Am J Epidemiol 1993;137: 235-41.
19. Jerrett M, Burnett RT, Willis A, et al. Spatial analysis of the air pollution-mortality relationship in the context of ecologic confounders. J Toxicol Environ Health A 2003;66:1735-77.
20. Willis A, Krewski D, Jerrett M, Goldberg MS, Burnett RT. Selection of ecologic covariates in the American Cancer Society study. J Toxicol Environ Health A 2003; 66:1563-89.
21. Ma R, Krewski D, Burnett RT. Random effects Cox models: a Poisson modelling approach. Biometrika 2003;90:157-69.
22. Siemiatycki J, Krewski D, Shi Y, Goldberg MS, Nadon L, Lakhani R. Controlling for potential confounding by occupational exposures. J Toxicol Environ Health A 2003;66:1591-603.
23. Chao A, Thun MJ, Jacobs EJ, Henley SJ, Rodriguez C, Calle EE. Cigarette smoking and colorectal cancer mortality in the Cancer Prevention Study II. J Natl Cancer Inst 2000;92:1888-96.
24. Mudway IS, Kelly FJ. An investigation of inhaled ozone dose and the magnitude of airway inflammation in healthy adults. Am J Respir Crit Care Med 2004;169:1089-95.
25. Brown JS, Bateson TF, McDonnell WF. Effects of exposure to 0.06 ppm ozone on FEV1 in humans: a secondary analysis of existing data. Environ Health Perspect 2008;116:1023-6.
26. McConnell R, Berhane K, Gilliland F, et al. Asthma in exercising children exposed to ozone: a cohort study. Lancet 2002;359:386-91. [Erratum, Lancet 2002; 359:896.]
27. Delfino RJ, Quintana PJ, Floro J, et al. Association of FEV1 in asthmatic children with personal and microenvironmental exposure to airborne particulate matter. Environ Health Perspect 2004;112:932-41.
28. Thurston GD, Lippmann M, Scott MB, Fine JM. Summertime haze air pollution and children with asthma. Am J Respir Crit Care Med 1997;155:654-60.
29. Spektor DM, Lippmann M, Lioy PJ, et al. Effects of ambient ozone on respiratory function in active, normal children. Am Rev Respir Dis 1988;137:313-20.
30. Tager IB, Balmes J, Lurmann F, Ngo L, Alcorn S, Künzli N. Chronic exposure to ambient ozone and lung function in young adults. Epidemiology 2005;16:751-9.
31. Yang Q, Chen Y, Shi Y, Burnett RT, McGrail KM, Krewski D. Association between ozone and respiratory admissions among children and the elderly in Vancouver, Canada. Inhal Toxicol 2003;15: 1297-308.
32. Rojas-Martinez R, Perez-Padilla R, Olaiz-Fernandez G, et al. Lung function growth in children with long-term exposure to air pollutants in Mexico City. Am J Respir Crit Care Med 2007;176:377-84.
33. Galizia A, Kinney PL. Long-term residence in areas of high ozone: associations with respiratory health in a nationwide sample of nonsmoking young adults. Environ Health Perspect 1999;107:675-9.
34. Chen C, Arjomandi M, Balmes J, Tager IB, Holland N. Effects of chronic and acute ozone exposure on lipid peroxidation and antioxidant capacity in healthy young adults. Environ Health Perspect 2007;115:1732-7.
35. Ackermann-Liebrich U, Leuenberger P, Schwartz J, et al. Lung function and long term exposure to air pollutants in Switzerland. Am J Respir Crit Care Med 1997;155:122-9.
36. McConnell R, Berhane K, Yao L, Lurmann FW, Avol E, Peters JM. Predicting residential ozone deficits from nearby traffic. Sci Total Environ 2006;363:166-74.
37. Zidek JV, Wong H, Le ND, Burnett R. Causality: measurement error and multicollinearity in epidemiology. Environmetrics 1996;7:441-51.
38. Schachter J. Geographical mobility: population characteristics. March 1999 to March 2000. Current population reports PPL-144. Washington, DC: Census Bureau, May 2001. (Accessed February 17, 2009, at http://www.census.gov/prod/2001pubs/p20-538.pdf.)

Chronic Exposure to Ambient Ozone and Asthma Hospital Admissions among Children

Shao Lin,[1] Xiu Liu,[1] Linh H. Le,[2] and Syni-An Hwang[1]

[1]Center for Environmental Health, New York State Department of Health, Troy, New York, USA; [2]Bureau of Healthcom Network System Management, New York State Department of Health, Menands, New York, USA

Background: The association between chronic exposure to air pollution and adverse health outcomes has not been well studied.

Objective: This project investigated the impact of chronic exposure to high ozone levels on childhood asthma admissions in New York State.

Methods: We followed a birth cohort born in New York State during 1995–1999 to first asthma admission or until 31 December 2000. We identified births and asthma admissions through the New York State Integrated Child Health Information System and linked these data with ambient ozone data (8-hr maximum) from the New York State Department of Environmental Conservation. We defined chronic ozone exposure using three indicators: mean concentration during the follow-up period, mean concentration during the ozone season, and proportion of follow-up days with ozone levels > 70 ppb. We performed logistic regression analysis to adjust for child's age, sex, birth weight, and gestational age; maternal race/ethnicity, age, education, insurance status, smoking during pregnancy, and poverty level; and geographic region, temperature, and copollutants.

Results: Asthma admissions were significantly associated with increased ozone levels for all chronic exposure indicators (odds ratios, 1.16–1.68), with a positive dose–response relationship. We found stronger associations among younger children, low sociodemographic groups, and New York City residents as effect modifiers.

Conclusion: Chronic exposure to ambient ozone may increase the risk of asthma admissions among children. Younger children and those in low socioeconomic groups have a greater risk of asthma than do other children at the same ozone level.

Key words: air pollution, asthma, children, chronic, hospital admissions, ozone. *Environ Health Perspect* 116:1725–1730 (2008). doi:10.1289/ehp.11184 available via *http://dx.doi.org/* [Online 10 September 2008]

The acute health effects of exposure to ambient ozone have been examined in many geographic regions. Although the findings are inconsistent, potential adverse effects reported include decrements in lung function, airway inflammation, symptoms of asthma, increases in hospitalization for respiratory diseases, and excess mortality (Schwela 2000). On the other hand, the health effects of chronic exposure to ozone have been less studied, and the results are inconclusive. Several studies have reported that long-term exposure to ozone may reduce lung function in school children and adults (Galizia and Kinney 1999; Peters et al. 1999; Qian et al. 2005; Rojas-Martinez et al. 2007) and increase the prevalence of asthma and asthmatic symptoms (Hwang et al. 2005; Ramadour et al. 2000; Wang et al. 1999). In contrast, other studies found an insignificant or negative association between respiratory health effects and chronic ozone exposure (Gauderman et al. 2004; Karr et al. 2007; Zemp et al. 1999). No studies have examined health effects of chronic ozone exposure among a birth cohort. Biologic studies provided plausibility that chronic exposure to ozone is associated with elevated oxidative damage, which might be involved in development of asthma and decrement of lung function (Chen et al. 2007; Mudway and Kelly 2000).

In New York State, asthma hospitalization rates remain considerably higher (20.4 per 10,000) than the U.S. rate of 16.9 per 10,000 population in 2002 (American Lung Association 2004; New York State Department of Health 2005). Young children are a vulnerable population with respect to air pollutants, given their narrow airways, higher breathing rate, developing lungs and immune systems, and more time spent outdoors. Most prior studies have focused on adults and school-age children and analyzed less severe health outcomes than hospitalizations. The effect of chronic exposure to high levels of air pollution in early life and its subsequent impact on childhood asthma admissions is unclear. In addition, the interactive effects between maternal/birth characteristics and air pollution on childhood asthma hospital admissions have rarely been studied. The purpose of this study was to investigate the association between chronic exposure to ozone and childhood asthma admissions. We also examined whether maternal and birth characteristics interacted with the impact of air pollution on asthma hospitalization in early life.

Materials and Methods

Study population and health outcome. In this retrospective cohort study we analyzed a New York State birth cohort born between 1 January 1995 and 31 December 1999 and followed each individual until the first asthma hospital admission or 31 December 2000. We defined asthma hospital admissions as children who were first admitted to a hospital from 1 January 1996 through 31 December 2000 with a principal diagnosis of *International Classification of Diseases, 9th Revision*, code 493 (U.S. Department of Health and Human Services 1991). We excluded children residing in Staten Island from the study cohort because a substantial amount of data was missing for ambient ozone in that area. We did not consider admitted children who were < 1 year of age because of difficulties in differentiating asthma from bronchiolitis in this age group (Kramarz et al. 2000). This study was approved by the New York State Department of Health Institutional Review Board and complied with all applicable U.S. regulations.

We obtained information on hospital admissions and maternal and birth characteristics from the New York State Integrated Child Health Information System (ICHIS). The ICHIS links various sources of New York State data, including the immunization records, birth certificates, hospital discharges, and death certificates. The birth certificate portion included individual-level information on residential address, maternal demographics, and birth characteristics; the hospital discharge portion contained the cause and date of hospital admission and home address at admission. We obtained regional demographic information from the 2000 U.S. Census (U.S. Census Bureau 2000), including land area, population density, hospital density, percentage of individuals living below poverty level, and median household income. Thus, potentially important individual and neighborhood confounders can be

Address correspondence to S. Lin, Bureau of Environmental and Occupational Epidemiology, New York State Department of Health, 547 River St., Room 200, Troy, NY 12180 USA. Telephone: (518) 402-7990. Fax: (518) 402-7959. E-mail: sxl05@health.state.ny.us

We thank R. Walker, M. Herdt-Losavio, W. Liu, and R. Jones for their contributions to the manuscript.

This work was supported by a grant from National Environmental Public Health Tracking Program, Centers for Disease Control and Prevention (u50/ccu422440).

The authors declare they have no competing financial interests.

Received 17 December 2007; accepted 10 September 2008.

controlled when assessing the relationship between childhood asthma admissions and chronic exposure to ambient ozone.

Air pollution data and exposure indicators. We obtained hourly ambient ozone data from the New York State Department of Environmental Conservation (NYSDEC). These data (reported in parts per billion) were measured hourly for each day. We used the 8-hr maximum hourly value during the peak outdoor exposure time (1000 to 1800 hours) in this study to represent the daily ozone level. We included 32 ozone monitoring sites and divided them into 11 ozone regions in New York State (Figure 1) according to their spatial and temporal correlations, wind direction, and traffic pattern. In general, we used a linear regression model with a fixed-origin intercept to assess the spatial correlation among monitor pairs as a function of distance. We performed empirical semivariance analysis and a total count of occurrences above a specific concentration to evaluate the spatial variation. The resulting 11 ozone regions are very similar to the air quality health advisory regions developed by NYSDEC (2008). If more than one monitoring site was located in one ozone region, we used the average value of the 8-hr maximum from multiple monitoring sites to represent the regional data. We assessed children's chronic ozone exposure as both continuous and categorical variables by identifying the individual ozone region based on their residential histories. The continuous ozone variable included the mean concentrations and the exceedance proportion. Mean concentration was the arithmetic mean of the regional 8-hr ozone maximum for each child during two different time periods: the entire follow-up period and ozone seasons (April–October) during the follow-up period. For children who had hospital admissions during the defined periods, we calculated the mean concentration between the date of birth and the date of admission. For children who had no hospital admissions, we calculated the mean concentration of the follow-up period and the ozone season between the date of birth and the end of the study. We assessed the risk of hospital admissions associated with chronic ozone exposure using a 1-ppb increase in mean concentration during the defined period. The exceedance proportion is the proportion of follow-up days with ozone levels > 70 ppb, which is our 90th percentile of year-round ozone over the entire follow-up period. This indicator not only reflects the specific days exposed to high ozone levels, but also includes the proportion of days exposed to high ozone levels for each child over the follow-up period. Therefore, it captures both the cumulative and chronic nature of exposures. We used the interquartile range (IQR; 75th to 25th quartile) as the unit change in the models for the continuous exceedance proportion exposure.

To estimate the potential dose–response effect, we categorized children as having low, medium, or high ozone exposure based on the tertile ranking of their mean ozone concentration during the follow-up period in New York City and the rest of New York State separately to adjust for geographic differences. The ranges for low, medium, and high exposure were 31.46–37.29 ppb, 37.30–38.11 ppb, and 38.12–50.13 ppb, respectively, for children living in New York City; and 33.50–42.57 ppb, 42.58–45.06 ppb, and 45.07–55.19 ppb for children living in other New York State regions.

Data linkage methods and geocoding. According to the enrollment criteria described above, we identified 1,433,826 children from the ICHIS database. We geocoded residential addresses at birth (from the birth certificate database) at the street level to determine the geographic region of air pollution using Map Marker (Mapinfo Corp., Troy, NY). In general, we geocoded 84% of the residential addresses automatically; we could not geocode 16% and excluded them from analysis. To assign an ozone region to individual residential addresses, we overlaid the map of geocoded addresses onto the map of ozone regions using Mapinfo (Mapinfo Corp.). Finally, we linked the ambient ozone data from NYSDEC to the asthma outcome, individual risk factors from ICHIS data, and regional level factors from the U.S. Census (U.S. Census Bureau 2000).

To evaluate study population dynamics, we compared exposure regions based on the original residential addresses retrieved from the birth certificate database to the secondary residences extracted from the immunization record and hospital discharge databases. Our study population was very stable, and we found a consistent ozone region (i.e., change in address did not affect exposure region classification) for 72.6% of children. For 27.2% of children, address information could be obtained from only one source: 18.9% from the birth certificate only and 8.3% from the immunization record only. For these children, we geocoded the residential address from the unique database. Only 0.2% of children had address changes that placed them in a different ozone region. For these children, we calculated the effective exposure corresponding to the time window across these regions. If a child was born in ozone region "A" and was admitted to the hospital at a later date in region "B," we considered the child spent half the time in region "A" and half the time in region "B."

Statistical analysis. In this study we aimed to predict the risk of having asthma admissions in a birth cohort, but the time to the first admission in children that is usually analyzed in survival models was not our primary interest. We therefore used a multivariate logistic regression model rather than a survival analysis. By incorporating children's ages (at admission or the end of the study) in the logistic regression analysis, we also appropriately considered and controlled the time dimension of exposure. We computed adjusted odds ratios (ORs) and 95% confidence intervals (CIs) while controlling for birth and maternal confounding variables and geographic regions. We fitted regression models separately for continuous and categorical chronic ozone exposures. We selected confounding variables based on the epidemiologic literature and the exploratory results using univariate analyses that suggested possible associations with asthma admissions at p-values ≤ 0.05. These confounders included child's sex, birth weight (≤ 2,500 g, > 2,500 g), gestational age (< 260 days, ≥ 260 days), age at admission or end of the study (range, 1–6 years) maternal

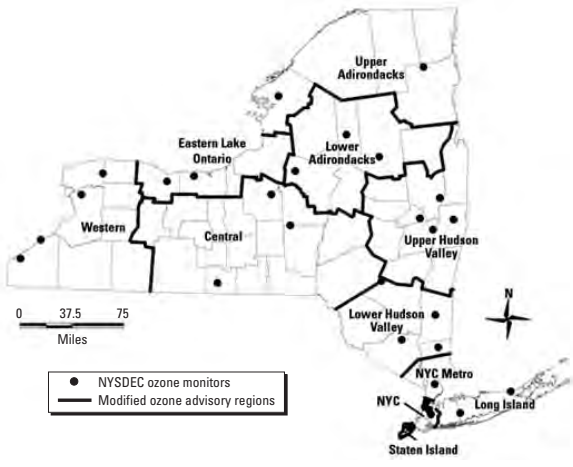

Figure 1. Ozone exposure regions in New York State used in this study. NYC, New York City.

age at delivery (< 20 or > 35 years, 20–35 years) and smoking status during pregnancy (yes, no). As a measure of sociodemographic status, we controlled for individual-level risk factors such as maternal race (black, other), ethnicity (Hispanic, non-Hispanic), education level (< 12 years, ≥ 12 years), insurance type during pregnancy (Medicaid, self-paid, and other) and geographic area (New York City vs. other). We also ascertained census block–group information such as median household income, percentage of population living below poverty level (the highest quartile vs. others), and hospital density (i.e., number of hospitals per 100 km^2 in each ozone region) to control for medical care access at the neighborhood level. Because hospital density was highly correlated with geographic region (Pearson correlation $r = 0.99$), and median household income was correlated with percent below poverty (Pearson correlation $r = 0.69$), we retained all confounders except for hospital density and median household income in the final multivariate regression models because of significant p-values (< 0.01). We also adjusted the proportion of days during the entire follow-up period with extreme temperatures, defined as the 90th percentile of the daily average temperature (72.3°F), in the final model, in which we compared children in the highest quartile of extreme temperature days (high-temperature group) with all others (low-temperature group).

We also assessed and controlled for the effects of copollutants by using the Air Quality Index (AQI) (U.S. Environmental Protection Agency 1999), which is a standard system representing the levels of multiple air pollutants, including ambient particulate matter (particulate matter with aerodynamic diameters ≤ 10 and 2.5 μm), nitrogen dioxide, carbon monoxide, and sulfur dioxide. We calculated the AQI for each pollutant in each ozone region and chose the maximum value to represent the daily AQI for that region. Cumulative AQI was the average level of daily AQI during the follow-up period. We used the AQI variable only in the analysis for children born between 1996 and 1999, but did not retain it in the final analysis model because AQI data were not available for 1995 and we would have missed 250,000 eligible births if we had included AQI.

We further added interaction terms to the logistic regression model with continuous ozone exposure to assess potential effect modifications. We used mean ozone concentration during the entire follow-up period to create the interaction terms with all dichotomous confounders. Once we identified significant interaction terms (p-value < 0.05), we performed stratified analysis to assess the differential impacts of birth and maternal risk on the association between air pollution and asthma admissions. The Hosmer–Lemeshow test showed that the models fitted reasonably well. We performed all statistical analyses with SAS software, version 9.1 (SAS Institute, Inc., Cary, NC).

Results

We included 1,204,396 eligible births in the analysis, with 10,429 (0.87%) children admitted to the hospital for asthma by 31 December 2000. Children in this study were between 1 and 6 years of age. Overall, the average follow-up time was 26.6 months for children with asthma admissions and 42 months for all births. The mean ozone level during the entire follow-up period (41.06 ppb) was lower than the mean concentration in the ozone season (50.62 ppb) (data not shown). The average exceedance proportion was 9.72% among the study population, ranging from 1.66% to 26.27%. Table 1 summarizes the average ozone levels, total area of region, and key population characteristics by exposure regions. The western region had the highest ozone level in New York State (47.8 ppb), and New York City had the lowest ozone level among 10 New York State regions (37.5 ppb). However, population density, birth density, percentages of blacks and Hispanics, and low level of maternal education in New York City were significantly higher than in the rest of New York State.

As described in Table 2, we found significant positive associations between chronic ozone level and asthma hospital admissions for all exposure indicators after adjusting for

Table 2. Association between ozone exposure indicators, birth and maternal risk factors, and asthma hospitalizations.

Characteristic	Adjusted OR (95% CI)
Ozone exposure (1-ppb increase/day)[a]	
Mean concentration during the follow-up period	1.16 (1.15–1.17)
Mean concentration during the ozone season	1.22 (1.21–1.23)
Exceedance proportion (%) > 70 ppb with IQR increase[b]	1.68 (1.64–1.73)
Other risk factors[c]	
Temperature	1.06 (1.00–1.13)
Child's age (month)	0.93 (0.93–0.94)
Race: black vs. other	1.97 (1.88–2.07)
Sex: female vs. male	0.58 (0.56–0.61)
Ethnicity: Hispanic vs. non-Hispanic	1.99 (1.89–2.09)
Birth weight: low vs. normal	1.55 (1.44–1.67)
Gestational age: preterm vs. full term	1.36 (1.27–1.45)
Maternal education: < high school vs. ≥ high school	1.18 (1.12–1.24)
Maternal smoking during pregnancy: yes vs. no	1.39 (1.29–1.49)
Geographic region: New York City vs. other regions	4.21 (3.77–4.70)
Maternal age (years): < 20 or > 35 vs. 20–35	1.06 (1.00–1.11)
Poverty level: highest 25th quartile vs. other	1.21 (1.15–1.27)
Maternal insurance	
Medicaid vs. other	1.26 (1.19–1.33)
Self-paid vs. other	1.19 (1.10–1.29)

[a]Adjusted for geographic region, child's sex, child's age, birth weight, gestational age, maternal race, ethnicity, maternal age, education, maternal insurance, smoking status during pregnancy, poverty level, and temperature. [b]IQR is a 2.51% increase. [c]ORs are from the model including the mean concentration during the follow-up period.

Table 1. Summary of ozone levels, land use, and population characteristics by ozone region in New York State.

Ozone region	Mean ozone[a] (ppb) during follow-up	Land area[b] (km^2)	Population density[b] (per km^2)	Birth density in cohort (per km^2)	Percent black in cohort	Percent Hispanic in cohort	Percent maternal low education in cohort
Upper Adirondacks	44.45	21,820	18.0	0.20	3.46	3.20	15.52
Lower Adirondacks	43.86	16,806	23.5	0.26	4.70	2.67	17.27
Central	45.38	30,414	52.6	0.60	7.08	2.36	16.58
Upper Hudson Valley	46.21	15,118	73.0	0.81	7.97	4.17	14.15
Lower Hudson Valley	44.74	10,218	94.8	1.16	8.18	11.95	15.09
Western	47.78	16,699	95.3	1.15	12.96	4.11	14.47
Eastern Lake Ontario	41.84	5,741	165.7	2.16	16.33	6.87	16.64
New York City metro[c]	40.49	1,572	769.7	10.70	15.57	24.51	12.66
Long Island	42.69	3,105	886.9	11.76	10.15	16.14	10.49
New York City[d]	37.51	634	11929.4	174.76	34.32	41.27	25.49

[a]The average of the maximum hourly concentration measured between 1000 and 1800 hours during the follow-up period (1 January 1995 to 31 December 2000). [b]We used 2000 census data (U.S. Census 2000) to obtain land area and population density information. [c]Includes Rockland and Westchester Counties. [d]Includes Bronx, New York, Kings, and Queens Counties.

potential confounding variables (ORs = 1.16–1.68). The risk of hospital admissions increased 22% with a 1-ppb increase in mean ozone concentration during the ozone season. Indicators using the entire follow-up period (OR = 1.16) showed similar but weaker elevated risks for asthma admissions. When estimating the ozone effect using the exceedance proportion, we observed a significant increase (OR = 1.68; 95% CI, 1.64–1.73) in hospital admissions associated with an IQR (2.51%) increase in ozone.

Because the effects of other risk factors on asthma admissions were similar when using three ozone indicators, to simplify the results Table 2 shows the effects of other risk factors using only the mean concentration during the entire follow-up period as the exposure included in the model. Children who are black or Hispanic, whose mother had a lower level of education, Medicaid, or self-paid insurance, and those residing in areas with a high percentage of below-poverty populations had a higher risk of asthma admissions. Low birth weight, preterm birth, and maternal smoking during pregnancy were associated with increased asthma admissions. Geographic region was the strongest risk factor associated with asthma admissions in this study. Children living in New York City were 4.21 (95% CI, 3.77–4.70) times more likely to be admitted to a hospital than children living in other regions of New York State. Child's age and female sex were negatively associated with asthma admissions. Maternal age and extreme temperature were not associated with increased asthma admissions. Additionally, we also examined the ozone–asthma association during the entire follow-up period after controlling for AQI and other confounders. The adjusted OR after controlling for AQI increased slightly (data not shown; OR = 1.24; 95% CI, 1.23–1.25) compared with the unadjusted OR of 1.16.

To control for the impacts of other confounders such as admission policy, home environment, and disease management, which are unavailable in ICHIS data but are related to hospital admissions, we used a "negative control," admissions due to gastroenteritis, in a sensitivity analysis. We found that chronic exposure to ozone was not positively associated with hospital admissions due to gastroenteritis (OR = 0.57; 95% CI, 0.54–0.59) after adjusting for confounders similar to those used in the asthma analysis.

To address the relationship between ozone dose and health effects, we analyzed dose response separately with categorical exposures in New York City and other regions of New York State (Figure 2). After adjustment for other covariates, we observed significantly positive dose–response relationships in both regions; that is, higher ozone exposure was associated with a higher risk of admissions.

We first identified the interactive effect of maternal/infant factors and chronic ozone levels on asthma hospital admissions from the logistic regression model and then investigated it using stratification analysis (Figure 3). We found the largest disparity for geographic regions; that is, the ozone-asthma association was stronger among New York City residents (OR = 1.43) than among other regions (OR = 1.11). Similarly, the effects of ozone on asthma admission were significantly higher among children 1–2 years of age (OR = 1.29), children living in poor neighborhoods (i.e., highest quartile of percent below poverty; OR = 1.25), children whose mothers had low education (OR = 1.22), Medicaid/self-paid births (OR = 1.22), and Hispanics (OR = 1.27) compared with older children (OR = 1.03), children in good neighborhoods (OR = 1.14), mothers with high school education (OR = 1.14), births covered by other insurance (OR = 1.11), and non-Hispanic children (OR = 1.13). However, we found the ozone–asthma association to be weaker among children born to smokers than among those born to nonsmokers (OR = 1.10 and 1.18, respectively).

Discussion

In this study, we found that chronic exposure to ambient ozone in early life was significantly and positively associated with an increased risk of asthma hospital admissions among a birth cohort in New York State. Multivariate analyses using three different exposure indicators produced similar results. We also observed positive dose–response trends in New York City and the remainder of New York State.

Many time-series studies have found that hospitalizations or emergency visits due to asthma may increase during the periods of short-term exposure to increased ozone levels (Burnett et al. 2001; Gent et al. 2003; Tolbert et al. 2000). Although few other studies have assessed the risk of childhood asthma hospitalizations associated with chronic ozone exposure, the findings of this study are consistent with several previous studies among children. Three cross-sectional studies observed a positive relationship between chronic exposure to ozone, and prevalence of asthma and asthmatic symptoms in school children (Hwang et al. 2005; Ramadour et al. 2000; Wang et al. 1999). Peters et al. (1999) and Rojas-Martinez et al. (2007) have reported a reduction in lung function associated with higher ozone concentration among school-age children in two prospective studies. One cohort study in Southern California found that in communities with high ozone levels, children who played sports outdoors had 3.3 (95% CI, 1.9–5.8) times the risk of developing asthma compared with children not playing sports (McConnell et al. 2002). Another birth cohort study by Brauer et al. (2007) also reported a significant association (OR = 1.26) between traffic-related pollution and both doctor-diagnosed asthma and self-reported wheeze among children < 4 years of age, but ozone was not measured in that project. No previous studies examined a similar health effect from chronic ozone exposure among young children in a birth cohort for direct comparison with our study. Taken together with the present study, all study findings in the current literature indicate that ozone might have both acute and chronic effects on the development of asthma and cause a subsequent increase in asthma

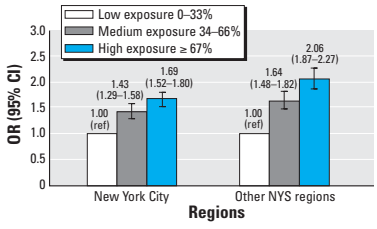

Figure 2. Ozone–asthma dose–response relationship using the mean concentration during the entire follow-up period, adjusted for child's sex, age, birth weight, and gestational age; maternal race, ethnicity, age, education, insurance, and smoking status during pregnancy; and regional poverty level and temperature. NYS, New York State. ref, referent.

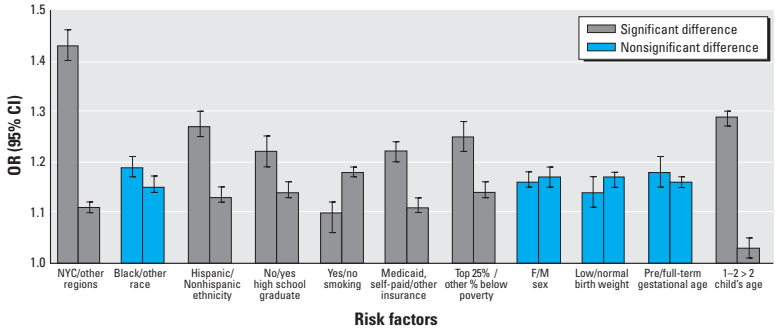

Figure 3. Stratified analysis of ozone–asthma association, using the mean concentration during the entire follow-up period. NYC, New York City.

hospital admissions. On the other hand, other studies (Gauderman et al. 2004; Zemp et al. 1999) found no significant association between exposure to ozone and respiratory morbidity, and Karr et al. (2007) reported a reduced risk (OR = 0.92; 95% CI, 0.88–0.97) of hospitalization for infant bronchiolitis with a 14-ppb increase in ozone exposure. Despite these studies showing no effect, our study has contributed another confirmation of positive associations between ozone exposure and respiratory outcomes.

Interestingly, in the present study, the associations between elevated ozone and increased asthma hospital admissions were stronger in young children, Medicaid/self-paid births, Hispanics, children living in poor communities or whose mothers had low education levels, and New York City residents. These results suggest that chronic exposure to ambient ozone did not have an equal asthma effect on children. Specifically, very young children were more susceptible to ozone exposure, and children with low socioeconomic status (SES) had a greater risk of asthma admissions at the same ozone level. Children < 2 years of age have been reported to be more susceptible to air pollutants compared with other children (Braga et al. 2001). Son et al. (2006) found a similar interactive effect of SES characteristics on the relationship between short-term exposure to high ozone levels and asthma hospital admissions. In New York State, Lin et al. (1999) found that areas with a high proportion of low-income, low-education level and high population density (i.e., crowded living conditions) experience higher rates of asthma hospitalizations. In the present study, maternal smoking status during pregnancy weakened the ozone effect on asthma admissions. This finding has not been reported in previous air pollution studies and should be interpreted with caution because maternal smoking information from the birth certificate was based on self-report. Smoking tends to be underreported by study participants in general, and smoking while pregnant is stigmatized. In addition, some quitters might go back to smoking after their children were born or some time before the child's hospital admission.

Although survival analysis is a method commonly used to examine time-varying events, logistic regression analysis has also been widely used in many air pollution and environmental epidemiologic studies (Andersen et al. 2008; Brauer et al. 2007; Hwang et al. 2005; Kumar et al. 2008; Morgenstern et al. 2008; Ramadour et al. 2000; Wang et al. 1999). Because the purpose of the present study is to predict the probability of occurrence of a hospital admission for asthma rather than time to disease occurrence, logistic regression analysis is an appropriate option. Additionally, in a survival analysis of a birth cohort, time to event is directly correlated with child's age. However, asthma hospital admissions are also strongly associated with age. Therefore, by including child's age in our logistic regression model, we could not only control for the confounding (and/or independent) effect of age but also incorporate the varying time dimension of exposure—that is, the length of time exposed for each child—which is the same as child's age. To validate our analytical method and the findings, we conducted a proportional hazards model for the same data in New York City. This sensitivity analysis yielded similar results between asthma admissions and chronic exposure to ozone.

This is one of the largest studies (n = 1,204,396 births) to date examining the relationship between chronic exposure to ambient ozone during early life and asthma hospital admissions among children. Data obtained from ICHIS had health, birth, and maternal information and were then combined with air pollution data. This integrated environmental health database provides a unique birth cohort to follow health end points and to estimate incidence. We selected a vulnerable subgroup, children < 6 years of age, as our study population. Unlike adults, children may be more affected by air pollutants because of higher vulnerability and different behavior (Trasande and Thurston 2005). Children's lungs and immune systems are developing, and exposure to high ozone levels may impair the normal process of development (Plopper and Fanucchi 2000; Trasande and Thurston 2005). In addition, children are more active than adults are and tend to be outside in the summer and the afternoon, which may result in higher individual exposure to ozone (Trasande and Thurston 2005; U.S. Environmental Protection Agency 2002). This study also used asthma hospital admissions from an existing file as the health outcome, which comes from the hospitals and is not subject to self-reporting bias. Although some studies have used cumulative ozone as an exposure indicator, to our knowledge this is the first study to specifically examine the association between chronic exposure to ambient ozone and first asthma hospital admission in children. This study also assessed the interactive effects of maternal/infant factors on the ozone–asthma association, the confounding effects of temperature and AQI, and the ozone effect on a control disease to estimate confounding bias.

Several limitations should be considered when interpreting these findings. First, hospital admissions data capture only the most severe cases of asthma and may not be representative of mild or less severe cases. Second, we have no personal activity information, so we are unable to calculate individual cumulative exposure accurately. Third, although many important confounding variables have been controlled in the analysis, further adjustment of other confounders such as genetic susceptibility may alter the associations. Finally, ICHIS data can identify the address changes over time only when a hospital admission occurred or if immunization data are available. For children who have a residential address from only one database, the accuracy of their exposure calculation is questionable. However, this misclassification bias would be nondifferential and toward the null. Our data also suggested stability in the study population, because most of the population did not change their exposure region over time, and few children lived in multiple ozone regions.

This study provides evidence of a positive association between chronic exposure to ozone and childhood asthma hospital admissions. Children who are exposed to high ozone levels over time are more likely to develop asthma severe enough to be admitted to the hospital. Further adjustment for temperature, AQI, and maternal/birth factors did not alter the ozone–asthma association. This study also found that socioeconomic characteristics may contribute to differential ozone–asthma associations and should be of special concern. The findings from the present study not only will help health professionals identify environmental risk factors for asthma admission, but also will help discern the impairment from chronic exposure to high ozone levels over time. Minimizing outdoor exposure opportunities on high-ozone days may be a viable strategy for reducing the burden of asthma hospital admissions in children. Further studies in a birth cohort examining health effect of chronic ozone exposure are needed to confirm our findings.

References

American Lung Association. 2004. Trends in Asthma Morbidity and Mortality. American Lung Association Epidemiology and Statistics Unit. Available: http://www.lungusa.org/atf/cf/%7B7A8D42C2-FCCA-4604-8ADE-7F5D5E762256%7D/ASTHMA1.PDF [accessed 1 June 2008].

Andersen ZJ, Loft S, Ketzel M, Stage M, Scheike T, Hermansen MN, et al. 2008. Ambient air pollution triggers wheezing symptoms in infants. Thorax 63(8):710–716.

Braga AL, Saldiva PH, Pereira LA, Menezes JJ, Conceicao GM, Lin CA, et al. 2001. Health effects of air pollution exposure on children and adolescents in São Paulo, Brazil. Pediatr Pulmonol 31:106–113.

Brauer M, Hoek G, Smit HA, de Jongste JC, Gerritsen J, Postma DS, et al. 2007. Air pollution and development of asthma, allergy and infections in a birth cohort. Eur Respir J 29:879–888.

Burnett RT, Smith-Doiron M, Stieb D, Raizenne ME, Brook JR, Dales RE, et al. 2001. Association between ozone and hospitalization for acute respiratory diseases in children less than 2 years of age. Am J Epidemiol 153:444–452.

Chen C, Arjomandi M, Balmes J, Tager I, Holland N. 2007. Effects of chronic and acute ozone exposure on lipid peroxidation and antioxidant capacity in healthy young adults. Environ Health Perspect 115:1732–1737.

Galizia A, Kinney PL. 1999. Long-term residence in areas of high ozone: associations with respiratory health in a nationwide sample of nonsmoking young adults. Environ Health Perspect 107:675–679.

Gauderman WJ, Avol E, Gilliland F, Vora H, Thomas D, Berhane K,

et al. 2004. The effect of air pollution on lung development from 10 to 18 years of age. N Engl J Med 351:1057–1067.

Gent JF, Triche EW, Holford TR, Belanger K, Bracken MB, Beckett WS, et al. 2003. Association of low-level ozone and fine particles with respiratory symptoms in children with asthma. JAMA 290:1859–1867.

Hwang BF, Lee YL, Lin YC, Jaakkola JJ, Guo YL. 2005. Traffic related air pollution as a determinant of asthma among Taiwanese school children. Thorax 60:467–473.

Karr C, Lumley T, Schreuder A, Davis R, Larson T, Ritz B, et al. 2007. Effects of subchronic and chronic exposure to ambient air pollutants on infant bronchiolitis. Am J Epidemiol 165:553–560.

Kramarz P, DeStefano F, Gargiullo PM, Davis RL, Chen RT, Mullooly JP, et al. 2000. Influenza vaccination in children with asthma in health maintenance organizations. Vaccine Safety Datalink Team. Vaccine 18:2288–2294.

Kumar R, Yu Y, Story RE, Pongracic JA, Gupta R, Pearson C, et al. 2008. Prematurity, chorioamnionitis, and the development of recurrent wheezing: a prospective birth cohort study. J Allergy Clin Immunol 121(4):878–884.

Lin S, Fitzgerald E, Hwang SA, Munsie JP, Stark A. 1999. Asthma hospitalization rates and socioeconomic status in New York State (1987–1993). J Asthma 36:239–251.

McConnell R, Berhane K, Gilliland F, London SJ, Islam T, Gauderman WJ, et al. 2002. Asthma in exercising children exposed to ozone: a cohort study. Lancet 359:386–391.

Morgenstern V, Zutavern A, Cyrys J, Brockow I, Koletzko S, Krämer U, et al. 2008. Atopic diseases, allergic sensitization, and exposure to traffic-related air pollution in children. Am J Respir Crit Care Med. 2008 Jun 15;177(12):1331–1337.

Mudway IS, Kelly FJ. 2000. Ozone and the lung: a sensitive issue. Mol Aspects Med 21:1–48.

New York State Department of Health. 2005. New York State Asthma Surveillance Summary Report. Available: http://www.health.state.ny.us/diseases/asthma/pdf/asthmareport.pdf [accessed 1 June 2008].

NYSDEC (New York State Department of Environmental Conservation). 2008. Air Quality Index (AQI) Forecast and Current Observations for New York State. Available: http://www.dec.ny.gov/chemical/34985.html [accessed 1 June 2008].

Peters JM, Avol E, Gauderman WJ, Linn WS, Navidi W, London SJ, et al. 1999. A study of twelve southern California communities with differing levels and types of air pollution. II. Effects on pulmonary function. Am J Respir Crit Care Med 159:768–775.

Plopper CG, Fanucchi MV. 2000. Do urban environmental pollutants exacerbate childhood lung diseases? Environ Health Perspect 108:A252–A253.

Qian Z, Liao D, Lin HM, Whitsel EA, Rose KM, Duan Y. 2005. Lung function and long-term exposure to air pollutants in middle-aged American adults. Arch Environ Occup Health 60:156–163.

Ramadour M, Burel C, Lanteaume A, Vervloet D, Charpin D, Brisse F, et al. 2000. Prevalence of asthma and rhinitis in relation to long-term exposure to gaseous air pollutants. Allergy 55:1163–1169.

Rojas-Martinez R, Perez-Padilla R, Olaiz-Fernandez G, Mendoza-Alvarado L, Moreno-Macias H, Fortoul T, et al. 2007. Lung function growth in children with long-term exposure to air pollutants in Mexico city. Am J Respir Crit Care Med 176:377–384.

Schwela D. 2000. Air pollution and health in urban areas. Rev Environ Health 15:13–42.

Son JY, Kim H, Lee JT, Kim SY. 2006. Relationship between the exposure to ozone in Seoul and the childhood asthma-related hospital admissions according to the socio-economic status. J Prev Med Pub Health 39:81–86.

Tolbert PE, Mulholland JA, MacIntosh DL, Xu F, Daniels D, Devine OJ, et al. 2000. Air quality and pediatric emergency room visits for asthma in Atlanta, Georgia, USA. Am J Epidemiol 151:798–810.

Trasande L, Thurston GD. 2005. The role of air pollution in asthma and other pediatric morbidities. J Allergy Clin Immunol 115:689–699.

U.S. Census Bureau. 2000. 2000 Census of Population and Housing. Summary File 3. Available: http://www.census.gov/prod/cen2000/doc/sf3.pdf [accessed 1 June 2008].

U.S. Department of Health and Human Services. 1991. The International Classification of Diseases, 9th Revision. Washington, DC:U.S. Department of Health and Human Services.U.S. Environmental Protection Agency. 1999. Air Quality Index Reporting: Final Rule. Available: http://www.epa.gov/ttn/oarpg/t1/fr_notices/airqual.pdf [accessed 1 June 2008].

U.S. Environmental Protection Agency. 2002. Child-Specific Exposure Factors Handbook. Available: http://fn.cfs.purdue.edu/fsq/WhatsNew/KidEPA.pdf [accessed 1 June 2008].

Wang TN, Ko YC, Chao YY, Huang CC, Lin RS. 1999. Association between indoor and outdoor air pollution and adolescent asthma from 1995 to 1996 in Taiwan. Environ Res 81:239–247.

Zemp E, Elsasser S, Schindler C, Kunzli N, Perruchoud AP, Domenighetti G, et al. 1999. Long-term ambient air pollution and respiratory symptoms in adults (SAPALDIA Study). The SAPALDIA Team. Am J Respir Crit Care Med 159:1257–1266.

ORIGINAL ARTICLE

Impact of ambient air pollution on birth weight in Sydney, Australia

T Mannes, B Jalaludin, G Morgan, D Lincoln, V Sheppeard, S Corbett

Occup Environ Med 2005;**62**:524–530. doi: 10.1136/oem.2004.014282

See end of article for authors' affiliations

Correspondence to: Ms T F Mannes, NSW Public Health Officer Training Program, New South Wales Health Department, LMB 961 North Sydney, Australia; paman@doh.health.nsw.gov.au

Accepted 24 February 2005

Background: Studies in Asia, Europe, and the Americas have provided evidence that ambient air pollution may have an adverse effect on birth weight, although results are not consistent.
Methods: Average exposure during pregnancy to five common air pollutants was estimated for births in metropolitan Sydney between 1998 and 2000. The effects of pollutant exposure in the first, second, and third trimesters of pregnancy on risk of "small for gestational age" (SGA), and of pollutant exposure during pregnancy on birth weight were examined.
Results: There were 138 056 singleton births in Sydney between 1998 and 2000; 9.7% of babies (13 402) were classified as SGA. Air pollution levels in Sydney were found to be quite low. In linear regression models carbon monoxide and nitrogen dioxide concentrations in the second and third trimesters had a statistically significant adverse effect on birth weight. For a 1 part per million increase in mean carbon monoxide levels a reduction of 7 (95% CI −5 to 19) to 29 (95% CI 7 to 51) grams in birth weight was estimated. For a 1 part per billion increase in mean nitrogen dioxide levels a reduction of 1 (95% CI 0 to 2) to 34 (95% CI 24 to 43) grams in birth weight was estimated. Particulate matter (diameter less than ten microns) in the second trimester had a small statistically significant adverse effect on birth weight. For a 1 microgram per cubic metre increase in mean particulate matter levels a reduction of 4 grams (95% CI 3 to 6) in birth weight was estimated.
Conclusion: These findings of an association between carbon monoxide, nitrogen dioxide, and particulate matter, and reduction in birth weight should be corroborated by further study.

Epidemiological studies addressing the relation between ambient air pollution and fetal development are accumulating worldwide. Studies conducted in China,[1] the Czech Republic,[2 3] Korea,[4] the UK,[5] Brazil,[6] and North America[7–11] have examined the link between ambient air pollution levels during pregnancy and reduction in birth weight or intrauterine growth retardation (IUGR). There is evidence to suggest that air pollutant exposure during pregnancy has an adverse impact on birth weight, although the findings are inconsistent; the effect of individual pollutants and the period(s) during pregnancy when pollutant levels are likely to have most impact on birth weight is not clear.

It is useful, then, to examine the impact of ambient air pollution and birth weight in a variety of different sites to clarify the nature of the relation. We examined this relation in Sydney as there is complete, routinely collected data available. In the present study we evaluated the effect of prenatal exposure (in early, mid, and late pregnancy) to five common urban air pollutants: particulate matter (PM_{10} and $PM_{2.5}$), carbon monoxide (CO), nitrogen dioxide (NO_2), and ozone (O_3) from routine air monitoring in the Sydney metropolitan area on birth weight.

METHODS

Information on all births in metropolitan Sydney between 1 January 1998 and 31 December 2000 was obtained from the Midwives Data Collection (MDC) at the New South Wales Department of Health. The MDC is a population based surveillance system covering all live births and stillbirths of at least 20 weeks gestation and at least 400 grams birth weight. Birth data includes maternal demographic factors (age, smoking status, country of birth, postcode of residence at time of delivery), pregnancy factors (date of the last menstrual period, gestational hypertension and diabetes, parity, time of first antenatal visit to a healthcare provider), details about the delivery (type of delivery), and infant factors (birth weight, gestational age). Other known causes of low birth weight including multiple births, hypertension of pregnancy, and gestational diabetes were excluded.

We obtained daily air pollution data from the New South Wales Environment Protection Authority (EPA) and daily meteorological data from the Australian Bureau of Meteorology. Air pollution data included concentrations of PM_{10}, $PM_{2.5}$, NO_2, O_3, and CO recorded at 14 monitoring stations in metropolitan Sydney. Monitoring stations were excluded if less than 80% of readings were available for each pollutant. Pollutant concentrations were analysed as continuous variables.

For each birth, exposure to each air pollutant during gestation was estimated by calculating the average of each pollutant over 30 days (last month) and 90 days (third trimester) before birth, the mid 90 days of gestation (second trimester), and 90 days (first trimester) after the estimated date of conception. Pollutant concentrations from monitoring stations were averaged to provide an estimate for the whole of metropolitan Sydney, using an approach similar to the APHEA2 (Short-term Effects of Air Pollution and Health: A European Approach) studies.[12–14] The process was repeated

Abbreviations: ABS, Australian Bureau of Statistics; APHEA, Short-term Effects of Air Pollution and Health: A European Approach; CI, confidence interval; EPA, Environment Protection Authority; IRSD, Index of Relative Socioeconomic Disadvantage; IUGR, intrauterine growth retardation; LBW, low birth weight; LMP, last menstrual period; MDC, midwives data collection; NSW, New South Wales; $PM_{2.5}$, particulate matter less than 2.5 microns diameter; PM_{10}, particulate matter less than 10 microns diameter; ppb, parts per billion (10^{-9}); ppm, parts per million (10^{-6}); SD, standard deviation; SE, standard error; SES, socioeconomic status; SGA, small for gestational age; OR, odds ratio; Temp, temperature; TSP, total suspended particulates

Table 1 Characteristics of all singleton births in Sydney from 1998 to 2000 by "small for gestational age"

	Small for gestational age (n = 13 402)		Not small for gestational age (n = 138 056)		
Variable	**No.**	**%**	**No.**	**%**	**Adjusted OR (95% CI)**
Maternal age (years)					
<24	2762	20.6	19460	14.1	1.02 (0.97 to 1.08)
25–34*	8340	62.2	93828	68.0	1.00
35–44	2285	17.0	24639	17.8	1.01 (0.95 to 1.01)
>45	15	0.1	129	0.1	1.55 (0.84 to 2.84)
Maternal smoker					
Yes	2659	19.8	14254	10.3	1.97 (1.87 to 2.08)
No	10741	80.1	110375	79.9	
Sex of infant					
Female	6456	48.2	60381	43.7	1.01 (0.97 to 1.05)
Male	6946	51.8	64273	46.6	
Maternal Aboriginality		0.0		0.0	
Yes	117	0.9	806	0.6	1.03 (0.83 to 1.28)
No	13275	99.1	123758	89.6	
Gestation at first antenatal visit					
>20 weeks	1803	13.5	13854	10.0	1.12 (1.05 to 1.18)
⩽20 weeks	11486	85.7	110014	79.7	
Previous pregnancy					
No	7427	55.4	53102	38.5	0.57 (0.54 to 0.59)
Yes	5973	44.6	71517	51.8	
IRSD quintile					
5 (least disadvantaged; high SES)*	3843	28.7	58638	42.5	1.00
4	2857	21.3	27395	19.8	1.24 (1.17 to 1.13)
3	2374	17.7	19997	14.5	1.38 (1.30 to 1.46)
2	1684	12.6	13826	10.0	1.50 (1.41 to 1.61)
1 (most disadvantaged; low SES)	2644	19.7	18200	13.2	1.73 (1.63 to 1.83)
Season of birth					
Summer (Dec–Feb)*	3265	24.4	43727	31.7	1.00
Autumn (Mar–May)	3456	25.8	31109	22.5	1.05 (0.99 to 1.11)
Winter (Jun–Aug)	3375	25.2	31469	22.8	1.00 (0.95 to 1.06)
Spring (Sep–Nov)	3306	24.7	31751	23.0	0.99 (0.94 to 1.05)

*Referent group.
OR, odds ratio adjusted for other covariates; SD, standard deviation; SES, socioeconomic status.
Note that in Australia, autumn is in March, April, May; winter is in June, July, August; spring is in September, October, November; and summer is in December, January, February.

matching air pollution concentrations from each eligible monitoring station and births to mothers residing in postcodes within 5 km of the monitoring station.

The following covariates were included in regression models: sex of child, maternal age (in year groupings), gestational age (only included in linear regression models), maternal smoking (yes/no), gestational age at first antenatal visit (⩽20 weeks or >20 weeks), maternal indigenous status (whether mother identifies as being Aboriginal or Torres Strait Islander), whether first pregnancy, season of birth, and socioeconomic status (SES). SES was measured using the Index of Relative Socioeconomic Disadvantage (IRSD) of postcode of maternal residence. The Australian Bureau of Statistics (ABS) constructs the IRSD to classify geographical areas on the basis of social and economic information collected in the population census. Each postcode in New South Wales (population of approximately 1000–5000 people) is assigned an IRSD index. We then ranked the postcodes and divided the list into quintiles.

A variable "small for gestational age" (SGA) was calculated based on the Australian national birth weight centile for gestational age 1991–94.[15] SGA was defined as greater than two standard deviations below the mean birth weight according to gestational age as SGA. SGA was analysed as a categorical variable in logistic regression models using the SAS System for Windows v8.02. Linear regression models were also developed using birth weight as a continuous variable. Following the development of the basic model, air pollutants were then added to the model to determine the association between ambient air pollutants and birth weight. Single and multi-pollutant pollutant models were assessed and we investigated interactions between air pollution variables and covariates. The impact of pollutant exposures in other pregnancy periods on key findings was also analysed.

RESULTS

There were 138 056 singleton births in Sydney between 1998 and 2000; 9.7% of babies (13 402) were classified as SGA. Mean (SD) birth weight for babies born in Sydney between 1998 and 2000 was 3418 (531) grams. After adjusting for other maternal and infant characteristics, SGA was significantly associated with maternal smoking, gestational age greater than 20 weeks at first antenatal visit, and first pregnancy (table 1). All SES variables exhibit a statistically significant association with SGA. Compared to the high SES category, there was increasing risk of SGA with decreasing SES.

Pollutant concentrations in Sydney from 1 April 1997 to 31 December 2000 are presented in table 2. A correlation matrix of air pollution variables is presented in table 3 to show correlations between pollutants. Correlation coefficients above 0.8 were observed between PM_{10} and $PM_{2.5}$. Correlation coefficients were also calculated to determine the correlations between air monitoring stations. Correlation coefficients between the 14 monitoring stations ranged from 0.68 to 0.85 for CO. Correlation coefficients between the 14 monitoring stations ranged from 0.46 to 0.85 for NO_2; from 0.53 to 0.94 for O_3; from 0.67 to 0.91 for PM_{10}; and from 0.66 to 0.93 for $PM_{2.5}$. All pollutants differed according to season ($p < 0.01$) and post hoc analysis revealed that all seasons were different to all others ($p < 0.05$). Concentrations of CO, NO_2, and $PM_{2.5}$ were highest in winter and lowest in summer. Concentrations of PM_{10} and O_3 were highest in summer and lowest in winter.

Table 2 Daily average pollutant concentrations for air monitoring stations in Sydney, 1 April 1997–31 December 2000

	Australian National Standard	Mean (SD)	Minimum	25th centile	Median	75th centile	Maximum
Pollutant							
PM_{10} (μg/m^3)							
24 hour av	50 μg/m^3	16.8 (7.1)	3.8	12.3	15.7	19.9	104.0
$PM_{2.5}$ (μg/m^3)							
24 hour av	25 μg/m^3*	9.4 (5.1)	2.4	6.5	8.4	11. 2	82.1
CO (ppm)							
8 hour av	9.0 ppm	0.8 (0.7)	0.0	0.4	0.6	1.1	4.6
O_3 (ppb)							
1 hour max	100 ppb	31.6 (14.6)	3.2	22.7	27.7	36.3	126.7
NO_2 (ppb)							
1 hour max	120 ppb	23.2 (7.4)	56.2	18.0	23.0	27.5	59.4

*Advisory reporting standard from 2003.
ppb, parts per billion (10^{-9}); ppm, parts per million (10^{-6}); CO, carbon monoxide, 8 hour average in ppm; O_3, ozone, 1 hour max in ppb; PM_{10}, particulate matter less than 10 microns, 24 hour average in μg/m^3; $PM_{2.5}$, particulate matter less than 2.5 microns, 24 hour average in μg/m^3; NO_2, nitrogen dioxide, 24 hour average in ppb.

Citywide average air pollutant concentrations in the last month, third trimester, and first trimester of pregnancy had no statistically significant effect on SGA after adjusting for infant and maternal characteristics (table 4). Concentrations of PM_{10}, $PM_{2.5}$, and O_3 in the second trimester of pregnancy had a small but statistically significant adverse effect on SGA (OR 1.01, 95% CI 1.00 to 1.04; OR 1.03, 95% CI 1.01 to 1.05; and OR 1.01, 95% CI 1.00 to 1.01, respectively).

Eleven metropolitan air monitoring stations were eligible for inclusion in the analysis of babies born to women residing within 5 km of an air monitoring station (table 4). There were 51 460 eligible births in 1998–2000. Of these, 5985 (11.6%) were classified as SGA. NO_2 concentrations in the second and third trimesters and one month before birth had a statistically significant adverse effect on risk of SGA (ORs between 1.07 and 1.14) (table 4). The NO_2 effects were robust to controlling for exposures in other pregnancy periods (ORs between 1.1 (95% CI 1.0 to 1.2) and 1.1 (95% CI 1.0 to 1.2) for second and third trimesters respectively). Exposure to PM_{10} in the second trimester of pregnancy had a small but statistically significant adverse effect on risk of SGA (OR 1.02, 95% CI 1.01 to 1.03) (table 4), although these findings were not robust to analysis when controlling for exposures to PM_{10} in other periods of pregnancy (OR 1.01, 95% CI 0.99 to 1.02).

In multivariate linear regression models, the effect of pollutant concentrations on birth weight (in grams) was examined for all births in Sydney during the study period and for babies born to women residing within 5 km of an air monitoring station (table 5). Citywide average levels of PM_{10} and $PM_{2.5}$ in the second trimester and last month of pregnancy had a small but statistically significant adverse effect on birth weight. When analysing only babies born to women residing within 5 km of an air monitoring station, we observed a small adverse effect of PM_{10} exposure during the second trimester on birth weight (regression coefficient −4.3, 95% CI −5.8 to −2.8). Thus, for every 1 μg/m^3 increase in 24 hour average PM_{10} during the second trimester of pregnancy, a 4 gram reduction in birth weight was estimated. This finding persisted after controlling for exposures in other pregnancy periods and analysis in multi-pollutant models (table 6).

Citywide average levels of CO in the last month of pregnancy had a statistically significant adverse effect on birth weight, whereas the 5 km results reveal an adverse effect of CO exposure on birth weight for the second and third trimesters of pregnancy. Linear regression coefficients for the 5 km analysis ranged from −23 (95% CI −44.6 to −1.2) to −29 (95% CI −51.0 to −6.8); thus, for every 1 part per million increase in 8 hour average CO during pregnancy, a 23–29 gram reduction in birth weight was estimated. Analysis of second trimester CO findings in two and three pollutant models and controlling for exposures in other pregnancy periods are presented in table 6. CO findings in the second trimester did not remain statistically significant when analysed in multi-pollutant models.

Citywide average levels of NO_2 in the first and third trimesters of pregnancy resulted in a small but statistically significant adverse effect on birth weight, whereas the 5 km results reveal an adverse effect of NO_2 exposure on birth weight for all periods of pregnancy. Linear regression coefficients for the 5 km analysis ranged from −20 (95% CI −27.8 to −11.5) to −34 (95% CI −43.4 to −24.3). NO_2 findings in the second trimester remained when analysed in two pollutant models, but did not remain when analysed in the four pollutant model (table 6).

Table 3 Matrix of Pearson correlation coefficients of pollutant concentrations (averaged across all air monitoring stations) in Sydney, April 1997–December 2000, and birth outcomes for term births in Sydney, 1998–2000

Pollutant	Birth weight	CO	NO_2	O_3	PM_{10}	$PM_{2.5}$	Temp
Birth weight	1.00						
CO	0.00	1.00					
NO_2	0.01	0.57	1.00				
O_3	0.01	−0.20	0.29	1.00			
PM_{10}	0.01	0.26	0.47	0.52	1.00		
$PM_{2.5}$	0.01	0.53	0.66	0.36	0.81	1.00	
Temp	0.00	−0.42	−0.16	0.60	0.38	0.05	1.00

Temp, temperature; ppb, parts per billion (10^{-9}); ppm, parts per million (10^{-6}); CO, carbon monoxide, 8 hour average in ppm; O_3, ozone, 1 hour max in ppb; PM_{10}, particulate matter less than 10 microns, 24 hour average in μg/m^3; $PM_{2.5}$, particulate matter less than 2.5 microns, 24 hour average in μg/m^3; NO_2, nitrogen dioxide, 24 hour average in ppb.

Table 4 Association (OR point estimate, 95% CI) between pollutant concentrations in Sydney and risk of small for gestational age (SGA) for infants born in Sydney between 1998 and 2000 by exposure period

		Exposure period							
		One month before birth		Third trimester		Second trimester		First trimester	
Pollutant	No. of infants (SGA/total)	OR	95% CI	OR	95% CI	OR	95% CI	OR	95% CI
All births									
PM_{10}	13402/138056	1.01	1.00 to 1.03	1.00	0.99 to 1.013	1.01	1.00 to 1.04	1.00	0.98 to 1.02
$PM_{2.5}$	13402/138056	1.01	0.99 to 1.03	0.99	0.97 to 1.02	1.03	1.01 to 1.05	0.99	0.97 to 1.01
CO	13402/138056	1.06	0.98 to 1.16	1.01	0.91 to 1.11	0.99	0.90 to 1.10	0.95	0.88 to 1.04
NO_2	13402/138056	1.00	1.00 to 1.01	1.01	1.00 to 1.02	1.00	0.99 to 1.01	1.00	0.99 to 1.01
O_3	13402/138056	1.00	0.99 to 1.01	1.00	1.00 to 1.01	1.01	1.00 to 1.01	1.00	1.00 to 1.01
5 km births									
PM_{10}	5391/44891	1.00	0.99 to 1.02	1.01	0.99 to 1.02	1.02	1.01 to 1.03	1.01	0.99 to 1.02
$PM_{2.5}$	1595/13855	1.01	0.97 to 1.04	1.00	0.95 to 1.05	1.00	0.96 to 1.05	0.99	0.94 to 1.04
CO	2892/22684	1.10	0.96 to 1.27	1.05	0.90 to 1.23	1.06	0.90 to 1.25	0.99	0.86 to 1.14
NO_2	5985/51460	1.07	1.00 to 1.14	1.13	1.05 to 1.21	1.14	1.07 to 1.22	1.06	0.99 to 1.14
O_3	5460/45730	1.01	0.97 to 1.06	1.01	0.96 to 1.07	1.00	0.95 to 1.06	0.99	0.93 to 1.03

OR estimates adjusted for: maternal age, maternal smoking, indigenous status, SES, gestational age at first antenatal visit, season of birth, and parity.
OR per 1 unit increase in pollutant concentration.
ppb, parts per billion (10^{-9}); ppm, parts per million (10^{-6}).
Units and averaging periods:
PM_{10} ($\mu g/m^3$): 24 hour av
$PM_{2.5}$ ($\mu g/m^3$): 24 hour av
CO (ppm): 8 hour av
O_3 (ppb): 1 hour max
NO_2 (ppb): 1 hour max

DISCUSSION

We examined associations between birth weight and exposure to air pollution concentrations at various stages of pregnancy across all of Sydney and for those infants born to women residing within 5 km of air monitoring stations. We showed a small effect of PM_{10} concentration in the second trimester of pregnancy, on birth weight in both linear and logistic regression models. We also showed that CO and NO_2 concentrations in the second and third trimesters of pregnancy (most pronounced in the second trimester), had a statistically significant effect on birth weight. The effect of NO_2 concentrations was only seen when examining births to women residing within 5 km of an air monitoring station. The effect of CO concentrations was only seen in the linear regression analysis and was most pronounced when examining births to women residing within 5 km of an air monitoring station.

There are a number of strengths to our study. We were able to investigate the association between low birth weight and pollutant concentrations for a large number of births in metropolitan Sydney between 1998 and 2000, and we were able to test this association using information on infants born to women residing within 5 km of an air monitoring station, again for a large number of births. We were also able to analyse the effect of five common air pollutants (PM_{10}, $PM_{2.5}$, CO, NO_2, and O_3), as these pollutants are routinely monitored at many air monitoring stations in metropolitan Sydney. One strength of this study is that we have been able to control for maternal smoking, indigenous status, gestational age at first antenatal visit, and parity among other potential confounders.

Although our analysis controlled for a number of important potential confounders, we did not have the information to adjust for some known risk factors for low birth weight; for example, maternal nutrition, maternal occupation, or pre-pregnancy maternal weight. Also, residual confounding by SES cannot be ruled out. Our SES estimate is a group level variable assigned to postcode of maternal residence at time of birth.

The most important source of bias in our study is due to measurement of exposure. By using air pollutant concentrations averaged across Sydney, we assume that ambient pollutant concentrations represent an individual's actual exposure to pollutants. This assumption does not account for time-activity patterns that may mediate exposure such as commuting habits, place or type of work, or time spent outdoors.

The use of citywide average exposure does not account for variations in pollutant concentrations across Sydney or even within the 5 km zone around an air monitoring station. It is likely that pollutants, particularly primary pollutants such as nitrogen dioxide and carbon monoxide, are not homogeneously distributed across Sydney. The distribution of primary pollutants will largely depend on the presence of combustion sources such as roads or industry. Thus we also examined the impact of pollutant concentrations only for births to women residing within 5 km of an air monitoring station to attempt to provide a better estimate of exposure for pollutants with large geographic variability. Analysis of the effect of CO and NO_2 shows a clear pattern of increased effect when examining only births to

Table 5 Changes in birth weight (in grams) for a 1 unit change in exposure to air pollutants (PM_{10} and $PM_{2.5}$ in $\mu g/m^3$; CO in ppm; O_3, NO_2 in ppb) at each trimester, and last month of pregnancy; results of linear regression models adjusted for covariates

	Exposure period									
	One month before birth		Third trimester		Second trimester		First trimester			
Pollutant	Multiple linear regression coefficient	95% confidence limits	Multiple linear regression coefficient	95% confidence limits	Multiple linear regression coefficient	95% confidence limits	Multiple linear regression coefficient	95% confidence limits		
All births										
PM_{10}	−1.21	−2.31	−0.11	−0.95	−2.30	0.40	−2.05	−3.36	−0.74	−0.14	−1.37	1.09
$PM_{2.5}$	−2.48	−4.58	−0.38	−0.98	−3.74	1.78	−4.10	−6.79	−1.41	0.36	−2.29	3.01
CO	−15.28	−25.59	−4.97	−6.63	−18.57	5.31	−10.72	−23.09	1.65	1.86	−8.31	12.03
NO_2	−0.76	−1.72	0.20	−1.48	−2.70	−0.26	−0.95	−2.07	0.17	−1.07	−2.07	−0.07
O_3	−0.11	−0.56	0.34	−0.45	−1.08	0.18	−0.75	−1.38	−0.12	−0.09	−0.66	0.48
5 km births										
PM_{10}	−2.98	−4.25	−1.71	−3.84	−5.35	−2.33	−4.28	−5.79	−2.77	−2.57	−4.04	−1.10
$PM_{2.5}$	−2.70	−6.80	1.40	−2.83	−9.00	3.34	1.54	−4.59	7.67	1.89	−1.99	5.77
CO	−10.41	−30.03	9.21	−22.88	−44.58	−1.18	−28.87	−50.98	−6.76	−8.96	−28.60	10.68
NO_2	−19.68	−27.83	−11.53	−32.17	−41.81	−22.53	−33.85	−43.38	−24.32	−26.22	−35.41	−17.03
O_3	−0.65	−6.51	5.21	−2.00	−9.64	5.64	8.77	1.05	16.49	8.99	−0.59	18.57

ppb, parts per billion (10^{-9}); ppm, parts per million (10^{-6}).
Units and averaging periods:
PM_{10} ($\mu g/m^3$): 24 hour av
$PM_{2.5}$ ($\mu g/m^3$): 24 hour av
CO (ppm): 8 hour av
O_3 (ppb): 1 hour max
NO_2 (ppb): 1hour max

women residing within 5 km of an air monitoring station. Ozone and $PM_{2.5}$ are secondary pollutants and thus should be more homogeneously distributed throughout metropolitan Sydney. The effects of concentrations of $PM_{2.5}$ and O_3 change little when analysing only births to women residing within 5 km of an air monitoring station.

Our findings of an adverse effect of particulates in the second trimester and of NO_2 and CO at various stages of pregnancy on birth weight have been replicated in previous studies. In a meta-analysis of studies examining the impact of particulate exposure on birth weight, Glinianaia and colleagues[16] concluded that in those studies where an effect of particulates in birth outcomes has been shown, there is considerable variability in the stage of pregnancy that the impact occurs.[16] The same can be said of those studies examining the impact of other pollutants on birth weight.

Chen and colleagues[9] examined the impact of ambient PM_{10} and other pollutant concentrations on birth weight in Northern Nevada (USA) between 1991 and 1999, and found that exposure to PM_{10} in the third trimester of pregnancy was negatively associated with birth weight in Nevada.[9] Gouveia and colleagues[6] examined the impact of O_3, CO, and PM_{10} concentrations on birth weight in Sao Paolo, Brazil in 1997, and found that first trimester exposure to CO and PM_{10} had an adverse affect on birth weight. No association between O_3 concentrations in any trimester and birth weight was observed.

IUGR, defined as birth weight below the 10th centile of recorded birth weight, was associated with exposure to $PM_{2.5}$ and PM_{10} concentrations in the first trimester of pregnancy in Northern Bohemia.[3] In the Czech Republic, IUGR was not associated with exposure to sulphur dioxide (SO_2) and total suspended particulate (TSP) concentrations during pregnancy.[2] Bobak[2] also reported that exposure to SO_2, TSP, and oxides of nitrogen (NO_x) during pregnancy had no affect on risk of low birth weight, after adjusting for gestational age (as well as other maternal characteristics). Ha and colleagues[4] examined the effect of exposure to CO, NO_2, TSP, and SO_2 in the first trimester of pregnancy on low birth weight in Seoul, South Korea. For each inter-quartile increase in pollutant the relative risk of low birth weight was 1.08 for CO, 1.07 for NO_2, 1.06 for SO_2, and 1.04 for TSPs.[4] No effect of exposure to these pollutants in the third trimester of pregnancy was noted.

Liu and colleagues[11] examined the effect of SO_2, NO_2, CO, and O_3 concentrations on IUGR, low birth weight, and preterm birth in Vancouver, Canada. Low birth weight was associated with exposure to SO_2 during the first month of pregnancy (OR 1.1 for a 5 ppb increase). IUGR was associated with exposure to SO_2 (OR 1.1 for a 5 ppb increase), NO_2 (OR 1.1 for a 10 ppb increase), and CO (OR 1.1 for a 1 ppm increase) in the first month of pregnancy.

Last trimester exposure to CO in Los Angeles, USA was reported to result in an increased risk of low birth weight in term births after adjusting for maternal characteristics including commuting habits (OR = 1.22).[7] Maisonet and colleagues[10] reported an increased risk of term low birth weight due to exposure to CO and SO_2 in all trimesters of pregnancy in six cities in North Eastern United States. No effect of exposure to PM_{10} was noted.[10] Concentrations of TSP and SO_2 in the last trimester of pregnancy were

associated with low birth weight in four residential areas of Beijing, China.[1]

In a recent study in Poland, Jedrychowski and colleagues[17] monitored individual exposure to fine particles over 48 hours during the second trimester of pregnancy of 362 women who gave birth between 34 and 43 weeks gestation. $PM_{2.5}$ exposures in this study averaged 43 μg/m^3 (with a range of 10–147 μg/m^3), thus were much higher than those observed in the present study. The authors observed an association between birth weight, birth length, and head circumference, and $PM_{2.5}$ exposure in the second trimester of pregnancy. A reduction in birth weight at an increased exposure from 10 to 50 μg/m^3 of 140 grams was estimated.

The hypothesised effect of air pollutants on reproductive health relate to a decreased in utero oxygen supply, resulting from a reduction of oxygen carrying capacity induced by air pollution.[4] Another possibility is that the production of free radicals induced by air pollution might cause an inflammatory response, increasing blood viscosity.[18 19] Suboptimal placenta perfusion from blood viscosity changes may cause adverse pregnancy outcomes, including low birth weight and preterm birth.[20] The possible biological mechanisms involved in the reduction in birth weight associated with maternal exposure to air pollution are likely to vary according to the timing of this exposure. The implantation of the fetus and the formation of the placenta occur during the first trimester, while weight gain occurs predominantly during the third trimester. In the first trimester genetic mutations are generally considered the most important cause of placental abnormalities, and in the second and third trimesters complex vascular alterations are considered to be the main cause of placental abnormalities and consequent fetal growth retardation.[21] Pollutants are recognised as being able to have an effect on both dimensions.[21] The effect of air pollutant exposure during pregnancy on birth weight has a plausible biological basis; however, the reported studies fail to show consistency in pollutants and periods during pregnancy where an effect occurs.

The lack of consistency in findings may be due to difficulties distinguishing between pollutants. In this study, when examining multiple pollutant models it appears that NO_2 is the most important pollutant, despite the fact that NO_2 levels in Sydney are well below the national standard. The lack of consistency in findings among countries may also be accounted for by differences in pollutant levels and mix. Air quality in the Sydney metropolitan area is generally good. Concentrations of pollutants measured at air monitoring sites in Sydney are typically well below standards, although seasonal conditions can cause the occasional exceedence of the national air quality standards.[22] In Sydney, motor vehicles are a major source of air pollutants, although solid fuel heating for domestic purposes in winter and occasional bush fires in summer also add to the fine particle concentrations.[22] Given the number of comparisons made in this study, the positive findings may be spurious. It is important, then, to corroborate these finding with future research.

Future research should involve the formation of individual testable hypotheses to avoid the problem of multiple tests. Research should also focus on obtaining higher quality exposure data, for example, modelling air pollution concentrations to smaller geographical areas using emission inventory, traffic density, and meteorological data in the presence of improved time activity data.

In conclusion, we observed that CO and NO_2 concentrations, particularly in the second trimester of pregnancy, have an adverse effect on birth weight. We also observed that $PM_{2.5}$ and PM_{10} concentrations in the second trimester of pregnancy have a small adverse effect on birth weight. While the number of studies in this area is accumulating, a

Table 6 Key second trimester findings of multivariate linear regression analysis (multiple linear regression coefficients (SE)) using multi-pollutant models and controlling for pollutant exposures in other pregnancy periods for babies born to women residing within 5 km of an air monitoring station; birth weight is expressed in grams

	Single pollutant model	95% confidence limits		Two pollutant models (PM_{10} and CO)	95% confidence limits	Two pollutant models (PM_{10} and NO_2)	95% confidence limits	Two pollutant models (CO and NO_2)	95% confidence limits	Two pollutant models (PM_{10} and O_3)	95% confidence limits	Four pollutant model	95% confidence limits	Controlling for exposures in other pregnancy periods	95% confidence limits	
PM_{10}	−4.28	−5.79	−2.77	−3.72	−6.29	−1.15	−2.65	−4.32	−0.98			−5.47	−7.06	−3.88	−3.27	−7.05	0.51	−3.03	−4.85	−1.21
NO_2	−33.85	−43.38	−24.32				−26.21	−37.46	−14.96	−26.74	−45.75	−7.73			−9.91	−35.10	15.28	−25.26	−35.63	−14.89
CO	−28.87	−50.98	−6.76	−27.31	−55.30	0.68				−20.17	−43.12	2.78			−25.97	−54.15	2.21	−24.38	−47.33	−1.43
O_3	8.77	1.05	16.49										18.28	10.03	26.53	−14.81	−33.65	4.03	8.84	1.10	16.58

ppb, parts per billion (10^{-9}); ppm, parts per million (10^{-6})
Units and averaging periods:
PM_{10} (μg/m^3), 24 hour av
CO (ppm), 8 hour av
NO_2 (ppb), 1 hour max

consistent pattern of pollutants and exposure times is not emerging. Further research is required to corroborate our findings.

ACKNOWLEDGEMENTS

Environmental Health Branch, NSW Health, and *Health Research Foundation*, South Western Sydney Area Health Service provided funding for this project. Sharyn Lymer assisted with SAS code. NSW Environment Protection Authority and Australian Bureau of Meteorology provided pollutant and meteorological data. The Australian Research Council and collaborators on the ARC SPIRT project *''The Assessment of the impact of air pollution on daily mortality and morbidity in Australian cities using a protocol based on international benchmarking''* provided valuable assistance with this project.

Authors' affiliations

T Mannes, NSW Public Health Officer Training Program, New South Wales Health Department, Australia
B Jalaludin, Epidemiology Unit, South Western Sydney Area Health Service, Australia and School of Public Health and Community Medicine, University of New South Wales, Australia
G Morgan, Northern Rivers Department of Rural Health, Sydney University, Australia
D Lincoln, NSW Biostatistical Officer Training Program, New South Wales Health Department, Australia
V Sheppeard, S Corbett, Environmental Health Branch, New South Wales Health Department, Australia

Competing interests: none

REFERENCES

1 **Wang X**, Ding H, Ryan L, *et al*. Association between air pollution and low birth weight: a community based study. *Environ Health Perspect* 1997;**105**:105–15.
2 **Bobak M**. Outdoor air pollution, low birth weight and prematurity. *Environ Health Perspect* 2000;**108**:173–6.
3 **Dejmek J**, Selevan SG, Benes I, *et al*. Fetal growth and maternal exposure to particulate matter during pregnancy. *Environ Health Perspect* 1999;**107**:475–80.
4 **Ha EH**, Hong YC, Lee BE, *et al*. Is air pollution a risk factor for low birth weight in Seoul? *Epidemiology* 2001;**12**:643–8.
5 **Bobak M**, Richards M, Wadsworth M. Air pollution and birth weight in Britain in 1946. *Epidemiology* 2001;**16**:358–9.
6 **Gouveia N**, Bremner SA, Noveas HMD. Association between ambient air pollution and birth weight in Sao Paulo, Brazil. *J Epidemiol Community Health* 2004;**58**:11–17.
7 **Ritz B**, Yu F. The effect of ambient carbon monoxide on low birth weight among children born in Southern California between 1989 and 1993. *Environ Health Perspect* 1999;**107**:17–25.
8 **Rogers JF**, Thompson SJ, Addy CL, *et al*. Association of very low birth weight with exposures to environmental sulfur dioxide and total suspended particulates. *Am J Epidemiol* 2000;**151**:602–13.
9 **Chen L**, Yang W, Jennison BJ, *et al*. Air pollution and birth weight in Northern Nevada, 1991–1999. *Inhal Toxicol* 2002;**14**:141–57.
10 **Maisonet M**, Bush T, Correa A, *et al*. Relation between ambient air pollution and low birth weight in the North-Eastern United States. *Environ Health Perspect* 2001;**109**(suppl 3):351–6.
11 **Liu S**, Krewski D, Shi Y, *et al*. Association between gaseous ambient air pollutants and adverse pregnancy outcomes in Vancouver, Canada. *Environ Health Perspect* 2003;**111**:1773–8.
12 **Atkinson RW**, Anderson HR, Sunyer J, *et al*. Acute effects of particulate air pollution on respiratory admissions: results from APHEA 2 project. *Am J Respir Crit Care Med* 2001;**164**(10 pt 1):1860–6.
13 **Katsouyanni K**, Touloumi G, Samoli E, *et al*. Confounding and effect modification in the short-term effects of ambient particles on total mortality: results from 29 European cities within the APHEA2 project. *Epidemiology* 2001;**12**:521–31.
14 **Le Tertre A**, Medina S, Samoli E, *et al*. Short-term effects of particulate air pollution on cardiovascular diseases in eight European cities. *J Epidemiol Community Health* 2002;**56**:773–9.
15 **Roberts CL**, Lancaster PAL. Australian national birth weight percentiles by gestational age. *Med J Aust* 1999;**170**:114–18.
16 **Glinianaia SV**, Rankin J, Bell R, *et al*. Particulate air pollution and fetal health: a systematic review of the epidemiologic evidence. *Epidemiology* 2004;**15**:36–45.
17 **Jedrychowski W**, Bendkowska I, Flak E, *et al*. Estimated risk for altered fetal growth resulting from exposure to fine particles during pregnancy: an epidemiologic prospective cohort study in Poland. *Environ Health Perspect* 2004;**112**:1398–402.
18 **Peters A**, Doering A, Wichmann HE, *et al*. Increased plasma viscosity during an air pollution episode: a link to mortality. *Lancet* 1997;**349**:1582–7.
19 **Bouthillier L**, Vincent R, Goegan P, *et al*. Acute effects of inhaled urban particles and ozone: lung morphology, macrophage activity, and plasma enothelin-1. *Am J Pathol* 1998;**153**:1873–84.
20 **Knottnerus JA**, Delgado LR, Knipschild PG, *et al*. Haematologic parameters and pregnancy outcome: a prospective cohort study in the third trimester. *J Clin Epidemiol* 1990;**43**:461–6.
21 **Lin CC**, Santolaya-Forgas J. Current concepts of fetal growth restriction: Part 1: Causes, classification and pathophysiology. *Obstet Gynaecol* 1998;**92**:1044–55.
22 **New South Wales Environment Protection Authority**. *State of the environment 2000*. Sydney: NSW Environment Protection Authority, December 2000, Available: http://www.epa.nsw.gov.au/index.htm [accessed July, 2003].

Impact of ambient air pollution on birth weight in Sydney, Australia

T Mannes, B Jalaludin, G Morgan, D Lincoln, V Sheppeard and S Corbett

Occup Environ Med 2005 62: 524-530
doi: 10.1136/oem.2004.014282

Environmental Research Section A **89,** 29–37 (2002)
doi:10.1006/enrs.2002.4357, available online at http://www.idealibrary.com on IDEAL®

Short-Term Effects of Low-Level Air Pollution on Respiratory Health of Adults Suffering from Moderate to Severe Asthma

Hélène Desqueyroux,* Jean-Claude Pujet,† Michel Prosper,† Fabien Squinazi,‡ and Isabelle Momas*,[1]

Laboratoire d'Hygiène et de Santé Publique, Faculté de Pharmacie, Université René Descartes, Paris, France; †Centre de Traitement des Affections Respiratoires, Paris, France; and ‡Laboratoire d'Hygiène de la Ville de Paris, Paris, France

Received August 16, 2001

Only a few studies have been carried out on the health effects of air pollution on patients suffering from severe asthma. We wanted to test the sensitivity of these patients to Paris air pollution. During 13 months, 60 severe asthmatics (62% female; mean age 55 years) were monitored by their physician, who filled in a follow-up form at each consultation and reported any asthma attacks. Daily levels of SO_2, PM10, NO_2, and O_3 were provided by the air quality network. Statistical analysis (generalized estimating equation models that accounted for autocorrelation of responses, temporal, meteorological, and aerobiological variables, and some individual characteristics) revealed significant associations between PM10, O_3, and incident asthma attacks. Odds Ratio (OR) for an increase of 10 μg/m^3 of PM10 was 1.41; 95% confidence interval (CI) [1.16; 1.71]. An increase of 10 μg/m^3 of O_3 was significantly associated with asthma attacks; OR = 1.20; 95% CI [1.03; 1.41]. These relations were observed after a delay between exposure and asthma attacks of 3 to 5 days for PM10 and 2 days for O_3, and they tended to differ according to atopic status. The results of our study suggest that ambient Paris levels of PM10 and O_3 affected health of severe asthmatics, despite their treatment.

Key Words: **asthma; ozone; particles; nitrogen dioxide; sulfur dioxide.**

INTRODUCTION

Exposure to ambient air pollutants has been associated with the short-term impairment of respiratory health all over the world. In Europe, ecological studies into this subject (Anderson *et al*., 1997; Dab *et al*., 1996; Ponce de Leon *et al*., 1996; Shouten *et al*., 1996; Spix *et al*., 1998; Vigotti *et al*., 1996) have shown that moderately elevated levels of air pollutants can lead to increases in the mortality rate and the number of hospital admissions for patients with asthma and respiratory symptoms.

Panel studies have been carried out often on sensitive populations: 24 on asthmatic adults and 17 on asthmatic children (Desqueyroux and Momas, 1999). These studies are generally based upon daily diaries and have shown the effect of particles upon health as judged by an increase in respiratory symptoms, degree of medication, and impairment of pulmonary function. Ozone (O_3) levels were associated with a decrease in forced expiratory volume (FEV1) and peak expiratory flow (PEF). A relation with sulfur and nitrogen dioxides (SO_2, NO_2) was less often observed.

Only two panels of asthmatics have been constituted in Paris, the first with children (Ségala *et al*., 1998) and the second with adults (Neukirch *et al*., 1998). The adult patients were mild to moderate asthmatics who were followed up over a 6-month winter period and who filled in a diary to record their symptoms and PEF. The authors found consistent and significant associations between pollutants and asthma attacks and symptoms in the entire study group. The subgroup of asthmatics who took inhaled beta2 agonists as needed exhibited even more consistent relations. Weaker associations were found in the subgroup of asthmatics who received regularly scheduled inhaled beta2 agonists; these patients were likely to be less susceptible to pollutants, their symptoms being better managed by more regular treatment.

We wanted to test this hypothesis by studying a new panel of adult asthmatics suffering from moderate to severe asthma, with regularly scheduled treatment. The aim of this study was to follow up

[1]To whom reprint requests and correspondence should be addressed. Fax: 33 1 43 25 38 76. E-mail: Isabelle.Momas@pharmacie.univ-paris5.fr.

0013-9351/02 $35.00

this new panel of asthmatics over a 1-year period, to determine the short-term effects of winter air pollution (particles with an aerodynamic diameter less than 10 μm; PM10, SO_2, and NO_2) and the estival photochemical air pollution (O_3 and NO_2). The study is based on medical data collected by a pulmonary physician at the time of clinical examinations, thus limiting biases resulting from patients' goodwill to fill in a daily questionnaire for several months.

MATERIALS AND METHODS

Study Design

The panel study was carried out from November 1995 to November 1996 on Paris patients having moderate to severe asthma. The panel comprised patients selected by two chest physicians who each completed a standardized inclusion questionnaire and subsequently used a follow-up form to report incident episodes of asthma attacks each time a patient came in for consultation. Patients were included up until December 1995.

At inclusion, subjects received a detailed explanation of the study and written consent was obtained. To blind subjects to the study objective and thus minimize selection biases, participants were told that they were enrolling in a study designed to investigate whether their way of life could influence bronchial hyperresponsiveness.

Study Population

Participants were recruited from patients regularly attending the Center for Treatment of Respiratory Diseases in Paris for several years. Eligibility criteria to enter the study included (1) moderate to severe physician-diagnosed asthma based on history and signs of airway obstruction: recurrent wheezing and cough, with an increase in FEV1 after beta2 agonist inhalation higher than 15% of the expected value or a greater than 20% FEV1 drop after provocative dose of methacholine; and (2) dwelling in Paris and its suburbs (six departments close to Paris). Any asthma consecutive to an underlying pathology, such as cardiac asthma, was excluded. Sixty adults participated in this study.

Demographic and Health Data

The inclusion questionnaire contained demographic (age, gender, residence, occupation) and medical management data. Baseline pulmonary function parameters [FEV1, forced vital capacity, (FVC), pulmonary total capacity (PTC)] were noted and compared to predicted values according to age, gender, and height. Regularly scheduled medications such as inhaled or systemic beta2 agonists and steroids were registered, as were smoking habits and allergy, allergy being reported by the physician.

The physician noted at the time of each consultation (regularly scheduled or emergency) whether the patient was enduring an asthma attack. Asthma attacks were defined as the need to increase twofold the dose of inhaled beta2 agonist and were objectified by clinical examination. Every acute exacerbation of the disease was thus confirmed by one or more of the following: wheezing on examination, expiratory brake, thoracic distension, hypertension with tachycardia, and polypnea.

The data of the first day of the attack and data on the potential aggravating factors of this attack were also reported by the patient, so that crises where no explanatory factor was noted could be compared with crises where a cause was suspected. These variables were dichotomous (infection, change of smoking habits, stress, exposure to allergen, unusual indoor pollution such as do-it-yourself).

Environmental Data Measurements

Information about ambient air pollution was obtained from daily measurements in urban background stations of the existing monitoring network (AIRPARIF), all located in the Greater Paris area. These stations were calibrated every 2 weeks. Air pollution data recorded included values for SO_2, PM10, NO_2, and O_3. Daily values were given by 28 stations for SO_2, 7 stations for PM10, 15 stations for NO_2, and 6 stations for O_3. SO_2 was measured by ultraviolet flurescence, PM10 by beta-radiometry, NO_2 by chemiluminescence, and O_3 by ultraviolet photometry, all measured with continuously recording monitors. Ambient concentrations of air pollutants were provided by the closest station to every participant's home. Twenty-four-hour average levels were calculated from midnight to midnight every day for SO_2, PM10, and NO_2. Eight-hour average levels (10 am–6 pm) were used for O_3. One-hour maximum value was also studied for NO_2 and O_3.

Daily average temperature and relative humidity were measured at the Paris weather station (Météo France).

Pollen data were obtained from the RNSA (National network of Aerobiologic Monitoring) and collected with a volumetric sampler (HIRST type).

Statistical Analysis

The association between air pollutants and health outcomes, i.e., incident episodes of asthma attacks (the index day being the reported date when the attack started), were examined using marginal logistic regressions based on the Generalized Estimating Equations (GEE) proposed by Liang and Zeger (1986). These models take into account reported measurements in response data. The correlation structure selected was exchangeable. All analyses were performed using the SAS procedure GEE (GENMOD).

Our approach was to carry out the analysis step by step. The procedure first determined by bivariate analysis and synthesis of the literature the covariates that belong to the regression models; subject characteristics and temporal, meteorological, and aerobiological variables. Different lags for temperature, humidity, and pollen count were investigated (up to 5 days). The final model included individual characteristics: age (continuous variable), ratio of FEV1 to its expected value (classified according to the median value of the distribution; 68%), smoking habits (current or former smokers versus nonsmokers), allergy (yes versus no), oral steroid treatment (yes versus no), weather (mean daily temperature for the index day and its previous 5 days, deviation between the maximum temperature and the minimum value during the same 6-day period (0 to -5 days), and relative humidity of the day), pollen counts (maximum of the previous days), season, and holiday periods (yes versus no).

Then, every pollutant effect on health was estimated by entering it separately into the model and into two-pollutant models. The possibility of a nonlinear relationship between pollution and health outcomes was considered by examining logarithmic transformation of pollutants. Since the analysis of log-transformed data did not improve the model, untransformed data were used for further results. Lags of up to 5 days were examined. We also explored the effect of cumulative exposure, defined as a mean of the previous days (up to 5 days). Odds Ratios (ORs) for exacerbation were given for an increase of 10 $\mu g/m^3$ in pollutant concentration. Interaction terms among variables were also tested. The fit to the model was checked by deviance, scaled deviance, and Pearson χ^2.

Analyses were conducted for the whole period and by season: winter (from October to March) and summer (from April to September), but only in summer for O_3.

RESULTS

Subjects and Visits

The panel was composed of 37 women and 23 men. Subjects were relatively old (55 ± 17 years). The smokers (5%) and former smokers (28%) were not excluded from the panel. All subjects had a bronchoconstriction with an average FEV1 of $71 \pm 29\%$ of the expected value, a slightly decreased FVC ($89 \pm 29\%$), and a normal PTC ($101 \pm 16\%$). A little more than half of the subjects were allergic (55%), especially to pollens (43%) and house dust mites (37%). All subjects used inhaled beta2 agonists and steroids as maintenance medication; nearly 20% took scheduled oral steroids.

The 13 months of the study made it possible to collect data on 406 visits (31 visits per month on average) including 93 asthma attacks (an average of 7 asthma attacks per month). Forty-nine asthmatics had at least 1 asthma attack during the study period. Nearly one third of these asthma attacks (30.1%, $n = 28$) was associated with none of the potential aggravating factors indexed in the questionnaire. For the two thirds of asthma attacks with an aggravating factor, this factor was generally an infection, in about half of the asthma attacks. The second factor reported either by the patient or the physician was stress (nearly 20% of cases). The other potential causes, such as modification of the treatment, unusual indoor pollution (do-if-yourself, insecticide), geographical change, or allergen, related to only 4 to 6 attacks (from 4 to 7% of the cases) each.

Pollution Levels

Daily concentrations of PM10 and NO_2, respectively, 26 and 54 $\mu g/m^3$, were homogeneous over the year. There were seasonal patterns in daily levels of SO_2 and O_3 with an increase of SO_2 in winter (average 24-h level of 19 $\mu g/m^2$ versus 7 $\mu g/m^3$ in summer) and of O_3 in summer (average 8-h level of 41 $\mu g/m^3$ versus 11 $\mu g/m^3$ in winter) (Table 1). Environmental data were strongly intercorrelated. There was a highly significant positive correlation between PM10, NO_2, and SO_2 whatever the season. In summer, O_3 was correlated with PM10 and NO_2 and not with SO_2. The temperature was generally associated negatively with atmospheric pollutants SO_2, PM10, and NO_2 and positively with O_3. Relative humidity was usually associated negatively with the other variables.

Relation between Air Pollution and Asthma Attacks

No association could be shown between asthma attacks and SO_2 (Table 2) whatever the lag or season

TABLE 1

Descriptive Statistics Relating to the Concentrations of Atmospheric Pollutants According to Estival[a] and Winter[a] Period (in µg/m³) (November 1995–November 1996)

	SO_2		PM10		NO_2		O_3	
	Summer	Winter	Summer	Winter	Summer	Winter	Summer	Winter
Mean	7	19	23	28	49	59	41	11
Standard deviation	5	12	9	14	15	16	18	10
Minimum	2	3	6	9	21	30	6	2
Maximum	27	81	63	84	106	128	85	51

[a]Summer, from April to September; winter, from October to March.

studied. The levels being weak in summer, the analysis according to the quartiles was carried out in winter. No association was observed (results not given).

An increase of PM10 was associated with an increase in the incidence of the asthma attacks. We observed effects after lags of 3–5 days and for mean exposure of these days (Table 2). The effect was highly significant in winter, but did not appear in summer (OR = 1.41; 95% confidence interval [CI] [1.16; 1.71] versus OR = 1.03; 95% CI [0.72; 1.47]).

The relation with particles was higher for asthma attacks for which no explanatory factor was noted compared to asthma attacks for which a cause was suspected (OR = 1.71; 95% CI [1.20; 2.43] versus OR = 1.27; 95% CI [1.06; 1.52]), especially for asthma attacks without infection (OR = 1.52; 95% CI [1.16; 2.00]) compared to asthma attacks with infection (OR = 1.30; 95% CI [1.03; 1.65]). Although the action of PM10 tended to be higher in allergic than in nonallergic people, no interaction was found. A similar effect of PM10 was observed whatever the importance of the obstructive syndrome, and patients taking or not taking oral steroids were equally sensitive to the influence of the PM10 (Table 3).

No effect of the average daily concentration of NO_2 was found on the incidence of asthma attacks over the whole period of study, over both winter and summer periods, whatever the lag after exposure (Table 2). The maximum 1-h level of NO_2 was also tested but did not show significant association with the incidence of asthma attacks.

The 8-h average level of O_3, for the previous day and up to 5 days before, did not show any association with asthma attacks. On the other hand, an increase of 10 µg/m³ of the maximum 1-h level, after a lag of 2 days, was significantly associated with an increase in the incidence of asthma attacks (OR = 1.20; 95% CI [1.03; 1.41]) (Table 2). The study by group (Table 3) highlighted a stronger effect among

TABLE 2

Odds Ratios (95% Confidence Interval)[a] of a 10-µg/m³ Increase in Pollutants on Incident Asthma Attacks in Paris Panel Study (November 1995–November 1996)

	Mean 24-h SO_2		Mean 24-h PM10		Mean 24-h NO_2		Maximum 1-h O_3[b]	
	OR	95% CI	OR	95% CI	OR	95% CI	OR	95% CI
Lag day-1	0.98	[0.76; 1.27]	0.87	[0.71; 1.06]	1.04	[0.94; 1.15]	0.94	[0.76; 1.15]
Lag day-2	0.92	[0.72; 1.19]	0.93	[0.80; 1.08]	0.99	[0.86; 1.13]	1.20	[1.03; 1.41]
Lag day-3	1.01	[0.82; 1.23]	1.11	[0.98; 1.26]	1.03	[0.93; 1.14]	1.14	[0.94; 1.39]
Lag day-4	1.01	[0.86; 1.19]	1.17	[1.03; 1.33]	1.07	[0.95; 1.20]	1.00	[0.84; 1.19]
Lag day-5	1.05	[0.85; 1.29]	1.16	[1.01; 1.34]	1.01	[0.88; 1.16]	0.88	[0.75; 1.04]
Cumulative exposure	Mean (− 1 to − 5d)		Mean (− 3 to − 5d)		Mean (− 1 to − 5d)		Max (− 1 to − 3d)	
	0.99	[0.76; 1.30]	1.21	[1.04; 1.40]	1.07	[0.91; 1.25]	1.08	[0.88; 1.33]

[a]Each odds ratio (OR), accompanied by its 95% confidence interval (95% CI), was obtained using a generalized estimating equation logistic model, adjusted for the effect of season and holiday periods, individual characteristics (age, FEV1, smoking habits, allergy, oral steroids), weather (mean temperature and relative humidity), and pollen counts.

[b]From April to September 1996.

TABLE 3
Influence of a 10-µg/m^3 Increase of Pollutant on Incident Asthma Attacks According to Patient Characteristics in the Paris Panel Study (November 1995–November 1996)

	Mean (− 3 to − 5 day) PM10[a]			Maximum 1-h (lag − 2 day) O_3[a]		
	n[b]	OR[c]	95% CI	n[b]	OR[c]	95% CI
Baseline pulmonary function (individual percentage of the predicted FEV1)						
FEV1 ⩾ 68%	114	1.38	[1.06; 1.79]	91	1.22	[1.04; 1.43]
FEV1 < 68%	112	1.45	[1.11; 1.90]	89	1.18	[0.93; 1.50]
Smoking habits						
Nonsmokers	160	1.53	[1.18; 1.98]	121	1.19	[1.02; 1.39]
Current and exsmokers	66	1.18	[0.90; 1.54]	59	1.22	[0.97; 1.54]
Allergy						
Nonallergic	100	1.29	[0.94; 1.77]	91	1.13	[0.93; 1.37]
Allergic	126	1.49	[1.17; 1.90]	89	1.31	[1.10; 1.55]
Regularly scheduled oral steroids						
no	175	1.41	[1.15; 1.73]	128	1.21	[1.00; 1.46]
yes	51	1.41	[0.88; 2.25]	52	1.20	[1.05; 1.38]

[a]Analyses were conducted from October 1995 to March 1996 for PM10 and from April to September 1996 for O_3.
[b]Number of observations, patients visits.
[c]Each odds ratio (OR), accompanied by its 95% confidence interval (95% CI), was obtained using a generalized estimating equation logistic model, adjusted for the effect of season and holiday periods, individual characteristics (age, FEV1, smoking habits, allergy, oral steroids), weather (mean temperature and relative humidity), and pollen counts, except the variable used for stratification.

allergic subjects, as for PM10. Baseline pulmonary function, smoking habits, and treatment by oral corticoids did not modify the effect of O_3. O_3 acted in the same way on concomitant asthma attacks with or without an infection (OR of asthma attacks without infection = 1.20; 95% CI [0.98; 1.45]; OR of asthma attacks with infection = 1.19; 95% CI [0.97; 1.46]).

The effect of PM10 and O_3 remained constant and statistically significant when both of these pollutants and another one entered the two-pollutant models (Table 4).

DISCUSSION

The methodology used in our study contributed two advantages: the homogeneity of patients with regard to their age and the severity of asthma and the evaluation of the medical variable on an individual scale. This variable was always objectively assessed by one of the two Center physicians, who standardized their medical practices. This appears to be a real advantage compared to the diary, which depends on the subjectivity and goodwill of the patient, the main risk being the involvement of declaration biases. On the other hand, by considering only the most severe crises, the study could be less sensitive.

The confounding and modifying factors, particularly subject characteristics, were also studied at an individual level; 55% of our patients had an allergic asthma, a rate consistent with results from a recent meta-analysis (Pearce *et al*., 1999) specifying that 30 to 40% of asthmatics are allergic. Smoking habits were another factor to be taken into account. Even if this factor did not vary daily at the same time as the pollutants and thus was not a confounding factor for short-term effect in panel studies, we can suppose that an asthmatic smoker or exsmoker could react differently to air pollution compared to a nonsmoking asthmatic. Asthmatics are light smokers; 15 to 20% smoke, but often with a relatively moderate consumption of less than 10 cigarettes per day (Pujet *et al*., 1994). According to the baseline pulmonary function parameter (FEV1) and maintenance medication, asthmatics from our panel generally suffer from more severe asthma than asthmatics from other panels. Individual normal indoor pollution has not been studied because it is regarded as being constant during the study and therefore unlikely to explain asthma attacks. The knowledge of all these individual characteristics is a real advantage for the semi-individual studies on which Künzli and Tager (1997) confer an inferential validity equivalent to that of individual studies.

The last important advantage of the study was that it covered the whole range of seasons, with their different types of air pollution, “estival” (spring and summer) and “winter” (autumn and winter). Other

TABLE 4

Influence of a 10-μg/m^3 Increase of PM10 or O_3 in Two-Pollutant Models in the Paris Panel Study (November 1995–November 1996)

	OR[a]	95% CI
Multipollutant model with PM10 and SO_2[b]		
PM10[d]	1.51	[1.20; 1.90]
SO_2[d]	0.84	[0.58; 1.21]
Multipollutant model with PM10 and NO_2[b]		
PM10[d]	1.43	[1.16; 1.76]
NO_2[d]	0.96	[0.71; 1.67]
Multipollutant model with O_3 and SO_2[c]		
O_3[d]	1.21	[1.03; 1.42]
SO_2[d]	0.70	[0.28; 1.78]
Multipollutant model with O_3 and PM10[c]		
O_3[d]	1.21	[1.03; 1.42]
PM10[d]	1.09	[0.71; 1.67]
Multipollutant model with O_3 and NO_2[c]		
O_3[d]	1.20	[1.03; 1.41]
NO_2[d]	0.96	[0.66; 1.39]

[a]Each odds ratio (OR), accompanied by its 95% confidence interval (95% CI), was obtained using a generalized estimating equation logistic model, adjusted for the effect of season and holiday periods, individual characteristics (age, FEV1, smoking habits, allergy, oral steroids), weather (mean temperature and relative humidity), and pollen counts.

[b]In winter from October to March.

[c]In summer from April to September.

[d]Average PM10 from the 3 to 5 previous days; average NO_2 and SO_2 from the 1 to 5 previous days; maximum 1 h O_3 from 2 days preceding the asthma attacks.

panel studies have generally been limited to shorter periods: winter season (Neukirch *et al*., 1998; Ostro *et al*., 1991; Peters *et al*., 1997), estival season (Taggart *et al*., 1996; Hiltermann *et al*., 1998), 8 months (Moseholm *et al*., 1993), 8 or 4 weeks (Delfino *et al*., 1997; Higgins *et al*., 1995), and two to four 3-month periods over 2 years (Lebowitz *et al*., 1987).

While we only had an ecological evaluation of the exposure, based on a fixed-site ambient monitor, we did try to have it be as close as possible to subjects by using the station closest to their home. Given the 1-year duration of the study, it was not possible to equip the whole panel with personal samplers, especially since we studied several pollutants.

Our study, in line with previous ecological studies (Anderson *et al*., 1997; Dab *et al*., 1996; Ponce de Leon *et al*., 1996; Shouten *et al*., 1996; Spix *et al*., 1998; Vigotti *et al*., 1996), clearly shows the effect of particles on the incidence of asthma attacks. Our results are also consistent with those of other panel studies, but only 10 teams have studied the relation between respiratory symptoms in asthmatic adults and ambient levels of particles, and the ORs that they found were weaker. For example (Hiltermann *et al*., 1998), waking up with breathing problems and shortness of breath were associated with PM10; relative risk = 1.24, 95% CI [1.01; 1.54] and 1.17, 95% CI [1.03; 1.34] per 50 μg/m^3 increase. Neukirch *et al*. (1998) found an OR of incidence of nocturnal cough of 1.73, 95% CI [1.29; 2.32], but also for an increase of 50 μg/m^3 of PM10. The panel population that those authors used was different, since it included only mild to moderate asthmatics. In our panel study, the effect of particles was highlighted even among asthmatics suffering from severe asthma, who were receiving a treatment adapted to the severity of their asthma. This effect appeared after lags of 3 to 5 days. This delayed effect is also reported in other studies. An impact of the concentration of PM10 is perceptible after a lag of 2 or 3 days (Pope *et al*., 1991; Pekkanen *et al*., 1997) or 4 to 6 days (Neukirch *et al*., 1998). The effect of the cumulated exposure observed in our study was also noted by Peters *et al*. (1997). Those authors report a more significant association between the fact of feeling ill during the day and the concentrations of PM10, taking into account not only the concentration of the current day when the medical effect was observed, but also the average concentration of the previous 4 days (or the average of the daily concentrations over these 5 days).

In our study, this delayed effect was consistent with an action of PM10 on inflammatory mechanisms. This hypothesis is corroborated by toxicological studies *in vitro* and *in vivo* in animals. Many authors have observed that particles generate an oxidative stress, production of reactive oxygen species by polymorphonuclear leukocytes (Hitzfeld *et al*., 1997; Rahman *et al*., 1997; Gavett *et al*., 1997), an inflammatory response with recruitment of neutrophils, eosinophils, and monocytes into the airways, impairment of particles clearance, and deficits in macrophage function (Warheit *et al*., 1997; Afaq *et al*., 1998; Dreher *et al*., 1997; Kodavanti *et al*., 1998).

Effects of PM10 tended to differ according to atopic status, although no effect of pollens was observed, perhaps due to low levels of pollen counts during the study period. However, different assumptions about the roles of particles and allergens in the aggravation of health of asthmatic people can be found in the literature. An action of particles, especially diesel emission particles (DEP), has been highlighted in IgE immunoglobin production (Nilsen *et al*., 1997; Lovik *et al*., 1997; Ichinose *et al*., 1997; Steinsvik *et al*., 1998). In men, combined intranasal challenge with DEP plus allergen induced a large increase in allergen-specific IgE production in allergic subjects (Diaz-Sanchez *et al*., 1994; Fujieda *et al*.,

1998). The effect observed could also result from the adsorption of allergens on particles (Steinsvik *et al*., 1998). Allergens can interact with other particles, such as DEP, which provide them with a means of transport for reaching lower airways (Suphioglu, 1998). Furthermore, the connection of allergens with particles involves a prolonged exposure to the allergen, which is slowly released from the particulate surface, thus increasing the risk of bronchial reactivity.

Despite low O_3 levels, concentrations being lower than standard guidelines (the maximum of the 1-h concentrations of O_3 was 163 $\mu g/m^3$ during summer 1996 and the threshold of information of the population of 180 $\mu g/m^3$ was never reached), an effect was observed in our panel. This effect appeared after a 2-day lag, a lag having also been described by Gielen *et al*. (1997). All the other teams highlighted instead an effect of the day before, but only one team studied adults (Higgins *et al*., 1995). Their results were very similar for respiratory symptoms; in particular they showed an aggravation of the lower respiratory symptoms, wheezing and coughing (Lebowitz *et al*., 1987) and trouble breathing and phlegm (Hiltermann *et al*., 1998). The relation that we observed with O_3 was more marked among allergic asthmatics than among nonallergic people. This effect of O_3 on allergic asthma was studied by Molfino *et al*. (1991), during controlled human experiments. Their results suggested that weak concentrations of O_3, similar to those encountered in large cities, may increase bronchial reactivity with an allergen in atopic asthmatic patients.

No effect of SO_2 was found in our study, presumably due to the fact that ambient concentrations have greatly decreased over recent decades, following regulations on air quality. Annual average levels of SO_2 have decreased by more than 85% in Paris and its suburbs in 35 years (Conseil Départemental d'Hygiène de Paris, 1997). Ambient concentrations in Paris are now 19 $\mu g/m^3$ in winter, whereas concentrations studied in the toxicological studies are over 500 $\mu g/m^3$. In other countries, such as the United Kingdom (Higgins *et al*., 1995; Taggart *et al*., 1996) and countries in Eastern Europe (Peters *et al*., 1996), authors have observed an impact of SO_2 on pulmonary function and on the bronchial hyperreactivity of asthmatic adults. However, SO_2 levels were higher (maximum 24 h higher than 100 $\mu g/m^3$), particularly in Eastern Europe where WHO value guides (average 24 h of 125 $\mu g/m^3$) were exceeded from 35 to 145 times per winter depending on the cities. In Paris, Neukirch *et al*. (1998) found a positive association between SO_2 and incident and prevalent episodes of wheeze and nocturnal cough in a panel of asthmatic adults and an association between SO_2 and prevalent episodes of shortness of breath. But ORs are calculated for an increase of 50 $\mu g/m^3$ in the concentrations of SO_2, which very seldom happened in our study period, the 1st and 3rd quartiles being, respectively, 10 and 26 $\mu g/m^3$ for the winter period. Moreover, they did not use two-pollutant models, adjusting for PM10.

CONCLUSION

In summary, our panel study has quantified the short-term effects of various urban atmospheric pollutants on asthma attacks for 60 adults suffering from moderate to severe asthma and receiving treatment adapted to the severity of their asthma. All data collected and analyzed show clear effects of PM10 and O_3. These effects could be observed with a delay between exposure and incidence of asthma attacks of 3 to 5 days for PM10 and 2 days for O_3. An increase of 10 $\mu g/m^3$ of pollutant resulted in ORs reaching a value close to 1.5 for PM10 and 1.3 for O_3. This result highlights the interest, for patients suffering from moderate to severe asthma, in reinforcing maintenance medication according to air pollution levels.

ACKNOWLEDGMENTS

The authors are grateful to Mr. Yvon Le Moullec from the Hygiene Laboratory of Paris City for the environmental data that he gave us and for his advice. We also thank Dr. Jacques Bourcereau for his help in medical data collection and Vérane Roig for her comments on the manuscript.

REFERENCES

Afaq, F., Abidi, P., Matin, R., and Rahman, Q. (1998). Cytotoxicity, pro-oxidant effects and antioxidant depletion in rat lung alveolar macrophages exposed to ultrafine titanium dioxide. *J. Appl. Toxicol.* **18,** 307–312.

Anderson, H., Spix, C., Medina, S., Shouten, J., Castellsague, J., Rossi, G., Zmirou, D., Touloumi, G., Wojtyniak, B., Ponka, A., Bacharova, L., Schwartz, J., and Katsouyanni, K. (1997). Air pollution and daily admissions for chronic obstructive pulmonary disease in 6 European cities: Results from the APHEA project. *Eur. Respir. J.* **10,** 1064–1071.

Conseil Départemental d'Hygiène de Paris. (1997). "La Qualité de l'air à Paris en 1996, Rapport Élaboré à Partir des Données de: AIRPARIF, Laboratoire Central de la Préfecture de Police, Laboratoire d'Hygiène de la Ville de Paris, Paris."

Dab, W., Medina, S., Quénel, P. Le Moullec, Y., Le Tertre, A., Thelot, B., Monteil, C., Lameloise, P., Pirard, P., Momas, I., Ferry, R., and Festy, B. (1996). Short term respiratory health effects of ambient air pollution: Results of the APHEA project in Paris. *J. Epidemiol. Commun. Health* **50**(Suppl. 1), S42–S46.

Delfino, R. J., Zeiger, R. S., Seltzer, J. M., Street, D. H., Matteucci, R. M., Anderson P. R., and Koutrakis, P. (1997). The effect of outdoor spore concentration on daily asthma severity. *Environ. Health Perspect.* **105,** 622–635.

Desqueyroux, H., and Momas, I. (1999). Air pollution and health: A synthesis of longitudinal panel studies published from 1987 to 1998. *Rev. Epidemiol. Sante Publ.* **47,** 361–375.

Diaz-Sanchez, D., Dotson, A. R., Takenaka, H., and Saxon, A. (1994). Diesel exhaust particles induce local IgE production in vivo and alter the pattern of IgE messenger RNA isoforms. *J. Clin. Invest.* **94,** 1417–1425.

Dreher, K. L., Jaskot, R. H., Lehmann, J. R., Richards, J. H., McGee, J. K., Ghio, A. J., and Costa, D. L. (1997). Soluble transition metals mediate residual oil fly ash induced acute lung injury. *J. Toxicol. Environ. Health* **50,** 285–305.

Fujieda, S., Diaz-Sanchez, D., and Saxon, A. (1998). Combined nasal challenge with diesel exhaust particles and allergen induces in vivo IgE isotype switching. *Am. J. Respir. Cell Mol. Biol.* **19,** 507–512.

Gavett, S. H., Madison, S. L., Dreher, K. L., Winsett, D. W., McGee, J. K., and Costa, D. L. (1997). Metal and sulfate composition of residual oil fly ash determines airway hyperreactivity and lung injury in rats. *Environ. Res.* **72,** 162–172.

Gielen, M. H., van der Zee, S. C., van Wijnen, J. H., van Steen, C. J., and Brunekreef, B. (1997). Acute effects of summer air pollution on respiratory health of asthmatic children. *Am. J. Respir. Crit. Care Med.* **157,** 2105–2108.

Higgins, B. G., Francis, H. C., Yates, C. J., Warburton, C. J., Fletcher, A. M., Read, J. A., Pickering, C. A. C., and Woodcock, A. A. (1995). Effects of air pollution on symptoms and peak expiratory flow measurements in subjects with obstructive airways disease. *Thorax* **50,** 149–155.

Hiltermann, T. J. N., Stolk, J., van der Zee, S. C., Brunekreef, B., de Bruijne, C. R., Fisher, P. H., Ameling, C. B., Sterk, P. J., Hiemstra, P. S., and van Bree, L. (1998). Asthma severity and susceptibility to air pollution. *Eur. Respir. J.* **11,** 686–693.

Hitzfeld, B., Friedrichs, K. H., Ring, J., and Behrendt, H. (1997). Airborne particulate matter modulates the production of reactive oxygen species in human polymorphonuclear granulocytes. *Toxicology* **120,** 185–195.

Ichinose, T., Takano, H., Miyabara, Y., Yanagisawa, R., and Sagai, M. (1997). Murine strain differences in allergic airway inflammation and immunoglobulin production by a combination of antigen and diesel exhaust particles. *Toxicology* **122,** 183–192.

Kodavanti, U. P., Hauser, R., Christiani, D. C., Meng, Z. H., McGee, J., Ledbetter, A., Richards, J., and Costa, D. L. (1998). Pulmonary responses to oil fly ash particles in the rat differ by virtue of their specific soluble metals. *Toxicol. Sci.* **43,** 204–212.

Künzli, N. and Tager, I. B. (1997). The semi-individual study in air pollution epidemiology: A valid design as compared to ecologic studies. *Environ. Health Perspect.* **105,** 1078–1083.

Lebowitz, M. D., Collins, L., and Holberg, C. J. (1987). Times series analyses of respiratory responses to indoor and outdoor environmental phenomena. *Environ. Res.* **43,** 332–341.

Liang, K. Y. and Zeger, S. L. (1986). Longitudinal data analysis using generalized linear models. *Biometrika* **73,** 13–22.

Lovik, M., Hogseth, A. K., Gaarder, P. I., Hagemann, R., and Eide, I. (1997). Diesel exhaust particles and carbon black have adjuvant activity on the local lymph node response and systematic IgE production to ovalbumin. *Toxicology* **121,** 165–178.

Molfino, N. A., Wright, S. C., Katz, I., Tarlo, S., Silverman, F., McClean, P. A., Szalai, J. P., Raizenne, M., Slutsky, A. S., and Zamel, N. (1991). Effect of low concentrations of ozone on inhaled allergen responses in asthmatic subjects. *Lancet* **338,** 199–203.

Moseholm, L., Taudorf, E., and Frosig, A. (1993). Pulmonary function changes in asthmatics associated with low-level SO_2 and NO_2 air pollution, weather, and medicine intake. *Allergy* **48,** 334–344.

Neukirch, F., Ségala, C., Le Moullec, Y., Korobaeff, M., and Aubier, M. (1998). Short-term effects of low-level winter pollution on respiratory health of asthmatic adults. *Arch. Environ. Health* **53,** 320–328.

Nilsen, A., Hagemann, R., and Eide, I. (1997). The adjuvant activity of diesel exhaust particles and carbon black on systemic IgE production to ovalbumin in mice after intranasal instillation. *Toxicology* **124,** 225–232.

Ostro, B. D., Lipsett, M. J., Wiener, M. B., and Selner, J. C. (1991). Asthmatic responses to airborne acid aerosols. *Am. J. Public Health* **81,** 694–702.

Pearce, N., Pekkanen, J., and Beasley, R. (1999). How much asthma is really attributable to atopy. *Thorax* **54,** 268–272.

Pekkanen, J., Timonen, K. L., Ruuskanen, J., Reponen, A., and Mirme, A. (1997). Effects of ultrafine and fine particles in urban air on peak expiratory flow among children with asthmatic symptoms. *Environ. Res.* **74,** 24–33.

Peters, A., Goldstein, I. F., Beyer, U., Franke, K., Heinrich, J., Dockery, D. W., Spengler, J. D., and Wichmann, H. E. (1996). Acute health effects of exposure to high levels of air pollution in Eastern Europe. *Am. J. Epidemiol.* **144,** 570–581.

Peters, A., Wichmann, H. E., Tuch, T., Heinrich, J., and Heyder, J. (1997). Respiratory effects are associated with the number of ultrafine particles. *Am. J. Respir. Crit. Care Med.* **155,** 1376–1383.

Ponce de Leon, A., Anderson, H., Bland, J., Strachan, D., and Bower, J. (1996). Effects of air pollution on daily hospital admissions for respiratory disease in London between 1987–88 and 1991–92. *J. Epidemiol. Commun. Health* **50**(Suppl. 1), S63–S70.

Pope, C. A., Dockery, D. W., Spengler, J. D., Raizenne, M. E. (1991). Respiratory health and PM10 pollution. *Am. Ref. Respir. Dis.* **144,** 668–674.

Pujet, J. C., Racineux, J. L., Dubosq-Mathieu, B., and Michel, F. B. (1994). Large survey on the quality of life of 18500 French asthmatics. First international conference on asthma education and management.

Rahman, Q., Norwood, J., and Hatch, G. (1997). Evidence that exposure of particular air pollutants to human and rat alveolar macrophages leads to differential oxidative response. *Biochem. Biophys. Res. Commun.* **240,** 669–672.

Ségala, C., Fauroux, B., Just, J., Pascual, L., Grimfeld, A., and Neukirch, F. (1998). Short-term effect of winter air pollution on respiratory health of asthmatic children in Paris. *Eur. Respir. J.* **11,** 677–685.

Shouten, J., Vonk, J., and de Graaf, A. (1996). Short term effects of air pollution on emergency hospital admissions for respiratory disease: Results of the APHEA project in two major cities in The Netherlands, 1977–89. *J. Epidemiol. Commun. Health* **50** (Suppl. 1), S22–S29.

Spix, C., Anderson, H. R., Schwartz, J., Vigotti, M., Le Tertre, A., Vonk, J., Touloumi, G., Balducci, F., Piekarski, T., Bacharova, L., Tobias, A., Pönkä, A., and Katsouyanni, K. (1998). Short-term effects of air pollution on hospital admissions of respiratory diseases in Europe: A quantitative summary of APHEA study results. *Arch. Environ. Health* **53,** 54–64.

Steinsvik, T. E., Ormstad, H., Gaarder, P. I., Aaberge, I. S., Bjonness, U., and Lovik, M. (1998). Human IgE production in hu-PBL-SCID mice injected with birch pollen and diesel exhaust particles. *Toxicology* **128,** 219–230.

Suphioglu, C. (1998). Thunderstorm asthma due to grass pollen. *Int. Arch. Allergy Immunol.* **116,** 253–260.

Taggart, S. C. O., Custovic, A., Francis, H. C., Faragher, E. B., Yates, C. J., Higgins, B. G., and Woodcock, A. (1996). Asthmatic bronchial hyperresponsiveness varies with ambient levels of summertime air pollution. *Eur. Respir. J.* **9,** 1146–1154.

Vigotti, M., Rossi, G., Bisanti, L., Zanobetti, A., and Schwartz, J. (1996). Short term effects of urban air pollution on respiratory health in Milan, Italy, 1980–1989. *J. Epidemiol. Commun. Health* **50**(Suppl. 1), S71–S75.

Warheit, D. B., Hansen, J. F., Yuen, I. S., Kelly, D. P., Snajdr, S. I., and Hartsky, M. A. (1997). Inhalation of high concentrations of low toxicity dusts in rats results in impaired pulmonary clearance mechanisms and persistent inflammation. *Toxicol. Appl. Pharmacol.* **145,** 10–22.

THESIS FOR THE DEGREE OF LICENTIATE OF ENGINEERING

Application of solar FTIR spectroscopy for quantifying gas emissions

Manne Kihlman

CHALMERS

Department of Radio and Space Science
Chalmers University of Technology
Göteborg, Sweden 2005

Application of solar FTIR spectroscopy for quantifying gas emissions
MANNE KIHLMAN

ISSN 1652-9103

Technical report No. 4L
Department of Radio and Space Science
Chalmers University of Technology
SE-412 96 Göteborg, Sweden
Telephone +46 (0) 31-772 1000

Cover:
The cover picture shows a 3D representation of a measurement done with the Solar Occultation Flux method to determine the total emission from a refinery. The red vertical lines correspond to solar lines. The colors in between the solar lines (blue to red) correspond to the integrated concentration of alkane (blue is low concentration while green and red are higher). The wind vectors are shown as green horizontal lines pointing into the measurement-surface. *(Aerial photo: Copyright Lantmäteriet 2004-11-09. Ur Din Karta och SverigeBilden)*

Printed by Chalmers reproservice
Göteborg, Sweden 2005

Application of solar FTIR spectroscopy for quantifying gas emissions

MANNE KIHLMAN
Department of Radio and Space Science
Chalmers University of Technology

Abstract

In environmental science there is an interest in quantifying gas emission rates to the lower atmosphere from anthropogenic and biogenic sources since there are many gases that constitute a potential short or long-term threat for human health.

Optical remote sensing methods give the possibility to get real time measurements of gases in the lower atmosphere where the instrument need not be located at the place where the gas is located. These methods also have the possibility to measure the concentration integrated along a line or a surface. This may be of more relevance for risk assessment than a measurement in one point. IR, visible or UV light is detected with a spectrometer and the molecules cause a fingerprint on the measured spectra by absorption of light on the molecules.

The Solar Occultation Flux (SOF) method is a relatively new method to measure gas emission rates. The method is based on recording broadband infrared spectra of the sun with a FTIR spectrometer that is connected to a solar-tracker. The latter is a mirror device that tracks the sun and reflects the light into the spectrometer independent of its position. From the solar spectra it is possible to retrieve the line-integrated concentration (molecules/cm^2) between the sun and the spectrometer. To obtain the gas emission from a source, the instrument is placed in a car and is driven in such way that the detected solar light cuts through the emission plume. To calculate the gas emission, the wind direction and speed is also required.

In the years 2002 to 2005, a project (KORUS) was run in cooperation with four industries to explore the possibilities to measure gas emissions of volatile organic compounds (VOC) with the SOF method. The four industries were three refineries, Preemraff-Göteborg, Preemraff-Lysekil and Shellraff-Göteborg, and the Oil harbour of Göteborg. All industries are located on the west coast of Sweden. The project aimed at lifting the usability of the method to commercially competitive performance, by increasing reliability and automatization. Simultaneously with the work to improve the method, an extensive measurement-program was run to put the method into a full-scale test to demonstrate its capacity for routine measurements.

This thesis gives an overview of the SOF method. It describes the technical challenges that have been solved to make the method more operative. General conclusions from the measurements are presented. A special report not appended in this thesis has been published that contain detailed results of all measurements. A detailed error analysis of the method is presented.

Keywords: Remote sensing, VOC, refinery, emission, solar occultation, FTIR

List of publications

Appended papers

Paper A

Kihlman M., Mellqvist J., Samuelsson J., Tang L., Chen D., **Monitoring of VOC emissions from refineries in Sweden using the SOF method**. *Manuscript in preparation for Environmental Science & Technology.*

Paper B

Mellqvist J., Kihlman M., Galle B., Fransson K., Samuelsson J., **The Solar Occultation Flux method, a nouvelle technique for quantifying fugitive gas emissions.** *Manuscript in preparation for Environmental Science & Technology.*

Related paper

Kihlman M., Mellqvist J., Samuelsson J., **Monitoring of VOC emissions from three refineries in Sweden and the Oil harbour of Göteborg using the Solar Occultation Flux method**, *Technical Report,* Optical Remote Sensing Group, Department of Radio and Space Science, Chalmers University of Technology, 2005.

Acknowledgments

I thank:

my supervisors Dr. Johan Mellqvist and Bo Galle,

Jerker Samuelsson,

Lin Tang and Deliang Chen at Gothenburg University for providing the TAPM data,

Karin Fransson for having performed the SF_6 measurements presented in chapter 6,

Anders Strandberg, Andreas Nilsson, Elisabeth Undén, Gunner Hanehöj, Karin Fransson Samuel Brohede, Åke Fält that have participated in the field measurements,

the personnel involved at the different industries,

Klas Folkesson for showing how an Acknowledgment chapter can be written,

all the people at the Department of Radio and Space Science,

my family and friends.

Table of contents

1 Introduction

This chapter argues that gas measurements are needed to assess the impact of biogenic and anthropogenic gas emissions. It then focuses on the formation of ozone in the lower troposphere where anthropogenic emission of VOC plays an important role. This motivates why VOC emissions from industries should be controlled.

1.1 General introduction

Emission of gases to the lower atmosphere from anthropogenic and biogenic activities constitute a potential hazard for human health and the environment. Some gases constitute a direct threat for human health, for example H_2S, that may lead to direct death in high concentration. Other gases constitute a long-term threat for example carcinogenic benzene. There are also long-term threats to the environment. One example is the global warming that is possibly an effect of emissions of green-house gases, for example carbon-dioxide and methane. Another example is the annual ozone losses at the south pole discovered in the mid eighties by Farman et al. [1], that is driven by human emissions of chlorofluorocarbons (CFC). Furthermore, acid rain, which causes forest decline, is the result of emissions of sulfur dioxide occurring both from anthropogenic sources by burning fossil fuels, and from biogenic sources by emissions from volcanoes.

Gas measurements are essential when determining what actions should be taken to lower the anthropogenic emissions of hazardous gases and to verify that the actions had the desired effect. Measurements on biogenic sources are of importance to warn the population if concentrations reach dangerous levels. Geophysical activity may also change the composition of gases as is the case with volcanic gases before an eruption. Gas detections can thus be used to alarm the population and in that way prevent a catastrophe.

The emission of volatile organic compounds (VOC) to air is a potential hazard for human health and the environment. The formation of ozone in the lower troposphere takes place through a photochemical reaction driven by VOC and nitrogen oxides. The formed ozone is a powerful oxidant that causes inflammation of the respiratory tract and exacerbates existing lung disease [2]. There are also indications that ozone in the lower troposphere may contribute to forest decline [3]. Furthermore, VOC can react with ozone and form secondary organic aerosols [4] that are also a threat to human health. Furthermore, some of the anthropogenic emissions of VOC are in the form of carcinogenic benzene. It is therefore of importance that the anthropogenic emissions of VOC should be minimized. This thesis is focused on measurements of VOC and a closer study of how the ozone is formed will therefore be presented.

1.2 The process of ozone formation

In the lower troposphere, ozone is formed in the presence of VOC and NO_x and sunlight. However, the chemistry behind the ozone formation is complex. Ozone is actually formed by the photolysis of nitrogen dioxide (NO_2). Instead of actually playing a role in the formation of ozone, the presence of VOC affect the efficiency with which NO_x forms ozone. The reaction scheme will here be presented as is given

in the report by SMHI [5]. A steady state between the following four reactions determines the concentration of O_3:

$$NO_2 + h\nu \rightarrow NO + O \quad (1.1)$$
$$NO + O_3 \rightarrow NO_2 + O_2 \quad (1.2)$$
$$O_3 + h\nu \rightarrow O_2 + O \quad (1.3)$$
$$O_2 + O \rightarrow O_3 \quad (1.4)$$

A steady state is typically settled between these reactions within a few minutes during daytime. The stable concentration of O_3 is then dependent of the sun radiation and temperature. If NO_2 is added to the air by emissions, there is no net production of O_3 since as much O_3 is consumed by reaction 1.2 as is produced by reaction 1.1 followed by 1.4. However, if new reactions are added that also consumes NO without consuming O_3, this balance is not stable anymore and the presence of NO_x will then produce additional O_3. One such reaction that consumes NO is the reaction with peroxy-radicals:

$$RO_2 + NO \rightarrow NO_2 + RO \quad (1.5)$$

where R can be either a hydrogen atom or a hydrocarbon. Peroxy-radicals are produced from the atmospheric decomposition of hydrocarbons. An example is the reaction between ethane (C_2H_6) and OH:

$$C_2H_6 + OH \rightarrow C_2H_5 + H_2O \quad (1.6)$$
$$C_2H_5 + O_2 \rightarrow C_2H_5O_2 \quad (1.7)$$

If NO is present it will then be converted to NO_2 by the following reaction system:

$$C_2H_5O_2 + NO \rightarrow C_2H_5O + NO_2 \quad (1.8)$$
$$C_2H_5O + O_2 \rightarrow CH_3CHO + HO_2 \quad (1.9)$$
$$HO_2 + NO \rightarrow OH + NO_2 \quad (1.10)$$

The scheme will thus not consume any OH-radicals if it goes all the way from reaction 1.6 to reaction 1.10. The presence of an ethane molecule will thus convert two NO molecules to NO_2 without consuming any O_3 and will thus disturb the balance that was settled by reactions 1.1 to 1.4. The potential of a specific hydrocarbon to increase the O_3 concentration is to first order dependent on its reaction rate with OH. A study based on this approach was presented by Darnall 1976 [6]. A more complete study based on the reaction scheme called the Master Chemical Mechanism (MCM) was presented in a paper by Derwent et al. [7]. The ozone creation potential presented there describes the increase in ozone concentration compared to the increase in ozone caused by ethylene if an additional term of 4.7 kg/km^2 of the hydrocarbon is employed in the MCM. This thesis will concentrate on alkanes which is the dominant hydrocarbon emitted from refineries. The ozone creation potential for some alkanes is presented in Table 1 together with some other hydrocarbons for comparison. Since the ozone creation potential of methane is low it is most often excluded in environmental VOC measurements and is then called

NMVOC (Non-Methane-VOC). Isoprene is emitted by biogenic emissions, for example tropical forests, and can cause high O_3 increase due to its high ozone creation potential if it resides together with high NO_x concentrations.

Table 1. Ozone creation potentials derived by Derwent et al. [7].

Organic compound	Ozone creation potential
Methane	0.6
Ethane	12.3
Propane	17.6
n-Butane	35.2
n-Pentane	39.5
n-Hexane	48.2
n-Heptane	49.4
n-Octane	45.3
n-Nonane	41.4
n-Decane	38.4
Isoprene	109.2
Benzene	21.8
Toluene	63.7
o-Xylene	105.3
m-Xylene	110.8
p-Xylene	101.0
Acetylene	8.5
Ethylene	100.0 (reference)

Since the ozone is produced in a photochemical reaction, the concentration is highest in the summer. The concentration limits recommended by WHO (from year 2000) are relatively often exceeded during sunny summer days in Sweden according to a study by SMHI [5]. Because of the complexity of the O_3 production, the relationship between VOC and NO_x emissions and O_3 concentration is not linear. A computer simulation by SMHI [5] based on emission estimates from 1999, showed that if the NO_x emissions were reduced with 45% in western Sweden, it would actually increase O_3 in areas with high NO_x emissions, for example in the neighborhood of Gothenburg but would reduce O_3 concentrations outside Gothenburg. Reducing VOC emissions would decrease the O_3 emissions on all places, but the reduction in O_3 outside Gothenburg were 7 times smaller than the reduction in O_3 caused by reducing the NO_x emissions. The isopleth diagram shown in Figure 1 is commonly used to show the complex relationship between O_3 concentration and the concentrations of VOC and NO_x. In regions with high VOC concentrations, the O_3 production will be NO_x limited and not sensitive to variations in VOC concentration. In high NO_x concentrations, it will be VOC limited. At a VOC concentration of around 0.3 ppmC, the isopleth diagram shows that the O_3 concentration will decrease if the NO_x concentration were increased. This is what was observed for the neighborhood of Gothenburg in the study by SMHI. The ratio VOC/NO_x=8/1 that defines the rim of maximum O_3 in the figure, is actually dependent on the kind of VOC in the mixture and many times a much higher ratio is observed for the rim.

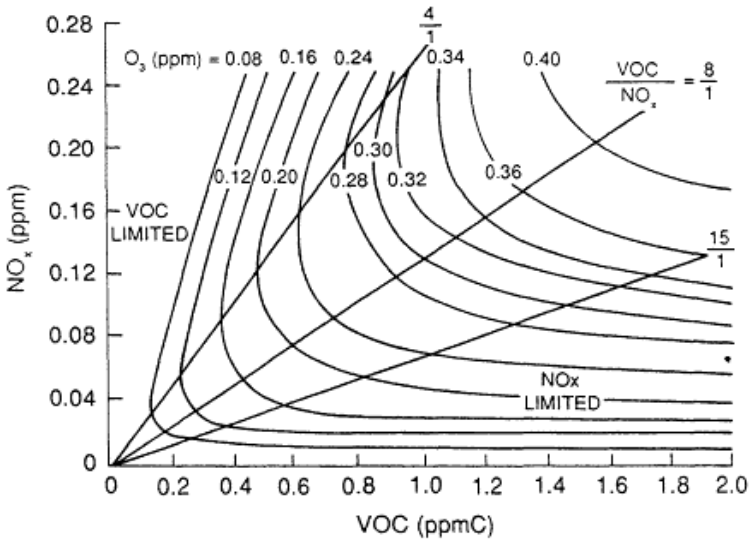

Figure 1. The isopleth diagram describing the relationship between O_3 concentration and its precursors. Picture is taken from Finlaysson-Pitts [8].

1.3 Sources for VOC emissions

Both anthropogenic and biogenic emissions from the European countries were compiled in the Corinair 94 inventory [9]. The total emission of NMVOC from Sweden was reported to 787 Kton/y and the anthropogenic emissions to 381 Kton/y. The emissions from 11 categories are shown in Table 2. Category 4 is represented by petroleum industries (12 Kton/y), organic chemical industries (3 Kton/y) and wood, paper pulp, food, drink and other industries (19 Kton/y). Thus petroleum industries are responsible for 3% of the anthropogenic emissions in Sweden.

Table 2. The emissions of NMVOC from Sweden in the Corinair 94 inventory.

Source	NMVOC (Kton/year)
1. Combustion in energy and transformation industries	4
2. Non-industrial combustion plants	0
3. Combustion in manufacturing industry	4
4. Production processes	34
5. Extraction and distribution of fossil fuels/geothermal energy	6
6. Solvent and other product use	152
7. Road transport	45
8. Other mobile sources and machinery	36
9. Waste treatment and disposal	0
10. Agriculture and forestry, land use and wood stock changes	*388*
11. Nature	*17*
Total:	***787***

2 Optical remote sensing

This chapter introduces the methods of optical remote sensing to measure gases and then concentrates on methods where the sun is used as the light source. This gives a preparation for the discussion of the SOF method that has been extensively used to monitor VOC emissions from industries.

2.1 Optical remote sensing for gas measurements

Historically, measurements of gases have been done by collecting gas in a point with some kind of absorber or a container. The samples are later analyzed with a gas chromatograph (GC) and mass spectrometry (MS). However, these methods fall short when used for real-time process monitoring and control. Historically, gas chromatographs produce useful data only a small fraction of their working time because of the sample collection requirements and in some cases the sample preparation. The sensitivity and selectivity of these method are however superior to most other methods.

Optical remote sensing methods gives the capability to get results in real time without the need to first collect a sample. Typically, repetitive measurements can be retrieved with a time resolution faster than 1 minute. These methods also have the possibility to measure the concentration integrated along a line or a surface and this may be of more relevance for risk assessment than a measurement in one point.

The methods are based on that IR, visible or UV light is detected with a spectrometer and the molecules cause a fingerprint on the measured spectra either by thermal emission of light from the molecules or by absorption of light on the molecules. Thermal emission from molecules is generally weak and measurements using emission spectroscopy are therefore considered more troublesome. It is therefore more common to use absorption spectroscopy to measure gases in the lower atmosphere. However, the analyzed gas must then be located between a light source and the spectrometer. The light source can either be a lamp or a natural object. The sun and the moon can be used as natural object when measuring with IR, visible and UV light. When measuring with visible and UV light the “blue sky” can also be used as a natural light source. Depending on what compounds that one wants to measure, the wavelength interval must be chosen so that the compounds have absorption structures in that region. With visible and UV light, three categories of compounds can be measured [10]:

- NO_x, O_3, HNO_2, CH_2O, SO_2
- Some aromatic hydrocarbons
- Radicals: BrO, OClO, IO, and OH

In the IR region, nearly all volatile compounds can be measured except atomic species. For a gas to have strong absorption structures in the IR region, the molecules must have a permanent magnetic dipole moment. Therefore, homonuclear diatomic species (e.g. Cl_2, N_2, O_2, H_2, etc.) should in theory not be detectable in IR. Similarly symmetrical linear polyatomic molecules (having a center of inversion) such as S=C=S and H-C≡C-H should not be detectable in IR. However, these molecules are still detectable if the concentrations are high due to much weaker magnetic dipole

moment caused by fine structures in these molecules [11]. For instance, it is possible to measure the total column of N_2 and O_2 in the atmosphere [12].

2.2 Light absorption on gas and particles

In absorption spectroscopy, the attenuation of light on molecules and particles is determined by Beer-Lambert's law:

$$I_m(\nu) = I_L(\nu) \cdot \exp\left(-\nu^4 \cdot \alpha_R \cdot L_R - \alpha_{Mie} \cdot L_{Mie} - \sum_i \sigma_i(\nu) \cdot conc_i \cdot L_i \right) \quad (2.1)$$

$I_m(\nu)$ is the light intensity at each wave number ν after it has passed through the gas.

$I_L(\nu)$ is the light intensity at each wave number ν for the light source.

$\sigma_i(\nu)$ is the absorption cross section (cm^2/molecule) of the gas with index i.

L_i is the path length where the gas with index i is present.

$conc_i$ is the concentration of the gas with index i. (molecules/m^3)

α_R, L_R represents the Rayleight scattering which occurs on particles and molecules with a size smaller than the wavelength of the light. The strength of the scattering depends on ν^4 and is therefore much higher at higher wave numbers.

α_{Mie}, L_{Mie} represents the Mie scattering which occurs on particles and molecules with a size larger than the wavelength of the light. For large particles, the strength of scattering is independent on the wave number. Scattering on particles of a size that lies in the intermediate region between Rayleigh scattering and Mie scattering will show a more complicated dependence on the wave number and particles size.

When measuring at high wave numbers and when high concentrations of scattering particles is present, it is also required to include a term in the equation that represents the light scattered into the light path by multiple scattering from particles and molecules located outside the observed light path. Using the sun as light source has the benefit that the shape of the light source as seen on earth is relatively small and has a huge contrast compared to other light sources. This makes the light path well defined and scattering has to occur at least two times instead of just one time for the light to be scattered into the observed light path. Using infrared light in comparison to UV/visible light also has the benefit that Rayleigh scattering is much weaker due to the ν^4 dependence. However, cloud droplets have a particle size distribution with a maximum between 1 and 2,5 μm [13] and thus falls between the Rayleigh and Mie scattering regions when using infrared light at 3 μm. The dependence of the scattering strength on the wave number will therefore vary between independent and ν^4 dependent.

In this thesis, there has been no effort to further determine Rayleigh and Mie scattering. However, particle loads in the atmosphere is varying and the varying scattering imposes changes in the measured spectra. Typically, when the sun is used as the light source and when faint clouds block the light path, a tilt in the measured spectra with a wave number dependence of approximately $\nu^{1.5}$ is observed. This must be compensated for when evaluating the spectra and is done by including a polynomial in the spectral fitting algorithm.

2.3 The solar occultation method

Retrieving the contents of trace gases in the atmosphere has been done with solar occultation techniques both with instruments onboard aeroplanes (already 1952 [14]) on satellites (in 1977 [15]) and from ground [16] . The systems consist of a solar tracker and an infrared spectrometer. 50 years ago, infrared grating spectrometers with low resolutions were used but the resolution of the spectrometers has been constantly improving since then. Today, very high-resolution FTIR spectrometers are commonly used for these studies.

From the solar spectra it is possible to retrieve the path-integrated concentration (molecules/cm^2) between the sun and the spectrometer. The concentrations of the gases of interest is determined by looking at how the solar light is absorbed in the atmosphere and to synthesize a spectra from guessed concentration profiles that fits the measured spectra in the best possible way. From high-resolution spectra (<0.125 cm^{-1}) it is also possible to derive height information by considering the temperature and pressure broadening of the spectral absorption lines. When synthesizing spectra, the atmosphere is usually divided in many layers stacked in altitude and the concentration, pressure and temperature broadening in each layer is taken into account to synthetically calculate how solar spectra in the infrared region would be observed by the instrument after it has passed through the atmosphere. The gas concentration in each layer is calculated with an optimum estimation method [17]. Usually, one measurement takes up to 10 minutes due to the high resolution required, and also requires a very stable optical system.

Another application of the solar-occultation technique is to study emission sources at ground level. When measuring localized emissions, the background atmosphere is no longer of interest but instead low concentrations of emitted compounds at low altitudes are of interest. Local wind situations will be of primary concern in such studies since it decides how the emission is transported and diluted. Therefore, pure concentration measurements are of little interest in such measurements. However, concentration ratios between different compounds can be of relevance. For example, volcanoes have been extensively studied by monitoring the ratios between SO_2, HCl and HF [18]. This can also be combined with controlled releases of trace gases at the same location as the emission source to determine the gas emission rate from localized sources by simultaneously measuring the trace gas and the gas of interest.

2.4 The HITRAN database

To calculate how a gas in the atmosphere absorbs light, the HITRAN database [12] can be used. It contains parameters for each absorption line for the 63 most common gases in the atmosphere, including parameters for the pressure and temperature broadening effects. From this it is possible to calculate how a specific gas at a specific temperature and pressure absorbs light. The absorption cross section for a single absorption line can be described by:

$$\sigma(\nu) = S(T) \cdot g\left(\nu - \nu_{\eta\eta'} - \delta\right) \tag{2.2}$$

where g is a function describing the broadening of the line. Figure 2 describes the different parameters in this equation. $\nu_{\eta\eta'}$ is the center frequency for the absorption line. $S_{\eta\eta'}$ is the line strength i.e. the total shaded area in the figure. δ is a shift in frequency caused by air-broadened pressure shift.

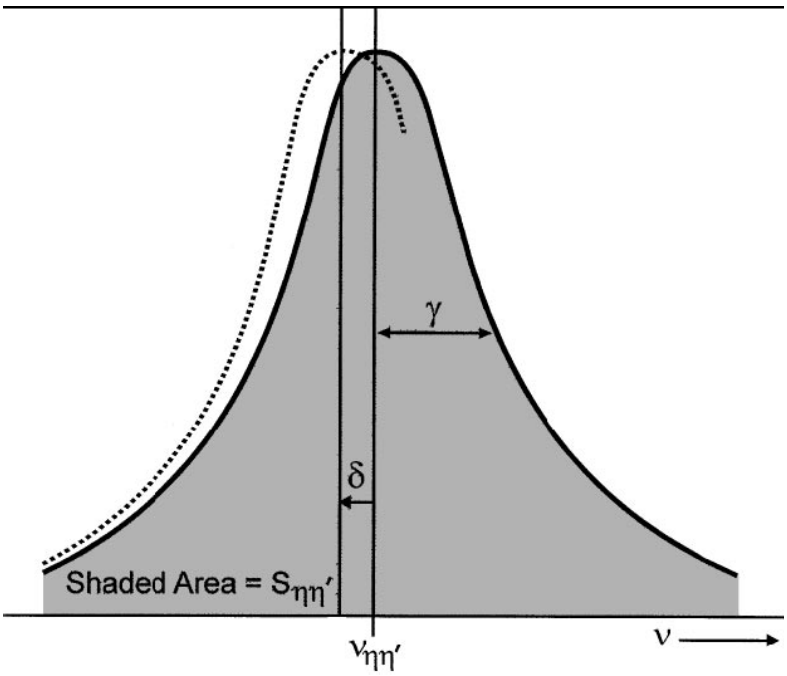

Figure 2. The figure show fundamental spectroscopic parameters of a line transition in HITRAN. The dotted line refers to a perturbed transition (with a negative δ). Picture is from the HITRAN paper [12].

The line strength S(T) used in equation 2.2 is dependent on the temperature since the temperature determines how strongly the upper and lower energy levels are populated:

$$S(T) = S_{\eta\eta'} \cdot \exp\left(-c_1 \cdot E_\eta \cdot \left(\frac{1}{T} - \frac{1}{296}\right)\right) \cdot \left(\frac{296}{T}\right)^m \cdot \frac{1-\exp\left(-c_1 \frac{\nu_{\eta\eta'}}{T}\right)}{1-\exp\left(-c_1 \frac{\nu_{\eta\eta'}}{296}\right)} \tag{2.3}$$

This equation is based on the Blotzmann equation for the distribution on the rotational and vibrational levels. Here c_1=hc/k=1.4388 cm·K. E_η is the energy (cm^{-1}) of the lower energy level. The parameter m represents the temperature dependence of the rotational partition function and has the value 1 for linear molecules and 1.5 otherwise.

There are two effects that contribute to the line broadening represented by function g in equation 2.2. The first is the doppler broadening due to random molecular motion and lead to a Gaussian line shape [19]:

$$f_G(\Delta\nu) = \frac{1}{\alpha_G\sqrt{\pi}} \cdot \exp\left(-\frac{(\Delta\nu)^2}{{\alpha_G}^2}\right) \tag{2.4}$$

where α_G is the Gaussian half-width at half-height:

$$\alpha_G = \frac{\nu_{\eta\eta'}}{c}\sqrt{\frac{2kT}{m}} \tag{2.5}$$

where m is the molecular mass. This is commonly called the temperature broadening effect and increases with increasing temperature. Pressure broadening is due to collisions perturbing the molecular energy levels and leads to a Lorentzian line shape:

$$f_L(\Delta\nu) = \frac{\alpha_L/\pi}{(\Delta\nu)^2 + {\alpha_L}^2} \tag{2.6}$$

where α_L is the Lorentzian half-width at half-height and is calculated by:

$$\alpha_L = \left(\frac{296}{T}\right)^n \left(\gamma_{air} \cdot (p - p_s) + \gamma_{self} \cdot (p_s)\right) \tag{2.7}$$

where γ_{air} represents the broadening due to collisions with other molecules and γ_{self} the brodening due to collisions of molecules of the same kind. p is the pressure of the air and p_s is the pressure if the specific gas were the only present gas. The coefficient n is transition dependent.

Typical values are around 0.07 cm^{-1} for α_L and 0.003 cm^{-1} for α_G for medium-sized molecules at room temperature and 1 atmosphere pressure [19]. If couplings between these broadening effects are neglected, the combined broadening can be calculated by the convolution between them. This is commonly called the voigt line profile:

$$g_{voigt}(\nu) = \int f_L(\nu') \cdot f_G(\nu - \nu') \cdot d\nu' \tag{2.8}$$

This is the commonly used line broadening function used in equation 2.2 above. All parameters are individually given for each absorption line in the HITRAN database. By calculating the line profiles for all absorption lines and summing up, an absorption spectrum can be calculated based on these parameters.

2.5 Methods to retrieve gas emission rates

In environmental and geological work there is often need to quantify the amount of gas emitted from biogenic or anthropogenic sources. There is a method for this where the gas concentration is measured and integrated over a surface that is selected in air. The mass-flow of gas through that surface is then determined by multiplying the surface integrated concentration with the wind transport through that surface. If the ambient concentrations of the studied gases are zero, the flux through the surface is equal to the emission on the leeward side of the surface.

One way to cut out this surface is to use a scanning system that measures the line integrated concentration in different directions as is commonly done with DIAL [20-22] and scanning DOAS [23]. Another method is to look in one direction but to move the platform the system resides on, commonly a car, an aeroplane or a ship. This was for example done from a ship to quantify the SO_2 emission from volcanoes both with DIAL, DOAS and COSPEC by Weibring et al. [24]. All three gas-monitoring instruments were then configured to look in the vertical direction and measured the total line integrated column of molecules through the whole atmosphere. The DIAL also has the added capability to resolve the variation in concentration along the line where the instrument is looking.

2.6 The SOF method

When scanning the surface by moving the platform, it is also possible to use solar-occultation spectroscopy. This is the Solar Occultation Flux method (SOF). The Optical Remote Sensing group at Chalmers has been working with this method since 1997. From the beginning the focus of the work was to develop a method to estimate VOC gas emission rates [25, 26]. However, the group has also demonstrated other applications with the method such as volcanic and agricultural measurements.

There is limited publication on studies where the solar-occultation method has been used to quantify gas emission rates. Duffel et al. measured volcanic gas emission rates with solar occultation and FTIR [27]. Weibring et al. [28] used solar occultation and DOAS for the same purpose. Appended **paper A** reports a monitoring project where the method was extensively used during three years to monitor the emissions of alkanes from four industries. Furthermore, appended **paper B** gives more examples where the method has been used to quantify the emissions of various gases from various sources.

The surface integrated concentration of gas is determined by cutting the surface into many parallelograms by continuously measuring spectrum after spectrum while moving the instrument. Each spectrum is evaluated separately to derive the line-integrated concentration represented by each spectrum. The position of the instrument during the traverse is measured with a GPS at the beginning and at the end of each measured spectrum and determines the base of each parallelogram. The surface integration is done by multiplying each line-integrated concentration with this base and summing up. The flow of gas through the surface is determined by a scalar-multiplication in vector representation between the wind-vector and the normal to each parallelogram. A look at Figure 3 gives an intuitive feeling for the surface where the measurement is done. The solar rays detected by the SOF instrument are shown as vertical lines. The area between these lines corresponds to the surface integrated

concentration observed, which if multiplied by the local wind-speed, corresponds to the mass-flux through the area.

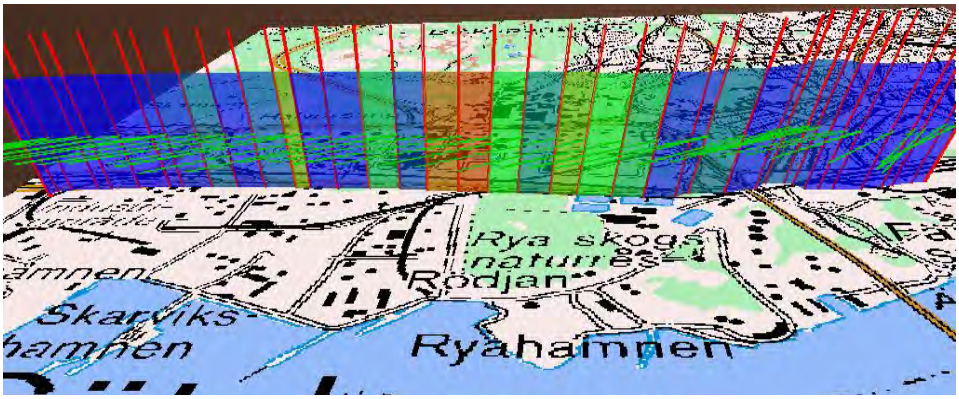

Figure 3. A 3D plot of a SOF measurement conducted at the oil harbour.

Here follows a more rigorous derivation of the equations that has been implemented in a real time software (QESOF) to calculate the flux. The position of the system is at the beginning and at the end of the collection of a spectrum defines a vector of movement $\vec{m} = \vec{V}_{stop} - \vec{V}_{start}$. This vector defines the short side of a parallelogram. The long side of the parallelogram is determined by the vector pointing towards the sun from the instrument. This can be calculated if the time, date and the position of the instrument are known. There are many algorithms for doing this, some more exact than others. In the QESOF software the following simplified equations has been used:

$$
\begin{aligned}
&d = 2\pi \cdot \text{daynr} / 365.0 \\
&\text{DEC} = \frac{\pi}{180}\begin{pmatrix} \cdot 0.322003 - 22.9711 \cdot \cos(d) - 0.357898 \cdot \cos(2d) - 0.14398 \cdot \cos(3d) \\ + 3.94638 \cdot \sin(d) + 0.019334 \cdot \sin(2d) + 0.05928 \cdot \sin(3d) \end{pmatrix} \\
&\text{eqTime} = \begin{pmatrix} 9.87 \cdot \sin(4\pi \cdot (\text{daynr} - 81)/365.0) - 7.53 \cdot \cos(2\pi \cdot (\text{daynr} - 81)/365.0) \\ -1.50 \cdot \sin(2\pi \cdot (\text{daynr} - 81)/365.0) \end{pmatrix} \\
&\text{LHA} = \frac{\pi}{180^\circ} \cdot (\text{second}_{\text{GMT}} / 3600 + \text{eqTime} / 60 - 12) \cdot 15^\circ + \text{Longitude} \\
&\text{solar\_zenith} = \arccos[\sin(\text{DEC}) \cdot \sin(\text{Latitude}) + \cos(\text{DEC}) \cdot \cos(\text{Latitude}) \cdot \cos(\text{LHA})] \\
&\text{ca} = \frac{\cos(\text{solar\_zenith}) \cdot \sin(\text{Latitude}) - \sin(\text{DEC})}{\sin(\text{solar\_zenith}) \cdot \cos(\text{Latitude})} \\
&\textit{if}\ (\text{LHA} < 0) \rightarrow \text{solar\_azim} = \pi - \arccos(\text{ca}) \\
&\textit{else} \rightarrow \text{solar\_azim} = \pi + \arccos(\text{ca})
\end{aligned}
\qquad (2.9)
$$

The input parameters are the time in seconds from mindnight according to Greenwich-Mean-Time ($\text{second}_{\text{GMT}}$), the day number of the year (daynr) and the position in degrees (Latitude, Longitude). The results are given as zenith and azimuth angles to the sun in radians where solar_zenith=0 corresponds to that the sun is straight up and solar_azim=π corresponds to that the sun is at its southmost position in

the day (assuming northern hemisphere). The direction to the sun can also be represented with a vector:

$$\vec{S} = \begin{bmatrix} \hat{x} \cdot \sin(solar\_zen) \cdot \sin(solar\_azim) \\ \hat{y} \cdot \sin(solar\_zen) \cdot \cos(solar\_azim) \\ \hat{z} \cdot \cos(solar\_zen) \end{bmatrix} \quad (2.10)$$

The cross multiplication between the vector of movement $\vec{m}$ and the vector to the sun $\vec{S}$ determines the normal of the parallelogram and its length is equal to the area of the parallelogram. The results of the spectral evaluation is a line integrated concentration that will here be represented by $[conc \cdot L]$ where L is supposed to represent a fiction height of the side of the parallelogram. The following formula calculates the normal to the parallelogram area and the normal vector has a length that is equal to the concentration integrated over the area of the parallelogram:

$$\vec{n} = \vec{m} \times \vec{S} \cdot [conc \cdot L] \quad (2.11)$$

The length of $\vec{n}$ has unit mass/length. It is then assumed that the flow of the gases is following the wind. By a scalar multiplication of the vector $\vec{n}$ with the wind vector $\vec{v}$, the flow of the gas through the parallelogram is calculated:

$$F = \vec{n} \cdot \vec{v} = \vec{m} \times \vec{S} \cdot \vec{v} \cdot [conc \cdot L] \quad (2.12)$$

The flux F has unit mass/time, typically kg/h. In most circumstances it can be assumed that the z component of $\vec{m}$ and $\vec{v}$ are zero and this simplifies the calculation of the flux to:

$$F = (m_y \cdot v_x \cdot S_z - m_x \cdot v_y \cdot S_z) \cdot [conc \cdot L] \quad (2.13)$$

Rewriting this in polar coordinates it becomes:

$$F = \cos(solar\_zen) \cdot \sin(v_\alpha - m_\alpha) \cdot v_S \cdot m_L \cdot [conc \cdot L] \quad (2.14)$$

where v_α and m_α are the wind and driving directions, v_S the wind speed and m_L the length of movement.

If there exists a strong difference in the wind on different heights, then a mass weighted wind must be used. This can be calculated by splitting equation 2.14 into smaller segments stacked in height and considering the wind in each segment:

$$F = \cos(solar\_zen) \cdot m_L \cdot \sum_j \sin(v_{\alpha,j} - m_\alpha) \cdot v_{S,j} \cdot [conc_j \cdot L_j] \quad (2.15)$$

$$[conc \cdot L] = \sum_j [conc_j \cdot L_j] \quad (2.16)$$

Only the total column $[conc \cdot L]$ is measured with SOF. The concentration in each height segment must be determined by other methods.

3 FTIR spectroscopy

This chapter gives an introduction to the FTIR (Fourier Transform Infrared) spectrometer and how the data collected from a FTIR is handled to retrieve a spectrum and how this should be done to get good quality in the spectra. In particular, resampling spectra to different wavelengths and the imposed side-lobes for different apodization functions are considered. This is presented here to give a preparation to the discussions in chapter 6 about the algorithm that have been implemented in the real time evaluation software (QESOF) that was developed to make the SOF method more operative.

3.1 The FTIR spectrometer

A FTIR spectrometer is an interferometer for IR light. The incoming light beam in the interferometer is divided into two separate light paths in a beam-splitter where half of the radiation is reflected and the rest is transmitted. The transmitted light travels to a movable mirror and the reflected light to a fixed mirror. The reflected light from the fixed mirror and the transmitted light from the moving mirror recombine at the beamsplitter, and hit the detector. The components of the interferometer are shown in Figure 4. All mirrors must be reflective in the infrared region. The beamsplitter is typically made of KBr or ZnSe to be able to handle infrared light. The detector must be sensitive to infrared radiation and is therefore made of HgCdTe, InSb, InAs, InGaAs, PbS or PbSe. The first four versions must be cooled by liquid nitrogen to work. The last two works at room temperature but has lower sensitivity.

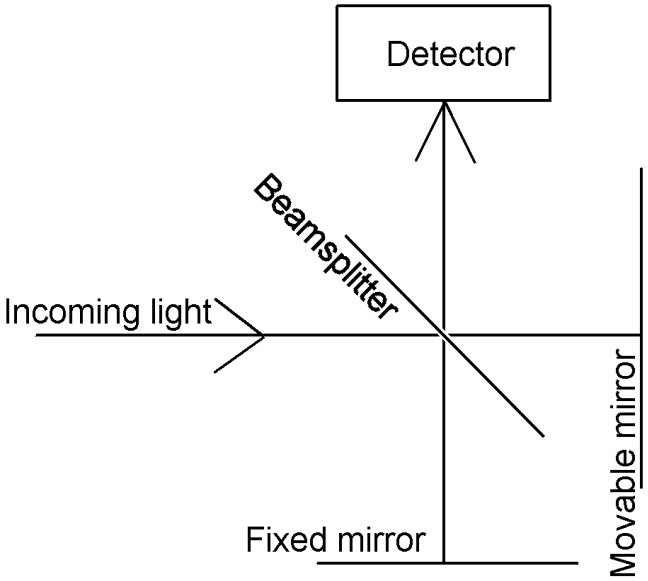

Figure 4. A common construction of a FTIR spectrometer (a Michelson interferometer).

The electrical signal from the detector represents the light intensity on the detector for different positions of the movable mirror and is called an interferogram. Figure 5

shows a typical interferogram. The spectrum is calculated in a computer by Fourier-transforming the interferogram. Figure 6 shows an example of a solar spectrum measured with a FTIR equipped with an InSb detector. This type of detector is not sensitive to wavelengths longer than 1700 cm^{-1}.

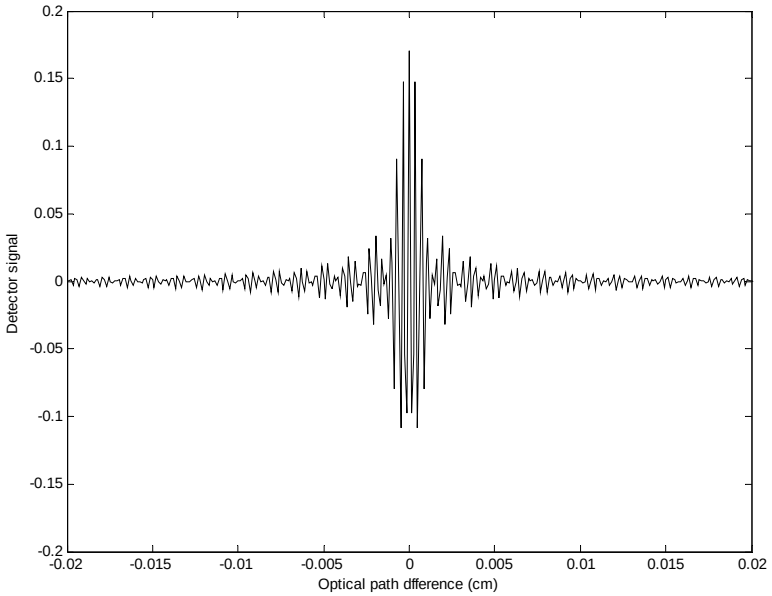

Figure 5. The figure shows the center of a typical interferogram.

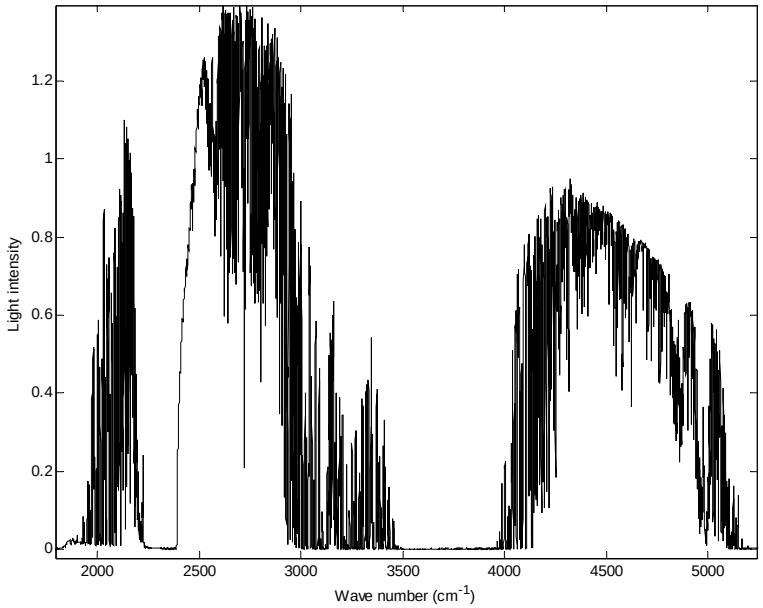

Figure 6. A solar spectrum measured on ground. The absence of light between 3000 to 4000 cm^{-1} is due to strong absorption on atmospheric H_2O and CO_2.

3.2 FTIR theory

The resolution of a spectrum is first of all restricted by the maximum optical path difference (OPD) in the movement of the movable mirror. The optical path difference is always measured in relation to the zero point where there is equal distance for the light to travel along the two paths to the two mirrors. If an interferogram is measured both at positive and negative path differences it is called a double sided interferogram. If it is only measured on one side of the zero point it is called single sided. If the interferometer is perfect then the interferogram is symmetric. A single sided interferrogram will therefore give the same resolution as a double sided interferogram but with only half the amount of movement of the mirror. Therefore, to get the highest resolution, single sided interferograms are commonly used. However, if the mirrors are misaligned, the interferogram will not be perfectly symmetric. Therefore, if these effects are strong, double sided interferograms should be used. If a single sided interferogram is measured, one side is mirrored around the zero point and copied to the other side to create a symmetric double sided interferogram.

From a direct discrete Fourier transform of the double sided interferogram, the spectral points will be separated with a wave number of $v_1 = 1/(2 \cdot OPD)$. A direct discrete Fourier transform is here defined to be the Fourier transform that contains as many output parameters as the number of sampling points in the interferogram and therefore defines a linear equation system:

$$A_n = \sum_{k=0}^{N} I_k \cdot \cos\left(\frac{v_n}{v_1} \cdot \frac{2\pi k}{N}\right) \tag{3.1}$$

$$B_n = \sum_{k=0}^{N} I_k \cdot \sin\left(\frac{v_n}{v_1} \cdot \frac{2\pi k}{N}\right) \tag{3.2}$$

$$v_n = v_1 \cdot n = \frac{n}{2 \cdot OPD} \tag{3.3}$$

where N is the number of sampling points in the interferogram. The vector I with indexes k represents the interferogram. The vector A represents the cosine term and the B vector represents the sine terms. Each index n represents the signal strength at the wave-number ν_n. If the interferogram is perfectly symmetric then all B components in equation 3.2 will become zero, and the components A_n alone represents the light intensity at different wave numbers. However if the interferogram is unsymmetric, the light intensity must be calculated by:

$$S_n = \sqrt{A_n^{\,2} + B_n^{\,2}} \tag{3.4}$$

Component number zero of A represents the bias component of the interferogram and component number N/2 represents the highest wave number that can be represented by the interferogram. The corresponding two numbers in the B vector will always be zero and can therefore be omitted. The spectrum S_n will contain light intensities at equal number of equidistant wave numbers (ν_n) as there are equidistant sampling points in the interferogram on one side of the zero point.

The discrete Fourier transform can be calculated by fast algorithms if the number of points in the interferogram (N) can be represented by $N=2^m$ where m is an integer. Even faster algorithms can be applied if N can be represented by $N=4^m$. The algorithms take advantage of the periodicity of the sine and cosine functions that occurs at these specific choices of N and thereby reduces the number of multiplications required.

The resolution of a spectrum is usually defined as the full width at half maximum of an individual peak in the spectrum and according to this definition, the resolution will be lower than the wave-number separation between each point in the direct Fourier-transform. The spectrum can be evaluated at different wave numbers than what is represented by the direct Fourier-transform by assuming the interferogram to be larger than what is actually measured and forcing the interferogram to be zero outside the limits of the measured interferogram. This is called zero-fill and has the effect of interpolating the spectrum based on the assumption that the original interferogram can be constructed by a sum of the cosine and sine functions that is represented by the non-zerofilled Fourier-transform. The zerofilling has the same effect as convoluting the spectrum with a *sinc* function. Thus, each peak S_n of the spectrum will have the following shape:

$$S(\nu) = S_n \frac{\sin\left(\pi \cdot (\nu - \nu_n)/\nu_1\right)}{\pi \cdot (\nu - \nu_n)/\nu_1} \tag{3.5}$$

In this way, the complete spectrum defined by all spectral points can be interpolated to any wave-number ν of interest:

$$S(\nu) = \sum_n S_n \frac{\sin\left(\pi \cdot (\nu - \nu_n)/\nu_1\right)}{\pi \cdot (\nu - \nu_n)/\nu_1} \tag{3.6}$$

An individual peak will have the shape of the function *sinc(x)=sin(x)/x* shown in Figure 7. Solving *sinc(x)=0.5* gives *x=0.6034* which corresponds to a full width at half maximum (FWHM) of 0.6034/OPD.

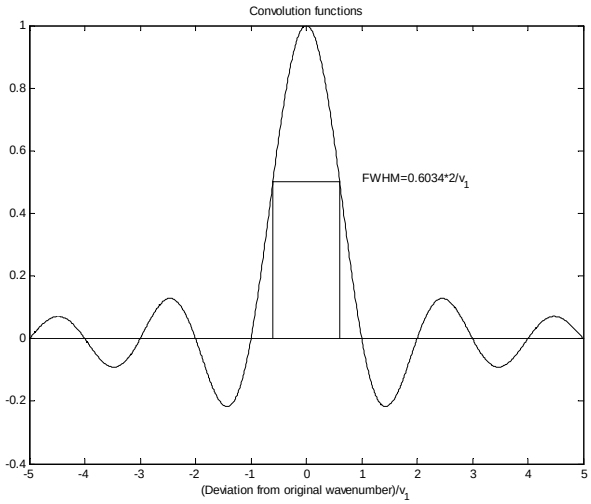

Figure 7. The figure shows the sinc function and the full width at half maximum.

Figure 7 shows the side-lobes that will occur if the wave-number of the incoming light does not exactly match one of those wave-numbers that is represented by the direct discrete Fourier transform. In a real measurement, a perfect match will never occur and there will therefore always be side-lobes. The side-lobes are strongest if the incoming light has a wave number that falls just in the middle between two of the wave-numbers in the direct discrete Fourier-transform. This coincides with that the wave-number causes maximum difference in signal strength between the end-points in the interferogram. For high quality evaluations of spectra, these side-lobes must be considered and there are two ways to do this. The two methods can also be used simultaneously. In the first method, a high-resolution spectrum is synthesized from guessed concentration profiles at typically around 16 times higher resolution than the actual measurement. The resolution is then degraded to the same resolution as the measurement in such a way that the side-lobes are synthesized as well. This can be done directly from equation 3.6. The best fit for the guessed concentration profiles is then searched for by a non-linear method. Thus, this method requires high-resolution absorption profiles for all the gases that has prominent absorption features in the measured spectra. It also requires a non-linear search algorithm. Another method to deal with the side-lobes is to multiply the interferogram with a function to force the signal strength to approach zero at the ends of the interferogram. This method, called apodization, has the disadvantage of reducing the resolution since the information contained at the ends of the interferogram is suppressed. A set of apodization functions that are commonly used is the Norton-Beer functions in its three versions: weak, medium and strong. These functions has been selected to minimize the effect of side lobes on discrete line spectra, see paper [29] by Norton and Beer from 1976. Another function commonly used is the triangular apodization, which however does not result in optimal suppression of side-lobes of a discrete line. Equation 3.7-3.9 shows the Norton-Beer functions and equation 3.10 the triangular function. The variable L represents the length of the interferogram. Figure 8 shows the apodization functions.

$$F_1(x) = 0.384093 - 0.087577 \cdot \left(1 - \frac{x^2}{L^2}\right) + 0.703484 \cdot \left(1 - \frac{x^2}{L^2}\right)^2 \tag{3.7}$$

$$F_2(x) = 0.152442 - 0.136176 \cdot \left(1 - \frac{x^2}{L^2}\right) + 0.983734 \cdot \left(1 - \frac{x^2}{L^2}\right)^2 \tag{3.8}$$

$$F_3(x) = 0.045335 - 0.554883 \cdot \left(1 - \frac{x^2}{L^2}\right)^2 + 0.399782 \cdot \left(1 - \frac{x^2}{L^2}\right)^3 \tag{3.9}$$

$$F_4(x) = 1 - \frac{|x|}{L} \tag{3.10}$$

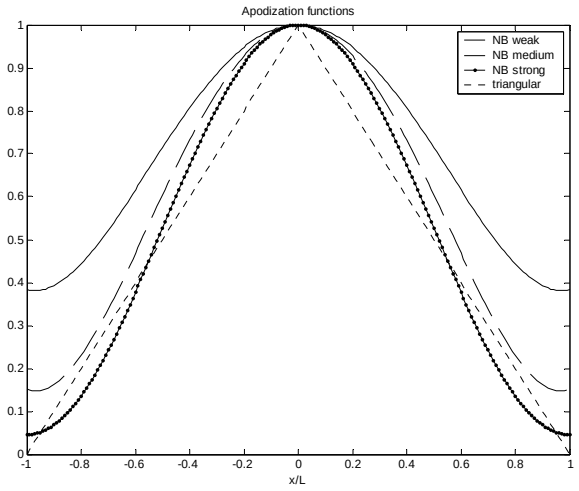

Figure 8. The Norton-Beer apodization functions and the triangular apodization function.

Multiplicating the interferogram with an apodization function has the same effect as convoluting the spectrum with the Fourier transform of the apodization-function. Figure 9 shows the convolution functions corresponding to the apodizations given in Figure 8. The FWHM for the convolution functions then becomes 0.715/OPD, 0.838/OPD, 0.941/OPD for Norton-Beer weak, medium and strong and 0.886/OPD for triangular apodization.

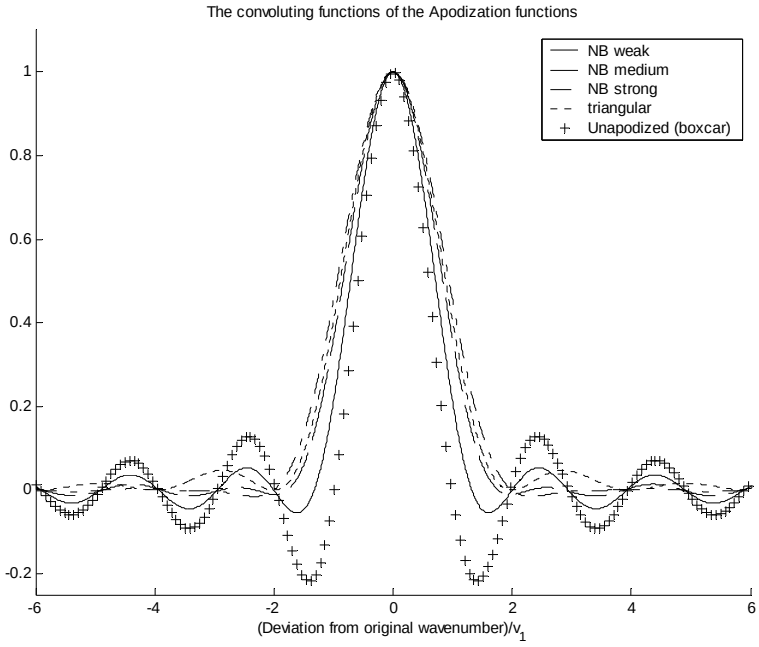

Figure 9. The Fourier transform of the apodization functions i.e. the functions that convolutes the spectra.

When measuring spectra with the OPUS software, the resolution is defined as the FWHM when using triangular apodization. For example, when measuring at 8 cm^{-1} an optical path difference of OPD=0.886/8 cm^{-1}=0.1108 cm is required. For the FTIR-spectrometers it is common to trigger the sampling of the interferogram by detecting the zero-crossings of the interferrogram from a Helium-Neon laser with a wavelength of 15798.84 cm^{-1} (632nm). The interferogram will consist of 15798.84 cm^{-1} × 0.1108 cm=1751 discretization points if it is single sided, or 3502 points if it is double sided. The shortest wavelength represented in such a spectra is twice the laser wavelength i.e. 7900 cm^{-1} (1.26 μm). However, the commonly used detectors do not work at such short wavelengths.

3.3 The effect of nonzero incidence angle

If it is assumed that the incoming light is perfectly parallel but the direction is tilted compared to the optical axis of the FTIR-spectrometer, it will cause a squeezing effect of the measured spectra in such a way that emission lines will show up at lower wave-numbers than the true wave-numbers. Figure 10 describes the principle behind this. The upper part shows the traditional way to picture an interferometer. An observer at the position of the detector will see both mirrors simultaneously. In the lower picture, the interferometer has been redrawn as if the elements were in a straight line. Assume that mirror 1 is fixed and that mirror 2 moves a distance *dx*. If the incoming light is tilted with an angle α, the movement of the mirror 2 with a distance *dx* will then cause the path difference between path 1 and 2 to change with a factor cos(α) lower than if the light were not tilted. This will produce less interference points in the recorded interferogram and this corresponds to that a monochromatic light source of wave number ν will cause a peak at wave number $\nu \cdot \cos(\alpha)$ in the spectrum.

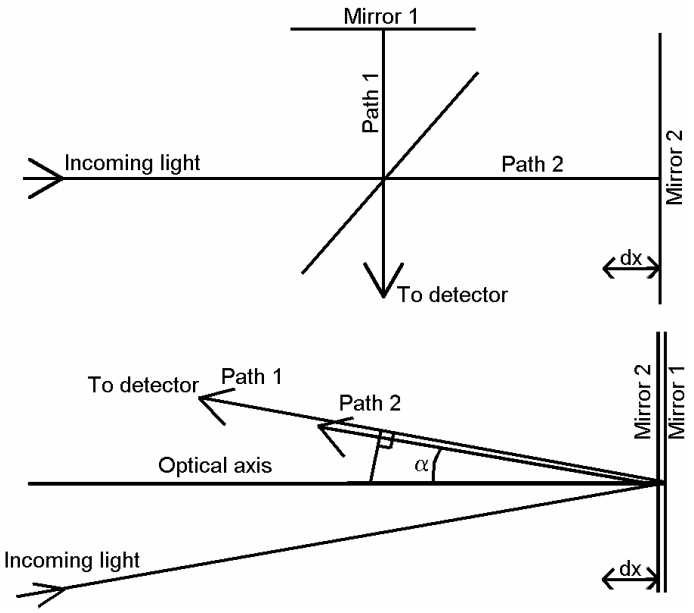

Figure 10. The figure shows the principle behind the squeezing effect when the incoming light is tilted with an angle α in comparison with the optical axis.

This reasoning can be extended to consider the case when the incoming light is coming from a distribution of angles. This will cause a broadening of the lines towards lower wave-numbers since the incoming light has a distribution inside a maximum angle Ω. If R(α) is the normalized distribution of light intensity over the different angles of incidence, then the spectra F will be distorted according to the following equation:

$$G(\nu) = \int_0^{\Omega} \frac{3 \cdot \alpha^2}{\Omega^2} \cdot R(\alpha) \cdot F(\nu \cdot \cos(\alpha)) \cdot d\alpha \qquad (3.11)$$

The dependence of α^2 is a result of that the light is entering through a bigger area at high angles. If there is an even distribution of light over all angles then $R(\alpha) = 1/\Omega$ for $0<\alpha<\Omega$.

The optical set up used for the measurements presented in this thesis includes an aperture before the spectrometer to limit the field of view of the spectrometer to force a well defined incidence angle that optimally should be zero. When using a large aperture, a larger squeeze factor is many times observed. However, even at the highest resolution used, 0.5cm^{-1}, it is difficult to observe a broadening of the lines when a large aperture is chosen.

4 This thesis

In the years 2002 to 2005, a project (KORUS) was run in cooperation with four industries to explore the possibilities to measure gas emissions of volatile organic compounds (VOC) with the SOF method. The four industries were three refineries, Preemraff-Göteborg, Preemraff-Lysekil and Shellraff-Göteborg, and the Oil harbour of Göteborg. All industries are located on the west coast of Sweden. The project aimed at lifting the usability of the method to commercially competitive performance, by increasing reliability and automatization. Simultaneously with the work to improve the method, an extensive measurement-program was run to put the method into a full-scale test to demonstrate its capacity for routine measurements. The success of the project is a result of the combined effort from many people in the Optical Remote Sensing group and many years of preparations.

Detailed results of the measurements on the industries are presented in the report: **Monitoring of VOC emissions from three refineries in Sweden and the Oil harbour of Göteborg using the Solar Occultation Flux method** [30]. This report is not appended to this thesis because it is too long. A summary of the results and general conclusions from the measurements are presented in the appended **paper A**. Some additional information that did not fit in **paper A** is given in chapter 7. A detailed error analysis of the measurements on the industries is presented in chapter 8 and a much shorter version is also included in appended **paper A**.

The SOF method and some examples of applications are described in the appended **paper B**.

To validate and test what precision that could be expected with the SOF method, two experiments were done where known amount of SF_6 trace gas was released and then measured with the SOF method. This is presented in chapter 5.

To make the SOF method more operative, development of the hardware and software of the measurement system was done. A new software for real time evaluation of the measurement was developed which made the measurements more efficient since it was possible to directly see if a measurement was successful or not. Also, the real time information has shown to be beneficial since it is possible to quickly scan through an industry and in real time detect leaks. This has resulted in that unexpected emission sources inside the industries have been discovered.

The newly developed QESOF software is described in chapter 6. Also, new post processing software was required to be able to handle and compile the results from the large number of measurements done on the industries. These are however not presented further in this thesis.

A new active solar tracker-was built that allowed 540° rotation. The old solar tracker only allowed 30° rotation and the heavy instrument must be moved by hand each time the measurement car made a turn. With the new solar tracker, this is not required anymore. The new solar tracker is described in chapter 9.

5 Validation of the SOF method with SF_6

The method to retrieve fluxes from traverses with a mobile solar-occultation system was tested on two experiments, carried out in year 2002 by Karin Fransson and Johan Mellqvist. In the first experiment, a trace gas (SF_6) was emitted from the top of a 17 m tall mast in the middle of an open field at Åby in Göteborg. Traverses were then done downwind with the measurement system at varying distances from the emission source. The wind was measured with a wind-meter located in the top of the same mast. The true amount of emitted trace gas was estimated by weighting the gas tube before and after the experiment and also measuring the time when the gas was emitted. The emitted gas was always approximately 2 kg/h. The measured peak concentrations were about 10 mg/m^2 for most scans.

The spectral evaluation was done in the region 925-975 cm^{-1} and included H_2O, CO_2, SF_6 and a fitted sky-reference spectra. Spectra for H_2O and CO_2 were created from the HITRAN database at a temperature of 288K and a pressure of 1 atm. SF_6 spectra was taken from the NIST database [31]. Figure 11 shows the transmission spectra for 1 mg/m^2 of SF_6. As can be seen, SF_6 is absorbing about 1% of the light in its peak at this concentration and this should be easily detected in the measured spectra. There is however a strong absorption-line of H_2O at wave number 948 cm^{-1} that is causing some trouble in the SF_6 retrieval. For the results presented here, non-linear spectral evaluation was used, Norton-Beer strong apodization [29] was used and a polynomial of 4th order was also fitted.

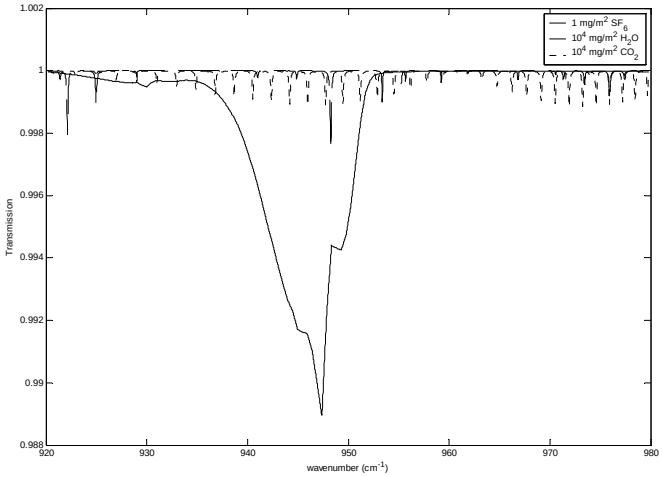

Figure 11. The transmission spectra of H_2O, CO_2 and the reference spectrum for SF_6.

Table 3 shows the results from the four days when the field experiment was done. The standard deviations for the calculated averages indicates that the result of just one traverse is uncertain and that averaging of many traverses are required to get reasonable results. As can be seen, each traverse has a low reliability but the average over many traverses comes close to the true value. Figure 12 shows a plot of the emissions derived from all the traverses for each day plotted towards the average wind speed during the traverse.

Table 3. Summary for each day in year 2002, when measurements on the Åby field were done.

Day	Emitted SF_6 (kg/h)	Calculated average (kg/h)	Number of accepted traverses	Average wind speed (m/s)	Average wind direction	Error
May-22	1.92	2.3±1.3	4	4.9-8.6	152°-169°	20%
May-23	1.97	2.2±0.6	15	3.9-5.6	120°-142°	10%
June-03	1.97	1.6±0.9	16	2.7-5.3	235°-273°	-20%
Jun-04	1.89	2.0±1.4	9	5.9-7.8	152°-191°	5%

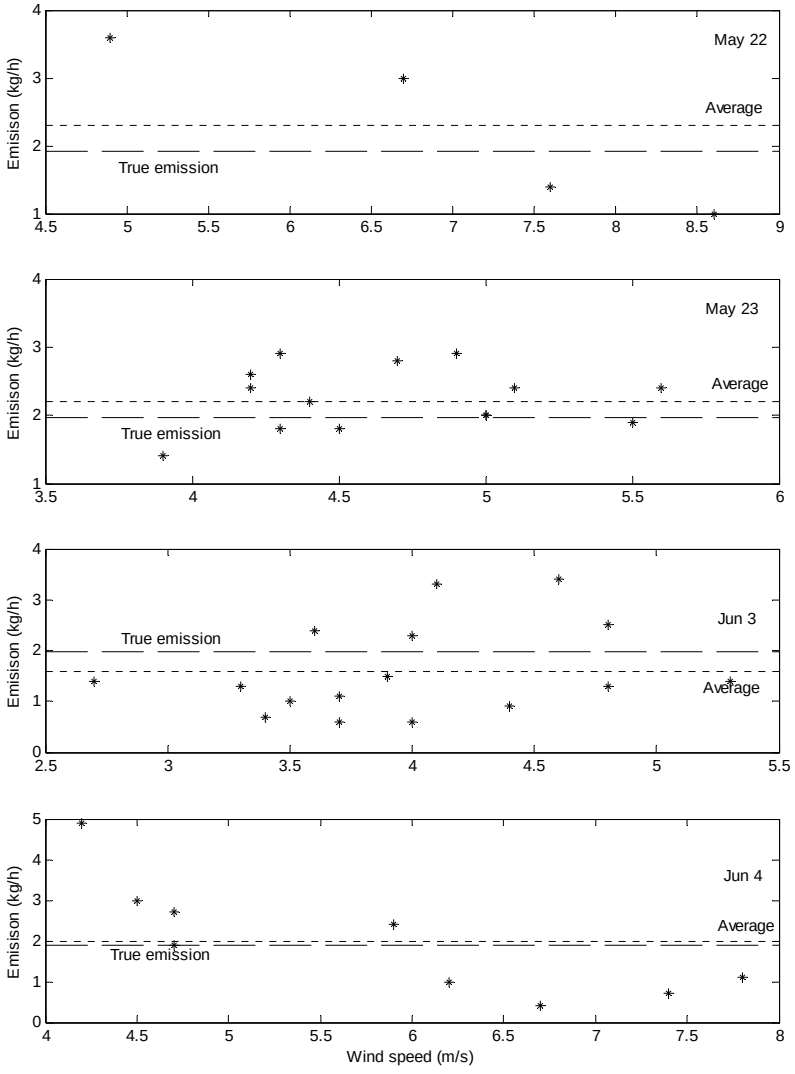

Figure 12. The figure shows the calculated SF_6 emission versus wind speed on all traverses.

Another experiment was done where SF_6 was emitted from the roof of a crude oil tank. The tank (Tank 105 at Preemraff-Göteborg) is located in a tank-park where nine tanks are standing close together, see Figure 13. It can be expected that the wind field is irregular close to the ground inside the tank-park. Traverses were done on a road along the side of the tank park, approximately 150 m away from the emission point. Figure 13 shows the location of a typical traverse on a map. During day 24-June 2002, eight traverses were successfully retrieved. Table 4 shows all the traverses done during that day. The true released amount of SF_6 was estimated to 2.0 kg/h by weighting the gas-tube before and after the experiment and the retrieved average emission was 3.0±1.1 kg/h which corresponds to an error of 50%.

Table 4. The traverses done on day 24-June 2002. True emitted amount of SF_6 has been determined to 2.0 kg/h.

Time (24 h)	**Emission SF_6 (kg/h)**	**Average wind speed (m/s)**	**Average wind direction**
12:45	3.1	6.5	252°
12:54	1.8	7.2	252°
13:05	1.3	6.0	259°
13:17	2.7	7.5	253°
13:29	3.1	5.4	255°
13:56	5.2	7.4	264°
14:05	3.7	7.2	251°
14:24	2.6	7.3	262°
14:31	3.4	6.5	260°
Average	**3.0±1.1**		

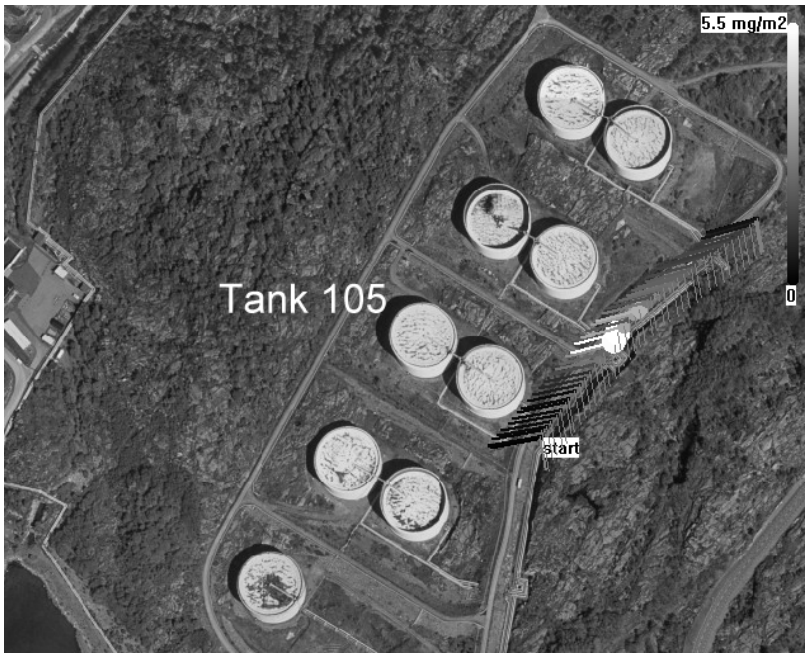

Figure 13. A typical traverse done when the SF_6 gas was emitted on top of tank 105. The broad lines along the traverse points towards the wind direction. *(Aerial photo: Copyright Lantmäteriet 2004-11-09. Ur Din Karta och SverigeBilden)*

6 The QESOF program

To render the SOF method more effective, an on line software was developed to allow real time evaluation when measuring gas emissions. The program waits for interferograms to be ready for evaluation, loads them, Fourier transform them and retrieves the line-integrated concentrations of the gases of interest from the spectra with a nonlinear algorithm. It combines this with the position of the vehicle retrieved by GPS, and wind information from wind-meters and calculates the flux of gas through the surface that is sliced out along the path the vehicle is driving. Linear interpolation is used both for the position, wind speed and wind-direction. It gives a graphical representation of the measured flux on a map while the measurement is running. The software was tailored to work with the Bruker OPAG and the Bruker IrCube spectrometers, and to do spectral evaluation with a resolution between 0.5 and 12 cm^{-1}. Two separate measurement systems were built with these two spectrometers.

6.1 The user interface

In Figure 14 the screen of the measurement-computer is shown. The upper left window shows a map of the measurement, with lines pointing toward the wind along the driving route. The measured and fitted absorption spectra are shown in the lower left window, and the retrieved data on the right side. All parameters are given to the program by text-files and results for post processing are saved as text files.

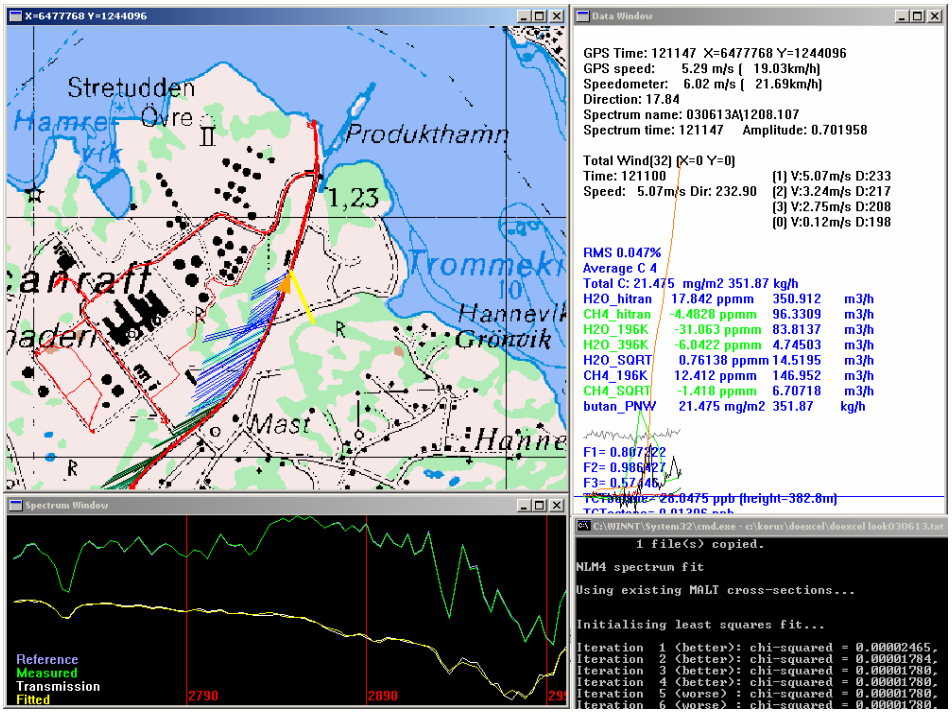

Figure 14. The figure shows the screen of the measurement computer with the presentation by the automatic retrieval software that has been developed, allowing online evaluation of the measured spectra. In the upper left is shown a map of the measurement with lines pointing toward the wind, the measured and fitted absorption spectra in the lower left, and the retrieved data on the right side.

6.2 Spectral evaluation in QESOF

Figure 15 shows a schematic view of the internal functions of the retrieval of the line-integrated concentrations in the QESOF-software. Each part will be described in this section. Each part has been numbered in the figure to simplify the discussion.

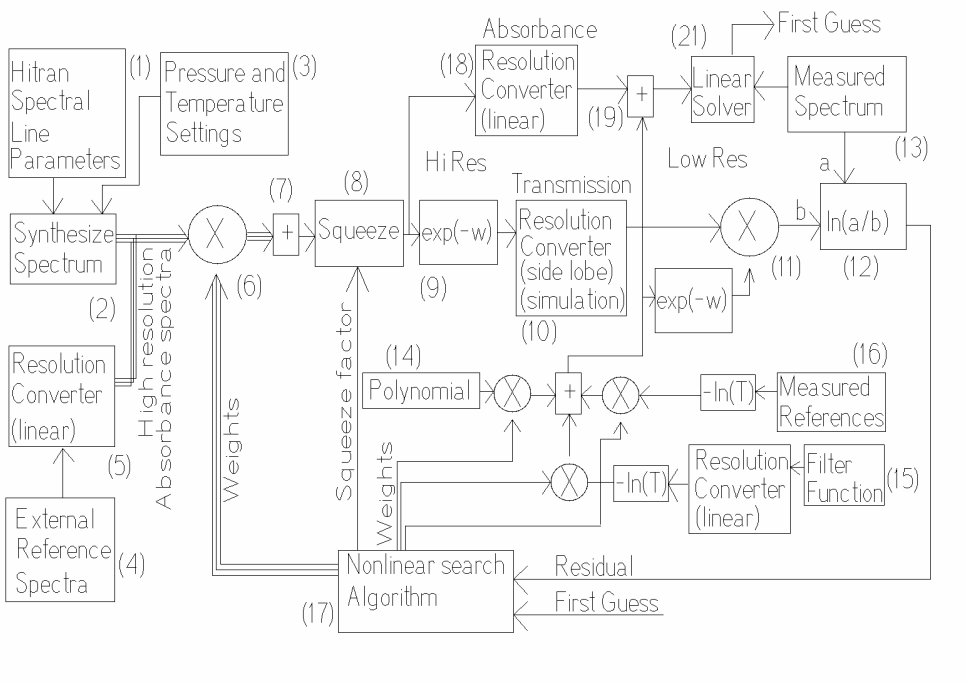

Figure 15. The internal functions of the spectral evaluation code in the QESOF software.

6.2.1 Hitran spectral line parameters - Part 1

The HITRAN database is probably the most exact and useful database for calculating cross sections of the most abundant compounds in the atmosphere at the date when this report was written. It is constantly updated when new and better information is available. Current version contains 63 compounds including most compounds that are of importance for studying the chemical properties of the atmosphere. The strength and wavelength of each absorption line is given as well as parameters that describe the pressure and temperature broadening of each line.

6.2.2 Synthesize spectrum - Part 2

The user chooses what compounds to be included in the spectral fit and the temperature and pressure for each compound (part 3). High-resolution spectra are then calculated for each compound based on the line parameters from the HITRAN database. For molecules with many absorption lines, this may require lots of computation. Therefore a buffert of the synthesized spectra is stored in a file the first time the program is run with new parameters. An old existing file is read in if it exists

and parameters are unchanged to reduce start-up time of the program. The resolution is set to 16 times higher than the distance between each discrete point in the measured spectrum that is entering in part 13. This determines what resolution is used in all parts that are working with high resolution.

6.2.3 External Reference Spectra - Part 4

QESOF was primarily developed to measure emission of alkanes from refineries. Unfortunately, data for the important alkanes are not present in the HITRAN database and therefore has to be retrieved from other database in the form of measured absorbance spectra. Spectra for propane and butane with 0.25 cm^{-1} resolution from the Pacific North West database and octane spectra with 0.5 cm^{-1} resolution from the QASoft database was used. External spectra can be provided to the program in either Galactic SPC format or in OPUS format. The spectra is converted to the same resolution as the synthetisized HITRAN spectra in part 5. To reduce calculations at start-up, buffers containing spectra with already converted resolution is maintained in a file and is used as long as parameters are not changed. The resolution of the absorbance spectra is converted with a linear interpolation that only considers the two points on each side of a wave number to calculate the absorbance at the new wave number. There is a possibility that this conversion can induce distortion if dealing with narrow absorption lines. For measurements at 0.5 cm^{-1} the internal high resolution will be 0.03 cm^{-1} and anticipating a safety factor of 4, spectral lines sharper than 0.12 cm^{-1} is possibly distorted. This can be neglected when dealing with compounds with broad spectral features, for example the alkanes.

6.2.4 Mixing of reference spectra - Part 6

The weight for each high-resolution reference spectra is provided by the non-linear fitting algorithm (part 17) and represents the guessed line integrated concentration of each compound. All absorbance spectra are then summed (part 7) to give the guessed synthesized high-resolution spectrum.

6.2.5 Squeezing of synthesized spectra - Part 8

When evaluating high-resolution spectra (0.5 cm^{-1}) it is most times required to compensate for nonzero incidence angle in the spectrometer. As described in section 3.3, this causes a squeeze of the spectra so that spectral lines will show up at lower wave numbers. This is anticipated by also squeezing the synthesized spectra by either forcing the squeeze factor to a value chosen by the user or letting the non-linear algorithm find the best squeeze to get the best fit between the final low-resolution synthesized spectra and the measured spectra.

The algorithm used for squeezing the high-resolution absorbance spectra rearranges the vector that is representing the individual intensity values in the spectra and uses linear interpolation that only considers the two points on each side of a wave number to calculate the absorbance at the new wave number. Just like mentioned with part 5, this can cause some errors when dealing with spectra with narrow absorption lines.

6.2.6 Conversion to transmission of synthesized spectra - Part 9

The synthesized absorbance spectra is converted to transmission:

$$Transmission = \exp(-Absorbance) = \exp(-\sum_i conc_i \cdot L_i \cdot \sigma_i) \qquad (6.1)$$

This is the same as equation 2.1 except that scattering has not been considered. The effect of scattering will be removed by including a polynomial with part 14.

6.2.7 Resolution conversion with side lobe simulation - Part 10

When the concentrations of all compounds, and pressure, temperature and squeeze parameters is close to a perfect match to the conditions imposed on the measured spectra, the high resolution synthesized spectra reaching part 10 is hopefully a high resolution representation of the light that is actually reaching the spectrometer. As previously shown in Figure 7, each wavelength will induce side-lobes in the spectra especially if the wavelength causes high light intensities at the edge of the sampled interferogram. This is simulated by convoluting with the modified *sinc* functions that was previously shown in Figure 9 when converting from the high resolution to the low resolution. The convolution functions representing the different apodization functions are calculated in advance and the desired one is read by the code depending on what apodization function the user has chosen. The conversion to low resolution is done to the same set of wave numbers as in the measured spectra. Then, a direct comparison between synthesized spectra and measured spectra is possible, point for point. When the user has chosen no apodization, then the convolution with the sinc function is done in the following way:

$$G(\nu_L) = \frac{\sum_j S(\nu_j) \cdot Sinc\left(\pi \cdot (\nu_j - \nu_L) \cdot \frac{zf}{\Delta\nu}\right)}{\sum_j Sinc\left(\pi \cdot (\nu_j - \nu_L) \cdot \frac{zf}{\Delta\nu}\right)} \qquad (6.2)$$

$$Sinc(x) = \frac{\sin(x)}{x} \qquad (6.3)$$

$G(\nu_L)$ is the resulting low resolution transmission at one data point with wave number ν_L. The data points in the vector G have a wave number separation of $\Delta\nu$.

zf is the zero-filling factor chosen by the user. Thus, the combination $\frac{zf}{\Delta\nu}$ represents the wave number separation as if no zero-filling was chosen. If the user has chosen to use apodization then the *sinc* function shown in equation 6.3 is replaced with the functions shown in Figure 9. These must however be calculated numerically by Fourier-transforming the apodization functions. $S(\nu_j)$ is the high resolution spectra that has data points at the wave numbers ν_j, not necessarily coinciding with ν_L. The summation over j is done at all data points on the high resolution spectra that lies inside the spectral interval where the spectral evaluation is done plus 320 extra points on each side of that interval. The extra 320 points is included to avoid side-lobe

effects at the edges of the chosen interval. It is required that $S(\nu_j)$ has valid spectral-information these extra 320 spectral points. The resulting low-resolution spectrum has spectral information at the same wave numbers as the measured spectra and a direct comparison point by point is therefore possible. Before a comparison is done, the multiplicator marked 11 will incorporate optional components in the synthesized spectra.

6.2.8 Calculation of residual – Part 12

The residual is calculated i.e. the discrepancies between the measured and the synthesized spectra by the following formula:

$$\vec{R} = \log\left(\frac{\vec{T}_{measured}}{\vec{T}_{synthesized}}\right) \tag{6.4}$$

The letter T has been chosen to represent the spectra to indicate that they represent transmission. Equation 6.4 is the residual in represented as absorbance and this representation has been chosen since it will make the search for the next guess more linear in the non-linear algorithm (part 17).

6.2.9 Measured spectrum – Part 13

The software will automatically wait for new measurements to be evaluated. It can either be set up to load files generated by the Bruker OPUS software in a continuous way. The OPUS software is then set up to take spectra with the spectrometer, store it in a file and unloading them in a repetitive way. When the file is valid for reading, QESOF will automatically load it and evaluate it. QESOF can also be set up to directly communicate with the IrCube spectrometer by its web-server interface, without using OPUS, and request new spectra in a repetitive way.

The user has the choice to prefer interferogram information or already Fourier transformed spectra in the retrieved files. If the user prefer interferogram and an interferogram is present in the file, then a Fourier transform is done inside the QESOF software with the zero-filling and apodization parameters that the user has chosen even if a spectra is also present in the file. If an interferogram is not present then a spectrum will be read if it is present in the file. If the user prefers already existing transformed spectra and a spectra is present in the file, then the spectra will be read from the file. Otherwise an interferogram will be read and Fourier-transformed if it is present in the file.

When Fourier-transforming in the software, the user can choose to perform a slow discrete Fourier transform with the same number of data points as the interferogram or optionally cut the interferogram before its actual ends. This is useful if one wants to study the consequences of lowering the resolution. This is also useful if the interferogram is noisy close to its edges and therefore should be omitted. The user also has the choice to zero-fill the interferogram to the closest higher exponential of 4. The software will then use a much faster Radix-4 algorithm for the Fourier-transform.

6.2.10 Polynomial – Part 14

An optional polynomial can be multiplied to the low-resolution spectra. Fitting of a bias term is always required to take care of varying light intensities in the measurement. Fitting of a linear term takes care of most variations caused by scattering. Even the Rayleigh scattering that has v^4 dependence can be approximated with a line if the wave-number interval for the evaluation is small. Fitting of higher polynomials is possible but may lead to errors due to that compounds with broad absorption structures is partly fitted with a polynomial instead. This has been observed when using polynomials with four terms when evaluating measurements containing alkanes of low concentrations.

6.2.11 Optical filter – Part 15

With both the Bruker OPAG and the IrCube spectrometer, optical filters has been placed just before the entrance to the spectrometer to test if it will result in better signal to noise ratio. The benefit of using optical filters is that more light at the interesting wavelength interval can be used without saturating the infrared detector. Unfortunately, the use of optical filters has shown to cause problems if the filter function has structures in the neighborhood of the evaluation interval. Even faint structures in the filter function can be huge in comparison to the absorption on the molecules of interest. The effects of these are difficult to compensate for due to the rough and varying situation imposed by the environment in a field measurement, where vibrations are strong and where temperature and the incidence angle into the spectrometer is varying.

The spectral shape of the filter function of the optical filter can be measured in lab. One or many filter functions can then be incorporated into the synthesizing if needed. The optimal strength for each filter function is then found by the non-linear algorithm. It has been observed that the strength of the filter function is dependent on if the filter is slightly tilted, which is many times the case when doing field measurements. This is taken care of by fitting the strength of the filter function. It has also been observed that the shape of the filter function is temperature dependent. This has been taken care of to a first degree by heating the filter in the lab to 30K above room temperature and dividing the measured filter function with the filter function measured at room temperature. This deviation is then also included as a filter function where the strength is decided by the non-linear algorithm. This temperature dependence is quite severe since the filter is usually exposed and thereby heated by concentrated sunlight. Due to the mentioned problems, it has most times been decided that optical filters should not be used.

The filter functions should be given as transmittance and can be provided to the program as Galactic SPC files or OPUS files in any desired resolution. The resolution of each filter function is converted to the same resolution as the measured spectra with linear interpolation. The weight of each filter function is decided by the non-linear algorithm and is then multiplied by the synthesized low-resolution spectra.

6.2.12 Measured references – Part 16

When the study of localized emission sources at ground level is the prime focus, the upper atmosphere is of no interest. However, with the SOF method the influence of

the upper atmosphere will always be present. This can be a problem if there are strong absorption structures overlapping with the absorption structures of the molecules of interest. One approach that is sometimes used to solve this is to find a match for all the spectral properties, by simulating an atmosphere with many layers and determining concentrations in each layer. This is difficult to do when working at low resolution due to the limited amount of information in the measured spectra. Another approach is to measure a spectrum at a place where one can assume that the concentrations are zero of the compounds that one wants to study. This spectral measurement then represents the sky and is included in the spectral evaluation where the weighting of the spectrum representing the sky is decided by the spectral evaluation. The fitting of the weight makes the measurement of the sky usable even if the path length through the atmosphere varies. If the sky spectrum is evaluating itself in the spectral evaluation, all other compounds will evaluate to zero since it represents a perfect fit. This method is not limited to one measurement of the sky but any number of measured spectra throughout a day can be used as sky references. These points are thereby forced to give zero alkane concentration. By choosing a few sky references throughout a day where it can be assumed that the alkane concentration is zero, it has been observed that an efficient removal of the influence of the upper atmosphere can be done. However, this method will cause errors in the retrieval if any of the chosen references have nonzero alkane concentration and should therefore be used with care. A strategy that has shown to give reasonable results is to start the measurements at a clean place and then drive into the contaminated area. The scan should if possible also be ended at a clean place. The first measured spectrum is then taken as the sky. If this is not enough to remove the influence of the upper atmosphere, the last measured spectrum is also taken as a reference. This also has the benefit that time variations occurring in the atmosphere during the traverse can to a first order be simulated by the weighted superposition of the first and last spectra.

6.2.13 Non-linear search algorithm – Part 17

The input to the non-linear search algorithm is the residual from the last guess. The outputs are the weights to all the selected compounds and polynomial in part 6, 14, 15 and 16. The guessed squeeze factor is also output to part 8 if fitting of the squeeze is selected. The step taken in the next iteration is given by finding the best least square solution of the vector $\vec{x}$ to the following equation system:

$$\vec{\vec{A}} \cdot \vec{x} = \vec{R} = \log\left(\frac{\vec{T}_{measured}}{\vec{T}_{synthesized}}\right) \tag{6.5}$$

The last identity is the same as equation 6.4. The equation is solved in the code by an implementation of the Householder algorithm. The equation requires some further explanations:

$$\vec{\vec{A}} = \begin{bmatrix} | & | & | & | \\ \vec{a}_1 & \vec{a}_2 & ... & \vec{a}_n \\ | & | & | & | \end{bmatrix} \tag{6.6}$$

$$\vec{a}_i = \log\left(\frac{\frac{d\vec{T}_{synthesized}}{dx_i}}{\vec{T}_{synthesized}}\right) \quad (6.7)$$

$\vec{T}_{synthesized}$ is the synthesized spectra from last iteration. $\vec{T}_{measured}$ is the measured spectra. $\frac{d\vec{T}_{synthesized}}{dx_i}$ represents the change in the total synthesized spectra if the weight x_i is changed.

Equation 6.5 is then solved so that the values of x_i are determined. The solved values of x_i are then multiplied by 0.9 and added to the weights that were used in the last iteration. An approximate solution is often found after just two iterations. The iterations are forced to stop after 100 iterations or if the last solution caused a higher RMS error than the previous guess.

To make the algorithm more stable and to speed up evaluation, a linear solution is always first calculated and is used as the first guess in the non-linear search. The non-linear search can also be completely skipped if the concentrations of the studied compounds as retrieved by the linear method are lower than a threshold defined by the user. In this way, the results from the faster linear method will be used if the concentrations are low, and the results from the non-linear method will be used if the concentrations are high. This is motivated by that non-linear effects typically become important when absorptions are strong.

The linear method is based on a variation of the non-linear code. The columns of the A matrix in equation 6.6 is instead built one at at time by simulating a spectra with the same code but only with one weight set to nonzero and the others set to zero. The synthesized spectrum is not converted to transmission in part 9 but takes another route through a linear resolution converter that does not simulate side lobes. The production of side lobes is a non-linear effect and cannot be considered when doing a linear fit. The polynomial, filter function and measured references from part 14, 15 and 16 are instead treated as absorbance. Equation is then replaced with the corresponding equation:

$$\vec{\vec{A}} \cdot \vec{x} = -\log\left(\vec{T}_{measured}\right) \quad (6.8)$$

The vector $\vec{x}$ representing the weights of the compounds is found by finding the best least square solution. The values of $\vec{x}$ are taken as the first guess for the non-linear search algorithm. The fitting of the squeeze factor is highly non linear and the squeeze-factor must therefore be forced to a default value chosen by the user when finding the linear solution. The default value will also be the first guess for the squeeze factor in the non-linear search algorithm.

6.2.14 Non-linear fit of the squeeze factor

The search for the best squeeze factor is slightly different. First guess for the squeeze factor is given by the default value chosen by the user. A perfect, undistorted spectra, corresponds to a squeeze factor of 1. The result is highly dependent on the choice of the first guess since there is a risk that the algorithm finds a local minimum instead of

the best solution. The diagram in Figure 16 describes the search algorithm. It first makes two iterations for the non-linear fitting to get a good first guess for the concentrations. It then tests if lowering or increasing the squeeze will cause a better fit to the measurement. After it has found the optimum squeeze for the current set of guessed concentrations it retrieves new guesses for the concentrations by making just one iterative step in the non-linear algorithm. This continues until no better solution is found.

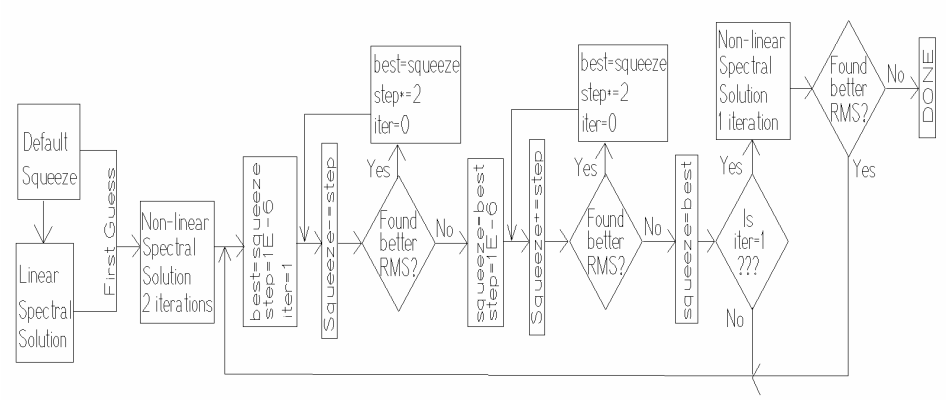

Figure 16. The diagram describes the algorithm used for finding the best squeeze.

6.3 Mathematical presentation of the algorithm

In section 6.2 all the blocks of the spectral evaluation algorithm was presented in detail. The algorithm implements some new ideas that are more clearly presented with equations, which here will follow. The linear solver can be described with the following method:

$$\ln\left(\vec{T}_{measured}(\nu)\right) - A + B + C + D = residual \tag{6.9}$$

$$A = \sum_i w_{sky,i} \cdot \ln\left(\vec{T}_{sky,i}(\nu)\right)$$

$$B = \sum_j w_{filter,j} \cdot \ln\left(\vec{T}_{filter,j}(\nu)\right)$$

$$C = \sum_k w_{ref,k} \cdot \sigma_{ref,k}(\nu)$$

$$D = \sum_{l=0} w_{polynomial,l} \cdot \nu^l$$

$\vec{T}_{measured}$ is the measured spectra.

$\vec{T}_{sky,i}$ are the selected reference measurements that are used to eliminate the atmosphere.

$\vec{T}_{filter,j}$ are the transmission functions of the optical filters (optional).

$\sigma_{ref,k}$ is the cross sections for the molecules that one wants to quantify.

The linear system is then solved by selecting the weights $w_{sky,i}$, $w_{filter,j}$, $w_{ref,k}$, $w_{polynomial,l}$ so that the length of the residual vector is minimized.

The non-linear algorithm can also be represented by equation 6.9 but with factor C replaced with the factor F here described:

$$\ln\left(\vec{T}_{measured}(\nu)\right) - A + B + F + D = residual \qquad (6.10)$$
$$F = -\ln\left[Distort\left[\exp(-C)\right]\right]$$

where *Distort* is an operator that represents the distortion in the spectra due to instrument line-shape factors, the incidence angle of the light, and the side lobes. These effects should be simulated in the software and applied to the synthesized spectra. These effects are weak for spectra with smooth properties, and has therefore little importance for the smooth structures in the filter function and the polynomial.

6.4 Validation of the spectral algorithm in QESOF

The results of the spectral fitting algorithm has been compared and verified with the results retrieved from other software, a Classical Least Square (CLS) method in the Grams software [32] and the non-linear NLM4 software developed by Griffith [19]. Comparisons were also done with a software used for FTIR measurements of volcanic gases by INGV (Istituto Nationale di Geofisica e Vulcanologia) [18], where the spectral evaluation of QESOF showed a very good agreement with the INGV results.

Figure 17 shows a comparison between the QESOF, NLM4 and CLS. The comparison was done on the total alkane concentration in a traverse done with a mobile solar occultation system outside a refinery. At the point of maximum concentration, the figure indicates that the values from QESOF are very similar to the NLM4 code and 10% higher than for the CLS code. The discrepancy towards the CLS algorithm is understandable for two reasons. First, since the CLS is a linear algorithm it underestimates the concentrations at high values. Second, close examination at the points of maximum concentrations shows that evaluating a mixture of propane and butane gives a much better spectral fitting to the measured spectra and this should therefore also give a higher total alkane mass.

The parameters used in the evaluation are the same as the standard parameters in the refinery application but with the addition that an optical filter was used in the set up. This was compensated for in the evaluation by adding two filter functions representing the filter to the evaluation in the QESOF and NLM4 evaluation. In the NLM4 evaluation, the filter functions were treated as external absorption spectra to be included in the evaluation. For the CLS evaluation, no filter function for the filter was provided to the evaluation. For NLM4, and CLS, Fourier-transforming was done with OPUS. For QESOF, Fourier-transform was done with the internal code. In all cases were no zero-fill and Norton-Beer strong apodization chosen. For the QESOF and NLM4 evaluation the evaluated alkanes were propane, butane and octane while butane was the only alkane included in the CLS evaluation.

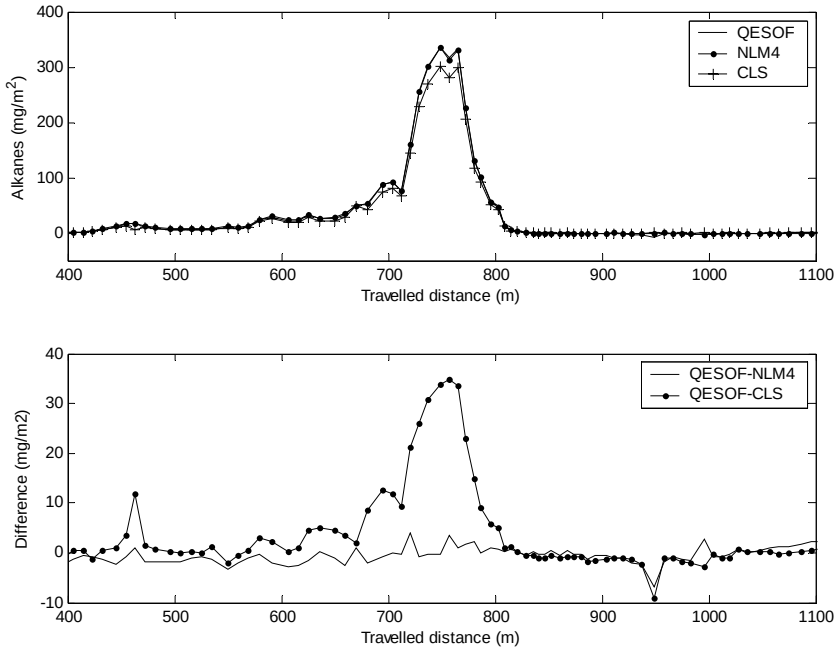

Figure 17. Comparison between three spectral algorithms when evaluating total alkane concentration in a traverse done with a mobile solar-occultation system outside a refinery. The results from QESOF and NLM4 are coinciding over almost the whole scan in the upper picture.

Figure 18 shows comparisons between the QESOF code and the INGV code when evaluating SO_2 and HCl from emissions from the Etna volcano. For the INGV data presented in the figure, a bias of 6 mg/m^2 in the HCl concentrations and 118 mg/m^2 has been subtracted to force the baseline to zero. There is no bias present in the QESOF results. This indicates that the inclusion of a "sky" reference is able to eliminate the influence of the atmosphere without distorting the measurements of SO_2 and HCl. For the QESOF results, the two isotopes ^{35}HCl and ^{37}HCl were retrieved separately and then added to get the total concentration of HCl. For the QESOF code, fitting of the stretch parameter was used and no zero-fill was used. Apart from the sky reference, H_2O, CH_4, O_3 and N_2O were also fitted.

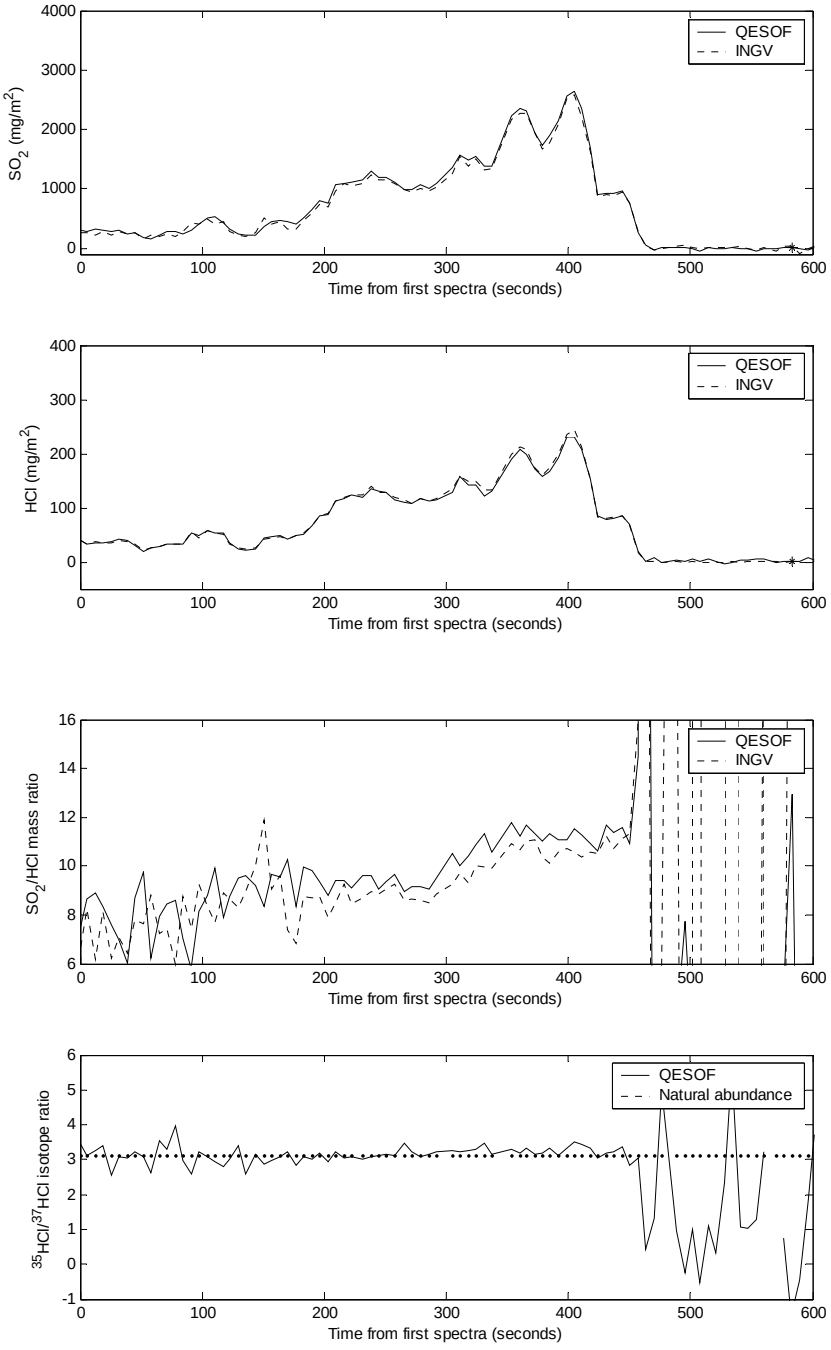

Figure 18. Comparison between the QESOF code and the INGV code for a traverse done with a mobile solar-occultation system 17 km away from the Etna Volcano on Sicily. The selected "sky" reference for QESOF is taken 570 seconds after first spectra and is indicated with a star.

7 Measurement of VOC from refineries

In the appended **Paper A** the method and the essential results from the monitoring project on the refineries are presented. Some additional information and some more examples of interesting measurements that did not fit in the paper are given in this chapter.

7.1 More on spectral evaluation of alkanes

In **Paper A** it is concluded that most of the VOC emitted from refineries is in the form of alkanes. A spectroscopic approach was therefore chosen for the refinery measurements that measure the emission of total mass of alkanes in the emitted gas. Measuring the total mass of alkanes independent on the exact alkane compound is possible with low resolution FTIR in the 3.3 μm region since the absorption occurring in this region is specific for the vibration/rotation occurring in a bond between a hydrogen atom and a carbon atom. The SOF instrument is sensitive to the alkanes shown in Figure 19. The figure shows the transmission structures for these alkanes. A transmission below one indicates that absorption has occurred. When measuring at a spectral resolution of 8 cm^{-1} it is difficult to resolve the individual types of alkanes from each other since their spectral shapes are overlapping and similar in shape to each other. However, the absorption strength is approximately proportional to the number of C-H bonds in the molecule. In addition, the molecular mass of an alkane is approximately proportional to the number of C-H bonds in the molecule. Absorption strength will therefore be approximately proportional to the mass of alkanes.

The time it takes to retrieve a spectrum with the FTIR-spectrometer grows with the square of the resolution. Measurements can therefore be performed much faster if performed at low spectral resolution. Alkanes have wide absorption structures and this makes it possible to use low spectral resolution for the quantification. For the measurements on the refineries, it is important that measurements are taken with a high repetitive speed because it is advisable that a traverse is done within a short time so that the local wind direction is kept the same during the whole traverse. Therefore a relatively low resolution of 8 cm^{-1} has been chosen since it has shown to give the highest repetitive speed in the measurements without loosing the capability to identify the average number of carbon atoms in the measured alkane. Spectra are measured with a repetition of 3.2 seconds. When doing leakage search inside the industry area, the distance between measurements need to be short in order to be able to identify the source of a registered emission. Therefore the car is then driven at approximately 10 km/h. When measuring total emissions from a whole industry at a far away distance of approximately 1 km, the car is driven at approximately 40 km/h. The car should not be driven slower than this in order to avoid that the local wind direction changes during the traverse.

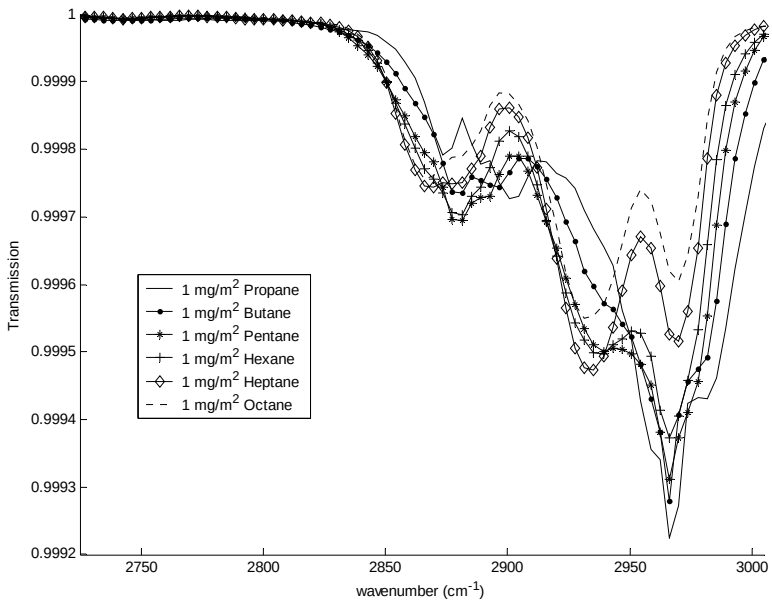

Figure 19. The picture shows the transmission for 1 mg/m^2 of the alkanes. The shown spectral region is the same as the region where the spectral fitting is performed. The spectral resolution shown has been degraded to the same resolution as for the measurements.

7.2 More on determination of carbon count number

It was realized that the kind of alkane observed in the SOF-measurements is an indication of the origin of the gas. If propane, butane and octane (with respectively 3, 4 and 8 carbon atoms in the molecule) are simultaneously included in the spectral fitting, the average number of carbon atoms in the measured alkane can be calculated by the following equation:

$$C_{avg} = \frac{3 \cdot m_{propane} + 4 \cdot m_{butane} + 8 \cdot m_{octane}}{m_{propane} + m_{butane} + m_{octane}} \qquad (7.1)$$

where m stands for the line integrated mass concentration of each compound. Typical observed carbon count numbers were 3.7 for crude-oil tanks, 4 for gasoline tanks, 6 for kerosene tanks, 5 for process and 6.5 for the water treatment facility. An example of how this was determined is shown in Figure 20 where the measured alkane plume and the calculated average carbon count for a water treatment facility is shown.

To evaluate propane, butane and octane simultaneously thus give valuable information but is done at the expense of more noise in the baseline i.e. registered alkane concentration even though no alkanes can be expected. A more sophisticated method has therefore been used that first evaluates the spectrum as butane only. If the evaluated butane concentration is higher than 12 mg/m^2, a new spectral evaluation is done with propane butane and octane. The sum of the three is taken as the total concentration of alkanes and is sensitive to the presence of all alkanes since other alkanes have spectral absorption structures similar to these three.

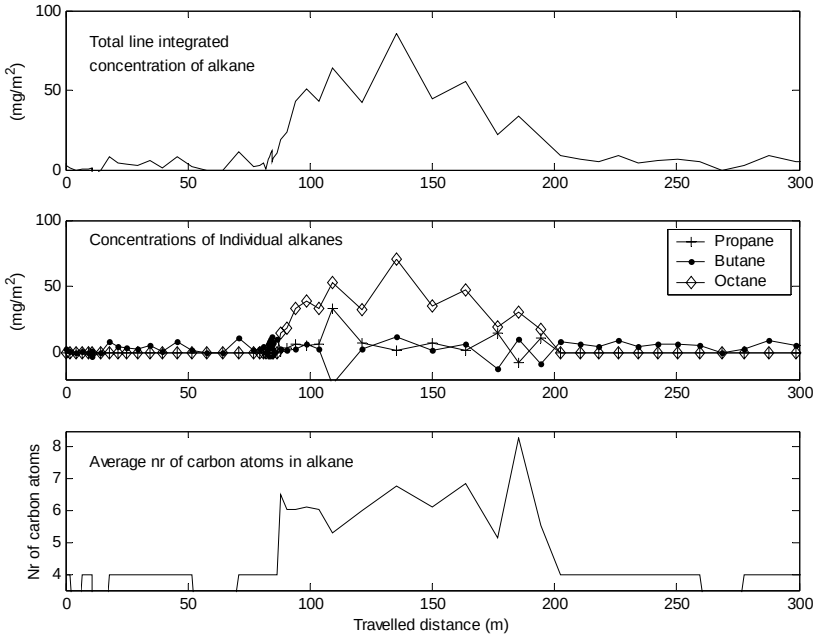

Figure 20. The figure shows the measured concentration of alkanes in a traverse of the plume from a water treatment facility (Preemraff-Göteborg, day 040910, time 15:13). When located in the plume, the average number of carbon atoms can be calculated and used for determining the source of the gas emission. Observe that only butane is evaluated when the alkane concentration is below 12 mg/m^2 and the average carbon count is then 4.

7.3 More on the parameters for spectral evaluation

Table 5 and Table 6 show the parameters that have been used with the QESOF software to retrieve the total alkane concentration in the measurements on the refineries. Is has been observed that some of the nonlinear effects due to the strong absorption lines of atmospheric H_2O, CH_4 and HDO can be removed if the square-root of the absorption spectra of compounds are also fitted. The square-root of the absorption spectra have been created by changing the line-strengths in the HITRAN database to the square root of its original value. This approach is valid since the aim is to remove the spectral structures of the species and not to evaluate the column values.

Table 5. The following table summarizes the standard parameters used for the spectral fitting of the alkanes in the KORUS-project.

Wavenumber interval	2725-3005 cm^{-1}
Resolution	8 cm^{-1}
Nr of averaged interferograms per sample	16
Apodization	Norton-Beer Strong
Fitting of a linear polynomial.	
No fitting of the spectrum stretch.	

Table 6. The gases included in the spectral fitting for the standard parameters in the KORUS-project.

Gas	Temperature (K)	Pressure (atm)	Database
H_2O	283	1	HITRAN ([12])
H_2O	253	0.5	HITRAN
Square root of H_2O	273	1	HITRAN
CH_4	253	0.5	HITRAN
Square root of CH_4	273	1	HITRAN
HDO	253	0.5	HITRAN
Square root of HDO	273	1	HITRAN
Propane	298	1	PNW ([33])
Butane	298	1	PNW
Octane	298	1	QAsoft ([34])
Reference	-	-	Typically first measured spectrum in a traverse. See section 6.2.12.

7.4 More on calculation of the yearly averages

Paper A describes how total measurements and sub-sector measurements are done. Daily averages of emission are calculated for all total measurements and sub-sector measurements done on the same day. During one year, total measurements on an industry were typically collected on four days and close measurements on each sub-sector were done at least on two days. Low variation in the measured emissions over a day is an indication of high quality in the measurements that day and that no exceptional activity was taking place at the industry on that day. A day with low variation of the total emission over the traverses during the day should therefore be more important when determining the total emission during that year. The main purpose of the measurements in the KORUS project was to determine emissions when the refinery was running under normal conditions. Therefore, the daily averages of the emissions for all days during a year are averaged in such a way that the weight of the average of a day is inversely proportional to the standard deviation among the traverses during that day. This will lead to that a day with low variation of the emission over the traverses will be more important when determining the total emission during that year.

7.5 Examples of unexpected emission sources

When a traverse was done to the north-most corner of Preemraff-Lysekil one day in 2004 a new emission source was by coincidence discovered that was identified to be the rock cavern exhaust. When this was discovered, the old measurements from 2003 were reevaluated to try to find signs of emissions source at the same place but no emissions was then found. However, it is possible that the source was completely missed in 2003.

Another unexpected source was found while measuring on the same refinery in summer 2004. It was discovered that the preskimmer was a significant point source. The preskimmer is a part of the waste water treatment system. It is constructed as a sewer with a filter where large debris is removed from the water before it gets to the waste water facility. From old measurements from year 2003, a few measurements could be retrieved but these measurements do not have as high quality as from year

2004. However they indicates clearly that the preskimmer had lower emissions year 2003. In year 2003 another unexpected emission source was found in the corner of the crude-oil tank park on Preemraff-Göteborg and were identified to be a sewer. However, in year 2004 almost no emissions were found from the sewer. There were no measurements found from year 2002 that indicated emissions from the sewer. However, emissions from the sewer were not anticipated then and may therefore have been missed.

7.6 Examples of observed changes in the emissions

Shellraff had a routine total maintenance stop in year 2003 and the refinery was restarted two weeks before the measurements started. Figure 21 shows the change of emissions from the hysomer[1] and process during year 2003 and 2004. The reason for the reductions in emissions is believed to be that process-equipment was leaking after the total maintenance stop and the leaking equipments were later found and repaired. In August-2003 there is a drop in the hysomer emission that can be explained by three documented repairs that have been done because leaks were detected. Between August-2003 and May-2004 there is a drop in the emission from the process that can be explained by seven documented repairs that have been done because leaks were detected or because of equipment breakdown. These measurements gave new insight of the emission picture after a total maintenance stop. The measurements showed that the emission picture returned to normal within less than a year. This would not have been detected if measurements were only done every third year, as was the routine before on the refinery. Thus, measuring every year has shown to give new valuable information. The relatively low cost of the method motivates that routine measurements should be done every year on the refineries in order to quickly detect changes in the emission picture.

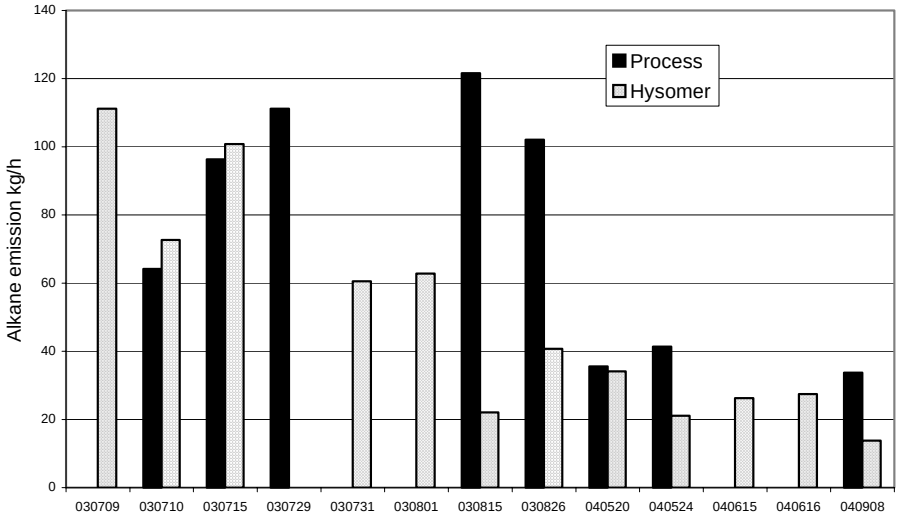

Figure 21. The figure shows the change of emissions from process and hysomer. Notice the drop in hysomer emission after 1-August-2003 and the drop in process emission after 26-August-2003.

[1] Hysomer is an abbreviation for hydro-isomerisation and is a part of the process where normal and mono-branched paraffins are converted into higher branched (high octane) components.

Measurements on the flare were done on day 14-July-2003 during 1.5 hours by driving back and forth about 50 meters in such way that the sun-ray traversed the flare. This resulted in 73 traverses and the average of all traverses were 15 kg/h. Figure 22 shows the variation over the whole set of traverses. The emission is higher than what has been observed on other measurements. After the total maintenance stop earlier year 2003, there was an error in the control of the flare that caused it to pulsate. This can probably explain the high measured emission. The problem with the flare was fixed later in year 2003.

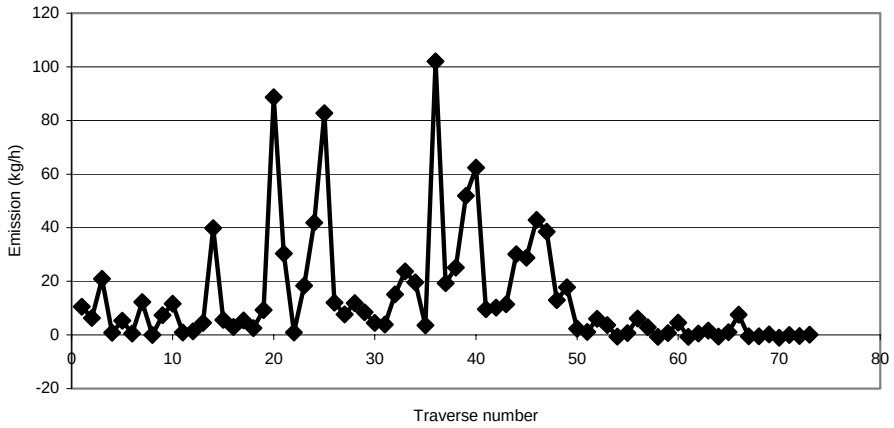

Figure 22. Results of individual traverses to measure the emission from the flare.

During day 8-June-2004, traverses for measuring total emissions were done along Oljevägen. It was quickly observed that emissions were much higher than normal. The measurements indicated a strong emission source inside the west tank-park. Measurements were then done inside the west tank-park and the point source was identified to be tank 105 containing residues of water mixed with oil. This was immediately reported to the personnel-in-charge. After investigations, it was found out that the tank-roof was tilting. This was fixed just a few hours later. Table 7 shows the total measurements done along Oljevägen before the roof was fixed. Total emissions should be compared to the average emission for 2004 that were 122.1 kg/h.

Table 7. Results of individual traverses on day 8-June-2004 when the roof of tank 105 was tilting.

Time	Total emission Shellraff (kg/h)	Tank 105 (kg/h)	Wind speed (m/s)	Wind direction
12:45	1490		5.0	36°
12:55	541		4.6	59°
13:15	691	126	4.7	44°
13:25	830	186	4.5	39°
13:40	199		3.3	55°
13:50	714		3.9	39°
14:10	633		3.1	42°

Crude oil tank 1406 on Preemraff-Lysekil was of special interest since earlier measurements with the DIAL method had shown high emissions from this tank and it was known that the floating roof on the tank was not tight. Before year 2003 a second

seal was built around the tank-roof in hope that it would decrease the emissions. Figure 23 shows how the emissions were still high in 2003 after the second seal was fitted but much lower in 2004. No construction changes or maintenance work was done with the tank between 2003 and 2004. However, the type of crude oil in the tank changed from 2003 to 2004. It is possible that this is the cause for the reduction in the emissions.

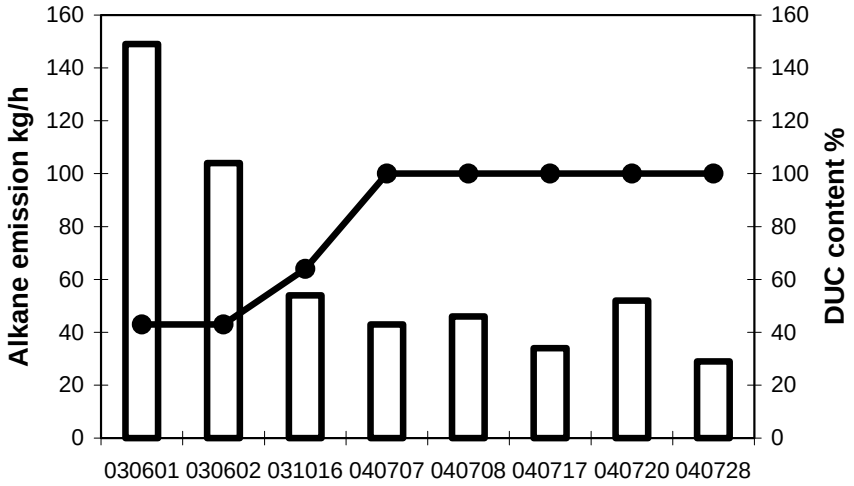

Figure 23. The figure shows the change of emission from crude-oil tank 1406. The crude-oil type changed from a mixture of Gullfaks® A&C and DUC® in 2003 to 100% DUC in 2004. The tank-roof level was at top on all days except 8-July when it was at 70% and 20-July when it was low.

7.7 The mobile wind meter

A new method was tested to measure the local wind speed at ground level where an ultrasonic wind meter was mounted in the front of the measurement car, see Figure 24. The true wind was then calculated by subtracting the velocity vector for the car from the measured wind vector. The resulting wind vector is then averaged over 60 seconds to get an average wind. The speed of the vehicle was either measured by a speedometer mounted on one wheel on the car, or by differentiating the GPS positions. The driving direction of the car was determined by differentiating the GPS positions. According to the manufacturer of the wind-meter (Waisala), the WAS425 has an error of ±0.135 m/s (0.3 mph) or 3% whichever is greater, up to 144 mph. This is a very good precision for a wind meter.

Figure 24. The ultrasonic wind meter.

An experiment was conducted by Jerker Samuelsson in our group, in order to

validate the method. This was done by driving at different speeds on a straight road and simultaneously measuring the wind-speed and wind direction with a traditional wind-meter located 3 m above the surface. Figure 25 shows a comparison where the wind speed was varying and shows good agreement with the fixed wind-meter at high wind speeds.

It was found that this method was not usable at wind speed below 3 m/s or at driving speeds above 5 m/s. However, at strong winds or low driving speed, the method was giving useful information. When measuring the emissions from the water treatments on the refineries, where the plume is located close to ground, the wind information from this method was commonly used.

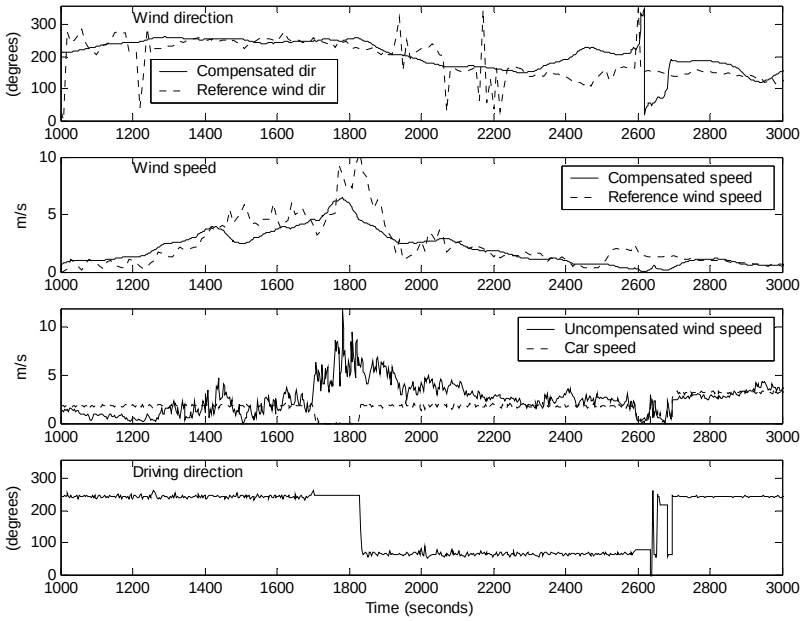

Figure 25. The two top figures shows the compensated wind speed and wind direction and the wind measured with the fixed wind meter.

7.8 Conclusions on VOC measurements

This chapter and **paper A** makes some general statements on the alkane emissions from the four industries based on the collected data. The alkane emission was divided into five groups and compared between the industries. Table 8 shows the emission from these five groups and also the total emissions of alkanes measured on the four industries. The annual throughput of refined crude oil is 10 Mton/y for Preemraff-Lysekil, 5 Mton/y for Shellraff and 3 Mton/y for Preemraff-Göteborg. Reflecting this, the emissions have been normalized to annual throughput in Table 9 to give the emission in each sector as ton alkanes per Mton refined crude oil.

Table 8. Summary of the measured emissions of alkanes from the four industries. First number in parenthesis indicates number of measurement days. Second number indicates total number of traverses.

Emission each year (ton/y)	Preemraff-Lysekil	Shellraff-Göteborg	Preemraff-Göteborg	Oil Harbour
Total 2002	-	-	3464 *(3, 13)*	-
Total 2003	4818 *(2, 22)*	3051 *(4, 19)*	2014 *(5, 27)*	1771 *(2, 11)*
Total 2004	4704 *(5, 42)*	1070 *(3, 18)*	2683 *(6, 38)*	1788 *(4, 15)*

Averages all years (ton/y)				
Total	4760 *(7, 64)*	2060 *(7, 37)*	2720 *(14, 78)*	1780 *(6, 26)*
Process	760 *(6, 23)*	930 *(12, 140)*	610 *(7, 54)*	0
Crude-oil tanks	1470 *(8, 93)*	410 *(9, 61)*	1000 *(10, 66)*	0
Product-tanks	2080 *(16, 115)*	260 *(7, 39)*	940 *(14, 78)*	1115 *(6, 26)*
Water treatment Facility	140 *(6, 32)*	390 *(7, 37)*	160 *(7, 91)*	0
Transport related activity	240 *(2, 17)*	80 *(3,11)*	0 (1)	665 *(12, 60)*

(1) Transport to/from Preemraff-Göteborg is only done through pipelines to the oil harbour.

Table 9. Normalized alkane emission in ton per megaton refined crude oil.

	Preemraff-Lysekil	Shellraff-Göteborg	Preemraff-Göteborg	Average
Process	76	186	203	155 (26%)
Crude-oil tanks	147	82	333	187 (31%)
Product tanks	208	52	310	190 (32%)
Water treatment facility	14	78	53	48 (8%)
Transport related activity	24	16	0	13 (2%)
Total (ton/Mton)	476	412	907	598

Thus for a typical refinery, about 0.06% (598 ton/Mton) of the mass of the crude oil is lost due to vaporization to the atmosphere. Of the emitted gas, 26% originates from the process, 31% from crude-oil tanks, 32% from product tanks, 8% from the water treatment facility and 2% from transport related activities. As transport related activity was counted loading/unloading to/from ships and trucks inside the industry areas. Transport related activities are typically intermittent and are therefore difficult to quantify. Therefore, this value has a high uncertainty.

8 Error estimation

This chapter gives a detailed error estimation of the calculated yearly average emissions for the industry measurements due to the limitation in measurement time, spectral errors and wind properties. A much shorter and less detailed version of this chapter is presented in the end of **paper A.**

8.1 Errors due to limitation in measurement time

One aim of the measurements is to make an estimation of the total emission from a refinery during a whole year. Since total measurements have only been done on two to six days within a time-span of a month, it must be assumed that the emissions on those days can represent the average emission the whole year.

Since year 1972, the U.S. Environmental Protection Agency (EPA) has contracted an extensive study to determine the parameters that decides the emissions from organic liquid storage tanks [35]. The results show that emissions from tanks with external floating roofs are increasing with the wind speed [35]. It also shows that emissions from fixed roof tanks are dependent on the level of the liquid surface in the tank. For floating roof tanks, it has also been observed that emissions increase when a tank is emptying i.e. when the roof is on the way down. Emission from all tanks is also dependent on vapor pressure of the stored liquid and is therefore also dependent on the liquid temperature. Emission is also dependent on outer temperature and therefore varies slightly with the seasonal variation. Equations to calculate the dependence from all these factors are presented in [35] but reliable results are dependent on that correct parameters for each tank is determined.

Thus, this dependence is complicated and the parameters for the EPA equations must more or less be determined for each tank individually. It has been outside the scope of this project to try to compensate the measured emissions to the winds, tank-roof heights and liquid temperature that was present during the days when the measurements were performed. All calculated emissions are therefore presented without compensations to these variations over the year.

If using the strategy of measuring each tank individually during a short time, and then summing the measured emissions from all tanks to determine the total emission from a tank-park, each tank must be compensated for the factors mentioned above individually, to give a reliable total emission estimate. This approach has previously been used with the DIAL method. However in the KORUS project, the whole tank-park is measured at once and the measurements are repeated on different days. It can then be expected that there is a variation in the activity between the tanks in the tank-park and also variations between days that will cancel out each other. This situation causes an average that is relevant for the emission of the whole tank park. The activity on each individual tank can then be neglected.

The variation of the emission from tanks due to changes in outer temperature has not been taken into account. For the DIAL measurements by Shell Global Solutions [36], correction factors for the tank emissions were applied that represented the changes of emission due to temperature variations over the year as calculated by the EPA model. Comparing this to the DIAL measurements and the temperature when the DIAL measurements took place, the correction factors for the tanks were determined to values between 0.91 and 0.99 depending on the tank-roof construction

and the content. Since the error is low compared to the total expected error, it has not been further considered.

VOC emission from a refinery can be divided into continuous emissions and intermittent emissions caused by short-term activities. On many occasions when higher emissions than normal was observed, it could be explained by short-term activities taking place inside the industries. If higher emissions than normal were found during a day and could be explained by short-term activity, then the measurements from that day were discarded. It is therefore believed that the average emission from all days will represent the continuous emission of the industry. For the cases where short term emissions were discovered, some sporadic tests were done afterwards to try to identify how big the emissions are in comparison to the continuous emissions. It has however become clear that a thorough study of this issue requires much more time and effort than what was available within this project. An example of one such study was done when an increased emission of 70 kg/h was measured a few hours after opening a tank for maintenance at Shellraff. Shellraff has reported that opening of a tank for maintenance work was done in the eastern tank park at 11 times during the period from summer 2003 to summer 2004. If assuming that the increased emission is maintained during 12 hours after opening the tank, then this will cause an increased emission of 9 ton/year. This should be compared to the average measured emission from the east-tank park of 146 ton/year for 2004. If the assumptions are correct then this indicates that the emission increase related to maintenance of tanks cause a 6% increase in the yearly emissions.

The impression gained during the project indicates that intermittent emissions correspond to 1-10% of the continuous emissions. To simplify the picture, the values presented later in this report correspond to the continuous emissions and do not include intermittent emissions on the industries. There is however a potential error source in that one may fail to detect a situation as intermittent, and the emission estimations will then be too high. Representatives from the industries with knowledge of the activities have been participating in the interpretation of the measurements in order to avoid this.

Since there are just a few measurement days each year, the situation is heavily under-sampled and there will be an error in the estimated annual emission due to this. The best dataset produced from the KORUS-project to estimate the variation of the continuous emission is probably five days of total measurements from Preemraff-Lysekil during July-September 2004. This dataset gives an average emission of 509.6 kg/h with a variance of 85.3 kg/h between the average emissions of the five days thus giving a standard deviation of 17% between days. It is possible that some of this variation is due to errors in the measurements but it is still safe to assume that the true variation in the total emission has a standard deviation of less than 17% between days for this case.

8.2 Spectral evaluation errors

Three different studies are presented to further describe the errors done with the chosen spectroscopy method. The first simulates the error in the spectral evaluation if the gas contains just one kind of alkane. The second simulates the errors on the gas-mixture of VOC that were measured with bag-samples in a crude-oil tank-park. The third investigates the baseline error due to imperfect incidence angle of the light into the spectrometer.

8.2.1 Error simulation of pure alkanes

Table 10 shows the total alkanes reported by the method if 1 mg/m^2 of each alkane is present in the sample. A sample consisting of 1000 mg/m^2 of water was also analyzed to check the sensitivity to changes in water concentration. The study has been performed by synthetically applying the transmission of each alkane/water to a measured sky spectrum and then evaluating the resulting spectrum. The standard parameters for the alkane evaluation were used including fitting of methane and water. The original sky spectrum were taken as the reference and included in the fitting. Spectra for ethane, pentane, hexane, heptane, octane and water were taken from the PNW database [33]. Spectra for methane, propane, butane and water were taken from the QASoft database [34]. The results show that the largest error (30%) for the non-linear method can be expected if the sample contains hexane. No cross-sensitivity to methane is observed. Methane is included in the fitting in both methods but the evaluated concentration is not included in the sum of the alkanes.

The non-linear method is more disturbed by water than the linear method. The total atmospheric water vapor column is typically in the range 1200 to 3600 g/m^2 [37]. Therefore the change in water vapor concentration during a traverse is probably more than 1 g/m^2. It is surprising to see a disturbance due to water since spectra for water at two different temperatures (283K and 253K) are included in the fitting. However, the water spectrum applied in the test was measured at room temperature. The spectral properties of water have strong temperature dependence in the used wavelength interval, and this is possibly the reason for the disturbance. This issue needs some further investigation.

Table 10. The table shows the interpreted concentration of total alkanes for a synthetically calculated spectrum that contains 1 mg/m^2 of a single alkane or 1 g/m^2 of water superimposed on a measured sky spectrum.

	Linear method Interpreted concentration of Butane (mg/m^2)	**Non-linear method** Interpreted concentration of Propane, Butane and Octane and the sum of the three (mg/m^2)
1 mg/m^2 Methane	0.000	0+0+0=**0.00**
1 mg/m^2 Ethane	0.195	0.032+0.087+0.157=**0.28**
1 mg/m^2 Propane	0.825	1.027-0.007+0.020=**1.04**
1 mg/m^2 Butane	1.004	0.101+0.847+0.065=**1.01**
1 mg/m^2 Pentane	1.133	-0.006+0.801+0.431=**1.23**
1 mg/m^2 Hexane	1.086	0.104+0.472+0.725=**1.30**
1 mg/m^2 Heptane	0.861	-0.07928+0.187+1.0383=**1.16**
1 mg/m^2 Octane	0.700	0.004-0.004+0.999=**1.00**
1 g/m^2 Water	-0.106	0.041-0.118-0.107=**-0.18**

8.2.2 Error simulation of a typical gas mixture from a crude-oil tank

A field measurement was done where approximately 2 liters of gas were collected into two aluminum-coated bags from the west side of the crude-oil tank-park at Preemraff-Göteborg. The gas in the two bags was analyzed with a GC system by IVL (Swedish Environmental Research Institute) within two hours to determine the mix of different hydrocarbons in the sampled gas mixture. Table 11 shows the average retrieved fraction by molecules and the fraction by mass for each compound. The total fraction by mass was 98.5% for the alkanes, 1.1% for aromatic hydrocarbons and 0.5% for alkenes/alkynes.

Cross sensitivity calculations for the measured compounds has been carried out by Jerker Samuelsson in our group. Table 11 shows the cross sensitivity of each compound in a spectral evaluation of butane. For example 1 mg/m^2 of pure ethylbenzene will be interpreted as 0.27 mg/m^2 of butane by the SOF evaluation. The emissions presented in the KORUS-project are the estimation of emitted alkanes. However, it is possible that other compounds than the alkanes are interpreted as alkanes and therefore causes an error. To determine this, the cross sensitivity was multiplied with the mass ratios given in Table 11. It was found out that the cross sensitivity of the most abundant alkenes/alkynes and aromatics are low and therefore result in very low errors. In the sample gas-mixture, the alkenes/alkynes only causes an error of 0.07% and the aromatics an error of 0.06% in the spectral evaluation of alkanes. These errors are therefore neglected in the following discussions.

Table 11. Gas mixture of the emissions from a crude-oil tank-park obtained by collecting air in bags followed by GC-analysis.

Compound	Mixing ratio by molecules (%)	Mass ratio (%)	Cross sensitivity as mass of Butane
Alkanes			
Propane	38.78	32.50	0.98
n-Butane	20.28	22.41	1.00
Ethane	14.48	8.28	0.26
Iso-Butane	8.69	9.59	1.60
n-Pentane	6.20	8.49	1.01
Iso-Pentane	5.66	7.76	1.29
Decane	1.44	3.88	0.74
Hexane	1.12	1.82	0.94
2-Methylpentane	0.98	1.60	1.05
3-Methylpentane	0.47	0.76	1.02
Cyclohexane	0.45	0.72	0.21
n-Heptane	0.27	0.51	0.76
Octane	0.05	0.11	0.55
Nonane	0.01	0.03	0.42
Aromatics			
Benzene	0.09	0.13	0.00
Toluene	0.21	0.37	0.04
Ethylbenzene	0.06	0.12	0.27
1,2,4-TMB	0.11	0.24	0.00
1,3,5-TMB	0.01	0.02	0.00
M+p-xylene	0.07	0.14	0.03
o-xylene	0.03	0.05	0.10
Alkenes/alkynes			
Etene	0.10	0.05	0.02
Etyne	0.05	0.02	0.24
Propene	0.23	0.18	0.11
Iso-Butene	0.11	0.12	0.19
c-2-Butene	0.01	0.01	0.34
1,3-Butadiene	0.01	0.01	0.09
t-2-Pentene	0.01	0.02	0.00
c-2-Pentene	0.01	0.02	0.42
1-Butene	0.01	0.01	0.28
t-2-Butene	0.01	0.01	0.75
Propyne	0.01	0.01	0.27
Total:	100	100	

(TMB=Trimethylbenzene)

The error in the spectral evaluation of a typical VOC gas-mixture was determined by a simulation, by creating a spectrum where absorption on the concentrations of the alkanes shown in Table 12 were applied. These have been set to the same concentrations that were measured with bag-samples in the crude-oil tank-park on Preemraff-Göteborg presented in Table 11. Reference spectrum for Propane and n-Butane were taken from the QASoft database [33] and the other spectra were taken from the PNW database [34]. The absorption was then applied to a measured solar spectrum and the resolution degraded to the same resolution as the measured spectrum ($8cm^{-1}$).

The spectral fitting of n-Butane represents compounds with similar absorption structures as n-Butane (iso-Butane, n-Pentane, iso-Pentane and to some degree n-Hexane). The spectral fitting of n-Octane represents compounds having similar broad absorption structures as n-Octane (n-Heptane, Cyclohexane, 2-Methylpentane, 3-Methylpentane and to some degree n-Hexane)

As can be seen in Table 12, the spectral evaluation overestimates the total simulated alkane-concentration with a factor 1.10 (231.1/210.4). Thus, the conclusion is that for a typical gas-mixture of hydrocarbons emitted from a crude-oil tank-park, the total mass of alkane in the gas-mixture will be determined with an error of **10%**. There is also an uncertainty in the spectral cross sections used that also contributes with an error of 10% .

Table 12. Concentration of alkanes in the error simulation.

Alkane compund	**Simulated concentration (mg/m^2)**	**Evaluated concentration (mg/m^2)**
Ethane	18.4	
Propane	72.3	97.1
n-Butane	49.9	114.6
Iso-Butane	21.3	
n-Pentane	18.9	
Iso-Pentane	17.3	
n-Hexane	4.0	
2-Methylpentane	3.6	
3-Methylpentane	1.7	
Cyclohexane	1.6	
n-Heptane	1.13	
n-Octane	0.24	19.4
Total:	**210.4**	**231.1**

8.2.3 Baseline error

When conducting SOF measurements, the flux is obtained by adding all columns above the baseline of the traverses. If the baseline drifts around, which was the case in many earlier measurements it will cause an error. The drift in the baseline occurs if the tilt of the path of the incoming light into the spectrometer is changed during a traverse. Changes in the tilt during a traverse is caused by imperfect aligning of the solar-tracker which causes the output angle to wobble around as the solar-tracker looks in different direction i.e. when the car is changing its direction or the sun moves over the sky. During the KORUS project, the solar-tracker has been under constant development. Therefore, this problem was big in the beginning but is almost not present at all with the latest version of the solar-tracker. Optical filter were also used

in earlier measurements but it was found that it also caused baseline drifts. The drift due to the filter could partially be compensated for in the software but it was later decided that optical filters should not be used so that baseline drifts were as much as possible avoided.

It was first believed that the broad structures of the alkanes would make the spectral evaluation almost insensitive to changes in the tilt of the incoming light. However, it was found out that since the stretch and smear effect also distorts the spectral lines of water and methane and since these have strong absorption lines overlapping with the alkanes in the spectral-evaluation range, it also disturbs the evaluation of the alkanes. It is difficult to completely compensate for this effect by fitting the stretch since the spectrum has a low resolution and single lines of water and methane are not resolved. The problem is not completely understood but is believed to be related to the big slant that is present in a solar spectrum around 2990 cm^{-1} due to that water in the atmosphere is absorbing strongly above this wave number, and that this slant coincides with the slant in the spectral shape of the alkanes around this wave number.

Figure 26 represents a traverse with a high baseline error. The traverse in the figure was not used to determine the emission that day but the average from 9 other traverses gives an average emission of 170 kg/h. A baseline error of 10 mg/m^2 over a traveled distance of 3000m and a wind speed of 5 m/s would have given an incorrect flux of about 150 kg/h and thus would have caused an error of 90% for that traverse. In the KORUS project, traverses with a baseline error of more than 3 mg/m^2 have been manually rejected and this gives an upper limit for the error of 30%. The evaluation method relies on that the user selects a zero point on the traverse and the baseline error is thus dependent on the choice of the user. Especially for traverses with high noise, it is difficult to locate the zero-point with high certainty. It is however believed that the error will be Gaussian distributed and will thus decrease when taking average of many traverses in the same day. Typically, 10 traverses are averaged and the error for the average due to baseline errors will then reduce and become $9.5\% = 30\% / \sqrt{10}$.

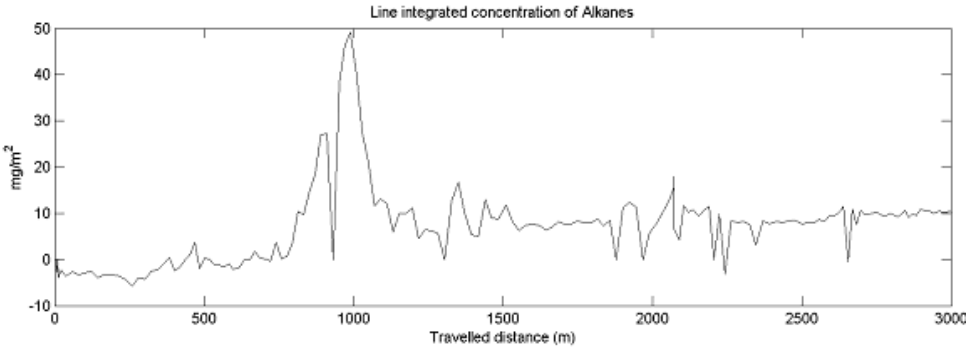

Figure 26. The figure shows the line-integrated concentration along a traverse. This shows a big baseline error since the concentration at the endpoint is evaluated to 10 mg/m^2 in a location where no alkane concentration is expected.

8.3 Errors in the retrieved flux due to wind properties

Calculation of emission relies on information of how the wind varies over the whole surface where the gas is measured. Since this information is not possible to completely retrieve, errors in the calculated emission will be induced. In the monitoring project, wind information was typically taken from a wind meter located 25 m above ground taking averages of wind speed and direction every 30 seconds. Since there are height variations both in wind speed and direction, there is a discrepancy between the wind at the position of the plume and the wind measured at 25 m. This error is difficult to determine since the height of the plume cannot be determined by the gas measurements.

A study of the errors due to the wind was made by looking at the variation in a dataset retrieved by a simulation of the micrometeorology model TAPM [38]. The data from the TAPM model simulations was provided by Lin Tang and Deliang Chen at Gothenburg University. Simulations were done for the time-span from 1st August to 30th September 2001 for three selected positions of relevance for the monitoring project. The used data from the simulation consists of wind speed and wind direction for every hour at 16 different altitudes between 10 and 1000 m and also the solar radiation at the surface.

For validation, the wind speed and wind direction retrieved for the TAPM model at an altitude of 100 m at the location of Oljehamnen was compared to the wind measured at Älvsborgsbron on an altitude of 100 m. The comparison is shown in Figure 27 and indicates a good correlation between measured wind and modelled wind.

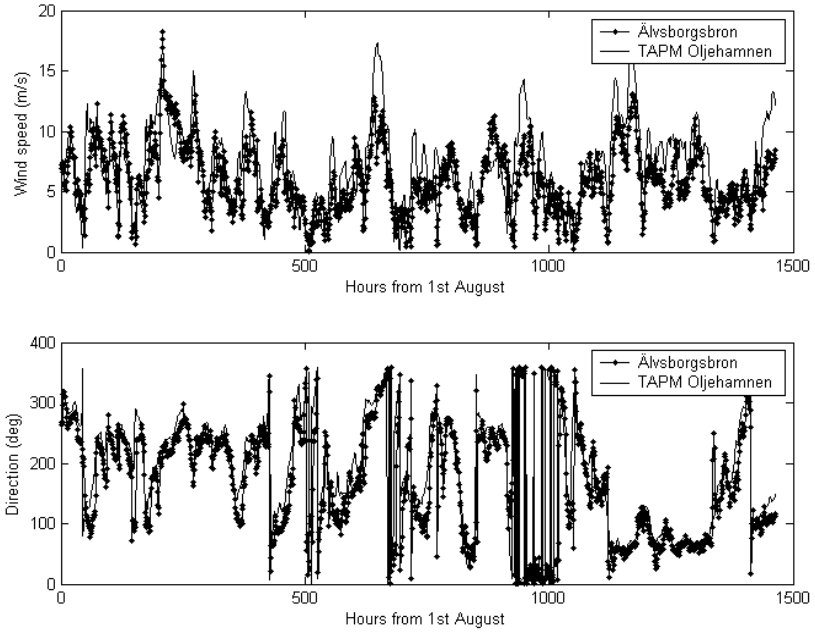

Figure 27. Comparison between measured wind at 100m at Älvsborgsbron and modelled wind at Oljehamnen.

Figure 28 shows the average solar radiation reaching the ground according to the model data between time 9:00 to 17:00 in the day. The days were grouped into three groups representing low, mid, and high average radiation during the day. The limits are shown by two tilting lines in the figure. Among the 61 days the distribution of the days in the different groups were according to Table 13.

Table 13. Number of days in each group. Sorted by average solar radiation.

Location	Low sun intensity	Middle sun intensity	High sun intensity
Oljehamnen	19	25	17
Risholmen	16	28	17
Preemraff-Lysekil	15	21	25

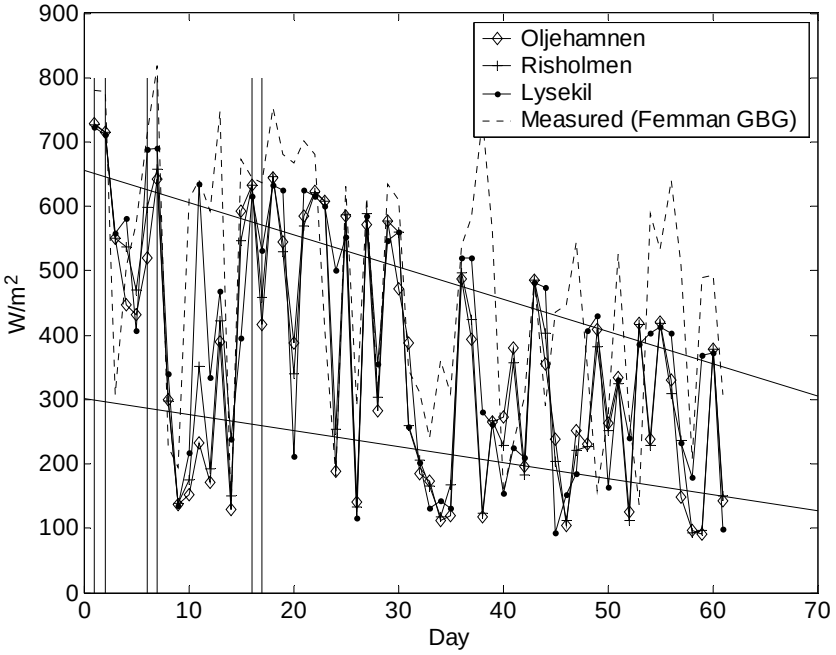

Figure 28. The average solar radiation reaching the ground between time 9:00 and 17:00 each day according to the TAPM simulations. Days are numbered with 1 starting on 1st August 2001. The vertical lines indicate days where SOF-measurements took place. The dashed line shows maximum intensity during a day measured at Femman in Gothenburg. The data from Femman was downloaded from Luftnet [39].

Usually, SOF measurements are only practically efficient during days with high sun radiation. The amount of turbulence in the lower troposphere is typically higher on such days, and this could potentially lead to stronger coupling between the wind speeds on different altitudes. Figure 29 shows as expected that the average difference in wind velocity with height is lower on days with high sun radiation. However the figure also shows that the variance in wind profile is stronger on sunny days.

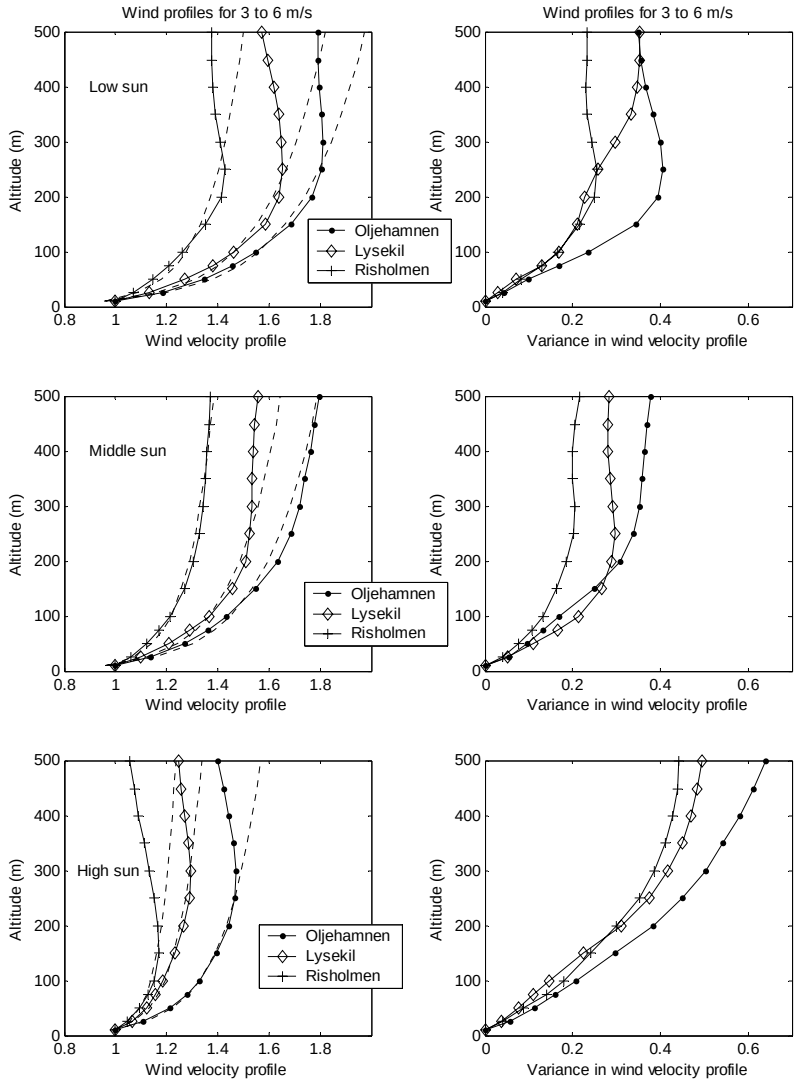

Figure 29. The averaged wind speed profile from all hours in a day between 9:00 and 17:00 when the wind speed at 10 meters were between 3 m/s and 6 m/s. Top figure shows average over days belonging to the low sun intensity group. Lowest figure shows average over days belonging to the high sun intensity group. Dotted lines shows log-profiles fitted to the lowest 7 data-points.

For simulating the error of a typical total measurement on a refinery, a case is simulated where a process and a tank-park is assumed to emit the same amount of VOC. It is assumed that the plume from the tank-park can be distributed anywhere between 0 and 100 m above ground with equal probability. It is further assumed that the plume from the process can be distributed anywhere between 100 and 300 m above ground. The wind data from all hours between 9:00 and 17:00 on days with

high sun-radiation and with a wind speed of 3-6 m/s at an altitude of 25 m are then selected. There are valid wind data on 25 days that fulfilled these criteria. Figure 30 shows the average wind profile retrieved by the selected data. The error bars show the standard deviation between daily averages.

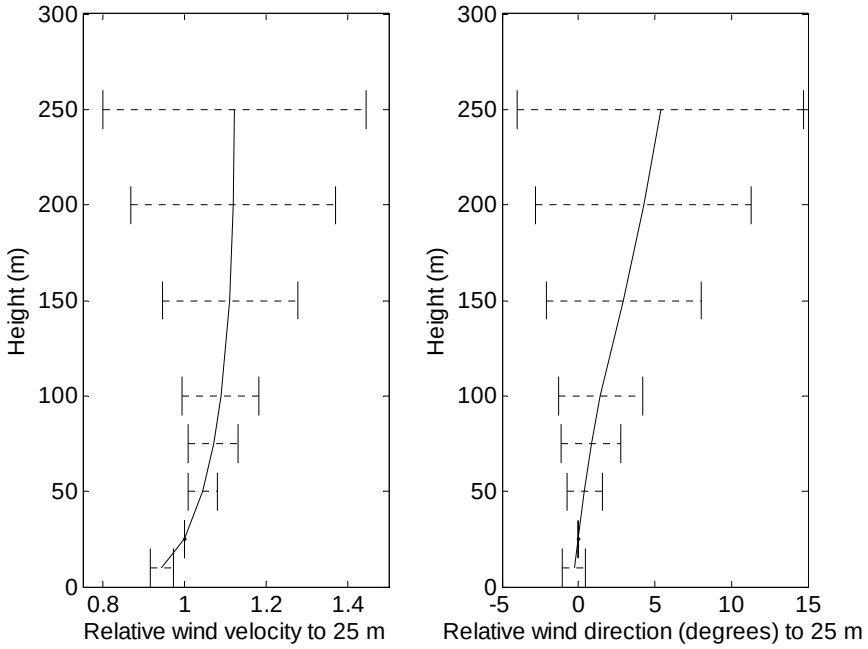

Figure 30. The figure shows the wind velocity and wind direction profile retrieved by simulation and averaged over daytime all sunny days with a wind-speed of 3-6 m/s at ground. The error bars indicate standard deviation between daily averages.

The selected data is then combined with the probability distributions of the process plume and the tank-park plume and a combined probability distribution curve is finally calculated. The average of the distributions and the variance is shown in Table 14 and corresponds to the overestimation done when calculating the emission. An overestimation below one tells that the calculated emission is lower than the true emission and is thus actually an underestimation. The error due to wind velocity and direction is individually presented as well as the combined error due to both. The probability function for the bolded case in Table 14 is shown in Figure 31. A slot-size of width 0.01 has been used for the distribution. Some examples might explain this figure. The figure shows that there is 5% chance to have a overestimation factor in the range 0.9±0.005 and 0,12% chance of having an overestimation in the range 1.2±0.005. For the error in wind direction, it is assumed that the car is driven at an angle of 45° to the wind direction and always in the direction that causes an underestimation and represents an upper limit on the expected error. The error factor for the tank-park and the process are given individually as well as the case where the two emission sources are both considered.

Table 14. Error factors in the retrieved flux due to wind variations with height.

	Factor due to wind velocity	Factor due to wind direction	Combined factor due to wind velocity and direction
Tank-park (0-100 m)	0.97±0.06	0.98±0.02	0.95±0.07
Process (100-300 m)	0.92±0.18	0.85±0.11	0.80±0.23
50% tank-park 50% process	0.95±0.13	0.91±0.07	**0.86±0.15**

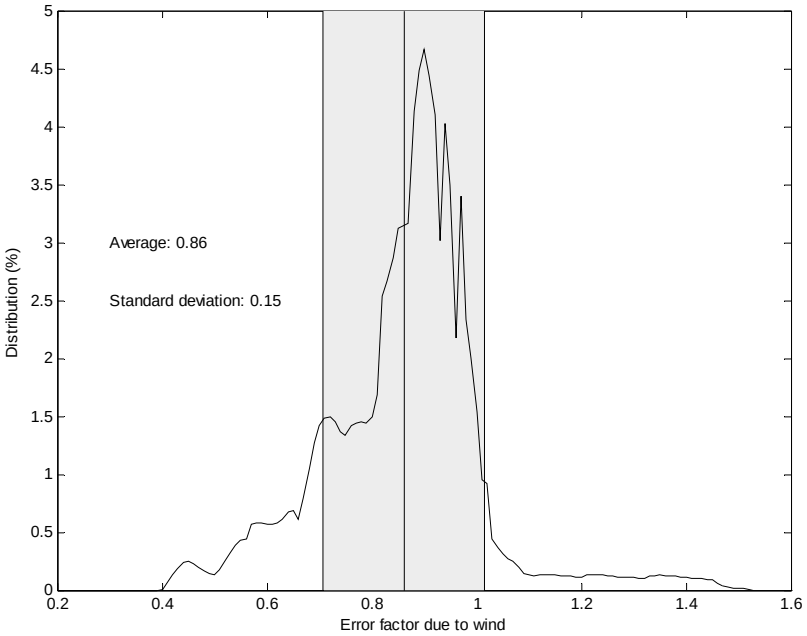

Figure 31. The distribution of the error factor for the simulated case when including all data-points between time 9:00 and 17:00 on days with high sun-radiation. The shaded area represents the standard deviation around the average value 0.86. Both the effect of wind-speed and wind-direction has been included.

For determining the total error in the yearly estimate from a refinery the case that is bolded in Table 14 is used. Thus the systematic error is expected to be $\sigma_{wind,sys} = -14\%$ and the standard deviation between days to $\sigma_{wind,day} = 15\%$.

Errors in calculated flux due to variations of the wind with location is another consideration but this issue was not possible to study with the available dataset. There are also variations in the wind with a much shorter timescale than 1 hour. The induced errors in calculated flux from the short timescale variations in wind can however be expected to reduce by taking the average of many traverses in one day. About 10 traverses of the same kind are done on a good measurement-day and are averaged to represent the emission on that day. The errors due to short timescale variations are therefore expected to be much lower than the errors due to the altitude and wind profile variations and will therefore be ignored hereafter.

8.4 Conclusion about total error

The combined errors from all expected error sources for the total emission measurements can be calculated by:

$$\sigma_{total} = \sigma_{wind,sys} + \sqrt{\sigma_{alkane}{}^2 + \sigma_{cross}{}^2 + \frac{\sigma_{wind,day}{}^2 + \sigma_{BL}{}^2 + \sigma_{true}{}^2}{N}} \qquad (8.1)$$

As concluded in previous chapters, the error in the spectral evaluation is $\sigma_{alkane} = 10\%$ (chapter 8.2.2). There is also an uncertainty in the spectral cross section used that contributes with an error $\sigma_{cross} = 10\%$ (chapter 8.2.2) and the systematic error due to wind is $\sigma_{wind,sys} = -14\%$ (chapter 8.3). These three errors are systematic and do not reduce by averaging the measurements over many days. The statistical error in the daily averages due to the wind is $\sigma_{wind,day} = 15\%$ (chapter 8.3), the variation between days induced by the baseline error is $\sigma_{BL} = 9.5\%$ (chapter 8.2.3) and the true variation between days $\sigma_{true} < 17\%$ (chapter 8.1). The true variation is possibly less than 17% but setting it to 17% will give an upper limit of the expected error. These three errors are not systematic and will reduce when averaging over the number of measurement days, here denoted by letter N. Measurements are typically done on four days (N=4) and the total error in the estimate of yearly emission will then be calculated by equation 8.1 to $\sigma_{total} = 19\%$. Measurements will however on average be underestimated with a factor 14% due to the systematic error in the wind.

The errors associated with leakage-search measurements will here be handled with the same equation for a comparison. The measurements on subsections of the industry, for example on a crude oil tank are typically done on four days but a higher true variation between days is also expected from a single crude oil tank. Due to the complexity of the wind-situation close to ground, the errors in the measurements of both wind-direction and wind-speed are expected to be high. This was observed in the trace gas experiment in chapter 5 where the flux was determined with an error of 50%. Assuming no systematic error and a standard deviation of 50% due to the wind and a variation in the true emission of 40% between days, the error for a tank measurement is:

$$\sigma_{\tan k} = \sqrt{0.10^2 + 0.10^2 + \frac{0.5^2 + 0.4^2 + 0.095^2}{4}} = 35\% \qquad (8.2)$$

Thus there will be more errors in the estimation from individual tanks than for the total emission-measurements.

For the measurement on the water treatment it is also expected that the error caused by the spectral evaluation is larger since the gas-mixture of alkanes have been observed to be quite different there than on the rest of the refinery. Since no bag-measurements have been done to determine this gas-mixture, it is unknown. However, the observed carbon count number (6.5) indicates that the plume contains hexane and Table 10 indicates that the spectral method makes an error of 30% when measuring hexane.

9 The solar tracker

To make the SOF-method more operative, a new active solar tracker was developed. Figure 32 shows a schematic figure of the solar tracker. The solar light is first reflected on the tilt mirror that is mounted directly on a motor axis. With the motor, the tilt of the path of the incoming light is decided so that the reflection hits another mirror (upper mirror). The upper mirror is tilted with 15° so that the reflected light goes straight vertical down the tower of the solar tracker. In the bottom of the solar tracker, the light reflects on a mirror mounted at a 45° angle so that the light exits in the horizontal direction.

The upper part of the tower is mounted on a ball bearing and is free to rotate. The tower is turned by a timing belt driven by the rotation motor. The electronics in the upper part of the tower is connected by a spiral cable to the lower part and this limits the freedom in rotation to 540°.

In the upper mirror, there is a 5mm drilled hole and behind that there is a small aperture of ∅0.5 mm. A small part of the solar light enters a black box through the aperture and is imaged as a small spot on a photosensitive plate after having traveled 6 cm inside the box. In front of the photosensitive plate there is a thin black plastic tape to dampen the intensity of the light. The photosensitive plate is a so called XY-plate with an active surface of 10x10 mm. The active surface corresponds to a field of view of ±5°.

The XY plate has been purchased from the manufacturer Sitek located in Gothenburg. The XY-plate can be considered as a large photodiode located between two high-resistive plates. The bottom resistive plate has electrodes along two opposite sides of the plate and the top plate has electrodes along the other two sides. When a current is created in the photodiode, different amounts of current will go to each electrode depending on the distance from the light spot to the electrode. By taking the difference in currents between two opposite electrodes, the position of average light intensity can be determined in two dimensions. The total light intensity can also be determined by measuring the total current created between the bottom and top plate.

The solar tracker determines if it has found the sun by comparing the total light intensity to a threshold value. When the solar tracker has successfully found the sun, the positions derived from the XY plate is used to drive the two motors to compensate so that the tiny light spot is always in the middle of the XY plate. The solar tracker also has a manual mode where the position can be manually controlled. Furthermore, it has an automatic seek-mode where it scans the rotation ±60° in order to find the sun.

The rotation motor is a synchronous motor with a maximum power of 109 W and is powered by 12 V and driven by a digital motor controller. The motor and the controller are manufactured by Faulhaber. The motor controller is working in analog mode when the tracker has successfully found the sun. When in seek and manual mode, it is digitally controlled by the microprocessor (PIC16C84) in the solar tracker.

The tilt motor is also a synchronous motor manufactured by Faulhaber with three outer windings and a magnet as rotor. This motor is however not controlled in conventional ways. Only two of the windings are controlled and the third winding is connected by a resistor to ground, see Figure 33. By balancing the two active windings, the force on the magnet in the rotor can be controlled and this determines the angle of the tilt mirror.

After the light exits the solar tracker it is focused on a 3 mm aperture with a mirror. After the aperture, optical filter can be mounted if needed. The light is then defocused into parallel light by a second mirror and then enters the spectrometer.

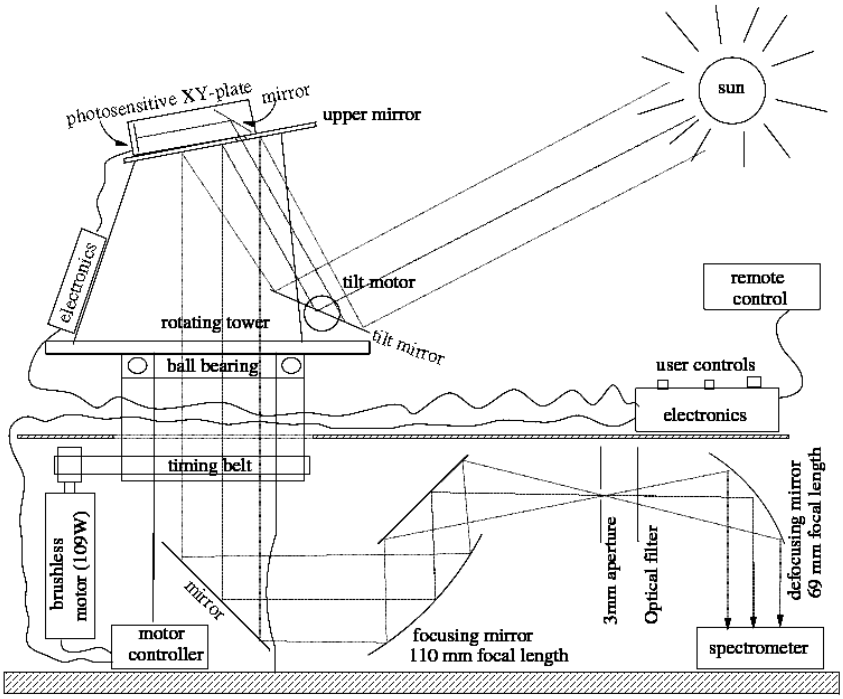

Figure 32. Schematic picture of the solar-tracker and the optics between the solar-tracker and spectrometer.

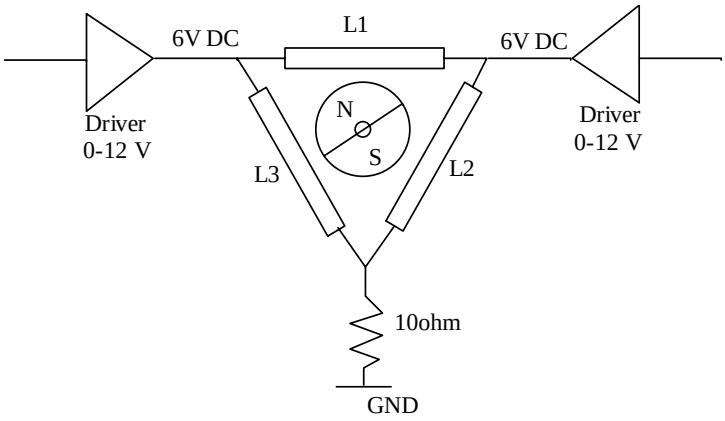

Figure 33. Schematic picture of the steering of the tilt motor. The two analog drivers can deliver a voltage between 0 and 12 V in reference to ground. The mirror obtains its center position when both drivers outputs 6 V.

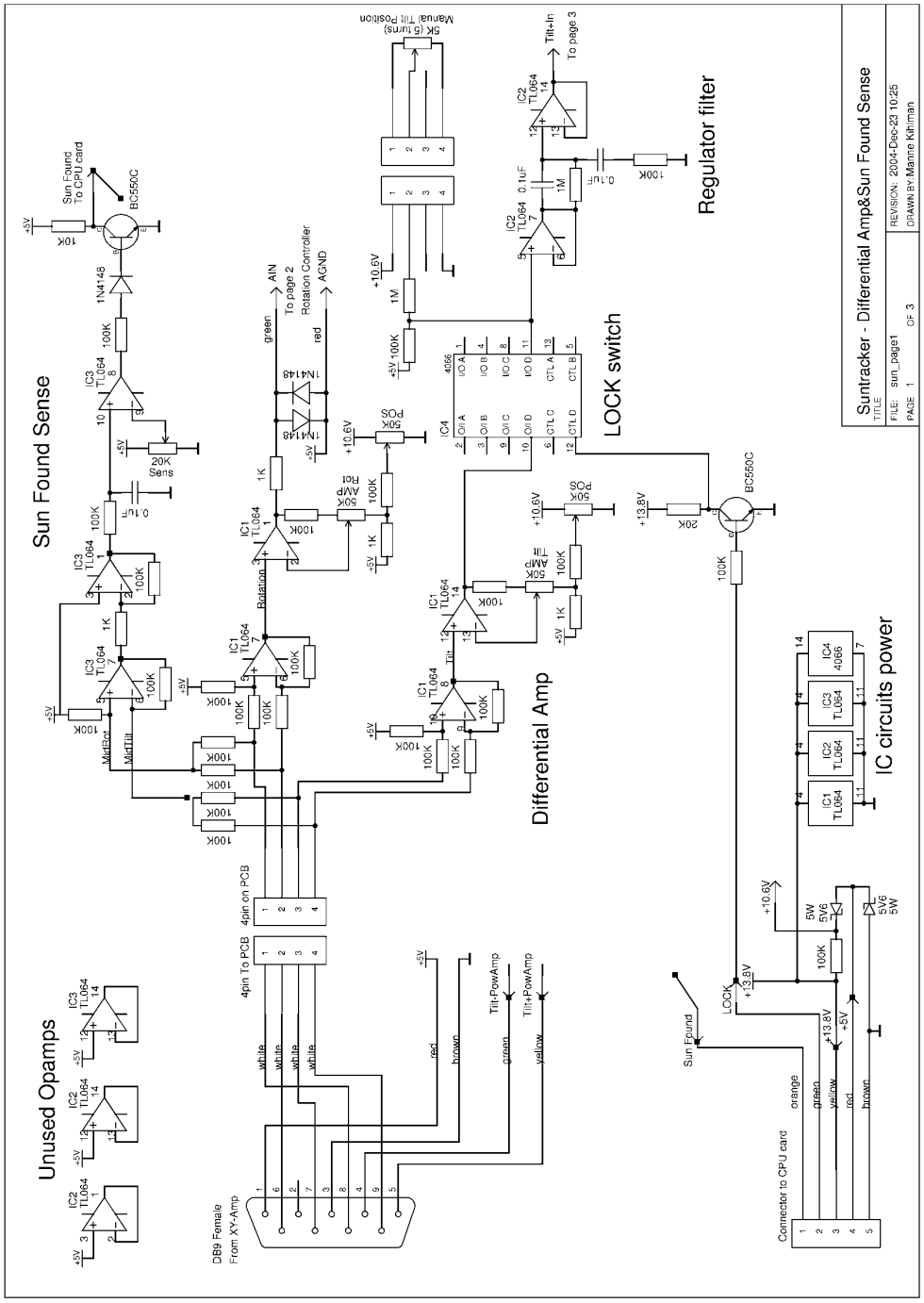

Figure 34. Drawing 1 of the electronics of the solar tracker.

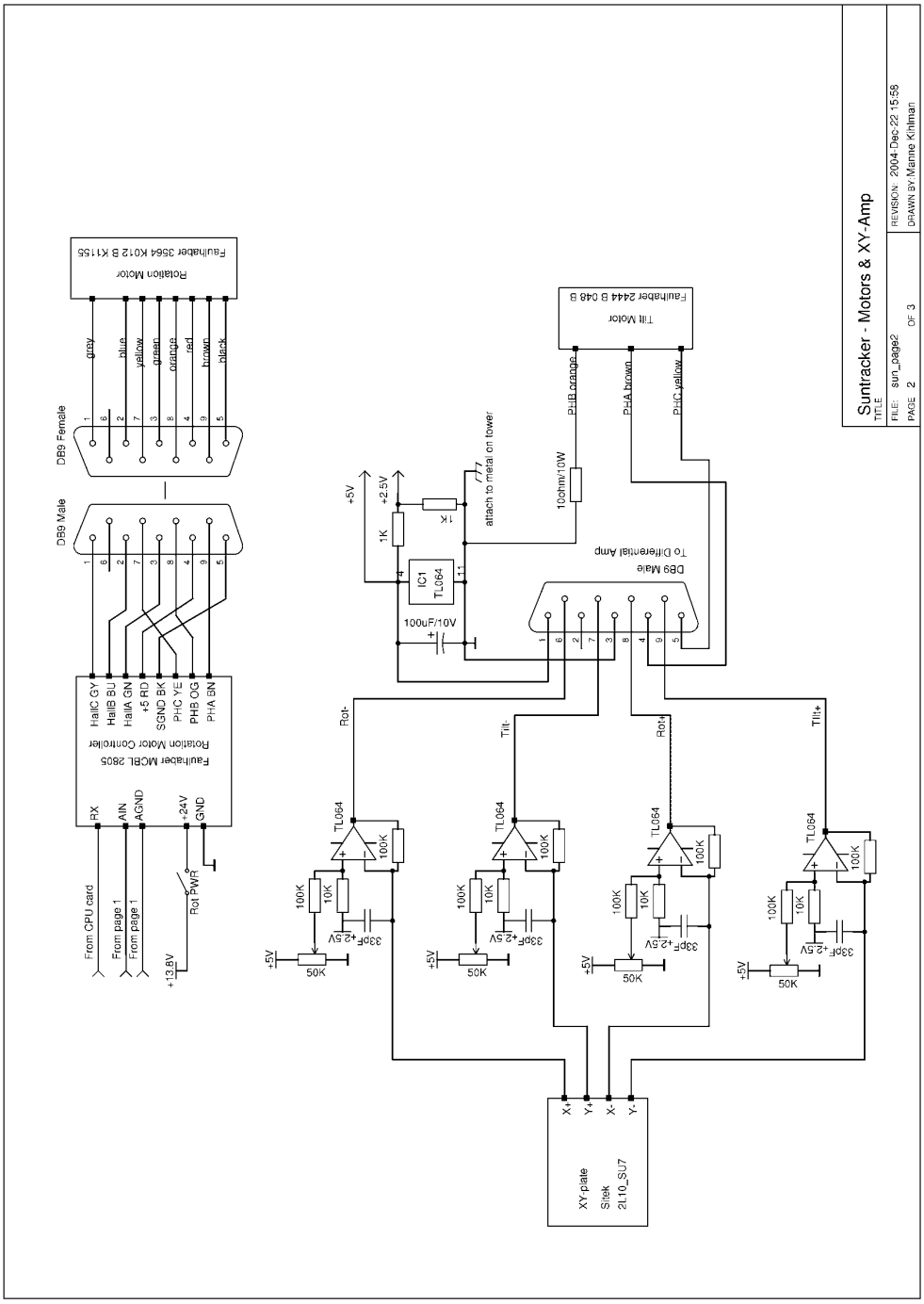

Figure 35. Drawing 2 of the electronics of the solar tracker.

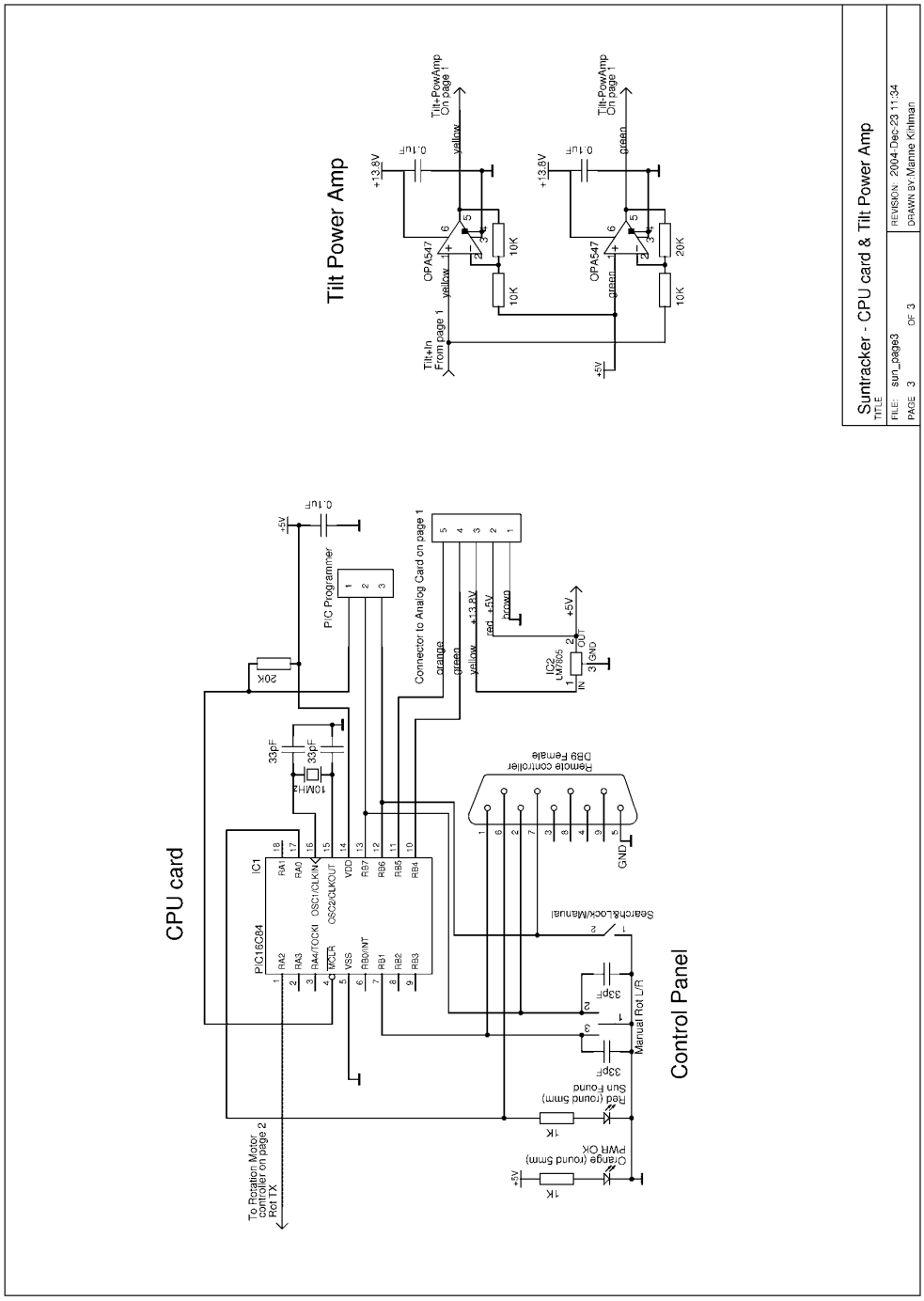

Figure 36. Drawing 3 of the electronics of the solar tracker.

10 Conclusions and outlook

The results from the KORUS project have proven that it is possible to make routine monitoring with the SOF method on industries. However, the results from the measurements show that intermittent emissions from industries were more common than first anticipated. Therefore, more measurements dedicated to the study of the intermittent emissions should preferably be done in the future. Since the available time for this was very limited within the project, this issue was more or less put aside.

The use of the SOF method to quantify the alkane emissions on industries have shown to both have strengths and weaknesses. The strength can be summarized into the following:

1 It is possible to quickly scan through an industry in the search for potential emission sources. As a result, new emission sources have been discovered that were not anticipated before.
2 Relatively inexpensive and not technically complicated.
3 Some capability to identify the kind of VOC in the measured gas.
4 Low noise in the measurement of gas concentration. This makes far-away measurements possible, where the concentrations are low.

The weakness can be summarized into the following:

1 No possibility to determine the height of the plume. This must therefore be assumed and can thus cause an error if done incorrectly.
2 Since only spatially resolved in one dimension, it gives limited possibility to separate emissions sources that are close to each other.

Paper A describes measurements of the concentration profile versus height and concludes that emissions from tank parks stay close to the ground. However, these measurements were not done high enough to be able to determine the typical plume height for the process emissions. This would have been relevant information since it affects what wind information that should be used and the estimation of the error that was determined in chapter 8.3. Therefore, similar measurements should be done again and then higher up to more accurately determine the plume height for a process plume.

In chapter 8.2.1 it was indicated that the current spectral evaluation of alkanes is sensitive to changes in water vapor. Typical changes in water vapor should be determined and the errors due to this should be determined and reduced if possible.

The measurements after the total maintenance stop at Shellraff-Göteborg gave new insight of the emission picture after a total stop. The measurements showed that the emission picture returned to normal within less than a year. This would not have been detected if measurements were only done every third year, as was the routine before on the refinery. Thus, measuring every year has shown to give new valuable information. The relatively low cost of the method motivates that routine measurements should be done every year on the refineries in order to quickly detect changes in the emission picture.

Experience has shown that much more work is required the first year measurements are done at a new industry. It takes time to learn which surrounding sources that can interfere, both from sources inside the same industry, or from

neighboring industries. The latter was the case with Shellraff-Göteborg and the Oil harbour in Göteborg that are located beside each other. It also takes time to see what variability that can be expected from the different sources. With knowledge about these factors, it is much easier to repeat measurements the following years at the same industries.

The newly developed hardware reduces the amount of work required to make measurements with the SOF method. Also, the newly developed software for real time information and post processing makes the compilation of the results more efficient. However, current versions of the programs are not user friendly and require much training by the personnel in the beginning. There is a need for more user-friendly versions of the programs. This would make the method more available and useful for other people.

Measurements with the SOF method require a human to drive the car. This human must constantly make decisions since the optimal location for a measurement within an industry is determined by the position of the sun in the sky (i.e. the time and day of the year), the wind direction and the activity inside the industry. It is difficult to automate this task and measurements with the SOF-method are therefore labor intensive.

Bibliography

1. Farman J.C., Gardiner B.G., and Shanklin J.D., *Large Losses Of Total Ozone In Antarctica Reveal Seasonal Clox/Nox Interaction.* Nature, 1985. **315**(6016): p. 207-210.
2. Yang C.Y., et al., *Respiratory and irritant health effects of a population living in a petrochemical-polluted area in Taiwan.* Environmental Research, 1997. **74**(2): p. 145-149.
3. Pye J.M., *Impact Of Ozone On The Growth And Yield Of Trees - A Review.* Journal Of Environmental Quality, 1988. **17**(3): p. 347-360.
4. Odum J.R., et al., *Aromatics, Reformulated Gasoline, and Atmospheric Organic Aerosol Formation.* Environ. Sci. Technol., 1997. **31**(7): p. 1890 - 1897.
5. Langner J., et al., *Nuläge och scenarier för inverkan på marknära ozon av emissioner från Västra Götalands län*. 2004, SMHI.
6. Darnall K.R., et al., *Reactivity Scale For Atmospheric Hydrocarbons Based On Reaction With Hydroxyl Radical.* Environmental Science & Technology, 1976. **10**(7): p. 692-696.
7. Derwent R.G., et al., *Photochemical ozone creation potentials for organic compounds in northwest Europe calculated with a master chemical mechanism.* Atmospheric Environment, 1998. **32**(14-15): p. 2429-2441.
8. Finlaysson-Pitts B.J. and Finlaysson-Pitts J., *Chemistry of the upper and lower atmosphere*. 2000, San Diego: Academic Press Inc.
9. *Corinair 94: Summary report: Report to the European Environment Agency*. 1997: Copenhagen.
10. Galle B., *Developement and application of methods based on DOAS and FTIR absorption spectroscopy for atmospheric research, Ph.D. thesis*. 1999, Chalmers University of Technology: Gothenburg, Sweden.
11. Tinkham M. and Strandberg M.W.P., *Theory of fine structure of molecular oxygen ground state and measurement of its paramagnetic spectrum.* Physical Review, 1955. **97**(4): p. 937.
12. Rothman L.S., et al., *The HITRAN Molecular Database and HAWKS (HITRAN atmospheric workstation) 1996 Edition.* J Quant. Spectrosc. Radiat. Transfer, 1998. **60**: p. 665-710.
13. Benayahu Y., et al., *Cloud-droplet-size distribution from lidar multiple-scattering measurements.* Applied Optics, 1995. **34**(9): p. 1569.
14. Yarnell J. and Goody R.M., *Infra-red solar spectroscopy in high-altitude aircraft.* Journal of Scientific Instruments, 1952. **29**(11): p. 352.
15. Russell J.M., Park J.H., and Drayson S.R., *Global Monitoring Of Stratospheric Halogen Compounds From A Satellite Using Gas Filter Spectroscopy In Solar Occultation Mode.* Applied Optics, 1977. **16**(3): p. 607-612.
16. Goldberg L., et al., *Carbon Dioxide In The Infra-Red Solar Spectrum.* Physical Review, 1949. **76**(12): p. 1848-1858.
17. Rodgers C.D., *Inverse methods for atmospheric sounding: Theory and practice, 1 ed.* 2000: World Scientific Publishing.
18. Burton M.R., et al., *Diurnal changes in volcanic plume chemistry observed by lunar and solar occultation spectroscopy*. Geophysical Research Letters, 2001. **28**: p. 843-846.

19. Griffith D.W.T., *Synthetic calibration and quantitative analysis of gas-phase FT-IR spectra.* Applied Spectroscopy, 1996. **50**(1): p. 59-70.
20. Milton M.J.T., et al. *Measurements of fugitive hydrocarbon emissions with a tunable infrared dial*. 1992. Cambridge, MA, USA: Publ by NASA, Washington, DC, USA.
21. Robinson R.A., Woods P.T., and Milton M.J. *DIAL measurements for air pollution and fugitive-loss monitoring*. 1995. Munich, Ger: Society of Photo-Optical Instrumentation Engineers, Bellingham, WA, USA.
22. Walmsley H.L. and O'Connor S.J. *The measurement of atmospheric emissions from process units using differential absorption LIDAR.* 1997. Munich, Germany: The International Society for Optical Engineering.
23. McGonigle A., et al., *Walking traverse and scanning DOAS measurements of volcanic gas emission rates.* Geophysical Research Letters, 2002. **29**(20): p. 46.
24. Weibring P., et al., *Monitoring of volcanic sulphur dioxide emissions using differntial absorption lidar (DIAL), differential optical absorption spectroscopy (DOAS), and correlation spectroscopy (COSPEC).* Applied Physics B Lasers and Optics, 1998(67): p. 419-426.
25. Fransson K. and Mellqvist J., *Measurements of VOCs at Refineries Using the Solar Occultation Flux Technique*. 2002, Chalmers report: Gothenburg.
26. Mellqvist J., *Fackelmätning med SOF vid Borealis Polyeten sommaren 2000*. 2001, Chalmers report: Gothenburg.
27. Duffell H., Oppenheimer C., and Burton M., *Volcanic gas emission rates measured by solar occultation spectroscopy.* Geophysical Research Letters, 2001. **28**(16): p. 3131.
28. Weibring P., et al., *Optical monitoring of volcanic sulphur dioxide emissions - comparison between four different remote-sensing spectroscopic techniques.* Optics and Lasers in Engineering, 2002. **37**: p. 267-284.
29. Norton R.H. and Beer R., *New Apodizing Functions For Fourier Spectrometry.* Journal Of The Optical Society Of America, 1976. **66**(3): p. 259-264.
30. Kihlman M., Mellqvist J., and Samuelsson J., *Monitoring of VOC emissions from three refineries in Sweden and the Oil harbour of Göteborg using the Solar Occultation Flux method*. 2005, Chalmers: Gothenburg.
31. Chu P.M., et al., *The NIST Quantitative Infrared Database.* J. Res. Natl. Inst. Stand. Technol., 1999. **104**(59).
32. *GRAMS/AI*. 2004, Galactic Industries Corporation.
33. *Pacific Northwest National Laboratory*. 2004 [cited; Available from: https://secure.pnl.gov/nsd/nsd.nsf/Welcome.
34. Hanst P.L., *QASoft ´96, Database and quantitative analysis program for measurements of gases.* Infrared Analysis Inc., 1996.
35. EPA. *AP42, Fifth Edition. Organic Liquid Storage Tanks*. 1997 [cited; Available from: http://www.epa.gov/ttn/chief/ap42/].
36. *Measurement of the VOC emissions from Shell Raffinaderi, Göteborg, Autumn 1999*. 2000, Shell Global Solutions.
37. Tomasi C., et al., *Mean vertical profiles of temperature and absolute humidity from a 12-year radiosounding data set at Terra Nova Bay (Antarctica).* Atmospheric Research, 2004. **71**(3): p. 139.

38. Hurley P.J., Physick W.L., and Luhar A.K., *TAPM: A practical approach to prognostic meteorological and air pollution modelling.* Environmental Modelling and Software, 2005. **20**(6): p. 737.
39. *Väder och luftkvalitet i Göteborg*. 2001 [cited 2005; Available from: http://www.miljo.goteborg.se/luftnet/].

Paper A

Monitoring of VOC emissions from refineries in Sweden using the SOF method
Kihlman M., Mellqvist J., Samuelsson J., Tang L., Chen D.

Manuscript

Monitoring of VOC emissions from refineries in Sweden using the Solar Occultation Flux method

Manne Kihlman[1], Johan Mellqvist*[1], Jerker Samuelsson[1], Lin Tang[2], Deliang Chen[2]

[1] Chalmers University of Technology, Göteborg, Sweden
[2] Gothenburg University, Sweden

* Corresponding author Johan.mellqvist@rss.chalmers.se, +46317724855

Short title: Mon. of VOCs from refineries using SOF

Abstract

A new spectroscopic technique for mobile gas flux measurements of VOCs, the Solar Occultation Flux method, has been further developed and successfully tested for its capability of conducting large scale monitoring of fugitive gas emissions from industries. During 2002-2004 three refineries and an oil harbour in Sweden were monitored. The measurement errors were, at good conditions, estimated to be around 25%, caused mainly by uncertainties of the wind field. The SOF instrument was tuned to detect alkanes, which contributes to the dominant fraction of the VOCs emitted from a refinery. Complimentary measurements were conducted to assess the emissions also of the aromatic species, typically 5-10% by mass of the alkanes. Each industry was divided into smaller sectors and the emission from each sector was determined as well as the total emission. With this method, it is possible to quickly scan through an industry and in real time detect leaks. For a typical refinery 0.06% of the mass of the crude oil is lost due to vaporization. Of the emitted gas 26% originates from the process, 31% from crude-oil tanks, 32% from product tanks, 8% from the water treatment facility and 2% from transport related activities.

Keywords: VOC, refinery, emission, SOF, solar occultation, FTIR

Introduction

Emission of volatile organic compounds (VOC) to air is a potential hazard for human health and the environment. The formation of ozone in the lower troposphere takes place through a photochemical reaction driven by VOCs and nitrogen oxides. The formed ozone is a powerful oxidant that causes inflammation of the respiratory tract and exacerbates existing lung disease [1], a serious health problem in many large cities of the world. Ozone in the lower troposphere also has negative impact on the vegetation [2] and contributes to global warming. In Europe, and other parts of the world, the levels of ozone exceed critical levels. Therefore a European protocol exists for abatement of ground level ozone by reducing VOCs and other compounds. (Convention on Long range transboundary pollution, UNECE).

The refineries are the single largest point sources of VOCs, and may contribute significantly to ozone formation on a regional scale. For instance, recent studies [3] have shown that the refineries in Houston may have a major impact on the ozone formation in Texas, although car traffic is the largest emission source of VOCs. In the Corinair 94 inventory [4], the emission of NMVOC from Swedish refineries and petrochemical industries was reported to 12 Kton/year, representing 3% of the anthropogenic emissions in Sweden. In Europe the emission from refineries and petrochemical industries are regulated by the authorities and control programs are required for reporting the VOC leakages.

A commonly used method to estimate the annual emissions from a refinery-process is the EPA method 21 [5]. The concentration of VOC is measured in a point close to valves, pumps and flanges etc. and the measured concentrations are used as screening values. These values are then incorporated into calculations that are based on the typical emission picture for that specific kind of equipment. The calculated emissions from all valves, pumps and flanges etc. on the whole refinery are then summed to estimate the total emission. The most widely used methods for estimations of the emissions of storage tanks and loading and unloading is the EPA AP42 model [6]. This method is completely based on calculations with equations derived from previous measurements on typical tanks where parameters related to the design of the tank, the product in the tank and the meteorological conditions at the site are considered. There are also examples [7,8] where concentration measurements have been done with GC combined with FID or MS. The prime interests in these studies were to identify what concentrations of VOC is expected in the neighborhood of a refinery and to identify the gas mixture of VOC that is emitted. Measurements on refineries have also been done with long-path systems, with FTIR [9,10] and UV-DOAS [8,11]. However, if the emitted amount of gas should be estimated with these methods, they must be complemented with a plume model.

Measurements with the DIAL method [12-14] provide a direct measure of the gas emission when combined with wind measurements. DIAL measurements have been performed both for the estimation of total emissions and to identify the emission from each sector inside a refinery. The measurements conducted in the past has shown that the emissions estimated by calculations were commonly underestimated with a factor 3 to 18 [15], hence indicating the need for more measurements. The DIAL method is however rather complex and expensive which has lead to little usage of this method during the more than 15 years it has been available for VOC flux measurements. In 1997 the development of a new method called SOF (Solar Occultation Flux) was started at Chalmers University, as described in a parallel paper [16]. The SOF equipment can be placed inside a small car, making it possible to quickly scan through an industry and in real time detect leaks. Compared to DIAL the

SOF method has better mobility and cost effectiveness, lower technical complexity, higher specificity and higher signal-to-noise making remote (far away) measurements possible. The weakness of the SOF-method is that the plume height is not determined and there is less possibility to separate emissions sources that are close to each other.

In this study the aim was to investigate whether the SOF method could be employed for large scale monitoring, and to understand the uncertainties involved in the measurements. This has included dedicated technical work building a new solar tracker and automation software for real time analysis that has proven vital for the ability to conduct measurements on larger scale. Results from an extensive monitoring project, denoted KORUS, are presented where the SOF method was applied during 3 years at three refineries and an oil harbour in Sweden. The results have contributed with information that is guiding when determining what actions should be taken to further reduce the emissions on the industries. A report with more details of the conducted measurements in the monitoring program has been published [17].

Methodology

The SOF method is thoroughly described in a separate paper [16]. It is based on recording broadband infrared spectra of the sun with a FTIR spectrometer that is connected to a solar-tracker, Figure 1. The latter is a mirror device that tracks the sun and reflects the light into the spectrometer independent of its position. From the solar spectra it is possible to retrieve the path-integrated concentration (molecules/cm^2) between the sun and the spectrometer. To obtain the gas emission from a source, the instrument is placed in a car and is driven in such way that the detected solar light cuts through the emission plume. To calculate the gas emission, the wind direction and speed is also required. The wind was measured from high masts and towers but also using an ultrasonic wind meter positioned on the car.

An additional point measuring FTIR has been utilized in order to obtain information about the plume height and to extend the number of compounds measured. This system has also been used for flux measurements using tracer gas [18].

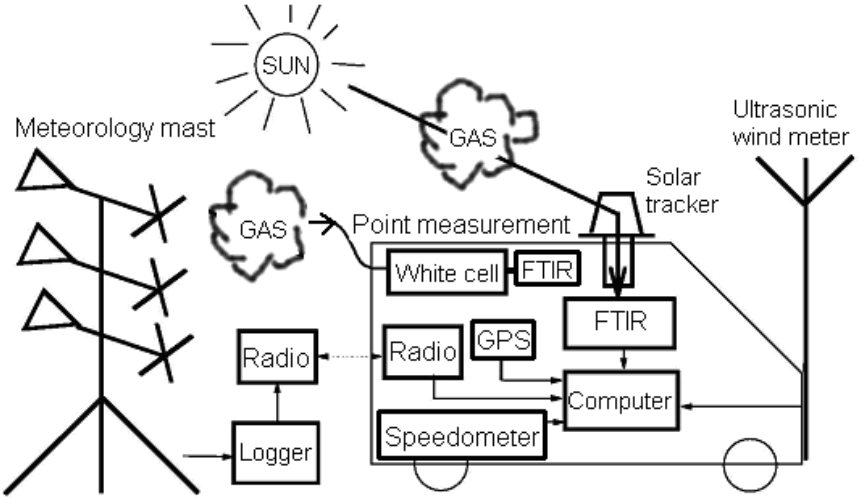

Figure 1. Schematic picture of the mobile measurement-system.

Spectroscopy

The VOCs leaking from refineries correspond mostly to alkanes. These compounds can be measured in the infrared region around 2950 cm^{-1}, using the vibration transition in the carbon and hydrogen bond (CH stretch). The absorption features of the alkanes are similar and interfere with each other. A study of the cross sensitivity of various compounds to butane was conducted by fitting absorbance spectra of butane to other compounds [17]. The results showed that alkanes (C3-C9), had cross sensitivities around one (0.7-1.6), while other compounds had considerably smaller cross sensitivities, around 0.03-0.27 for aromatics and 0.02-0.11 for olefines, respectively. The concentrations of these interfering compounds were then determined by sampling the hydrocarbon mixture in the plume from a crude oil tank. This was conducted by bag sampling followed by quantitative analysis by gas chromatography within 2 hours by an accredited laboratory. The mass fractions in the samples were 98.5% alkanes, 1.1% aromatic hydrocarbons and 0.5 % alkenes/alkynes. Taking the cross sensitivities and gas composition into account shows that interference from non-alkanes is of little importance when measuring on a refinery. It is also clear that the measurements in the CH stretch region within certain error bars, corresponds to the sum of the number of C-H bonds, independently of the assumption of alkanes in the mixture. Both these issues are further discussed in the error analysis section.

Even though the alkane spectra are similar, they are still significantly different so that molecular specificity can be partly obtained. If propane, butane and octane are simultaneously included in the spectral fitting, the average number of carbon atoms in the measured alkane can be calculated. In this study typical observed number of carbon atoms was 3.7 for crude-oil tanks, 4 for gasoline tanks, 6 for kerosene tanks, 5 for process and 6.5 for the water treatment facility. The simultaneous fitting of multiple reference spectra yields valuable information but it is done at the expense of more noise in the baseline. A two-step method has therefore been used that first evaluates the spectrum as butane only. If the evaluated butane concentration is higher than 12 mg/m^2, a new spectral evaluation is done with propane, butane and octane. The sum of the three is taken as the total concentration of alkanes and is sensitive to the presence of all alkanes since other alkanes have spectral absorption structures similar to these three. In addition to the alkanes, for which reference spectra from PNW database were used [19], synthesized spectra of H_2O, HDO and CH_4 were also included in the spectral fitting obtained by using line parameters in the HITRAN database [20]. The spectral retrieval was conducted in the interval 2725-3005 cm^{-1} at 8 cm^{-1} resolution.

To render the SOF method more effective, an on line software was developed to allow real time evaluation of alkanes when measuring gas emissions from the refineries. The program retrieves the line-integrated concentrations of the gases of interest from the spectra with a nonlinear algorithm [21]. It combines this with the position of the vehicle retrieved by GPS, and wind information from wind-meters and calculates the flux of gas through the surface that is sliced out along the path the vehicle is driving. It gives a graphical representation of the measured flux on a map while the measurement is running. The software was tailored to work with the Bruker OPAG and the Bruker IrCube spectrometers, and to do spectral evaluation with a resolution between 0.5 and 12 cm^{-1}. Two separate measurement systems were built with these two spectrometers.

Aromatic emissions

It is difficult to measure aromatic compounds using the SOF method. In order to be able to estimate emissions of the latter compounds an approach was adapted in which the ratios of aromatic hydrocarbons to alkanes was measured in different parts of the refinery such as in the plumes from the waste water treatment area, process area, and crude oil tanks. The aromatic compounds were sampled with TENAX® absorption tubes that were later analyzed with GC. The alkanes were measured by the point FTIR shown in Figure 1. The results showed that the average mass fraction of aromatic hydrocarbons were 3% in a crude-oil tank-park, 11% from a process, 14% from a product tank-park and 15% from a water treatment facility Thus, most of the VOC emission on a refinery is in the form of alkanes. Aromatic emissions were later obtained by multiplying the aromatic/alkane ratios with the emission values of alkanes obtained from the SOF method.

Flux measurements of sub-sectors and total industry

The wind field inside an industry area is expected to be very complex since there are many large buildings that cause disturbances in the wind-field. It is therefore difficult to determine the wind field inside the industry area. When determining the total emission from a refinery it has therefore been done with measurements approximately 1 km away from the industry, where it is expected that the plume has risen to altitudes where the turbulence imposed by the structures and the ground has decreased. When measuring the emission far away, the errors induced by the variation in height of the wind-speed and direction will however be present. Total industry measurements are typically done over 3 hours and about 10 traverses can then be collected during good conditions. All traverses done in one day are averaged and are taken to represent the average emission that day. Figure 2 shows an example of how the measurement car was driven to measure the total emission from Refinery A. When conducting far away measurements the speed of the car was 40 km/h, to minimize wind changes, and 10 km/h for close by measurements. Typically 16 spectra were coadded, yielding a sampling time of 3 s.

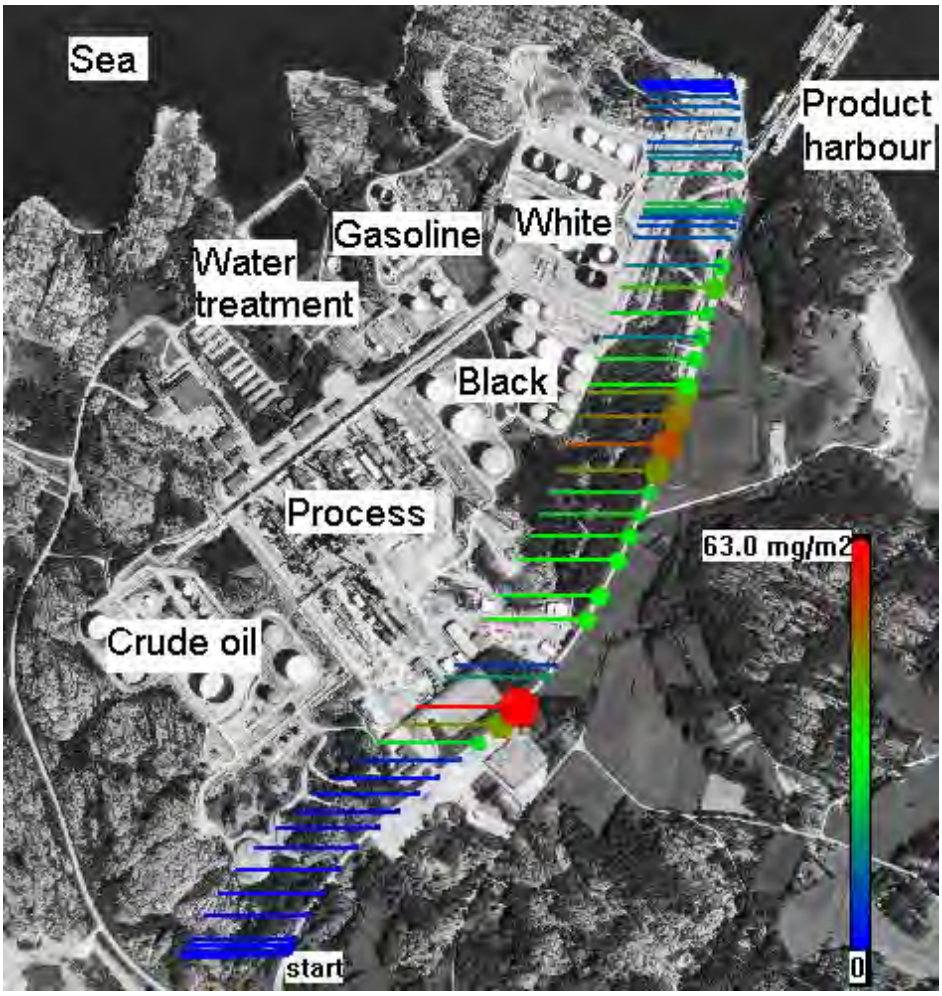

Figure 2. The figure shows how the measurement car was driven to do a total measurement on Refinery A. The car was driven along the road to the product harbour. The position of the car when the measurement of a new spectrum was started is indicated with dots with attached lines. The lines indicate the wind direction (they point towards a possible emission source). Dark dots indicates points where high line integrated concentrations have been measured. *(Aerial photo: Copyright Lantmäteriet 2004-11-09. Ur Din Karta och SverigeBilden)*

It is also of interest to know the emission of each sub-sector inside the industry and measurements inside the industry area are done to get the proportions of the emissions from each area. It is preferred that many sectors are measured within a limited time-period so that the meteorological conditions remain the same for the measurements on all sectors. The calculated emissions for the sub-sectors will typically be too high since the wind-speed just behind a tank is lower than the average wind-field. However, the size proportions between the sub-sectors can be decided. The estimated emission for all sub-sectors are summed and a normalization factor is determined by dividing this sum with the total emission measured approximately 1 km away. The errors in the absolute emission on each sub-sector are then compensated by dividing the value with the normalization factor. With this approach, much less labor is required for the meteorological measurements since a few single wind-meters

representing the average wind field can be used. These are typically permanently mounted in existing towers in the industry area or mobile masts.

The subsectors correspond to areas with similar products or processes and these were usually chosen by the industries themselves. However, there are limitations in how the sub-sectors can be chosen since it must be possible to drive between each sub sector in order to separate them and there must not be strong emission sources behind a weak source.

For Refinery A, the emissions were divided into nine sectors and the emission from each sector is shown in Table 1. Figure 3 shows how a measurement was done on a sub-sector, in this case the crude oil tank-park on Refinery A. The emissions have been further divided into individual tanks, when this was possible and of interest to the industries.

Table 1. Emissions of alkanes (kg/h) from the different sectors on Refinery A. First number in parenthesis indicates number of measurement days. Second number indicates total number of traverses the whole year.

Source	**Year 2003**		**Year 2004**	
Process	88	*(1, 6)*	85	*(5, 17)*
Crude-oil tank-park	209	*(2, 25)*	126	*(6, 68)*
Black components tank-park	124	*(2, 8)*	108	*(2, 14)*
White components tank-park	49	*(3, 21)*	36	*(2,19)*
Gasoline components tank-park	27	*(2, 24)*	37	*(5, 29)*
Water treatment facility	12	*(4, 22)*	19	*(2, 10)*
Preskimmer	3.5	*(2, 17)*	14	*(5, 32)*
Rock cavern exhaust	8.0	*(1, 4)*	85	*(3, 12)*
Product harbour	27	*(2, 17)*	27*	
Total	**550**	*(2, 22)*	**537**	*(5, 42)*

* The product harbour was not measured 2004 and the same emission as 2003 was assumed.

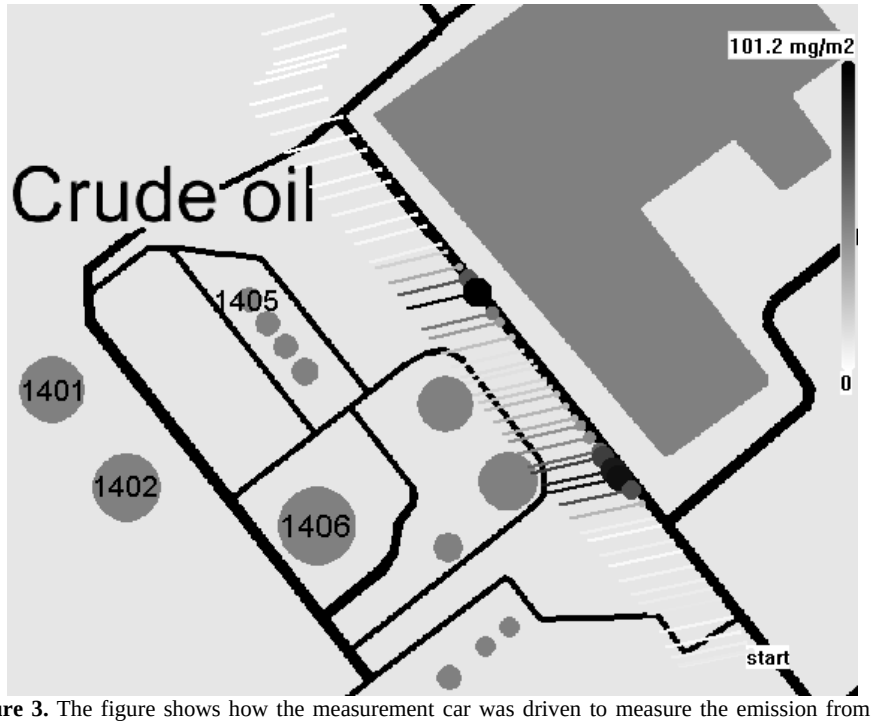

Figure 3. The figure shows how the measurement car was driven to measure the emission from the crude-oil tank-park on Refinery A.

Results

Continuous emissions

One aim of the measurements is to make an estimation of the total emission from a refinery during a whole year. Since total measurements have only been done on a few days within a time-span of a month, it must be assumed that the emissions on those days can represent the average emission for the whole year.

VOC emission from a refinery can be divided into continuous emissions and intermittent emissions caused by short-term activities. On many occasions when higher emissions than normal were observed it could be explained by short-term activities taking place and the measurements from that day were then discarded.

The best data produced from the industry monitoring project to estimate the variation of the continuous emission is five days of total measurements from Refinery A during July-September 2004. This data gives an average emission of 509.6 kg/h with a variance of 85.3 kg/h between the five days thus giving a standard deviation of 17% between days. It is possible that some of this variation is due to errors in the measurements but it is still safe to assume that the true variation in the total emission has a standard deviation of less than 17% between days for this case. With this approach, variations in the wind were partly captured which may have an impact on the emissions. However, the effect of the annual variation in the temperature was not captured.

Intermittent emissions

Intermittent emissions were more frequently observed at the oil harbour than at the refineries. The reason is that more than ten different companies are working independently with activities in the area that temporarily causes emissions, such as loading of trucks and ships, filling of caverns, and cleaning of tanks and pipes. An example of measurements during an intermittent emission in the oil harbour is shown in Figure 4, illustrating both a strong short-term emission and how the emission returns to the average emission. On several occasions high emissions were found which originated from loading of ships. When ships are loading low volatile products (class II and III) in the harbour this is generally done without vapor recovery unit. High emissions from such loading were found on cases where the ships had previous loads with high volatile products (class I). The reason is probably that the old volatile load was pushed out when the ship was refilled with a low volatile product. Emissions were varying between 10-300 kg/h. Measurements over a full loading cycle are needed to more accurately determine the average emission. There is a potential error source in that one may fail to detect a situation as intermittent, and the estimation of continuous emission will then be too high.

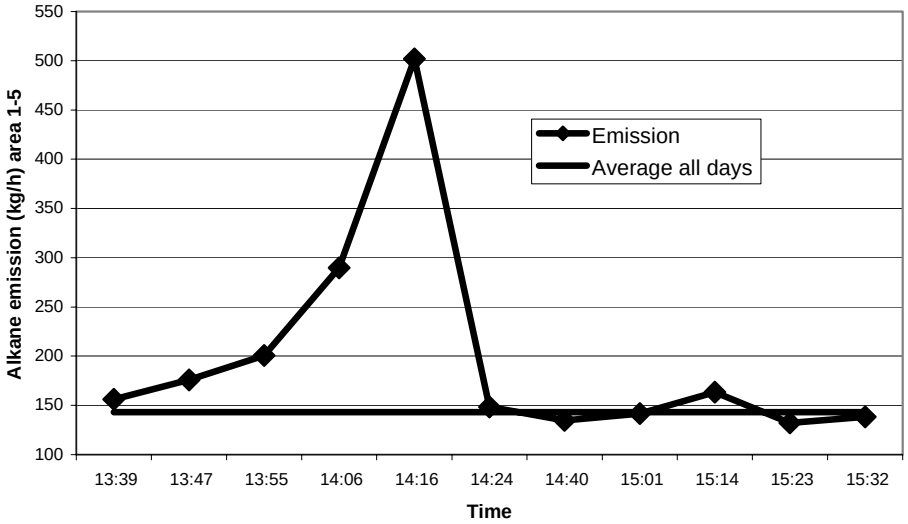

Figure 4. Measured emission of alkanes from an oil harbour. The emission values gradually increased with a peak around 14:10 and then stabilized close to the continuous emission average of 143 kg/h. The reason for the peak in the emission is either loading of a ship with gas-oil or filling of a tank, both finishing at around 14:00.

When short-term emissions were discovered, some sporadic tests were done afterwards to try to identify how big the emissions are in comparison to the continuous emissions. It has however become clear that a thorough study of this issue requires much more time and effort than what was available. Some calculations of the contribution of short-term activity are shown in Table 2. All examples are based on measured emissions, the frequency of each short-term activity has been based on statistics but the duration of the short-term emissions have been guessed.

Table 2. Calculated examples of the relevance of intermittent emissions compared to the continuous emission, based on the measurements and the here given assumptions.

Assumptions	Intermittent emission compared to continuous emission
Cleaning activities causing emissions of 100 kg/h during 2 h every day at the oil harbour.	(73 ton of total 1600) 5%
Loading of ships in the oil harbour causing emissions of 100 kg/h for 12 h every third day.	(146 ton of total 1600) 10%
Rock cavity in the oil harbour is filled causing emission of 149 kg/h and is done 3 times a year during 48 hours.	(21 ton of total 1600) 1%
Cleaning a tank at Refinery B causing emission of 70 kg/h for 12 h and is done 11 times during a year.	(9 ton of total 146) 6%

General results from 3 years of monitoring

From the collected data some general statements of the VOC emissions from the four studied industries can be done. The alkane emission was divided into five groups and compared between the industries. Table 3 shows the emission from these five groups and also the total emissions of alkanes measured on the four industries. The annual throughput of refined crude oil is 10 Mton/y for Refinery A, 5 Mton/y for Refinery B and 3 Mton/y for Refinery C. Reflecting this, the emissions have been normalized to

annual throughput in Table 4 to give the emission in each sector as ton alkanes per Mton refined crude oil.

Table 3. Summary of the measured emissions of alkanes from the four industries. First number in parenthesis indicates number of measurement days. Second number indicates total number of traverses.

Emission each year (ton/y)	Refinery A	Refinery B	Refinery C	Oil Harbour
Total 2002	-	-	3464 *(3, 13)*	-
Total 2003	4818 *(2, 22)*	3051 *(4, 19)*	2014 *(5, 27)*	1771 *(2, 11)*
Total 2004	4704 *(5, 42)*	1070 *(3, 18)*	2683 *(6, 38)*	1788 *(4, 15)*
Averages all years (ton/y)				
Total	4760 *(7, 64)*	2060 *(7, 37)*	2720 *(14, 78)*	1780 *(6, 26)*
Process	760 *(6, 23)*	930 *(12, 140)*	610 *(7, 54)*	0
Crude-oil tanks	1470 *(8, 93)*	410 *(9, 61)*	1000 *(10, 66)*	0
Product-tanks	2080 *(16, 115)*	260 *(7, 39)*	940 *(14, 78)*	1115 *(6, 26)*
Water treatment Facility	140 *(6, 32)*	390 *(7, 37)*	160 *(7, 91)*	0
Transport related activity	240 *(2, 17)*	80 *(3,11)*	0 (1)	665 *(12, 60)*

(1) Transport to/from Refinery C is only done through pipelines to the oil harbour

Table 4. Normalized alkane emission in ton per megaton refined crude oil.

	Refinery A	Refinery B	Refinery C	Average
Process	76	186	203	155 (26%)
Crude-oil tanks	147	82	333	187 (31%)
Product tanks	208	52	310	190 (32%)
Water treatment facility	14	78	53	48 (8%)
Transport related activity	24	16	0	13 (2%)
Total (ton/Mton)	476	412	907	598

Thus for a typical refinery, about 0.06% (598 ton/Mton) of the mass of the crude oil is lost due to vaporization to the atmosphere. Of the emitted gas, 26% originates from the process, 31% from crude-oil tanks, 32% from product tanks, 8% from the water treatment facility and 2% from transport related activities. As transport related activity was counted loading/unloading to/from ships and trucks inside the industry areas. Transport related activities are typically intermittent and are therefore difficult to quantify. Therefore, this value has a high uncertainty.

Figure 5 shows the measured daily averaged total emission from each industry. The emissions from Refinery B were substantial during the early part of 2003, probably caused by leaks that emerged in an isomerisation process area during a complete maintance stop conducted 2 weeks prior to the first SOF measurements. The emissions were reduced after having conducted several documented repairs of the process equipment. In 2004 the emission decreased even more, probably caused by a tenfold of documented repairs in the main process area. The measurements showed that the emission picture returned to normal within less than a year and that measuring every year yields valuable information. The relatively low cost of the method motivates annual routine measurements in order for rapid assessment of new leaks and better control of the plant. The apparent low variability in the Oil harbour is a result of that days with unusually high emissions has been discarded and treated as intermittent activity.

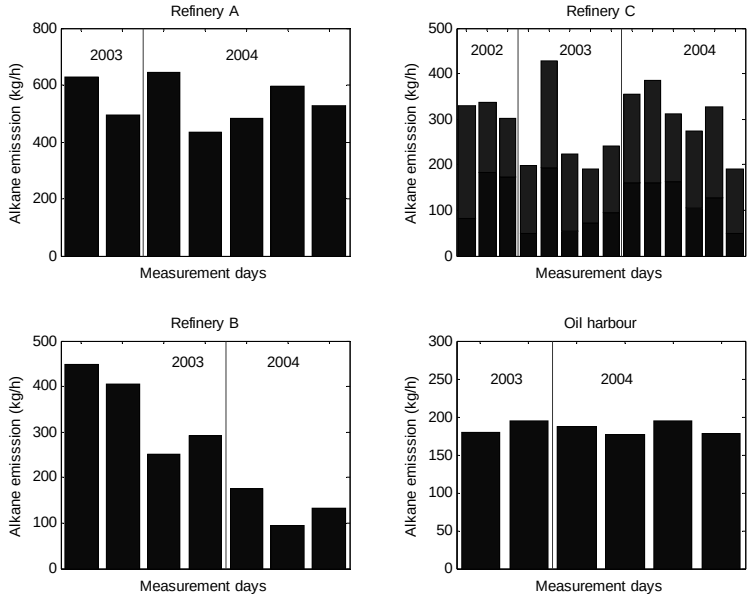

Figure 5. The figure shows the measured daily averaged total emission on each industry.

Discussion

The SOF method is based on two parts, mobile spectroscopic measurements and measurements of the wind at the plume height. Both parts cause uncertainties in the flux values and this will be further discussed here.

Plume height determination

The plume height cannot be determined by the SOF method. Since the wind should be measured at the plume height to determine the gas emission rate, this must therefore be assumed and can thus cause errors if done incorrectly. In order to get more height information the point measuring system shown in Figure 1 was applied. With this system it was possible to obtain the ratio between the alkane concentration on the ground and the alkane column measured in the solar beam with the SOF. In general the plume from the process areas seems to raise very quickly, since little gas was found at ground level, while the plumes from a tank park seems to be well mixed from tank height (25 m) to the ground. In order to quantify this better an experiment was done to determine the plume height from a refinery process and a product tank park. Air was sucked in through a long teflon tube connected to a point measurement system located in the car and the tube end was lifted between the ground and 50 m height. The expected center of emission was located 250 m from the measurement point both for the process and product tank park. The local wind direction determined if a measurement was done on the process or the tank park. Figure 6 shows the distribution of all measurements and the average profile. This indicates that the tank park plume is located close to ground and the concentration decreases at 50 m. The center of the plume is located at approximately 25 m. From the process there is zero concentration on ground and the plume starts at 25 m. The center of the plume is probably located well above 50 m but measurements higher up is required to actually tell.

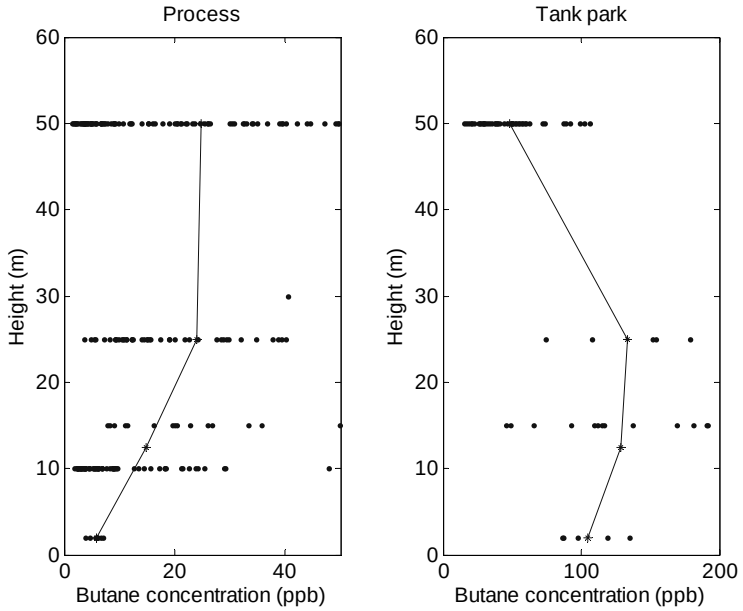

Figure 6. The dots indicate the concentration measurements. The lines indicate the average concentration profile.

In Figure 7 results from a plume height experiment is shown in which simultaneous measurements with the SOF and the point measuring system were conducted downwind a crude oil tank. The points with maximum concentrations were measured to 370 mg/m^2 and 3 mg/m^3 in the SOF and point measurement respectively. Assuming a constant concentration from ground and up, this gives a path-length of around 120 m. By taking into account the slant column to the sun, the height of the column is halved to 60 m. Note that the positions do not coincide due to the slant angle of the SOF measurements and a time delay in the point measuring system.

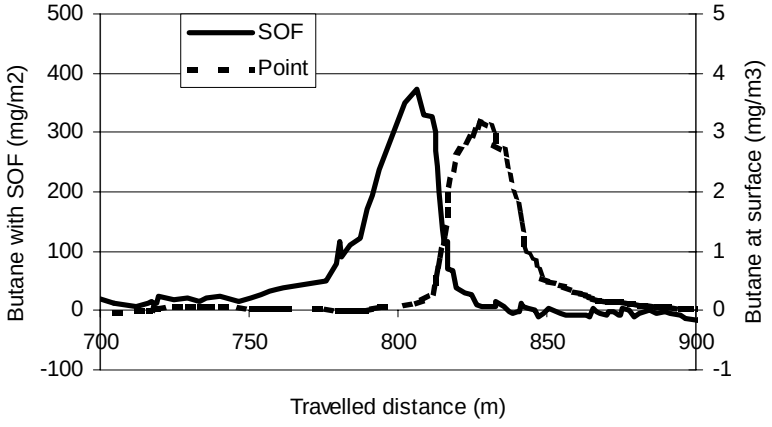

Figure 7. Simultaneous measurement with the SOF (left peak) and the point measurement at the surface (right peak) close to a crude oil tank.

Spectral evaluation errors

The error in the spectral evaluation of a typical VOC gas-mixture was determined by a simulation, by creating a synthetic spectrum at 8 cm^{-1} resolution that included absorption of the alkanes given in Table 6, superimposed on a real measured solar spectrum. The concentrations of the alkanes correspond to the ones measured by bag-samples in the crude-oil tank-park on Refinery C. Reference spectrum for Propane and n-Butane were taken from the QASoft database [22] and the other spectra were taken from the PNW database [19]. The total amout of alkanes in the synthetic spectrum was then obtained by simultaneous fitting of 3 compounds: propane, n-butane and octane.

The spectral fitting of n-Butane represents compounds with similar absorption structures as n-Butane (iso-Butane, n-Pentane, iso-Pentane and to some degree n-Hexane). The spectral fitting of n-Octane represents compounds having similar broad absorption structures as n-Octane (n-Heptane, Cyclohexane, 2-Methylpentane, 3-Methylpentane and to some degree n-Hexane).

As can be seen in Table 5, the spectral evaluation overestimates the total simulated alkane-concentration with 10%, for this typical crude oil gas-mixture. We assume that the overall uncertainty in the total alkane estimation at a refinery is of the same size. There is also an uncertainty in the spectral cross sections used that contributes with an error of 10% .

Table 5. Concentration of alkanes in the error simulation. Here 3 compounds, propane, n-butane and octane were fitted simultaneously to a synthetic spectrum corresponding to the concentration in the left column.

Alkane compund	**Simulated concentration (mg/m^2)**	**Evaluated concentration (mg/m^2)**
Ethane	18	
Propane	72	97
n-Butane	50	115
Iso-Butane	21	
n-Pentane	19	
Iso-Pentane	17	
n-Hexane	4.0	
2-Methylpentane	3.6	
3-Methylpentane	1.7	
Cyclohexane	1.6	
n-Heptane	1.1	
n-Octane	0.24	19
Total:	**210**	**231**

When conducting SOF measurements, the flux is obtained by adding all columns above the baseline of the traverses. The baseline is the registered concentration at a position with zero alkane concentration. If the baseline drifts around, which was the case in many earlier measurements, it will cause an error. The drift in the baseline occurs if the tilt of the incoming light into the spectrometer is changed during a traverse. This will occur if the solar-tracker is misaligned causing the output angle to wobble around at different viewing directions. Baseline drift is also caused by temperature variations in the transmittance properties of the optical filters if this is used. The size of this effect is dependent on the spectral characteristics of the filter and can be partly compensated for in the software.

In the monitoring project, traverses with a baseline error of more than 3 mg/m^2 were manually rejected and this gives an upper limit for the error of 30%. It is here assumed that the error is Gaussian distributed and will thus decrease when taking average of many traverses in the same day. Typically, 10 traverses are averaged and the error for the average due to baseline errors will then reduce to $9.5\% = 30\% / \sqrt{10}$. The uncertainties caused by baseline drift are applicable for the results here, but today this problem has been minimized.

Errors in the retrieved flux due to wind properties

Calculation of emission relies on information of how the wind varies over the whole surface where the gas is measured. Since this information is not possible to completely retrieve, errors in the calculated emission will be induced. In the monitoring project, wind information was typically taken from a wind meter located 25 m above ground recording averages of wind speed and direction every 30 seconds. Since there are variations both in wind speed and direction with height, there is a discrepancy between the wind at the position of the plume and the wind measured at 25 m. This error is difficult to determine since the height of the plume cannot be determined by the gas measurements.

A study of the errors due to the wind was made by looking at the variation in a dataset retrieved by a simulation of the micrometeorology model TAPM [23]. Simulations were done for the time-span from 1st August to 30th September 2001 for three selected positions of relevance for the monitoring project. The used data from the simulation consists of wind speed and wind direction for every hour at 16 different altitudes between 10 and 1000 m and also the solar radiation at the surface.

For simulating the error of a typical total measurement of an industry, a case is simulated where a process and a tank-park is assumed to emit the same amount of VOC. It is assumed that the plume from the tank-park is equally distributed from the ground to 100 m above. It is further assumed that the plume from the process is equally distributed between 100 and 300 m above ground. The wind data from all hours between 9 and 17 on days with high-sun radiation and with a wind speed of 3-6 m/s at an altitude of 25 m are then selected. There are valid wind data on 25 days that fulfilled these criteria. Figure 8 shows the average wind profile retrieved by the filtered data. The error bars show the standard deviation between daily averages.

The selected wind data is then combined with the height distributions of the VOCs in the process plume and the tank-park plume and a combined height distribution curve is finally calculated. The average of the distributions and the variance is shown in Table 6 and corresponds to the overestimation done when calculating the emission. The error due to wind velocity and direction is individually presented as well as the combined error due to both. For the error in wind direction, it is assumed that the car is driven at an angle of 45° to the wind direction and always in the direction that causes an underestimation and this represents an upper limit on the expected error. The overestimation for the tank-park and the process are given individually as well as the case where the two emission sources are both considered.

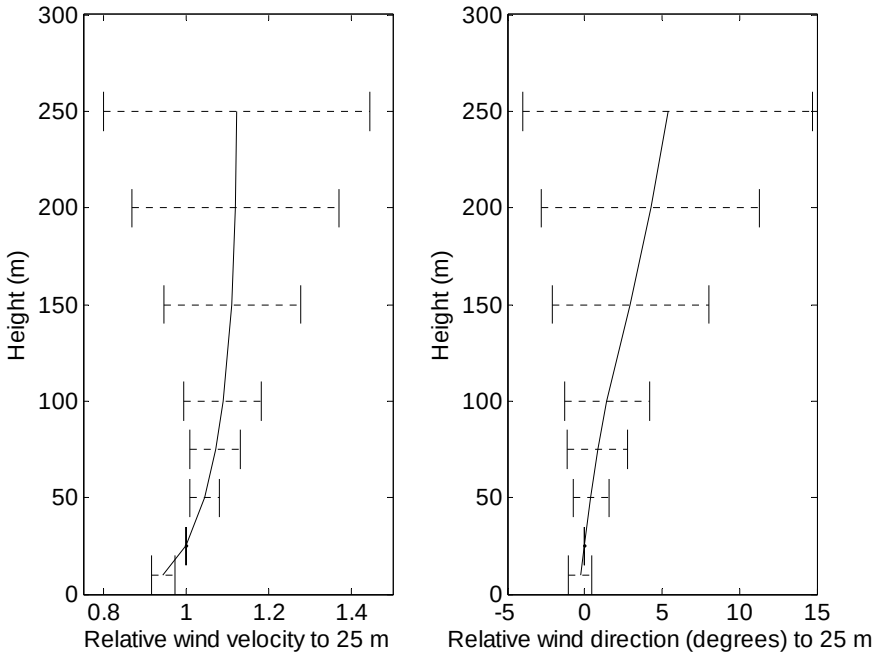

Figure 8. The figure shows the wind velocity and wind direction profile retrieved by simulation and averaged over daytime all sunny days with a wind-speed of 3-6 m/s at ground. The error bars indicate standard deviation between daily averages.

Table 6. Error factors in the retrieved flux due to wind variations with height.

	Factor due to wind velocity	Factor due to wind direction	Combined factor due to wind velocity and direction
Tank-park (0-100 m)	0.97±0.06	0.98±0.02	0.95±0.07
Process (100-300 m)	0.92±0.18	0.85±0.11	0.80±0.23
50% tank-park 50% process	0.95±0.13	0.91±0.07	**0.86±0.15**

For determining the total error in the yearly estimate from a refinery, the case that is bolded in Table 6 is used. Thus the systematic error is expected to be -14% and the standard deviation between days 15%.

Conclusion on total error

The total error is calculated by taking into account the three systematic errors: the error in the spectral evaluation of alkane, the error in spectral cross section and error due to the wind, and the three temporarily errors that occur due to variation between days: true variation, baseline error and variation due to wind. Measurements are typically done on four days and the total error in the estimate of yearly emission will then be 19%, obtained as the square root sum of the quadratic errors. Measurements will however on average be underestimated with a factor 14% due to the systematic error in the wind.

The measurements on sub-sectors of the industry, for example on a crude oil tank are typically conducted over four individual days but a higher true variation between days is also expected from a single crude oil tank. Due to the complexity of the wind-situation close to the ground, the errors in the measurements of the wind are expected to be high. Assuming a systematic error of 25% and a standard deviation of 50% due to the wind and a variation in the true emission of 40% between days, the error for a tank measurement will be 35%. For close by measurements of tanks this uncertainty is probably low, as has been shown elsewhere by tracer experiments [16, 21].

Acknowledgment
The authors would like to thank Anders Strandberg, Andreas Nilsson, Bo Galle, Elisabeth Undén, Gunner Hanehöj, Karin Fransson, Samuel Brohede and Åke Fält that have participated in the field measurements.

References

1. Yang C.Y., et al., Respiratory and irritant health effects of a population living in a petrochemical-polluted area in Taiwan. Environmental Research, 1997. **74**(2): p. 145-149.
2. Pye J.M., *Impact Of Ozone On The Growth And Yield Of Trees - A Review.* Journal Of Environmental Quality, 1988. **17**(3): p. 347-360.
3. Ryerson T.B., et al., *Effect of petrochemical industrial emissions of reactive alkenes and NOx on tropospheric ozone formation in Houston, Texas.* Journal Of Geophysical Research-Atmospheres, 2003. **108**(D8).
4. *Corinair 94: Summary report: Report to the European Environment Agency*. 1997: Copenhagen.
5. EPA, *EIIP-Volume II, chapter 4 – Preferred and alternative methods for estimating emissions from equipment leaks*. 1996.
6. EPA. *AP42, Fifth Edition. Organic Liquid Storage Tanks*. 1997 Available from: http://www.epa.gov/ttn/chief/ap42/.
7. Domeno C., et al., *Sampling and analysis of volatile organic pollutants emitted by an industrial stack.* Analytica Chimica Acta, 2004. **524**(1-2): p. 51-62.
8. Lin T.Y., et al., *Volatile organic compound concentrations in ambient air of Kaohsiung petroleum refinery in Taiwan.* Atmospheric Environment, 2004. **38**(25): p. 4111-4122.
9. Wu R.T., et al., *FTIR remote sensor measurements of air pollutants in the petrochemical industrial park.* 1995. San Diego, CA, USA: Society of Photo-Optical Instrumentation Engineers, Bellingham, WA, USA.
10. Yan Li H.X., et al., *Path Concentration Distribution of Toluene using Remote Sensing FTIR and One-Dimensional Reconstruction Method.* Journal of Environmental Science and Health, Part A, 2005. **40**: p. 183 - 191.
11. Lee C., et al., *Measurement of atmospheric monoaromatic hydrocarbons using differential optical absorption spectroscopy: Comparison with on-line gas chromatography measurements in urban air.* Atmospheric Environment, 2005. **39**(12): p. 2225-2234.
12. Milton M.J.T., et al. *Measurements of fugitive hydrocarbon emissions with a tunable infrared dial*. 1992. Cambridge, MA, USA: Publ by NASA, Washington, DC, USA.

13. Robinson R.A., Woods P.T., and Milton M.J. *DIAL measurements for air pollution and fugitive-loss monitoring*. 1995. Munich, Ger: Society of Photo-Optical Instrumentation Engineers, Bellingham, WA, USA.
14. Walmsley H.L. and O'Connor S.J. *The measurement of atmospheric emissions from process units using differential absorption LIDAR*. 1997. Munich, Germany: The International Society for Optical Engineering.
15. IMPEL, *Diffuse VOC emissions*. 2000: Brussels.
16. Mellqvist J., et al., *The Solar Occultation Flux method, a nouvelle technique for quantifying fugitive gas emissions.* To be published.
17. Kihlman M., Mellqvist J., and Samuelsson J., *Monitoring of VOC emissions from three refineries in Sweden and the Oil harbour of Göteborg using the Solar Occultation Flux method. 2005*, Chalmers, Göteborg.
18. Galle B., et al., *Measurements of methane emissions from landfills using a time correlation tracer method based on FTIR absorption spectroscopy*. Environmental Science & Technology, 2001. **35**(1): p. 21-25.
19. *Pacific Northwest National Laboratory*. 2004 Available from: https://secure.pnl.gov/nsd/nsd.nsf/Welcome.
20. Benner D.C., et al., *The HITRAN molecular spectroscopic database: Edition of 2000 including updates through 2001*. Journal of Quantitative Spectroscopy and Radiative Transfer, 2003. **82**(1-4): p. 5.
21. Kihlman M., *Application of solar FTIR spectroscopy for quantifying gas emissions*. 2005, Licentiate thesis at Chalmers University of Technology: Gothenburg.
22. Hanst P.L., *QASoft ´96, Database and quantitative analysis program for measurements of gases.* Infrared Analysis Inc., 1996.
23. Hurley P.J., Physick W.L., and Luhar A.K., *TAPM: A practical approach to prognostic meteorological and air pollution modelling.* Environmental Modelling and Software, 2005. **20**(6): p. 737.

Paper B

The Solar Occultation Flux method, a nouvelle technique for quantifying fugitive gas emissions

Mellqvist J., Kihlman M., Galle B., Fransson K., Samuelsson J.

Manuscript

The Solar Occultation Flux method, a nouvelle technique for quantifying fugitive gas emissions

Johan Mellqvist*, Manne Kihlman, Bo Galle, Karin Fransson and Jerker Samuelsson

[1] Chalmers University of Technology, Göteborg, Sweden
* Corresponding author Johan.mellqvist@rss.chalmers.se, +46317724855

Short title: The SOF method, a new technique for quantifying gas emissions

Abstract

A new remote sensing method named SOF (Solar Occultation Flux) has been developed since 1997 and applied to locate and quantify fugitive hydrocarbon emissions from industry. The method is based on measuring infrared (2.5-15 μm) intensity spectra of the sun from a moving platform, vehicle or ship. In order to obtain the flux from a particular emission source, the vehicle is driven in such as way that the detected solar light traverses across the actual emission plume. The flux is then obtained as the integrated sum of the retrieved path averaged concentrations, multiplied by the wind speed. The main uncertainty for the method is in the assessment of the wind field. The retrieval code has been tested and compared to other published codes for alkanes, HCl and SO_2, with generally good agreement. Results from a validation experiment utilizing SF_6 trace gas shows that if averaging enough data, 10 traverses, accuracies of 10-20% are obtained from simple emissions sources. Another tracer experiment, simulating emission from a crude oil tank showed an error of 50% when measuring in the *near field* where meteorological disturbances are caused by the tanks. The good performance of the method for estimation of ammonia emissions from fertilized land is demonstrated, with fluxes of 6 kg ammonia per hour, 24 hours after fertilization. A ship traverse in the Göteborg harbor in 2001, passing one refinery and the oil harbor showed an emission of 900 kg/h of alkanes, with average carbon number of 4.5.

Keywords: gas, emission, fugitive, solar, occultation, flux, FTIR, ammonia, fertilized land, VOC, alkanes

Introduction

In environmental work there is a need to quantify the amount of gas emitted from biogenic or anthropogenic sources. Often the emissions occur over a certain area from multiple emissions points, such as a process area in a refinery, where releases occur from leaking valves and vents (*fugitive emissions*), a crude oil tank with a floating roof or a fertilized field from which ammonia is leaking. To quantify such emissions is often very difficult and requires combining the measurements with a dispersion model [1] or simulation of the leakage by using a tracer gas in combination with measurements of the ratio between the tracer and the leaking gas [2-4]. There is a family of methods where the gas concentration is measured and integrated over a surface corresponding to the cross section of the emission plume. The mass-flow of gas through that surface is then determined by multiplying the integrated concentration with the wind transport through that surface. One way to determine the gas concentration over the cross section of the plume is to actively look in different angles with a scanning system based on reflected solar light [5] or DIAL [6-8], a technique sending out laser pulses and receiving them after reflection and absorption on the molecules of interest. Another method is to look in one direction but to move the platform the system resides on, commonly a car or a boat. For example, this has been done from a boat to quantify the SO_2 emission from the volcano MtEtna both with DIAL and passive UV/visible methods such as DOAS and COSPEC [9].

Since 1997 a measurement approach, denoted the Solar Occultation Flux method (SOF), has been developed in our group based on measuring infrared solar light in occultation mode. The aim was to develop a method for the estimation of fugitive emissions of volatile hydrocarbons which only are measurable in the infrared region, but also other applications have been demonstrated such as volcanic and agricultural ones. The method is based on experience gained working with high resolution solar FTIR [10, 11] and industrial measurements using long path FTIR [4]. In the recent years other groups have also used solar occultation measurements both in the UV and infrared spectral region to quantify emissions from volcanoes of SO_2 [12] and HCl [13].

Here the SOF method and several examples, as applied in our group for industrial measurements, are for the first time presented in a scientific paper. In two parallel papers a more detailed description of VOC measurements from refineries together with an error analysis is given [14-16].

Methodology

Flux measurement

The Solar Occultation Flux method (SOF) is based on recording broadband infrared spectra of the sun with a FTIR spectrometer that is connected to a solar-tracker. The latter is a mirror device that tracks the sun and reflects the light into the spectrometer independent of its position. From the solar spectra it is possible to retrieve the path-integrated concentration (molecules/cm^2) between the sun and the spectrometer. To obtain the gas emission from a source, the instrument is placed in a car and is driven in such way that the detected solar light cuts through the emission plume. In this way, the solar-ray going between the sun and the mobile instrument is cutting out an area in the sky. The surface integrated concentration of alkanes on this surface is determined. This is done by cutting the surface into many parallelograms by continuously measuring spectrum after spectrum while driving. Each spectrum is evaluated separately to derive the line-integrated concentration represented by each spectrum

[conc·L]. The position of the car during the traverse is measured with a GPS at the beginning and at the end of each measured spectrum and determines the base of each parallelogram, x. The surface integration is done by multiplying each line-integrated concentration with this base and summing up. The flow of gas through the surface is determined by a scalar-multiplication in vector representation between the wind-vector, and the normal to each parallelogram, as shown in Eq. 1. A more thorough description can be found elsewhere [15].

$$F = \cos(SZA) \cdot \sin(u_\alpha - x_\alpha) \cdot u \cdot x_L \cdot [conc \cdot L] \quad (1)$$

Where u_α and x_α are the wind and driving directions, u the wind speed, x_L the length of movement and SZA corresponds to the solar zenith angle. Thus, the calculation of flux also requires information about the wind on the surface. A look at Figure 1 gives an intuitive feeling for the surface where the measurement is done. The solar rays detected by the SOF instrument are shown as vertical lines. The area between these lines corresponds to the surface integrated concentration observed. If these values are multiplied by the local wind-speed the mass-flux through the area is obtained.

Figure 1. A 3D plot of a SOF measurement conducted at the oil harbor. The lines correspond to the solar light, which together with the movement defines the area cut out through the atmosphere.

The wind through the surface is not straightforward to obtain, since the wind is usually complex and varies with the height. The situation is simpler for a plume without extension in height (flue gas plume) but for a complex one the appropriate wind value to use corresponds to the mass weighted wind over the plume. This in turn requires knowledge about the concentration height profile of the plume and of the wind profile, neither of which are measured by the SOF technique. In applications we have often used complimentary measurements by a point measuring system [3] to obtain more height information. The SOF method can only be applied in sunny conditions. This is advantageous since this corresponds to *unstable meteorological conditions* for which wind gradients due to convection are smoothed out. For flat conditions the wind on average, varies less than 20% between 20 and 100 m height, using standard calculations of logarithmic wind. The best approach to minimize the problem with wind gradients for complex gas plumes, is to measure at distances far away, i.e. 0.5-2 km downwind the releases, so that most of the plume have had time to rise to heights above the first 20-40 m, where the wind is usually disturbed due to various structures (building, trees, tanks). In the SOF method the direction of

movement through the plume is seldom horizontal due to the slant observation angle of the sun, in contrast to vertically observing techniques, such as UV/DOAS [5]. For instance at 45^{o} SZA the movement through the plume will be equally upwards and sidewards. This fact makes it difficult to resolve plumes from different emission sources late in the day. On the other hand for steady wind conditions, it can also be of advantage, since it might provide height information.

Equipment

Three different SOF systems were built around a commercial Fourier Transform spectrometer (Bruker-OPAG 22) having a spectral resolution of 0.5 cm^{-1}, a field of view of 30 mrad and an entrance aperture of 38 mm, Figure 2. With this instrument two cryogenically cooled detectors InSb and MCT are used, with 1 mm^2 detector area. The first system (top left) utilizes a 10 cm diameter solar tracker, from the National Physics Laboratory (NPL) in UK, and uses focusing and defocusing optics to obtain 5 times higher light intensity, which is valuable in the 10 µm region. With this system the detector views only half the sun diameter. The light is focused on an aperture and optical filters can be placed after the aperture. This system is relatively large and the solar tracker allows only a 30° rotation wherefore the whole instrument has to be rotated for each turn of the car. A more mobile system is shown in the top right panel in Figure 2, as applied on a refinery measurement at Tula near Mexico city. This system uses the same solar tracker and spectrometer as above but only flat front optics. The throughput is considerably smaller than the previous system and it detects 4 sun diameters, and the latter may introduce spectral shifts in the spectra due to possible variations of the incidence angle into the spectrometer. This system has recently been rebuilt and instead uses a smaller spectrometer (Bruker IrCube) with the same resolution. This spectrometer is conveniently interfaced through an Ethernet connection and has its own web interface. It has a smaller entrance aperture of 25 mm but the direct solar light is strong enough to saturate the detector in the 3 µm region. A metal grating has been placed in front of the opening to reduce the light if no optical filters are used. Figure 2 (lower panel) shows the most recent system that has been developed during the last years [15]. A new active solar tracker with 540° freedom in rotation has been developed. The light is first focused with a 90° off axis parabolic mirror with 110 mm focal length onto a 3 mm aperture. Optical filters can be inserted after the aperture. The light is then defocused by a 69 mm off-axis mirror into the spectrometer OPAG-22 spectrometer. The detector views 2 sun diameters and the instrument is susceptible to variations in the incidence angle, putting considerable requirements on the solar tracker.

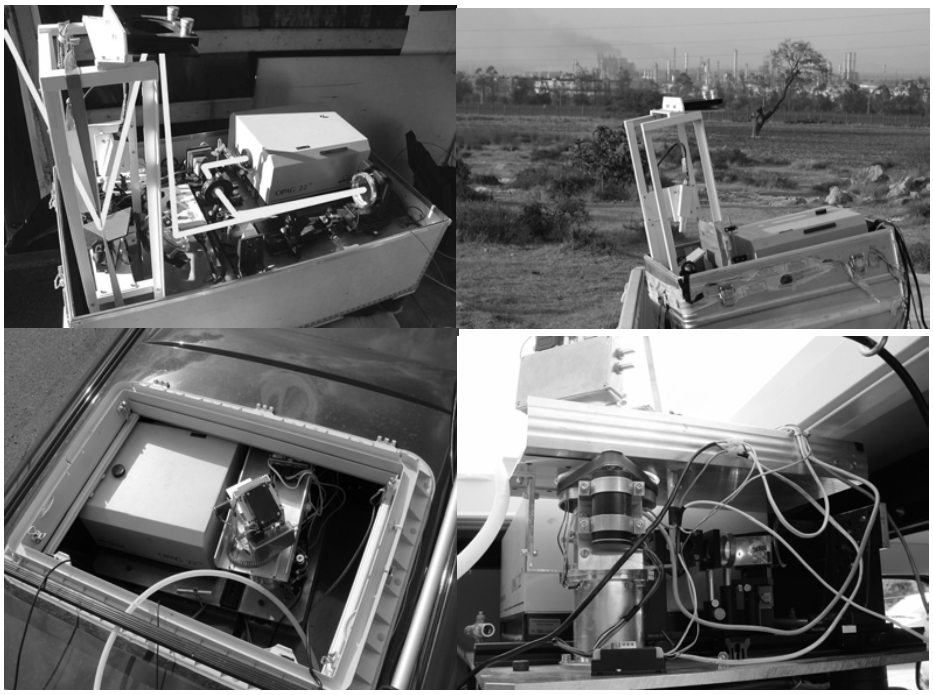

Figure 2. Several SOF systems are shown that have been utilized during the last years. The top left panel shows the oldest system, including a schematic of the light path. The top right panel shows a mobile system with flat entrance optics. The bottom left and right panels show the new system with 540^{o} rotating solar tracker positioned inside a VW bus.

The benefit of introducing optical filters in the solar light beam, is that more light at the interesting wavelength-interval can be used without saturating the infrared detector. When tested in the alkane measurement application, the filters cause problems if they have spectral structures in the neighborhood of the evaluation interval. Even faint structures in the filter function can be large in comparison to the absorption on the molecules of interest. This was the case with one of our filters for which the strength of the filter function was varying with the incident angle and the shape varied with temperature. This dependence is severe since the filter is usually exposed to concentrated sunlight. These two effects could only be partly compensated for by the software, but fortunately the measurements worked well without. A second filter with less structure has been working well, however. Filters are more essential for the 10 μm region, since the solar light is weak. A filter with a cutoff at 10.2 μm has successfully been used when measuring SF_6 and ethylene in this region.

Spectroscopy

The spectral lines of the gas will cause a fingerprint on the measured spectra according to Beer-Lambert's law, as shown below:

$$A(\nu) = -\ln\left[I(\nu)/I_0(\nu)\right] = \sum_i \sigma_i(\nu) \cdot \int conc_i(x) \cdot dx \tag{2}$$

here we define A as absorbance, I is the measured light intensity at wave number ν, I_0 is the light intensity before the light enters the gas and σ_i are the absorption spectra of the gas. By fitting known fingerprints of the gases to the measured absorbance spectrum, in a linear least squares fit, the line-integrated concentration of the gas is retrieved. Reference spectra are possible to simulate for the atmospheric species using the HITRAN database [17]. Additional spectra such as volatile hydrocarbons can be found in other databases, such as PNW [18] or Hanst [19]. When studying localized emission sources one approach is to measure a reference spectrum at ground on a place with zero concentration of the gases of interest and use that spectrum as I_0. This is the method we have applied in several of the measurements shown in this paper, i.e. for alkanes and ammonia. Linear evaluation of spectra was performed with the Classical Least Square (CLS) algorithm in the GRAMS software [20]. Later, non-linear evaluation was also used with the help of the NLM4 and MALT software [21]. One disadvantage with this approach is that the reference measurement of I_0 will only be useful as long as the path length through the atmosphere is constant, which is the case only for a limited time due to the movement of the sun. One way to solve this is to let the spectral evaluation determine the change of path length by representing I_0 as an absorbance. This also makes it possible to use more than one measured references $I_{0,j}$, to include filter functions in the fit and to shift the wavenumber scale of the reference spectrum.

$$\ln\left[I(\nu)\right] = \sum_j F_j \cdot \ln\left[I_{0,j}(\nu)\right] - \sum_i \sigma_i(\nu) \cdot \int conc_i(x) \cdot dx \tag{3}$$

where the factors F_j are determined in the same way as the concentrations. If the spectra $I_{0,j}$ are evaluated they are forced to give zero gas concentrations since they represent a perfect fit. By choosing a few sky references throughout a day, such as in the beginning and end of the traverses, where it can be assumed that the gas concentration is zero, it has been observed that an efficient removal of the influence of the upper atmosphere can be done. However, this method will cause errors in the retrieval if any of the chosen references have nonzero gas concentration and should therefore be used with care.

The SOF measurements are presently evaluated with a new software (QESOF) based on Eq. 3. Non-linear effects will be present, however, as a result of the fact that the spectrometer broadens and distorts the spectral absorption lines. This can be simulated by a broadening operator *D* that is applied to the synthetic spectra, according to Eq. 4. Since this problem is non-linear it must be solved in an iterative way.

$$\ln\left[I(\nu)\right] = \sum_j F_j \cdot \ln\left[I_{0,j}(\nu)\right] + \ln\left(D\left[\exp\left(-\sum_i \sigma_i(\nu) \cdot \int conc_i(x) \cdot dx \right) \right] \right) \tag{4}$$

Results

Validation

The method to retrieve fluxes from traverses with a mobile solar-occultation system was tested on two tracer experiments. In the first one, a trace gas (SF_6) was emitted from the top of a 17 m tall mast in the middle of a large open parking lot in Göteborg, Figure 3. Traverses were done downwind with the measurement system at varying distances from the emission source. The wind was measured with a Yong wind-meter located in the top of the same mast, averaging the wind for 1 minute. The true amount of emitted trace gas was estimated by weighing the gas tube before and after the experiment and also measuring the duration time of the gas release. The emitted gas was always around 1.9 kg/h. The measured peak concentrations were slightly less than 10 mg/m^2 for most scans. The spectral evaluation was done using the non-linear algorithm QESOF in the region 925-975 cm^{-1} and included H_2O, CO_2, SF_6 and a fitted sky-reference spectra [15]. Spectra for H_2O and CO_2 were created from the HITRAN database at a temperature of 288K and a pressure of 1 atm. SF_6 spectra were taken from the NIST database [22]. A polynomial of 4th order was also fitted.

Table 1 shows the results from the four days when the field experiment was done and the individual data points for May 23 is shown in Figure 3. There is considerable scatter in the individual data but for May 23 the average lies within 10% from the real release rate. Most of this scatter is not caused by the spectroscopic measurements, but rather by short term turbulence in the wind field, not captured by the 1 minute averages of the wind that was used. This turbulence can be seen in the plume measurements. For this type of measurements with a narrow plume such turbulence may cause more effect than on a broader one. The average error varied over the days, as can be seen in Table 1. This is not well understood but may be caused by variations in the atmospheric conditions.

Table 1. Summary for each day in year 2002, for which tracer release experiments measurements were conducted at the Åby field.

Day	Emitted SF_6 (kg/h)	Calculated average (kg/h)	Number of accepted traverses	Average wind speed (m/s)	Average wind direction	Error
May-22	1.9	2.3±1.3	4	4.9-8.6	152°-169°	21%
May-23	2.0	2.2±0.6	15	3.9-5.6	120°-142°	10%
June-03	2.0	1.6±0.9	16	2.7-5.3	235°-273°	-20%
June-04	1.9	2.0±1.4	9	5.9-7.8	152°-191°	5%

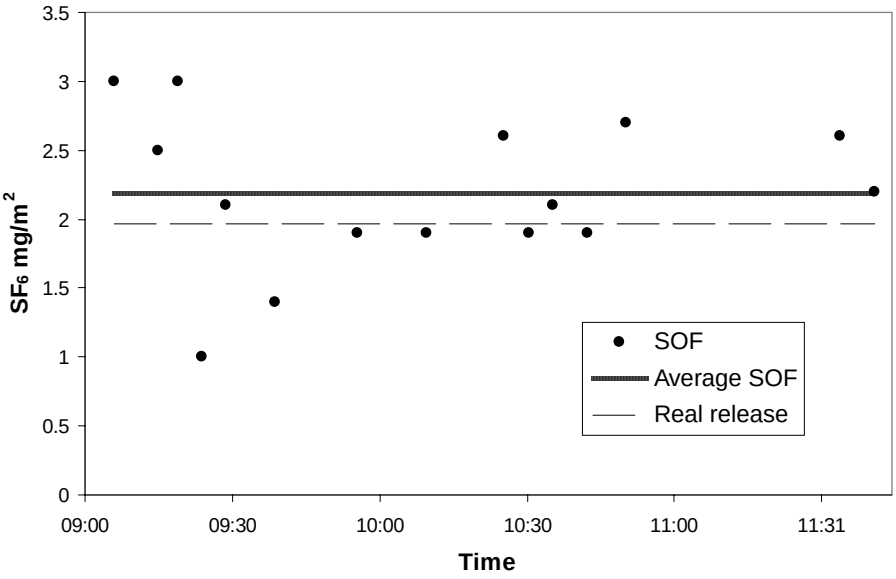

Figure 3. Results from a validation experiment in which SF_6 was emitted from a 17 m mast on May 23 2002 at an open field. The average of the measured emissions was 11% higher than the real release rate.

Another experiment was conducted in which SF_6 was emitted from the roof of a crude oil tank, in June 2002. The tank is located in a tank-park where nine tanks are standing close together, see Figure 4. It can be expected that the wind field is irregular close to the ground inside the tank-park. Traverses were done on a road along the side of the tank park, approximately 150 m away from the emission point, but close to the other tanks. The wind was measured from a Yong windmeter on a 5 m mast on the top of a small mountain just west of the tanks, as indicated by the arrow in the picture.

Table 2 shows all the traverses done during that day. The released amount of SF_6 was estimated to 2.0 kg/h by weighing the gas-tube before and after the experiment and the retrieved average emission was 3±1 kg/h, i.e. 50% overestimation of the flux. Figure 4 shows an example of a typical traverse. The plumes were in many cases broad, as shown in Table 2, indicating a downwash of the plume into the wake of the tanks. This reduces the retrieved flux because the plume will reside leeward of the tanks were the wind is much weaker. The narrow plumes on the other hand had flux values much closer to the true value, probably corresponding to occasions when little downwash occurred. The windmeter used here was noisy and probably causes a certain amount of the scatter. Nevertheless, even though this measurement was conducted in the near field, where we anticipate great difficulties in conducting the measurements, the value were *only* 50% off. Usually the measurements are conducted further away from the sources.

Table 2. Trace gas experiment in which SF_6 was emitted from tank 105, on June 24, 2002. SOF measurements were conducted in the near field. The release rate of SF_6 has been determined to 2.0 kg/h.

Time	Emission SF_6 (kg/h)	Average wind speed (m/s)	Average wind direction	Plume width	Error
12:45	3.1	6.5	252°	80	55%
12:54	1.8	7.2	252°	70	-10%
13:05	1.3	6	257o	30	-35%
13:17	2.7	7.5	253°	72	35%
13:29	3.1	5.4	255°	80	55%
14:05	5.2	7.4	264°	70	160%
14:10	3.7	7.2	251°	100	85%
14:24	2.6	7.3	262°	75	30%
14:31	3.4	6.5	260°	40	70%
Average	**3 ±1.0**				**50%**

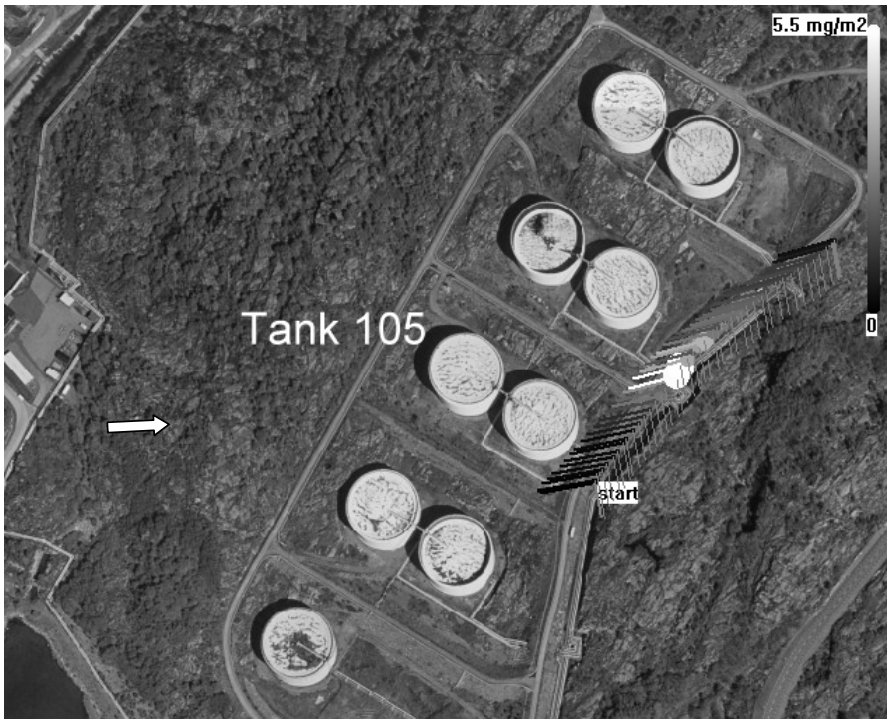

Figure 4. A traverse conducted during a tracer release of SF_6 on top of tank 105. The lines point towards the wind, towards a potential emission source. The position of the wind meter is indicated by an arrow. *(Aerial photo: Copyright Lantmäteriet 2004-11-09. Ur Din Karta och SverigeBilden)*

Results from intercomparison exercises with other flux measuring techniques are not available. An indication, however, of the validity of the SOF technique is the following: During 1995 and 1999 the DIAL technique, operated by a commercial company, was applied to estimate emission from a certain refinery in Sweden. According to official reports to the provincial government they estimated fugitive emission from the whole process area corresponding to 64 and 87 kg/h of alkanes during 1995 and 1999, respectively, with reported error bars of 15-20%. The SOF

method was applied two years later, in 2001, to our knowledge measuring in a similar geometry along the main refinery road. Measurements of the process area during two days yielded a total flux of 74±20 kg/h. This falls surprisingly close to the values spanned by the DIAL measurements. The measurements were not conducted at the same occasion, but the process area seems quite constant since the values for 2002, 2003 and 2004 were 57, 75 and 76 kg/h, respectively [15, 16]. Also, the process area is a good test case since it shows less intermittent emissions and it is less susceptible to variations in wind and temperature, which may the case for emissions from storage tanks.

Another type of validation test is to compare the retrieval algorithms used. The results of the spectral fitting algorithm for alkanes in our software QESOF [15] has been compared and verified with the results retrieved from other software, a Classical Least Square (CLS) method in the Grams software [32] and the non-linear NLM4 software developed by Griffith [19]. The agreement between NLM4 and QESOF was very good, within a few percent. The CLS code agreed less well with the other codes, with discrepancies of 30% in the plume, but this can be explained by several reasons. Verification of the software has also been conducted for the volcanic species HCl and SO_2. Solar spectra measured in the plume of Mt Etna in Sicily in October 2000 were analyzed by two independent retrieval algorithms, i.e. QESOF and a code developed by Mike Burton at INGV [23] for spectral evaluation on measurements of volcanic gases. This comparison shows very good agreement, with differences of a few percent, both for SO_2 and HCl, if the column amount above the baseline is considered.

Ammonia emissions from fertilized fields

A field test was conducted using SOF in the summer of 1998 measuring the amount of ammonia released when fertilizing fields with manure. A first prototype of a SOF system was used similar to the old system in Figure 2, but with a 1 cm^{-1} FTIR spectrometer (Bomem MB100) having an MCT detector, and an optical interference filter. Emissions of ammonia from agriculture cause eutrophication, decrease in the biological variety and acidification on local and regional scale. Ammonia emissions also represent a loss of nitrogen otherwise available as fertilizer. To find methods to reduce ammonia emissions from agriculture is therefore of high concern. In order to evaluate the effects of such methods quantitative measurements of the emissions needs to be done. Ammonia is difficult to measure by point sampling techniques, since it is relatively reactive compound. In addition, will the spreading of manure cause emissions over a whole area and there are few techniques for estimating such emissions.

Measurements were done during the summer of 1998, approximately 24 hours after spreading fertilizer on a field corresponding to 1.5 ha. In Figure 5 an absorbance spectrum of ammonia is shown, measured downwind the field. In addition, a spectral fit of ammonia, and H_2O is shown using the codes MALT [21] combined with CLS [20], and the retrieval yields a column of ammonia of around 5 mg/m^2.

The detection limit of the ammonia is here estimated to 0.3 mg/m^2. In Figure 6 the retrieved total column of ammonia along the measurements path is shown, as well as the accumulated mass flux. The wind was measured with a single wind meter to 5.4 m/s, but considering the open field situation, this is ideal for the SOF method. The total massflux corresponds to 6 kg/h. This application is suitable for the SOF method, and rather straightforward.

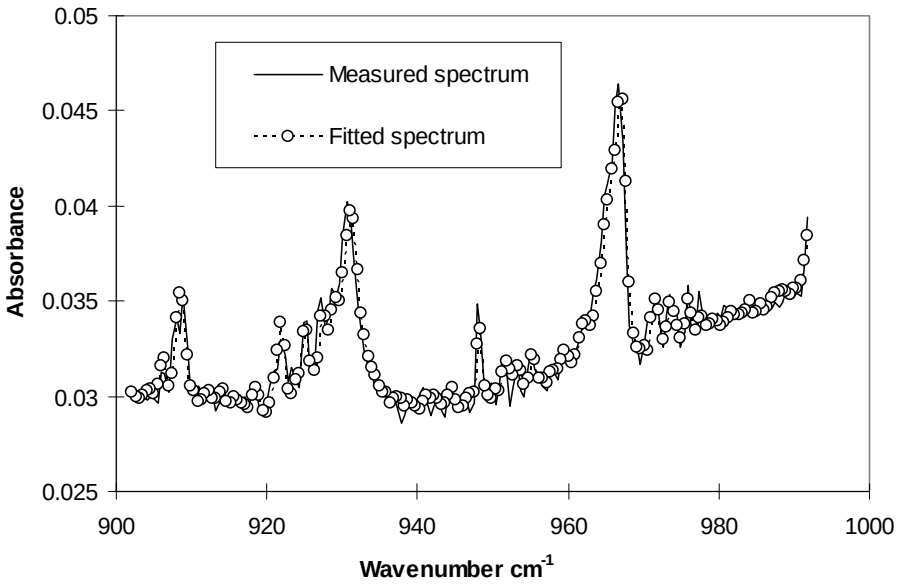

Figure 5. An absorbance spectrum of ammonia ($-\log(I/I_0)$), corresponding to 5 mg/m^2, measured downwind a fertilized field of 5 ha, together with a spectral fit of ammonia and water.

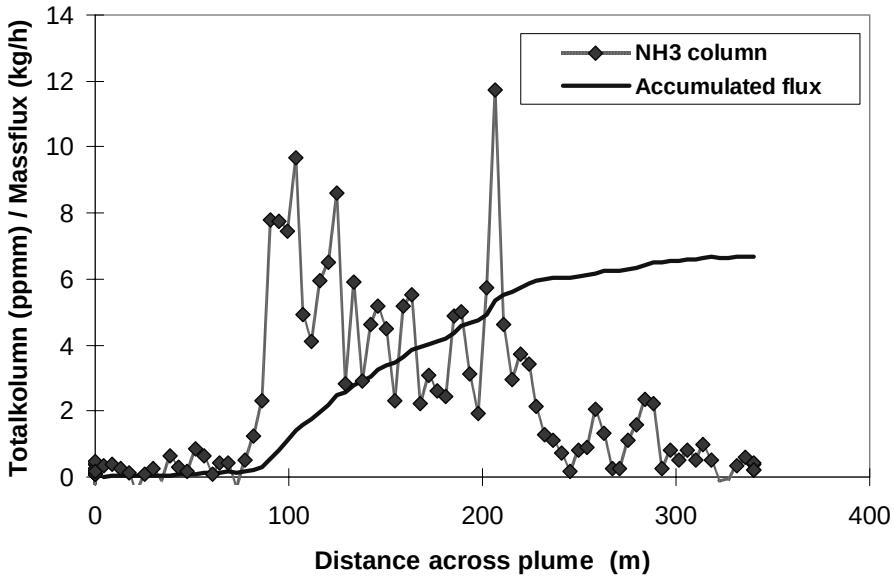

Figur 6 . Total column and mass flux of ammonia from a fertilized field, measured using the SOF method, 24 h after fertilization.

Total flux estimate of VOCs from Göteborg harbour

The combination of volatile organic compounds (VOC), nitrogen oxides and sunlight causes secondary production of ground level ozone, a species that has negative effect on both the health and the environment. The largest point sources for VOCs are refineries and petrochemical industries and the emissions from these occur from a number of points such as: process equipment, crude oil tanks, storage tanks, dockside loading operation, water treatment facilities and flaring. The SOF method is suitable, and has been demonstrated for quite a few VOC compounds, both olefins measured around 10 µm (ethylene and propylene) and straight chained alkanes measured around 3.3. µm. In a separate paper results from an extensive study of VOC measurements is given [16]. In Figure 7 is shown a SOF traverse conducted from a ship, R/V Arne Tiselius, in the Göteborg harbor on June 19, 2001. The measurements were conducted using the instrument shown in the top left panel in Figure 2. A measurement was carried out beginning east of Älvsborgsbron and ending at Skandiahamnen, passing by the Port of Göteborg and a refinery. The wind was northerly with a velocity of 2.8 m/s. It can be seen in Figure 7, that a plume was traversed south of the oil harbour, situated in the middle of picture. Figure 8 shows the total column of alkanes and the accumulated total flux. The emission, originating from the whole industrial complex including the oil harbour and a refinery, was estimated to 900 kg/h. There are however uncertainties in the wind speed. The spectral analysis was conducted using CLS [20] and a composition of alkanes with a mean carbon number of 4.5 was retrieved by fitting several species (propane, butane, 2-methylbutane and 3-metylpentane), as shown in Figure 9 for the spectrum with the highest column in Figure 8.

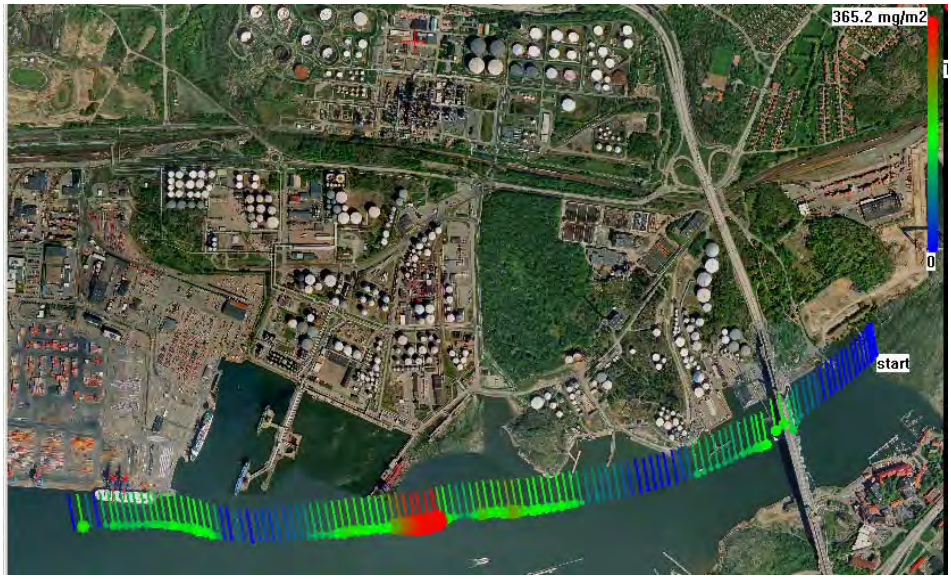

Figure 7. SOF measurement from R/V Arne Tiselius on June 19, 2001, at 10:30. The arrows point towards the wind, which was northerly. The colorscale corresponds to the column of alkanes. "*Copyright Lantmäteriet 2004-11-09. Ur Din Karta och SverigeBilden™*",

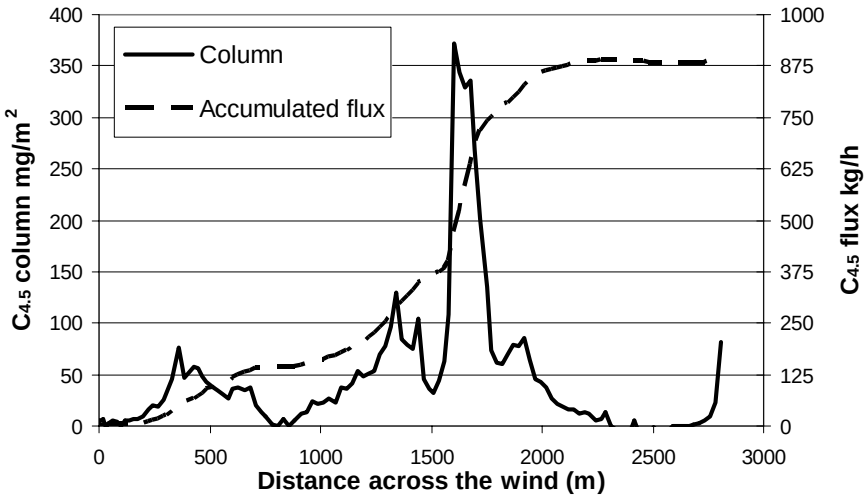

Figure 8. The column and accumulated mass flux across the Göteborg harbour is shown here. The data corresponds to the one in Figure. 7.

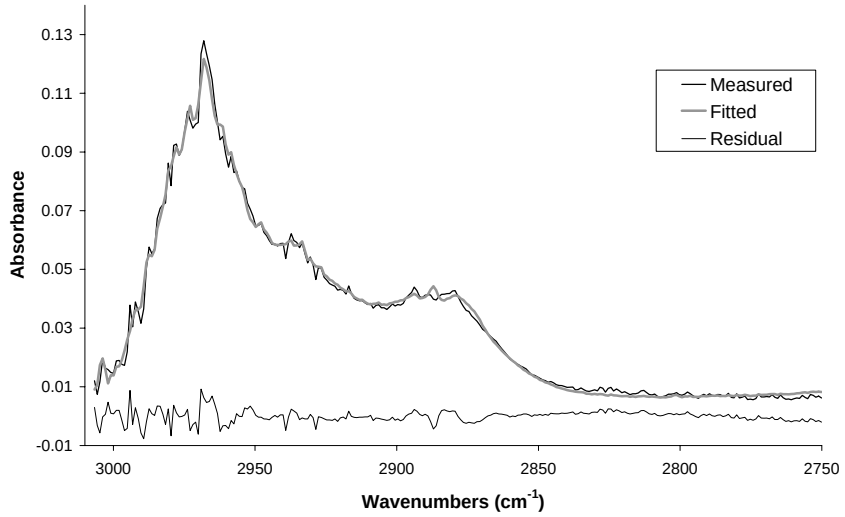

Figure 9. A spectrum measured with a resolution of 2 cm^{-1} together with a fitted spectrum consisting of four different alkanes (propane, butane, 2-methylbutane and 3-metylpentane) with a mean carbon number of 4.5. The difference between the two absorption spectra (the residual) is also shown.

Acknowledgement

Financial support from Vinnova research council and Preem environmental foundation is acknowledged. We also thank Elisabeth Unden and Gunner Hanehoj for participating in the measurements.

References

1. Sommer, S.G., Mikkelsen, H. and Mellqvist, J., *Evaluation of meteorological Techniques for Measurements of Ammonia Loss from Pig Slurry*. Agric. For. Meteorol., 1994(74), p 169-179
2. Siversten, B., *Estimation of Diffuse Hydrocarbon Leakages from Petrochemical Factories*. J. of Air. Poll. Cont. Assoc, 1983. 33(4)
3. Galle B., et al., *Measurements of methane emissions from landfills using a time correlation tracer method based on FTIR absorption spectroscopy.* Environmental Science & Technology, 2001. **35**(1): p. 21-25.
4 Mellqvist., Johan, *Application of infrared and UV-visible remote sensing techniques for studying the stratosphere and for estimating anthropogenic emissions*, Chalmers Dissertation, ISBN 91-7197-765-I, Göteborg, 1999
5. Galle B., Oppenheimer C., Geyer A., McGonigle A. and Edmonds M., *A miniaturised ultravioletspectrometer for remote sensing of SO2 fluxes: a new tool for volcano surveillance*. Journal of Volcanology, 2002. 119: p. 241-254
6 Milton M.J.T., et al. *Measurements of fugitive hydrocarbon emissions with a tunable infrared dial*. 1992. Cambridge, MA, USA: Publ by NASA, Washington, DC, USA.
7. Robinson R.A., Woods P.T., and Milton M.J. *DIAL measurements for air pollution and fugitive-loss monitoring*. 1995. Munich, Ger: Society of Photo-Optical Instrumentation Engineers, Bellingham, WA, USA.
8. Walmsley H.L. and O'Connor S.J. *The measurement of atmospheric emissions from process units using differential absorption LIDAR*. 1997. Munich,
9. Weibring P., et al., *Monitoring of volcanic sulphur dioxide emissions using differential absorption lidar (DIAL), differential optical absorption spectroscopy (DOAS), and correlation spectroscopy (COSPEC)*. Applied Physics B Lasers and Optics, 1998. 67: p. 419-426.
10. Mellqvist, J., et al., *Ground-based FTIR observations of chlorine activation and ozone depletion inside the Arctic vortex during the winter of 1999/2000*, JGR, 2002. 107(D20)
11. Galle, B.; Mellqvist, J., et al., *Ground Based FTIR Measurements of Stratospheric Trace Species from Harestua, Norway during Sesame and Comparison with a 3-D Model*, JAC, **1999**. 32(1): p147-164.
12. Weibring P., et al., *Optical monitoring of volcanic sulphur dioxide emissions - comparison between four different remote-sensing spectroscopic techniques. Optics and Lasers in Engineering*, 2002. 37: p. 267-284.
13. Duffell H., Oppenheimer C., and Burton M., *Volcanic gas emission rates measured by solar occultation spectroscopy*. Geophysical Research Letters, 2001. 28(16): p. 3131.
14. Kihlman M., Mellqvist J., and Samuelsson J., *Monitoring of VOC emissions from three refineries in Sweden and the Oil harbour of Göteborg using the Solar Occultation Flux method*. 2005. Chalmers: Gothenburg.
15. Kihlman, M., *Application of solar FTIR spectroscopy for quantifying gas emissions*, Technical report No. 4L, ISSN 1652-9103 Department of Radio and Space Science, Chalmers University of Technology, 2005
16. Kihlman M ., Mellqvist J., Samuelsson J., Tang L., Chen D., *Monitoring of VOC emissions from refineries in Sweden using the SOF method*, in manuscript, 2005

17. Benner D.C., et al., *The HITRAN molecular spectroscopic database: Edition of 2000 including updates through 2001*. Journal of Quantitative Spectroscopy and Radiative Transfer, 2003. 82(1-4): p. 5
18. *Pacific Northwest National Laboratory*. 2004 Available from: https://secure.pnl.gov/nsd/nsd.nsf/Welcome.
19. Hanst P.L., *QASoft ´96, Database and quantitative analysis program for measurements of gases.* Infrared Analysis Inc., 1996.
20. GRAMS/AI. 2004, Galactic Industries Corporation.
21. Griffith D.W.T., *Synthetic calibration and quantitative analysis of gas-phase FT-IR spectra.* Applied Spectroscopy, 1996. **50**(1): p. 59-70.
22. Chu P.M., et al., *The NIST Quantitative Infrared Database.* J. Res. Natl. Inst. Stand. Technol., 1999. **104(**59).
23 Burton M.R., et al., *Diurnal changes in volcanic plume chemistry observed by lunar and solar occultation spectroscopy.* Geophysical Research Letters, 2001. **28**: p. 843-846.

Research report

The temporal pattern of mortality responses to ambient ozone in the APHEA project

E Samoli,[1] A Zanobetti,[2] J Schwartz,[2] R Atkinson,[3] A LeTertre,[4] C Schindler,[5] L Pérez,[6] E Cadum,[7] J Pekkanen,[8,9] A Paldy,[10] G Touloumi,[1] K Katsouyanni[1]

► Supplemental file published online only at http://jech.bmj.com/content/vol63/issue12

[1] Departement of Hygiene, Epidemiology & Medical Statistics, University of Athens, Greece; [2] Harvard School of Public Health, Boston, USA; [3] St George's, University of London, UK; [4] Environmental Health Unit, National Institute of Public Health Surveillance, Paris, France; [5] Institute of Social and Preventive Medicine, University of Basel, Switzerland; [6] CREAL-Barcelona, Spain; [7] Center for Epidemiology and Environmental Health, Regional Agency for Environmental Protection, Turin, Italy; [8] Department of Environmental Health, National Public Health Institute (KTL), Finland; [9] School of Public Health and Clinical Nutrition, University of Kuopio, Finland; [10] National Institute of Environmental Health, Budapest, Hungary

Correspondence to:
Dr E Samoli, Department of Hygiene and Epidemiology, University of Athens Medical School, 75 Mikras Asias Street, 115 27 Athens, Greece;
esamoli@med.uoa.gr

Accepted 27 April 2009
Published Online First 30 July 2009

ABSTRACT

Background: The temporal pattern of effects of summertime ozone (O_3) in total, cardiovascular and respiratory mortality were investigated in 21 European cities participating in the APHEA-2 (Air Pollution and Health: a European Approach) project, which is fundamental in determining the importance of the effect in terms of life loss.

Methods: Data from each city were analysed separately using distributed lag models with up to 21 lags. City-specific air pollution estimates were regressed on city-specific covariates to obtain overall estimates and to explore sources of possible heterogeneity.

Results: Stronger effects on respiratory mortality that extend to a period of 2 weeks were found. A 10 $\mu g/m^3$ increase in O_3 was associated with a 0.36% (95% CI −0.21% to 0.94%) increase in respiratory deaths for lag 0 and with 3.35% (95% CI 1.90% to 4.83%) for lags 0–20. Significant adverse health effects were found of summer O_3 (June–August) on total and cardiovascular mortality that persist up to a week, but are counterbalanced by negative effects thereafter.

Conclusions: The results indicate that studies on acute health effects of O_3 using single-day exposures may have overestimated the effects on total and cardiovascular mortality, but underestimated the effects on respiratory mortality.

Previous research has demonstrated that the adverse health effects of tropospheric ozone (O_3), a dominant pollutant in the photochemical air pollution mixture in urban centres, are mainly encountered in the summer period.[1–3] This finding may be due to the higher concentration levels during the warmer period, since O_3 is a strong oxidising agent formed in the troposphere through a complex series of reactions involving the action of sunlight on nitrogen dioxide and hydrocarbons. Furthermore, O_3 is very reactive, and its concentrations indoors are much lower than those outdoors, hence people are exposed to O_3 outdoors. Thereafter the higher summer effect of O_3 may also be a result of longer time spent outside in the warmer periods, or more commonly open windows, which results in higher exposures.

Examination of specific causes of death indicates that a major part of the excess mortality related to elevated O_3 levels is from cardiovascular and respiratory deaths. There are several underlying potential mechanisms: inflammation of pulmonary tissues, which can introduce a spectrum of mediators that may also alter cardiac function, or irritant receptor-mediated stimulation of parasympathetic pathways.[4]

Earlier studies reported the association between daily deaths and O_3 concentrations on the same day, a couple of days before death to up to a week before death.[1 5–7] At the same time the results from air pollution epidemiological studies have been criticised as reflecting a small mortality displacement, that is, affecting only frail people who would have died within a few days anyway. If this were true, and air pollution did not simultaneously increase the number of people who become frail, the size of the frail pool would decrease after the air pollution episode and this would result in a reduction in the number of deaths at longer lags. This mortality displacement effect has been described before, particularly for high temperatures.[8] Only Zanobetti and Schwartz[9] have analysed mortality displacement due to O_3, in US cities and found no indication of a displacement pattern. Behaviour and ventilation patterns, as well as co-pollutant exposures differ between the USA and other areas of the world, suggesting the importance of confirming these results in other locales.

The aim of this study was to investigate the temporal pattern (up to 21 days) in health effects of exposure to summertime O_3. We present the results of analyses investigating the effects of O_3 on mortality from all cardiovascular and respiratory causes within the APHEA-2 project (Air Pollution and Health: a European Approach), which uses an extensive European database of cities spanning across the continent.

DATA AND METHODS

APHEA-2 is a multicentre project including 30 cities across Europe and associated regions which studies short-term health effects of air pollution. Data were collected on daily counts of all-cause mortality excluding deaths from external causes (International Classification of Disease (ICD-9) > 800), cardiovascular mortality (ICD-9 390–459) and respiratory mortality (ICD-9 460–519). The data covered at least three consecutive years for each city within the years 1990 to 1997. We analysed daily deaths that occurred in June–August, so that all the lags were still in the warm season to ensure that any changes in the effect estimate reflect the effects of lags and not possible weather effects, especially in the upper and lower time limits of the data. In total, 571 798 deaths occurred in the studied cities during the summer period (June–August). Details about the data have been published elsewhere.[1]

Daily air pollution measurements were provided by the monitoring networks established in each town participating in the APHEA-2 project.[10] According to the APHEA protocol[10] we used the average daily concentration from fixed monitors

that were not located at traffic sites and fulfilled certain data completeness criteria. We present results using the daily maximum of average exposure to O_3 during eight consecutive hours (8 h), because this is the indicator recommended by the World Health Organization for reflecting the most health-relevant exposure to O_3.[11] In total, 21 cities throughout Europe provided daily time series data for O_3 (8 h) concentrations. Time series data on daily temperature (°C, daily mean) and relative humidity (%) were used to control for the potential confounding effects of weather.

Table 1 presents descriptive characteristics of the individual city data sets. The total population exposed is more than 60 million. The Netherlands is considered as one urban area because of its relative small size and dense population. The mean daily total number of deaths in the period analysed ranged from 5 (in Geneva) to 331 (in The Netherlands). For respiratory mortality, mean daily counts ranged from <1 (eg, in Ljubliana, Geneva) to 28 (Netherlands). The median levels of summer O_3 (8 h max) ranged from 39 μg/m^3 in Rome to 123 μg/m^3 in Turin. There was substantial variability among cities in the levels of all pollutants, as well as in the mean daily temperature and humidity.

Methods

According to the APHEA-2 methodology,[12] we used a hierarchic modelling approach. First, we fit regression models for each city separately to allow specific control for seasonal effects, weather and other potential confounders. We then used the individual city results in a second-stage analysis to obtain overall estimates and to investigate potential effect modifiers.

The O_3 (8 h) mortality associations for each city were investigated using Poisson regression models allowing for overdispersion. In order to control for season and long-term patterns we used dummy variables per month per year of data included in the analyses. To evaluate how sensitive our results were to the degree of seasonality control we also applied a natural spline function with 2 degrees of freedom per summer per year, as proposed by Zanobetti and Schwatrz,[9] and 3 degrees of freedom per summer per year. We did not control for influenza epidemics since previously published results[8 13] have shown that these do not bias the association between air pollution and mortality, and since they do not occur in the summer. We used day of the week indicator variables, a linear term for humidity and an unconstrained distributed lag function (ie, multiple linear lags[14]) for temperature to take into account the effect of temperature today and the previous three days (ie, lags 0–3). We chose the number of lags for temperature based on previous results on the acute health effects of summer temperature in Europe, which showed that they extend only for a couple of days.[15] Our initial models included the O_3 level of the day of death (lag 0) as a linear term. There was no significant temporal autocorrelation in the residuals of the city-specific models. We also present results on the effects of O_3 exposure from the average of the same and previous day of death for comparability purposes with previously reported APHEA-2 effect estimates.[1]

For the distributed lags analysis, we used the methodology proposed by Zanobetti and Schwartz[9] and Zanobetti *et al*.[16] Hence, we refit models using O_3 on the day of death and up to the previous 20 days using an unconstrained distributed lag model, that is, a model in which each lag is entered as a separate variable. If there is a mortality displacement effect, we expect to see negative associations between air pollution and deaths several days to weeks after exposure. The overall effect of O_3, is the sum of the positive and negative estimates for all 21 days. We also applied a penalised quasi-likelihood to smooth the coefficients of the distributed lags.[16] This allows us to better examine the temporal pattern of the association with lag, since the unconstrained distributed lag model has too much collinearity to accurately estimate the individual lag effects, although it is precise enough to estimate the sum of all lagged effects.

In the second-stage of the analysis, we assumed the city-specific effect estimates to be normally distributed around an overall estimate. To see whether some of the variability in the city-specific estimates was explained by city characteristics, we

Table 1 Characteristics of the city-specific data sets

	Study period	No of data	Population×1000	Mean no of deaths per day			O_3 (8 h) (μg/m^3) Median (27th to 75th centile)	Mean summer temperature (°C)
				Total	CVD	Respiratory		
Athens	1/92–12/96	460	3073	67	32	4	100.8 (88.0–114.5)	26.8
Barcelona	1/91–12/96	552	1644	36	13	3	75.9 (63.7–91.5)	23.3
Basel	1/90–12/95	552	360	9	4	1	83.5 (63.2–111.4)	19.0
Birmingham	1/92–12/96	460	2300	54	24	7	55.0 (42.6–66.8)	15.7
Budapest	1/92–12/95	368	1931	74	36	3	107.0 (92.8–125.0)	23.3
Geneva	1/90–12/95	552	317	5	2	0	90.9 (71.9–115.6)	19.5
Helsinki	1/93–12/96	644	828	17	8	1	57.2 (46.2–70.1)	15.8
Ljubljana	1/92–12/96	460	322	6	3	0	60.0 (45.0–75.0)	20.4
London	1/92–12/96	460	6905	149	62	22	41.5 (31.0–60.1)	18.2
Lyon	1/93–12/97	460	416	8	3	1	81.8 (60.3–105.5)	20.8
Madrid	1/92–12/95	368	3012	55	18	5	67.1 (55.2–81.2)	23.8
Milan	1/90–12/96	644	1343	26	9	2	84.7 (63.8–110.0)	22.9
Netherlands	1/90–9/95	552	15400	331	130	28	75.9 (60.9–102.0)	16.9
Paris	1/91–12/96	552	6700	116	35	7	54.2 (36.5–84.3)	20.0
Prague	2/92–12/96	460	1213	36	21	1	106.9 (79.3–140.5)	19.4
Rome	1/92–12/96	460	2775	52	20	3	39.2 (29.1–53.4)	25.0
Stockholm	1/90–12/96	644	1126	27	13	2	67.5 (57.3–80.3)	16.8
Teplice	1/90–12/97	736	625	17	10	1	72.3 (52.0–96.6)	18.2
Turin	1/90–12/96	644	926	19	8	1	123.2 (95.8–146.6)	23.5
Valencia	1/94–12/96	276	753	15	5	1	58.6 (50.0–70.4)	25.2
Zurich	1/90–12/95	552	540	12	5	1	92.1 (68.5–119.4)	18.0

CVD, mortality from cardiovascular diseases.

regressed the city-specific effect estimates on potential effect modifiers (at city level), giving each city a weight inversely proportional to the variance of its effect estimate. If substantial ($p<0.20$) heterogeneity remained across city results beyond the variation associated with the effect modifiers, random-effects regression models were applied. In these models, it was assumed that city-specific estimates were a sample of independent observations from a normal distribution with the same mean and with variances equal to the sum of the between-cities variance and the squared standard error of the city-specific estimate. The random variance component was estimated by iteratively reweighted least squares.[17] We applied the χ^2 test and the I^2 statistic, proposed by Higgins and Thompson,[18] to examine heterogeneity. There was a general agreement between the two measures concerning the amount of observed heterogeneity attributed to the between cites variability.

Potential effect modifiers considered in the analysis included variables describing the air pollution level and mix in each city, the exposure and the health status of the population, the geographical area (north, western, and central-eastern European cities) and the climatic conditions. There are very sparse comparable socioeconomic status (SES) indicators across the different countries in Europe available at city level. The only SES indicator available for all cities in this study was the percentage of unemployment.

All models were fit in R v.2.6 (R development Core Team (2007), www.R-project.org).

RESULTS

Table 2 shows the overall percent increase in the daily mortality associated with an increase of 10 μg/m³ in the levels of the daily maximum 8-h O_3. Under the different lag structures except for lag 0 (for which there was no heterogeneity), there was significant to moderate (χ^2 $p<0.20$ and $I^2>20\%$) heterogeneity among the estimates on total and cardiovascular mortality, while there was no heterogeneity in the O_3 effects on respiratory deaths resulting in identical fixed and random effect estimates. We will comment on the random effects estimates that take into account heterogeneity if present or coincide with fixed-effects estimates in case of its absence. The unconstrained distributed lag model gave similar results to the penalised distributed lag. For total mortality when we considered only same-day O_3 exposure a 10 μg/m³ increase was associated with a 0.28% (95% CI 0.07 to 0.48) increase in deaths. The effect of the average of 2 days' exposure was slightly lower but still significant while the sum of lags 0–20 was associated with a small decrease in the daily number of deaths. The same pattern was observed for cardiovascular mortality. Opposite results were found for respiratory mortality: the effect of O_3 seemed to persist over the whole period examined (0–20 days). More specifically, a 10 μg/m³ increase in same-day O_3 yields a non-significant increase in respiratory mortality of 0.36% (95% CI −0.21 to 0.94) and a similar and significant increase after 2 day's exposure. The effect of O_3 on respiratory deaths increased to 3.66% (95% CI 2.25 to 5.08) and to 3.35% (95% CI 1.90 to 4.83) when looking at the penalised and unconstrained distributed lag model, respectively, indicating a prolonged effect of O_3 on respiratory deaths.

In order to test for the robustness of the O_3 effect we performed two sensitivity analyses. We used the same unconstrained distributed lag model as before, but instead of summing all the coefficients from lag 0 to lag 20 and meta-analysing the sum across cities, we created two sums of coefficients in each city, from lag 0 to lag 3 and from lag 4 to lag 20 and meta-analysed both sums across cities. We repeated the same analysis using a cut-off of 7 days, hence we created the sums for lags 0–6 and lags 7–20. For all-cause mortality we found an effect size of 0.40% (95% CI −0.01 to 0.80) for lags 0–3 and −0.96% (95% CI −1.5 to −0.37) for lags 4–20. Correspondingly, we found an effect size of 0.43% (95% CI 0.05 to 0.81) for lags 0–6 and −0.99% (95% CI −1.5 to −0.40) for lags 7–20. These findings indicate a positive O_3 effect on total mortality that persists up to a week, which is followed by negative effects thereafter. Since deaths from cardiovascular causes account for about 45% of the total number of deaths in the analysed cities, the corresponding patterns for cardiovascular mortality followed the ones of total mortality.

Table 2 Estimated percent increase in mortality outcomes (and 95% CIs) for a 10 μg/m³ increase in maximum 8-h ozone during June–August, for the same day, the average of the same and previous day, the unconstrained distributed lag model for the sum of 0–20 days and the penalised distributed lag model (lags 0–20)

	Fixed effects	Random effects
	Per cent increase (95% CI)	Per cent increase (95% CI)
Total mortality		
Lag 0	0.28 (0.11 to 0.45)	0.28 (0.07 to 0.48)
Average lags 0–1	0.24 (0.15 to 0.34)	0.22 (0.08 to 0.35)
Sum lags 0–20, unconstrained	0.01 (−0.40 to 0.41)	−0.54 (−1.28 to 0.20)
Sum lags 0–20, penalised	0.01 (−0.41 to 0.42)	−0.56 (−1.30 to 0.19)
Cardiovascular mortality		
Lag 0	0.43 (0.18 to 0.69)	0.37 (0.05 to 0.69)
Average lags 0–1	0.33 (0.19 to 0.48)	0.25 (0.03 to 0.47)
Sum lags 0–20, unconstrained	−0.33 (−0.93 to 0.29)	−0.62 (−1.47 to 0.24)
Sum lags 0–20, penalised	−0.32 (−0.92 to 0.28)	−0.57 (−1.39 to 0.26)
Respiratory mortality		
Lag 0	0.36 (−0.21 to 0.94)	0.36 (−0.21 to 0.94)
Average lags 0–1	0.40 (0.11 to 0.70)	0.40 (0.11 to 0.70)
Sum lags 0–20, unconstrained	3.35 (1.90 to 4.83)	3.35 (1.90 to 4.83)
Sum lags 0–20, penalised	3.66 (2.25 to 5.08)	3.66 (2.25 to 5.08)

Our results were also robust to the city-specific model choice. We tested excluding humidity from our models and our estimates changed only slightly. The estimate from the unconstrained distributed lag model for total daily number of deaths decreased to −0.56% (95% CI −0.92 to 0.17), that is, decreased by less than 4%, indicating the stronger effect of temperature—compared with humidity—with regard to the model fit. Our results were also robust to the inclusion of a larger number of temperature lags, since when we allowed for up to nine lags the estimate for respiratory mortality remained significant and decreased only by 10%, while there was a similar increase for total mortality. We also applied a natural cubic spline with 2 degrees of freedom per summer per year of data to control for seasonality and long-term trends as suggested by Zanobetti and Schwartz.[9] The total mortality estimate from the unconstrained distributed lag model increased slightly to −0.47% (95% CI −1.18 to 0.24). There was a similar increase in the estimate of cardiovascular mortality and a decrease in comparable magnitude in respiratory mortality, not affecting the essence of the conclusions. When we applied a natural cubic spline with 3 degrees of freedom per summer per year of data to control for seasonality, the estimate from the unconstrained distributed lag model for total mortality increased to −0.35% (95% CI −1.20 to 0.51), not altering the direction or the magnitude of the results.

Figure 1 presents the percentage increase in the daily number of all (A) and respiratory (B) deaths and their 95% CI associated with an increase of 10 μg/m³ in O_3 levels during June–August in

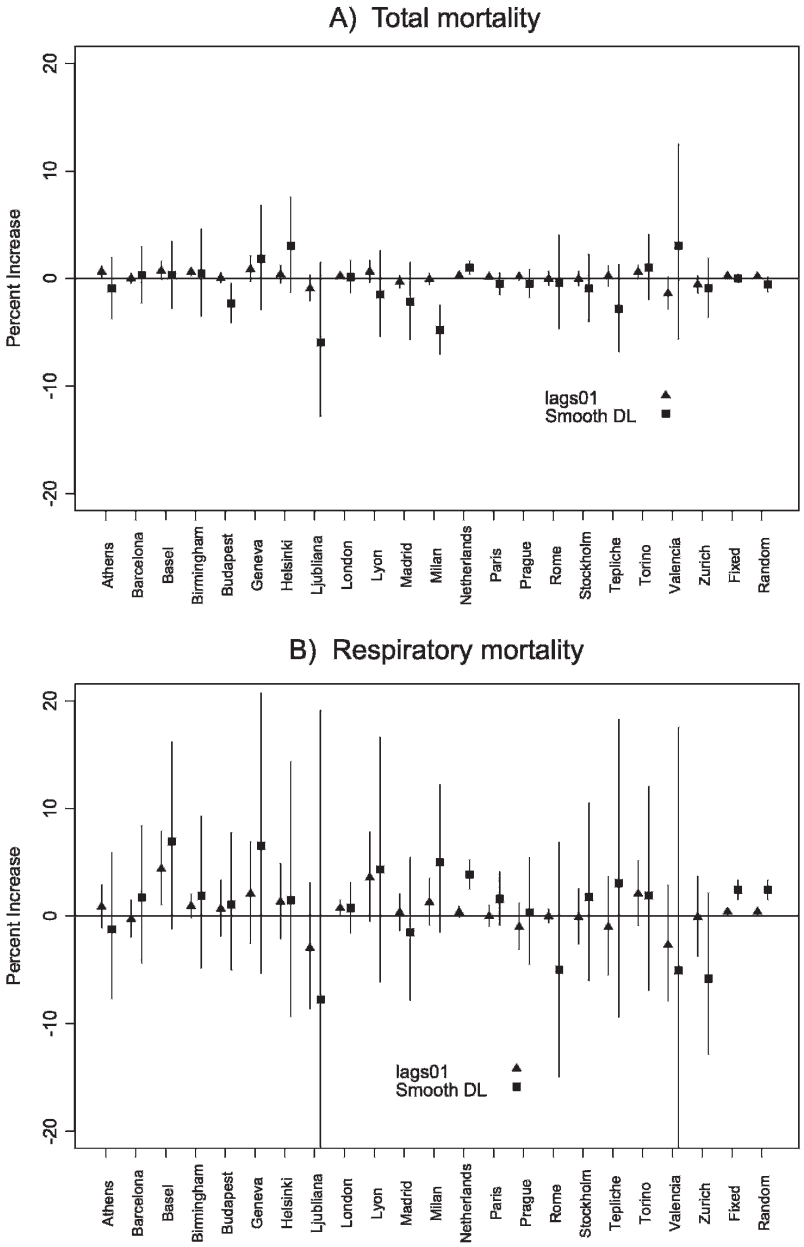

Figure 1 City-specific and overall percent increase (and 95% CIs) in total (A) and respiratory (B) mortality per 10 μg/m^3 increase in O_3 (8 h) during June–August. Triangles represent the effect of the average of lags 0 and 1 and squares the smooth distributed lag effect. DL, distributed lag.

each city and in all cities, as estimated from the models using mean exposure of 2 days (triangles represent average of same and previous day) and from the smooth distributed lag model (squares). The statistically significant estimated increases in total mortality per 10 μg/m^3 increase in summer O_3 average of lags 0–1 ranged from 0.30% in The Netherlands to 0.65% in Athens, while the corresponding increases from the distributed lag model ranged from −4.75% in Milan to 1.02% in The Netherlands. The plot demonstrates the heterogeneity of the total mortality results especially under the distributed lag model. As shown in table 2 the average of the same and previous day of O_3 exposure yields larger and comparably less heterogeneous effect estimates for total mortality, while the opposite is true for respiratory mortality. The larger cities tend to have the smaller CIs (such as The Netherlands, London and Paris).

Figure 2 presents the shape of the smoothed distributed lag pattern for total mortality across the 21 European cities. Each triangle represents the percent increase in total mortality per 10 μg/m^3 increase in O_3 for each of the 21 lags. We found the highest effect at lag 0 declining to zero by day 4. The values between lags 5 and 17 are almost zero while the last lags have high CIs that make extrapolation unreliable. The temporal pattern between O_3 and cardiovascular mortality is almost identical to the one for total mortality.

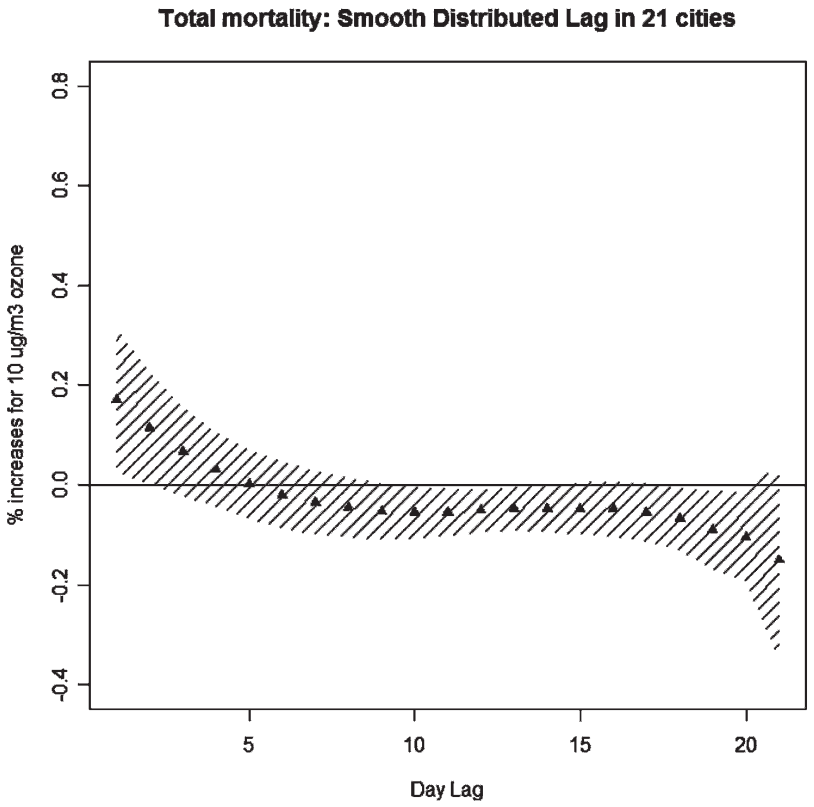

Figure 2 Plot of the combined smooth distributed lag in 21 European cities during June–August. The triangles represent the percent increase in total mortality per 10 μg/m³ increase in O_3 (8 h), and the shaded area represents the 95% CIs.

Figure 3 presents the corresponding plot for respiratory mortality. The highest effect is observed in the first 2 days while the effect of O_3 persists up to lag 12. Again the next four values are almost zero while the last lags are poorly estimated. However, the whole curve has larger CIs than the plot for total mortality due to the smaller death counts. The plot illustrates the extended effect of O_3 on respiratory mortality as also indicated by the results in table 2.

We investigated the observed heterogeneity in the estimates of the short-term effects of summer O_3 on total and cardiovascular mortality by examining potential effect modifiers in second-stage regression models. For the distributed lag effect estimates and for respiratory mortality we did not investigate effect modification, as O_3 did not have an overall significant effect on daily total and cardiovascular mortality or there was no heterogeneity in the estimates. When investigating the source of heterogeneity in the association between O_3 and total and cardiovascular mortality using the average of 2 day's exposure the only significant effect modifiers were the mean level of PM_{10} for total mortality and the age structure of the population for cardiovascular mortality. More specifically, the effect of summer O_3 on total mortality was higher in cities with lower levels of PM_{10} (particulate matter <10 μm in aerodynamic diameter); on cardiovascular mortality the effect was greater for cities with a smaller proportion of older people and the association was inverse in cities with younger populations.

DISCUSSION

In the last few years, several meta-analyses on acute mortality and O_3 have been published, and the results showed (quite consistently) significant increases in risks for the warm season. For all causes of mortality the reported increase (per 10 μg/m³ increase of O_3) has swayed among 0.1%,[19–21] 0.2%[22] and 0.3%.[1–3 6 23 24] For cardiovascular causes the magnitude of effects ranged between an increase of 0.4%[1 6 23] and 0.2%,[24] but the Italian meta-analysis considered a different period (May–September).

Our study investigated a more prolonged time period of effects. We have found significant adverse health effects of summer O_3 (June–August) on total and cardiovascular mortality that persist up to a week. We found stronger effects on respiratory mortality that extend to a period of 2 weeks. These findings complement those previously reported from APHEA-2,[1] where an increase of 10 μg/m³ in O_3 (8 h), average of lags 0 and 1, in the warm period of the year (April–September) was associated with 0.31%, 0.46% and 1.13% increases in total, cardiovascular and respiratory mortality, respectively. Our estimates for the same period of exposure (average of same and previous day) are slightly lower. This may be attributed to the difference between the months analysed as well as to the methodology applied within APHEA-2.

When we examined models for the cumulative effect of 21 days of O_3 exposure either using an unconstrained or a penalised smooth distributed lag model we found no effect of summer O_3 on total and cardiovascular mortality but a significant adverse effect on respiratory mortality. Thus, there seems to be mortality displacement in the effects of O_3 on total and cardiovascular but not on respiratory mortality. Zanobetti and Schwartz,[9] in their investigation of mortality displacement in the association of O_3 and mortality in 48 US cities found effect size estimates for total, cardiovascular and respiratory mortality after 21 lags (0–20 days) that were somewhat larger

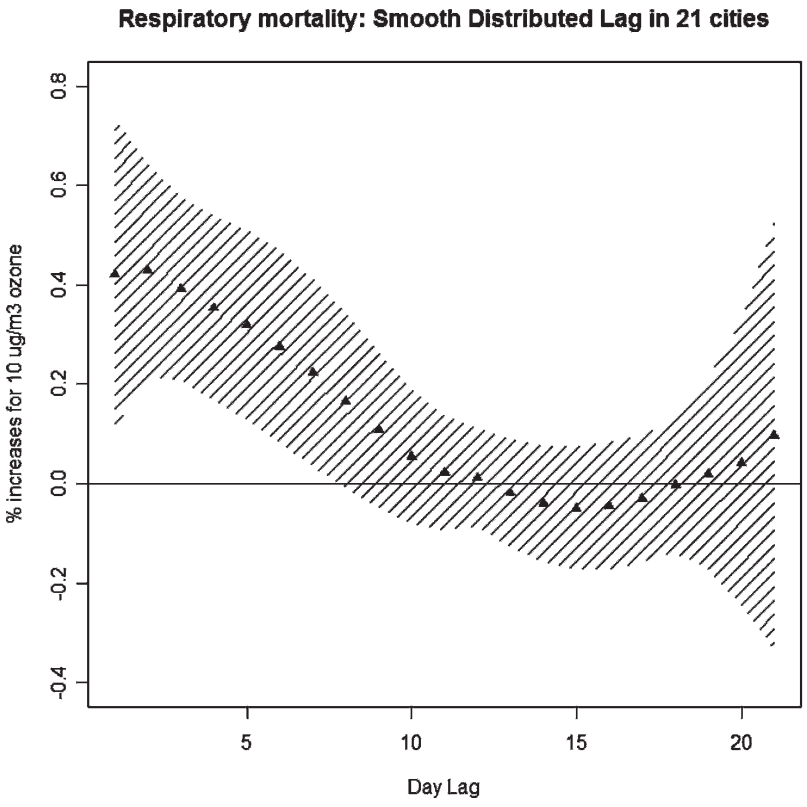

Figure 3 Plot of the combined smooth distributed lag in 21 European cities during June–August. The triangles represent the percent increase in respiratory mortality per 10 μg/m^3 increase in O_3 (8 h), and the shaded area represents the 95% CIs.

(though non-significant except for total mortality) than those using a single day's concentration, indicating no evidence of short-term mortality displacement. Although these findings indicate a different magnitude of exposure–response between the USA and Europe, the comparison of the smooth plots for the two regions produced for the association between summer O_3 and total mortality reveals a similar shape slightly shifted upwards in the USA. Hence the overall pattern is quite similar—both studies find the summer O_3 effect on total mortality is in the first week.

Several factors may explain the upward shift of the curve in the US cities. First, the US cities presented in the Zanobetti and Schwartz study[9] seem to have higher O_3 levels than the European ones in our analysis. Another difference between the US and the European results is that the latter are more heterogeneous than the former. In that context we have tried to identify city-specific characteristics that may contribute to the observed heterogeneity especially in the O_3–total mortality association. Since there was moderate heterogeneity when we considered two days' exposure, the only effect modifier identified for total mortality was the mean level of PM_{10} and for cardiovascular mortality the age structure of the population, expressed either as the proportion above 75 or inversely the proportion under 15. The higher effects of 2 days' O_3 on total mortality in cities with lower PM level is unclear and may reflect the air pollution mix, while the higher effect in younger populations may reflect exposure patterns in the sense that during hot days on which O_3 concentration is higher elderly people tend to stay indoors or even leave urban areas. The effect modification patterns identified were not driven by outliers in the distribution of the variables under investigation. The exploration of effect modification was limited by the number of variables that extended across the full data set. Although previous investigation of effect modification patterns in the effects of O_3 on total and cardiovascular mortality[1] indicated the standardised mortality rate and the geographical area as modifiers, respectively, we have not replicated these findings in our restricted summer period analysis.

Our analysis is constrained by the nature of time-series studies that can only extend up to about a monthly time period. Since there is evidence of adaptation to O_3 with reduced effects on lung function[25] there is reason to believe that any effect would occur in the first weeks. Nevertheless, it is not possible to test such a hypothesis within this framework. Another inherent disadvantage of time-series studies is exposure misclassification. Especially for the analysis of O_3 effects, the location of the monitoring stations may be important due to the scavenging characteristic of the pollutant. However, even if the absolute levels in each city may be affected by the monitoring station's location (and consequently the ranking of the cities according to the pollutant's level may not reflect the reality), the day-to-day variability is unlikely to be affected. Therefore, our results, based on the analysis of daily variability, should not have been affected. Finally, we have not controlled for PM_{10} since there is good evidence that this would not confound the association.[1 26]

We found that ozone effects are more prolonged for respiratory than for cardiovascular deaths. It is interesting to note that Goodman *et al*[27] have reported similar time patterns

What is already known on this subject

- Previous research has demonstrated adverse health effects of tropospheric ozone (O_3), a dominant pollutant in the photochemical air pollution mixture in urban centres, mainly encountered in the summer period.
- At the same time the results from air pollution epidemiological studies have been criticised as reflecting a small mortality displacement, that is, affecting only frail people who would have died within a few days anyway.

What this study adds

- We investigated the temporal pattern of effects up to 21 days of summertime ozone (O_3) in total, cardiovascular and respiratory mortality in 21 European cities participating in the APHEA-2 project, which is fundamental in determining the importance of the effect in terms of life loss.
- We found that O_3 effects are more prolonged for respiratory compared with cardiovascular deaths.
- Our results indicate that studies on acute health effects of O_3 using single day exposures may have overestimated the effects on total and cardiovascular mortality, but underestimated the effects on respiratory mortality.

for exposure to particulate pollution and indicated a different time response for cardiovascular mortality compared with respiratory mortality, where cardiovascular mortality occurred within the first few days of exposure, whereas respiratory mortality showed a lag of up to 2 weeks. This makes some sense, since air pollution can be associated with the triggering of cardiovascular events,[28] while exacerbation of respiratory infections would be expected to take more time. Wheeler *et al*[29] found direct evidence of heterogeneity in the autonomic response to ambient pollution that is dependent on the underlying health status of the study population. Mudway and Kelly[30] point out that the rules that govern the balance between beneficial and detrimental interactions between O_3 and antioxidants in the lung lining fluid compartment are not well established but these may contribute in part to sensitivity. Hence, the biological mechanisms responsible for the adverse health effects of O_3, particularly on the basis of individual susceptibility, are still unclear.

In conclusion, there was indication of mortality displacement for total and cardiovascular mortality but not for respiratory mortality. The extended follow-up effects of O_3 on respiratory mortality were more than three times greater than acute effects previously reported. Our results indicate that studies on acute health effects of O_3 using single-day exposures may have underestimated the effects of air pollution on respiratory mortality.

Funding: This work was funded through two grants from the European Commission (EC) Environment and Climate Programme (contract numbers ENV4-CT97-0534 and QLK4-CT-2001-30055).

Competing interests: None.

Provenance and peer review: Not commissioned; externally peer reviewed.

REFERENCES

1. **Gryparis A,** Forsberg B, Katsouyanni K, *et al*. Acute effects of ozone on mortality from the "air pollution and health: European approach" project. *Am J Respir Crit Care Med* 2004;**170**:1080–7.
2. **Ito K,** De Leon SF, Lippmann M. Associations between ozone and daily mortality: analysis and meta-analysis. *Epidemiology* 2005;**16**:446–57.
3. **Levy JL,** Chemerynski SM, Sarnat JA. Ozone exposure and mortality: an empiric Bayes metaregression analysis. *Epidemiology* 2005;**16**:458–68.
4. **Watkinson WP,** Campen MJ, Nolan JP, *et al*. Cardiovascular and systemic responses to inhaled pollutants in rodents: effects of ozone and particulate matter. *Environ Health Perspect* 2001;**109**:539–46.
5. **Huang Y,** Dominici F, Bell ML. Bayesian hierarchical distributed lag models for summer ozone exposure and cardio-respiratory mortality. *Environmentrics* 2005;**16**:547–62.
6. **Bell ML,** Dominici F, Samet JM. A meta-analysis of time-series studies of ozone and mortality with comparison to the national Morbidity, Mortality and Air Pollution Study. *Epidemiology* 2005;**16**:436–45.
7. **Bell ML,** Dominici F. Effect modification by community characteristics on the short-term effects of ozone exposure and mortality in 98 US communities. *Am J Epidemiology* 2008;**167**:986–97.
8. **Braga A,** Zanobetti A. Do respiratory epidemics confound the association between air pollution and daily deaths? *Eur Respir J* 2000;**16**:723–6.
9. **Zanobetti A,** Schwartz J. Mortality displacement in the association of ozone with mortality: An analysis of 48 US cities. *Am J Respir Crit Care Med* 2008;**177**:184–9.
10. **Katsouyanni K,** Touloumi G, Samoli E, *et al*. Confounding and effect modification in the short-term effects of ambient particles on total mortality: results from 29 European cities within the APHEA2 project. *Epidemiology* 2001;**12**:521–31.
11. **WHO (World Health Organization)**. *Air quality guidelines for Europe*, 2nd edn. WHO Regional Publications European Series No 91, Copenhagen. 2000.
12. **Touloumi G,** Atkinson R, Le Tertre A, *et al*. Analysis of health outcome time series data in epidemiological studies. *Environmetrics* 2003;**15**:101–17.
13. **Touloumi G,** Samoli E, Quenel P, *et al*. Short-term effects of air pollution on total and cardiovascular mortality: the confounding effects of influenza epidemics. *Epidemiology* 2005;**16**:49–57.
14. **Schwartz J.** The distributed lag between air pollution and daily deaths. *Epidemiology* 2000;**11**:320–6.
15. **Baccini M,** Biggeri A, Accetta G, *et al*. Effects of apparent temperature on summer mortality in 15 European cities: results of the PHEWE project. *Epidemiology* 2008;**19**:711–19.
16. **Zanobetti A,** Wand MP, Schwartz J, *et al*. Generalised additive distributed lag models: quantifying mortality displacement. *Biostatistics* 2000;**1**:279–92.
17. **Berkey CS,** Hoaglin DC, Mosteller F, *et al*. A random-effects regression model for meta-analysis. *Stat Med* 1995;**14**:395–411.
18. **Higgins JP,** Thompson SG. Quantifying heterogeneity in a meta-analysis. *Stat Med* 2002;**21**:1539–58.
19. **Thurston GD,** Ito K. Epidemiological studies of acute ozone exposures and mortality. *J Expo Anal Environ Epidemiol* 2001;**11**:286–94.
20. **Stieb DM,** Judek S, Burnett RT. Meta-analysis of time-series studies of air pollution and mortality: effects of gases and particles and the influence of cause of death, age, and season. *J Air Waste Manag Assoc* 2002;**52**:470–84.
21. **Bell ML,** McDermott A, Zeger SL, *et al*. Ozone and short-term mortality in 95 US urban communities, 1987–2000. *JAMA* 2004;**292**:2372–8.
22. **Schwartz J.** How sensitive is the association between ozone and daily deaths to control for temperature? *Am J Respir Crit Care Med* 2005;**171**:627–31.
23. **Anderson HR,** Atkinson R, Peacock J, *et al*. *Meta-analysis of time-series studies and panel studies of particulate matter (PM) and ozone (O3): report of a WHO task group*. Copenhagen: WHO Regional Office for Europe 2004. (document EUR/04/5042688) www.euro.who.int/document/E82792.pdf (accessed 1 Jul 2008).
24. **Biggeri A,** Bellini P, Terracini B. Meta-analysis of the Italian studies on short-term effects of air pollution – MISA 1996–2002 (in Italian). *Epidemiol Prev* 2004;**28**(S4–5):4–100.
25. **Zanobetti A,** Schwartz J. Is there adaptation in the ozone-mortality relationship: A multi-city case crossover analysis. *Environ Health* 2008;**30**:7–22.
26. **Bell ML,** Kim JY, Dominici F. Potential confounding of particulate matter on the short-term association between ozone and mortality in multisite time-series studies. *Environ Health Perspect* 2007;**115**:1591–5.
27. **Goodman PG,** Dockery DW, Clancy L. Cause-specific mortality and the extended effects of particulate pollution and temperature exposure. *Environ Health Perspect* 2004;**112**:179–85.
28. **Peters A,** von Klot S, Heier M, *et al*, Cooperative Health Research in the Region of Augsburg Study Group. Exposure to traffic and the onset of myocardial infarction. *N Engl J Med* 2004;**351**:1721–30.
29. **Wheeler A,** Zanobetti A, Gold DR, *et al*. The relationship between ambient air pollution and heart rate variability differs for individuals with heart and pulmonary disease. *Environ Health Perspect* 2006;**114**:560–6.
30. **Mudway IS,** Kelly FJ. Ozone and the lung: a sensitive issue. *Mol Aspects Med* 2000;**21**(1–2):1–48.

The temporal pattern of mortality responses to ambient ozone in the APHEA project

E Samoli, A Zanobetti, J Schwartz, R Atkinson, A LeTertre, C Schindler, L Pérez, E Cadum, J Pekkanen, A Paldy, G Touloumi and K Katsouyanni

J Epidemiol Community Health 2009 63: 960-966 originally published online July 30, 2009
doi: 10.1136/jech.2008.084012

See the Best and Worst Places for Breathable Air in the U.S.

New rankings of air quality in cities show the cleanest air isn't always rural.

Los Angeles has long struggled with air quality.

Photograph by Peter Bohler, Redux

By **Laura Parker**

PUBLISHED APRIL 19, 2017

The air Americans breathe is cleaner than ever, thanks to cleaner power plants and cleaner vehicles. That milestone is all the more impressive when considering progress has been achieved in spite of increases in population, energy use, and miles driven.

Yet nearly 40 percent of Americans—125 million people—still live where the air is unhealthy to breathe. Those findings are contained in the American Lung Association's annual State of the Air report, released Wednesday.

This year's survey tracks air quality measurements between 2013 and 2015 of ozone and particle pollution, short-term and year-round. Cities and counties are ranked on three separate lists for levels of those pollutants. More than 18 million people live in 12 counties with all three air pollution conditions.

Ozone, otherwise known as smog, is created by gases, including tailpipe and smokestack emissions. People at risk from inhaling ozone are children, teens, seniors age 65 and older, people who work outdoors, and people with heart and lung diseases, including asthma and lung cancer.

Particle pollution is a mixture of solid and liquid particles, one-thirtieth the diameter of a human hair, that circulate in the air. Inhaling particle pollution can increase the risk of lung cancer and cause heart attacks, strokes, emergency room visits for people with asthma, heart disease, and early death.

Both particles and ozone increase the risk of lower birth weight in newborns.

"You don't have to have pollution day in and day out to harm you," says Janice Nolen, an American Lung Association assistant vice president. "The classic example is the 1952 killer fog in London."

Toxic fog, mixed with tons of poisonous soot from coal-burning fireplaces, settled over the city for five days, creating the worst air pollution disaster in British history. An estimated 4,000 people died, though some concluded that the bad air eventually caused 12,000 deaths.

Nolen says the Clean Air Act of 1970 accounts for the progress that's been made in cleaning up America's air. But with success has come pushback from industries that "don't want to do more," she says. "We're concerned about that." (See 46 environmental victories since the first Earth Day.)

1. California is still air pollution king

Los Angeles maintains its rank as the city with the worst ozone pollution. The City of Angels has remained at the top of the worst pollution list for 17 out of the 18-year history of the report. Bakersfield is holding steady as the city with the worst short-term particle pollution and Visalia-Porterfield-Hanford rounds out a California trifecta in the pollution rankings by becoming the most-polluted city for year-round particle pollution for the first time this year.

California also retains its ranking with seven of the 10 most-polluted metropolitan areas and 11 of the worst 25 cities. But the pollution isn't caused just by the millions of cars driven by the 39 million people who live in California. The state's weather and geography complicate efforts to reduce emissions. Wildfire smoke and high inversions that trap particles behind ridges and mountains are becoming year-round conditions. After California, nine of the 25 most ozone-polluted cities are in the Southwest, where wildfires and drought are now also regular occurrences.

2. Progress in the Rust Belt and the industrial East

The eastern portion of the country, where coal-fired power plants have been cleaned up and the use of old diesel engines has declined, has seen a shift in rankings. Dirty manufacturing cities such as Pittsburgh, Pennsylvania, which had been ranked as the most polluted city for year-round particle pollution in 2008, experienced its fewest unhealthy days ever, thanks to clean-up of industrial sites. Likewise, three Tennessee cities, including Knoxville, home to the Tennessee Valley Authority power plants, are no longer on the worst-polluted lists. Knoxville once had 111 unhealthy air days, but just one for the new report.

3. Climate change will make it difficult to protect human health

Despite the improvements in air quality, a handful of cities reported their highest number of unhealthy days since the report began, in part because of extreme weather events. Drought prompts dust storms and wildfires, which, in turn, increase short-term particle pollution. Warmer daily temperatures make it more difficult to reduce ozone pollution. Stagnant weather patterns contributed to the extraordinarily high number of days the air contained unhealthy particulate matter. Inversions in the San Joaquin Valley in southern California and in the Wasatch Ridge in Utah worsened bad air days in both states.

4. The cleanest cities are not all rural

Six cities ranked on all three pollutant lists for cleanest cities. They had no high ozone or high particle pollution days, and were among the 25 cities with the lowest year-round particle levels. Five cities are repeaters: Burlington, Vermont, Cape Coral-Fort Myers, Florida, Elmira-Corning, New York, Honolulu, Hawaii, and Melbourne-Titusville-Palm Bay on Florida's Space Coast. For the first time, Wilmington, North Carolina made the top clean cities list.

AMERICAN LUNG ASSOCIATION®

STATE OF THE AIR 2017

Acknowledgments

The American Lung Association "State of the Air® 2017" is the result of the hard work of many people:

In the American Lung Association National Office: Paul G. Billings, who supervised the work; Janice E. Nolen, M.A., who directed the project, analyzed data, wrote the text, and coordinated print and web presentations; Lyndsay Moseley Alexander, Laura Kate Bender and Diana Van Vleet who integrated the Healthy Air Campaign with this report; Zach Jump, M.A., who converted the raw data into meaningful tables and comparisons and calculated all the population data; Susan Rappaport, MPH, who supervised the data analysis; Norman Edelman, M.D., and Al Rizzo, M.D., who reviewed the science and health discussions; Neil Ballentine, who directed the online presentation; Todd Nimirowski, who designed and created the user experiences online; Lauren Innocenzi and Valerie Wojs, who managed content production online; Laura Lavelle, Thomas Venhuizen and Corey Clark who developed social sharing and digital engagement strategy; Kim Lacina, Allison MacMunn, Gregg Tubbs and Erin Meyer who coordinated internal and external communications and media outreach; Michael Albiero, who designed the logo and report cover; and Craig Finstad, who coordinated sharing the data with direct mail donors.

In the nationwide American Lung Association: All Lung Association charters reviewed and commented on the data for their states. Hardworking staff across the nation went out of their way to ensure that their state and local air directors were informed and had a chance to review the draft data.

Outside the American Lung Association: Allen S. Lefohn of A.S.L. and Associates, who compiled the data; Deborah Shprentz, who assisted with the research; Beaconfire RedEngine Consulting, who uploaded the data to the website; and Our Designs, Inc., who designed the print version.

Great appreciation goes to the National Association of Clean Air Agencies, who along with their Executive Director Bill Becker, strove to make this report better through their comments, review and concerns. Many of their members reviewed and commented on the individual state data presented and the methodology to make this report more accurate. We also appreciate the assistance of the Association of Air Pollution Control Agencies, whose members also assisted in the review of the data from their states. We appreciate them as our partners in the fight against air pollution. This report should in no way be construed as a comment on the work any of these agencies do.

The American Lung Association assumes sole responsibility for the content of the American Lung Association "State of the Air® 2017."

American Lung Association
National Headquarters
55 W. Wacker Drive, Suite 1150
Chicago, IL 60601

Advocacy Office
1331 Pennsylvania Avenue, NW, Suite 1725 North
Washington, DC 20004

Phone: 1 (800) 586-4872
Fax: (202) 452-1805

www.stateoftheair.org
www.Lung.org

Fighting for Air

Designed by Our Designs, Inc., Nashville, TN

Contents

The State of the Air 2017

The "State of the Air 2017" found continued improvement in air quality in 2013-2015 in ozone and year-round particle pollution, but an unrelenting increase in dangerous spikes in particle pollution. These trends demonstrate the continued need to support and enforce the Clean Air Act to protect the nation from unhealthy air.

The "State of the Air 2017" report shows that cleaning up pollution continues successfully in much of the nation. In the 25 cities with the worst ozone and year-round particle pollution, the majority saw improvements from last year. Many again reached their lowest levels ever of these widespread air pollutants.

Yet, even as most cities experienced strong improvement, too many cities suffered worse episodes of unhealthy air. While most of the nation has much cleaner air quality than even a decade ago, many cities reported their highest number of unhealthy days since the report began, including some that experienced extreme weather events.

"State of the Air 2017" shows that more than four in 10 people had unhealthy air quality in their communities.

The "State of the Air 2017" report shows that, even with continued improvement, too many people in the United States live where the air is unhealthy for them to breathe. Despite that continued need and the nation's progress, some people seek to weaken the Clean Air Act, the public health law that has driven the cuts in pollution since 1970, and to undermine the ability of the nation to fight for healthy air.

The "State of the Air 2017" report looks at levels of ozone and particle pollution found in official monitoring sites across the United States in 2013, 2014 and 2015. The report uses the most current quality-assured nationwide data available for these analyses.

The report examines particle pollution ($PM_{2.5}$) in two different ways: averaged year-round (annual average) and over short-term levels (24-hour). For both ozone and short-term particle pollution, the analysis uses a weighted average number of days that allows recognition of places with higher levels of pollution. For the year-round particle pollution rankings, the report uses averages calculated and reported by the U.S. Environmental Protection Agency (EPA). For comparison, the "State of the Air 2016" report covered data from 2012, 2013 and 2014.[1]

Overall Trends

The "State of the Air 2017" found continued improvement in air quality in 2013-2015 in ozone and year-round particle pollution, but an unrelenting increase in dangerous spikes in particle pollution. The number of people exposed to unhealthy levels of air pollution dropped to more than 125 million people, from 166 million in the years covered in the 2016 report (2012-2014).

Four in 10 people live where the air is unhealthy.

Overall, **the best progress came in the continued reduction of ozone and year-round particle pollution,** thanks to cleaner power plants and increased use of cleaner vehicles and engines. Continued progress to cleaner air remains crucial to reduce the risk of premature death, asthma attacks and lung cancer. However, a changing climate is making it harder to protect human health.

Nearly four in 10 people (38.9 percent) in the United States live in counties that have unhealthful levels of either ozone or particle pollution. More than 125 million Americans live in 204 counties where they are exposed to unhealthful levels of air pollution in the form of either ozone or short-term or year-round levels of particles.

Still, this represents a major improvement: One-quarter fewer people now live where the air quality hit unhealthy levels.

Still, this represents a major improvement: **One-quarter fewer people now live where the air quality hit unhealthy levels in 2013-2015** than in the 2016 report. In last year's report, covering 2012-2014, more than 166 million Americans lived in counties with unhealthful levels of air pollution.

Los Angeles improved over last year and again had its best ozone report in the history of the "State of the Air."

More than 18 million people (5.6 percent) live in 12 counties with unhealthful levels of all three: ozone and short-term and year-round particle pollution. This is nearly 1.9 million fewer people than in the 2016 report when approximately 6.3 percent were exposed. However, we continue to lack data on particle pollution in all or parts of two states.

Los Angeles remains the city with the worst ozone pollution as it has for nearly the entire history of the report. **Bakersfield, CA, maintains its rank as the city with the worst short-term particle pollution,** while **Visalia-Porterfield-Hanford, CA,** moved for the first time to rank as the **most-polluted city for year-round particle pollution.**

The "State of the Air 2017" report shows the sustained success of the Clean Air Act, continuing to clean up pollution in much of the nation, as it nearly completes its fifth decade of service. Many cities reported fewer days of high ozone and lower levels of year-round particle pollution. Several cities again reported their cleanest years ever during this period, while others had their worst periods of air pollution.

Thanks to the provisions in the Clean Air Act, the United States has continued to **reduce ozone and particle pollution** as well as other pollutants for decades. Figure 1 from EPA shows that since 1970, the air has gotten cleaner while the population, the economy, energy use and miles driven increased greatly. As the economy continues to grow, overall air emissions that create the six most-widespread pollutants continue to drop.

Comparison of Growth Areas and Emissions, 1970–2015

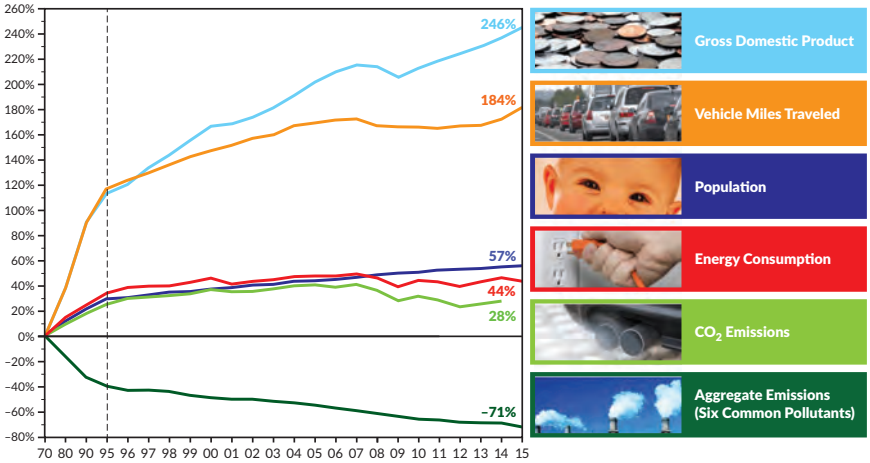

Figure 1: Air pollution emissions continue to drop steadily since 1970 thanks to the Clean Air Act. As the economy continues to grow, emissions that cause ozone and particle pollution continue to drop. Source: U.S. EPA, Air Trends: Air Quality National Summary, 2017.

The Clean Air Act must remain intact and enforced to enable the nation to continue to protect all Americans from the dangers of air pollution. This law has driven improvements in air quality for 47 years, as shown in Figure 1. Since first issued in 2000, the "State of the Air" reports have also documented these improvements, as shown in trend charts for counties and cities available at www.stateoftheair.org. The nation must ensure that the Clean Air Act's tools remain in place, funded and followed.

The "State of the Air 2017" report adds to the evidence that a changing climate in making it harder to protect human health. While most of the nation has much cleaner air quality than even a decade ago, a few cities reported their worst number of unhealthy days since the report began, including many that experienced wildfire smoke.

As climate change continues, cleaning up these pollutants will become ever more challenging. Climate change poses many threats to human health, including worsened air quality and extreme weather events. The nation must continue to reduce emissions that worsen climate.

Ozone Pollution

Twenty of the 25 cities with the worst ozone pollution reduced the number of high-ozone days they experienced each year, improving over the previous report. Twelve experienced their best ozone seasons ever during 2013-2015, reaching their lowest weighted average number of days of unhealthy levels each year.

Los Angeles remains at the top of this list as it has for all but one of the 18 reports. Los Angeles also continues its success at cleaning up ozone, dropping its average number of unhealthy days to its lowest level ever.

Also **experiencing their fewest high-ozone days on average were 10 other cities** among the 25 most polluted by ozone. They include Bakersfield, CA; Visalia-Porterville-Hanford, CA; Modesto-Merced, CA; Sacramento, CA; Las Vegas; Dallas-Fort Worth; El Centro, CA; San Jose-San Francisco; Philadelphia; and Chico, CA.

Nine others improved, though not reaching their lowest level: Fresno-Madera, CA; Phoenix; Denver-Aurora, CO; El Centro, CA; Fort Collins, CO; El Paso-Las Cruces, TX-NM; San Antonio; Hartford, CT; Sheboygan, WI. One city—Redding-Red Bluff, CA—had the same number of unhealthy ozone days on average in this year's report.

Four cities suffered more high-ozone days on average than in last year's report: San Diego; Houston; Salt Lake City; and Baton Rouge, LA.

These comparisons are all based on the Air Quality Index adopted with the 2015 ozone standard. Although EPA has yet to designate any places for cleanup based on that standard, it remains the current official national ambient air quality standard.

Regional differences. Cities in the West and Southwest continue to dominate the most ozone-polluted list. California retains its historic challenge with seven of the 10 most polluted metropolitan areas in that state and 11 of the worst 25. California's weather and geography complicate the strong effort the state continues to make to reduce emissions. The Southwest continues to fill most of the remaining slots, with nine of the 25 most ozone-polluted cities. Texas has four cities in the 25 most-polluted list: Houston, Dallas-Fort Worth, El Paso and San Antonio. Colorado has two: Denver and Fort Collins. Arizona, Nevada and Utah each have one. The Northeast also has three metro areas on the list, two of which cover parts of multiple states: New York City, Philadelphia, and Hanford, CT. The Midwest has only Sheboygan, WI. in the 25 most-polluted list. The only southern city to remain on the list is Baton Rouge, LA.

Those changes reflect changes seen in the past two reports, where increased oil and gas extraction especially in the Southwest and cleanup of power plants in the eastern U.S. have shifted the cities that experienced the greatest number of unhealthy air days.

Twelve cities improved to their lowest levels of year-round particle pollution.

Year-round Particles

Fifteen of the 25 cities with the highest year-round particle pollution reduced their levels, including 12 that reached or matched their lowest levels ever in 2013-2015. The 10 most polluted remain the only metropolitan areas in the nation that fail to meet the official national limits on annual fine particle pollution.

Eight of the 25 cities suffered higher annual particle pollution levels, including Visalia-Porterfield-Hanford, CA, the city that ranked as the most polluted for year-round levels. In addition to Visalia, three other California cities—Bakersfield; San Jose-San Francisco; and San Luis Obispo—and two other cities in the western states—Medford-Grants Pass, OR, and Fairbanks, AK—had worse year-round levels. The two remaining cities with higher year-round average levels were in the east: Johnstown-Somerset, PA and New York City metro area. San Luis Obispo reached its worst level ever.

Two cities in the list of the 25 most-polluted maintained the same level as in the 2016 report: Cleveland and Houston.

Regional differences. Much of the eastern and middle parts of the country have improved significantly since the report first started to track these fine particles. Much of that improvement came from reducing emissions from coal-fired power plants, as well as benefiting from nationwide cleanup of diesel engines. However, the western states' burden of so much wildfire smoke and high inversions seems to have moved from just being a short-term problem to adding to the burden year-round. Cities in California's San Joaquin valley were hit hard, as were other locations where particle pollution is usually limited to short spikes, including Fairbanks, AK, and Medford-Grants Pass, OR.

Data remain missing in all of Illinois, most of Tennessee and parts of Maine. That means that millions of people, including in large cities Chicago, Memphis and St. Louis (which is missing suburban counties in Illinois), cannot know how much particulate matter they are breathing.

Eight cities suffered their highest number of spikes in particle pollution since the reporting began.

Short-Term Particle Pollution

Bakersfield, CA retains its ranking as the most polluted city for spikes in particle pollution in this report, as it had in the 2016 report and in four other reports since 2010. Unfortunately, Bakersfield suffered more unhealthy days on average in this year's report.

Fifteen of the 25 most-polluted cities had more days with higher episodes of particle pollution, including eight that suffered their most days since the report started and one that maintained its worst report ever.

Cities recording their worst short-term particle episodes in 2013-2015 concentrated in the western states: Visalia-Porterfield-Hanford, CA; Fairbanks, AK; San Jose-San Francisco; Reno, NV; El Centro, CA; Lancaster, PN; Anchorage, AK; and Bend-Redmond-Prineville, OR, marking that city's first time on this list.

Seven other western cities recorded more unhealthy days than in the previous report: Bakersfield, CA; Salt Lake City, UT; Logan, UT-ID; Los Angeles; Sacramento, CA; Seattle-Tacoma, WA; and Medford-Grants Pass, OR.

Fortunately, **eight cities improved with fewer days of spikes in particle levels** in 2013-2015 than in 2012-2014. Six of these are western cities: Fresno-Madera, CA; Modesto-Merced, CA; Missoula, MT; Yakima, WA; Eugene, OR; and Phoenix, AZ. Two cities in Pennsylvania also improved: Harrisburg-York-Lebanon; and notably, Pittsburgh. Pittsburgh, which had been ranked the most polluted city in the same category in the 2008 report, experienced its fewest unhealthy days ever in 2013-2015.

Philadelphia and South Bend, IN recorded the same number of days in this year's report as in last year's report. However, as noted above, that kept South Bend stuck at its worst average number of unhealthy particle pollution days.

Regional differences. Locations with many days of spikes shows the burden of **concentrated smoke from wildfires, brushfires and wood-burning devices**. For example, Reno, NV, suffered wildfires, and Logan, UT-ID; Eugene, OR, and Fairbanks and Anchorage, AK, rely heavily on wood burning devices for heat. Wildfires have increased, in part, from drought and heat enhanced by climate change. Inversions trap particles in place behind mountains and ridgelines. For example, inversions in the San Joaquin Valley in California and in the Wasatch Ridge in Utah contributed to high pollution days in both states.

Cleanest Cities

Six cities ranked on all three cleanest cities lists in 2013-2015. These cities had zero high ozone or high particle pollution days, and were among the 25 cities with the lowest year-round particle levels. Five have repeated their ranking on this list, but Wilmington, NC, joins this list for the first time. Listed alphabetically below, these six cities are:

- Burlington-South Burlington, VT
- Cape Coral-Fort Myers-Naples, FL
- Elmira-Corning, NY
- Honolulu, HI
- Palm Bay-Melbourne-Titusville, FL
- Wilmington, NC

Eleven other cities ranked among the cleanest cities for both year-round and short-term levels of particle pollution. That means they had no days in the unhealthy level for short-term particle pollution and were on the list of the cleanest cities for year-round particle pollution. They are:

- Bangor, ME
- Casper, WY
- Colorado Springs, CO
- Farmington, NM
- Homosassa Springs, FL
- Lakeland Winter Haven, FL
- North Port Sarasota, FL
- Orlando-Deltona-Daytona Beach, FL
- Pueblo-Canon City, CO
- Sierra Vista-Douglas, AZ
- Syracuse-Auburn, NY

Twenty-three other cities ranked among the cleanest for ozone and short-term particle pollution. That means they had no days in the unhealthy level for ozone or short-term particle pollution. They are:

- Bellingham, WA
- Brunswick, GA
- Charlottesville, VA
- Columbia-Orangeburg-Newberry, SC
- Des Moines-Ames-West Des Moines, IA
- Dothan-Enterprise-Ozark, AL
- Eau Claire-Menomonie, WI
- Fayetteville-Springdale-Rogers, AK-MO
- Florence, SC
- Florence-Muscle Shoals, AL
- Gadsden, AL
- Gainesville-Lake City, FL
- Greenville-Washington, NC
- Harrisonburg-Staunton-Waynesboro, VA
- Jackson-Vicksburg-Brookhaven, MS
- La Crosse-Onalaska, WI-MN
- McAllen-Edinburg, TX
- Monroe-Ruston-Bastrop, LA
- Rome-Summerville, GA
- Savannah-Hinesville-Statesboro, GA
- Springfield-Branson, MO
- Tuscaloosa, AL
- Waterloo-Cedar Falls, IA

Two cities ranked on both lists for ozone and year-round particle pollution levels. Fargo-Wahpeton, ND-MN and Salinas, CA had no days in the unhealthy level for ozone pollution and were on the list of the cleanest cities for year-round particle pollution.

People at Risk

Looking at the nation as a whole, the **"State of the Air 2017" shows that, even with ongoing improvement, too many people in the United States live where the air is unhealthy for them to breathe.**

Nearly four in 10 people (38.9 percent) in the United States live in counties that have unhealthful levels of either ozone or particle pollution. More than 125 million Americans live in 204 counties where they breathe unhealthful levels of air pollution in the form of either ozone or short-term or year-round levels of particles.

This represents a major improvement: One-quarter fewer people now live where the air quality hit unhealthy levels in 2013-2015 than in the 2016 report. In last year's report, covering 2012-2014, more than 166 million Americans lived in counties with unhealthful levels of air pollution.

This improvement reflects continued progress in reducing harmful air pollution under the Clean Air Act. Progress would have been greater if climate change had not helped to create conditions that can worsen air quality.

More than one-third (36 percent) of the people in the United States live in areas with unhealthy levels of ozone pollution, but that is far fewer in 2013-2015 than in the previous report. Approximately 116.5 million people live in 161 counties that earned an F for ozone this year's report, a significant drop from the approximately 162.9 million who lived in counties earning an F in 2012-2014.

More than 18 million people in the U.S. live in counties where the outdoor air failed all three tests.

Nearly 19.9 million people (6.2 percent) suffered from unhealthy year-round levels of particle pollution in 2013-2015. These people lived in 18 counties where the annual average concentration of particle pollution was too high. Although still too high, fewer people face those dangerous year-round concentrations during this period than in last year's report. That report covered 2012-2014 when approximately 22.8 million people lived where monitors recorded unhealthy levels of year-round particle pollution.

More than 13 percent of people in the United States—more than 43 million—live in an area with too many days with unhealthful levels of particle pollution. Slightly fewer people lived where those episodes of unhealthy spikes in particle pollution in 2013-2015, despite many cities reaching their worst number of spikes since the report began. The total population exposed to unhealthy air dropped slightly to 43.03 million, down from 44.97 million in the 2016 report. Some counties with large populations had fewer high days, so they no longer received an F, while smaller population counties had more high pollution days. Those shifts resulted in slight changes to the population totals.

More than 18 million people (5.6 percent) live in 12 counties with unhealthful levels of all three: ozone and short-term and year-round particle pollution. This is nearly 1.9 million fewer people than in the 2016 report when approximately 6.3 percent were exposed. However, data on particle pollution remains missing in all or parts of three states.

With the risks from airborne pollution so great, the Lung Association seeks to inform people who may be in danger. Many people are at greater risk because of their age or because they have asthma or other chronic lung disease, cardiovascular disease or diabetes. The following list identifies the numbers of people in each at-risk group. Because of the missing data on particle pollution in Illinois, Tennessee and Maine, the numbers of people living in counties that fail all three tests may be actually higher.

Older and Younger—Nearly 16.7 million adults age 65 and over and more than 29.5 million children under 18 years old live in counties that received an F for at least one pollutant. More than 2.3 million seniors and more than 4.3 million children live in counties failing all three tests.

People with Asthma—Nearly 2.5 million children and nearly 8.3 million adults with asthma live in counties of the United States that received an F for at least one pollutant. Nearly 322,000 children and close to 1.1 million adults with asthma live in counties failing all three tests.

Chronic Obstructive Pulmonary Disease (COPD)—More than 5.1 million people with COPD live in counties that received an F for at least one pollutant. More than 575,000 people with COPD live in counties failing all three tests.

Lung Cancer—More than 68,000 people with lung cancer live in counties that received an F for at least one pollutant. More than 8,000 people with lung cancer live in counties failing all three tests.

Cardiovascular Disease—More than 7.1 million people with cardiovascular diseases live in counties that received an F for at least one pollutant; more than 88,000 people live in counties failing all three tests.

Diabetes—Nearly 3.3 million people with diabetes live in counties that received an F for either short-term or year-round particle pollution; more than 1.3 million live in counties failing both tests. Having diabetes increases the risk of harm from particle pollution.

Poverty—More than 17.7 million people with incomes meeting the federal poverty definition live in counties that received an F for at least one pollutant. Nearly 3.2 million people in poverty live in counties failing all three tests. Evidence shows that people who have low incomes may face higher risk from air pollution.

What Needs to Be Done

Our nation has made significant strides in cleaning up our air, as the progress in the 18 years of this report has shown. Stopping or retreating cannot be an option. Our nation's historic, legal commitment to protect the health of millions of Americans requires more work to reduce the burden of air pollution. Cleaning up air pollution requires a strong and coordinated effort on the part of our federal and state leaders. The President, the EPA administrator, members of Congress, governors and state leaders all have a key role to play. These leaders must support steps to improve the air we breathe so that it does not cause or worsen lung disease. The American Lung Association urges our nation's leaders to stand up for public health and take these important steps to improve the air we all breathe.

Protect the Clean Air Act

Congress must make certain that the Clean Air Act remains strong, fully implemented and enforced.

Our nation's continued air quality improvement shown in the "State of the Air 2017" report is possible only because of the Clean Air Act, a strong public health law put in place by an overwhelming bipartisan majority in Congress more than 45 years ago. Congress wrote the Clean Air Act to set up science-based, technology-fostering steps to protect public health by reducing pollution. Under the Clean Air Act, Congress directed that the EPA and each state take steps to clean up the air. As the "State of the Air 2017" report documents, those steps have reduced ozone and particle pollution in much of the nation.

Unfortunately, some in Congress seek changes to the Clean Air Act that would dismantle key provisions of the law and threaten progress made over nearly five decades. To protect the lives and health of millions of Americans, Congress must protect the Clean Air Act—making certain it remains strong, fully implemented and enforced.

Fight Climate Change by Reducing Carbon Pollution from Power Plants

Power plants comprise the largest stationary source of carbon pollution in the United States. The electric sector contributed 30 percent of all energy-related carbon dioxide (CO_2) emissions in 2014.[2] Scientists tell us that carbon pollution contributes to a warming climate, enhancing conditions for ozone formation and making it harder to reduce this lethal pollutant. Climate change also leads to particle pollution from increased droughts and wildfires. Taking steps to reduce carbon pollution from electricity generation will also reduce ozone and particle pollution from these plants at the same time. EPA's analysis shows that these co-benefits can prevent up to 3,600 premature deaths and up to 90,000 asthma attacks in children in 2030. The American Lung Association calls on governors to direct their states to develop strong plans to reduce carbon pollution from power plants and protect public health.

In 2015, EPA adopted the Clean Power Plan, a flexible, practical tool kit for the states to reduce carbon pollution from power plants approximately 32 percent (below 2005 levels) by 2030. States can choose a variety of ways to cut carbon pollution with the Clean Power Plan. They can choose to require cleaner fuels for existing utilities, improve energy efficiency, produce more clean energy and partner with other states to jointly reduce carbon pollution. In February 2015, the Supreme Court issued a stay on the plan, putting EPA's enforcement of the plan on a temporary hold while the courts hear the case.

Even before the lower court released its decision on the Clean Power Plan, President Trump issued an Executive Order directing EPA Administrator Scott Pruitt to roll back the plan. However, the Lung Association and others will continue to fight to secure reductions in carbon dioxide emissions from power plants and other sources.

Retain the Clean Vehicle Emissions Standards.

Transportation produces more than one quarter of the nation's greenhouse gases that worsen climate change.[3] In 2012, EPA and the National Highway Traffic Safety Administration announced new standards for reducing greenhouse gas emissions from cars, SUVs and light-duty trucks in model years 2017-2025. The emissions standards would reduce 2 billion metric tons of carbon dioxide emissions over the lifetime of the vehicles and would improve fuel efficiency. EPA committed to doing an interim review after the initial phase was in place to see if the longer-term standards for 2012-2025 should still be in place. In January 2017, EPA announced that it had completed its mid-term review and that these emissions standards were appropriate and achievable by the automobile industry for model years 2022-2025. However, in March 2017, EPA Administrator Scott Pruitt and Transportation Secretary Elaine Chao announced the reconsideration of the final determination and reopened EPA's review.

The Lung Association opposed the decision to reopen the review, as EPA had taken an extensive, in-depth examination with public comments before reaching their conclusion. Based on the evidence EPA found before, the Lung Association expects EPA to conclude, again, that the targets should remain in place.

Reduce Emissions from Existing and New Oil and Gas Operations

Oil and gas production wells, processing plants, transmission pipelines and storage units have long emitted harmful gases including methane, volatile organic compounds and other pollutants. As noted earlier, this report found high levels of unhealthy ozone in places where oil and gas production has expanded in the last few years. In May 2016, EPA adopted health-protective standards to reduce harmful emissions of these gases from new and modified sources within the oil and natural gas industry.

However, that action did not affect emissions from the existing oil and gas infrastructure. In November 2016, EPA requested essential information from the oil and gas industry about the location and size of their facilities. Gathering this information is a required step for EPA to eventually limit harmful emissions from these existing sources. The industry objected and, unfortunately, in March 2017, the EPA withdrew its request to the updated information on their facilities, with the explanation that the administrator needed to review the request. The Lung Association calls on the administrator to move forward and set strong pollution control standards for existing oil and gas operations.

These standards would not only help to mitigate climate change and its associated health risks by curtailing emissions of methane—an especially potent greenhouse gas—but would also limit emissions of major precursors to ozone, as well as other toxic and carcinogenic air pollutants, benefiting public health in communities across the country.

Improve the Air Pollution Monitoring Network

The grades in this report come from information from the nationwide air pollution-monitoring network. That network forms the infrastructure for healthy air. States and local governments use monitors to accurately measure the amount of air pollution in the community.

Less than one-third of all counties have ozone or particle pollution monitors, seriously limiting the ability to adequately detect and track the levels of harmful air pollution. Unfortunately, funds for existing air pollution monitors have been cut across the nation. More monitoring is needed near roadways to measure the highest levels of exposures from air pollution related to traffic. Communities that have expanded oil and gas extraction operations need more monitoring.

The President has proposed to cut EPA's budget by 31 percent, including dramatic cuts for state air pollution grants that fund monitoring. With such challenges to our monitoring infrastructure, it may be harder for the nation to ensure accurate, reliable quality data in the future.

What You Can Do

You can do a great deal to help reduce air pollution outdoors. Here's how to speak up and step up:

Speak up for Healthy Air Protections.

Send a message to Congress and to the White House: Protect the Clean Air Act! Urge the President and Congress to support cleaner, healthier air and oppose measures to block or delay the cleanup of air pollution. The President and all members of Congress should support and protect the Clean Air Act.

Tell Congress to support adequate funds for the EPA to implement and enforce the Clean Air Act. EPA works with the states to make sure that the pollution is cleaned up, but they need the resources to do that work.

Tell EPA to follow the law to protect your health. EPA is required to follow the Clean Air Act, completing regular reviews of the science and putting in place steps to clean up sources of pollution to provide that protection. That includes taking steps to reduce pollution that causes climate change. You can provide comments to EPA at public hearings or in writing online. Sign up for more information about times when your voice is needed at www.FightingForAir.org.

Share your story. Do you or any member of your family have a personal reason to fight for healthier, cleaner air? Go to www.FightingForAir.org to let us know how healthy air affects you. Your story helps us remind decision makers what is at stake when it comes to clean air.

Get involved locally. Participate in state and local efforts to clean up air pollution and address climate change. To find your local air pollution control agency, go to www.4cleanair.org.

Step up to Curb Pollution in Your Community.

Drive less. Combine trips, walk, bike, carpool or vanpool, and use buses, subways or other alternatives to driving. Vehicle emissions are a major source of air pollution. Support community plans that provide ways to get around that don't require a car, such as more sidewalks, bike trails and transit systems.

Use less electricity. Turn out the lights and use energy-efficient appliances. Generating electricity is one of the biggest sources of pollution, particularly in the eastern United States.

Don't burn wood or trash. Burning firewood and trash is among the largest sources of particle pollution in many parts of the country. If you must use a fireplace or stove for heat, convert your woodstove to natural gas, which has far fewer polluting emissions. Compost and recycle as much as possible and dispose of other waste properly; don't burn it. Support efforts in your community to ban outdoor burning of construction and yard wastes. Avoid the use of outdoor hydronic heaters, also called outdoor wood boilers, which are frequently much more polluting than woodstoves.

Make sure your local school system requires clean school buses, which includes replacing or retrofitting old school buses with filters and other equipment to reduce emissions. Make sure your local schools don't idle their buses, a step that can immediately reduce emissions.

1 A complete discussion of the sources of data and the methodology is included in Methodology.

2 U.S. Environmental Protection Agency. *Inventory of Greenhouse Gas Emissions and Sinks: 1990-2014.* Washington, DC: U.S. EPA, 2016. EPA 430-R-16-002.

3 EPA, 2016.

RANKINGS

People at Risk from Short-Term Particle Pollution (24-Hour $PM_{2.5}$)

	Chronic Diseases							Age Groups			
In Counties where the Grades were:	Adult Asthma	Pediatric Asthma	COPD	Lung Cancer	CV Disease	Diabetes	Poverty	Under 18	65 and Over	Total Population	Number of Counties
Grade A (0.0)	5,992,655	1,802,928	4,289,711	53,062	5,519,300	6,813,373	12,296,314	19,154,928	12,637,796	85,841,453	288
Grade B (0.3-0.9)	2,487,361	710,302	1,707,641	22,079	2,257,763	2,798,334	5,296,773	8,482,854	5,136,291	36,961,630	111
Grade C (1.0-2.0)	1,497,678	418,793	1,017,268	13,031	1,354,796	1,698,140	3,133,628	5,062,225	3,014,053	21,607,181	54
Grade D (2.1-3.2)	1,034,136	260,265	627,358	8,067	847,006	1,130,589	2,203,289	3,452,500	2,064,381	15,344,010	23
Grade F (3.3+)	2,758,254	821,980	1,571,574	20,540	2,256,027	3,140,522	6,585,074	10,434,818	5,634,316	43,036,931	69
National Population in Counties with $PM_{2.5}$ Monitors	15,156,120	4,405,144	10,236,303	129,977	13,557,088	17,166,636	32,430,455	51,249,670	31,374,325	223,082,364	636

People at Risk from Year-Round Particle Pollution (Annual $PM_{2.5}$)

	Chronic Diseases							Age Groups			
In Counties where the Grades were:	Adult Asthma	Pediatric Asthma	COPD	Lung Cancer	CV Disease	Diabetes	Poverty	Under 18	65 and Over	Total Population	Number of Counties
Pass	11,727,392	3,421,296	7,938,618	100,393	10,429,084	13,115,687	24,212,629	38,997,449	23,983,876	170,682,208	468
Fail	1,215,259	349,400	673,296	9,220	1,011,474	1,495,671	3,455,844	4,738,182	2,612,834	19,870,106	18
National Population in Counties with $PM_{2.5}$ Monitors	15,156,120	4,405,144	10,236,303	129,977	13,557,088	17,166,636	32,430,455	51,249,670	31,374,325	223,082,364	636

People at Risk from Ozone

	Chronic Diseases					Age Groups			
In Counties where the Grades were:	Adult Asthma	Pediatric Asthma	COPD	CV Disease	Poverty	Under 18	65 and Over	Total Population	Number of Counties
Grade A (0.0)	2,135,734	592,588	1,591,631	2,084,164	4,515,103	7,034,893	4,934,132	31,578,049	218
Grade B (0.3-0.9)	1,866,933	547,662	1,429,515	1,831,132	4,001,141	6,187,522	4,137,336	27,423,560	159
Grade C (1.0-2.0)	2,625,700	740,239	1,949,579	2,496,364	4,762,756	8,192,247	5,655,800	36,787,108	167
Grade D (2.1-3.2)	1,752,575	487,238	1,199,321	1,527,279	3,307,983	5,233,129	3,456,203	23,537,106	62
Grade F (3.3+)	7,629,719	2,304,667	4,743,298	6,576,087	16,529,442	27,566,927	15,417,092	116,502,119	161
National Population in Counties with Ozone Monitors	16,218,750	4,732,885	11,069,317	14,726,495	33,546,429	54,859,943	34,098,150	238,804,343	803

Note: *The State of the Air 2017* covers the period 2013-2015. The Appendix provides a full discussion of the methodology.

RANKINGS

People at Risk In 25 U.S. Cities Most Polluted by Short-Term Particle Pollution (24-hour $PM_{2.5}$)

2017 Rank[1]	Metropolitan Statistical Areas	Total Population[2]	Under 18[3]	65 and Over[3]	Pediatric Asthma[4,6]	Adult Asthma[5,6]	COPD[7]	Lung Cancer[8]	CV Disease[9]	Diabetes[10]	Poverty[11]
1	Bakersfield, CA	882,176	257,727	88,992	18,417	47,777	23,732	384	36,297	57,322	185,990
2	Visalia-Porterville-Hanford, CA	610,828	185,471	63,293	13,253	32,579	16,291	266	24,985	39,208	154,039
2	Fresno-Madera, CA	1,129,859	322,159	132,448	23,021	62,047	31,883	490	49,778	77,435	274,927
4	Modesto-Merced, CA	806,843	226,215	95,841	16,165	44,619	23,071	350	36,214	56,432	171,672
5	Fairbanks, AK	99,631	24,116	8,349	2,045	7,139	2,756	56	3,943	4,891	7,671
6	San Jose-San Francisco-Oakland, CA	8,713,914	1,877,655	1,214,016	134,173	526,751	280,172	3,779	448,510	696,765	933,311
7	Salt Lake City-Provo-Orem, UT	2,467,709	757,422	231,853	53,789	154,727	60,714	653	90,218	115,839	255,652
8	Logan, UT-ID	133,857	41,508	12,489	3,008	8,322	3,200	38	4,693	5,854	19,910
9	Los Angeles-Long Beach, CA	18,679,763	4,383,662	2,376,130	313,246	1,099,027	571,985	8,096	902,929	1,409,515	2,928,894
10	Reno-Carson City-Fernley, NV	605,706	131,049	102,549	7,661	38,311	33,137	356	39,626	49,111	81,422
11	El Centro, CA	180,191	51,119	22,442	3,653	9,934	5,187	78	8,178	12,647	41,685
12	Lancaster, PA	536,624	128,793	89,727	14,397	41,751	28,456	353	38,439	42,053	55,725
13	Missoula, MT	114,181	22,154	16,172	1,404	8,203	4,628	66	5,905	6,350	17,461
14	Sacramento-Roseville, CA	2,544,026	593,452	374,195	42,407	150,701	81,902	1,102	132,685	204,433	379,600
14	Anchorage, AK	399,790	101,387	38,009	8,596	27,941	11,714	223	17,279	21,498	34,981
16	Yakima, WA	248,830	74,063	32,662	4,838	16,416	10,504	138	13,029	14,296	46,794
17	Pittsburgh-New Castle-Weirton, PA-OH-WV	2,648,605	509,215	497,830	56,223	218,112	158,026	1,748	213,287	232,472	327,752
17	Seattle-Tacoma, WA	4,602,591	1,000,111	626,375	65,324	339,697	216,668	2,557	263,773	293,479	482,638
19	Medford-Grants Pass, OR	297,312	60,886	65,587	5,714	26,407	14,726	167	21,709	28,402	58,695
20	Philadelphia-Reading-Camden, PA-NJ-DE-MD	7,183,479	1,592,239	1,085,893	162,777	525,438	349,693	4,605	470,916	542,896	916,171
21	South Bend-Elkhart-Mishawaka, IN-MI	725,065	178,459	113,087	13,523	56,107	43,911	511	54,707	62,712	109,079
21	Harrisburg-York-Lebanon, PA	1,247,235	272,926	209,814	30,509	99,682	68,539	820	92,638	101,485	126,887
23	Eugene, OR	362,895	68,799	64,973	6,456	33,296	16,555	204	23,240	31,518	67,777
24	Phoenix-Mesa-Scottsdale, AZ	4,574,531	1,127,596	670,488	122,981	324,484	214,829	2,233	264,628	340,926	727,788
25	Bend-Redmond-Prineville, OR	196,898	41,110	38,464	3,858	17,521	9,377	111	13,392	17,982	26,721

Notes:

1. Cities are ranked using the highest weighted average for any county within that Combined Metropolitan Statistical Area or Metropolitan Statistical Area.
2. **Total Population** represents the at-risk populations for all counties within the respective Combined Metropolitan Statistical Area or Metropolitan Statistical Area.
3. Those **under 18** and **65 and over** are vulnerable to $PM_{2.5}$ and are, therefore, included. They should not be used as population denominators for disease estimates.
4. **Pediatric asthma** estimates are for those under 18 years of age and represent the **estimated** number of people who had asthma in 2015 based on state rates (BRFSS) applied to population estimates (U.S. Census).
5. **Adult asthma** estimates are for those 18 years and older and represent the **estimated** number of people who had asthma in 2015 based on state rates (BRFSS) applied to population estimates (U.S. Census).
6. Adding across rows does not produce valid estimates. Adding the disease categories (asthma, COPD, etc.) will double-count people who have been diagnosed with more than one disease.
7. **COPD** estimates are for adults 18 and over who have been diagnosed within their lifetime, based on state rates (BRFSS) applied to population estimates (U.S. Census).
8. **Lung cancer** estimates are the number of new cases diagnosed in 2013 .
9. **CV disease** is cardiovascular disease and estimates are for adults 18 and over who have been diagnosed within their lifetime, based on state rates (BRFSS) applied to population estimates (U.S. Census).
10. **Diabetes** estimates are for adults 18 and over who have been diagnosed within their lifetime, based on state rates (BRFSS) applied to population estimates (U.S. Census).
11. **Poverty** estimates come from the U.S. Census Bureau and are for all ages.

RANKINGS

People at Risk In 25 U.S. Cities Most Polluted by Year-Round Particle Pollution (Annual $PM_{2.5}$)

2017 Rank[1]	Metropolitan Statistical Areas	Total Population[2]	Under 18[3]	65 and Over[3]	Pediatric Asthma[4,6]	Adult Asthma[5,6]	COPD[7]	Lung Cancer[8]	CV Disease[9]	Diabetes[10]	Poverty[11]
1	Visalia-Porterville-Hanford, CA	610,828	185,471	63,293	13,253	32,579	16,291	266	24,985	39,208	154,039
2	Bakersfield, CA	882,176	257,727	88,992	18,417	47,777	23,732	384	36,297	57,322	185,990
3	Fresno-Madera, CA	1,129,859	322,159	132,448	23,021	62,047	31,883	490	49,778	77,435	274,927
4	San Jose-San Francisco-Oakland, CA	8,713,914	1,877,655	1,214,016	134,173	526,751	280,172	3,779	448,510	696,765	933,311
5	Los Angeles-Long Beach, CA	18,679,763	4,383,662	2,376,130	313,246	1,099,027	571,985	8,096	902,929	1,409,515	2,928,894
6	Modesto-Merced, CA	806,843	226,215	95,841	16,165	44,619	23,071	350	36,214	56,432	171,672
7	El Centro, CA	180,191	51,119	22,442	3,653	9,934	5,187	78	8,178	12,647	41,685
8	Pittsburgh-New Castle-Weirton, PA-OH-WV	2,648,605	509,215	497,830	56,223	218,112	158,026	1,748	213,287	232,472	327,752
9	Cleveland-Akron-Canton, OH	3,493,596	756,784	597,001	54,482	274,623	222,765	2,401	263,764	312,145	497,987
10	San Luis Obispo-Paso Robles-Arroyo Grande, CA	281,401	50,837	51,231	3,633	17,910	10,097	122	16,633	25,113	38,448
11	Medford-Grants Pass, OR	297,312	60,886	65,587	5,714	26,407	14,726	167	21,709	28,402	58,695
11	Philadelphia-Reading-Camden, PA-NJ-DE-MD	7,183,479	1,592,239	1,085,893	162,777	525,438	349,693	4,605	470,916	542,896	916,171
13	Indianapolis-Carmel-Muncie, IN	2,372,530	583,997	313,675	43,916	184,825	139,575	1,738	171,702	200,542	329,297
13	Louisville/Jefferson County—Elizabethtown—Madison, KY-IN	1,504,559	346,616	219,919	35,200	133,941	130,160	1,365	133,904	150,903	200,814
13	Johnstown-Somerset, PA	211,933	40,095	44,363	4,482	17,358	12,999	140	18,031	19,502	29,615
16	Houston-The Woodlands, TX	6,855,069	1,829,561	703,418	144,776	382,312	248,754	3,705	381,501	552,311	988,741
17	Fairbanks, AK	99,631	24,116	8,349	2,045	7,139	2,756	56	3,943	4,891	7,671
18	Detroit-Warren-Ann Arbor, MI	5,319,913	1,196,787	801,027	92,712	424,024	314,167	3,379	372,872	436,925	847,421
18	Altoona, PA	125,593	25,939	24,852	2,900	10,102	7,381	82	10,174	11,031	18,616
20	Lancaster, PA	536,624	128,793	89,727	14,397	41,751	28,456	353	38,439	42,053	55,725
20	Cincinnati-Wilmington-Maysville, OH-KY-IN	2,216,735	531,163	311,427	42,406	176,287	145,299	1,650	160,014	188,672	287,495
22	Birmingham-Hoover-Talladega, AL	1,360,082	312,528	209,403	41,245	103,803	110,714	933	116,412	141,142	222,890
22	Harrisburg-York-Lebanon, PA	1,247,235	272,926	209,814	30,509	99,682	68,539	820	92,638	101,485	126,887
22	New York-Newark, NY-NJ-CT-PA	23,723,696	5,178,719	3,461,559	505,108	1,708,629	1,001,947	14,302	1,340,765	1,727,386	3,178,139
25	Erie-Meadville, PA	364,529	78,960	61,087	8,827	29,248	19,931	240	26,881	29,464	57,949

Notes:

1. Cities are ranked using the highest weighted average for any county within that Combined Metropolitan Statistical Area or Metropolitan Statistical Area.
2. **Total Population** represents the at-risk populations for all counties within the respective Combined Metropolitan Statistical Area or Metropolitan Statistical Area.
3. Those **under 18** and **65 and over** are vulnerable to PM2.5 and are, therefore, included. They should not be used as population denominators for disease estimates.
4. **Pediatric asthma** estimates are for those under 18 years of age and represent the **estimated** number of people who had asthma in 2015 based on state rates (BRFSS) applied to population estimates (U.S. Census).
5. **Adult asthma** estimates are for those 18 years and older and represent the **estimated** number of people who had asthma in 2015 based on state rates (BRFSS) applied to population estimates (U.S. Census).
6. Adding across rows does not produce valid estimates. Adding the disease categories (asthma, COPD, etc.) will double-count people who have been diagnosed with more than one disease.
7. **COPD** estimates are for adults 18 and over who have been diagnosed within their lifetime, based on state rates (BRFSS) applied to population estimates (U.S. Census).
8. **Lung cancer** estimates are the number of new cases diagnosed in 2013 .
8. **CV disease** is cardiovascular disease and estimates are for adults 18 and over who have been diagnosed within their lifetime, based on state rates (BRFSS) applied to population estimates (U.S. Census).
9. **Diabetes** estimates are for adults 18 and over who have been diagnosed within their lifetime, based on state rates (BRFSS) applied to population estimates (U.S. Census).
10. **Poverty** estimates come from the U.S. Census Bureau and are for all ages.

RANKINGS

People at Risk In 25 Most Ozone-Polluted Cities

2017 Rank[1]	Metropolitan Statistical Areas	Total Population[2]	Under 18[3]	65 and Over[3]	Pediatric Asthma [4,6]	Adult Asthma[5,6]	COPD[7]	CV Disease[8]	Poverty[9]
1	Los Angeles-Long Beach, CA	18,679,763	4,383,662	2,376,130	313,246	1,099,027	571,985	8,096	1,409,515
2	Bakersfield, CA	882,176	257,727	88,992	18,417	47,777	23,732	384	57,322
3	Fresno-Madera, CA	1,129,859	322,159	132,448	23,021	62,047	31,883	490	77,435
4	Visalia-Porterville-Hanford, CA	610,828	185,471	63,293	13,253	32,579	16,291	266	39,208
5	Phoenix-Mesa-Scottsdale, AZ	4,574,531	1,127,596	670,488	122,981	324,484	214,829	2,233	340,926
6	Modesto-Merced, CA	806,843	226,215	95,841	16,165	44,619	23,071	350	56,432
7	San Diego-Carlsbad, CA	3,299,521	728,037	431,999	52,024	197,708	102,514	1,433	250,288
8	Sacramento-Roseville, CA	2,544,026	593,452	374,195	42,407	150,701	81,902	1,102	204,433
9	New York-Newark, NY-NJ-CT-PA	23,723,696	5,178,719	3,461,559	505,108	1,708,629	1,001,947	14,302	1,727,386
10	Las Vegas-Henderson, NV-AZ	2,362,015	543,472	358,944	33,670	149,068	120,361	1,367	179,273
11	Denver-Aurora, CO	3,418,876	802,008	408,996	68,001	237,472	108,795	1,453	169,116
12	Houston-The Woodlands, TX	6,855,069	1,829,561	703,418	144,776	382,312	248,754	3,705	552,311
13	Dallas-Fort Worth, TX-OK	7,538,055	1,990,630	826,555	157,759	422,482	282,033	4,071	625,563
14	El Centro, CA	180,191	51,119	22,442	3,653	9,934	5,187	78	12,647
15	Fort Collins, CO	333,577	67,793	47,570	5,748	24,144	11,356	142	17,585
16	El Paso-Las Cruces, TX-NM	1,053,267	288,219	129,282	23,423	61,859	39,643	538	84,514
17	Redding-Red Bluff, CA	242,841	53,749	47,109	3,841	14,771	8,761	105	22,350
18	San Jose-San Francisco-Oakland, CA	8,713,914	1,877,655	1,214,016	134,173	526,751	280,172	3,779	696,765
19	San Antonio-New Braunfels, TX	2,384,075	612,614	296,086	48,477	134,762	91,254	1,286	202,041
20	Salt Lake City-Provo-Orem, UT	2,467,709	757,422	231,853	53,789	154,727	60,714	653	115,839
21	Hartford-West Hartford, CT	1,483,187	305,454	239,202	35,791	123,794	60,395	936	109,140
22	Baton Rouge, LA	830,480	197,739	105,468	17,303	51,764	45,903	579	76,252
22	Philadelphia-Reading-Camden, PA-NJ-DE-MD	7,183,479	1,592,239	1,085,893	162,777	525,438	349,693	4,605	542,896
24	Sheboygan, WI	115,569	26,084	19,254	1,917	8,460	4,412	69	7,810
25	Chico, CA	225,411	45,348	39,543	3,240	13,978	7,812	98	19,274

Notes:

1. Cities are ranked using the highest weighted average for any county within that Combined Metropolitan Statistical Area or Metropolitan Statistical Area.
2. **Total Population** represents the at-risk populations for all counties within the respective Combined Metropolitan Statistical Area or Metropolitan Statistical Area.
3. Those **under 18** and **65 and over** are vulnerable to $PM_{2.5}$ and are, therefore, included. They should not be used as population denominators for disease estimates.
4. **Pediatric asthma** estimates are for those under 18 years of age and represent the **estimated** number of people who had asthma in 2015 based on state rates (BRFSS) applied to population estimates (U.S. Census).
5. **Adult asthma** estimates are for those 18 years and older and represent the **estimated** number of people who had asthma in 2015 based on state rates (BRFSS) applied to population estimates (U.S. Census).
6. Adding across rows does not produce valid estimates. Adding the disease categories (asthma, COPD, etc.) will double-count people who have been diagnosed with more than one disease.
7. **COPD** estimates are for adults 18 and over who have been diagnosed within their lifetime, based on state rates (BRFSS) applied to population estimates (U.S. Census).
8. **CV disease** is cardiovascular disease and estimates are for adults 18 and over who have been diagnosed within their lifetime, based on state rates (BRFSS) applied to population estimates (U.S. Census).
9. **Poverty** estimates come from the U.S. Census Bureau and are for all ages.

RANKINGS

People at Risk in 25 Counties Most Polluted by Short-Term Particle Pollution (24-hour $PM_{2.5}$)

				At-Risk Groups								High $PM_{2.5}$ Days in Unhealthy Ranges, 2013–2015	
2017 Rank[1]	County	ST	Total Population[2]	Under 18[3]	65 and Over[3]	Pediatric Asthma[4,6]	Adult Asthma[5,6]	COPD[7]	Lung Cancer[8]	CV Disease[8]	Diabetes[9]	Poverty[10]	Weighted Avg.[11]	Grade[12]
1	Kern	CA	882,176	257,727	88,992	18,417	47,777	23,732	384	36,297	57,322	185,990	52.7	F
2	Fresno	CA	974,861	279,544	112,074	19,976	53,384	27,289	423	42,457	66,139	241,669	41.2	F
2	Kings	CA	150,965	41,435	14,146	2,961	8,357	4,026	66	6,015	9,555	30,117	41.2	F
4	Stanislaus	CA	538,388	146,063	67,324	10,437	30,189	15,817	233	25,049	38,935	103,646	29.8	F
5	Fairbanks North Star Borough	AK	99,631	24,116	8,349	2,045	7,139	2,756	56	3,943	4,891	7,671	25.8	F
6	Madera	CA	154,998	42,615	20,374	3,045	8,663	4,595	67	7,321	11,296	33,258	24.7	F
7	San Joaquin	CA	726,106	199,894	87,579	14,284	40,454	21,053	315	33,228	51,852	124,606	22.8	F
8	Salt Lake	UT	1,107,314	311,386	109,258	22,113	72,084	28,671	293	42,720	54,993	117,311	21.7	F
9	Cache	UT	120,783	37,123	10,685	2,636	7,531	2,768	32	4,057	5,140	18,657	20.2	F
10	Merced	CA	268,455	80,152	28,517	5,727	14,430	7,254	117	11,165	17,497	68,026	19.5	F
11	Shoshone	ID	12,432	2,464	2,772	209	909	576	6	892	988	2,577	16.8	F
12	Utah	UT	575,205	198,953	42,066	14,129	33,832	12,002	152	17,123	21,908	70,537	15.5	F
13	Lemhi	ID	7,735	1,398	2,193	119	574	398	4	642	694	1,347	14.3	F
14	Riverside	CA	2,361,026	612,848	320,086	43,793	134,810	71,829	1,024	114,813	177,144	377,244	14.0	F
15	Douglas	NV	47,710	8,500	12,234	497	3,145	3,277	28	4,072	4,863	4,459	13.3	F
16	Franklin	ID	13,074	4,385	1,804	372	791	432	6	636	714	1,253	12.7	F
17	Tulare	CA	459,863	144,036	49,147	10,292	24,222	12,265	200	18,970	29,653	123,922	12.5	F
17	Ravalli	MT	41,373	8,214	9,904	521	2,901	2,193	24	3,088	3,060	6,129	12.5	F
19	Plumas	CA	18,409	3,149	4,729	225	1,206	785	8	1,395	2,065	2,503	11.3	F
20	Weber	UT	243,645	70,325	27,606	4,994	15,725	6,546	64	10,045	12,791	29,768	11.0	F
20	Santa Cruz	CA	274,146	54,183	38,794	3,872	16,944	8,989	119	14,364	22,322	40,480	11.0	F
22	Los Angeles	CA	10,170,292	2,279,839	1,277,335	162,912	606,055	312,736	4,407	490,888	767,731	1,675,802	10.5	F
23	Inyo	CA	18,260	3,769	4,044	269	1,139	706	8	1,227	1,827	2,222	9.7	F
23	Lincoln	MT	19,052	3,491	4,903	221	1,360	1,072	11	1,523	1,499	3,817	9.7	F
25	Washoe	NV	446,903	99,275	67,548	5,804	28,100	23,194	263	27,431	34,367	61,017	9.5	F

Notes:

1. Counties are ranked by weighted average. See note 11 below.
2. **Total Population** represents the at-risk populations in counties with PM2.5 monitors.
3. Those **under 18** and **65 and over** are vulnerable to PM2.5 and are, therefore, included. They should not be used as population denominators for disease estimates.
4. **Pediatric asthma** estimates are for those under 18 years of age and represent the estimated number of people who had asthma in 2015 based on state rates (BRFSS) applied to population estimates (U.S. Census).
5. **Adult asthma** estimates are for those 18 years and older and represent the estimated number of people who had asthma in 2015 based on state rates (BRFSS) applied to population estimates (U.S. Census).
6. Adding across rows does not produce valid estimates. Adding the disease categories (asthma, COPD, etc.) will double-count people who have been diagnosed with more than one disease.
7. **COPD** estimates are for adults 18 and over who have been diagnosed within their lifetime, based on state rates (BRFSS) applied to population estimates (U.S. Census).
8. **Lung cancer** estimates are the number of new cases diagnosed in 2013 .
9. **CV disease** is cardiovascular disease and estimates are for adults 18 and over who have been diagnosed within their lifetime, based on state rates (BRFSS) applied to population estimates (U.S. Census).
10. **Diabetes** estimates are for adults 18 and over who have been diagnosed within their lifetime, based on state rates (BRFSS) applied to population estimates (U.S. Census).
11. **Poverty** estimates come from the U.S. Census Bureau and are for all ages.
12. The **Weighted Average** was derived by counting the number of days in each unhealthful range (orange, red, purple, maroon) in each year (2013-2015), multiplying the total in each range by the assigned standard weights (i.e., 1 for orange, 1.5 for red, 2.0 for purple, 2.5 for maroon), and calculating the average.
13. **Grade** is assigned by weighted average as follows: A=0.0, B=0.3-0.9, C=1.0-2.0, D=2.1-3.2, F=3.3+.

RANKINGS

People at Risk In 25 Counties Most Polluted by Year-Round Particle Pollution (Annual $PM_{2.5}$)

				At-Risk Groups									$PM_{2.5}$ Annual, 2013–2015	
2017 Rank[1]	County	ST	Total Population[2]	Under 18[3]	65 and Over[3]	Pediatric Asthma[4,6]	Adult Asthma[5,6]	COPD[7]	Lung Cancer[8]	CV Disease[9]	Diabetes[10]	Poverty[11]	Design Value[12]	Pass/ Grade[13]
1	Kings	CA	150,965	41,435	14,146	2,961	8,357	4,026	66	6,015	9,555	30,117	22.2	Fail
2	Kern	CA	882,176	257,727	88,992	18,417	47,777	23,732	384	36,297	57,322	185,990	20.8	Fail
3	Tulare	CA	459,863	144,036	49,147	10,292	24,222	12,265	200	18,970	29,653	123,922	17.6	Fail
4	Fresno	CA	974,861	279,544	112,074	19,976	53,384	27,289	423	42,457	66,139	241,669	15.4	Fail
5	Madera	CA	154,998	42,615	20,374	3,045	8,663	4,595	67	7,321	11,296	33,258	15.2	Fail
6	Plumas	CA	18,409	3,149	4,729	225	1,206	785	8	1,395	2,065	2,503	14.9	Fail
7	San Joaquin	CA	726,106	199,894	87,579	14,284	40,454	21,053	315	33,228	51,852	124,606	14.2	Fail
8	Riverside	CA	2,361,026	612,848	320,086	43,793	134,810	71,829	1,024	114,813	177,144	377,244	14.1	Fail
9	Stanislaus	CA	538,388	146,063	67,324	10,437	30,189	15,817	233	25,049	38,935	103,646	13.8	Fail
10	Shoshone	ID	12,432	2,464	2,772	209	909	576	6	892	988	2,577	13.7	Fail
11	Imperial	CA	180,191	51,119	22,442	3,653	9,934	5,187	78	8,178	12,647	41,685	13.1	Fail
12	Lemhi	ID	7,735	1,398	2,193	119	574	398	4	642	694	1,347	12.7	Fail
13	Allegheny	PA	1,230,459	233,675	217,210	26,121	102,088	69,398	807	93,646	102,520	145,454	12.6	Fail
14	Merced	CA	268,455	80,152	28,517	5,727	14,430	7,254	117	11,165	17,497	68,026	12.5	Fail
15	Cuyahoga	OH	1,255,921	268,170	210,832	19,306	99,147	79,368	861	93,526	110,646	224,256	12.4	Fail
16	Los Angeles	CA	10,170,292	2,279,839	1,277,335	162,912	606,055	312,736	4,407	490,888	767,731	1,675,802	12.3	Fail
17	San Luis Obispo	CA	281,401	50,837	51,231	3,633	17,910	10,097	122	16,633	25,113	38,448	12.1	Fail
17	Hawaii	HI	196,428	43,217	35,851	4,291	15,151	6,892	99	10,359	13,874	35,294	12.1	Fail
19	San Bernardino	CA	2,128,133	572,173	228,666	40,886	119,170	59,986	923	92,725	146,418	394,031	12.0	Pass
20	Jackson	OR	212,567	44,332	44,244	4,160	18,855	10,252	119	14,926	19,715	40,427	11.8	Pass
20	Philadelphia	PA	1,567,442	346,932	198,475	38,782	127,499	74,034	1,024	94,862	106,183	385,781	11.8	Pass
22	Lincoln	MT	19,052	3,491	4,903	221	1,360	1,072	11	1,523	1,499	3,817	11.7	Pass
22	Marion	IN	939,020	234,220	108,060	17,613	73,292	52,169	686	63,121	75,137	189,323	11.7	Pass
22	Jefferson	KY	763,623	171,811	113,444	18,636	70,483	70,948	727	70,423	78,758	115,246	11.7	Pass
22	Cambria	PA	136,411	26,377	28,534	2,949	11,114	8,324	90	11,550	12,488	19,450	11.7	Pass
22	Washington	PA	208,261	41,143	40,169	4,599	16,954	12,373	137	17,016	18,497	20,501	11.7	Pass

Notes:

1. Counties are ranked by Design Value. See note 11 below.
2. **Total Population** represents the at-risk populations in counties with $PM_{2.5}$ monitors.
3. Those under 18 and 65 and over are vulnerable to $PM_{2.5}$ and are, therefore, included. They should not be used as population denominators for disease estimates.
4. **Pediatric asthma** estimates are for those under 18 years of age and represent the estimated number of people who had asthma in 2014 based on state rates (BRFSS) applied to population estimates (U.S. Census).
5. **Adult asthma** estimates are for those 18 years and older and represent the estimated number of people who had asthma in 2014 based on state rates (BRFSS) applied to population estimates (U.S. Census).
6. Adding across rows does not produce valid estimates. Adding the disease categories (asthma, COPD, etc.) will double-count people who have been diagnosed with more than one disease.
7. **COPD** estimates are for adults 18 and over who have been diagnosed within their lifetime, based on state rates (BRFSS) applied to population estimates (U.S. Census).
8. **Lung cancer** estimates are the number of new cases diagnosed in 2013 .
9. **CV disease** is cardiovascular disease and estimates are for adults 18 and over who have been diagnosed within their lifetime, based on state rates (BRFSS) applied to population estimates (U.S. Census).
10. **Diabetes** estimates are for adults 18 and over who have been diagnosed within their lifetime, based on state rates (BRFSS) applied to population estimates (U.S. Census).
11. **Poverty** estimates come from the U.S. Census Bureau and are for all ages.
12. The **Design Value** is the calculated concentration of a pollutant based on the form of the Annual $PM_{2.5}$ National Ambient Air Quality Standard, and is used by EPA to determine whether the air quality in a county meets the current (2012) standard (U.S. EPA).
13. **Grades** are based on EPA's determination of meeting or failure to meet the NAAQS for annual $PM_{2.5}$ levels during 2012-2014. Counties meeting the NAAQS received grades of Pass; counties not meeting the NAAQS received grades of Fail.

People at Risk in 25 Most Ozone-Polluted Counties

2017 Rank[1]	County	ST	Total Population[2]	At-Risk Groups: Under 18[3]	65 and Over[3]	Pediatric Asthma[4,6]	Adult Asthma[5,6]	COPD[7]	CV Disease[8]	Poverty[9]	High Ozone Days in Unhealthy Ranges, 2013–2015: Weighted Avg.[10]	Grade[11]
1	San Bernardino	CA	2,128,133	572,173	228,666	40,886	119,170	59,986	92,725	394,031	142.3	F
2	Riverside	CA	2,361,026	612,848	320,086	43,793	134,810	71,829	114,813	377,244	122.0	F
3	Los Angeles	CA	10,170,292	2,279,839	1,277,335	162,912	606,055	312,736	490,888	1,675,802	108.3	F
4	Kern	CA	882,176	257,727	88,992	18,417	47,777	23,732	36,297	185,990	100.5	F
5	Fresno	CA	974,861	279,544	112,074	19,976	53,384	27,289	42,457	241,669	92.8	F
6	Tulare	CA	459,863	144,036	49,147	10,292	24,222	12,265	18,970	123,922	92.5	F
7	Madera	CA	154,998	42,615	20,374	3,045	8,663	4,595	7,321	33,258	46.8	F
8	Kings	CA	150,965	41,435	14,146	2,961	8,357	4,026	6,015	30,117	44.5	F
9	Maricopa	AZ	4,167,947	1,030,669	592,961	112,410	295,494	193,792	237,849	667,637	34.7	F
10	Uintah	UT	37,928	12,923	3,410	918	2,262	889	1,322	3,733	34.0	F
11	Merced	CA	268,455	80,152	28,517	5,727	14,430	7,254	11,165	68,026	33.3	F
12	San Diego	CA	3,299,521	728,037	431,999	52,024	197,708	102,514	161,074	445,948	31.2	F
13	El Dorado	CA	184,452	37,919	34,393	2,710	11,424	6,776	11,581	16,634	31.0	F
14	Stanislaus	CA	538,388	146,063	67,324	10,437	30,189	15,817	25,049	103,646	30.0	F
15	Sacramento	CA	1,501,335	361,617	198,168	25,840	87,748	46,278	73,651	250,325	26.0	F
16	Nevada	CA	98,877	17,428	24,201	1,245	6,422	4,090	7,193	12,137	25.7	F
17	Fairfield	CT	948,053	220,906	137,799	25,884	76,395	36,729	51,524	83,612	24.0	F
18	Clark	NV	2,114,801	498,564	290,001	29,147	130,554	103,810	121,424	321,755	23.8	F
19	Jefferson	CO	565,524	116,627	85,287	9,889	40,386	20,708	29,549	44,068	23.7	F
20	Harris	TX	4,538,028	1,224,413	428,697	96,889	252,264	158,961	240,522	744,712	23.3	F
21	Tarrant	TX	1,982,498	533,475	208,355	42,215	110,194	72,657	111,992	255,993	23.2	F
21	Denton	TX	780,612	201,646	70,965	15,957	44,046	27,885	42,057	61,186	23.2	F
23	Imperial	CA	180,191	51,119	22,442	3,653	9,934	5,187	8,178	41,685	22.5	F
24	Duchesne	UT	20,862	7,230	2,283	513	1,236	517	802	2,247	21.3	F
25	Larimer	CO	333,577	67,793	47,570	5,748	24,144	11,356	16,259	39,648	19.7	F

Notes:

1. Counties are ranked by weighted average. See note 10 below.
2. **Total Population** represents the at-risk populations in counties with $PM_{2.5}$ monitors.
3. Those **under 18** and **65 and over** are vulnerable to $PM_{2.5}$ and are, therefore, included. They should not be used as population denominators for disease estimates.
4. **Pediatric asthma** estimates are for those under 18 years of age and represent the **estimated** number of people who had asthma in 2015 based on state rates (BRFSS) applied to population estimates (U.S. Census).
5. **Adult asthma** estimates are for those 18 years and older and represent the **estimated** number of people who had asthma in 2015 based on state rates (BRFSS) applied to population estimates (U.S. Census).
6. Adding across rows does not produce valid estimates. Adding the disease categories (asthma, COPD, etc.) will double-count people who have been diagnosed with more than one disease.
7. **COPD** estimates are for adults 18 and over who have been diagnosed within their lifetime, based on state rates (BRFSS) applied to population estimates (U.S. Census).
8. **CV disease** is cardiovascular disease and estimates are for adults 18 and over who have been diagnosed within their lifetime, based on state rates (BRFSS) applied to population estimates (U.S. Census).
9. **Poverty** estimates come from the U.S. Census Bureau and are for all ages.
10. The **Weighted Average** was derived by counting the number of days in each unhealthful range (orange, red, purple) in each year (2013-2015), multiplying the total in each range by the assigned standard weights (i.e., 1 for orange, 1.5 for red, 2.0 for purple), and calculating the average.
11. Grade is assigned by weighted average as follows: A=0.0, B=0.3-0.9, C=1.0-2.0, D=2.1-3.2, F=3.3+.

RANKINGS

Cleanest U.S. Cities for Short-Term Particle Pollution (24-hour $PM_{2.5}$)[1]

Metropolitan Statistical Area	Population
Albany-Schenectady, NY	1,173,891
Alexandria, LA	154,484
Asheville-Brevard, NC	480,051
Atlanta—Athens-Clarke County—Sandy Springs, GA	6,365,108
Augusta-Richmond County, GA-SC	590,146
Austin-Round Rock, TX	2,000,860
Bangor, ME	152,692
Beckley, WV	122,507
Bellingham, WA	212,284
Birmingham-Hoover-Talladega, AL	1,360,082
Bowling Green-Glasgow, KY	221,915
Brunswick, GA	116,003
Buffalo-Cheektowaga, NY	1,213,152
Burlington-South Burlington, VT	217,042
Cape Coral-Fort Myers-Naples, FL	1,059,287
Casper, WY	82,178
Charleston-Huntington-Ashland, WV-OH-KY	693,726
Charlotte-Concord, NC-SC	2,583,956
Charlottesville, VA	229,514
Chattanooga-Cleveland-Dalton, TN-GA-AL	950,005
Colorado Springs, CO	697,856
Columbia-Orangeburg-Newberry, SC	937,288
Columbus-Auburn-Opelika, GA-AL	504,865
Columbus-Marion-Zanesville, OH	2,424,831
Corpus Christi-Kingsville-Alice, TX	526,068
Des Moines-Ames-West Des Moines, IA	782,390
Dothan-Enterprise-Ozark, AL	248,947
Eau Claire-Menomonie, WI	210,133
Edwards-Glenwood Springs, CO	129,487
Elmira-Corning, NY	184,702
Erie-Meadville, PA	364,529
Evansville, IN-KY	315,693
Farmington, NM	118,737
Fayetteville-Lumberton-Laurinburg, NC	546,215
Fayetteville-Springdale-Rogers, AR-MO	513,559
Florence, SC	206,448
Florence-Muscle Shoals, AL	146,950
Fort Smith, AR-OK	280,241
Gadsden, AL	103,057
Gainesville-Lake City, FL	345,511
Goldsboro, NC	124,132
Grand Island, NE	85,066
Greensboro—Winston-Salem—High Point, NC	1,642,506
Greenville-Washington, NC	223,493
Gulfport-Biloxi-Pascagoula, MS	389,255
Harrisonburg-Staunton-Waynesboro, VA	251,352
Homosassa Springs, FL	141,058
Hot Springs-Malvern, AR	130,603
Houma-Thibodaux, LA	212,297
Huntsville-Decatur-Albertville, AL	763,287
Jackson-Vicksburg-Brookhaven, MS	670,061
La Crosse-Onalaska, WI-MN	136,985
Lafayette-Opelousas-Morgan City, LA	627,146
Lake Charles-Jennings, LA	237,044
Lakeland-Winter Haven, FL	650,092
Lansing-East Lansing-Owosso, MI	540,895
Lexington-Fayette—Richmond—Frankfort, KY	723,849
Lima-Van Wert-Celina, OH	219,831
Longview-Marshall, TX	284,527
Lynchburg, VA	259,950
McAllen-Edinburg, TX	906,099
Milwaukee-Racine-Waukesha, WI	2,046,692
Mobile-Daphne-Fairhope, AL	619,104
Monroe-Ruston-Bastrop, LA	253,407
Montgomery, AL	373,792
Morgantown-Fairmont, WV	195,101
New Orleans-Metairie-Hammond, LA-MS	1,493,205
North Port-Sarasota, FL	977,491
Oklahoma City-Shawnee, OK	1,430,327
Orlando-Deltona-Daytona Beach, FL	3,129,308
Owensboro, KY	117,463
Palm Bay-Melbourne-Titusville, FL	568,088
Parkersburg-Marietta-Vienna, WV-OH	153,444
Pensacola-Ferry Pass, FL-AL	515,832
Pittsfield, MA	127,828
Pueblo-Cañon City, CO	210,283
Richmond, VA	1,271,334
Rochester-Batavia-Seneca Falls, NY	1,175,724
Rome-Summerville, GA	121,426
Saginaw-Midland-Bay City, MI	382,598
Salisbury, MD-DE	395,300
San Antonio-New Braunfels, TX	2,384,075
Santa Maria-Santa Barbara, CA	444,769
Savannah-Hinesville-Statesboro, GA	532,048
Scranton—Wilkes-Barre—Hazleton, PA	558,166
Sierra Vista-Douglas, AZ	126,427
Springfield-Branson, MO	541,991
Springfield-Greenfield Town, MA	702,583
St. George, UT	155,602
Syracuse-Auburn, NY	738,746
Tampa-St. Petersburg-Clearwater, FL	2,975,225
Texarkana, TX-AR	149,769
Tulsa-Muskogee-Bartlesville, OK	1,151,172
Tuscaloosa, AL	239,908
Urban Honolulu, HI	998,714
Valdosta, GA	142,875
Virginia Beach-Norfolk, VA-NC	1,828,187
Waterloo-Cedar Falls, IA	170,612
Wilmington, NC	277,969

Note:

1. Monitors in these cities reported no days when $PM_{2.5}$ levels reached the unhealthful range using the Air Quality Index based on the 2006 NAAQS.

Top 25 Cleanest U.S. Cities for Year-Round Particle Pollution (Annual $PM_{2.5}$)[1]

Rank[2]	Design Value[3]	Metropolitan Statistical Area	Population
1	4.1	Cheyenne, WY	97,121
1	4.1	Farmington, NM	118,737
3	4.6	Casper, WY	82,178
4	4.8	Kahului-Wailuku-Lahaina, HI	164,726
5	5.3	Bismarck, ND	129,517
6	5.4	Urban Honolulu, HI	998,714
7	5.6	Palm Bay-Melbourne-Titusville, FL	568,088
8	5.7	Colorado Springs, CO	697,856
8	5.7	Elmira-Corning, NY	184,702
10	5.8	Pueblo-Cañon City, CO	210,283
11	5.9	Cape Coral-Fort Myers-Naples, FL	1,059,287
12	6.0	Miami-Fort Lauderdale-Port St. Lucie, FL	6,654,565
13	6.1	North Port-Sarasota, FL	977,491
14	6.2	Redding-Red Bluff, CA	242,841
14	6.2	Homosassa Springs, FL	141,058
14	6.2	Orlando-Deltona-Daytona Beach, FL	3,129,308
17	6.3	Salinas, CA	433,898
17	6.3	Burlington-South Burlington, VT	217,042
19	6.4	Fargo-Wahpeton, ND-MN	256,634
19	6.4	Yuma, AZ	204,275
19	6.4	Bangor, ME	152,692
19	6.4	Syracuse-Auburn, NY	738,746
23	6.5	Lakeland-Winter Haven, FL	650,092
23	6.5	Sierra Vista-Douglas, AZ	126,427
23	6.5	Wilmington, NC	277,969

Notes:

1 This list represents cities with the lowest levels of annual $PM_{2.5}$ air pollution.

2. Cities are ranked by using the highest design value for any county within that metropolitan area.

3. The **Design Value** is the calculated concentration of a pollutant based on the form of the Annual $PM_{2.5}$ National Ambient Air Quality Standard, and is used by EPA to determine whether the air quality in a county meets the current (2012) standard (U.S. EPA).

RANKINGS

Cleanest U.S. Cities for Ozone Air Pollution[1]

Metropolitan Statistical Area	Population
Bellingham, WA	212,284
Blacksburg-Christiansburg-Radford, VA	181,747
Brownsville-Harlingen-Raymondville, TX	444,059
Brunswick, GA	116,003
Burlington-South Burlington, VT	217,042
Cape Coral-Fort Myers-Naples, FL	1,059,287
Cedar Rapids-Iowa City, IA	432,538
Charleston-North Charleston, SC	744,526
Charlottesville, VA	229,514
Columbia-Moberly-Mexico, MO	226,174
Columbia-Orangeburg-Newberry, SC	937,288
Decatur, IL	107,303
Des Moines-Ames-West Des Moines, IA	782,390
Dothan-Enterprise-Ozark, AL	248,947
Eau Claire-Menomonie, WI	210,133
Elmira-Corning, NY	184,702
Fairbanks, AK	99,631
Fargo-Wahpeton, ND-MN	256,634
Fayetteville-Springdale-Rogers, AR-MO	513,559
Florence, SC	206,448
Florence-Muscle Shoals, AL	146,950
Fort Wayne-Huntington-Auburn, IN	626,124
Gadsden, AL	103,057
Gainesville-Lake City, FL	345,511
Greenville-Washington, NC	223,493
Harrisonburg-Staunton-Waynesboro, VA	251,352
Hickory-Lenoir, NC	407,499
Idaho Falls-Rexburg-Blackfoot, ID	235,829
Ithaca-Cortland, NY	153,420
Jackson-Vicksburg-Brookhaven, MS	670,061
Jefferson City, MO	151,145

Metropolitan Statistical Area	Population
Johnson City-Kingsport-Bristol, TN-VA	507,768
La Crosse-Onalaska, WI-MN	136,985
Lincoln-Beatrice, NE	345,478
McAllen-Edinburg, TX	906,099
Missoula, MT	114,181
Monroe-Ruston-Bastrop, LA	253,407
New Bern-Morehead City, NC	195,124
Ocala, FL	343,254
Palm Bay-Melbourne-Titusville, FL	568,088
Peoria-Canton, IL	413,717
Quincy-Hannibal, IL-MO	116,296
Rapid City-Spearfish, SD	168,961
Roanoke, VA	314,560
Rochester-Austin, MN	252,989
Rome-Summerville, GA	121,426
Salinas, CA	433,898
Savannah-Hinesville-Statesboro, GA	532,048
Sebring, FL	99,491
Sioux City-Vermillion, IA-SD-NE	183,033
Sioux Falls, SD	251,854
Springfield-Branson, MO	541,991
Springfield-Jacksonville-Lincoln, IL	314,212
Steamboat Springs-Craig, CO	37,067
Tallahassee-Bainbridge, FL-GA	405,098
Terre Haute, IN	171,019
Tuscaloosa, AL	239,908
Urban Honolulu, HI	998,714
Utica-Rome, NY	295,600
Waterloo-Cedar Falls, IA	170,612
Williamsport-Lock Haven, PA	155,489
Wilmington, NC	277,969

Notes:

1. This list represents cities with no monitored ozone air pollution in unhealthful ranges using the Air Quality Index based on 2015 NAAQS.

RANKINGS

Cleanest Counties for Short-Term Particle Pollution (24-hour $PM_{2.5}$)[1]

County	State	MSAs and Respective CSA[2]
Baldwin	AL	Mobile-Daphne-Fairhope, AL
Clay	AL	
Colbert	AL	Florence-Muscle Shoals, AL
DeKalb	AL	Huntsville-Decatur-Albertville, AL
Etowah	AL	Gadsden, AL
Houston	AL	Dothan-Enterprise-Ozark, AL
Jefferson	AL	Birmingham-Hoover-Talladega, AL
Madison	AL	Huntsville-Decatur-Albertville, AL
Mobile	AL	Mobile-Daphne-Fairhope, AL
Montgomery	AL	Montgomery, AL
Morgan	AL	Huntsville-Decatur-Albertville, AL
Russell	AL	Columbus-Auburn-Opelika, GA-AL
Shelby	AL	Birmingham-Hoover-Talladega, AL
Talladega	AL	Birmingham-Hoover-Talladega, AL
Tuscaloosa	AL	Tuscaloosa, AL
Arkansas	AR	
Ashley	AR	
Garland	AR	Hot Springs-Malvern, AR
Jackson	AR	
Polk	AR	
Union	AR	
Washington	AR	Fayetteville-Springdale-Rogers, AR-MO
Cochise	AZ	Sierra Vista-Douglas, AZ
Mohave	AZ	Las Vegas-Henderson, NV-AZ
Pima	AZ	Tucson-Nogales, AZ
San Benito	CA	San Jose-San Francisco-Oakland, CA
Santa Barbara	CA	Santa Maria-Santa Barbara, CA
Sonoma	CA	San Jose-San Francisco-Oakland, CA
Ventura	CA	Los Angeles-Long Beach, CA
Yolo	CA	Sacramento-Roseville, CA
Arapahoe	CO	Denver-Aurora, CO
El Paso	CO	Colorado Springs, CO
Garfield	CO	Edwards-Glenwood Springs, CO
La Plata	CO	
Montezuma	CO	
Pueblo	CO	Pueblo-Cañon City, CO
Rio Blanco	CO	
Hartford	CT	Hartford-West Hartford, CT
Litchfield	CT	New York-Newark, NY-NJ-CT-PA
District of Columbia	DC	Washington-Baltimore-Arlington, DC-MD-VA-WV-PA
Kent	DE	Philadelphia-Reading-Camden, PA-NJ-DE-MD
Sussex	DE	Salisbury, MD-DE
Alachua	FL	Gainesville-Lake City, FL
Brevard	FL	Palm Bay-Melbourne-Titusville, FL
Broward	FL	Miami-Fort Lauderdale-Port St. Lucie, FL
Citrus	FL	Homosassa Springs, FL
Escambia	FL	Pensacola-Ferry Pass, FL-AL
Hillsborough	FL	Tampa-St. Petersburg-Clearwater, FL
Lee	FL	Cape Coral-Fort Myers-Naples, FL
Orange	FL	Orlando-Deltona-Daytona Beach, FL
Palm Beach	FL	Miami-Fort Lauderdale-Port St. Lucie, FL
Pinellas	FL	Tampa-St. Petersburg-Clearwater, FL
Polk	FL	Lakeland-Winter Haven, FL
Sarasota	FL	North Port-Sarasota, FL
Seminole	FL	Orlando-Deltona-Daytona Beach, FL
Volusia	FL	Orlando-Deltona-Daytona Beach, FL
Chatham	GA	Savannah-Hinesville-Statesboro, GA
Clarke	GA	Atlanta—Athens-Clarke County—Sandy Springs, GA
Clayton	GA	Atlanta—Athens-Clarke County—Sandy Springs, GA
Cobb	GA	Atlanta—Athens-Clarke County—Sandy Springs, GA
DeKalb	GA	Atlanta—Athens-Clarke County—Sandy Springs, GA
Floyd	GA	Rome-Summerville, GA
Fulton	GA	Atlanta—Athens-Clarke County—Sandy Springs, GA
Glynn	GA	Brunswick, GA
Gwinnett	GA	Atlanta—Athens-Clarke County—Sandy Springs, GA
Hall	GA	Atlanta—Athens-Clarke County—Sandy Springs, GA
Houston	GA	Macon-Bibb County—Warner Robins, GA
Lowndes	GA	Valdosta, GA
Muscogee	GA	Columbus-Auburn-Opelika, GA-AL
Paulding	GA	Atlanta—Athens-Clarke County—Sandy Springs, GA
Richmond	GA	Augusta-Richmond County, GA-SC
Walker	GA	Chattanooga-Cleveland-Dalton, TN-GA-AL
Washington	GA	
Honolulu	HI	Urban Honolulu, HI
Kauai	HI	
Black Hawk	IA	Waterloo-Cedar Falls, IA
Delaware	IA	
Lee	IA	
Palo Alto	IA	
Polk	IA	Des Moines-Ames-West Des Moines, IA
Van Buren	IA	
Dubois	IN	

Notes:

1. Monitors in these counties reported no days when $PM_{2.5}$ levels reached the unhealthful range using the Air Quality Index based on the current (2006) standard (U.S. EPA).
2. MSA and CSA are terms used by the U.S. Office of Management and Budget for statistical purposes. MSA stands for Metropolitan Statisical Area and includes one or more counties. CSA stands for Combined Statistical Area and may include multiple MSAs and individual counties.

Cleanest Counties for Short-Term Particle Pollution (24-hour $PM_{2.5}$)[1] (cont.)

County	State	MSAs and Respective CSA[2]
Greene	IN	
Spencer	IN	
Vanderburgh	IN	Evansville, IN-KY
Johnson	KS	Kansas City-Overland Park-Kansas City, MO-KS
Bell	KY	
Boyd	KY	Charleston-Huntington-Ashland, WV-OH-KY
Campbell	KY	Cincinnati-Wilmington-Maysville, OH-KY-IN
Carter	KY	
Christian	KY	Clarksville, TN-KY
Daviess	KY	Owensboro, KY
Fayette	KY	Lexington-Fayette—Richmond—Frankfort, KY
Hardin	KY	Louisville/Jefferson County—Elizabethtown—Madison, KY-IN
Henderson	KY	Evansville, IN-KY
Madison	KY	Lexington-Fayette—Richmond—Frankfort, KY
McCracken	KY	Paducah-Mayfield, KY-IL
Perry	KY	
Pulaski	KY	
Warren	KY	Bowling Green-Glasgow, KY
Calcasieu Parish	LA	Lake Charles-Jennings, LA
Iberville Parish	LA	Baton Rouge, LA
Jefferson Parish	LA	New Orleans-Metairie-Hammond, LA-MS
Lafayette Parish	LA	Lafayette-Opelousas-Morgan City, LA
Ouachita Parish	LA	Monroe-Ruston-Bastrop, LA
Rapides Parish	LA	Alexandria, LA
St. Bernard Parish	LA	New Orleans-Metairie-Hammond, LA-MS
Tangipahoa Parish	LA	New Orleans-Metairie-Hammond, LA-MS
Terrebonne Parish	LA	Houma-Thibodaux, LA
West Baton Rouge Parish	LA	Baton Rouge, LA
Berkshire	MA	Pittsfield, MA
Bristol	MA	Boston-Worcester-Providence, MA-RI-NH-CT
Essex	MA	Boston-Worcester-Providence, MA-RI-NH-CT
Hampden	MA	Springfield-Greenfield Town, MA
Plymouth	MA	Boston-Worcester-Providence, MA-RI-NH-CT
Suffolk	MA	Boston-Worcester-Providence, MA-RI-NH-CT
Worcester	MA	Boston-Worcester-Providence, MA-RI-NH-CT
Anne Arundel	MD	Washington-Baltimore-Arlington, DC-MD-VA-WV-PA
Baltimore	MD	Washington-Baltimore-Arlington, DC-MD-VA-WV-PA
Dorchester	MD	Washington-Baltimore-Arlington, DC-MD-VA-WV-PA
Garrett	MD	
Harford	MD	Washington-Baltimore-Arlington, DC-MD-VA-WV-PA
Kent	MD	
Montgomery	MD	Washington-Baltimore-Arlington, DC-MD-VA-WV-PA
Prince George's	MD	Washington-Baltimore-Arlington, DC-MD-VA-WV-PA
Penobscot	ME	Bangor, ME
Allegan	MI	Grand Rapids-Wyoming-Muskegon, MI
Bay	MI	Saginaw-Midland-Bay City, MI
Berrien	MI	South Bend-Elkhart-Mishawaka, IN-MI
Chippewa	MI	
Ingham	MI	Lansing-East Lansing-Owosso, MI
Lenawee	MI	Detroit-Warren-Ann Arbor, MI
Missaukee	MI	
Washtenaw	MI	Detroit-Warren-Ann Arbor, MI
Dakota	MN	Minneapolis-St. Paul, MN-WI
Scott	MN	Minneapolis-St. Paul, MN-WI
Wright	MN	Minneapolis-St. Paul, MN-WI
Cedar	MO	
Greene	MO	Springfield-Branson, MO
Grenada	MS	
Hancock	MS	Gulfport-Biloxi-Pascagoula, MS
Harrison	MS	Gulfport-Biloxi-Pascagoula, MS
Hinds	MS	Jackson-Vicksburg-Brookhaven, MS
Jackson	MS	Gulfport-Biloxi-Pascagoula, MS
Alamance	NC	Greensboro—Winston-Salem—High Point, NC
Buncombe	NC	Asheville-Brevard, NC
Caswell	NC	
Catawba	NC	Hickory-Lenoir, NC
Cumberland	NC	Fayetteville-Lumberton-Laurinburg, NC
Davidson	NC	Greensboro—Winston-Salem—High Point, NC
Duplin	NC	
Durham	NC	Raleigh-Durham-Chapel Hill, NC
Forsyth	NC	Greensboro—Winston-Salem—High Point, NC
Gaston	NC	Charlotte-Concord, NC-SC
Guilford	NC	Greensboro—Winston-Salem—High Point, NC
Haywood	NC	Asheville-Brevard, NC
Jackson	NC	
Johnston	NC	Raleigh-Durham-Chapel Hill, NC
Martin	NC	
Mecklenburg	NC	Charlotte-Concord, NC-SC
Mitchell	NC	
Montgomery	NC	
New Hanover	NC	Wilmington, NC
Pitt	NC	Greenville-Washington, NC
Rowan	NC	Charlotte-Concord, NC-SC
Swain	NC	

Notes:

1. Monitors in these counties reported no days when $PM_{2.5}$ levels reached the unhealthful range using the Air Quality Index based on the current (2006) standard (U.S. EPA).
2. MSA and CSA are terms used by the U.S. Office of Management and Budget for statistical purposes. MSA stands for Metropolitan Statisical Area and includes one or more counties. CSA stands for Combined Statistical Area and may include multiple MSAs and individual counties.

Cleanest Counties for Short-Term Particle Pollution (24-hour $PM_{2.5}$)[1] (cont.)

County	State	MSAs and Respective CSA[2]
Wayne	NC	Goldsboro, NC
Hall	NE	Grand Island, NE
Scotts Bluff	NE	
Belknap	NH	Boston-Worcester-Providence, MA-RI-NH-CT
Grafton	NH	
Hillsborough	NH	Boston-Worcester-Providence, MA-RI-NH-CT
Rockingham	NH	Boston-Worcester-Providence, MA-RI-NH-CT
Atlantic	NJ	Philadelphia-Reading-Camden, PA-NJ-DE-MD
Bergen	NJ	New York-Newark, NY-NJ-CT-PA
Gloucester	NJ	Philadelphia-Reading-Camden, PA-NJ-DE-MD
Mercer	NJ	New York-Newark, NY-NJ-CT-PA
Middlesex	NJ	New York-Newark, NY-NJ-CT-PA
Morris	NJ	New York-Newark, NY-NJ-CT-PA
Passaic	NJ	New York-Newark, NY-NJ-CT-PA
Warren	NJ	New York-Newark, NY-NJ-CT-PA
San Juan	NM	Farmington, NM
Albany	NY	Albany-Schenectady, NY
Bronx	NY	New York-Newark, NY-NJ-CT-PA
Chautauqua	NY	
Erie	NY	Buffalo-Cheektowaga, NY
Essex	NY	
Kings	NY	New York-Newark, NY-NJ-CT-PA
Monroe	NY	Rochester-Batavia-Seneca Falls, NY
New York	NY	New York-Newark, NY-NJ-CT-PA
Onondaga	NY	Syracuse-Auburn, NY
Orange	NY	New York-Newark, NY-NJ-CT-PA
Queens	NY	New York-Newark, NY-NJ-CT-PA
Richmond	NY	New York-Newark, NY-NJ-CT-PA
Steuben	NY	Elmira-Corning, NY
Suffolk	NY	New York-Newark, NY-NJ-CT-PA
Allen	OH	Lima-Van Wert-Celina, OH
Athens	OH	
Butler	OH	Cincinnati-Wilmington-Maysville, OH-KY-IN
Clark	OH	Dayton-Springfield-Sidney, OH
Franklin	OH	Columbus-Marion-Zanesville, OH
Greene	OH	Dayton-Springfield-Sidney, OH
Lake	OH	Cleveland-Akron-Canton, OH
Lawrence	OH	Charleston-Huntington-Ashland, WV-OH-KY
Lorain	OH	Cleveland-Akron-Canton, OH
Mahoning	OH	Youngstown-Warren, OH-PA
Medina	OH	Cleveland-Akron-Canton, OH
Portage	OH	Cleveland-Akron-Canton, OH
Preble	OH	
Scioto	OH	Charleston-Huntington-Ashland, WV-OH-KY
Trumbull	OH	Youngstown-Warren, OH-PA
Oklahoma	OK	Oklahoma City-Shawnee, OK
Sequoyah	OK	Fort Smith, AR-OK
Tulsa	OK	Tulsa-Muskogee-Bartlesville, OK
Armstrong	PA	Pittsburgh-New Castle-Weirton, PA-OH-WV
Erie	PA	Erie-Meadville, PA
Lackawanna	PA	Scranton—Wilkes-Barre—Hazleton, PA
Monroe	PA	New York-Newark, NY-NJ-CT-PA
Westmoreland	PA	Pittsburgh-New Castle-Weirton, PA-OH-WV
Kent	RI	Boston-Worcester-Providence, MA-RI-NH-CT
Washington	RI	Boston-Worcester-Providence, MA-RI-NH-CT
Chesterfield	SC	
Edgefield	SC	Augusta-Richmond County, GA-SC
Florence	SC	Florence, SC
Lexington	SC	Columbia-Orangeburg-Newberry, SC
Richland	SC	Columbia-Orangeburg-Newberry, SC
Spartanburg	SC	Greenville-Spartanburg-Anderson, SC
Brown	SD	
Hamilton	TN	Chattanooga-Cleveland-Dalton, TN-GA-AL
McMinn	TN	Chattanooga-Cleveland-Dalton, TN-GA-AL
Bexar	TX	San Antonio-New Braunfels, TX
Bowie	TX	Texarkana, TX-AR
Ellis	TX	Dallas-Fort Worth, TX-OK
Galveston	TX	Houston-The Woodlands, TX
Harrison	TX	Longview-Marshall, TX
Hidalgo	TX	McAllen-Edinburg, TX
Nueces	TX	Corpus Christi-Kingsville-Alice, TX
Travis	TX	Austin-Round Rock, TX
Washington	UT	St. George, UT
Albemarle	VA	Charlottesville, VA
Arlington	VA	Washington-Baltimore-Arlington, DC-MD-VA-WV-PA
Bristol City	VA	Johnson City-Kingsport-Bristol, TN-VA
Charles City	VA	Richmond, VA
Chesterfield	VA	Richmond, VA
Fairfax	VA	Washington-Baltimore-Arlington, DC-MD-VA-WV-PA
Hampton City	VA	Virginia Beach-Norfolk, VA-NC
Henrico	VA	Richmond, VA
Loudoun	VA	Washington-Baltimore-Arlington, DC-MD-VA-WV-PA
Lynchburg City	VA	Lynchburg, VA
Norfolk City	VA	Virginia Beach-Norfolk, VA-NC
Page	VA	
Rockingham	VA	Harrisonburg-Staunton-Waynesboro, VA

Notes:

1. Monitors in these counties reported no days when $PM_{2.5}$ levels reached the unhealthful range using the Air Quality Index based on the current (2006) standard (U.S. EPA).
2. MSA and CSA are terms used by the U.S. Office of Management and Budget for statistical purposes. MSA stands for Metropolitan Statisical Area and includes one or more counties. CSA stands for Combined Statistical Area and may include multiple MSAs and individual counties.

Cleanest Counties for Short-Term Particle Pollution (24-hour $PM_{2.5}$)[1] (cont.)

County	State	MSAs and Respective CSA[2]
Salem City	VA	Roanoke, VA
Virginia Beach City	VA	Virginia Beach-Norfolk, VA-NC
Bennington	VT	
Chittenden	VT	Burlington-South Burlington, VT
Kitsap	WA	Seattle-Tacoma, WA
Skagit	WA	Seattle-Tacoma, WA
Whatcom	WA	Bellingham, WA
Ashland	WI	
Dodge	WI	Milwaukee-Racine-Waukesha, WI
Eau Claire	WI	Eau Claire-Menomonie, WI
Forest	WI	
Grant	WI	
La Crosse	WI	La Crosse-Onalaska, WI-MN
Milwaukee	WI	Milwaukee-Racine-Waukesha, WI
Ozaukee	WI	Milwaukee-Racine-Waukesha, WI
Sauk	WI	Madison-Janesville-Beloit, WI
Taylor	WI	
Vilas	WI	
Waukesha	WI	Milwaukee-Racine-Waukesha, WI
Brooke	WV	Pittsburgh-New Castle-Weirton, PA-OH-WV
Cabell	WV	Charleston-Huntington-Ashland, WV-OH-KY
Hancock	WV	Pittsburgh-New Castle-Weirton, PA-OH-WV
Harrison	WV	
Kanawha	WV	Charleston-Huntington-Ashland, WV-OH-KY
Marion	WV	Morgantown-Fairmont, WV
Marshall	WV	Wheeling, WV-OH
Monongalia	WV	Morgantown-Fairmont, WV
Raleigh	WV	Beckley, WV
Wood	WV	Parkersburg-Marietta-Vienna, WV-OH
Albany	WY	
Carbon	WY	
Natrona	WY	Casper, WY
Park	WY	
Sublette	WY	
Sweetwater	WY	
Teton	WY	

Notes:

1. Monitors in these counties reported no days when $PM_{2.5}$ levels reached the unhealthful range using the Air Quality Index based on the current (2006) standard (U.S. EPA).
2. MSA and CSA are terms used by the U.S. Office of Management and Budget for statistical purposes. MSA stands for Metropolitan Statistical Area and includes one or more counties. CSA stands for Combined Statistical Area and may include multiple MSAs and individual counties.

Top 25 Cleanest Counties for Year-Round Particle Pollution (Annual $PM_{2.5}$)[1]

2017 Rank[2]	County	State	Design Value[3]
1	Custer	SD	3.2
2	McKenzie	ND	3.4
3	Kauai	HI	3.9
3	Lake	CA	4.0
4	San Juan	NM	4.1
4	Laramie	WY	4.1
4	Essex	NY	4.1
4	Park	WY	4.1
9	Campbell	WY	4.2
10	Albany	WY	4.3
11	Fergus	MT	4.5
12	Natrona	WY	4.6
13	Jackson	SD	4.7
13	Teton	WY	4.7
15	Sweetwater	WY	4.8
15	Lake	MN	4.8
15	Maui	HI	4.8
18	Kent	RI	4.9
18	Oliver	ND	4.9
18	Phillips	MT	4.9
18	Billings	ND	4.9
22	San Benito	CA	5.0
22	Vilas	WI	5.0
22	Sublette	WY	5.0
22	Belknap	NH	5.0

Notes:

1. This list represents counties with the lowest levels of monitored long term $PM_{2.5}$ air pollution.
2. Counties are ranked by Design Value.
3. The Design Value is the calculated concentration of a pollutant based on the form of the Annual PM2.5 National Ambient Air Quality Standard, and is used by EPA to determine whether the air quality in a county meets the current (2012) standard (U.S. EPA).

Cleanest Counties for Ozone Air Pollution[1]

County	State	Metropolitan Statistical Area
Denali Borough	AK	
Fairbanks North Star Borough	AK	Fairbanks, AK
Colbert	AL	Florence-Muscle Shoals, AL
Etowah	AL	Gadsden, AL
Houston	AL	Dothan-Enterprise-Ozark, AL
Madison	AL	Huntsville-Decatur-Albertville, AL
Morgan	AL	Huntsville-Decatur-Albertville, AL
Sumter	AL	
Tuscaloosa	AL	Tuscaloosa, AL
Newton	AR	
Polk	AR	
Washington	AR	Fayetteville-Springdale-Rogers, AR-MO
Colusa	CA	
Humboldt	CA	
Lake	CA	
Marin	CA	San Jose-San Francisco-Oakland, CA
Mendocino	CA	
Monterey	CA	Salinas, CA
San Francisco	CA	San Jose-San Francisco-Oakland, CA
Santa Cruz	CA	San Jose-San Francisco-Oakland, CA
Sonoma	CA	San Jose-San Francisco-Oakland, CA
Moffat	CO	Steamboat Springs-Craig, CO
Montezuma	CO	
Alachua	FL	Gainesville-Lake City, FL
Baker	FL	Jacksonville-St. Marys-Palatka, FL-GA
Brevard	FL	Palm Bay-Melbourne-Titusville, FL
Collier	FL	Cape Coral-Fort Myers-Naples, FL
Columbia	FL	Gainesville-Lake City, FL
Flagler	FL	Orlando-Deltona-Daytona Beach, FL
Highlands	FL	Sebring, FL
Holmes	FL	
Lee	FL	Cape Coral-Fort Myers-Naples, FL
Leon	FL	Tallahassee-Bainbridge, FL-GA
Liberty	FL	
Marion	FL	Ocala, FL
Seminole	FL	Orlando-Deltona-Daytona Beach, FL
Wakulla	FL	Tallahassee-Bainbridge, FL-GA
Chatham	GA	Savannah-Hinesville-Statesboro, GA
Chattooga	GA	Rome-Summerville, GA
Clarke	GA	Atlanta—Athens-Clarke County—Sandy Springs, GA
Columbia	GA	Augusta-Richmond County, GA-SC
Glynn	GA	Brunswick, GA
Muscogee	GA	Columbus-Auburn-Opelika, GA-AL
Paulding	GA	Atlanta—Athens-Clarke County—Sandy Springs, GA
Richmond	GA	Augusta-Richmond County, GA-SC
Sumter	GA	
Honolulu	HI	Urban Honolulu, HI
Bremer	IA	Waterloo-Cedar Falls, IA
Linn	IA	Cedar Rapids-Iowa City, IA
Polk	IA	Des Moines-Ames-West Des Moines, IA
Scott	IA	Davenport-Moline, IA-IL
Story	IA	Des Moines-Ames-West Des Moines, IA
Van Buren	IA	
Warren	IA	Des Moines-Ames-West Des Moines, IA
Butte	ID	Idaho Falls-Rexburg-Blackfoot, ID
Adams	IL	Quincy-Hannibal, IL-MO
Clark	IL	
Effingham	IL	
Hamilton	IL	
Macon	IL	Decatur, IL
Macoupin	IL	St. Louis-St. Charles-Farmington, MO-IL
Peoria	IL	Peoria-Canton, IL
Sangamon	IL	Springfield-Jacksonville-Lincoln, IL
Will	IL	Chicago-Naperville, IL-IN-WI
Allen	IN	Fort Wayne-Huntington-Auburn, IN
Delaware	IN	Indianapolis-Carmel-Muncie, IN
Elkhart	IN	South Bend-Elkhart-Mishawaka, IN-MI
Hamilton	IN	Indianapolis-Carmel-Muncie, IN
Hancock	IN	Indianapolis-Carmel-Muncie, IN
Hendricks	IN	Indianapolis-Carmel-Muncie, IN
Huntington	IN	Fort Wayne-Huntington-Auburn, IN
Johnson	IN	Indianapolis-Carmel-Muncie, IN
Knox	IN	
Madison	IN	Indianapolis-Carmel-Muncie, IN
Morgan	IN	Indianapolis-Carmel-Muncie, IN
Shelby	IN	Indianapolis-Carmel-Muncie, IN
Vigo	IN	Terre Haute, IN
Johnson	KS	Kansas City-Overland Park-Kansas City, MO-KS
Trego	KS	
Bell	KY	
Carter	KY	
Morgan	KY	
Perry	KY	
Pike	KY	
Pulaski	KY	
Warren	KY	Bowling Green-Glasgow, KY
Ouachita Parish	LA	Monroe-Ruston-Bastrop, LA
Androscoggin	ME	Portland-Lewiston-South Portland, ME
Aroostook	ME	
Oxford	ME	
Chippewa	MI	
Becker	MN	
Crow Wing	MN	

Notes:
1. This list represents counties with no monitored ozone air pollution in unhealthful ranges using the Air Quality Index based on 2015 NAAQS.

Cleanest Counties for Ozone Air Pollution[1] (cont.)

County	State	Metropolitan Statistical Area
Goodhue	MN	Minneapolis-St. Paul, MN-WI
Hennepin	MN	Minneapolis-St. Paul, MN-WI
Lake	MN	
Mille Lacs	MN	Minneapolis-St. Paul, MN-WI
Olmsted	MN	Rochester-Austin, MN
St. Louis	MN	Duluth, MN-WI
Stearns	MN	Minneapolis-St. Paul, MN-WI
Washington	MN	Minneapolis-St. Paul, MN-WI
Boone	MO	Columbia-Moberly-Mexico, MO
Callaway	MO	Jefferson City, MO
Cass	MO	Kansas City-Overland Park-Kansas City, MO-KS
Greene	MO	Springfield-Branson, MO
Taney	MO	Springfield-Branson, MO
Hinds	MS	Jackson-Vicksburg-Brookhaven, MS
Lauderdale	MS	
Fergus	MT	
Flathead	MT	
Lewis and Clark	MT	
Missoula	MT	Missoula, MT
Phillips	MT	
Powder River	MT	
Richland	MT	
Rosebud	MT	
Alexander	NC	Hickory-Lenoir, NC
Avery	NC	
Buncombe	NC	Asheville-Brevard, NC
Caldwell	NC	Hickory-Lenoir, NC
Carteret	NC	New Bern-Morehead City, NC
Chatham	NC	Raleigh-Durham-Chapel Hill, NC
Durham	NC	Raleigh-Durham-Chapel Hill, NC
Franklin	NC	Raleigh-Durham-Chapel Hill, NC
Granville	NC	Raleigh-Durham-Chapel Hill, NC
Johnston	NC	Raleigh-Durham-Chapel Hill, NC
Lenoir	NC	
Macon	NC	
Martin	NC	
Montgomery	NC	
New Hanover	NC	Wilmington, NC
Pitt	NC	Greenville-Washington, NC
Swain	NC	
Billings	ND	
Burke	ND	
Burleigh	ND	Bismarck, ND
Cass	ND	Fargo-Wahpeton, ND-MN
McKenzie	ND	
Mercer	ND	
Williams	ND	
Knox	NE	
Lancaster	NE	Lincoln-Beatrice, NE
Belknap	NH	Boston-Worcester-Providence, MA-RI-NH-CT
Sandoval	NM	Albuquerque-Santa Fe-Las Vegas, NM
Santa Fe	NM	Albuquerque-Santa Fe-Las Vegas, NM
Albany	NY	Albany-Schenectady, NY
Hamilton	NY	
Herkimer	NY	Utica-Rome, NY
Monroe	NY	Rochester-Batavia-Seneca Falls, NY
Onondaga	NY	Syracuse-Auburn, NY
Steuben	NY	Elmira-Corning, NY
Tompkins	NY	Ithaca-Cortland, NY
Lorain	OH	Cleveland-Akron-Canton, OH
Portage	OH	Cleveland-Akron-Canton, OH
Summit	OH	Cleveland-Akron-Canton, OH
Caddo	OK	
Columbia	OR	Portland-Vancouver-Salem, OR-WA
Bradford	PA	
Clearfield	PA	State College-DuBois, PA
Lycoming	PA	Williamsport-Lock Haven, PA
Abbeville	SC	Greenville-Spartanburg-Anderson, SC
Aiken	SC	Augusta-Richmond County, GA-SC
Anderson	SC	Greenville-Spartanburg-Anderson, SC
Berkeley	SC	Charleston-North Charleston, SC
Charleston	SC	Charleston-North Charleston, SC
Chesterfield	SC	
Colleton	SC	
Darlington	SC	Florence, SC
Oconee	SC	Greenville-Spartanburg-Anderson, SC
Pickens	SC	Greenville-Spartanburg-Anderson, SC
Richland	SC	Columbia-Orangeburg-Newberry, SC
York	SC	Charlotte-Concord, NC-SC
Brookings	SD	
Custer	SD	Rapid City-Spearfish, SD
Jackson	SD	
Meade	SD	Rapid City-Spearfish, SD
Minnehaha	SD	Sioux Falls, SD
Union	SD	Sioux City-Vermillion, IA-SD-NE
Anderson	TN	Knoxville-Morristown-Sevierville, TN
Claiborne	TN	
DeKalb	TN	
Sevier	TN	Knoxville-Morristown-Sevierville, TN
Sullivan	TN	Johnson City-Kingsport-Bristol, TN-VA
Wilson	TN	Nashville-Davidson—Murfreesboro, TN
Brewster	TX	
Cameron	TX	Brownsville-Harlingen-Raymondville, TX
Hidalgo	TX	McAllen-Edinburg, TX
Albemarle	VA	Charlottesville, VA

Notes:
1. This list represents counties with no monitored ozone air pollution in unhealthful ranges using the Air Quality Index based on 2015 NAAQS.

Cleanest Counties for Ozone Air Pollution[1] (cont.)

County	State	Metropolitan Statistical Area
Caroline	VA	Richmond, VA
Chesterfield	VA	Richmond, VA
Fauquier	VA	Washington-Baltimore-Arlington, DC-MD-VA-WV-PA
Frederick	VA	Washington-Baltimore-Arlington, DC-MD-VA-WV-PA
Giles	VA	Blacksburg-Christiansburg-Radford, VA
Madison	VA	
Page	VA	
Roanoke	VA	Roanoke, VA
Rockbridge	VA	
Rockingham	VA	Harrisonburg-Staunton-Waynesboro, VA
Wythe	VA	
Chittenden	VT	Burlington-South Burlington, VT
Clallam	WA	
Pierce	WA	Seattle-Tacoma, WA
Skagit	WA	Seattle-Tacoma, WA
Thurston	WA	Seattle-Tacoma, WA
Whatcom	WA	Bellingham, WA
Ashland	WI	
Eau Claire	WI	Eau Claire-Menomonie, WI
Forest	WI	
La Crosse	WI	La Crosse-Onalaska, WI-MN
Taylor	WI	
Berkeley	WV	Washington-Baltimore-Arlington, DC-MD-VA-WV-PA
Gilmer	WV	
Greenbrier	WV	
Big Horn	WY	
Campbell	WY	
Fremont	WY	
Teton	WY	
Weston	WY	

Notes:
1. This list represents counties with no monitored ozone air pollution in unhealthful ranges using the Air Quality Index based on 2015 NAAQS.

HEALTH EFFECTS

Health Effects of Ozone and Particle Pollution

Two types of air pollution dominate in the U.S.: ozone and particle pollution.[1] These two pollutants threaten the health and the lives of millions of Americans. Thanks to the Clean Air Act, the U.S. has far less of both pollutants now than in the past. Still, more than 125 million people live in counties where monitors show unhealthy levels of one or both—meaning the air a family breathes could shorten life or cause lung cancer.

So what are ozone and particle pollution?

Air pollution remains a major danger to the health of children and adults.

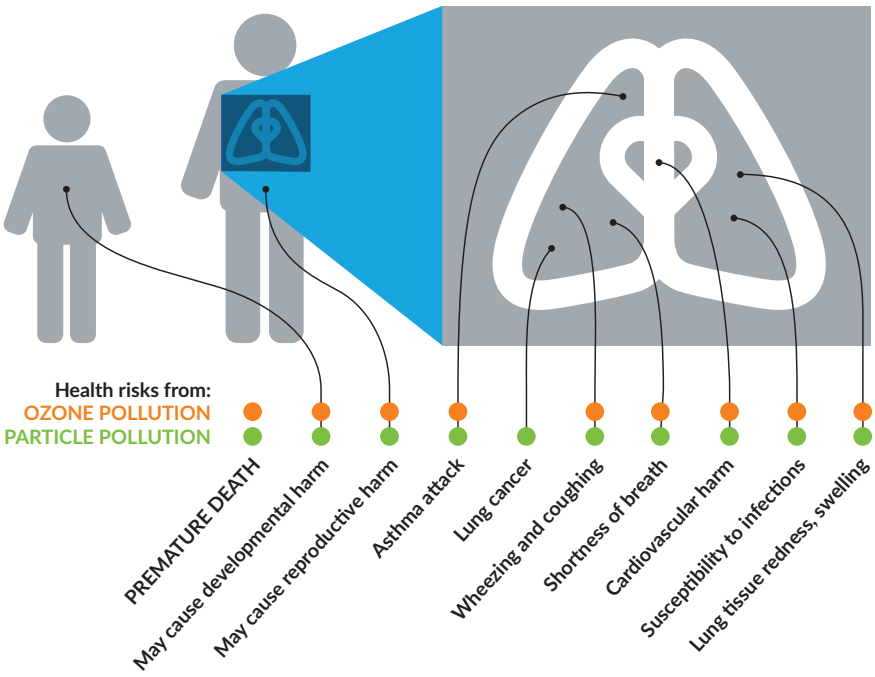

Ozone Pollution

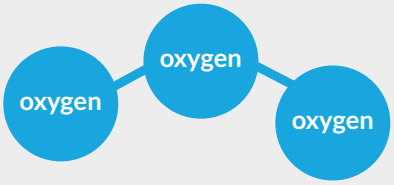

Ozone (O_3) is a gas molecule composed of three oxygen atoms.

It may be hard to imagine that pollution could be invisible, but ozone is. The most widespread pollutant in the U.S. is also one of the most dangerous.

Scientists have studied the effects of ozone on health for decades. Hundreds of research studies have confirmed that ozone harms people at levels currently found in the United States. In the last few years, we've learned that it can also be deadly.

What Is Ozone?

Ozone (O_3) is a gas molecule composed of three oxygen atoms. Often called "smog," ozone is harmful to breathe. Ozone aggressively attacks lung tissue by reacting chemically with it.

The ozone layer found high in the upper atmosphere (the stratosphere) shields us from much of the sun's ultraviolet radiation. However, ozone air pollution at ground level where we can breathe it (in the troposphere) causes serious health problems.

Where Does Ozone Come From?

Ozone develops in the atmosphere from gases that come out of tailpipes, smokestacks and many other sources. When these gases come in contact with sunlight, they react and form ozone smog.

The essential raw ingredients for ozone come from nitrogen oxides (NO_x); hydrocarbons, also called volatile organic compounds (VOCs); and carbon monoxide (CO). They are

When gases that come out of tailpipes and smokestacks come in contact with sunlight, they react and form ozone smog.

produced primarily when fossil fuels like gasoline, oil or coal are burned or when some chemicals, like solvents, evaporate. NOx is emitted from power plants, motor vehicles and other sources of high-heat combustion. VOCs are emitted from motor vehicles, chemical plants, refineries, factories, gas stations, paint and other sources. CO is also primarily emitted from motor vehicles.[2]

If the ingredients are present under the right conditions, they react to form ozone. And because the reaction takes place in the atmosphere, the ozone often shows up downwind of the sources of the original gases. In addition, winds can carry ozone far from where it began.

You may have wondered why "ozone action day" warnings are sometimes followed by recommendations to avoid activities such as mowing your lawn or driving your car. Lawn mower exhaust and gasoline vapors are VOCs that could turn into ozone in the heat and sun.

Who Is at Risk from Breathing Ozone?

Anyone who spends time outdoors where ozone pollution levels are high may be at risk. Five groups of people are especially vulnerable to the effects of breathing ozone:

- children and teens;[3]
- anyone 65 and older;[4]
- people who work or exercise outdoors;[5]
- people with existing lung diseases, such as asthma and chronic obstructive pulmonary disease (also known as COPD, which includes emphysema and chronic bronchitis);[6] and
- people with cardiovascular disease.[7]

In addition, some evidence suggests that other groups—including women, people who suffer from obesity and people with low incomes—may also face higher risk from ozone.[8] More research is needed to confirm these findings.

A major new study found evidence that people with lung cancer faced greater risk from ozone and other outdoor air pollutants. The 2016 study tracked the air pollution levels from 1988 to 2011 that more than 350,000 cancer patients in California experienced. The researchers found that the ozone and other air pollutants shortened their survival.[9]

The impact on your health can depend on many factors, however. For example, the risks would be greater if ozone levels are higher, if you are breathing faster because you're working outdoors or if you spend more time outdoors.

Lifeguards in Galveston, Texas, provided evidence of the impact of even short-term exposure to ozone on healthy, active adults in a study published in 2008. Testing the breathing capacity of these outdoor workers several times a day, researchers found that many lifeguards had greater obstruction in their airways when ozone levels were high. Because of this research, Galveston became the first city in the nation to install an air quality warning flag system on the beach.[10]

How Ozone Pollution Harms Your Health

Premature death. Breathing ozone can shorten your life. Strong evidence exists of the deadly impact of ozone in large studies conducted in cities across the U.S., in Europe and in Asia. Researchers repeatedly found that the risk of premature death increased with higher levels of ozone.[11] Newer research has confirmed that ozone increased the risk of premature death even when other pollutants also exist.[12]

Immediate breathing problems. Many areas in the United States produce enough ozone during the summer months to cause health problems that can be felt right away. Immediate problems—in addition to increased risk of premature death—include:

- shortness of breath, wheezing and coughing;
- asthma attacks;
- increased risk of respiratory infections;
- increased susceptibility to pulmonary inflammation; and
- increased need for people with lung diseases, like asthma or chronic obstructive pulmonary disease (COPD), to receive medical treatment and to go to the hospital.[13]

Cardiovascular effects. Inhaling ozone may affect the heart as well as the lungs. A 2006 study linked exposures to high ozone levels for as little as one hour to a particular type of cardiac arrhythmia that itself increases the risk of premature death and stroke.[14] A French study found that exposure to elevated ozone levels for one to two days increased the risk of heart attacks for middle-aged adults without heart disease.[15] Several studies around the world have found increased risk of hospital admissions or emergency department visits for cardiovascular disease.[16]

Long-term exposure risks. New studies warn of serious effects from breathing ozone over longer periods. With more long-term data, scientists are finding that long-term exposure—that is, for periods longer than eight hours, including days, months or years—may increase the risk of onset of asthma or early death.

- Examining the records from a long-term national database, researchers found a higher risk of death from respiratory diseases associated with increases in ozone.[17]
- New York researchers looking at hospital records for children's asthma found that the risk of admission to hospitals for asthma increased with chronic exposure to ozone. Younger children and children from low-income families were more likely than other children to need hospital admissions even during the same time periods.[18]
- California researchers analyzing data from their long-term Southern California Children's Health Study found that some children with certain genes were more likely to develop asthma as adolescents in response to the variations in ozone levels in their communities.[19]
- Studies link lower birth weight and decreased lung function in newborns to ozone levels in their community.[20] This research provides increasing evidence that ozone may harm newborns.

Breathing other pollutants in the air may make your lungs more responsive to ozone—and breathing ozone may increase your body's response to other pollutants. For example, research warns that breathing sulfur dioxide and nitrogen oxide—two pollutants common in the eastern U.S.—can make the lungs react more strongly than to just breathing ozone alone. Breathing ozone may also increase the response to allergens in people with allergies. A large study published in 2009 found that children were more likely to suffer from hay fever and respiratory allergies when ozone and $PM_{2.5}$ levels were high.[21]

Research shows lower level of ozone causes harm. The EPA released their latest complete review of the current research on ozone pollution in February 2013.[22] The EPA had engaged a panel of expert scientists, the Clean Air Scientific Advisory Committee, to help them assess the evidence; in particular, they examined research published between 2006 and 2012. The experts on the Committee and EPA concluded that ozone pollution posed multiple, serious threats to health. Their findings are highlighted in the box on the next page.

EPA Concludes Ozone Pollution Poses Serious Health Threats

- Causes respiratory harm (e.g., worsened asthma, worsened COPD, inflammation)
- Likely to cause early death (both short-term and long-term exposure)
- Likely to cause cardiovascular harm (e.g., heart attacks, strokes, heart disease, congestive heart failure)
- May cause harm to the central nervous system
- May cause reproductive and developmental harm

—U.S. Environmental Protection Agency, *Integrated Science Assessment for Ozone and Related Photochemical Oxidants*, 2013. EPA/600/R-10/076F.

Based on that review, the EPA set more protective limits, called national ambient air quality standards, on ozone pollution in October 2015. These official limits drive the cleanup of ozone pollution nationwide. The Clean Air Act requires EPA to review the standards every five years to make sure that they protect the health of the public.

Particle Pollution

Ever look at dirty truck exhaust?

The dirty, smoky part of that stream of exhaust is made of particle pollution. Overwhelming evidence shows that particle pollution—like that coming from that exhaust smoke—can kill. Particle pollution can increase the risk of heart disease, lung cancer and asthma attacks and can interfere with the growth and work of the lungs.

What Is Particle Pollution?

Particle pollution refers to a mix of very tiny solid and liquid particles that are in the air we breathe. But nothing about particle pollution is simple. And it is so dangerous, it can shorten your life.

Particle pollution refers to a mix of very tiny solid and liquid particles that are in the air we breathe. But nothing about particle pollution is simple. And it is so dangerous, it can shorten your life.

Size matters. Particles themselves are different sizes. Some are one-tenth the diameter of a strand of hair. Many are even tinier; some are so small they can only be seen with an electron microscope. Because of their size, you can't see the individual particles. You can only see the haze that forms when millions of particles blur the spread of sunlight.

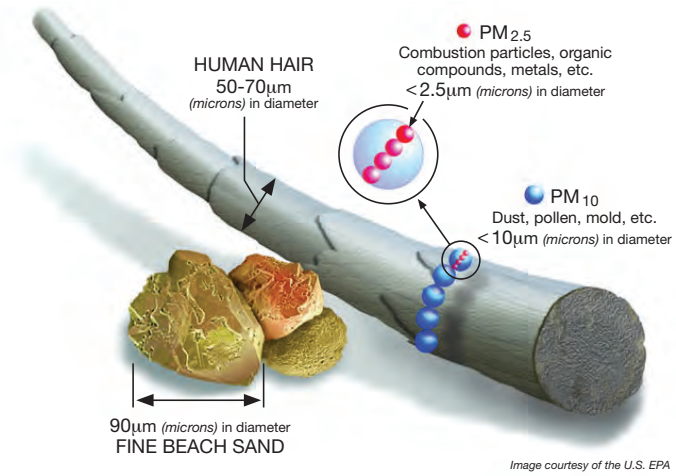

Image courtesy of the U.S. EPA

The differences in size make a big difference in how they affect us. Our natural defenses help us to cough or sneeze larger particles out of our bodies. But those defenses don't keep out smaller particles, those that are smaller than 10 microns (or micrometers) in diameter, or about one-seventh the diameter of a single human hair. These particles get

trapped in the lungs, while the smallest are so minute that they can pass through the lungs into the bloodstream, just like the essential oxygen molecules we need to survive.

Researchers categorize particles according to size, grouping them as coarse, fine and ultrafine. Coarse particles fall between 2.5 microns and 10 microns in diameter and are called $PM_{10-2.5}$. Fine particles are 2.5 microns in diameter or smaller and are called $PM_{2.5}$. Ultrafine particles are smaller than 0.1 micron in diameter[23] and are small enough to pass through the lung tissue into the blood stream, circulating like the oxygen molecules themselves. No matter what the size, particles can harm your health.

"A mixture of mixtures." Because particles form in so many different ways, they can be composed of many different compounds. Although we often think of particles as solids, not all are. Some are completely liquid; others are solids suspended in liquids. As the EPA puts it, particles are really "a mixture of mixtures."[24]

The mixtures differ between the eastern and western United States and in different times of the year. For example, the Midwest, Southeast and Northeast states have more sulfate particles than the West on average, largely due to the high levels of sulfur dioxide emitted by large, coal-fired power plants. By contrast, nitrate particles from motor vehicle exhaust form a larger proportion of the unhealthful mix in the winter in the Northeast, Southern California, the Northwest and North Central U.S.[25]

Who Is at Risk?

Anyone who lives where particle pollution levels are high is at risk. Some people face higher risk, however. People at the greatest risk from particle pollution exposure include:

- Infants, children and teens;[26]
- People over 65 years of age;[27]
- People with lung disease such as asthma and chronic obstructive pulmonary disease (COPD), which includes chronic bronchitis and emphysema;
- People with heart disease[28] or diabetes;[29]
- People with low incomes;[30] and
- People who work or are active outdoors.[31]

Diabetics face increased risk at least in part because of their higher risk for cardiovascular disease.[32]

People with lung cancer also appear to be at higher risk from particle pollution, according to the 2016 study of more than 350,000 patients in California. Researchers looked at the exposure they experienced between 1988 and 2011 and found that where higher concentrations of particle pollution existed, people with lung cancer had shorter life spans.[33]

What Can Particles Do to Your Health?

Particle pollution can be very dangerous to breathe. Breathing particle pollution may trigger illness, hospitalization and premature death, risks that are showing up in new studies that validate earlier research.

Breathing particle pollution may trigger illness, hospitalization and premature death.

Thanks to steps taken to reduce particle pollution, good news is growing from researchers who study the drop in year-round levels of particle pollution.

Looking at air quality in 545 counties in the U.S. between 2000 and 2007, researchers found that people had approximately four months added to their life expectancy on average due to cleaner air. Women and people who lived in urban and densely populated counties benefited the most.[34]

Another long-term study of six U.S. cities tracked from 1974 to 2009 added more evidence of the benefits. Their findings suggest that cleaning up particle pollution

had almost immediate health benefits. They estimated that the U.S. could prevent approximately 34,000 premature deaths a year if the nation could lower annual levels of particle pollution by 1 µg/m^3.[35]

Other researchers estimated that reductions in air pollution can be expected to produce rapid improvements in public health, with fewer deaths occurring within the first two years after reductions.[36]

These studies add to the growing research that cleaning up air pollution improves life and health.

Short-Term Exposure Can Be Deadly

First and foremost, short-term exposure to particle pollution can kill. Peaks or spikes in particle pollution can last for hours to days. Deaths can occur on the very day that particle levels are high, or within one to two months afterward. Particle pollution does not just make people die a few days earlier than they might otherwise—these are deaths that would not have occurred if the air were cleaner.[37]

Even low levels of particles can be deadly. A 2016 study found that people age 65 and older in New England faced a higher risk of premature death from particle pollution, even in places that met current standards for short-term particle pollution.[38] Another study in 2017 looked more closely at Boston and found a similar higher risk of premature death from particle pollution in a city that meets current limits on short-term particle pollution.[39]

Particle pollution also diminishes lung function, causes greater use of asthma medications and increased rates of school absenteeism, emergency room visits and hospital admissions. Other adverse effects include coughing, wheezing, cardiac arrhythmias and heart attacks. According to extensive research, short-term increases in particle pollution have been linked to:

- death from respiratory and cardiovascular causes, including strokes;[40, 41, 42, 43]
- increased mortality in infants and young children;[44]
- increased numbers of heart attacks, especially among the elderly and in people with heart conditions;[45]
- inflammation of lung tissue in young, healthy adults;[46]
- increased hospitalization for cardiovascular disease, including strokes and congestive heart failure;[47, 48, 49]
- increased emergency room visits for patients suffering from acute respiratory ailments;[50]
- increased hospitalization for asthma among children;[51, 52, 53] and
- increased severity of asthma attacks in children.[54]

Again, the impact of even short-term exposure to particle pollution on healthy adults was demonstrated in the Galveston lifeguard study. In addition to the harmful effects of ozone pollution, lifeguards had reduced lung volume at the end of the day when fine particle levels were high.[55]

Year-Round Exposure

Breathing high levels of particle pollution day in and day out can also be deadly, as landmark studies in the 1990s conclusively showed[56] and as other studies confirmed.[57] Chronic exposure to particle pollution can shorten life by one to three years.[58] Recent research has confirmed that long-term exposure to particle pollution still kills, even with the declining levels in the U.S. since 2000 [59] and even in areas, such as New England, that currently meet the official limit, or standard, for year-round particle pollution.[60]

In late 2013, the World Health Organization concluded that particle pollution could cause lung cancer.

In late 2013, the International Agency for Research on Cancer, part of the World Health Organization, concluded that particle pollution could cause lung cancer. The IARC reviewed the most recent research and reported that the risk of lung cancer increases as the particle levels rise.[61]

Year-round exposure to particle pollution has also been linked to:

- increased hospitalization for asthma attacks for children living near roads with heavy truck or trailer traffic;[62, 63]
- slowed lung function growth in children and teenagers;[64, 65]
- development of asthma in children up to age 14;[66]
- significant damage to the small airways of the lungs;[67]
- increased risk of death from cardiovascular disease;[68] and
- increased risk of lower birth weight and infant mortality.[69]

Research into the health risks of 65,000 women over age 50 found that those who lived in areas with higher levels of particle pollution faced a much greater risk of dying from heart disease than had been previously estimated. Even women who lived within the same city faced differing risks depending on the annual levels of pollution in their neighborhood.[70]

New research has found evidence that long-term exposure to particle pollution may increase the risk of developing diabetes. Two independent reviews of published research found that particle pollution may increase the risk of developing type 2 diabetes mellitus.[71]

Scientists have found links between particle pollution and mental health concerns. A study of 27,000 residents in Seoul, Korea, found that breathing particle pollution over a long time increased the risk of major depressive disorder. The risk was higher for those who also had a chronic disease such as asthma, COPD, or diabetes.[72] Older adults suffered more symptoms of depression and anxiety when particle pollution was higher in a large study looking at data from community living groups across the United States. Those who lived in lower socioeconomic situations or who had a history of respiratory illness or heart disease were more likely to have anxiety symptoms.[73]

The EPA completed their most recent review of the current research on particle pollution in December 2009.[74] The EPA had engaged a panel of expert scientists, the Clean Air Scientific Advisory Committee, to help them assess the evidence. The EPA concluded that particle pollution caused multiple, serious threats to health. Their findings are highlighted in the box below.

EPA Concludes Fine Particle Pollution Poses Serious Health Threats

- Causes early death (both short-term and long-term exposure)
- Causes cardiovascular harm (e.g., heart attacks, strokes, heart disease, congestive heart failure)
- Likely to cause respiratory harm (e.g., worsened asthma, worsened COPD, inflammation)
- May cause cancer
- May cause reproductive and developmental harm

—U.S. Environmental Protection Agency, *Integrated Science Assessment for Particulate Matter*, December 2009. EPA 600/R-08/139F

Chemical processes in the atmosphere create most of the tiniest particles.

Where Does Particle Pollution Come From?

Particle pollution is produced through two separate processes—mechanical and chemical.

Mechanical processes break down bigger bits into smaller bits with the material remaining essentially the same, only becoming smaller. Mechanical processes primarily create coarse particles.[75] Dust storms, construction and demolition, mining operations, and agriculture are among the activities that produce coarse particles. Tire, brake pad and road wear can also create coarse particles. Bacteria, pollen, mold, and plant and animal debris are also included as coarse particles.[76]

By contrast, chemical processes in the atmosphere create most of the tiniest fine and ultrafine particles. Combustion sources burn fuels and emit gases. These gases can vaporize and then condense to become a particle of the same chemical compound. Or they can react with other gases or particles in the atmosphere to form a particle of a different chemical compound. Particles formed by this latter process come from the reaction of elemental carbon (soot), heavy metals, sulfur dioxide (SO_2), nitrogen oxides (NO_x) and volatile organic compounds with water and other compounds in the atmosphere.[77] Burning fossil fuels in factories, power plants, steel mills, smelters, diesel- and gasoline-powered motor vehicles (cars and trucks) and equipment generate a large part of the raw materials for fine particles. So does burning wood in residential fireplaces and wood stoves or burning agricultural fields or forests.

Are Some Particles More Dangerous Than Others?

With so many sources of particles, researchers want to know if some particles pose greater risk than others. Researchers are exploring possible differences in health effects of the sizes of particles and particles from different sources, such as diesel particles from trucks and buses or sulfates from coal-fired power plants. Recent studies have tried to answer this question. So far, the answers are complicated.

Each particle may have many different components. The building blocks of each can include several biological and chemical components. Bacteria, pollen and other biological ingredients can combine in the particle with chemical agents, such as heavy metals, elemental carbon, dust and secondary species like sulfates and nitrates. These combinations mean that particles can have complex effects on the body.[78]

Some studies have found different kinds of particles may have greater risk for different health outcomes.

- For example, one 2015 study found that particles from burning fossil fuels, including coal-burning and diesel emissions, increased the risk of dying prematurely from ischemic heart disease, but that particles from wind-blown soil and biomass combustion did not.[79]
- Another recent study looked at older adults in Connecticut and Massachusetts and found that breathing black carbon, calcium and road dust particles was more likely to send them to the hospital for cardiovascular and respiratory problems than other particles.[80]
- Some of the same researchers found that when they looked at the risk of low birthweight for newborns in the Northeast and Mid-Atlantic states, different particles harmed some groups more than others.[81]

Other studies have identified the challenges of exploring all the kinds of particles and their health effects with the limited monitoring across the nation.[82] Some particles serve as carriers for other chemicals that are also toxic, and the combination may worsen the impact.[83, 84]

The best evidence shows that having less of all types of particles in the air leads to better health and longer lives.

Focusing on Children's Health

Children face special risks from air pollution because their lungs are growing and because they are so active.

Just like the arms and legs, the largest portion of a child's lungs will grow long after he or she is born. Eighty percent of their tiny air sacs develop after birth. Those sacs, called the alveoli, are where the life-sustaining transfer of oxygen to the blood takes place. The lungs and their alveoli aren't fully grown until children become adults.[85] In addition, the body's defenses that help adults fight off infections are still developing in young bodies.[86] Children have more respiratory infections than adults, which also seems to increase their susceptibility to air pollution.[87]

Furthermore, children don't behave like adults, and their behavior also affects their vulnerability. They are outside for longer periods and are usually more active when outdoors. Consequently, they inhale more polluted outdoor air than adults typically do.[88]

Air Pollution Affects Children Before They Are Born

Several studies have found air pollution linked to harm to children while they are still in the womb. A large study in California found that higher particle pollution levels increased the risk of preterm birth.[89] Pregnant women exposed to even low levels of particle pollution had higher risk factors for preterm birth in a Boston study.[90] Preterm births occurred more frequently when particle pollution spiked, as an Australian study found, even when they controlled for other risk factors.[91]

> The largest portion of a child's lungs will grow long after he or she is born.

Air Pollution Increases Risk of Underdeveloped Lungs

The Southern California Children's Health study looked at the long-term effects of particle pollution on teenagers. Tracking 1,759 children who were between ages 10 and 18 from 1993 to 2001, researchers found that those who grew up in more polluted areas face the increased risk of having underdeveloped lungs, which may never recover to their full capacity. The average drop in lung function was 20 percent below what was expected for the child's age, similar to the impact of growing up in a home with parents who smoked.[92]

Community health studies are pointing to less obvious, but serious effects from year-round exposure to ozone, especially for children. Scientists followed 500 Yale University students and determined that living just four years in a region with high levels of ozone and related co-pollutants was associated with diminished lung function and frequent reports of respiratory symptoms.[93] A much larger study of 3,300 schoolchildren in Southern California found reduced lung function in girls with asthma and boys who spent more time outdoors in areas with high levels of ozone.[94]

Cleaning Up Pollution Can Reduce Risk to Children

There is also real-world evidence that reducing air pollution can help protect children.

A 2015 follow-up to that Southern California Children's Health study showed that reducing pollution could improve children's health. This time they tracked a different group of 863 children living in the same area, but growing up between 2007 and 2011, when the air in Southern California was much cleaner. They compared these children to those who had been part of their earlier studies when the air was dirtier. Children growing up in the cleaner air had much greater lung function, a benefit that may help them throughout their lives. As the researchers noted, their study suggested that "all children have the potential to benefit from improvements in air quality." [95]

In Switzerland, particle pollution dropped during a period in the 1990s. Researchers there tracked 9,000 children over a nine-year period, following their respiratory symptoms. After taking other factors such as family characteristics and indoor air pollution into account, the researchers noted that during the years with less pollution, the children had fewer episodes of chronic cough, bronchitis, common cold and conjunctivitis symptoms.[96]

Disparities in the Impact of Air Pollution

Poorer people and some racial and ethnic groups often face higher exposure and greater responses to pollution.

The burden of air pollution is not evenly shared. Poorer people and some racial and ethnic groups are among those who often face higher exposure to pollutants and who may experience greater responses to such pollution. Many studies have explored the differences in harm from air pollution to racial or ethnic groups and people who are in a low socioeconomic position, have less education, or live nearer to major sources,[97] including a workshop the American Lung Association held in 2001 that focused on urban air pollution and health inequities.[98]

Many studies have looked at differences in the impact on premature death. Results have varied widely, particularly for effects between racial groups. Some studies have found no differences among races,[99] while others found greater responsiveness for whites and Hispanics, but not African Americans,[100] or for African Americans but not other races or ethnic groups.[101] Other researchers have found greater risk for African Americans from hazardous air pollutants, including those pollutants that also come from traffic sources.[102]

Socioeconomic position has been more consistently associated with greater harm from air pollution. Multiple large studies show evidence of that link. Low socioeconomic status consistently increased the risk of premature death from fine particle pollution among 13.2 million Medicare recipients studied in the largest examination of particle pollution mortality nationwide.[103] In the 2008 study that found greater risk for premature death for African Americans, researchers also found greater risk for people living in areas with higher unemployment or higher use of public transportation.[104] A 2008 study of Washington, DC, found that while poor air quality and worsened asthma went hand in hand in areas where Medicaid enrollment was high, the areas with the highest Medicaid enrollment did not always have the strongest association of high air pollution and asthma attacks.[105] A 2016 study of New Jersey residents found that the risk of dying early from long-term exposure to particle pollution was higher in communities with larger African-American populations, lower home values and lower median income.[106] However, two other studies in France have found no association with lower income and asthma attacks.[107]

Scientists have speculated that there are three broad reasons why disparities may exist. First, groups may face greater exposure to pollution because of factors ranging from racism to class bias to housing market dynamics and land costs. For example, pollution sources may be located near disadvantaged communities, increasing exposure to harmful pollutants. Second, low social position may make some groups more susceptible to health threats because of factors related to their disadvantage. Lack of access to health care, grocery stores and good jobs; poorer job opportunities; dirtier workplaces or higher traffic exposure are among the factors that could handicap groups and increase the risk of harm. Finally, existing health conditions, behaviors or traits may predispose some groups to greater risk. For example, diabetics are among the groups most at risk from air pollutants, and the elderly, African Americans, Mexican Americans and people living near a central city have higher incidence of diabetes.[108]

Communities of color also may be more likely to live in counties with higher levels of pollution. Non-Hispanic blacks and Hispanics were more likely to live in counties that had worse problems with particle pollution, researchers found in a 2011 analysis. Non-Hispanic blacks were also more likely to live in counties with worse ozone pollution. Income groups, by contrast, differed little in these exposures. However, since few rural counties have monitors, the primarily older, non-Hispanic white residents of those counties lack information about the air quality in their communities.[109]

Unemployed people, those with low income or low education and non-Hispanic blacks were found to be more likely to live in areas with higher exposures to particle pollution in a 2012 study. However, the different racial/ethnic and income groups were often breathing very different kinds of particles; the different composition and structure of these particles may have different health impacts.[110]

Highways May Be Especially Dangerous for Breathing

Being in heavy traffic or living near a road may be even more dangerous than being in other places in a community. Growing evidence shows that the vehicle emissions coming directly from those highways may be higher than in the community as a whole, increasing the risk of harm to people who live or work near busy roads.

The number of people living "next to a busy road" may include 30 to 45 percent of the urban population in North America, according to the most recent review of the evidence. In January 2010, the Health Effects Institute published a major review of the evidence by a panel of expert scientists. The panel looked at over 700 studies from around the world, examining the health effects. They concluded that traffic pollution causes asthma attacks in children, and may cause a wide range of other effects including the onset of childhood asthma, impaired lung function, premature death and death from cardiovascular diseases, and cardiovascular morbidity. The area most affected, they concluded, was roughly 0.2 to 0.3 miles (300 to 500 meters) from the highway.[111]

Children and teenagers are among the most vulnerable—though not the only ones at risk. A Danish study found that long-term exposure to traffic air pollution may increase the risk of developing chronic obstructive pulmonary disease (COPD). They found that those most at risk were people who already had asthma or diabetes.[112] Studies have found increased risk of premature death from living near a major highway or an urban road.[113] Another study found an increase in risk of heart attacks from being in traffic, whether driving or taking public transportation.[114] Urban women in a Boston study experienced decreased lung function associated with traffic-related pollution.[115]

Adults living closer to the road—within 300 meters—may risk dementia. In 2017, a study of residents of Ontario, Canada, found that those who lived close to heavy traffic had a higher risk of dementia, though not for Parkinson's disease or multiple sclerosis. Researchers found the strongest association among those who lived closest to the roads (less than 50 meters), who had never moved and who lived in major cities.[116] A study of older men in 2011 also found that long-term exposure to traffic pollution increased their risk of having poor cognition.[117]

How to Protect Yourself from Ozone and Particle Pollution

To minimize your exposure to ozone and particle pollution:

- Pay attention to forecasts for high air pollution days to know when to take precautions;
- Avoid exercising near high-traffic areas;
- Avoid exercising outdoors when pollution levels are high, or substitute an activity that requires less exertion;
- Do not let anyone smoke indoors and support measures to make all places smokefree; and
- Reduce the use of fireplaces and wood-burning stoves.

Bottom line: Help yourself and everyone else breathe easier. Support national, state and local efforts to clean up sources of pollution. Your life and the life of someone you love may depend on it.

Support national, state and local efforts to clean up sources of pollution. Your life and the life of someone you love may depend on it.

1 Ozone and particle pollution are the most widespread, but they aren't the only serious air pollutants. Others include carbon monoxide, lead, nitrogen dioxide, and sulfur dioxide, as well as scores of toxins such as mercury, arsenic, benzene, formaldehyde, and acid gases. However, the monitoring networks are not as widespread nationwide for the other pollutants.

2 U.S. Environmental Protection Agency. *Integrated Science Assessment of Ozone and Related Photochemical Oxidants (Final Report).* U.S. Environmental Protection Agency, Washington, DC, EPA/600/R-10/076F, 2013.

3 Mar TF, Koenig JQ. Relationship between visits to emergency departments for asthma and ozone exposure in greater Seattle, Washington. *Ann Allergy Asthma Immunol.* 2009; 103: 474-479. Villeneuve PJ, Chen L, Rowe BH, Coates F. Outdoor air pollution and emergency department visits for asthma among children and adults: A case-crossover study in northern Alberta, Canada. *Environ Health Global Access Sci Source.* 2007; 6: 40.

4 Medina-Ramón M, Schwartz J. Who is more vulnerable to die from ozone air pollution? *Epidemiology.* 2008; 19: 672-679.

5 Thaller EI, Petronell SA, Hochman D, Howard S, Chhikara RS, Brooks EG. Moderate increases in ambient $PM_{2.5}$ and ozone are associated with lung function decreases in beach lifeguards. *J Occp Environ Med.* 2008; 50: 202-211; Sawyer K, Brown J, Hazucha M, Bennett WD. The effect of exercise on nasal uptake of ozone in healthy human adults. *J Appl Physiol.* 2007;102: 1380-1386; Hu SC, Ben-Jebria A, Ultman JS. Longitudinal distribution of ozone absorption in the lung: Effects of respiratory flow. *J Appl Physiol.* 1994; 77: 574-583.

6 Horstman DH, Ball BA, Brown J, Gerrity T, Folinsbee LJ. Comparison of pulmonary responses of asthmatic and nonasthmatic subjects performing light exercise while exposed to a low level of ozone. *Toxicol Ind Health.* 1995; 11: 369-385; Kreit JW, Gross KB, Moore TB, Lorenzen TJ, D'Arcy J, Eschenbacher WL. Ozone-induced changes in pulmonary function and bronchial responsiveness in asthmatics. *J Appl Physiol.* 1989; 66: 217-222; Medina-Ramón M, Zanobetti A, Schwartz J. The effect of ozone and PM_{10} on hospital admissions for pneumonia and chronic obstructive pulmonary disease: A national multicity study. *Am J Epidemiol.* 2006; 163(6):579-588.

7 Peel JL, Metzger KB, Klein M, Flanders WD, Mulholland JA, Tolbert PE. Ambient air pollution and cardiovascular emergency department visits in potentially sensitive groups. *Am J Epidemiol.* 2007; 165: 625-633; Medina-Ramón and Schwartz, 2008; Medina-Ramón M, Zanobetti A, Schwartz J, 2006.

8 Medina-Ramón and Schwartz, 2008; Stafoggia M, Forastiere F, Faustini A, Biggeri A, Bisanti L, et al. Susceptibility factors to ozone-related mortality: A population-based case-crossover analysis. *Am J Respir Crit Care Med.* 2010; 182: 376-384; Jerrett M, Burnett RT, Pope CA III, Ito K, Thurston G, Krewski D, Shi Y, Calle E, Thun M. Long-term ozone exposure and mortality. *N Engl J Med.* 2009;360: 1085-1095; Alexeeff SE, Litonjua AA, Suh H, Sparrow D, Vokonas PS, Schwartz J. Ozone exposure and lung function: Effect modified by obesity and airways hyperresponsiveness in the VA Normative Aging Study. *Chest.* 2007; 132: 1890-1897; McDonnell WF, Stewart PW, Smith MV. Prediction of ozone-induced lung function responses in humans. *Inhal Toxicol.* 2010; 22: 160-168. Lin S, Liu X, Le LH, Hwang SA. Chronic exposure to ambient ozone and asthma hospital admissions among children. *Environ Health Perspect.* 2008; 116: 1725-1730; Burra TA, Moineddin R, Agha MM, Glazier RH. Social disadvantage, air pollution, and asthma physician visits in Toronto, Canada. *Environ Res.* 2009; 109: 567-574.

9 Eckel SP, Cockburn M, Shu Y-H, et al. F. Air pollution affects lung cancer survival. *Thorax.* 2016: 71: 891-898.

10 Thaller, et al., 2008.

11 Bell ML, McDermott A, Zeger SL, Samet JM, Dominici F. Ozone and short-term mortality in 95 US urban communities, 1987-2000. *JAMA.* 2004; 292:2372-2378. Gryparis A, Forsberg B, Katsouyanni K, et al. Acute Effects of Ozone on Mortality from the "Air Pollution and Health: a European approach" project. *Am J Respir Crit Care Med.* 2004; 170: 1080-1087. Bell ML, Dominici F, and Samet JM. A meta-analysis of time-series studies of ozone and mortality with comparison to the national morbidity, mortality, and air pollution study. *Epidemiology.* 2005; 16:436-445. Levy JI, Chermerynski SM, Sarnat JA. Ozone exposure and mortality: An empiric Bayes metaregression analysis. *Epidemiology.* 2005; 16:458-468. Ito K, De Leon SF, Lippmann M. Associations between ozone and daily mortality: Analysis and meta-analysis. *Epidemiology.* 2005; 16:446-429.

12 Zanobetti A, Schwartz J. Mortality displacement in the association of ozone with mortality: An analysis of 48 cities in the United States. *Am J Respir Crit Care Med.* 2008; 177:184-189; Katsouyanni K, Samet JM, Anderson HR, Atkinson R, Le Tertre A, et al. *Air pollution and health: A European and North American approach (APHENA).* Boston, MA: Health Effects Institute, 2009; Samoli E, Zanobetti A, Schwartz J, Atkinson R, Le Tertre A, et al. The temporal pattern of mortality responses to ambient ozone in the APHEA project. *J Epidemiol Community Health.* 2009; 63: 960-966; Stafoggia M, et al, 2010.

13 Gent JF, Triche EW, Holford TR, Belanger K, Bracken MB, Beckett WS, Leaderer BP. Association of low-level ozone and fine particles with respiratory symptoms in children with asthma. *JAMA.* 2003; 290:1859-1867; Desqueyroux H, Pujet JC, Prosper M, Squinazi F, Momas I. Short-term effects of low-level air pollution on respiratory health of adults suffering from moderate to severe asthma. *Environ Res.* 2002; 89:29-37; Burnett RT, Brook JR, Yung WT, Dales RE, Krewski D. Association between ozone and hospitalization for respiratory diseases in 16 Canadian cities. *Environ Res.* 1997; 72:24-31; Medina-Ramón M, Zanobetti A, Schwartz J. The effect of ozone and PM_{10} on hospital admissions for pneumonia and chronic obstructive pulmonary disease: A national multicity study. *Am J Epidemiol.* 2006; 163(6):579-588.

14 Rich DQ, Mittleman MA, Link MS, Schwartz J, Luttmann-Gibson H, Catalano PJ, Speizer FE, Gold DR, Dockery DW. Increased risk of paroxysmal atrial fibrillation episodes associated with acute increases in ambient air pollution. *Environ Health Perspect.* 2006; 114:120-123.

15 Ruidavets J-B, Cournot M, Cassadou S, Giroux M, Meybeck M, Ferrières J. Ozone air pollution is associated with acute myocardial infarction. *Circulation.* 2005; 111:563-569.

16 Azevedo JM, Gonçalves FL, de Fátima Andrade M. Long-range ozone transport and its impact on respiratory and cardiovascular health in the north of Portugal. *Int J Biometeorol.* 2011; 55: 187-202; Linares C, Díaz J. Short-term effect of concentrations of fine particulate matter on hospital admissions due to cardiovascular and respiratory causes among the over-75 age group in Madrid, Spain. *Public Health.* 2010; 124: 28-36; Middleton N, Yiallouros P, Kleanthous S, Kolokotroni O, Schwartz J, et al. A 10-year time-series analysis of respiratory and cardiovascular morbidity in Nicosia, Cyprus: The effect of short-term changes in air pollution and dust storms. *Environ Health.* 2008; 7: 39; Lee JT, Kim H, Cho YS, Hong YC, Ha EH, Park H. Air pollution and hospital admissions for ischemic heart diseases among individuals 64+ years of age residing in Seoul, Korea. *Arch Environ Health.* 2003; 58: 617-623; Wong TW, Lau TS, Yu TS, Neller A, Wong SL, Tam W, Pang SW. Air pollution and hospital admissions for respiratory and cardiovascular diseases in Hong Kong. *Occup Environ Med.* 1999; 56: 679-683.

17 Jerrett M, et al., 2009.

18 Lin S, Liu X, Le LH, Hwang S-A. Chronic exposure to ambient ozone and asthma hospital admissions among children. *Environ Health Perspect.* 2008; 116:1725-1730.

19 Islam T, McConnell R, Gauderman WJ, Avol E, Peters JM, Gilliland F. Ozone, oxidant defense genes, and risk of asthma during adolescence. *Am J Respir Crit Care Med.* 2009; 177(4):388-395.

20 Salam MT, Millstein J, Li YF, Lurmann FW, Margolis HG, Gilliland FD. Birth outcomes and prenatal exposure to ozone, carbon monoxide, and particulate matter: Results from the Children's Health Study. *Environ Health Perspect.* 2005; 113: 1638-1644; Morello-Frosch R, Jesdale BM, Sadd JL, Pastor M. Ambient air pollution exposure and full-term birth weight in California. *Environ Health.* 2010; 9: 44; Hansen CA, Barnett AG, Pritchard G. The effect of ambient air pollution during early pregnancy on fetal ultrasonic measurements during mid-pregnancy. *Environ Health Perspect.* 2008; 116: 362-369; Mannes T, Jalaludin B, Morgan G, Lincoln D, Sheppeard V, Corbett S. Impact of ambient air pollution on birth weight in Sydney, Australia. *Occup Environ Med.* 2005; 62: 524-530.

21 Parker JD, Akinbami LJ, Woodruff TJ. Air pollution and childhood respiratory allergies in the United States. *Environ Health Perspect.* 2009; 117:140-147.

22 U.S. EPA, 2013.

23 U.S. EPA. Integrated Science Assessment for Particulate Matter (Final Report). U.S. Environmental Protection Agency, Washington, DC, EPA/600/R-08/139F, 2009. Available at http://cfpub.epa.gov/ncea/cfm/recordisplay.cfm?deid=216546.

24 U.S. EPA. Air Quality Criteria for Particulate Matter, October 2004. Available at http://cfpub2.epa.gov/ncea/cfm/recordisplay.cfm?deid=87903.

25 U.S. EPA, 2009.

26 Mar TF, Larson TV, Stier RA, Claiborn C, Koenig JQ. An analysis of the association between respiratory symptoms in subjects with asthma and daily air pollution in Spokane, Washington. *Inhal Toxicol.* 2004; 16: 809-815; Peel JL, Tolbert PE, Klein M, Metzger KB, Flanders WD, Knox T, Mulholland JA, Ryan PB, Frumkin H. Ambient air pollution and respiratory emergency department visits. *Epidemiology.* 2005; 16: 164-174.

27 Barnett AG, Williams GM, Schwartz J, Best TL, Neller AH, Petroeschevsky AL, Simpson RW. The effects of air pollution on hospitalizations for cardiovascular disease in elderly people in Australian and New Zealand cities. *Environ Health Perspect.* 2006; 114: 1018-1023.

28 Peel JL, Metzger KB, Klein M, Flanders WD, Mulholland JA, Tolbert PE. Ambient air pollution and cardiovascular emergency department visits in potentially sensitive groups. *Am J Epidemiol.* 2007; 165: 625-633. Pope CA III, Dockery DW. Health effects of fine particulate air pollution: Lines that connect. *J Air Waste Mange Assoc.* 2006; 56: 709-742.

29 Zanobetti A, Schwartz J. Are diabetics more susceptible to the health effects of airborne particles? *Am J Respir Crit Care Med.* 2001; 164: 831-833. National Research Council. *Research Priorities for Airborne Particulate Matter: IV. Continuing Research Progress.* Washington, DC: The National Academies Press, 2004.

30 Ostro B, Broadwin R, Green S, Feng WY, Lipsett M. Fine particulate air pollution and mortality in nine California counties: results from CALFINE. *Environ Health Perspect.* 2006: 114: 29-33; Ostro B, Feng WY, Broadwin R, Malig B, Green S, Lipsett M. The Impact of Components of Fine Particulate Matter on Cardiovascular Mortality in Susceptible Subpopulations. *Occup Environ Med.* 2008; 65(11): 750-6.

31 U.S. EPA, 2009.

32 Miller, 2007; O'Neill MS, Veves A, Zanobetti A, Sarnat JA, Gold DR, Economides PA, Horton ES, Schwartz J. Diabetes enhances vulnerability to particulate air pollution-associated impairment in vascular reactivity and endothelial function. *Circulation.* 2005; 111: 2913-2920;

33 Eckel SP, et al. 2016

34 Correia AW, Pope CA III, Dockery DW, Wang Y, Ezzati M, Domenici F. Effect of air pollution control on life expectancy in the United States: An analysis of 545 U.S. Counties for the period from 2000 to 2007. *Epidemiology.* 2013; 24(1): 23-31.

35 Lepeule J, Laden F, Dockery D, Schwartz J. Chronic exposure to fine particles and mortality: An extended follow-up of the Harvard Six Cities Study from 1974 to 2009. *Environ Health Perspect.* 2012; 120: 965-970.

36 Schwartz J, Coull B, Laden F, Ryan L. The effect of dose and timing of dose on the association between airborne particles and survival. *Environ Health Perspect.* 2008; 116: 64-69.

37 Zanobetti A, Schwartz J, Samoli E, Gryparis A, Tuoloumi G, Peacock J, Anderson RH, Le Tertre A, Bobros J, Celko M, Goren A, Forsberg B, Michelozzi P, Rabczenko D, Perez Hoyos S, Wichmann HE, Katsouyanni K. The temporal pattern of respiratory and heart disease mortality in response to air pollution. *Environ Health Perspect.* 2003; 111:1188-1193; Dominici F, McDermott A, Zeger SL, Samet JM. Airborne particulate matter and mortality: Timescale effects in four US cities. *Am J Epidemiol.* 2003; 157: 1055-1065.

38 Shi L, Zanobetti A, Kloog I, Coull BA, Koutrakis P, Melly SJ, Schwartz JD. Low-concentration $PM_{2.5}$ and mortality: estimating acute and chronic effects in a population-based study. *Environ Health Perspect.* 2016; 124:46-52. http://dx.doi.org/10.1289/ehp.1409111

39 Schwartz J, Bind MA, Koutrakis P. Estimating causal effects of local air pollution on daily deaths: Effect of low levels. *Environ Health Perspect.* 2017; 125:23-29. http://dx.doi.org/10.1289/EHP232

40 Dominici F, McDermott A, Zeger SL, Samet JM. On the use of generalized additive models in time-series studies of air pollution and health. *Am J Epidemiol.* 2002; 156: 193-203.

41 Hong Y-C, Lee J-T, Kim H, Ha E-H, Schwartz J, Christiani DC. Effects of air pollutants on acute stroke mortality. *Environ Health Perspect.* 2002; 110: 187-191.

42 Tsai SS, Goggins WB, Chiu HF, Yang CY. Evidence for an association between air pollution and daily stroke admissions in Kaohsiung, Taiwan. *Stroke.* 2003; 34: 2612-6.

43 Wellenius GA, Schwartz J, Mittleman MA. Air Pollution and Hospital admissions for ischemic and hemorrhagic stroke among Medicare beneficiaries. *Stroke.* 2005; 36: 2549-2553.

44 Pope and Dockery, 2006.

45 D'Ippoliti D, Forastiere F, Ancona C, Agabity N, Fusco D, Michelozzi P, Perucci CA. Air pollution and myocardial infarction in Rome: A case-crossover analysis. *Epidemiology.* 2003; 14: 528-535. Zanobetti A, Schwartz J. The effect of particulate air pollution on emergency admissions for myocardial infarction: A multicity case-crossover analysis. *Environ Health Perspect.* 2005; 113: 978-982.

46 Ghio AJ, Kim C, Devlin RB. Concentrated ambient air particles induce mild pulmonary inflammation in healthy human volunteers. *Am J Respir Crit Care Med.* 2000; 162(3 Pt 1): 981-988.

47 Metzger KB, Tolbert PE, Klein M, Peel JL, Flanders WD, Todd K, Mulholland JA, Ryan PB, Frumkin H. Ambient air pollution and cardiovascular emergency department visits in Atlanta, Georgia, 1993-2000. *Epidemiology.* 2004; 15: 46-56.

48 Tsai, et al., 2003.

49 Wellenius GA, Schwartz J, Mittleman MA. Particulate air pollution and hospital admissions for congestive heart failure in seven United States cities. Am J Cardiol. 2006; 97 (3): 404-408; Wellenius GA, Bateson TF, Mittleman MA, Schwartz J. Particulate air pollution and the rate of hospitalization for congestive heart failure among Medicare beneficiaries in Pittsburgh, Pennsylvania. Am J Epidem. 2005; 161: 1030-1036.

50 Van Den Eeden SK, Quesenberry CP Jr, Shan J, Lurmann F. *Particulate Air Pollution and Morbidity in the California Central Valley: A High Particulate Pollution Region.* Final Report to the California Air Resources Board, 2002.

51 Lin M, Chen Y, Burnett RT, Villeneuve PJ, Kerwski D. The influence of ambient coarse particulate matter on asthma hospitalization in children: Case-crossover and time-series analyses. *Environ Health Perspect.* 2002; 110: 575-581.

52 Norris G, YoungPong SN, Koenig JQ, Larson TV, Sheppard L, Stout JW. An association between fine particles and asthma emergency department visits for children in Seattle. *Environ Health Perspect.* 1999; 107: 489-493.

53 Tolbert PE, Mulholland JA, MacIntosh DD, Xu F, Daniels D, Devine OJ, Carlin BP, Klein M, Dorley J, Butler AJ, Nordenberg DF, Frumkin H, Ryan PB, White MC. Air quality and pediatric emergency room visits for asthma in Atlanta, Georgia. *Am J Epidemiol.* 2000; 151: 798-810.

54 Slaughter JC, Lumley T, Sheppard L, Koenig JQ, Shapiro, GG. Effects of ambient air pollution on symptom severity and medication use in children with asthma. *Ann Allergy Asthma Immunol.* 2003; 91: 346-353.

55 Thaller, et al., 2008.

56 Dockery DW, Pope CA III, Xu X, Spengler JD, Ware JH, Fay ME, Ferris BG, Speizer FE. An association between air pollution and mortality in six U.S. cities. *N Engl J Med.* 1993; 329: 1753-1759. Pope CA, Thun MJ, Namboodiri MM, Dockery DW, Evans JS, Speizer FE, Heath CW. Particulate air pollution as a predictor of mortality in a prospective study of U.S. adults. *Am J Respir Crit Care Med.* 1995; 151: 669-674.

57 Zanobetti A, Schwartz J. The effect of fine and coarse particulate air pollution on mortality: A national analysis. *Environ Health Perspect.* 2009; 117: 1-40 2009; Krewski D; Jerrett M; Burnett RT; Ma R; Hughes E; Shi Y; Turner MC; Pope AC III; Thurston G; Calle EE; Thun MJ. *Extended follow-up and spatial analysis of the American Cancer Society study linking particulate air pollution and mortality.* Report Nr. 140 (Cambridge, MA: Health Effects Institute, 2009); Franklin M, Zeka A, Schwartz J. Association between $PM_{2.5}$ and all-cause and specific cause mortality in 27 U.S. communities. *J Expo Sci Environ Epidemiol.* 2007; 18: 1005-1011; Lepeule et al, 2012; Pope CA III, Burnett RT, Thun MJ, Calle EE, Krewski D, Ito K, Thurston GD. Lung cancer, cardiopulmonary mortality, and long-term exposure to fine particulate air pollution. *JAMA.* 2002; 287(9): 1132-1141.

58 Pope CA III. *Epidemiology* of fine particulate air pollution and human health: Biological mechanisms and who's at risk? *Environ Health Perspect.* 2000; 108: 713-723.

59 Thurston GD, Ahn J, Cromar KR, Shao Y, Reynolds H, et al. Ambient particulate matter air pollution exposure and mortality in the NIH-AARP Diet and Health Cohort. *Environ Health Perspect.* 2015 Advanced Publication; Lepeule J, Laden F, Douglas Dockery D, and Schwartz J. Chronic exposure to fine particles and mortality: An extended follow-up of the Harvard Six Cities Study from 1974 to 2009. *Environ Health Perspect.* 2012; 120: 965–970.

60 Shi, et al., 2016.

61 Hamra GB, Guha N, Cohen A, Laden F, Raaschou-Nielsen O, Samet JM, Vineis P, Forastiere F, Saldiva P, Yorifuji T, and Loomis D. Outdoor particulate matter exposure and lung cancer: A systematic review and meta-analysis. *Environ Health Perspect.* 2014: 122: 906-911.

62 Lin S, Munsie JP, Hwang SA, Fitzgerald E, Cayo MR. Childhood asthma hospitalization and residential exposure to state route traffic. *Environ Res.* 2002; 88: 73-81.

63 Gauderman WJ, Vora H, McConnell R, Berhane K, Gilliland GF, Thomas D, Lurmann F, Avol E, Küenzli N, Jarrett M, Peters J. Effect of exposure to traffic on lung development from 10 to 18 years of age: A cohort study. Lancet. 2007; 369: 571-577.

64 Gauderman WJ, Gilliland GF, Vora H, Avol E, Stram D, McConnell R, Thomas D, Lurmann F, Margolis HG, Rappaport EB, Berhane K, Peters JM. Association between air pollution and lung function growth in southern California children: Results from a second cohort. *Am J Respir Crit Care Med.* 2002; 166: 76-84.

65 Gauderman WJ, Avol E, Gilliland F, Vora H, Thomas D, Berhane K, McConnell R, Kuenzli N, Lurmann F, Rappaport E, Margolis H, Bates D, Peters J. The effect of air pollution on lung development from 10 to 18 years of age. *N Engl J Med.* 2004; 351: 1057-1067.

66 Gehring U, Wijga AH, Hoek G, Bellander T, et al. Exposure to air pollution and development of asthma and rhinoconjunctivitis throughout childhood and adolescence: a population-based birth cohort study. *Lancet Respiratory Medicine.* 2015; 3 (12): 933-942.

67 Churg, A Brauer, M, Avila-Casado, MdC, Fortoul TI, Wright JL. chronic exposure to high levels of particulate air pollution and small airway remodeling. *Environ Health Perspect.* 2003; 111: 714-718.

68 Pope CA III, Burnett RT, Thurston GD, Thun MJ, Calle EE, Krewski D, Godleski JJ. Cardiovascular mortality and year-round exposure to particulate air pollution: Epidemiological evidence of general pathophysiological pathways of disease. *Circulation.* 2004; 109: 71-77.

69 Bell ML, Ebisu K, Belanger K. Ambient air pollution and low birth weight in Connecticut and Massachusetts. *Environ Health Perspect.* 2007; 115: 118-24; Ritz B, Wilhelm M, Zhao Y. Air pollution and infant death in southern California, 1989-2000. *Pediatrics.* 2006; 118: 493-502; Woodruff TJ, parker JD, Schoendorf KC. Fine particulate matter ($PM_{2.5}$) air pollution and selected causes of postneonatal infant mortality in California. *Environ Health Perspect.* 2006; 114: 785-790.

70 Miller KA, Siscovick DS, Shepard L, Shepherd K, Sullivan JH, Anderson GL, Kaufman JD. Long-term exposure to air pollution and incidence of cardiovascular events in women. *N Engl J Med.* 2007; 356: 447-458.

71 Rao X, Patel P, Puett R and Rajogpalan S. Air pollution as a risk factor for type 2 diabetes. *Toxicological Sciences.* 2015; 143 (2): 231-241; Eze IC, Hemkens LG, Bucher HC, Hoffman B, et al. Association between ambient air pollution and diabetes mellitus in Europe and North America: Systematic review and meta-analysis. *Environ Health Perspect.* 2015; 123 (5): 381-389.

72 Kim KY, Lim YH, Bea HJ, Kim M, Jung K, Hong YC. Long-term fine particulate matter exposure and major depressive disorder in a community-based urban cohort. *Environ Health Perspect.* 2016; 124:1547-1553.

73 Pun VC, Manjourides J, Shh H. Association of ambient air pollution with depressive and anxiety symptoms in older adults: results from the NSHAP study. *Environ Health Perspect.* 2017; 125: 342-348.

74 U.S. EPA, 2009.

75 U.S. EPA, 2009.

76 U.S. EPA, 2009.

77 U.S. EPA, 2009.

78 Morakinyo OM, Mokgobu MI, Mukhola MS, Hunter RP. Review: Health outcomes of exposure to biological and chemical components of inhalable and respirable particulate matter. *Int. J. Environ. Res. Public Health.* 2016: 592.

79 Thurston GD, Burnett RT, Turner MC, Shi Y, Krewski D, Lall R, Ito K, Jerrett M, Gapstur SM, Diver WR, Pope CA III. Ischemic heart disease mortality and long-term exposure to source-related components of U.S. fine particle air pollution. *Environ Health Perspect*; Advance Publication as of 2 Dec 2015. http://dx.doi.org/10.1289/ehp.1509777

80 Bell ML, Ebisu K, Leaderer BP, Gent JF, Lee HJ, Koutrakis P, Wang Y, Dominici F, Peng RD. Associations of $PM_{2.5}$ constituents and sources with hospital admissions: analysis of four counties in Connecticut and Massachusetts (USA) for persons ≥ 65 years of age. *Environ Health Perspect.* 2014: 122: 138–144; http://dx.doi.org/10.1289/ehp.1306656

81 Ebisu K, Bell ML. Airborne $PM_{2.5}$ chemical components and low birth weight in the Northeastern and Mid-Atlantic regions of the United States. *Environ Health Perspect.* 2012; 120: 1746–1752; http://dx.doi.org/10.1289/ehp.1104763

82 Levy JI, Diez D, Dou Y, Barr CD, Dominici F. A meta-analysis and multisite time-series analysis of the differential toxicity of major fine particulate matter constituents. *Am J Epidemiology.* 2012; 175(11): 1091-1099. doi:10.1093/aje/kwr457; Dai L, Zanobetti A, Koutrakis P, Schwartz JD. Associations of fine particulate matter species with mortality in the United States: A multicity time-series analysis. *Environ Health Perspect.* 2014; 122(8): 837-842. doi:10.1289/ehp.1307568.

83 Morakinyo et al.

84 Cassee FR, Héroux M-E, Gerlofs-Nijland ME, Kelly FJ. Particulate matter beyond mass: recent health evidence on the role of fractions, chemical constituents and sources of emission. *Inhalation Toxicology.* 2013; 25(14): 802-812. doi:10.3109/08958378.2013.850127.

85 Dietert RR, Etzel RA, Chen D, et al. Workshop to identify critical windows of exposure for children's health: Immune and respiratory systems workgroup summary. *Environ Health Perspect.* 2000; 108 (supp 3): 483-490.

86 World Health Organization: The effects of air pollution on children's health and development: A review of the evidence E86575. 2005. Available at http://www.euro.who.int/document/E86575.pdf.

87 WHO, 2005.

88 American Academy of Pediatrics Committee on Environmental Health, Ambient Air Pollution: Health hazards to children. *Pediatrics.* 2004; 114: 1699-1707. Statement was reaffirmed in 2010.

89 Laurent O, Hu J, LI L, et al. A statewide nested case-control study of preterm birth and air pollution by source and composition: California, 2001-2008. *Environ Health Perspect.* 2016. 124:1479-1486. Doi: 10.1289/ehp.1510133.

90 Nach RM, Mao G, Zhang X, et al. Intrauterine inflammation and maternal exposure to ambient $PM_{2.5}$ during preconception and specific periods of pregnancy: the Boston Birth Cohort. *Environ Health Perspect.* 2016. 124:1608–1615; http://dx.doi.org/10.1289/EHP243

91 Li S, Guo Y, Williams G. Acute impact of hourly ambient air pollution on preterm birth. *Environ Health Perspect.* 2016. 124:1623–1629; http://dx.doi.org/10.1289/EHP200

92 Gauderman et al., 2004.

93 Galizia A, Kinney PL. Year-round residence in areas of high ozone: Association with respiratory health in a nationwide sample of nonsmoking young adults. *Environ Health Perspect.* 1999; 107: 675-679.

94 Peters JM, Avol E, Gauderman WJ, Linn WS, Navidi W, London SJ, Margolis H, Rappaport E, Vora H, Gong H, Thomas DC. A study of twelve southern california communities with differing levels and types of air pollution. II. Effects on pulmonary function. *Am J Respir Crit Care Med.* 1999; 159: 768-775.

95 Gauderman WJ, Urman R, Avol E, Berhane K, McConnell R, Rapport E, Chang R, Lurmann F, Gilliland F. Association of improved air quality with lung development in children. *N Eng J Med.* 2015; 372: 905-913.

96 Bayer-Oglesby L, Grize L, Gassner M, Takken-Sahli K, Sennhauser FH, Neu U, Schindler C, Braun-Fahrländer C. Decline of ambient air pollution levels and improved respiratory health in swiss children. *Environ Health Perspect.* 2005; 113: 1632-1637.

97 Institute of Medicine. *Toward Environmental Justice: Research, Education, and Health Policy Needs.* Washington, DC: National Academy Press, 1999; O'Neill MS, Jerrett M, Kawachi I, Levy JI, Cohen AJ, Gouveia N, Wilkinson P, Fletcher T, Cifuentes L, Schwartz J, et al. Health, wealth, and air pollution: Advancing theory and methods. *Environ Health Perspect.* 2003: 111: 1861-1870; Finkelstein MM, Jerrett M, DeLuca P, Finkelstein N, Verma DK, Chapman K, Sears MR. Relation between income, air pollution and mortality: A cohort study. *CMAJ.* 2003; 169: 397-402; Ostro B, Broadwin R, Green S, Feng W, Lipsett M. Fine particulate air pollution and mortality in nine California counties: Results from CALFINE. *Environ Health Perspect.* 2005: 114: 29-33; Zeka A, Zanobetti A, Schwartz J. Short term effects of particulate matter on cause specific mortality: effects of lags and modification by city characteristics. *Occup Environ Med.* 2006: 62: 718-725.

98 American Lung Association. Urban air pollution and health inequities: A workshop report. *Environ Health Perspect.* 2001: 109 (suppl 3): 357-374.

99 Zeka A, Zanobetti A, Schwartz J. Individual-level modifiers of the effects of particulate matter on daily mortality. *Am J Epidemiol.* 2006: 163: 849-859.

100 Ostro et al., 2006; Ostro et al., 2008.

101 Bell ML, Dominici F. Effect modification by community characteristics on the short-term effects of ozone exposure and mortality in 98 US communities. *Am J Epidemiol.* 2008; 167: 986-997.

102 Apelberg BJ, Buckley TJ, White RH. Socioeconomic and racial disparities in cancer risk from air toxics in Maryland. *Environ Health Perspect.* 2005: 113: 693-699.

103 Zeger SL, Dominici F, McDermott A, Samet J. Mortality in the Medicare population and chronic exposure to fine particulate air pollution in urban centers (2000-2005). *Environ Health Perspect.* 2008: 116: 1614-1619.

104 Bell and Dominici, 2008.

105 Babin S, Burkom H, Holtry R, Tabernero N, Davies-Cole J, Stokes L, Dehaan K, Lee D. Medicaid patient asthma-related acute care visits and their associations with ozone and particulates in Washington, DC, from 1994-2005. Int J Environ Health Res. 2008; 18 (3): 209-221.

106 Wang Y, Kloog I, Coul BA, Kosheleva A, Zanobetti A, Schwartz JD. Estimating causal effects of long-term $PM_{2.5}$ exposure on mortality in New Jersey. *Environ Health Perspect.* 2016; 124: 1182-1188.

107 Laurent O, Pedrono G, Segala C, Filleul L, Havard S, Deguen S, Schillinger C, Rivière E, Bard D. Air pollution, asthma attacks, and socioeconomic deprivation: a small-area case-crossover study. *Am J Epidemiol.* 2008; 168: 58-65; Laurent O, Pedrono G, Filleul L, Segala C, Lefranc A, Schillinger C, Riviere E, Bard D. Influence of socioeconomic deprivation on the relation between air pollution and beta-agonist sales for asthma. *Chest.* 2009; 135 (3): 717-716.

108 O'Neill et al., 2003.

109 Miranda ML, Edwards SE, Keating MH, Paul CJ. Making the environmental justice grade: The relative burden of air pollution exposure in the United States. Int J Environ Res *Public Health.* 2011; 8: 1755-1771.

110 Bell ML, Ebisu K. Environmental inequality in exposures to airborne particulate matter component in the United States. *Environ Health Perspect.* 2012; 120: 1699–1704.

111 Health Effects Institute Panel on the Health Effects of Traffic-Related Air Pollution, *Traffic-Related Air Pollution: A Critical Review of the Literature on Emissions, Exposure, and Health Effects.* Health Effects Institute: Boston, 2010. Available at www.healtheffects.org.

112 Andersen ZJ, Hvidberg M, Jensen SS, Ketzel M, Loft S, Sørensen M, Tjønneland A, Overvad K, Raaschou-Nielsen O. Chronic obstructive pulmonary disease and long-term exposure to traffic-related air pollution: A cohort study. *Am J Respir Crit Care Med.* 2011: 183: 455-461.

113 Finklestein MM, Jerrett M., Sears MR. Traffic air pollution and mortality rate advancement periods. *Am J Epidemiol.* 2004; 160: 173-177; Hoek G, Brunkreef B, Goldbohn S, Fischer P, van den Brandt. Associations between mortality and indicators of traffic-related air pollution in the Netherlands: a cohort study. Lancet. 2002; 360: 1203-1209.

114 Peters A, von Klot S, Heier M, Trentinaglia I, Cyrys J, Hormann A, Hauptmann M, Wichmann HE, Lowel H. Exposure to traffic and the onset of myocardial infarction. *N Engl J Med.* 2004; 351: 1721-1730.

115 Suglia SF, Gryparis A, Schwartz J, Wright RJ. Association between traffic-related black carbon exposure and lung function among urban women. *Environ Health Perspect.* 2008; 116 (10): 1333-1337.

116 Chen H, KJC, Capes R, et al. Living near major roads and the incidence of dementia, Parkinson's disease and multiple sclerosis: a population-based cohort study. Lancet. 2017. Published online http://dx.doi.org/10.1016/5014-6736(16)32596-X

117 Power MC, Weisskopf MG, Alexeeff SE, et al. Traffic-related air pollution and cognitive function in a cohort of older men. Environ Health Perspect 2011.119:682–687. doi:10.1289/ehp.1002767

METHODOLOGY

Statistical Methodology: The Air Quality Data

Data Sources

The data on air quality throughout the United States were obtained from the U.S. Environmental Protection Agency's Air Quality System (AQS), formerly called Aerometric Information Retrieval System (AIRS) database. The American Lung Association contracted with Dr. Allen S. Lefohn, A.S.L. & Associates, Helena, Montana, to characterize the hourly averaged ozone concentration information and the 24-hour averaged $PM_{2.5}$ concentration information for the three-year period for 2013-2015 for each monitoring site.

Design values for the annual $PM_{2.5}$ concentrations by county for the period 2013-2015 came from data posted on July 29, 2016, at the U.S. Environmental Protection Agency's website at https://www.epa.gov/sites/production/files/2016-07/pm25_designvalues_20132015_final_07_29_16.xlsx.

Ozone Data Analysis

The 2013, 2014 and 2015 AQS hourly ozone data were used to calculate the daily 8-hour maximum concentration for each ozone-monitoring site. The hourly averaged ozone data were downloaded on August 11, 2016, following the close of the authorized period for quality review and assurance certification of data. Only the hourly average ozone concentrations derived from FRM and FEM monitors were used in the analysis. The data were considered for a three-year period for the same reason that the EPA uses three years of data to determine compliance with the ozone standard: to prevent a situation in any single year, where anomalies of weather or other factors create air pollution levels, which inaccurately reflect the normal conditions. The highest 8-hour daily maximum concentration in each county for 2013, 2014 and 2015, based on the EPA-defined ozone season, was identified.

The current national ambient air quality standard for ozone is 70 parts per billion (ppb) measured over eight hours. The EPA's Air Quality Index reflects the 70 ppb standard. A.S.L. & Associates prepared a table by county that summarized, for each of the three years, the number of days the ozone level was within the ranges identified by the EPA based on the EPA Air Quality Index:

8-hour Ozone Concentration	Air Quality Index Levels
0 – 54 ppb	Good (Green)
55 – 70 ppb	Moderate (Yellow)
71 – 85 ppb	Unhealthy for Sensitive Groups (Orange)
86 – 105 ppb	Unhealthy (Red)
106 – 200 ppb	Very Unhealthy (Purple)
>201 ppb	Hazardous (Maroon)

The goal of this report was to identify the number of days that 8-hour daily maximum concentrations in each county occurred within the defined ranges. This approach provided an indication of the level of pollution for all monitored days, not just those days that fell under the requirements for attaining the national ambient air quality standards. Therefore, no data capture criteria were applied to eliminate monitoring sites or to require a number of valid days for the ozone season.

The daily maximum 8-hour average concentration for a given day is derived from the highest of the 17 consecutive 8-hour averages beginning with the 8-hour period from 7:00 a.m. to 3:00 p.m. and ending with the 8-hour period from 11:00 p.m. to 7:00 a.m. the following day. This follows the process EPA uses for the current ozone standard adopted in 2015, but differs from the form used under the previous 0.075 ppm 8-hour

average ozone standard that was established in 2008. All valid days of data within the ozone season were used in the analysis. However, for computing an 8-hour average, at least 75 percent of the hourly concentrations (i.e., 6-8 hours) had to be available for the 8-hour period. In addition, an 8-hour daily maximum average was identified if valid 8-hour averages were available for at least 75 percent of possible hours in the day (i.e., at least 13 of the possible 17 8-hour averages). Because the EPA includes days with inadequate data (i.e., not 75 percent complete) if the standard value is exceeded, our data capture methodology also included the site's 8-hour value if at least one valid 8-hr period were available and it was 71 ppb or higher.

As instructed by the Lung Association, A.S.L. & Associates included the exceptional and natural events that were identified in the database and identified for the Lung Association the dates and monitoring sites that experienced such events. Some data have been flagged by the state or local air pollution control agency to indicate that they had raised issues with EPA about those data. For each day across all sites within a specific county, the highest daily maximum 8-hour average ozone concentration was recorded and then the results were summarized by county for the number of days the ozone levels were within the ranges identified above.

Following receipt of the above information, the American Lung Association identified the number of days each county, with at least one ozone monitor, experienced air quality designated as orange (Unhealthy for Sensitive Groups), red (Unhealthy) or purple (Very Unhealthy).

Short-Term Particle Pollution Data Analysis

A.S.L. & Associates identified the maximum daily 24-hour AQS $PM_{2.5}$ concentration for each county in 2013, 2014 and 2015 with monitoring information. The 24-hour $PM_{2.5}$ data were downloaded on August 10, 2016, following the close of the authorized period for quality review and assurance certification of data. In addition, hourly averaged $PM_{2.5}$ concentration data were characterized into 24-hour average $PM_{2.5}$ values by the EPA and provided to A.S.L. & Associates. Using these results, A.S.L. & Associates prepared a table by county that summarized, for each of the three years, the number of days the maximum of the daily $PM_{2.5}$ concentration was within the ranges identified by the EPA based on the EPA Air Quality Index, as adopted by the EPA on December 14, 2012:

24-hour $PM_{2.5}$ Concentration	Air Quality Index Levels
0.0 mg/m^3 to 12.0 mg/m^3	Good (Green)
12.1 mg/m^3 to 35.4 mg/m^3	Moderate (Yellow)
35.5 mg/m^3 to 55.4 mg/m^3	Unhealthy for Sensitive Groups (Orange)
55.5 mg/m^3 to 150.4 mg/m^3	Unhealthy (Red)
150.5 mg/m^3 to 250.4 mg/m^3	Very Unhealthy (Purple)
greater than or equal to 250.5 mg/m^3	Hazardous (Maroon)

All previous data collected for 24-hour average $PM_{2.5}$ were characterized using the AQI thresholds listed above.

The goal of this report was to identify the number of days that the maximum in each county of the daily $PM_{2.5}$ concentration occurred within the defined ranges. This approach provided an indication of the level of pollution for all monitored days, not just those days that fell under the requirements for attaining the national ambient air quality standards. Therefore, no data capture criteria were used to eliminate monitoring sites. Both 24-hour averaged PM data, as well as hourly averaged PM data averaged over 24 hours were used. Included in the analysis are data collected using only FRM

and FEM methods, which reported hourly and 24-hour averaged data. As instructed by the Lung Association, A.S.L. & Associates included the exceptional and natural events that were identified in the database and identified for the Lung Association the dates and monitoring sites that experienced such events. Some data have been flagged by the state or local air pollution control agency to indicate that they had raised issues with EPA about those data. For each day across all sites within a specific county, the highest daily maximum 24-h $PM_{2.5}$ concentration was recorded and then the results were summarized by county for the number of days the concentration levels were within the ranges identified on the chart on the preceding page.

Following receipt of the above information, the American Lung Association identified the number of days each county, with at least one $PM_{2.5}$ monitor, experienced air quality designated as orange (Unhealthy for Sensitive Groups), red (Unhealthy), purple (Very Unhealthy) or maroon (Hazardous).

Description of County Grading System

Ozone and Short-Term Particle Pollution (24-hour $PM_{2.5}$)

The grades for ozone and short-term particle pollution (24-hour $PM_{2.5}$) were based on a weighted average for each county. To determine the weighted average, the Lung Association followed these steps:

1. First, assigned weighting factors to each category of the Air Quality Index. The number of orange days experienced by each county received a factor of 1; red days, a factor of 1.5; purple days, a factor of 2; and maroon days, a factor of 2.5. This allowed days where the air pollution levels were higher to receive greater weight.
2. Next, multiplied the total number of days within each category by their assigned factor, and then summed all the categories to calculate a total.
3. Finally, divided the total by three to determine the weighted average, since the monitoring data were collected over a three-year period.

The weighted average determined each county's grades for ozone and 24-hour $PM_{2.5}$.

- All counties with a weighted average of zero (corresponding to no exceedances of the standard over the three-year period) were given a grade of "A."
- For ozone, an "F" grade was set to generally correlate with the number of unhealthy air days that would place a county in nonattainment for the ozone standard.
- For short-term particle pollution, fewer unhealthy air days are required for an F than for nonattainment under the $PM_{2.5}$ standard. The national air quality standard is set to allow 2 percent of the days during the three years to exceed 35 $\mu g/m^3$ (called a "98th percentile" form) before violating the standard. That would be roughly 21 unhealthy days in three years. The grading used in this report would allow only about 1 percent of the days to be over 35 $\mu g/m^3$ (called a "99th percentile" form) of the $PM_{2.5}$. The American Lung Association supports using the tighter limits in a 99th percentile form as a more appropriate standard that is intended to protect the public from short-term spikes in pollution.

Grading System		
Grade	**Weighted Average**	**Approximate Number of Allowable Orange/Red/Purple/Maroon days**
A	0.0	None
B	0.3 to 0.9	1 to 2 orange days with no red
C	1.0 to 2.0	3 to 6 days over the standard: 3 to 5 orange with no more than 1 red OR 6 orange with no red
D	2.1 to 3.2	7 to 9 days over the standard: 7 total (including up to 2 red) to 9 orange with no red
F	3.3 or higher	9 days or more over the standard: 10 orange days or 9 total including at least 1 or more red, purple or maroon

Weighted averages allow comparisons to be drawn based on severity of air pollution. For example, if one county had nine orange days and no red days, it would earn a weighted average of 3.0 and a D grade. However, another county that had only eight orange days but also two red days, which signify days with more serious air pollution, would receive a F. That second county would have a weighted average of 3.7.

Note that this system differs significantly from the methodology the EPA uses to determine violations of both the ozone and the 24-hour $PM_{2.5}$ standards. The EPA determines whether a county violates the standard based on the fourth maximum daily 8-hour ozone reading each year averaged over three years. Multiple days of unhealthy air beyond the highest four in each year are not considered. By contrast, the system used in this report recognizes when a community's air quality repeatedly results in unhealthy air throughout the three years. Consequently, some counties will receive grades of "F" in this report, showing repeated instances of unhealthy air, while still meeting the EPA's 2015 ozone standard. The American Lung Association's position is that the evidence shows that the 2015 ozone standard, although stronger than the 2008 standard, still fails to adequately protect public health.

The Lung Association calculates the population at risk from these pollutants based on the population from the entire county where the monitor is located and the largest metropolitan area that contains that county. Not only do people from that county or metropolitan area circulate within the county and the metropolitan area, the air pollution circulates to that monitor through the county and metropolitan area.

Counties were ranked by weighted average. Metropolitan areas were ranked by the highest weighted average among the counties within a given Metropolitan Statistical Area as of 2015 as defined by the White House Office of Management and Budget (OMB).

Year-Round Particle Pollution (Annual $PM_{2.5}$)

Since no comparable Air Quality Index exists for year-round particle pollution (annual $PM_{2.5}$), the grading was based on the 2012 National Ambient Air Quality Standard for annual $PM_{2.5}$ of 12 µg/m^3. Counties that EPA listed as being at or below 12 µg/m^3 were given grades of "Pass." Counties EPA listed as being at or above 12.1 µg/m^3 were given grades of "Fail." Where insufficient data existed for EPA to determine a design value, those counties received a grade of "Incomplete."

EPA officially recognized that data collected in all Illinois counties, in some Maine counties and in most Tennessee counties were processed in certain laboratories where quality control issues meant that available data could not be considered for development of an official design value. For short-term and annual particle pollution, those counties received a grade of "Incomplete."

Design value is the calculated concentration of a pollutant based on the form of the national ambient air quality standard and is used by EPA to determine whether or not the air quality in a county meets the standard. Counties were ranked by design value. Metropolitan areas were ranked by the highest design value among the counties within a given Metropolitan Statistical Area as of 2015 as defined by the OMB.

The Lung Association received critical assistance from members of the National Association of Clean Air Agencies and the Association of Air Pollution Control Agencies. With their assistance, all state and local agencies were provided the opportunity to review and comment on the data in draft tabular form. The Lung Association reviewed all discrepancies with the agencies and, if needed, with Dr. Lefohn at A.S.L. & Associates. Questions about the annual PM design values were discussed with EPA; however, the Lung Association made final decisions to grade counties as "Incomplete" where EPA considered $PM_{2.5}$ data to have inadequate quality assurance. The American Lung Association wishes to express its continued appreciation to the state and local air directors for their willingness to assist in ensuring that the characterized data used in this report are correct.

Calculations of Populations at Risk

Presently county-specific measurements of the number of persons with chronic conditions are not generally available. In order to assess the magnitude of chronic conditions at the state and county levels, we have employed a synthetic estimation technique originally developed by the U.S. Census Bureau. This method uses age-specific national and state estimates of self-reported conditions to project disease prevalence to the county level. The exception to this is poverty, for which estimates are available at the county level.

Population Estimates

The Lung Association includes the total county population in discussions of populations at risk from exposure to pollution in each county. The Lung Association uses that conservative count based on several factors: the recognized limited number and locations of monitors in most counties and metropolitan areas; the movement of the population both in daily activities, including outdoor activities, such as exercise or work; and the transport of emission from sources into and across the county to reach the monitor.

The U.S. Census Bureau estimated data on the total population of each county in the United States for 2015. The Census Bureau also estimated the age-specific breakdown of the population and how many individuals were living in poverty by county. These estimates are the best information on population demographics available between decennial censuses.

Poverty estimates came from the Census Bureau's Small Area Income and Poverty Estimates (SAIPE) program. The program does not use direct counts or estimates from sample surveys, as these methods would not provide sufficient data for all counties. Instead, a model based on estimates of income or poverty from the Annual Social and Economic Supplement (ASEC) to the Current Population Survey (CPS) is used to develop estimates for all states and counties.

Prevalence Estimates

Chronic Obstructive Pulmonary Disease, Cardiovascular Disease, Asthma and Diabetes. In 2015, the Behavioral Risk Factor Surveillance System (BRFSS) survey found that approximately 21.6 million (8.9 percent) of adults residing in the United States and 8.5 percent of children from 30 states and Washington, D.C., reported currently having asthma. Among adults in the Unites States in 2015, 15.5 million (6.3 percent) had ever been diagnosed with chronic obstructive pulmonary disease (COPD), 20.4 million (8.4

percent) had ever been diagnosed with cardiovascular disease and 25.6 million (10.4 percent) had ever been diagnosed with diabetes.

The prevalence estimate for pediatric asthma is calculated for those younger than 18 years. Local area prevalence of pediatric asthma is estimated by applying 2015 state prevalence rates, or if not available, the national rate from the BRFSS to pediatric county-level resident populations obtained from the U.S. Census Bureau website. Pediatric asthma data from the 2015 BRFSS were available for thirty states and Washington D.C., from the 2014 BRFSS for seven states, from the 2013 BRFSS for one state, from the 2012 BRFSS for two states, from the 2011 BRFSS for one state, and national data were used for the nine states[1] that had no data available. Data from earlier years were not used due to changes in the 2011 survey methodology.

The prevalence estimate for COPD, cardiovascular disease, adult asthma and diabetes is calculated for those aged 18-44 years, 45-64 years and 65 years and older. Local area prevalence for these diseases is estimated by applying age-specific state prevalence rates from the 2015 BRFSS to age-specific county-level resident populations obtained from the U.S. Census Bureau website. Cardiovascular disease included ever having been diagnosed with a heart attack, angina or coronary heart disease, or stroke.

Incidence Estimates

Lung Cancer. State- and gender-specific lung cancer incidence rates for 2013 were obtained from StateCancerProfiles.gov, a system that provides access to statistics from both the National Cancer Institute's Surveillance, Epidemiology and End Results (SEER) program and the Center for Disease Control and Prevention's National Program of Cancer Registries.

Local area incidence of lung cancer is estimated by applying 2013 age-adjusted and sex-specific incidence rates to 2015 county populations obtained from the U.S. Census Bureau. Thereafter, the incidence estimates for each county within a state are summed to determine overall incidence. Estimates for Nevada are based on 2010 rates.

Limitations of Estimates. Since the statistics presented by the BRFSS and SAIPE are based on a sample, they will differ (due to random sampling variability) from figures that would be derived from a complete census or case registry of people in the U.S. with these diseases. The results are also subject to reporting, non-response and processing errors. These types of errors are kept to a minimum by methods built into the survey.

Additionally, a major limitation of the BRFSS is that the information collected represents self-reports of medically diagnosed conditions, which may underestimate disease prevalence since not all individuals with these conditions have been properly diagnosed. However, the BRFSS is the best available source for information on the magnitude of chronic disease at the state level. The conditions covered in the survey may vary considerably in the accuracy and completeness with which they are reported.

Local estimates of chronic diseases are scaled in direct proportion to the base population of the county and its age distribution. No adjustments are made for other factors that may affect local prevalence (e.g., local prevalence of cigarette smokers or occupational exposures) since the health surveys that obtain such data are rarely conducted on the county level. Because the estimates do not account for geographic differences in the prevalence of chronic and acute diseases, the sum of the estimates for each of the counties in the United States may not exactly reflect the national or state estimates derived from the BRFSS.

1 2014: Alabama, Kentucky, Maryland, North Carolina, Tennessee, Washington, West Virginia. 2013: Arizona. 2012: North Dakota and Wyoming. 2011: Iowa. National: Alaska, Arkansas, Colorado, Delaware, Florida, Idaho, South Carolina, South Dakota and Virginia.

References

Irwin, R. Guide to Local Area Populations. U.S. Bureau of the Census, Technical Paper Number 39 (1972).

Centers for Disease Control and Prevention. Behavioral Risk Factor Surveillance System, 2015.

StateCancerProfile.gov, 2016. Cancer Incidence by State and Gender, 2013.

Population Estimates Branch, U.S. Census Bureau. Annual Estimates of the Resident Population by Selected Age Groups and Sex for Counties: April 1, 2010 to July 1, 2015.

Office of Management and Budget. Revised Delineations of Metropolitan Statistical Areas, Micropolitan Statistical Areas, and Combined Statistical Areas, and Guidance on Uses of the Delineations of These Areas. OMB Bulletin 15-01 July 15, 2015.

U.S. Census Bureau. Small Area Income and Poverty Estimates. State and County Data, 2015.

State Table Notes

A full explanation of the sources of data and methodology is in **Methodology**.

Notes for all state data tables

1. **Total Population** is based on 2015 U.S. Census and represents the at-risk populations in counties with ozone or $PM_{2.5}$ pollution monitors; it does not represent the entire state's sensitive populations.
2. **Those 18 & under** and **65 & over** are vulnerable to ozone and $PM_{2.5}$. Do not use them as population denominators for disease estimates—that will lead to incorrect estimates.
3. **Pediatric asthma** estimates are for those under 18 years of age and represent the estimated number of people who had asthma in 2015 based on the state rates when available or national rates when not (Behavioral Risk Factor Surveillance System, or BRFSS), applied to county population estimates (U.S. Census).
4. **Adult asthma** estimates are for those 18 years and older and represent the estimated number of people who had asthma during 2015 based on state rates (BRFSS) applied to county population estimates (U.S. Census).
5. **COPD** estimates are for adults 18 and over who had ever been diagnosed with chronic obstructive pulmonary disease, which includes chronic bronchitis and emphysema, based on state rates (BRFSS) applied to county population estimates (U.S. Census).
6. **Lung cancer** estimates are for all ages and represent the estimated number of people diagnosed with lung cancer in 2013 based on state rates (StateCancerProfiles.gov) applied to county population estimates (U.S. Census).
7. **Cardiovascular disease** estimates are for adults 18 and over who have been diagnosed within their lifetime, based on state rates (BRFSS) applied to county population estimates (U.S. Census). CV disease includes coronary heart disease, stroke, and heart attack.
8. **Diabetes** estimates are for adults 18 and over who have been diagnosed within their lifetime based on state rates (BRFSS) applied to county population estimates (U.S. Census).
9. **Poverty** estimates include all ages and come from the U.S. Census Bureau's Small Area Income and Poverty Estimates program. The estimates are derived from a model using estimates of income or poverty from the Annual Social and Economic Supplement and the Current Population Survey, 2015.
10. Adding across rows does not produce valid estimates. Adding the at risk categories (asthma, COPD, poverty, etc.) will double-count people who fall into more than one category.

Notes for all state grades tables.

1. Not all counties have monitors for either ozone or particle pollution. If a county does not have a monitor, that county's name is not on the list in these tables. The decision about monitors in the county is made by the state and the U.S. Environmental Protection Agency, not by the American Lung Association.
2. **INC** (Incomplete) indicates that monitoring is underway for that pollutant in that county, but that the data are incomplete for all three years. Those counties are not graded. For particle pollution, some states collected data, but experienced laboratory quality issues that meant the data could not be used for assessing pollution levels.
3. **DNC** (Data Not Collected) indicates that data on that particular pollutant are not collected in that county.
4. The **Weighted Average (Wgt. Avg)** was derived by adding the three years of individual level data (2013-2015), multiplying the sums of each level by the assigned standard weights (i.e. 1=orange, 1.5=red, 2.0=purple and 2.5=maroon) and calculating the average. Grades are assigned based on the weighted averages as follows: A=0.0, B=0.3-0.9, C=1.0-2.0, D=2.1-3.2, F=3.3+.
5. The Design Value is the calculated concentration of a pollutant based on the form of the National Ambient Air Quality Standard, and is used by EPA to determine whether the air quality in a county meets the standard. The numbers refer to micrograms per cubic meter, or $\mu g/m^3$. Design values for the annual $PM_{2.5}$ concentrations by county for the period 2013-2015 are as posted on July 26, 2016 at EPA's website at https://www.epa.gov/air-trends/air-quality-design-values. The 2013-2015 design values were compared to the 2012 National Ambient Air Quality Standard for Annual $PM_{2.5}$, particularly to the EPA's assessment of data quality required, as discussed on EPA's website at https://www.epa.gov/pm-pollution/2012-national-ambient-air-quality-standards-naaqs-particulate-matter-pm. Many design values are missing because state data did not meet quality requirements.
6. The annual average National Ambient Air Quality Standard for $PM_{2.5}$ is 12 $\mu g/m^3$ as of December 14, 2012. Counties with design values of 12 or lower received a grade of "Pass." Counties with design values of 12.1 or higher received a grade of "Fail."

STATE TABLES

ALABAMA

American Lung Association in Alabama

www.lung.org/alabama

				AT-RISK GROUPS						
				Lung Diseases						
County	Total Population	Under 18	65 & Over	Pediatric Asthma	Adult Asthma	COPD	Lung Cancer	Cardiovascular Disease	Diabetes	Poverty
Baldwin	203,709	44,719	39,062	5,902	15,709	17,599	140	19,344	23,202	25,941
Clay	13,555	2,897	2,700	382	1,053	1,194	9	1,322	1,585	2,436
Colbert	54,354	11,698	10,232	1,544	4,217	4,700	37	5,139	6,174	9,732
DeKalb	71,130	17,539	11,383	2,315	5,306	5,730	49	6,101	7,372	14,481
Elmore	81,468	18,601	11,693	2,455	6,234	6,536	56	6,769	8,234	10,609
Etowah	103,057	22,585	18,278	2,981	7,961	8,752	71	9,456	11,391	19,146
Houston	104,173	24,547	17,147	3,240	7,880	8,515	71	9,090	10,969	18,829
Jefferson	660,367	152,511	96,633	20,127	50,335	52,865	451	54,982	66,751	115,897
Madison	353,089	78,771	49,684	10,396	27,236	28,736	243	29,667	36,236	45,877
Mobile	415,395	99,154	62,039	13,086	31,333	33,139	284	34,686	42,050	75,204
Montgomery	226,519	54,083	31,018	7,137	17,089	17,578	155	18,045	21,919	49,457
Morgan	119,565	27,527	19,529	3,633	9,117	9,914	82	10,564	12,787	19,250
Russell	59,660	15,352	7,574	2,026	4,396	4,501	41	4,579	5,584	13,575
Shelby	208,713	50,382	28,101	6,649	15,723	16,505	143	16,969	20,742	17,558
Sumter	13,103	2,553	2,197	337	1,043	1,101	9	1,164	1,401	4,073
Talladega	80,862	17,686	13,396	2,334	6,258	6,803	56	7,248	8,773	17,439
Tuscaloosa	203,976	42,579	24,553	5,619	15,992	15,511	140	15,316	18,631	38,704
Totals	**2,972,695**	**683,184**	**445,219**	**90,161**	**226,882**	**239,679**	**2,038**	**250,441**	**303,801**	**498,208**

STATE TABLES

ALABAMA

American Lung Association in Alabama

www.lung.org/alabama

	HIGH OZONE DAYS 2013–2015					HIGH PARTICLE POLLUTION DAYS 2013–2015						
						24-Hour					Annual	
County	Orange	Red	Purple	Wgt. Avg.	Grade	Orange	Red	Purple	Wgt. Avg.	Grade	Design Value	Pass/ Fail
Baldwin	3	0	0	1.0	C	0	0	0	0.0	A	8.6	PASS
Clay	DNC	DNC	DNC	DNC	DNC	0	0	0	0.0	A	8.4	PASS
Colbert	0	0	0	0.0	A	0	0	0	0.0	A	8.9	PASS
DeKalb	1	0	0	0.3	B	0	0	0	0.0	A	9.2	PASS
Elmore	1	0	0	0.3	B	DNC	DNC	DNC	DNC	DNC	DNC	DNC
Etowah	0	0	0	0.0	A	0	0	0	0.0	A	9.2	PASS
Houston	0	0	0	0.0	A	0	0	0	0.0	A	8.1	PASS
Jefferson	11	0	0	3.7	F	0	0	0	0.0	A	11.0	PASS
Madison	0	0	0	0.0	A	0	0	0	0.0	A	8.6	PASS
Mobile	7	0	0	2.3	D	0	0	0	0.0	A	8.6	PASS
Montgomery	1	0	0	0.3	B	0	0	0	0.0	A	9.3	PASS
Morgan	0	0	0	0.0	A	0	0	0	0.0	A	8.9	PASS
Russell	2	0	0	0.7	B	0	0	0	0.0	A	10.0	PASS
Shelby	4	0	0	1.3	C	0	0	0	0.0	A	INC	INC
Sumter	0	0	0	0.0	A	DNC	DNC	DNC	DNC	DNC	DNC	DNC
Talladega	DNC	DNC	DNC	DNC	DNC	0	0	0	0.0	A	9.5	PASS
Tuscaloosa	0	0	0	0.0	A	0	0	0	0.0	A	9.0	PASS

STATE TABLES

ALASKA

American Lung Association in Alaska

www.lung.org/alaska

				AT-RISK GROUPS						
				Lung Diseases						
County	Total Population	Under 18	65 & Over	Pediatric Asthma	Adult Asthma	COPD	Lung Cancer	Cardiovascular Disease	Diabetes	Poverty
Anchorage Municipality	298,695	73,959	28,001	6,271	21,084	8,706	166	12,779	15,881	25,305
Denali Borough	1,919	352	173	30	145	64	1	93	122	124
Fairbanks North Star Borough	99,631	24,116	8,349	2,045	7,139	2,756	56	3,943	4,891	7,671
Juneau City and Borough	32,756	7,216	3,594	612	2,372	1,060	18	1,597	1,992	2,542
Kenai Peninsula Borough	58,059	13,343	8,604	1,131	4,123	2,057	32	3,275	3,960	6,488
Matanuska-Susitna Borough	101,095	27,428	10,008	2,326	6,857	3,008	57	4,500	5,618	9,676
Totals	**592,155**	**146,414**	**58,729**	**12,414**	**41,720**	**17,651**	**331**	**26,188**	**32,463**	**51,806**

STATE TABLES

ALASKA

American Lung Association in Alaska

www.lung.org/alaska

	HIGH OZONE DAYS 2013–2015					HIGH PARTICLE POLLUTION DAYS 2013–2015						
						24-Hour					Annual	
Borough	Orange	Red	Purple	Wgt. Avg.	Grade	Orange	Red	Purple	Wgt. Avg.	Grade	Design Value	Pass/ Fail
Anchorage Municipality	DNC	DNC	DNC	DNC	DNC	0	1	0	0.5	B	5.7	PASS
Denali Borough	0	0	0	0.0	A	DNC	DNC	DNC	DNC	DNC	DNC	DNC
Fairbanks North Star Borough	0	0	0	0.0	A	26	33	1	25.8	F	11.5	PASS
Juneau City and Borough	DNC	DNC	DNC	DNC	DNC	3	0	0	1.0	C	6.8	PASS
Kenai Peninsula Borough	DNC	DNC	DNC	DNC	DNC	INC	INC	INC	INC	INC	INC	INC
Matanuska-Susitna Borough	INC	INC	INC	INC	INC	20	2	0	7.7	F	7.1	PASS

STATE TABLES

ARIZONA

American Lung Association in Arizona

www.lung.org/arizona

		AT-RISK GROUPS								
				Lung Diseases						
County	Total Population	Under 18	65 & Over	Pediatric Asthma	Adult Asthma	COPD	Lung Cancer	Cardiovascular Disease	Diabetes	Poverty
Apache	71,474	20,658	9,977	2,253	4,804	3,242	35	4,004	5,188	26,788
Cochise	126,427	28,038	26,125	3,058	9,240	6,964	62	8,939	11,020	20,439
Coconino	139,097	29,757	15,930	3,245	10,261	6,029	68	7,138	9,491	25,133
Gila	53,159	10,845	14,609	1,183	3,977	3,438	26	4,568	5,456	11,089
La Paz	20,152	3,451	7,491	376	1,545	1,505	10	2,069	2,342	4,398
Maricopa	4,167,947	1,030,669	592,961	112,410	295,494	193,792	2,033	237,849	307,832	667,637
Mohave	204,737	37,506	56,716	4,091	15,719	13,467	100	17,851	21,373	34,720
Navajo	108,277	29,874	17,825	3,258	7,398	5,271	53	6,633	8,407	29,810
Pima	1,010,025	218,540	185,865	23,835	74,267	52,701	492	66,528	83,206	184,628
Pinal	406,584	96,927	77,527	10,571	28,991	21,037	200	26,779	33,093	60,151
Santa Cruz	46,461	12,919	7,668	1,409	3,167	2,267	23	2,855	3,620	11,295
Yavapai	222,255	38,024	64,634	4,147	17,332	15,160	108	20,183	24,097	32,978
Yuma	204,275	52,433	36,813	5,719	14,162	9,995	100	12,659	15,606	41,159
Totals	**6,780,870**	**1,609,641**	**1,114,141**	**175,556**	**486,357**	**334,869**	**3,310**	**418,057**	**530,731**	**1,150,225**

STATE TABLES

ARIZONA

American Lung Association in Arizona

www.lung.org/arizona

	HIGH OZONE DAYS 2013–2015					HIGH PARTICLE POLLUTION DAYS 2013–2015						
						24-Hour					Annual	
County	Orange	Red	Purple	Wgt. Avg.	Grade	Orange	Red	Purple	Wgt. Avg.	Grade	Design Value	Pass/ Fail
Apache	DNC	DNC	DNC	DNC	DNC	INC	INC	INC	INC	INC	INC	INC
Cochise	7	0	0	2.3	D	0	0	0	0.0	A	6.5	PASS
Coconino	11	0	0	3.7	F	INC	INC	INC	INC	INC	INC	INC
Gila	20	0	0	6.7	F	DNC	DNC	DNC	DNC	DNC	DNC	DNC
La Paz	12	0	0	4.0	F	INC	INC	INC	INC	INC	INC	INC
Maricopa	101	2	0	34.7	F	7	3	1	4.5	F	10.0	PASS
Mohave	DNC	DNC	DNC	DNC	DNC	0	0	0	0.0	A	INC	INC
Navajo	2	0	0	0.7	B	DNC	DNC	DNC	DNC	DNC	DNC	DNC
Pima	7	0	0	2.3	D	0	0	0	0.0	A	5.5	PASS
Pinal	25	0	0	8.3	F	8	0	0	2.7	D	7.7	PASS
Santa Cruz	DNC	DNC	DNC	DNC	DNC	7	3	0	3.8	F	9.1	PASS
Yavapai	7	0	0	2.3	D	INC	INC	INC	INC	INC	INC	INC
Yuma	20	2	0	7.7	F	1	1	0	0.8	B	6.4	PASS

ARKANSAS

American Lung Association in Arkansas

www.lung.org/arkansas

		AT-RISK GROUPS								
				Lung Diseases						
County	Total Population	Under 18	65 & Over	Pediatric Asthma	Adult Asthma	COPD	Lung Cancer	Cardiovascular Disease	Diabetes	Poverty
Arkansas	18,433	4,255	3,280	361	1,443	1,447	15	1,668	1,897	3,748
Ashley	20,838	4,889	3,929	415	1,619	1,641	17	1,919	2,167	4,040
Clark	22,633	4,334	3,638	367	1,824	1,666	18	1,823	2,082	4,466
Crittenden	48,963	13,578	6,133	1,151	3,608	3,380	39	3,647	4,267	12,473
Garland	97,177	20,122	21,427	1,706	7,785	8,111	78	9,762	10,867	18,354
Jackson	17,338	3,488	2,948	296	1,405	1,366	14	1,541	1,764	4,150
Newton	7,913	1,563	1,976	133	643	698	6	866	955	1,894
Polk	20,216	4,766	4,438	404	1,562	1,647	16	2,000	2,220	4,869
Pulaski	392,664	92,607	55,006	7,852	30,450	28,558	315	31,092	36,114	74,375
Union	40,144	9,591	6,842	813	3,111	3,095	32	3,542	4,043	7,800
Washington	225,477	56,325	24,743	4,776	16,954	14,630	183	14,926	17,610	36,600
Totals	**911,796**	**215,518**	**134,360**	**18,273**	**70,403**	**66,239**	**733**	**72,787**	**83,988**	**172,769**

STATE TABLES

ARKANSAS

American Lung Association in Arkansas

www.lung.org/arkansas

	HIGH OZONE DAYS 2013–2015					HIGH PARTICLE POLLUTION DAYS 2013–2015						
						24-Hour					Annual	
County	Orange	Red	Purple	Wgt. Avg.	Grade	Orange	Red	Purple	Wgt. Avg.	Grade	Design Value	Pass/ Fail
Arkansas	DNC	DNC	DNC	DNC	DNC	0	0	0	0.0	A	9.1	PASS
Ashley	DNC	DNC	DNC	DNC	DNC	0	0	0	0.0	A	8.6	PASS
Clark	1	0	0	0.3	B	DNC	DNC	DNC	DNC	DNC	DNC	DNC
Crittenden	1	0	0	0.3	B	1	0	0	0.3	B	9.4	PASS
Garland	DNC	DNC	DNC	DNC	DNC	0	0	0	0.0	A	9.0	PASS
Jackson	DNC	DNC	DNC	DNC	DNC	0	0	0	0.0	A	8.9	PASS
Newton	0	0	0	0.0	A	DNC	DNC	DNC	DNC	DNC	DNC	DNC
Polk	0	0	0	0.0	A	0	0	0	0.0	A	9.2	PASS
Pulaski	4	0	0	1.3	C	1	0	0	0.3	B	10.7	PASS
Union	DNC	DNC	DNC	DNC	DNC	0	0	0	0.0	A	9.1	PASS
Washington	0	0	0	0.0	A	0	0	0	0.0	A	8.6	PASS

STATE TABLES

CALIFORNIA

American Lung Association in California

www.lung.org/california

		AT-RISK GROUPS								
				Lung Diseases						
County	Total Population	Under 18	65 & Over	Pediatric Asthma	Adult Asthma	COPD	Lung Cancer	Cardiovascular Disease	Diabetes	Poverty
Alameda	1,638,215	346,302	208,711	24,746	99,232	51,297	709	80,675	126,353	184,716
Amador	37,001	5,654	9,539	404	2,475	1,589	16	2,803	4,144	4,404
Butte	225,411	45,348	39,543	3,240	13,978	7,812	98	12,787	19,274	47,269
Calaveras	44,828	7,795	11,595	557	2,929	1,912	19	3,403	5,033	5,781
Colusa	21,482	5,958	2,889	426	1,198	646	9	1,042	1,611	2,800
Contra Costa	1,126,745	261,320	164,504	18,673	66,864	36,598	488	59,728	92,596	114,123
El Dorado	184,452	37,919	34,393	2,710	11,424	6,776	80	11,581	17,709	16,634
Fresno	974,861	279,544	112,074	19,976	53,384	27,289	423	42,457	66,139	241,669
Glenn	28,017	7,491	4,220	535	1,590	883	12	1,447	2,214	5,105
Humboldt	135,727	26,518	21,791	1,895	8,447	4,603	59	7,444	11,365	27,616
Imperial	180,191	51,119	22,442	3,653	9,934	5,187	78	8,178	12,647	41,685
Inyo	18,260	3,769	4,044	269	1,139	706	8	1,227	1,827	2,222
Kern	882,176	257,727	88,992	18,417	47,777	23,732	384	36,297	57,322	185,990
Kings	150,965	41,435	14,146	2,961	8,357	4,026	66	6,015	9,555	30,117
Lake	64,591	13,267	13,778	948	4,025	2,473	28	4,282	6,420	13,006
Los Angeles	10,170,292	2,279,839	1,277,335	162,912	606,055	312,736	4,407	490,888	767,731	1,675,802
Madera	154,998	42,615	20,374	3,045	8,663	4,595	67	7,321	11,296	33,258
Marin	261,221	53,520	52,327	3,824	16,244	9,837	113	16,960	25,706	19,100
Mariposa	17,531	2,875	4,421	205	1,157	744	8	1,316	1,952	2,627
Mendocino	87,649	18,982	17,382	1,356	5,368	3,203	38	5,454	8,187	17,508
Merced	268,455	80,152	28,517	5,727	14,430	7,254	117	11,165	17,497	68,026
Monterey	433,898	114,387	53,530	8,174	24,563	12,728	189	19,992	31,075	63,732
Napa	142,456	30,661	24,821	2,191	8,688	4,953	62	8,241	12,528	13,960
Nevada	98,877	17,428	24,201	1,245	6,422	4,090	43	7,193	10,664	12,137
Orange	3,169,776	716,153	430,447	51,175	188,995	100,412	1,374	160,772	250,372	398,428
Placer	375,391	84,957	69,332	6,071	22,644	13,266	162	22,400	33,857	32,093
Plumas	18,409	3,149	4,729	225	1,206	785	8	1,395	2,065	2,503
Riverside	2,361,026	612,848	320,086	43,793	134,810	71,829	1,024	114,813	177,144	377,244
Sacramento	1,501,335	361,617	198,168	25,840	87,748	46,278	650	73,651	114,506	250,325
San Benito	58,792	15,631	6,957	1,117	3,316	1,731	26	2,748	4,328	5,454
San Bernardino	2,128,133	572,173	228,666	40,886	119,170	59,986	923	92,725	146,418	394,031
San Diego	3,299,521	728,037	431,999	52,024	197,708	102,514	1,433	161,074	250,288	445,948
San Francisco	864,816	115,963	126,593	8,286	57,569	29,633	376	46,201	71,392	105,244
San Joaquin	726,106	199,894	87,579	14,284	40,454	21,053	315	33,228	51,852	124,606
San Luis Obispo	281,401	50,837	51,231	3,633	17,910	10,097	122	16,633	25,113	38,448
San Mateo	765,135	162,283	114,498	11,596	46,568	25,369	331	41,231	63,775	63,663
Santa Barbara	444,769	99,537	63,670	7,113	26,618	14,037	193	22,203	33,995	66,475
Santa Clara	1,918,044	436,397	239,977	31,184	113,823	59,008	833	93,034	145,834	156,430

CALIFORNIA (cont.)

American Lung Association in California

www.lung.org/california

				AT-RISK GROUPS						
				Lung Diseases						
County	Total Population	Under 18	65 & Over	Pediatric Asthma	Adult Asthma	COPD	Lung Cancer	Cardiovascular Disease	Diabetes	Poverty
Santa Cruz	274,146	54,183	38,794	3,872	16,944	8,989	119	14,364	22,322	40,480
Shasta	179,533	38,620	35,628	2,760	11,015	6,564	78	11,166	16,752	33,556
Siskiyou	43,554	8,813	10,231	630	2,737	1,734	19	3,039	4,503	9,725
Solano	436,092	99,381	61,524	7,102	25,974	13,988	189	22,587	35,069	50,972
Sonoma	502,146	102,120	87,731	7,297	31,075	17,715	217	29,511	45,011	54,563
Stanislaus	538,388	146,063	67,324	10,437	30,189	15,817	233	25,049	38,935	103,646
Sutter	96,463	25,170	14,342	1,799	5,517	3,029	42	4,928	7,539	16,721
Tehama	63,308	15,129	11,481	1,081	3,756	2,197	27	3,705	5,598	14,073
Trinity	13,069	2,207	3,209	158	856	549	6	970	1,445	2,523
Tulare	459,863	144,036	49,147	10,292	24,222	12,265	200	18,970	29,653	123,922
Tuolumne	53,709	8,959	12,976	640	3,523	2,209	23	3,851	5,703	7,305
Ventura	850,536	202,649	119,596	14,481	49,997	27,022	369	43,731	67,850	83,389
Yolo	213,016	45,741	24,994	3,269	12,808	6,335	92	9,602	14,965	35,877
Totals	**38,984,776**	**9,084,172**	**5,166,478**	**649,133**	**2,301,495**	**1,210,079**	**16,906**	**1,921,480**	**2,987,129**	**5,866,931**

STATE TABLES

CALIFORNIA

American Lung Association in California

www.lung.org/california

	HIGH OZONE DAYS 2013–2015					HIGH PARTICLE POLLUTION DAYS 2013–2015						
						24-Hour					Annual	
County	Orange	Red	Purple	Wgt. Avg.	Grade	Orange	Red	Purple	Wgt. Avg.	Grade	Design Value	Pass/ Fail
Alameda	19	0	0	6.3	F	11	0	0	3.7	F	10.8	PASS
Amador	20	0	0	6.7	F	DNC	DNC	DNC	DNC	DNC	DNC	DNC
Butte	23	1	0	8.2	F	4	1	0	1.8	C	9.3	PASS
Calaveras	23	1	0	8.2	F	2	1	1	1.8	C	8.6	PASS
Colusa	0	0	0	0.0	A	3	1	0	1.5	C	7.6	PASS
Contra Costa	13	0	0	4.3	F	3	0	0	1.0	C	10.5	PASS
El Dorado	87	4	0	31.0	F	DNC	DNC	DNC	DNC	DNC	DNC	DNC
Fresno	215	41	1	92.8	F	68	37	0	41.2	F	15.4	FAIL
Glenn	2	0	0	0.7	B	DNC	DNC	DNC	DNC	DNC	DNC	DNC
Humboldt	0	0	0	0.0	A	4	0	0	1.3	C	INC	INC
Imperial	63	3	0	22.5	F	22	4	0	9.3	F	13.1	FAIL
Inyo	9	0	0	3.0	D	6	14	1	9.7	F	7.6	PASS
Kern	232	45	1	100.5	F	81	50	1	52.7	F	20.8	FAIL
Kings	120	9	0	44.5	F	65	39	0	41.2	F	22.2	FAIL
Lake	0	0	0	0.0	A	0	1	0	0.5	B	4.0	PASS
Los Angeles	202	78	3	108.3	F	27	3	0	10.5	F	12.3	FAIL
Madera	124	11	0	46.8	F	47	18	0	24.7	F	15.2	FAIL
Marin	0	0	0	0.0	A	5	0	0	1.7	C	10.0	PASS
Mariposa	49	0	0	16.3	F	DNC	DNC	DNC	DNC	DNC	DNC	DNC
Mendocino	0	0	0	0.0	A	2	2	0	1.7	C	INC	INC
Merced	94	4	0	33.3	F	48	7	0	19.5	F	12.5	FAIL
Monterey	0	0	0	0.0	A	1	0	0	0.3	B	6.3	PASS
Napa	2	0	0	0.7	B	2	0	0	0.7	B	11.4	PASS
Nevada	74	2	0	25.7	F	1	1	0	0.8	B	5.3	PASS
Orange	26	4	0	10.7	F	8	0	0	2.7	D	7.8	PASS
Placer	49	5	0	18.8	F	5	6	1	5.3	F	7.8	PASS
Plumas	DNC	DNC	DNC	DNC	DNC	31	2	0	11.3	F	14.9	FAIL
Riverside	243	82	0	122.0	F	36	4	0	14.0	F	14.1	FAIL
Sacramento	72	4	0	26.0	F	23	0	0	7.7	F	10.2	PASS
San Benito	9	0	0	3.0	D	0	0	0	0.0	A	5.0	PASS
San Bernardino	220	126	9	142.3	F	18	0	0	6.0	F	12.0	PASS
San Diego	92	1	0	31.2	F	4	2	0	2.3	D	10.0	PASS
San Francisco	0	0	0	0.0	A	2	0	0	0.7	B	8.4	PASS
San Joaquin	39	2	0	14.0	F	52	11	0	22.8	F	14.2	FAIL
San Luis Obispo	21	0	0	7.0	F	7	0	0	2.3	D	12.1	FAIL
San Mateo	2	0	0	0.7	B	3	0	0	1.0	C	7.8	PASS

STATE TABLES

CALIFORNIA (cont.)

American Lung Association in California

www.lung.org/california

	HIGH OZONE DAYS 2013–2015					HIGH PARTICLE POLLUTION DAYS 2013–2015						
						24-Hour					Annual	
County	Orange	Red	Purple	Wgt. Avg.	Grade	Orange	Red	Purple	Wgt. Avg.	Grade	Design Value	Pass/ Fail
Santa Barbara	8	2	0	3.7	F	0	0	0	0.0	A	7.7	PASS
Santa Clara	13	0	0	4.3	F	9	2	0	4.0	F	10.2	PASS
Santa Cruz	0	0	0	0.0	A	33	0	0	11.0	F	5.6	PASS
Shasta	16	0	0	5.3	F	0	1	0	0.5	B	6.2	PASS
Siskiyou	1	0	0	0.3	B	4	2	0	2.3	D	INC	INC
Solano	4	0	0	1.3	C	14	0	0	4.7	F	9.8	PASS
Sonoma	0	0	0	0.0	A	0	0	0	0.0	A	INC	INC
Stanislaus	84	4	0	30.0	F	64	17	0	29.8	F	13.8	FAIL
Sutter	19	1	0	6.8	F	3	0	0	1.0	C	9.1	PASS
Tehama	42	1	0	14.5	F	DNC	DNC	DNC	DNC	DNC	DNC	DNC
Trinity	DNC	DNC	DNC	DNC	DNC	INC	INC	INC	INC	INC	INC	INC
Tulare	226	33	1	92.5	F	18	13	0	12.5	F	17.6	FAIL
Tuolumne	29	0	0	9.7	F	DNC	DNC	DNC	DNC	DNC	DNC	DNC
Ventura	37	1	0	12.8	F	0	0	0	0.0	A	9.4	PASS
Yolo	4	0	0	1.3	C	0	0	0	0.0	A	7.0	PASS

STATE TABLES

COLORADO

American Lung Association in Colorado

www.lung.org/colorado

				AT-RISK GROUPS						
				Lung Diseases						
County	Total Population	Under 18	65 & Over	Pediatric Asthma	Adult Asthma	COPD	Lung Cancer	Cardiovascular Disease	Diabetes	Poverty
Adams	491,337	135,138	47,987	11,458	32,466	13,882	209	19,244	21,576	61,980
Arapahoe	631,096	153,148	76,968	12,985	43,314	20,195	268	28,436	31,401	57,651
Boulder	319,372	63,682	40,331	5,399	23,227	10,580	136	14,899	16,431	38,046
Chaffee	18,658	2,848	4,366	241	1,409	858	8	1,275	1,329	2,006
Clear Creek	9,303	1,472	1,743	125	695	408	4	585	637	880
Denver	682,545	140,671	74,815	11,927	49,657	20,404	290	28,558	31,559	105,275
Douglas	322,387	89,885	33,895	7,621	20,957	9,951	137	13,757	15,563	10,917
El Paso	674,471	167,331	79,908	14,188	46,093	20,905	287	29,453	32,453	72,201
Garfield	58,095	14,941	6,534	1,267	3,902	1,825	25	2,543	2,846	5,909
Gunnison	16,067	2,807	1,851	238	1,211	515	7	718	799	1,892
Jackson	1,356	237	296	20	99	61	1	89	94	189
Jefferson	565,524	116,627	85,287	9,889	40,386	20,708	240	29,549	32,231	44,068
La Plata	54,688	10,531	8,129	893	3,981	1,996	23	2,843	3,105	4,993
Larimer	333,577	67,793	47,570	5,748	24,144	11,356	142	16,259	17,585	39,648
Mesa	148,513	33,122	25,879	2,808	10,389	5,551	63	8,110	8,600	20,326
Moffat	12,937	3,317	1,719	281	865	438	6	619	682	1,496
Montezuma	26,168	5,909	5,169	501	1,807	1,067	11	1,570	1,656	4,994
Park	16,510	2,744	2,844	233	1,215	723	7	1,023	1,136	1,511
Pitkin	17,787	2,772	2,908	235	1,347	707	8	1,008	1,101	1,243
Pueblo	163,591	37,836	28,497	3,208	11,311	6,102	69	8,917	9,456	31,501
Rio Blanco	6,571	1,561	916	132	452	224	3	319	348	607
San Miguel	7,879	1,444	929	122	579	277	3	382	434	865
Weld	285,174	76,551	32,528	6,491	18,940	8,642	121	12,144	13,430	31,531
Totals	**4,863,606**	**1,132,367**	**611,069**	**96,012**	**338,444**	**157,371**	**2,067**	**222,301**	**244,450**	**539,729**

STATE TABLES

COLORADO

American Lung Association in Colorado

www.lung.org/colorado

	HIGH OZONE DAYS 2013–2015					HIGH PARTICLE POLLUTION DAYS 2013–2015						
						24-Hour					Annual	
County	Orange	Red	Purple	Wgt. Avg.	Grade	Orange	Red	Purple	Wgt. Avg.	Grade	Design Value	Pass/ Fail
Adams	19	0	0	6.3	F	2	0	0	0.7	B	INC	INC
Arapahoe	21	0	0	7.0	F	0	0	0	0.0	A	6.3	PASS
Boulder	25	1	0	8.8	F	2	0	0	0.7	B	7.0	PASS
Chaffee	INC	INC	INC	INC	INC	DNC	DNC	DNC	DNC	DNC	DNC	DNC
Clear Creek	32	3	0	12.2	F	DNC	DNC	DNC	DNC	DNC	DNC	DNC
Denver	8	0	0	2.7	D	9	1	0	3.5	F	7.5	PASS
Douglas	41	3	0	15.2	F	1	0	0	0.3	B	5.5	PASS
El Paso	11	0	0	3.7	F	0	0	0	0.0	A	5.7	PASS
Garfield	2	0	0	0.7	B	0	0	0	0.0	A	INC	INC
Gunnison	1	0	0	0.3	B	DNC	DNC	DNC	DNC	DNC	DNC	DNC
Jackson	1	0	0	0.3	B	DNC	DNC	DNC	DNC	DNC	DNC	DNC
Jefferson	62	6	0	23.7	F	DNC	DNC	DNC	DNC	DNC	DNC	DNC
La Plata	7	0	0	2.3	D	0	0	0	0.0	A	INC	INC
Larimer	56	2	0	19.7	F	2	1	0	1.2	C	6.8	PASS
Mesa	1	0	0	0.3	B	4	0	0	1.3	C	7.4	PASS
Moffat	0	0	0	0.0	A	DNC	DNC	DNC	DNC	DNC	DNC	DNC
Montezuma	0	0	0	0.0	A	0	0	0	0.0	A	INC	INC
Park	5	0	0	1.7	C	INC	INC	INC	INC	INC	INC	INC
Pitkin	INC	INC	INC	INC	INC	DNC	DNC	DNC	DNC	DNC	DNC	DNC
Pueblo	DNC	DNC	DNC	DNC	DNC	0	0	0	0.0	A	5.8	PASS
Rio Blanco	9	4	1	5.7	F	0	0	0	0.0	A	8.2	PASS
San Miguel	INC	INC	INC	INC	INC	DNC	DNC	DNC	DNC	DNC	DNC	DNC
Weld	19	0	0	6.3	F	2	0	0	0.7	B	7.8	PASS

STATE TABLES

CONNECTICUT

American Lung Association in Connecticut

www.lung.org/connecticut

		AT-RISK GROUPS								
				Lung Diseases						
County	Total Population	Under 18	65 & Over	Pediatric Asthma	Adult Asthma	COPD	Lung Cancer	Cardiovascular Disease	Diabetes	Poverty
Fairfield	948,053	220,906	137,799	25,884	76,395	36,729	598	51,524	66,675	83,612
Hartford	895,841	192,728	142,573	22,583	73,932	35,966	565	51,006	64,973	96,763
Litchfield	183,603	35,040	34,949	4,106	15,442	8,423	116	12,149	15,281	13,383
Middlesex	164,063	30,985	29,944	3,631	13,892	7,288	103	10,464	13,197	10,744
New Haven	859,470	178,891	137,053	20,961	71,618	34,597	542	49,032	62,466	112,801
New London	271,863	54,507	44,994	6,387	22,836	11,233	172	15,975	20,290	28,760
Tolland	151,420	27,234	21,691	3,191	13,134	5,907	96	8,209	10,681	9,593
Windham	116,573	23,768	17,803	2,785	9,752	4,697	74	6,602	8,518	12,211
Totals	**3,590,886**	**764,059**	**566,806**	**89,528**	**297,001**	**144,841**	**2,265**	**204,962**	**262,081**	**367,867**

STATE TABLES

CONNECTICUT

American Lung Association in Connecticut

www.lung.org/connecticut

	HIGH OZONE DAYS 2013–2015					HIGH PARTICLE POLLUTION DAYS 2013–2015						
						24-Hour					Annual	
County	Orange	Red	Purple	Wgt. Avg.	Grade	Orange	Red	Purple	Wgt. Avg.	Grade	Design Value	Pass/ Fail
Fairfield	51	14	0	24.0	F	2	0	0	0.7	B	9.4	PASS
Hartford	23	1	0	8.2	F	0	0	0	0.0	A	7.3	PASS
Litchfield	11	0	0	3.7	F	0	0	0	0.0	A	5.2	PASS
Middlesex	28	3	0	10.8	F	DNC	DNC	DNC	DNC	DNC	DNC	DNC
New Haven	28	6	0	12.3	F	3	0	0	1.0	C	8.7	PASS
New London	15	4	0	7.0	F	1	0	0	0.3	B	INC	INC
Tolland	22	0	0	7.3	F	DNC	DNC	DNC	DNC	DNC	DNC	DNC
Windham	7	0	0	2.3	D	DNC	DNC	DNC	DNC	DNC	DNC	DNC

STATE TABLES

DELAWARE

American Lung Association in Delaware

www.lung.org/delaware

		AT-RISK GROUPS								
				Lung Diseases						
County	Total Population	Under 18	65 & Over	Pediatric Asthma	Adult Asthma	COPD	Lung Cancer	Cardiovascular Disease	Diabetes	Poverty
Kent	173,533	40,353	27,752	3,421	12,327	9,164	122	12,038	14,468	23,947
New Castle	556,779	122,224	78,983	10,363	40,396	29,290	391	37,276	46,136	65,503
Sussex	215,622	41,809	53,780	3,545	16,172	13,976	152	19,956	22,909	26,205
Totals	**945,934**	**204,386**	**160,515**	**17,330**	**68,894**	**52,430**	**665**	**69,271**	**83,513**	**115,655**

STATE TABLES

DELAWARE

American Lung Association in Delaware

www.lung.org/delaware

	HIGH OZONE DAYS 2013–2015					HIGH PARTICLE POLLUTION DAYS 2013–2015						
						24-Hour					Annual	
County	Orange	Red	Purple	Wgt. Avg.	Grade	Orange	Red	Purple	Wgt. Avg.	Grade	Design Value	Pass/ Fail
Kent	1	0	0	0.3	B	0	0	0	0.0	A	8.1	PASS
New Castle	17	1	0	6.2	F	9	1	0	3.5	F	9.6	PASS
Sussex	8	0	0	2.7	D	0	0	0	0.0	A	8.4	PASS

DISTRICT OF COLUMBIA

American Lung Association in the District of Columbia

www.lung.org/districtofcolumbia

		AT-RISK GROUPS								
				Lung Diseases						
County	Total Population	Under 18	65 & Over	Pediatric Asthma	Adult Asthma	COPD	Lung Cancer	Cardiovascular Disease	Diabetes	Poverty
District of Columbia	672,228	118,107	77,004	10,175	59,002	28,305	375	37,044	46,280	113,185
Totals	**672,228**	**118,107**	**77,004**	**10,175**	**59,002**	**28,305**	**375**	**37,044**	**46,280**	**113,185**

STATE TABLES

DISTRICT OF COLUMBIA

American Lung Association in the District of Columbia

www.lung.org/districtofcolumbia

	HIGH OZONE DAYS 2013–2015					HIGH PARTICLE POLLUTION DAYS 2013–2015						
						24-Hour					Annual	
County	Orange	Red	Purple	Wgt. Avg.	Grade	Orange	Red	Purple	Wgt. Avg.	Grade	Design Value	Pass/ Fail
District of Columbia	10	0	0	3.3	F	0	0	0	0.0	A	9.2	PASS

STATE TABLES

FLORIDA

American Lung Association in Florida

www.lung.org/florida

		AT-RISK GROUPS								
				Lung Diseases						
County	Total Population	Under 18	65 & Over	Pediatric Asthma	Adult Asthma	COPD	Lung Cancer	Cardiovascular Disease	Diabetes	Poverty
Alachua	259,964	46,861	33,506	3,973	16,007	11,918	155	15,044	18,257	52,258
Baker	27,420	6,769	3,636	574	1,567	1,313	16	1,700	2,073	4,189
Bay	181,635	39,234	29,823	3,327	10,763	9,517	108	12,574	15,154	29,301
Brevard	568,088	105,472	130,247	8,943	34,825	35,230	338	48,315	57,294	75,268
Broward	1,896,425	407,683	296,906	34,567	112,749	98,583	1,128	129,582	156,814	263,607
Citrus	141,058	21,032	50,225	1,783	8,877	10,724	84	15,432	17,779	24,249
Collier	357,305	63,956	107,485	5,423	21,743	24,126	213	34,140	39,548	48,198
Columbia	68,348	14,889	12,005	1,262	4,035	3,664	41	4,882	5,858	12,413
Duval	913,010	207,260	119,785	17,573	53,462	43,566	543	56,074	68,376	142,660
Escambia	311,003	64,885	50,304	5,502	18,556	15,977	186	21,003	25,283	44,835
Flagler	105,392	18,778	30,717	1,592	6,449	7,144	63	10,072	11,729	12,213
Highlands	99,491	17,476	33,952	1,482	6,037	7,096	59	10,196	11,699	22,419
Hillsborough	1,349,050	311,084	180,904	26,376	78,572	64,466	803	83,213	101,279	209,040
Holmes	19,324	3,848	3,762	326	1,166	1,091	12	1,468	1,752	4,535
Indian River	147,919	25,425	45,664	2,156	9,095	10,294	88	14,601	16,934	19,051
Lake	325,875	64,420	85,204	5,462	19,489	20,536	194	28,638	33,475	41,272
Lee	701,982	129,382	189,043	10,970	42,657	45,196	418	63,130	73,716	110,398
Leon	286,272	54,381	33,957	4,611	17,445	12,742	170	15,951	19,452	59,366
Liberty	8,331	1,609	1,004	136	510	400	5	508	624	1,422
Manatee	363,369	69,687	94,063	5,909	21,940	23,107	216	32,165	37,697	53,080
Marion	343,254	64,096	97,002	5,435	20,749	22,493	204	31,619	36,781	62,271
Martin	156,283	26,273	46,400	2,228	9,690	10,828	93	15,280	17,805	17,125
Miami-Dade	2,693,117	552,280	420,642	46,827	161,793	138,709	1,602	181,691	219,597	529,850
Okaloosa	198,664	43,993	30,682	3,730	11,671	9,957	119	13,045	15,737	21,966
Orange	1,288,126	290,689	141,831	24,647	75,573	57,410	768	72,218	88,804	196,882
Osceola	323,993	80,769	41,928	6,848	18,388	14,891	193	19,170	23,316	59,226
Palm Beach	1,422,789	276,718	326,763	23,462	85,823	85,174	846	116,804	137,780	189,355
Pasco	497,909	101,714	112,844	8,624	29,705	29,645	296	40,664	48,023	71,760
Pinellas	949,827	159,853	222,148	13,554	59,433	59,907	564	82,129	97,345	127,287
Polk	650,092	147,812	128,029	12,533	37,680	35,383	387	47,818	56,748	109,907
Santa Rosa	167,040	37,266	24,872	3,160	9,842	8,520	100	11,153	13,538	19,681
Sarasota	405,549	59,816	140,193	5,072	25,580	30,252	241	43,364	50,014	38,874
Seminole	449,144	95,641	66,050	8,109	26,795	22,857	267	29,808	36,207	51,205
St. Lucie	298,563	61,111	68,766	5,182	17,789	17,857	178	24,544	28,946	48,570
Volusia	517,887	92,727	122,495	7,862	31,901	32,178	308	44,218	52,234	82,326
Wakulla	31,535	6,596	4,347	559	1,896	1,599	19	2,072	2,532	4,623
Totals	**18,525,033**	**3,771,485**	**3,527,184**	**319,778**	**1,110,252**	**1,024,351**	**11,026**	**1,374,285**	**1,640,200**	**2,860,682**

STATE TABLES

FLORIDA

American Lung Association in Florida

www.lung.org/florida

	HIGH OZONE DAYS 2013–2015					HIGH PARTICLE POLLUTION DAYS 2013–2015						
						24-Hour					Annual	
County	Orange	Red	Purple	Wgt. Avg.	Grade	Orange	Red	Purple	Wgt. Avg.	Grade	Design Value	Pass/ Fail
Alachua	0	0	0	0.0	A	0	0	0	0.0	A	INC	INC
Baker	0	0	0	0.0	A	DNC	DNC	DNC	DNC	DNC	DNC	DNC
Bay	1	0	0	0.3	B	DNC	DNC	DNC	DNC	DNC	DNC	DNC
Brevard	0	0	0	0.0	A	0	0	0	0.0	A	5.6	PASS
Broward	2	0	0	0.7	B	0	0	0	0.0	A	INC	INC
Citrus	DNC	DNC	DNC	DNC	DNC	0	0	0	0.0	A	6.2	PASS
Collier	0	0	0	0.0	A	DNC	DNC	DNC	DNC	DNC	DNC	DNC
Columbia	0	0	0	0.0	A	DNC	DNC	DNC	DNC	DNC	DNC	DNC
Duval	4	0	0	1.3	C	1	0	0	0.3	B	7.7	PASS
Escambia	5	0	0	1.7	C	0	0	0	0.0	A	7.7	PASS
Flagler	0	0	0	0.0	A	DNC	DNC	DNC	DNC	DNC	DNC	DNC
Highlands	0	0	0	0.0	A	DNC	DNC	DNC	DNC	DNC	DNC	DNC
Hillsborough	10	0	0	3.3	F	0	0	0	0.0	A	7.8	PASS
Holmes	0	0	0	0.0	A	DNC	DNC	DNC	DNC	DNC	DNC	DNC
Indian River	1	0	0	0.3	B	DNC	DNC	DNC	DNC	DNC	DNC	DNC
Lake	3	0	0	1.0	C	DNC	DNC	DNC	DNC	DNC	DNC	DNC
Lee	0	0	0	0.0	A	0	0	0	0.0	A	5.9	PASS
Leon	0	0	0	0.0	A	0	1	0	0.5	B	8.3	PASS
Liberty	0	0	0	0.0	A	DNC	DNC	DNC	DNC	DNC	DNC	DNC
Manatee	3	0	0	1.0	C	DNC	DNC	DNC	DNC	DNC	DNC	DNC
Marion	0	0	0	0.0	A	DNC	DNC	DNC	DNC	DNC	DNC	DNC
Martin	INC	INC	INC	INC	INC	DNC	DNC	DNC	DNC	DNC	DNC	DNC
Miami-Dade	2	0	0	0.7	B	1	0	0	0.3	B	6.0	PASS
Okaloosa	1	0	0	0.3	B	DNC	DNC	DNC	DNC	DNC	DNC	DNC
Orange	3	0	0	1.0	C	0	0	0	0.0	A	6.2	PASS
Osceola	1	0	0	0.3	B	DNC	DNC	DNC	DNC	DNC	DNC	DNC
Palm Beach	3	0	0	1.0	C	0	0	0	0.0	A	5.3	PASS
Pasco	2	0	0	0.7	B	DNC	DNC	DNC	DNC	DNC	DNC	DNC
Pinellas	4	0	0	1.3	C	0	0	0	0.0	A	6.5	PASS
Polk	2	0	0	0.7	B	0	0	0	0.0	A	6.5	PASS
Santa Rosa	3	0	0	1.0	C	DNC	DNC	DNC	DNC	DNC	DNC	DNC
Sarasota	6	0	0	2.0	C	0	0	0	0.0	A	6.1	PASS
Seminole	0	0	0	0.0	A	0	0	0	0.0	A	6.1	PASS
St. Lucie	INC	INC	INC	INC	INC	DNC	DNC	DNC	DNC	DNC	DNC	DNC
Volusia	1	0	0	0.3	B	0	0	0	0.0	A	6.1	PASS
Wakulla	0	0	0	0.0	A	DNC	DNC	DNC	DNC	DNC	DNC	DNC

GEORGIA

American Lung Association in Georgia

www.lung.org/georgia

		AT-RISK GROUPS								
				Lung Diseases						
County	Total Population	Under 18	65 & Over	Pediatric Asthma	Adult Asthma	COPD	Lung Cancer	Cardiovascular Disease	Diabetes	Poverty
Bibb	153,721	38,331	22,157	4,261	10,747	8,295	101	11,020	13,528	39,343
Chatham	286,956	63,320	40,041	7,038	20,576	15,162	189	20,027	24,437	48,579
Chattooga	24,922	5,646	4,126	628	1,807	1,455	17	1,949	2,400	4,781
Clarke	123,912	21,518	12,223	2,392	9,081	5,512	81	7,032	8,370	42,773
Clayton	273,955	77,100	23,396	8,570	18,229	12,585	179	16,189	19,824	62,452
Cobb	741,334	182,064	81,302	20,237	52,131	37,970	488	49,492	60,804	83,213
Columbia	144,052	37,251	17,316	4,140	9,969	7,447	95	9,777	12,018	13,355
Coweta	138,427	35,281	17,659	3,922	9,689	7,436	91	9,804	12,086	14,976
Dawson	23,312	4,936	4,330	549	1,738	1,461	15	1,971	2,435	2,800
DeKalb	734,871	173,901	78,499	19,329	51,950	36,932	482	47,985	58,756	128,675
Dougherty	91,332	22,653	12,926	2,518	6,368	4,841	60	6,420	7,865	25,847
Douglas	140,733	37,540	15,015	4,173	9,654	7,098	92	9,256	11,392	19,638
Floyd	96,504	22,599	15,526	2,512	6,893	5,458	64	7,300	8,966	18,060
Fulton	1,010,562	231,537	108,711	25,736	71,920	50,682	666	65,813	80,451	156,705
Glynn	83,579	19,122	15,181	2,125	6,058	5,027	55	6,784	8,357	14,999
Gwinnett	895,823	247,554	79,872	27,516	60,468	42,829	592	55,273	67,944	112,026
Hall	193,535	50,521	27,256	5,615	13,315	10,249	128	13,608	16,702	32,263
Henry	217,739	57,991	23,693	6,446	14,976	11,108	143	14,506	17,871	21,377
Houston	150,033	38,453	18,150	4,274	10,384	7,705	99	10,116	12,416	22,510
Lowndes	112,865	28,087	12,987	3,122	7,710	5,316	75	6,935	8,405	28,460
Murray	39,565	10,027	5,446	1,115	2,766	2,143	26	2,839	3,494	6,960
Muscogee	200,579	48,646	24,713	5,407	13,983	10,088	133	13,232	16,148	42,678
Paulding	152,238	41,773	15,125	4,643	10,311	7,452	100	9,678	11,899	13,326
Pike	17,941	4,379	2,688	487	1,280	1,026	12	1,367	1,688	2,074
Richmond	201,793	47,511	26,108	5,281	14,261	10,493	133	13,808	16,888	46,401
Rockdale	88,856	22,656	11,700	2,518	6,237	4,853	58	6,414	7,916	14,009
Sumter	30,779	7,285	4,783	810	2,179	1,690	20	2,254	2,762	8,970
Walker	68,066	15,176	11,539	1,687	4,973	4,048	45	5,430	6,692	12,485
Washington	20,816	4,586	3,374	510	1,525	1,224	14	1,636	2,016	4,969
Wilkinson	9,155	2,095	1,670	233	670	568	6	767	949	1,891
Totals	**6,467,955**	**1,599,539**	**737,512**	**177,790**	**451,848**	**328,152**	**4,259**	**428,684**	**525,480**	**1,046,595**

STATE TABLES

GEORGIA

American Lung Association in Georgia

www.lung.org/georgia

	HIGH OZONE DAYS 2013–2015					HIGH PARTICLE POLLUTION DAYS 2013–2015						
						24-Hour					Annual	
County	Orange	Red	Purple	Wgt. Avg.	Grade	Orange	Red	Purple	Wgt. Avg.	Grade	Design Value	Pass/ Fail
Bibb	2	0	0	0.7	B	1	0	0	0.3	B	10.2	PASS
Chatham	0	0	0	0.0	A	0	0	0	0.0	A	8.9	PASS
Chattooga	0	0	0	0.0	A	DNC	DNC	DNC	DNC	DNC	DNC	DNC
Clarke	0	0	0	0.0	A	0	0	0	0.0	A	9.5	PASS
Clayton	DNC	DNC	DNC	DNC	DNC	0	0	0	0.0	A	10.0	PASS
Cobb	5	0	0	1.7	C	0	0	0	0.0	A	9.6	PASS
Columbia	0	0	0	0.0	A	DNC	DNC	DNC	DNC	DNC	DNC	DNC
Coweta	4	0	0	1.3	C	DNC	DNC	DNC	DNC	DNC	DNC	DNC
Dawson	3	0	0	1.0	C	DNC	DNC	DNC	DNC	DNC	DNC	DNC
DeKalb	8	0	0	2.7	D	0	0	0	0.0	A	9.4	PASS
Dougherty	DNC	DNC	DNC	DNC	DNC	7	0	0	2.3	D	9.8	PASS
Douglas	4	0	0	1.3	C	DNC	DNC	DNC	DNC	DNC	DNC	DNC
Floyd	DNC	DNC	DNC	DNC	DNC	0	0	0	0.0	A	9.9	PASS
Fulton	17	3	0	7.2	F	0	0	0	0.0	A	10.5	PASS
Glynn	0	0	0	0.0	A	0	0	0	0.0	A	8.0	PASS
Gwinnett	6	1	0	2.5	D	0	0	0	0.0	A	9.0	PASS
Hall	DNC	DNC	DNC	DNC	DNC	0	0	0	0.0	A	8.4	PASS
Henry	11	1	0	4.2	F	DNC	DNC	DNC	DNC	DNC	DNC	DNC
Houston	DNC	DNC	DNC	DNC	DNC	0	0	0	0.0	A	8.9	PASS
Lowndes	DNC	DNC	DNC	DNC	DNC	0	0	0	0.0	A	8.5	PASS
Murray	1	1	0	0.8	B	DNC	DNC	DNC	DNC	DNC	DNC	DNC
Muscogee	0	0	0	0.0	A	0	0	0	0.0	A	9.6	PASS
Paulding	0	0	0	0.0	A	0	0	0	0.0	A	8.2	PASS
Pike	4	1	0	1.8	C	DNC	DNC	DNC	DNC	DNC	DNC	DNC
Richmond	0	0	0	0.0	A	0	0	0	0.0	A	9.5	PASS
Rockdale	14	0	0	4.7	F	DNC	DNC	DNC	DNC	DNC	DNC	DNC
Sumter	0	0	0	0.0	A	DNC	DNC	DNC	DNC	DNC	DNC	DNC
Walker	DNC	DNC	DNC	DNC	DNC	0	0	0	0.0	A	9.9	PASS
Washington	DNC	DNC	DNC	DNC	DNC	0	0	0	0.0	A	9.2	PASS
Wilkinson	DNC	DNC	DNC	DNC	DNC	1	0	0	0.3	B	10.0	PASS

STATE TABLES

HAWAII

American Lung Association in Hawaii

www.lung.org/hawaii

		AT-RISK GROUPS								
				Lung Diseases						
County	Total Population	Under 18	65 & Over	Pediatric Asthma	Adult Asthma	COPD	Lung Cancer	Cardiovascular Disease	Diabetes	Poverty
Hawaii	196,428	43,217	35,851	4,291	15,151	6,892	99	10,359	13,874	35,294
Honolulu	998,714	214,852	161,966	21,333	79,203	33,353	505	47,503	64,243	88,536
Kauai	71,735	16,019	12,902	1,591	5,515	2,500	36	3,748	5,026	7,928
Maui	164,637	36,745	26,166	3,649	12,794	5,586	83	8,155	11,097	17,333
Totals	**1,431,514**	**310,833**	**236,885**	**30,864**	**112,663**	**48,331**	**724**	**69,765**	**94,239**	**149,091**

STATE TABLES

HAWAII

American Lung Association in Hawaii

www.lung.org/hawaii

	HIGH OZONE DAYS 2013–2015					HIGH PARTICLE POLLUTION DAYS 2013–2015						
						24-Hour					Annual	
County	Orange	Red	Purple	Wgt. Avg.	Grade	Orange	Red	Purple	Wgt. Avg.	Grade	Design Value	Pass/ Fail
Hawaii	DNC	DNC	DNC	DNC	DNC	2	0	0	0.7	B	12.1	FAIL
Honolulu	0	0	0	0.0	A	0	0	0	0.0	A	5.4	PASS
Kauai	DNC	DNC	DNC	DNC	DNC	0	0	0	0.0	A	3.9	PASS
Maui	DNC	DNC	DNC	DNC	DNC	1	0	0	0.3	B	4.8	PASS

STATE TABLES

IDAHO

American Lung Association in Idaho

www.lung.org/idaho

		AT-RISK GROUPS								
				Lung Diseases						
County	Total Population	Under 18	65 & Over	Pediatric Asthma	Adult Asthma	COPD	Lung Cancer	Cardiovascular Disease	Diabetes	Poverty
Ada	434,211	107,568	56,644	9,121	29,849	15,427	205	21,998	25,165	49,369
Bannock	83,744	22,302	11,020	1,891	5,594	2,864	40	4,112	4,655	18,179
Benewah	9,052	2,003	1,973	170	643	409	4	634	702	1,614
Butte	2,501	624	512	53	171	107	1	165	183	394
Canyon	207,478	61,522	26,566	5,216	13,298	6,883	98	9,906	11,224	32,329
Franklin	13,074	4,385	1,804	372	791	432	6	636	714	1,253
Jerome	22,814	7,115	2,811	603	1,434	748	11	1,073	1,224	3,577
Lemhi	7,735	1,398	2,193	119	574	398	4	642	694	1,347
Shoshone	12,432	2,464	2,772	209	909	576	6	892	988	2,577
Totals	**793,041**	**209,381**	**106,295**	**17,753**	**53,263**	**27,843**	**375**	**40,057**	**45,548**	**110,639**

STATE TABLES

IDAHO

American Lung Association in Idaho

www.lung.org/idaho

	HIGH OZONE DAYS 2013–2015					HIGH PARTICLE POLLUTION DAYS 2013–2015						
						24-Hour					Annual	
County	Orange	Red	Purple	Wgt. Avg.	Grade	Orange	Red	Purple	Wgt. Avg.	Grade	Design Value	Pass/ Fail
Ada	6	1	0	2.5	D	INC	INC	INC	INC	INC	INC	INC
Bannock	DNC	DNC	DNC	DNC	DNC	3	1	0	1.5	C	7.3	PASS
Benewah	DNC	DNC	DNC	DNC	DNC	INC	INC	INC	INC	INC	INC	INC
Butte	0	0	0	0.0	A	DNC	DNC	DNC	DNC	DNC	DNC	DNC
Canyon	DNC	DNC	DNC	DNC	DNC	INC	INC	INC	INC	INC	INC	INC
Franklin	DNC	DNC	DNC	DNC	DNC	20	12	0	12.7	F	INC	INC
Jerome	DNC	DNC	DNC	DNC	DNC	INC	INC	INC	INC	INC	INC	INC
Lemhi	DNC	DNC	DNC	DNC	DNC	34	6	0	14.3	F	12.7	FAIL
Shoshone	DNC	DNC	DNC	DNC	DNC	43	5	0	16.8	F	13.7	FAIL

STATE TABLES

ILLINOIS

American Lung Association in Illinois

www.lung.org/illinois

		AT-RISK GROUPS								
				Lung Diseases						
County	Total Population	Under 18	65 & Over	Pediatric Asthma	Adult Asthma	COPD	Lung Cancer	Cardiovascular Disease	Diabetes	Poverty
Adams	67,013	15,213	12,711	1,125	4,300	3,243	43	4,879	5,821	8,674
Champaign	208,861	39,693	23,639	2,935	14,382	8,428	135	10,735	13,579	38,751
Clark	15,979	3,632	3,029	269	1,024	782	10	1,178	1,408	2,171
Cook	5,238,216	1,175,147	692,946	86,906	341,993	224,961	3,377	306,619	381,122	833,241
DuPage	933,736	216,777	129,486	16,031	60,047	41,707	603	58,108	72,050	65,538
Effingham	34,371	8,103	5,870	599	2,187	1,608	22	2,362	2,852	3,313
Hamilton	8,200	1,815	1,678	134	528	413	5	633	750	1,055
Jersey	22,372	4,762	4,016	352	1,463	1,095	14	1,620	1,954	2,455
Jo Daviess	22,086	4,271	5,552	316	1,460	1,232	14	1,978	2,301	2,060
Kane	530,847	141,342	64,659	10,453	32,725	21,999	344	29,962	37,481	56,882
Lake	703,910	176,512	88,880	13,054	44,232	30,322	456	41,581	52,009	61,899
Macon	107,303	23,914	19,664	1,769	6,933	5,160	69	7,683	9,211	18,784
Macoupin	46,045	9,770	8,897	723	3,007	2,302	30	3,469	4,148	6,192
Madison	266,209	59,077	42,437	4,369	17,297	12,351	172	17,738	21,641	33,734
McHenry	307,343	75,431	38,883	5,578	19,422	13,535	199	18,604	23,327	24,659
McLean	173,166	38,016	20,468	2,811	11,432	7,115	112	9,355	11,766	18,969
Peoria	186,221	44,415	28,650	3,285	11,867	8,285	120	11,823	14,415	28,269
Randolph	32,852	6,300	5,782	466	2,214	1,602	22	2,336	2,826	4,049
Rock Island	146,133	32,595	26,190	2,410	9,450	6,954	94	10,290	12,363	18,596
Sangamon	198,712	45,433	31,830	3,360	12,791	9,198	128	13,260	16,158	29,798
St. Clair	264,052	63,022	37,645	4,661	16,833	11,705	170	16,430	20,263	42,464
Will	687,263	179,235	79,991	13,255	42,712	28,544	445	38,444	48,427	53,883
Winnebago	287,078	68,062	46,023	5,033	18,270	13,182	185	19,061	23,193	41,541
Totals	**10,487,968**	**2,432,537**	**1,418,926**	**179,893**	**676,570**	**455,721**	**6,771**	**628,146**	**779,067**	**1,396,977**

STATE TABLES

ILLINOIS

American Lung Association in Illinois

www.lung.org/illinois

	HIGH OZONE DAYS 2013–2015					HIGH PARTICLE POLLUTION DAYS 2013–2015						
						24-Hour					Annual	
County	Orange	Red	Purple	Wgt. Avg.	Grade	Orange	Red	Purple	Wgt. Avg.	Grade	Design Value	Pass/ Fail
Adams	0	0	0	0.0	A	DNC	DNC	DNC	DNC	DNC	DNC	DNC
Champaign	1	0	0	0.3	B	INC	INC	INC	INC	INC	INC	INC
Clark	0	0	0	0.0	A	DNC	DNC	DNC	DNC	DNC	DNC	DNC
Cook	17	1	0	6.2	F	INC	INC	INC	INC	INC	INC	INC
DuPage	3	0	0	1.0	C	INC	INC	INC	INC	INC	INC	INC
Effingham	0	0	0	0.0	A	DNC	DNC	DNC	DNC	DNC	DNC	DNC
Hamilton	0	0	0	0.0	A	INC	INC	INC	INC	INC	INC	INC
Jersey	3	1	0	1.5	C	INC	INC	INC	INC	INC	INC	INC
Jo Daviess	2	0	0	0.7	B	DNC	DNC	DNC	DNC	DNC	DNC	DNC
Kane	1	0	0	0.3	B	INC	INC	INC	INC	INC	INC	INC
Lake	15	0	0	5.0	F	DNC	DNC	DNC	DNC	DNC	DNC	DNC
Macon	0	0	0	0.0	A	INC	INC	INC	INC	INC	INC	INC
Macoupin	0	0	0	0.0	A	DNC	DNC	DNC	DNC	DNC	DNC	DNC
Madison	22	0	0	7.3	F	INC	INC	INC	INC	INC	INC	INC
McHenry	5	0	0	1.7	C	INC	INC	INC	INC	INC	INC	INC
McLean	1	0	0	0.3	B	INC	INC	INC	INC	INC	INC	INC
Peoria	0	0	0	0.0	A	INC	INC	INC	INC	INC	INC	INC
Randolph	4	0	0	1.3	C	INC	INC	INC	INC	INC	INC	INC
Rock Island	1	0	0	0.3	B	INC	INC	INC	INC	INC	INC	INC
Sangamon	0	0	0	0.0	A	INC	INC	INC	INC	INC	INC	INC
St. Clair	4	0	0	1.3	C	INC	INC	INC	INC	INC	INC	INC
Will	0	0	0	0.0	A	INC	INC	INC	INC	INC	INC	INC
Winnebago	3	0	0	1.0	C	INC	INC	INC	INC	INC	INC	INC

INDIANA

American Lung Association in Indiana

www.lung.org/indiana

	AT-RISK GROUPS									
				Lung Diseases						
County	Total Population	Under 18	65 & Over	Pediatric Asthma	Adult Asthma	COPD	Lung Cancer	Cardiovascular Disease	Diabetes	Poverty
Allen	368,450	96,167	49,434	7,232	28,100	21,417	270	26,495	30,756	52,689
Bartholomew	81,162	19,533	12,282	1,469	6,334	4,972	60	6,242	7,129	9,462
Boone	63,344	17,002	8,084	1,279	4,779	3,735	46	4,561	5,364	3,734
Brown	14,977	2,893	3,272	218	1,215	1,145	11	1,489	1,632	1,688
Carroll	19,856	4,508	3,604	339	1,561	1,347	15	1,723	1,925	1,855
Clark	115,371	26,683	16,811	2,007	9,130	7,129	85	8,860	10,229	11,832
Delaware	116,852	22,109	18,947	1,663	9,771	7,248	85	9,213	10,402	24,820
Dubois	42,461	10,185	6,962	766	3,296	2,768	31	3,490	3,961	3,179
Elkhart	203,474	56,889	27,717	4,278	15,101	11,658	149	14,513	16,730	27,906
Floyd	76,778	17,795	11,459	1,338	6,056	4,879	56	6,060	6,995	8,502
Greene	32,441	7,205	5,983	542	2,565	2,222	24	2,847	3,175	4,710
Hamilton	309,697	87,329	33,758	6,567	23,072	17,116	227	20,525	24,634	14,366
Hancock	72,520	17,226	11,199	1,295	5,665	4,640	53	5,797	6,648	4,272
Hendricks	158,192	40,662	20,089	3,058	12,146	9,245	116	11,296	13,285	8,477
Henry	48,985	10,256	8,982	771	3,945	3,337	36	4,274	4,771	6,636
Howard	82,556	18,761	15,225	1,411	6,489	5,535	60	7,127	7,911	13,724
Huntington	36,630	8,072	5,967	607	2,924	2,386	27	3,005	3,418	3,832
Jackson	44,069	10,778	6,811	810	3,414	2,742	32	3,447	3,929	5,250
Johnson	149,633	37,532	21,118	2,822	11,549	8,924	110	11,099	12,807	11,720
Knox	37,927	8,005	6,383	602	3,067	2,439	28	3,102	3,494	6,735
Lake	487,865	118,118	73,176	8,882	37,969	30,309	357	37,867	43,453	79,740
LaPorte	110,884	24,277	17,940	1,826	8,873	7,209	82	9,068	10,327	16,294
Madison	129,723	28,550	22,366	2,147	10,340	8,494	95	10,823	12,157	20,636
Marion	939,020	234,220	108,060	17,613	73,292	52,169	686	63,121	75,137	189,323
Monroe	144,705	23,002	16,832	1,730	12,779	7,869	106	9,570	11,380	30,425
Montgomery	38,227	8,829	6,489	664	3,003	2,491	28	3,166	3,564	4,543
Morgan	69,648	16,261	10,890	1,223	5,462	4,557	51	5,682	6,526	7,814
Perry	19,347	3,996	3,346	300	1,570	1,287	14	1,635	1,843	2,341
Porter	167,688	37,980	24,962	2,856	13,333	10,585	123	13,158	15,182	18,931
Posey	25,512	5,795	4,202	436	2,012	1,715	19	2,151	2,455	2,442
Shelby	44,478	10,203	7,078	767	3,507	2,912	33	3,644	4,170	5,205
Spencer	20,715	4,658	3,820	350	1,630	1,429	15	1,828	2,041	1,931
St. Joseph	268,441	64,242	39,260	4,831	21,028	16,236	196	20,287	23,296	42,922
Tippecanoe	185,826	38,439	19,501	2,891	15,485	9,570	137	11,530	13,844	32,336
Vanderburgh	181,877	39,873	28,248	2,998	14,597	11,442	133	14,364	16,408	30,123
Vigo	107,896	22,180	16,090	1,668	8,853	6,580	80	8,240	9,450	20,027

INDIANA (cont.)

American Lung Association in Indiana

www.lung.org/indiana

	AT-RISK GROUPS									
				Lung Diseases						
County	Total Population	Under 18	65 & Over	Pediatric Asthma	Adult Asthma	COPD	Lung Cancer	Cardiovascular Disease	Diabetes	Poverty
Wabash	32,138	6,905	6,374	519	2,560	2,213	24	2,882	3,160	3,625
Warrick	61,897	15,119	10,247	1,137	4,776	3,992	45	5,057	5,713	4,546
Whitley	33,406	7,743	5,457	582	2,622	2,194	25	2,759	3,140	2,598
Totals	**5,144,668**	**1,229,980**	**718,425**	**92,492**	**403,873**	**308,133**	**3,770**	**381,995**	**442,441**	**741,191**

STATE TABLES

INDIANA

American Lung Association in Indiana

www.lung.org/indiana

	HIGH OZONE DAYS 2013–2015					HIGH PARTICLE POLLUTION DAYS 2013–2015						
						24-Hour					Annual	
County	Orange	Red	Purple	Wgt. Avg.	Grade	Orange	Red	Purple	Wgt. Avg.	Grade	Design Value	Pass/ Fail
Allen	0	0	0	0.0	A	7	1	0	2.8	D	10.2	PASS
Bartholomew	3	0	0	1.0	C	INC	INC	INC	INC	INC	INC	INC
Boone	4	0	0	1.3	C	DNC	DNC	DNC	DNC	DNC	DNC	DNC
Brown	INC	INC	INC	INC	INC	DNC	DNC	DNC	DNC	DNC	DNC	DNC
Carroll	1	0	0	0.3	B	DNC	DNC	DNC	DNC	DNC	DNC	DNC
Clark	4	1	0	1.8	C	1	0	0	0.3	B	11.4	PASS
Delaware	0	0	0	0.0	A	2	0	0	0.7	B	9.7	PASS
Dubois	DNC	DNC	DNC	DNC	DNC	0	0	0	0.0	A	10.6	PASS
Elkhart	0	0	0	0.0	A	16	0	0	5.3	F	10.4	PASS
Floyd	6	0	0	2.0	C	1	0	0	0.3	B	10.0	PASS
Greene	3	0	0	1.0	C	0	0	0	0.0	A	9.5	PASS
Hamilton	0	0	0	0.0	A	INC	INC	INC	INC	INC	INC	INC
Hancock	0	0	0	0.0	A	DNC	DNC	DNC	DNC	DNC	DNC	DNC
Hendricks	0	0	0	0.0	A	DNC	DNC	DNC	DNC	DNC	DNC	DNC
Henry	DNC	DNC	DNC	DNC	DNC	1	0	0	0.3	B	9.1	PASS
Howard	DNC	DNC	DNC	DNC	DNC	INC	INC	INC	INC	INC	INC	INC
Huntington	0	0	0	0.0	A	DNC	DNC	DNC	DNC	DNC	DNC	DNC
Jackson	2	0	0	0.7	B	DNC	DNC	DNC	DNC	DNC	DNC	DNC
Johnson	0	0	0	0.0	A	DNC	DNC	DNC	DNC	DNC	DNC	DNC
Knox	0	0	0	0.0	A	DNC	DNC	DNC	DNC	DNC	DNC	DNC
Lake	5	0	0	1.7	C	8	2	0	3.7	F	11.0	PASS
LaPorte	8	0	0	2.7	D	2	0	0	0.7	B	9.5	PASS
Madison	0	0	0	0.0	A	3	0	0	1.0	C	9.6	PASS
Marion	4	0	0	1.3	C	10	1	0	3.8	F	11.7	PASS
Monroe	DNC	DNC	DNC	DNC	DNC	0	1	0	0.5	B	9.4	PASS
Montgomery	DNC	DNC	DNC	DNC	DNC	INC	INC	INC	INC	INC	INC	INC
Morgan	0	0	0	0.0	A	DNC	DNC	DNC	DNC	DNC	DNC	DNC
Perry	3	0	0	1.0	C	DNC	DNC	DNC	DNC	DNC	DNC	DNC
Porter	8	0	0	2.7	D	2	2	0	1.7	C	10.0	PASS
Posey	2	0	0	0.7	B	DNC	DNC	DNC	DNC	DNC	DNC	DNC
Shelby	0	0	0	0.0	A	DNC	DNC	DNC	DNC	DNC	DNC	DNC
Spencer	DNC	DNC	DNC	DNC	DNC	0	0	0	0.0	A	10.1	PASS
St. Joseph	3	0	0	1.0	C	5	1	0	2.2	D	9.7	PASS
Tippecanoe	DNC	DNC	DNC	DNC	DNC	1	0	0	0.3	B	9.8	PASS
Vanderburgh	13	0	0	4.3	F	0	0	0	0.0	A	10.7	PASS

STATE TABLES

INDIANA (cont.)

American Lung Association in Indiana

www.lung.org/indiana

	HIGH OZONE DAYS 2013–2015					HIGH PARTICLE POLLUTION DAYS 2013–2015						
						24-Hour					Annual	
County	Orange	Red	Purple	Wgt. Avg.	Grade	Orange	Red	Purple	Wgt. Avg.	Grade	Design Value	Pass/ Fail
Vigo	0	0	0	0.0	A	2	1	0	1.2	C	10.3	PASS
Wabash	6	0	0	2.0	C	DNC	DNC	DNC	DNC	DNC	DNC	DNC
Warrick	4	0	0	1.3	C	DNC	DNC	DNC	DNC	DNC	DNC	DNC
Whitley	DNC	DNC	DNC	DNC	DNC	3	0	0	1.0	C	9.3	PASS

STATE TABLES

IOWA

American Lung Association in Iowa

www.lung.org/iowa

				AT-RISK GROUPS						
				Lung Diseases						
County	Total Population	Under 18	65 & Over	Pediatric Asthma	Adult Asthma	COPD	Lung Cancer	Cardiovascular Disease	Diabetes	Poverty
Black Hawk	133,455	28,752	20,236	1,655	7,985	5,680	85	7,289	8,473	18,161
Bremer	24,722	5,422	4,661	312	1,462	1,149	16	1,548	1,757	1,791
Clinton	47,768	10,950	8,898	630	2,797	2,264	30	3,074	3,522	6,263
Delaware	17,403	4,134	3,170	238	1,010	823	11	1,119	1,288	1,743
Harrison	14,265	3,214	2,800	185	838	696	9	955	1,089	1,385
Johnson	144,251	29,208	15,003	1,681	8,840	5,358	92	6,265	7,568	24,908
Lee	35,089	7,594	6,698	437	2,088	1,693	22	2,301	2,633	5,358
Linn	219,916	52,166	32,289	3,003	12,826	9,353	140	12,093	14,166	23,524
Montgomery	10,234	2,280	2,172	131	601	515	6	716	809	1,339
Muscatine	43,011	10,915	6,676	628	2,450	1,857	27	2,445	2,847	4,871
Palo Alto	9,133	2,053	1,974	118	533	450	6	626	701	1,013
Polk	467,711	117,819	55,946	6,782	26,886	18,343	297	22,854	27,333	54,557
Pottawattamie	93,671	22,256	14,930	1,281	5,452	4,145	59	5,466	6,361	12,293
Scott	172,126	41,195	25,490	2,371	10,013	7,375	109	9,575	11,219	20,823
Story	96,021	16,276	10,417	937	6,112	3,587	62	4,132	4,950	15,717
Van Buren	7,344	1,697	1,534	98	427	365	5	508	575	1,154
Warren	48,626	12,180	7,409	701	2,785	2,097	31	2,750	3,212	3,641
Woodbury	102,782	26,929	14,335	1,550	5,802	4,192	65	5,397	6,331	13,957
Totals	**1,687,528**	**395,040**	**234,638**	**22,738**	**98,908**	**69,942**	**1,071**	**89,112**	**104,835**	**212,498**

STATE TABLES

IOWA

American Lung Association in Iowa

www.lung.org/iowa

	HIGH OZONE DAYS 2013–2015					HIGH PARTICLE POLLUTION DAYS 2013–2015						
						24-Hour					Annual	
County	Orange	Red	Purple	Wgt. Avg.	Grade	Orange	Red	Purple	Wgt. Avg.	Grade	Design Value	Pass/ Fail
Black Hawk	DNC	DNC	DNC	DNC	DNC	0	0	0	0.0	A	9.0	PASS
Bremer	0	0	0	0.0	A	DNC	DNC	DNC	DNC	DNC	DNC	DNC
Clinton	1	0	0	0.3	B	3	0	0	1.0	C	10.2	PASS
Delaware	DNC	DNC	DNC	DNC	DNC	0	0	0	0.0	A	8.7	PASS
Harrison	1	0	0	0.3	B	DNC	DNC	DNC	DNC	DNC	DNC	DNC
Johnson	DNC	DNC	DNC	DNC	DNC	2	0	0	0.7	B	8.8	PASS
Lee	DNC	DNC	DNC	DNC	DNC	0	0	0	0.0	A	10.0	PASS
Linn	0	0	0	0.0	A	3	0	0	1.0	C	9.3	PASS
Montgomery	1	0	0	0.3	B	1	0	0	0.3	B	7.6	PASS
Muscatine	DNC	DNC	DNC	DNC	DNC	11	0	0	3.7	F	10.4	PASS
Palo Alto	1	0	0	0.3	B	0	0	0	0.0	A	7.8	PASS
Polk	0	0	0	0.0	A	0	0	0	0.0	A	8.3	PASS
Pottawattamie	DNC	DNC	DNC	DNC	DNC	1	0	0	0.3	B	9.0	PASS
Scott	0	0	0	0.0	A	5	0	0	1.7	C	10.1	PASS
Story	0	0	0	0.0	A	DNC	DNC	DNC	DNC	DNC	DNC	DNC
Van Buren	0	0	0	0.0	A	0	0	0	0.0	A	8.0	PASS
Warren	0	0	0	0.0	A	DNC	DNC	DNC	DNC	DNC	DNC	DNC
Woodbury	DNC	DNC	DNC	DNC	DNC	3	0	0	1.0	C	8.4	PASS

STATE TABLES

KANSAS

American Lung Association in Kansas

www.lung.org/kansas

				AT-RISK GROUPS						
				Lung Diseases						
County	Total Population	Under 18	65 & Over	Pediatric Asthma	Adult Asthma	COPD	Lung Cancer	Cardiovascular Disease	Diabetes	Poverty
Johnson	580,159	145,597	76,022	12,903	37,954	26,585	365	33,371	41,203	31,474
Leavenworth	79,315	19,050	10,365	1,688	5,263	3,650	51	4,566	5,647	7,817
Linn	9,536	2,198	2,004	195	636	525	6	724	844	1,318
Neosho	16,346	4,044	3,030	358	1,067	835	10	1,127	1,330	2,995
Riley	75,247	13,025	6,256	1,154	5,394	2,707	48	2,986	3,925	15,560
Sedgwick	511,574	134,499	67,228	11,919	32,879	22,839	322	28,782	35,402	76,898
Shawnee	178,725	43,262	29,471	3,834	11,780	8,832	112	11,604	13,921	24,840
Sumner	23,535	5,821	4,135	516	1,540	1,200	15	1,600	1,904	2,701
Trego	2,927	545	707	48	206	177	2	248	286	298
Wyandotte	163,369	45,889	18,586	4,067	10,260	6,858	103	8,433	10,532	35,442
Totals	**1,640,733**	**413,930**	**217,804**	**36,682**	**106,979**	**74,210**	**1,033**	**93,440**	**114,993**	**199,343**

STATE TABLES

KANSAS

American Lung Association in Kansas

www.lung.org/kansas

	HIGH OZONE DAYS 2013–2015					HIGH PARTICLE POLLUTION DAYS 2013–2015						
						24-Hour					Annual	
County	Orange	Red	Purple	Wgt. Avg.	Grade	Orange	Red	Purple	Wgt. Avg.	Grade	Design Value	Pass/ Fail
Johnson	0	0	0	0.0	A	0	0	0	0.0	A	7.7	PASS
Leavenworth	4	0	0	1.3	C	DNC	DNC	DNC	DNC	DNC	DNC	DNC
Linn	INC	INC	INC	INC	INC	INC	INC	INC	INC	INC	INC	INC
Neosho	INC	INC	INC	INC	INC	INC	INC	INC	INC	INC	INC	INC
Riley	INC	INC	INC	INC	INC	DNC	DNC	DNC	DNC	DNC	DNC	DNC
Sedgwick	8	0	0	2.7	D	1	0	0	0.3	B	9.2	PASS
Shawnee	1	0	0	0.3	B	1	0	0	0.3	B	8.0	PASS
Sumner	5	0	0	1.7	C	1	0	0	0.3	B	7.8	PASS
Trego	0	0	0	0.0	A	DNC	DNC	DNC	DNC	DNC	DNC	DNC
Wyandotte	1	0	0	0.3	B	1	0	0	0.3	B	9.2	PASS

STATE TABLES

KENTUCKY

American Lung Association in Kentucky

www.lung.org/kentucky

		AT-RISK GROUPS								
				Lung Diseases						
County	Total Population	Under 18	65 & Over	Pediatric Asthma	Adult Asthma	COPD	Lung Cancer	Cardiovascular Disease	Diabetes	Poverty
Bell	27,337	5,809	4,852	630	2,552	2,718	26	2,784	3,050	11,772
Boone	127,712	34,843	14,808	3,779	11,106	10,927	122	10,493	12,018	10,304
Boyd	48,325	10,186	8,823	1,105	4,517	4,859	46	5,003	5,463	9,440
Bullitt	78,702	17,953	11,116	1,947	7,241	7,392	75	7,275	8,195	7,504
Campbell	92,066	20,046	13,096	2,174	8,588	8,562	88	8,414	9,476	12,805
Carter	27,158	6,102	4,620	662	2,498	2,635	26	2,685	2,952	5,203
Christian	73,309	20,014	8,410	2,171	6,384	5,498	71	5,242	5,985	13,750
Daviess	99,259	24,141	16,079	2,619	8,918	9,312	95	9,442	10,412	14,405
Edmonson	12,007	2,276	2,407	247	1,150	1,253	11	1,308	1,415	2,376
Fayette	314,488	66,246	37,689	7,186	29,741	26,994	300	25,619	29,457	57,637
Greenup	36,068	7,867	7,046	853	3,331	3,676	34	3,843	4,155	5,973
Hancock	8,692	2,186	1,479	237	771	830	8	851	932	1,189
Hardin	106,439	26,333	13,901	2,856	9,563	9,441	102	9,199	10,422	15,424
Henderson	46,407	10,857	7,419	1,178	4,223	4,445	44	4,484	4,966	7,688
Jefferson	763,623	171,811	113,444	18,636	70,483	70,948	727	70,423	78,758	115,246
Jessamine	51,961	12,805	7,098	1,389	4,670	4,648	49	4,565	5,143	9,129
Livingston	9,316	1,920	1,909	208	872	996	9	1,047	1,129	1,404
Madison	87,824	18,551	11,491	2,012	8,284	7,689	84	7,420	8,436	14,873
McCracken	65,018	14,201	12,169	1,540	6,012	6,528	62	6,767	7,355	9,671
Morgan	13,275	2,552	1,954	277	1,279	1,280	13	1,259	1,417	3,577
Oldham	64,875	16,641	7,791	1,805	5,765	5,842	63	5,627	6,441	3,688
Perry	27,565	6,064	4,404	658	2,555	2,682	26	2,696	2,994	7,675
Pike	61,792	13,066	10,260	1,417	5,786	6,128	59	6,192	6,852	15,082
Pulaski	63,782	14,325	11,539	1,554	5,856	6,331	61	6,528	7,122	14,448
Simpson	18,006	4,378	2,864	475	1,619	1,694	17	1,712	1,893	2,820
Trigg	14,233	3,061	3,072	332	1,315	1,519	14	1,618	1,729	2,129
Warren	122,851	27,678	15,030	3,002	11,394	10,379	117	9,920	11,347	20,992
Washington	12,063	2,761	2,102	299	1,102	1,184	12	1,213	1,329	1,992
Totals	**2,474,153**	**564,673**	**356,872**	**61,249**	**227,576**	**226,390**	**2,361**	**223,628**	**250,845**	**398,196**

STATE TABLES

KENTUCKY

American Lung Association in Kentucky

www.lung.org/kentucky

	HIGH OZONE DAYS 2013–2015					HIGH PARTICLE POLLUTION DAYS 2013–2015						
						24-Hour					Annual	
County	Orange	Red	Purple	Wgt. Avg.	Grade	Orange	Red	Purple	Wgt. Avg.	Grade	Design Value	Pass/ Fail
Bell	0	0	0	0.0	A	0	0	0	0.0	A	8.9	PASS
Boone	2	0	0	0.7	B	DNC	DNC	DNC	DNC	DNC	DNC	DNC
Boyd	5	0	0	1.7	C	0	0	0	0.0	A	9.1	PASS
Bullitt	4	0	0	1.3	C	DNC	DNC	DNC	DNC	DNC	DNC	DNC
Campbell	13	0	0	4.3	F	0	0	0	0.0	A	9.5	PASS
Carter	0	0	0	0.0	A	0	0	0	0.0	A	7.6	PASS
Christian	1	0	0	0.3	B	0	0	0	0.0	A	9.7	PASS
Daviess	1	0	0	0.3	B	0	0	0	0.0	A	10.3	PASS
Edmonson	1	0	0	0.3	B	DNC	DNC	DNC	DNC	DNC	DNC	DNC
Fayette	4	0	0	1.3	C	0	0	0	0.0	A	9.1	PASS
Greenup	1	0	0	0.3	B	DNC	DNC	DNC	DNC	DNC	DNC	DNC
Hancock	6	0	0	2.0	C	DNC	DNC	DNC	DNC	DNC	DNC	DNC
Hardin	1	0	0	0.3	B	0	0	0	0.0	A	9.8	PASS
Henderson	2	0	0	0.7	B	0	0	0	0.0	A	10.3	PASS
Jefferson	6	4	0	4.0	F	2	1	0	1.2	C	11.7	PASS
Jessamine	1	0	0	0.3	B	DNC	DNC	DNC	DNC	DNC	DNC	DNC
Livingston	2	0	0	0.7	B	DNC	DNC	DNC	DNC	DNC	DNC	DNC
Madison	DNC	DNC	DNC	DNC	DNC	0	0	0	0.0	A	8.1	PASS
McCracken	1	0	0	0.3	B	0	0	0	0.0	A	INC	INC
Morgan	0	0	0	0.0	A	DNC	DNC	DNC	DNC	DNC	DNC	DNC
Oldham	6	0	0	2.0	C	DNC	DNC	DNC	DNC	DNC	DNC	DNC
Perry	0	0	0	0.0	A	0	0	0	0.0	A	INC	INC
Pike	0	0	0	0.0	A	3	0	0	1.0	C	8.0	PASS
Pulaski	0	0	0	0.0	A	0	0	0	0.0	A	8.7	PASS
Simpson	1	0	0	0.3	B	DNC	DNC	DNC	DNC	DNC	DNC	DNC
Trigg	2	0	0	0.7	B	DNC	DNC	DNC	DNC	DNC	DNC	DNC
Warren	0	0	0	0.0	A	0	0	0	0.0	A	9.1	PASS
Washington	2	0	0	0.7	B	DNC	DNC	DNC	DNC	DNC	DNC	DNC

STATE TABLES

LOUISIANA

American Lung Association in Louisiana

www.lung.org/louisiana

		AT-RISK GROUPS								
				Lung Diseases						
Parish	Total Population	Under 18	65 & Over	Pediatric Asthma	Adult Asthma	COPD	Lung Disease	Cardiovascular Diabetes	Poverty	
Ascension Parish	119,455	32,905	12,536	2,879	7,071	6,217	83	8,674	10,209	12,695
Bossier Parish	125,175	31,423	16,527	2,750	7,674	6,838	87	9,879	11,416	17,765
Caddo Parish	251,460	61,152	38,375	5,351	15,547	14,636	174	21,587	24,857	54,405
Calcasieu Parish	198,788	49,384	27,852	4,321	12,205	11,288	139	16,419	19,009	34,103
East Baton Rouge Parish	446,753	101,773	57,272	8,906	28,269	24,506	310	35,101	40,586	80,662
Iberville Parish	33,095	7,047	4,648	617	2,126	1,971	23	2,841	3,307	6,538
Jefferson Parish	436,275	94,962	67,695	8,310	27,857	26,432	304	38,811	44,859	70,484
Lafayette Parish	240,098	57,778	27,678	5,056	14,923	12,910	167	18,189	21,229	39,876
Lafourche Parish	98,325	23,175	13,797	2,028	6,135	5,703	69	8,266	9,598	13,612
Livingston Parish	137,788	36,109	16,505	3,160	8,310	7,428	96	10,560	12,325	18,356
Orleans Parish	389,617	79,432	48,658	6,951	25,384	22,147	270	31,364	36,545	90,849
Ouachita Parish	156,761	39,935	21,430	3,494	9,553	8,692	109	12,628	14,594	34,836
Pointe Coupee Parish	22,251	5,032	4,156	440	1,402	1,439	15	2,180	2,502	4,264
Rapides Parish	132,141	33,075	20,183	2,894	8,087	7,698	92	11,361	13,098	27,768
St. Bernard Parish	45,408	12,355	4,547	1,081	2,703	2,319	32	3,215	3,783	9,179
St. Charles Parish	52,812	13,348	6,346	1,168	3,215	2,989	37	4,226	4,979	6,147
St. James Parish	21,567	5,009	3,347	438	1,349	1,317	15	1,934	2,245	3,902
St. John the Baptist Parish	43,626	10,928	5,681	956	2,666	2,489	30	3,567	4,172	8,829
St. Martin Parish	53,835	13,320	7,326	1,166	3,305	3,098	38	4,472	5,211	9,693
St. Tammany Parish	250,088	60,805	38,533	5,321	15,417	15,091	174	22,189	25,742	31,138
Tangipahoa Parish	128,755	31,859	16,932	2,788	7,924	7,133	90	10,276	11,915	30,092
Terrebonne Parish	113,972	29,354	14,655	2,569	6,910	6,320	80	9,073	10,567	22,587
West Baton Rouge Parish	25,490	6,258	3,120	548	1,570	1,421	18	2,017	2,361	3,754
Totals	**3,523,535**	**836,418**	**477,799**	**73,190**	**219,602**	**200,084**	**2,452**	**288,828**	**335,109**	**631,534**

STATE TABLES

LOUISIANA

American Lung Association in Louisiana

www.lung.org/louisiana

	HIGH OZONE DAYS 2013–2015					HIGH PARTICLE POLLUTION DAYS 2013–2015						
						24-Hour					Annual	
Parish	Orange	Red	Purple	Wgt. Avg.	Grade	Orange	Red	Purple	Wgt. Avg.	Grade	Design Value	Pass/ Fail
Ascension Parish	6	1	0	2.5	D	DNC	DNC	DNC	DNC	DNC	DNC	DNC
Bossier Parish	5	0	0	1.7	C	DNC	DNC	DNC	DNC	DNC	DNC	DNC
Caddo Parish	1	0	0	0.3	B	1	0	0	0.3	B	10.3	PASS
Calcasieu Parish	8	1	0	3.2	D	0	0	0	0.0	A	7.2	PASS
East Baton Rouge Parish	21	4	0	9.0	F	1	0	0	0.3	B	8.8	PASS
Iberville Parish	13	0	0	4.3	F	0	0	0	0.0	A	8.7	PASS
Jefferson Parish	7	0	0	2.3	D	0	0	0	0.0	A	7.9	PASS
Lafayette Parish	2	0	0	0.7	B	0	0	0	0.0	A	7.8	PASS
Lafourche Parish	1	0	0	0.3	B	DNC	DNC	DNC	DNC	DNC	DNC	DNC
Livingston Parish	11	0	0	3.7	F	DNC	DNC	DNC	DNC	DNC	DNC	DNC
Orleans Parish	INC	INC	INC	INC	INC	INC	INC	INC	INC	INC	INC	INC
Ouachita Parish	0	0	0	0.0	A	0	0	0	0.0	A	INC	INC
Pointe Coupee Parish	8	0	0	2.7	D	DNC	DNC	DNC	DNC	DNC	DNC	DNC
Rapides Parish	DNC	DNC	DNC	DNC	DNC	0	0	0	0.0	A	7.4	PASS
St. Bernard Parish	6	0	0	2.0	C	0	0	0	0.0	A	9.0	PASS
St. Charles Parish	INC	INC	INC	INC	INC	DNC	DNC	DNC	DNC	DNC	DNC	DNC
St. James Parish	2	1	0	1.2	C	DNC	DNC	DNC	DNC	DNC	DNC	DNC
St. John the Baptist Parish	5	0	0	1.7	C	DNC	DNC	DNC	DNC	DNC	DNC	DNC
St. Martin Parish	INC	INC	INC	INC	INC	DNC	DNC	DNC	DNC	DNC	DNC	DNC
St. Tammany Parish	9	1	0	3.5	F	DNC	DNC	DNC	DNC	DNC	DNC	DNC
Tangipahoa Parish	DNC	DNC	DNC	DNC	DNC	0	0	0	0.0	A	7.6	PASS
Terrebonne Parish	DNC	DNC	DNC	DNC	DNC	0	0	0	0.0	A	7.2	PASS
West Baton Rouge Parish	5	0	0	1.7	C	0	0	0	0.0	A	8.9	PASS

STATE TABLES

MAINE

American Lung Association in Maine

www.lung.org/maine

		AT-RISK GROUPS								
				Lung Diseases						
County	Total Population	Under 18	65 & Over	Pediatric Asthma	Adult Asthma	COPD	Lung Cancer	Cardiovascular Disease	Diabetes	Poverty
Androscoggin	107,233	23,468	17,615	2,271	9,491	6,529	82	7,587	7,883	15,668
Aroostook	68,628	12,778	15,032	1,237	6,197	4,798	52	5,829	5,875	12,342
Cumberland	289,977	56,068	49,183	5,426	26,504	18,210	220	21,155	21,985	30,030
Hancock	54,659	9,551	12,084	924	5,007	3,874	42	4,704	4,742	6,136
Kennebec	119,980	23,627	21,154	2,286	10,873	7,728	91	9,084	9,366	15,229
Knox	39,855	7,333	9,143	710	3,595	2,830	30	3,460	3,471	4,393
Oxford	57,202	11,150	11,363	1,079	5,145	3,883	44	4,666	4,739	9,579
Penobscot	152,692	28,318	26,256	2,740	14,095	9,622	116	11,160	11,609	24,822
Sagadahoc	35,149	6,793	7,136	657	3,165	2,383	27	2,865	2,909	3,915
Washington	31,625	5,998	7,145	580	2,834	2,230	24	2,724	2,735	5,779
York	201,169	39,427	37,449	3,815	18,177	13,211	153	15,665	16,055	16,376
Totals	**1,158,169**	**224,511**	**213,560**	**21,726**	**105,082**	**75,298**	**880**	**88,899**	**91,369**	**144,269**

STATE TABLES

MAINE

American Lung Association in Maine

www.lung.org/maine

	HIGH OZONE DAYS 2013–2015					HIGH PARTICLE POLLUTION DAYS 2013–2015						
						24-Hour					Annual	
County	Orange	Red	Purple	Wgt. Avg.	Grade	Orange	Red	Purple	Wgt. Avg.	Grade	Design Value	Pass/ Fail
Androscoggin	0	0	0	0.0	A	INC	INC	INC	INC	INC	INC	INC
Aroostook	0	0	0	0.0	A	INC	INC	INC	INC	INC	INC	INC
Cumberland	7	0	0	2.3	D	INC	INC	INC	INC	INC	INC	INC
Hancock	6	0	0	2.0	C	INC	INC	INC	INC	INC	INC	INC
Kennebec	1	0	0	0.3	B	INC	INC	INC	INC	INC	INC	INC
Knox	6	0	0	2.0	C	DNC	DNC	DNC	DNC	DNC	DNC	DNC
Oxford	0	0	0	0.0	A	INC	INC	INC	INC	INC	INC	INC
Penobscot	1	0	0	0.3	B	0	0	0	0.0	A	6.4	PASS
Sagadahoc	1	0	0	0.3	B	DNC	DNC	DNC	DNC	DNC	DNC	DNC
Washington	1	0	0	0.3	B	DNC	DNC	DNC	DNC	DNC	DNC	DNC
York	12	0	0	4.0	F	DNC	DNC	DNC	DNC	DNC	DNC	DNC

STATE TABLES

MARYLAND

American Lung Association in Maryland

www.lung.org/maryland

				AT-RISK GROUPS						
				Lung Diseases						
County	Total Population	Under 18	65 & Over	Pediatric Asthma	Adult Asthma	COPD	Lung Cancer	Cardiovascular Disease	Diabetes	Poverty
Anne Arundel	564,195	126,843	77,478	12,264	38,806	26,664	325	33,851	44,294	32,769
Baltimore	831,128	179,387	133,926	17,344	57,577	40,725	477	54,155	68,882	73,955
Baltimore City	621,849	131,353	77,919	12,700	43,408	28,201	357	34,916	45,727	135,850
Calvert	90,595	21,516	12,259	2,080	6,168	4,414	52	5,556	7,420	5,315
Carroll	167,627	37,047	26,540	3,582	11,612	8,518	97	11,173	14,536	10,235
Cecil	102,382	23,808	14,590	2,302	6,991	4,975	59	6,367	8,371	10,109
Charles	156,118	38,264	17,904	3,700	10,517	7,125	90	8,625	11,679	10,943
Dorchester	32,384	6,896	6,546	667	2,245	1,721	19	2,441	3,020	5,781
Frederick	245,322	58,104	32,623	5,618	16,659	11,593	141	14,594	19,310	17,749
Garrett	29,460	5,704	6,094	552	2,093	1,606	17	2,275	2,818	3,921
Harford	250,290	56,808	37,682	5,493	17,181	12,287	144	15,974	20,770	19,384
Howard	313,414	76,590	39,680	7,405	21,083	14,520	181	18,081	24,056	16,350
Kent	19,787	3,304	5,013	319	1,438	1,136	11	1,716	2,035	2,723
Montgomery	1,040,116	243,491	146,195	23,542	70,668	49,115	598	62,958	82,042	77,657
Prince George's	909,535	204,375	106,712	19,760	62,662	41,217	523	50,108	66,913	83,988
Washington	149,585	33,184	24,253	3,208	10,296	7,382	87	9,831	12,543	16,984
Totals	**5,523,787**	**1,246,674**	**765,414**	**120,537**	**379,403**	**261,199**	**3,178**	**332,622**	**434,417**	**523,713**

STATE TABLES

MARYLAND

American Lung Association in Maryland

www.lung.org/maryland

	HIGH OZONE DAYS 2013–2015					HIGH PARTICLE POLLUTION DAYS 2013–2015						
						24-Hour					Annual	
County	Orange	Red	Purple	Wgt. Avg.	Grade	Orange	Red	Purple	Wgt. Avg.	Grade	Design Value	Pass/ Fail
Anne Arundel	9	0	0	3.0	D	0	0	0	0.0	A	9.3	PASS
Baltimore	20	0	0	6.7	F	0	0	0	0.0	A	9.8	PASS
Baltimore City	6	0	0	2.0	C	1	0	0	0.3	B	9.6	PASS
Calvert	6	0	0	2.0	C	DNC	DNC	DNC	DNC	DNC	DNC	DNC
Carroll	3	0	0	1.0	C	DNC	DNC	DNC	DNC	DNC	DNC	DNC
Cecil	13	1	0	4.8	F	1	0	0	0.3	B	9.4	PASS
Charles	4	0	0	1.3	C	DNC	DNC	DNC	DNC	DNC	DNC	DNC
Dorchester	3	0	0	1.0	C	0	0	0	0.0	A	7.9	PASS
Frederick	2	0	0	0.7	B	DNC	DNC	DNC	DNC	DNC	DNC	DNC
Garrett	1	0	0	0.3	B	0	0	0	0.0	A	6.6	PASS
Harford	13	1	0	4.8	F	0	0	0	0.0	A	9.4	PASS
Howard	DNC	DNC	DNC	DNC	DNC	INC	INC	INC	INC	INC	INC	INC
Kent	10	0	0	3.3	F	0	0	0	0.0	A	8.8	PASS
Montgomery	6	0	0	2.0	C	0	0	0	0.0	A	8.9	PASS
Prince George's	16	1	0	5.8	F	0	0	0	0.0	A	9.4	PASS
Washington	4	0	0	1.3	C	3	0	0	1.0	C	9.4	PASS

STATE TABLES

MASSACHUSETTS

American Lung Association in Massachusetts

www.lung.org/massachusetts

		AT-RISK GROUPS								
				Lung Diseases						
County	Total Population	Under 18	65 & Over	Pediatric Asthma	Adult Asthma	COPD	Lung Cancer	Cardiovascular Disease	Diabetes	Poverty
Barnstable	214,333	33,534	61,137	4,053	17,645	12,686	136	19,120	21,136	16,030
Berkshire	127,828	22,400	27,597	2,707	10,567	6,708	81	9,544	10,858	17,453
Bristol	556,772	116,624	89,109	14,095	45,031	25,669	353	34,497	40,355	68,378
Dukes	17,299	3,158	3,617	382	1,419	905	11	1,282	1,469	1,456
Essex	776,043	169,296	123,799	20,461	62,022	35,610	491	47,962	56,131	87,669
Franklin	70,601	12,653	13,439	1,529	5,860	3,595	45	4,986	5,782	8,221
Hampden	470,690	105,014	72,932	12,692	37,479	21,025	298	28,133	32,860	77,818
Hampshire	161,292	24,587	24,700	2,972	14,134	7,399	102	9,645	11,270	21,232
Middlesex	1,585,139	322,638	226,108	38,994	130,333	70,034	1,004	91,480	107,969	116,761
Norfolk	696,023	149,465	111,124	18,065	55,890	31,991	440	43,046	50,370	48,042
Plymouth	510,393	113,432	85,389	13,710	40,386	23,953	323	32,672	38,155	48,231
Suffolk	778,121	133,727	86,473	16,162	67,807	31,251	493	37,909	45,273	144,867
Worcester	818,963	178,270	118,261	21,546	65,911	36,609	519	48,272	57,168	95,500
Totals	**6,783,497**	**1,384,798**	**1,043,685**	**167,368**	**554,483**	**307,435**	**4,295**	**408,549**	**478,798**	**751,658**

STATE TABLES

MASSACHUSETTS

American Lung Association in Massachusetts

www.lung.org/massachusetts

	HIGH OZONE DAYS 2013–2015					HIGH PARTICLE POLLUTION DAYS 2013–2015						
						24-Hour					Annual	
County	Orange	Red	Purple	Wgt. Avg.	Grade	Orange	Red	Purple	Wgt. Avg.	Grade	Design Value	Pass/ Fail
Barnstable	8	0	0	2.7	D	DNC	DNC	DNC	DNC	DNC	DNC	DNC
Berkshire	INC	INC	INC	INC	INC	0	0	0	0.0	A	6.8	PASS
Bristol	9	2	0	4.0	F	0	0	0	0.0	A	6.9	PASS
Dukes	4	0	0	1.3	C	DNC	DNC	DNC	DNC	DNC	DNC	DNC
Essex	14	0	0	4.7	F	0	0	0	0.0	A	6.3	PASS
Franklin	INC	INC	INC	INC	INC	INC	INC	INC	INC	INC	INC	INC
Hampden	7	0	0	2.3	D	0	0	0	0.0	A	7.3	PASS
Hampshire	6	0	0	2.0	C	INC	INC	INC	INC	INC	INC	INC
Middlesex	3	0	0	1.0	C	DNC	DNC	DNC	DNC	DNC	DNC	DNC
Norfolk	7	1	0	2.8	D	INC	INC	INC	INC	INC	INC	INC
Plymouth	INC	INC	INC	INC	INC	0	0	0	0.0	A	INC	INC
Suffolk	6	0	0	2.0	C	0	0	0	0.0	A	7.7	PASS
Worcester	3	0	0	1.0	C	0	0	0	0.0	A	6.9	PASS

STATE TABLES

MICHIGAN

American Lung Association in Michigan

www.lung.org/michigan

		AT-RISK GROUPS								
				Lung Diseases						
County	Total Population	Under 18	65 & Over	Pediatric Asthma	Adult Asthma	COPD	Lung Cancer	Cardiovascular Disease	Diabetes	Poverty
Allegan	114,625	28,179	17,738	2,183	8,866	6,785	73	8,142	9,463	12,668
Bay	105,659	21,934	19,842	1,699	8,544	6,759	67	8,346	9,546	15,161
Benzie	17,457	3,257	4,301	252	1,431	1,258	11	1,633	1,811	1,810
Berrien	154,636	34,521	28,115	2,674	12,265	9,639	98	11,873	13,603	25,854
Cass	51,657	10,899	10,254	844	4,145	3,399	33	4,247	4,817	7,530
Chippewa	38,033	7,100	6,330	550	3,181	2,316	25	2,775	3,242	6,502
Clinton	77,390	17,667	12,207	1,369	6,127	4,660	49	5,587	6,501	7,632
Genesee	410,849	95,474	65,992	7,396	32,345	24,536	261	29,550	34,316	83,172
Huron	31,883	6,218	7,574	482	2,590	2,254	20	2,911	3,238	3,662
Ingham	286,085	57,692	35,094	4,469	23,751	15,154	182	17,099	20,836	56,310
Kalamazoo	260,263	57,149	36,023	4,427	21,016	14,218	166	16,530	19,732	40,161
Kent	636,369	158,665	79,581	12,291	49,439	34,080	405	39,215	46,957	90,457
Lenawee	98,573	21,365	17,053	1,655	7,903	6,083	63	7,405	8,546	13,388
Macomb	864,840	187,442	137,131	14,521	69,546	52,417	549	62,721	73,101	99,879
Manistee	24,461	4,357	5,816	338	2,031	1,750	16	2,250	2,510	3,465
Mason	28,783	5,963	6,234	462	2,313	1,938	18	2,463	2,768	4,745
Missaukee	14,903	3,400	2,922	263	1,170	958	10	1,199	1,359	2,576
Monroe	149,568	33,218	24,353	2,573	11,919	9,249	95	11,143	12,913	15,717
Muskegon	172,790	40,701	26,801	3,153	13,565	10,150	110	12,149	14,167	26,695
Oakland	1,242,304	270,694	192,577	20,970	99,794	75,210	789	89,638	104,668	114,976
Ottawa	279,955	69,191	37,983	5,360	21,771	15,170	178	17,716	21,041	23,266
Schoolcraft	8,173	1,440	2,031	112	678	606	5	785	870	1,273
St. Clair	159,875	34,557	27,456	2,677	12,812	10,129	102	12,313	14,186	20,195
Tuscola	53,777	11,360	10,174	880	4,323	3,483	34	4,310	4,917	8,200
Washtenaw	358,880	69,537	44,917	5,387	30,063	19,495	228	22,065	26,801	48,525
Wayne	1,759,335	423,146	248,327	32,780	137,680	99,824	1,116	117,427	138,457	430,851
Wexford	33,003	7,725	5,915	598	2,580	2,048	21	2,522	2,888	4,827
Totals	**7,434,126**	**1,682,851**	**1,112,741**	**130,366**	**591,847**	**433,567**	**4,725**	**514,016**	**603,256**	**1,169,497**

STATE TABLES

MICHIGAN

American Lung Association in Michigan

www.lung.org/michigan

	HIGH OZONE DAYS 2013–2015					HIGH PARTICLE POLLUTION DAYS 2013–2015						
						24-Hour					Annual	
County	Orange	Red	Purple	Wgt. Avg.	Grade	Orange	Red	Purple	Wgt. Avg.	Grade	Design Value	Pass/ Fail
Allegan	17	2	0	6.7	F	0	0	0	0.0	A	8.1	PASS
Bay	DNC	DNC	DNC	DNC	DNC	0	0	0	0.0	A	7.8	PASS
Benzie	6	0	0	2.0	C	DNC	DNC	DNC	DNC	DNC	DNC	DNC
Berrien	14	0	0	4.7	F	0	0	0	0.0	A	8.2	PASS
Cass	7	0	0	2.3	D	DNC	DNC	DNC	DNC	DNC	DNC	DNC
Chippewa	0	0	0	0.0	A	0	0	0	0.0	A	6.1	PASS
Clinton	2	0	0	0.7	B	DNC	DNC	DNC	DNC	DNC	DNC	DNC
Genesee	5	0	0	1.7	C	1	0	0	0.3	B	8.2	PASS
Huron	4	0	0	1.3	C	DNC	DNC	DNC	DNC	DNC	DNC	DNC
Ingham	1	0	0	0.3	B	0	0	0	0.0	A	8.5	PASS
Kalamazoo	3	0	0	1.0	C	1	0	0	0.3	B	9.0	PASS
Kent	6	0	0	2.0	C	0	1	0	0.5	B	9.4	PASS
Lenawee	4	0	0	1.3	C	0	0	0	0.0	A	8.4	PASS
Macomb	15	0	0	5.0	F	0	1	0	0.5	B	8.9	PASS
Manistee	5	0	0	1.7	C	1	0	0	0.3	B	6.3	PASS
Mason	5	0	0	1.7	C	DNC	DNC	DNC	DNC	DNC	DNC	DNC
Missaukee	2	0	0	0.7	B	0	0	0	0.0	A	5.6	PASS
Monroe	DNC	DNC	DNC	DNC	DNC	1	0	0	0.3	B	INC	INC
Muskegon	17	1	0	6.2	F	INC	INC	INC	INC	INC	INC	INC
Oakland	8	0	0	2.7	D	1	0	0	0.3	B	9.0	PASS
Ottawa	7	0	0	2.3	D	INC	INC	INC	INC	INC	INC	INC
Schoolcraft	8	0	0	2.7	D	DNC	DNC	DNC	DNC	DNC	DNC	DNC
St. Clair	19	0	0	6.3	F	1	0	0	0.3	B	9.1	PASS
Tuscola	1	0	0	0.3	B	DNC	DNC	DNC	DNC	DNC	DNC	DNC
Washtenaw	5	0	0	1.7	C	0	0	0	0.0	A	9.2	PASS
Wayne	9	0	0	3.0	D	4	0	0	1.3	C	11.4	PASS
Wexford	2	0	0	0.7	B	DNC	DNC	DNC	DNC	DNC	DNC	DNC

STATE TABLES

MINNESOTA

American Lung Association in Minnesota

www.lung.org/minnesota

		AT-RISK GROUPS								
				Lung Diseases						
County	Total Population	Under 18	65 & Over	Pediatric Asthma	Adult Asthma	COPD	Lung Cancer	Cardiovascular Disease	Diabetes	Poverty
Anoka	344,151	83,424	42,705	5,248	19,301	11,354	198	16,473	19,048	24,058
Becker	33,386	8,227	6,532	518	1,834	1,277	19	2,020	2,185	3,728
Beltrami	45,672	11,516	6,826	724	2,541	1,509	26	2,252	2,515	7,081
Carlton	35,569	8,059	5,945	507	2,021	1,304	21	1,991	2,211	3,658
Crow Wing	63,428	13,940	13,464	877	3,604	2,552	36	4,072	4,371	6,500
Dakota	414,686	102,866	52,466	6,471	23,088	13,629	238	19,853	22,860	29,191
Goodhue	46,435	10,438	8,789	657	2,628	1,793	27	2,805	3,063	4,042
Hennepin	1,223,149	271,399	157,112	17,074	70,967	40,122	702	57,856	66,595	130,801
Lake	10,631	1,986	2,655	125	623	476	6	779	823	1,024
Lyon	25,673	6,424	3,787	404	1,428	857	15	1,279	1,435	3,009
Mille Lacs	25,788	6,154	4,744	387	1,437	966	15	1,505	1,644	3,125
Olmsted	151,436	37,346	21,771	2,349	8,453	5,084	87	7,554	8,523	13,255
Ramsey	538,133	125,750	71,450	7,911	30,770	17,476	309	25,385	28,983	78,920
Scott	141,660	40,341	13,602	2,538	7,549	4,150	81	5,802	6,891	7,203
St. Louis	200,431	38,344	35,413	2,412	11,947	7,587	115	11,579	12,809	25,821
Stearns	154,708	35,283	21,287	2,220	8,908	5,096	89	7,441	8,458	19,939
Washington	251,597	62,864	33,651	3,955	13,922	8,474	144	12,499	14,289	12,744
Winona	50,885	9,338	7,888	587	3,102	1,786	29	2,634	2,960	5,953
Wright	131,311	37,511	15,260	2,360	6,963	4,029	76	5,824	6,733	6,629
Totals	**3,888,729**	**911,210**	**525,347**	**57,325**	**221,085**	**129,523**	**2,234**	**189,602**	**216,396**	**386,681**

STATE TABLES

MINNESOTA

American Lung Association in Minnesota

www.lung.org/minnesota

	HIGH OZONE DAYS 2013–2015					HIGH PARTICLE POLLUTION DAYS 2013–2015						
						24-Hour					Annual	
County	Orange	Red	Purple	Wgt. Avg.	Grade	Orange	Red	Purple	Wgt. Avg.	Grade	Design Value	Pass/ Fail
Anoka	3	0	0	1.0	C	1	0	0	0.3	B	6.8	PASS
Becker	0	0	0	0.0	A	2	0	0	0.7	B	INC	INC
Beltrami	DNC	DNC	DNC	DNC	DNC	INC	INC	INC	INC	INC	INC	INC
Carlton	1	0	0	0.3	B	INC	INC	INC	INC	INC	INC	INC
Crow Wing	0	0	0	0.0	A	2	0	0	0.7	B	5.1	PASS
Dakota	DNC	DNC	DNC	DNC	DNC	0	0	0	0.0	A	7.0	PASS
Goodhue	0	0	0	0.0	A	DNC	DNC	DNC	DNC	DNC	DNC	DNC
Hennepin	0	0	0	0.0	A	1	0	0	0.3	B	8.1	PASS
Lake	0	0	0	0.0	A	1	0	0	0.3	B	4.8	PASS
Lyon	4	0	0	1.3	C	1	0	0	0.3	B	6.3	PASS
Mille Lacs	0	0	0	0.0	A	DNC	DNC	DNC	DNC	DNC	DNC	DNC
Olmsted	0	0	0	0.0	A	2	0	0	0.7	B	7.3	PASS
Ramsey	DNC	DNC	DNC	DNC	DNC	3	0	0	1.0	C	9.3	PASS
Scott	1	0	0	0.3	B	0	0	0	0.0	A	7.8	PASS
St. Louis	0	0	0	0.0	A	1	0	0	0.3	B	7.5	PASS
Stearns	0	0	0	0.0	A	0	1	0	0.5	B	6.1	PASS
Washington	0	0	0	0.0	A	2	0	0	0.7	B	8.4	PASS
Winona	DNC	DNC	DNC	DNC	DNC	INC	INC	INC	INC	INC	INC	INC
Wright	1	0	0	0.3	B	0	0	0	0.0	A	6.6	PASS

STATE TABLES

MISSISSIPPI

American Lung Association in Mississippi

www.lung.org/mississippi

		AT-RISK GROUPS								
				Lung Diseases						
County	Total Population	Under 18	65 & Over	Pediatric Asthma	Adult Asthma	COPD	Lung Cancer	Cardiovascular Disease	Diabetes	Poverty
Bolivar	33,322	8,403	4,779	747	1,929	1,892	26	2,762	3,604	11,380
DeSoto	173,323	45,833	21,065	4,073	9,912	9,623	135	13,634	18,017	17,169
Forrest	75,944	17,548	9,980	1,560	4,495	4,171	59	5,962	7,867	19,355
Grenada	21,578	5,133	3,658	456	1,278	1,331	17	1,999	2,572	4,539
Hancock	46,420	10,185	8,158	905	2,827	3,005	36	4,513	5,802	9,574
Harrison	201,410	48,920	27,525	4,348	11,829	11,575	157	16,684	21,885	43,019
Hinds	242,891	60,755	30,353	5,400	14,123	13,542	187	19,229	25,403	63,361
Jackson	141,425	34,092	20,634	3,030	8,356	8,445	110	12,307	16,048	22,511
Lauderdale	78,524	18,824	12,320	1,673	4,632	4,689	61	6,938	8,991	16,497
Lee	85,300	21,934	12,457	1,949	4,920	4,933	66	7,227	9,407	14,640
Yalobusha	12,447	2,895	2,301	257	742	789	10	1,204	1,538	2,747
Totals	**1,112,584**	**274,522**	**153,230**	**24,398**	**65,043**	**63,994**	**864**	**92,458**	**121,133**	**224,792**

STATE TABLES

MISSISSIPPI

American Lung Association in Mississippi

www.lung.org/mississippi

	HIGH OZONE DAYS 2013–2015					HIGH PARTICLE POLLUTION DAYS 2013–2015						
						24-Hour					Annual	
County	Orange	Red	Purple	Wgt. Avg.	Grade	Orange	Red	Purple	Wgt. Avg.	Grade	Design Value	Pass/ Fail
Bolivar	1	0	0	0.3	B	DNC	DNC	DNC	DNC	DNC	DNC	DNC
DeSoto	2	0	0	0.7	B	1	0	0	0.3	B	9.3	PASS
Forrest	DNC	DNC	DNC	DNC	DNC	1	0	0	0.3	B	10.0	PASS
Grenada	DNC	DNC	DNC	DNC	DNC	0	0	0	0.0	A	8.1	PASS
Hancock	2	0	0	0.7	B	0	0	0	0.0	A	8.6	PASS
Harrison	7	0	0	2.3	D	0	0	0	0.0	A	8.8	PASS
Hinds	0	0	0	0.0	A	0	0	0	0.0	A	INC	INC
Jackson	8	0	0	2.7	D	0	0	0	0.0	A	9.2	PASS
Lauderdale	0	0	0	0.0	A	DNC	DNC	DNC	DNC	DNC	DNC	DNC
Lee	1	0	0	0.3	B	DNC	DNC	DNC	DNC	DNC	DNC	DNC
Yalobusha	1	0	0	0.3	B	DNC	DNC	DNC	DNC	DNC	DNC	DNC

STATE TABLES

MISSOURI

American Lung Association in Missouri

www.lung.org/missouri

				AT-RISK GROUPS						
				Lung Diseases						
County	Total Population	Under 18	65 & Over	Pediatric Asthma	Adult Asthma	COPD	Lung Cancer	Cardiovascular Disease	Diabetes	Poverty
Andrew	17,296	3,984	3,022	345	1,272	1,174	13	1,521	1,633	1,612
Boone	174,974	35,803	18,998	3,096	13,586	10,170	131	11,594	12,960	29,347
Buchanan	89,100	20,210	13,356	1,748	6,634	5,710	67	7,113	7,733	14,578
Callaway	44,834	9,507	6,539	822	3,402	2,924	34	3,617	3,954	5,672
Cass	101,603	25,189	16,118	2,178	7,325	6,577	76	8,377	9,052	9,241
Cedar	13,934	3,246	3,352	281	1,012	1,014	10	1,408	1,458	2,727
Clay	235,637	58,322	30,934	5,044	17,111	14,431	176	17,614	19,358	18,212
Clinton	20,609	4,876	3,628	422	1,503	1,392	16	1,809	1,939	2,094
Greene	288,072	60,311	45,016	5,216	21,990	18,438	216	22,908	24,764	48,993
Jackson	687,623	165,286	95,014	14,295	50,363	42,820	514	52,688	57,659	119,421
Jasper	118,596	30,156	16,783	2,608	8,530	7,230	89	8,946	9,735	18,467
Jefferson	224,124	53,406	30,911	4,619	16,414	14,345	168	17,751	19,493	23,221
Lincoln	54,696	14,267	6,951	1,234	3,893	3,353	41	4,105	4,529	6,089
Monroe	8,583	1,912	1,839	165	633	620	6	838	882	1,182
Perry	19,183	4,604	3,242	398	1,395	1,271	14	1,637	1,759	2,088
St. Charles	385,590	93,004	52,662	8,043	28,177	24,240	289	29,863	32,763	23,775
St. Louis	1,003,362	223,088	169,017	19,294	74,774	67,336	748	86,170	92,819	101,692
St. Louis City	315,685	63,437	36,569	5,486	24,494	19,411	236	22,709	25,343	78,089
Ste. Genevieve	17,919	4,035	3,118	349	1,325	1,237	13	1,603	1,726	1,914
Taney	54,592	11,646	11,028	1,007	4,102	3,801	41	5,033	5,313	8,483
Totals	**3,876,012**	**886,289**	**568,097**	**76,650**	**287,936**	**247,496**	**2,899**	**307,306**	**334,871**	**516,897**

STATE TABLES

MISSOURI

American Lung Association in Missouri

www.lung.org/missouri

	HIGH OZONE DAYS 2013–2015					HIGH PARTICLE POLLUTION DAYS 2013–2015						
						24-Hour					Annual	
County	Orange	Red	Purple	Wgt. Avg.	Grade	Orange	Red	Purple	Wgt. Avg.	Grade	Design Value	Pass/ Fail
Andrew	3	0	0	1.0	C	DNC	DNC	DNC	DNC	DNC	DNC	DNC
Boone	0	0	0	0.0	A	DNC	DNC	DNC	DNC	DNC	DNC	DNC
Buchanan	DNC	DNC	DNC	DNC	DNC	1	0	0	0.3	B	10.5	PASS
Callaway	0	0	0	0.0	A	DNC	DNC	DNC	DNC	DNC	DNC	DNC
Cass	0	0	0	0.0	A	1	0	0	0.3	B	9.4	PASS
Cedar	1	0	0	0.3	B	0	0	0	0.0	A	7.9	PASS
Clay	13	0	0	4.3	F	1	0	0	0.3	B	8.6	PASS
Clinton	6	0	0	2.0	C	DNC	DNC	DNC	DNC	DNC	DNC	DNC
Greene	0	0	0	0.0	A	0	0	0	0.0	A	INC	INC
Jackson	DNC	DNC	DNC	DNC	DNC	3	0	0	1.0	C	9.1	PASS
Jasper	2	0	0	0.7	B	DNC	DNC	DNC	DNC	DNC	DNC	DNC
Jefferson	10	0	0	3.3	F	3	0	0	1.0	C	10.6	PASS
Lincoln	4	0	0	1.3	C	DNC	DNC	DNC	DNC	DNC	DNC	DNC
Monroe	1	0	0	0.3	B	DNC	DNC	DNC	DNC	DNC	DNC	DNC
Perry	1	0	0	0.3	B	DNC	DNC	DNC	DNC	DNC	DNC	DNC
St. Charles	15	1	0	5.5	F	DNC	DNC	DNC	DNC	DNC	DNC	DNC
St. Louis	11	0	0	3.7	F	3	0	0	1.0	C	10.7	PASS
St. Louis City	2	0	0	0.7	B	7	1	0	2.8	D	11.0	PASS
Ste. Genevieve	4	0	0	1.3	C	DNC	DNC	DNC	DNC	DNC	DNC	DNC
Taney	0	0	0	0.0	A	DNC	DNC	DNC	DNC	DNC	DNC	DNC

MONTANA

American Lung Association in Montana

www.lung.org/montana

				AT-RISK GROUPS						
				Lung Diseases						
County	Total Population	Under 18	65 & Over	Pediatric Asthma	Adult Asthma	COPD	Lung Cancer	Cardiovascular Disease	Diabetes	Poverty
Fergus	11,427	2,337	2,685	148	794	587	7	825	817	1,515
Flathead	96,165	21,452	17,068	1,360	6,633	4,416	56	5,933	6,135	13,270
Lewis and Clark	66,418	14,379	11,234	912	4,630	3,002	38	3,992	4,165	7,903
Lincoln	19,052	3,491	4,903	221	1,360	1,072	11	1,523	1,499	3,817
Missoula	114,181	22,154	16,172	1,404	8,203	4,628	66	5,905	6,350	17,461
Phillips	4,169	965	865	61	282	204	2	283	285	673
Powder River	1,773	302	435	19	129	99	1	139	138	185
Ravalli	41,373	8,214	9,904	521	2,901	2,193	24	3,088	3,060	6,129
Richland	11,960	3,091	1,504	196	796	466	7	594	643	835
Rosebud	9,398	2,763	1,326	175	593	373	5	490	517	1,750
Silver Bow	34,622	7,092	6,107	450	2,442	1,575	20	2,103	2,181	5,614
Yellowstone	157,048	36,826	24,786	2,335	10,690	6,650	91	8,761	9,193	15,995
Totals	**567,586**	**123,066**	**96,989**	**7,802**	**39,452**	**25,264**	**328**	**33,634**	**34,983**	**75,147**

STATE TABLES

MONTANA

American Lung Association in Montana

www.lung.org/montana

	HIGH OZONE DAYS 2013–2015					HIGH PARTICLE POLLUTION DAYS 2013–2015						
						24-Hour					Annual	
County	Orange	Red	Purple	Wgt. Avg.	Grade	Orange	Red	Purple	Wgt. Avg.	Grade	Design Value	Pass/ Fail
Fergus	0	0	0	0.0	A	7	3	0	3.8	F	4.5	PASS
Flathead	0	0	0	0.0	A	9	9	0	7.5	F	9.3	PASS
Lewis and Clark	0	0	0	0.0	A	12	5	0	6.5	F	8.3	PASS
Lincoln	DNC	DNC	DNC	DNC	DNC	9	12	1	9.7	F	11.7	PASS
Missoula	0	0	0	0.0	A	9	11	0	8.5	F	10.4	PASS
Phillips	0	0	0	0.0	A	5	4	0	3.7	F	4.9	PASS
Powder River	0	0	0	0.0	A	5	1	0	2.2	D	6.2	PASS
Ravalli	DNC	DNC	DNC	DNC	DNC	17	11	2	12.5	F	9.4	PASS
Richland	0	0	0	0.0	A	4	3	0	2.8	D	7.0	PASS
Rosebud	0	0	0	0.0	A	4	1	0	1.8	C	5.4	PASS
Silver Bow	DNC	DNC	DNC	DNC	DNC	10	7	0	6.8	F	9.7	PASS
Yellowstone	DNC	DNC	DNC	DNC	DNC	INC	INC	INC	INC	INC	INC	INC

NEBRASKA

American Lung Association in Nebraska

www.lung.org/nebraska

				AT-RISK GROUPS						
				Lung Diseases						
County	Total Population	Under 18	65 & Over	Pediatric Asthma	Adult Asthma	COPD	Lung Cancer	Cardiovascular Disease	Diabetes	Poverty
Douglas	550,064	142,366	64,743	9,416	29,437	20,470	338	27,534	32,882	77,869
Hall	61,680	16,673	8,902	1,103	3,241	2,456	38	3,402	3,973	8,182
Knox	8,543	2,077	2,039	137	462	438	5	646	720	1,141
Lancaster	306,468	70,379	38,425	4,655	17,054	11,578	189	15,724	18,567	39,383
Sarpy	175,692	49,226	18,645	3,256	9,137	6,234	108	8,293	9,997	10,095
Scotts Bluff	36,261	8,957	6,543	592	1,960	1,615	22	2,296	2,628	5,364
Washington	20,248	4,864	3,361	322	1,105	911	12	1,267	1,482	1,328
Totals	**1,158,956**	**294,542**	**142,658**	**19,480**	**62,396**	**43,703**	**713**	**59,162**	**70,249**	**143,362**

STATE TABLES

NEBRASKA

American Lung Association in Nebraska

www.lung.org/nebraska

	HIGH OZONE DAYS 2013–2015					HIGH PARTICLE POLLUTION DAYS 2013–2015						
						24-Hour					Annual	
County	Orange	Red	Purple	Wgt. Avg.	Grade	Orange	Red	Purple	Wgt. Avg.	Grade	Design Value	Pass/ Fail
Douglas	2	0	0	0.7	B	4	0	0	1.3	C	9.1	PASS
Hall	DNC	DNC	DNC	DNC	DNC	0	0	0	0.0	A	6.8	PASS
Knox	0	0	0	0.0	A	DNC	DNC	DNC	DNC	DNC	DNC	DNC
Lancaster	0	0	0	0.0	A	1	0	0	0.3	B	7.5	PASS
Sarpy	DNC	DNC	DNC	DNC	DNC	3	0	0	1.0	C	INC	INC
Scotts Bluff	DNC	DNC	DNC	DNC	DNC	0	0	0	0.0	A	5.3	PASS
Washington	DNC	DNC	DNC	DNC	DNC	1	0	0	0.3	B	7.5	PASS

STATE TABLES

NEVADA

American Lung Association in Nevada

www.lung.org/nevada

				AT-RISK GROUPS						
				Lung Diseases						
County	Total Population	Under 18	65 & Over	Pediatric Asthma	Adult Asthma	COPD	Lung Cancer	Cardiovascular Disease	Diabetes	Poverty
Carson City	54,521	11,140	10,792	651	3,492	3,226	32	3,913	4,779	8,457
Churchill	24,200	5,626	4,425	329	1,492	1,341	14	1,613	1,978	3,115
Clark	2,114,801	498,564	290,001	29,147	130,554	103,810	1,242	121,424	153,343	321,755
Douglas	47,710	8,500	12,234	497	3,145	3,277	28	4,072	4,863	4,459
Elko	51,935	14,459	5,043	845	3,058	2,226	31	2,562	3,328	5,065
Lyon	52,585	11,634	10,816	680	3,293	3,136	31	3,827	4,647	7,180
Washoe	446,903	99,275	67,548	5,804	28,100	23,194	263	27,431	34,367	61,017
White Pine	9,811	2,088	1,511	122	625	518	6	614	769	1,198
Totals	**2,802,466**	**651,286**	**402,370**	**38,075**	**173,759**	**140,729**	**1,647**	**165,456**	**208,074**	**412,246**

STATE TABLES

NEVADA

American Lung Association in Nevada

www.lung.org/nevada

	HIGH OZONE DAYS 2013–2015					HIGH PARTICLE POLLUTION DAYS 2013–2015						
						24-Hour					Annual	
County	Orange	Red	Purple	Wgt. Avg.	Grade	Orange	Red	Purple	Wgt. Avg.	Grade	Design Value	Pass/ Fail
Carson City	1	0	0	0.3	B	8	10	1	8.3	F	INC	INC
Churchill	2	0	0	0.7	B	DNC	DNC	DNC	DNC	DNC	DNC	DNC
Clark	64	5	0	23.8	F	5	1	0	2.2	D	10.1	PASS
Douglas	DNC	DNC	DNC	DNC	DNC	13	10	6	13.3	F	INC	INC
Elko	INC	INC	INC	INC	INC	DNC	DNC	DNC	DNC	DNC	DNC	DNC
Lyon	6	0	0	2.0	C	DNC	DNC	DNC	DNC	DNC	DNC	DNC
Washoe	18	0	0	6.0	F	18	7	0	9.5	F	9.6	PASS
White Pine	8	0	0	2.7	D	DNC	DNC	DNC	DNC	DNC	DNC	DNC

NEW HAMPSHIRE

American Lung Association in New Hampshire

www.lung.org/newhampshire

				AT-RISK GROUPS						
				Lung Diseases						
County	Total Population	Under 18	65 & Over	Pediatric Asthma	Adult Asthma	COPD	Lung Cancer	Cardiovascular Disease	Diabetes	Poverty
Belknap	60,641	11,714	12,451	845	4,872	3,532	40	4,079	4,424	5,217
Cheshire	75,909	13,972	13,574	1,008	6,283	4,172	50	4,648	5,073	7,064
Coos	31,212	5,412	7,018	390	2,554	1,910	21	2,236	2,410	4,792
Grafton	89,320	15,033	16,667	1,084	7,546	5,007	59	5,588	6,065	9,245
Hillsborough	406,678	87,109	58,512	6,283	32,660	20,524	267	22,154	24,704	31,984
Merrimack	147,994	28,984	24,880	2,091	12,059	7,973	97	8,834	9,732	11,691
Rockingham	301,777	61,163	47,679	4,412	24,310	16,094	198	17,762	19,803	15,687
Totals	**1,113,531**	**223,387**	**180,781**	**16,113**	**90,285**	**59,212**	**731**	**65,301**	**72,211**	**85,680**

STATE TABLES

NEW HAMPSHIRE

American Lung Association in New Hampshire

www.lung.org/newhampshire

	HIGH OZONE DAYS 2013–2015					HIGH PARTICLE POLLUTION DAYS 2013–2015						
						24-Hour					Annual	
County	Orange	Red	Purple	Wgt. Avg.	Grade	Orange	Red	Purple	Wgt. Avg.	Grade	Design Value	Pass/ Fail
Belknap	0	0	0	0.0	A	0	0	0	0.0	A	5.0	PASS
Cheshire	1	0	0	0.3	B	3	1	0	1.5	C	8.8	PASS
Coos	7	0	0	2.3	D	DNC	DNC	DNC	DNC	DNC	DNC	DNC
Grafton	1	0	0	0.3	B	0	0	0	0.0	A	6.3	PASS
Hillsborough	4	0	0	1.3	C	0	0	0	0.0	A	6.3	PASS
Merrimack	2	0	0	0.7	B	INC	INC	INC	INC	INC	INC	INC
Rockingham	9	0	0	3.0	D	0	0	0	0.0	A	8.2	PASS

STATE TABLES

NEW JERSEY

American Lung Association in New Jersey

www.lung.org/newjersey

		AT-RISK GROUPS								
				Lung Diseases						
County	Total Population	Under 18	65 & Over	Pediatric Asthma	Adult Asthma	COPD	Lung Cancer	Cardiovascular Disease	Diabetes	Poverty
Atlantic	274,219	60,077	44,800	5,175	15,459	10,901	160	15,917	19,885	37,923
Bergen	938,506	201,430	152,403	17,351	53,224	37,421	548	54,597	68,269	65,906
Camden	510,923	118,125	74,538	10,175	28,407	19,173	298	27,507	34,471	65,805
Cumberland	155,854	36,694	21,848	3,161	8,621	5,673	92	8,040	10,063	24,740
Essex	797,434	191,077	100,634	16,459	43,951	28,153	466	39,512	49,773	131,125
Gloucester	291,479	65,857	42,653	5,673	16,321	11,115	170	16,027	20,133	22,086
Hudson	674,836	136,696	73,318	11,775	39,100	22,716	395	30,321	38,252	117,828
Hunterdon	125,488	25,973	20,477	2,237	7,191	5,243	73	7,794	9,827	6,046
Mercer	371,398	80,663	52,076	6,948	21,047	13,868	217	19,699	24,736	39,354
Middlesex	840,900	183,992	115,274	15,849	47,569	31,018	492	43,846	55,073	69,660
Monmouth	628,715	138,218	100,935	11,906	35,431	25,248	368	37,103	46,557	46,641
Morris	499,509	109,736	78,501	9,452	28,166	19,849	292	29,039	36,453	25,917
Ocean	588,721	138,514	130,156	11,931	32,235	25,767	344	39,159	48,012	63,101
Passaic	510,916	124,017	68,264	10,682	28,014	18,301	299	25,890	32,510	86,457
Union	555,786	131,997	73,670	11,370	30,698	20,137	325	28,577	35,981	58,384
Warren	106,869	22,141	17,629	1,907	6,119	4,382	62	6,452	8,093	8,040
Totals	**7,871,553**	**1,765,207**	**1,167,176**	**152,050**	**441,554**	**298,964**	**4,602**	**429,480**	**538,088**	**869,013**

STATE TABLES

NEW JERSEY

American Lung Association in New Jersey

www.lung.org/newjersey

	HIGH OZONE DAYS 2013–2015					HIGH PARTICLE POLLUTION DAYS 2013–2015						
						24-Hour					Annual	
County	Orange	Red	Purple	Wgt. Avg.	Grade	Orange	Red	Purple	Wgt. Avg.	Grade	Design Value	Pass/ Fail
Atlantic	4	1	0	1.8	C	0	0	0	0.0	A	8.1	PASS
Bergen	22	0	0	7.3	F	0	0	0	0.0	A	9.1	PASS
Camden	18	1	0	6.5	F	1	0	0	0.3	B	10.4	PASS
Cumberland	3	0	0	1.0	C	DNC	DNC	DNC	DNC	DNC	DNC	DNC
Essex	10	0	0	3.3	F	2	0	0	0.7	B	8.9	PASS
Gloucester	12	0	0	4.0	F	0	0	0	0.0	A	8.9	PASS
Hudson	21	2	0	8.0	F	1	0	0	0.3	B	10.8	PASS
Hunterdon	10	0	0	3.3	F	DNC	DNC	DNC	DNC	DNC	DNC	DNC
Mercer	19	0	0	6.3	F	0	0	0	0.0	A	8.6	PASS
Middlesex	13	1	0	4.8	F	0	0	0	0.0	A	8.0	PASS
Monmouth	9	2	0	4.0	F	DNC	DNC	DNC	DNC	DNC	DNC	DNC
Morris	10	0	0	3.3	F	0	0	0	0.0	A	7.1	PASS
Ocean	15	1	0	5.5	F	1	0	0	0.3	B	7.7	PASS
Passaic	9	0	0	3.0	D	0	0	0	0.0	A	8.9	PASS
Union	DNC	DNC	DNC	DNC	DNC	5	0	0	1.7	C	10.4	PASS
Warren	3	0	0	1.0	C	0	0	0	0.0	A	8.3	PASS

STATE TABLES

NEW MEXICO

American Lung Association in New Mexico

www.lung.org/newmexico

		AT-RISK GROUPS								
				Lung Diseases						
County	Total Population	Under 18	65 & Over	Pediatric Asthma	Adult Asthma	COPD	Lung Cancer	Cardiovascular Disease	Diabetes	Poverty
Bernalillo	676,685	153,390	99,360	13,882	51,620	30,839	271	40,308	58,573	126,614
Doña Ana	214,295	54,119	31,444	4,898	15,811	9,174	86	12,034	17,463	53,968
Eddy	57,578	15,216	8,022	1,377	4,178	2,504	23	3,272	4,755	7,015
Grant	28,609	5,929	7,226	537	2,238	1,607	11	2,263	3,077	5,753
Lea	71,180	21,611	7,399	1,956	4,891	2,679	29	3,388	5,077	9,875
Luna	24,518	6,385	5,121	578	1,790	1,200	10	1,661	2,296	7,395
Rio Arriba	39,465	9,489	6,793	859	2,956	1,926	16	2,581	3,662	9,486
San Juan	118,737	31,403	16,654	2,842	8,614	5,179	48	6,774	9,836	22,047
Sandoval	139,394	33,821	22,113	3,061	10,410	6,576	56	8,716	12,494	15,572
Santa Fe	148,686	28,477	31,050	2,577	11,852	8,108	59	11,065	15,447	19,165
Valencia	75,737	18,383	12,106	1,664	5,655	3,590	30	4,764	6,821	14,643
Totals	**1,594,884**	**378,223**	**247,288**	**34,231**	**120,014**	**73,384**	**639**	**96,827**	**139,501**	**291,533**

STATE TABLES

NEW MEXICO

American Lung Association in New Mexico

www.lung.org/newmexico

HIGH OZONE DAYS 2013–2015

County	Orange	Red	Purple	Wgt. Avg.	Grade
Bernalillo	7	0	0	2.3	D
Doña Ana	47	1	0	16.2	F
Eddy	6	0	0	2.0	C
Grant	INC	INC	INC	INC	INC
Lea	3	0	0	1.0	C
Luna	INC	INC	INC	INC	INC
Rio Arriba	2	0	0	0.7	B
San Juan	6	0	0	2.0	C
Sandoval	0	0	0	0.0	A
Santa Fe	0	0	0	0.0	A
Valencia	5	0	0	1.7	C

HIGH PARTICLE POLLUTION DAYS 2013–2015

	24-Hour					Annual	
	Orange	Red	Purple	Wgt. Avg.	Grade	Design Value	Pass/ Fail
Bernalillo	1	0	0	0.3	B	7.5	PASS
Doña Ana	0	1	0	0.5	B	5.6	PASS
Eddy	DNC	DNC	DNC	DNC	DNC	DNC	DNC
Grant	DNC	DNC	DNC	DNC	DNC	DNC	DNC
Lea	1	1	0	0.8	B	7.8	PASS
Luna	DNC	DNC	DNC	DNC	DNC	DNC	DNC
Rio Arriba	DNC	DNC	DNC	DNC	DNC	DNC	DNC
San Juan	0	0	0	0.0	A	4.1	PASS
Sandoval	DNC	DNC	DNC	DNC	DNC	DNC	DNC
Santa Fe	INC	INC	INC	INC	INC	INC	INC
Valencia	DNC	DNC	DNC	DNC	DNC	DNC	DNC

STATE TABLES

NEW YORK

American Lung Association in New York

www.lung.org/newyork

		AT-RISK GROUPS								
				Lung Diseases						
County	Total Population	Under 18	65 & Over	Pediatric Asthma	Adult Asthma	COPD	Lung Cancer	Cardiovascular Disease	Diabetes	Poverty
Albany	309,381	58,304	48,270	5,820	25,045	14,222	187	18,365	24,127	36,827
Bronx	1,455,444	368,977	166,281	36,829	108,973	56,592	878	71,058	95,629	430,291
Chautauqua	130,779	26,957	24,195	2,691	10,265	6,506	79	8,608	11,130	21,630
Dutchess	295,754	58,429	47,326	5,832	23,510	14,221	179	18,470	24,379	28,978
Erie	922,578	189,903	154,748	18,955	72,679	43,998	558	57,512	75,126	139,581
Essex	38,478	6,501	8,240	649	3,148	2,108	23	2,824	3,617	4,418
Franklin	50,660	10,048	7,766	1,003	4,038	2,354	31	3,040	4,017	8,234
Hamilton	4,712	684	1,305	68	391	302	3	416	523	523
Herkimer	63,100	13,267	12,133	1,324	4,915	3,204	38	4,262	5,493	7,806
Jefferson	117,635	28,751	14,843	2,870	8,938	4,605	72	5,833	7,723	15,718
Kings	2,636,735	612,433	325,578	61,129	203,249	105,485	1,591	133,122	177,651	581,684
Monroe	749,600	159,513	119,145	15,922	58,648	34,647	453	45,035	59,058	107,747
New York	1,644,518	240,380	240,185	23,993	141,186	73,158	992	92,935	122,646	280,715
Niagara	212,652	43,176	37,547	4,310	16,742	10,569	129	13,900	18,134	32,421
Onondaga	468,463	101,865	73,407	10,168	36,408	21,602	283	28,054	36,875	66,114
Orange	377,647	97,462	48,796	9,728	27,867	15,918	229	20,341	27,220	44,395
Oswego	120,146	25,897	17,842	2,585	9,349	5,539	73	7,150	9,490	19,996
Putnam	99,042	20,747	15,070	2,071	7,722	4,803	60	6,219	8,298	5,897
Queens	2,339,150	476,985	323,755	47,610	185,952	102,666	1,415	130,999	174,342	320,712
Richmond	474,558	104,847	71,216	10,465	36,723	21,600	287	27,926	36,907	66,586
Rockland	326,037	90,294	49,160	9,013	23,402	14,047	197	18,331	23,965	44,933
Saratoga	226,249	47,460	36,846	4,737	17,692	10,863	137	14,164	18,634	14,149
Steuben	97,631	21,597	17,601	2,156	7,504	4,813	59	6,364	8,257	14,745
Suffolk	1,501,587	329,288	234,551	32,867	116,081	70,497	910	91,598	120,920	114,849
Tompkins	104,926	15,703	13,350	1,567	9,018	4,342	64	5,415	7,221	18,480
Wayne	91,446	20,039	15,562	2,000	7,042	4,489	55	5,894	7,727	11,008
Westchester	976,396	221,464	154,130	22,105	74,826	45,276	591	58,954	77,491	96,580
Totals	**15,835,304**	**3,390,971**	**2,278,848**	**338,465**	**1,241,312**	**698,426**	**9,575**	**896,789**	**1,186,604**	**2,535,017**

STATE TABLES

NEW YORK

American Lung Association in New York

www.lung.org/newyork

	HIGH OZONE DAYS 2013–2015					HIGH PARTICLE POLLUTION DAYS 2013–2015						
						24-Hour					Annual	
County	Orange	Red	Purple	Wgt. Avg.	Grade	Orange	Red	Purple	Wgt. Avg.	Grade	Design Value	Pass/ Fail
Albany	0	0	0	0.0	A	0	0	0	0.0	A	7.4	PASS
Bronx	14	0	0	4.7	F	0	0	0	0.0	A	9.4	PASS
Chautauqua	8	0	0	2.7	D	0	0	0	0.0	A	INC	INC
Dutchess	3	0	0	1.0	C	DNC	DNC	DNC	DNC	DNC	DNC	DNC
Erie	9	0	0	3.0	D	0	0	0	0.0	A	8.6	PASS
Essex	1	0	0	0.3	B	0	0	0	0.0	A	4.1	PASS
Franklin	4	0	0	1.3	C	DNC	DNC	DNC	DNC	DNC	DNC	DNC
Hamilton	0	0	0	0.0	A	DNC	DNC	DNC	DNC	DNC	DNC	DNC
Herkimer	0	0	0	0.0	A	DNC	DNC	DNC	DNC	DNC	DNC	DNC
Jefferson	1	0	0	0.3	B	DNC	DNC	DNC	DNC	DNC	DNC	DNC
Kings	DNC	DNC	DNC	DNC	DNC	0	0	0	0.0	A	9.1	PASS
Monroe	0	0	0	0.0	A	0	0	0	0.0	A	7.2	PASS
New York	8	0	0	2.7	D	0	0	0	0.0	A	11.0	PASS
Niagara	2	0	0	0.7	B	INC	INC	INC	INC	INC	INC	INC
Onondaga	0	0	0	0.0	A	0	0	0	0.0	A	6.4	PASS
Orange	4	0	0	1.3	C	0	0	0	0.0	A	7.2	PASS
Oswego	1	0	0	0.3	B	DNC	DNC	DNC	DNC	DNC	DNC	DNC
Putnam	3	0	0	1.0	C	DNC	DNC	DNC	DNC	DNC	DNC	DNC
Queens	11	0	0	3.7	F	0	0	0	0.0	A	8.1	PASS
Richmond	18	2	0	7.0	F	0	0	0	0.0	A	INC	INC
Rockland	8	0	0	2.7	D	DNC	DNC	DNC	DNC	DNC	DNC	DNC
Saratoga	1	0	0	0.3	B	DNC	DNC	DNC	DNC	DNC	DNC	DNC
Steuben	0	0	0	0.0	A	0	0	0	0.0	A	5.7	PASS
Suffolk	22	2	0	8.3	F	0	0	0	0.0	A	7.5	PASS
Tompkins	0	0	0	0.0	A	DNC	DNC	DNC	DNC	DNC	DNC	DNC
Wayne	1	0	0	0.3	B	DNC	DNC	DNC	DNC	DNC	DNC	DNC
Westchester	18	1	0	6.5	F	DNC	DNC	DNC	DNC	DNC	DNC	DNC

STATE TABLES

NORTH CAROLINA

American Lung Association in North Carolina

www.lung.org/northcarolina

				AT-RISK GROUPS						
				Lung Diseases						
County	Total Population	Under 18	65 & Over	Pediatric Asthma	Adult Asthma	COPD	Lung Cancer	Cardiovascular Disease	Diabetes	Poverty
Alamance	158,276	36,006	25,967	4,138	10,049	9,404	111	11,839	13,568	29,039
Alexander	37,325	7,735	7,268	889	2,439	2,402	27	3,142	3,539	5,555
Avery	17,689	2,743	3,691	315	1,229	1,186	13	1,554	1,741	2,997
Buncombe	253,178	48,656	47,089	5,591	16,815	15,971	178	20,538	23,256	37,433
Caldwell	81,287	17,004	14,831	1,954	5,301	5,202	57	6,696	7,622	12,963
Carteret	68,879	12,577	15,542	1,445	4,653	4,789	49	6,461	7,177	9,370
Caswell	22,941	4,390	4,658	504	1,532	1,542	16	2,029	2,285	4,353
Catawba	155,056	35,211	25,759	4,046	9,865	9,408	109	11,889	13,637	23,050
Chatham	70,928	14,114	17,716	1,622	4,698	4,963	50	6,923	7,548	8,111
Cumberland	323,838	82,868	36,625	9,523	19,664	16,254	228	18,698	22,260	59,320
Davidson	164,622	36,952	28,400	4,246	10,520	10,193	116	12,997	14,858	22,977
Davie	41,753	9,023	8,180	1,037	2,703	2,725	29	3,581	4,037	5,080
Duplin	59,159	14,471	9,762	1,663	3,676	3,487	42	4,424	5,056	14,603
Durham	300,952	65,360	34,465	7,511	19,232	15,910	211	18,150	21,740	49,310
Edgecombe	54,150	12,476	9,504	1,434	3,433	3,321	38	4,262	4,849	14,742
Forsyth	369,019	87,172	54,419	10,017	23,139	21,137	258	25,965	30,134	64,966
Franklin	63,710	14,466	9,945	1,662	4,054	3,839	45	4,777	5,532	9,909
Gaston	213,442	48,942	32,838	5,624	13,524	12,603	150	15,625	18,086	36,243
Graham	8,616	1,836	1,961	211	560	575	6	786	864	1,783
Granville	58,674	12,289	9,341	1,412	3,820	3,628	42	4,512	5,230	8,786
Guilford	517,600	117,471	73,066	13,499	32,807	29,322	362	35,488	41,440	78,783
Haywood	59,868	11,001	14,384	1,264	4,038	4,188	42	5,752	6,320	10,436
Jackson	41,265	7,064	7,473	812	2,801	2,531	29	3,206	3,634	7,879
Johnston	185,660	48,767	23,545	5,604	11,240	10,152	131	12,131	14,323	23,887
Lee	59,660	14,874	9,190	1,709	3,680	3,419	42	4,267	4,914	10,044
Lenoir	58,106	13,143	10,623	1,510	3,706	3,626	41	4,695	5,319	13,069
Lincoln	81,035	17,661	13,178	2,030	5,223	5,027	57	6,304	7,283	10,774
Macon	34,201	6,475	9,163	744	2,293	2,453	24	3,478	3,757	5,719
Martin	23,357	4,761	5,018	547	1,537	1,577	16	2,114	2,357	5,213
McDowell	44,989	9,263	8,484	1,064	2,945	2,888	32	3,744	4,240	8,183
Mecklenburg	1,034,070	251,972	106,570	28,956	63,888	52,936	726	59,508	72,056	145,693
Mitchell	15,246	2,815	3,644	323	1,028	1,073	11	1,471	1,620	2,516
Montgomery	27,548	6,329	5,233	727	1,748	1,717	19	2,249	2,529	5,296
New Hanover	220,358	42,336	35,679	4,865	14,586	13,082	155	16,201	18,628	36,967
Person	39,259	8,509	7,046	978	2,536	2,486	28	3,195	3,640	6,317
Pitt	175,842	38,695	20,590	4,447	11,183	9,139	123	10,466	12,467	43,954

NORTH CAROLINA (cont.)

American Lung Association in North Carolina

www.lung.org/northcarolina

	AT-RISK GROUPS									
				Lung Diseases						
County	Total Population	Under 18	65 & Over	Pediatric Asthma	Adult Asthma	COPD	Lung Cancer	Cardiovascular Disease	Diabetes	Poverty
Robeson	134,197	34,605	18,170	3,977	8,167	7,318	94	8,857	10,348	39,785
Rockingham	91,758	19,184	17,184	2,205	5,989	5,938	64	7,694	8,733	16,699
Rowan	139,142	31,310	23,306	3,598	8,871	8,407	98	10,636	12,177	23,342
Swain	14,434	3,222	2,727	370	922	889	10	1,160	1,304	2,295
Union	222,742	62,453	25,941	7,177	13,169	11,899	157	14,033	16,727	21,397
Wake	1,024,198	253,184	105,510	29,095	63,063	53,124	721	59,937	72,654	111,299
Watauga	52,906	6,990	7,728	803	3,739	3,045	37	3,581	4,183	11,956
Wayne	124,132	29,833	18,567	3,428	7,740	7,069	88	8,725	10,092	22,267
Yancey	17,587	3,332	4,208	383	1,178	1,225	12	1,683	1,849	3,359
Totals	**6,962,654**	**1,609,540**	**974,188**	**184,962**	**438,984**	**393,069**	**4,893**	**475,422**	**555,616**	**1,087,719**

STATE TABLES

NORTH CAROLINA

American Lung Association in North Carolina

www.lung.org/northcarolina

	HIGH OZONE DAYS 2013–2015					HIGH PARTICLE POLLUTION DAYS 2013–2015						
						24-Hour					Annual	
County	Orange	Red	Purple	Wgt. Avg.	Grade	Orange	Red	Purple	Wgt. Avg.	Grade	Design Value	Pass/ Fail
Alamance	DNC	DNC	DNC	DNC	DNC	0	0	0	0.0	A	INC	INC
Alexander	0	0	0	0.0	A	DNC	DNC	DNC	DNC	DNC	DNC	DNC
Avery	0	0	0	0.0	A	DNC	DNC	DNC	DNC	DNC	DNC	DNC
Buncombe	0	0	0	0.0	A	0	0	0	0.0	A	7.7	PASS
Caldwell	0	0	0	0.0	A	DNC	DNC	DNC	DNC	DNC	DNC	DNC
Carteret	0	0	0	0.0	A	DNC	DNC	DNC	DNC	DNC	DNC	DNC
Caswell	1	0	0	0.3	B	0	0	0	0.0	A	8.8	PASS
Catawba	DNC	DNC	DNC	DNC	DNC	0	0	0	0.0	A	8.9	PASS
Chatham	0	0	0	0.0	A	INC	INC	INC	INC	INC	INC	INC
Cumberland	1	0	0	0.3	B	0	0	0	0.0	A	8.5	PASS
Davidson	DNC	DNC	DNC	DNC	DNC	0	0	0	0.0	A	9.2	PASS
Davie	INC	INC	INC	INC	INC	DNC	DNC	DNC	DNC	DNC	DNC	DNC
Duplin	DNC	DNC	DNC	DNC	DNC	0	0	0	0.0	A	7.3	PASS
Durham	0	0	0	0.0	A	0	0	0	0.0	A	8.3	PASS
Edgecombe	1	0	0	0.3	B	INC	INC	INC	INC	INC	INC	INC
Forsyth	5	0	0	1.7	C	0	0	0	0.0	A	8.5	PASS
Franklin	0	0	0	0.0	A	DNC	DNC	DNC	DNC	DNC	DNC	DNC
Gaston	DNC	DNC	DNC	DNC	DNC	0	0	0	0.0	A	INC	INC
Graham	1	0	0	0.3	B	DNC	DNC	DNC	DNC	DNC	DNC	DNC
Granville	0	0	0	0.0	A	DNC	DNC	DNC	DNC	DNC	DNC	DNC
Guilford	2	0	0	0.7	B	0	0	0	0.0	A	8.4	PASS
Haywood	2	0	0	0.7	B	0	0	0	0.0	A	8.2	PASS
Jackson	2	0	0	0.7	B	0	0	0	0.0	A	7.3	PASS
Johnston	0	0	0	0.0	A	0	0	0	0.0	A	7.3	PASS
Lee	INC	INC	INC	INC	INC	INC	INC	INC	INC	INC	INC	INC
Lenoir	0	0	0	0.0	A	INC	INC	INC	INC	INC	INC	INC
Lincoln	5	0	0	1.7	C	DNC	DNC	DNC	DNC	DNC	DNC	DNC
Macon	0	0	0	0.0	A	DNC	DNC	DNC	DNC	DNC	DNC	DNC
Martin	0	0	0	0.0	A	0	0	0	0.0	A	6.9	PASS
McDowell	DNC	DNC	DNC	DNC	DNC	1	0	0	0.3	B	8.4	PASS
Mecklenburg	13	0	0	4.3	F	0	0	0	0.0	A	9.0	PASS
Mitchell	DNC	DNC	DNC	DNC	DNC	0	0	0	0.0	A	INC	INC
Montgomery	0	0	0	0.0	A	0	0	0	0.0	A	INC	INC
New Hanover	0	0	0	0.0	A	0	0	0	0.0	A	6.5	PASS
Person	1	0	0	0.3	B	DNC	DNC	DNC	DNC	DNC	DNC	DNC
Pitt	0	0	0	0.0	A	0	0	0	0.0	A	7.3	PASS

NORTH CAROLINA (cont.)

American Lung Association in North Carolina

www.lung.org/northcarolina

	HIGH OZONE DAYS 2013–2015					HIGH PARTICLE POLLUTION DAYS 2013–2015						
						24-Hour					Annual	
County	Orange	Red	Purple	Wgt. Avg.	Grade	Orange	Red	Purple	Wgt. Avg.	Grade	Design Value	Pass/ Fail
Robeson	DNC	DNC	DNC	DNC	DNC	INC	INC	INC	INC	INC	INC	INC
Rockingham	3	0	0	1.0	C	DNC	DNC	DNC	DNC	DNC	DNC	DNC
Rowan	2	0	0	0.7	B	0	0	0	0.0	A	8.7	PASS
Swain	0	0	0	0.0	A	0	0	0	0.0	A	7.6	PASS
Union	3	0	0	1.0	C	DNC	DNC	DNC	DNC	DNC	DNC	DNC
Wake	1	0	0	0.3	B	2	0	0	0.7	B	10.7	PASS
Watauga	DNC	DNC	DNC	DNC	DNC	0	1	0	0.5	B	6.7	PASS
Wayne	DNC	DNC	DNC	DNC	DNC	0	0	0	0.0	A	INC	INC
Yancey	1	0	0	0.3	B	DNC	DNC	DNC	DNC	DNC	DNC	DNC

NORTH DAKOTA

American Lung Association in North Dakota

www.lung.org/northdakota

				AT-RISK GROUPS						
				Lung Diseases						
County	Total Population	Under 18	65 & Over	Pediatric Asthma	Adult Asthma	COPD	Lung Cancer	Cardiovascular Disease	Diabetes	Poverty
Billings	936	173	163	11	69	42	1	62	72	66
Burke	2,308	562	401	37	159	98	1	149	169	192
Burleigh	92,991	21,222	13,612	1,381	6,465	3,702	54	5,307	6,195	8,048
Cass	171,512	38,045	18,870	2,475	11,893	6,161	99	7,969	9,723	17,733
Dunn	4,646	1,076	636	70	323	184	3	264	311	452
McKenzie	12,826	3,854	942	251	802	400	7	505	638	1,061
Mercer	8,853	2,011	1,502	131	624	383	5	588	672	630
Oliver	1,846	435	356	28	129	84	1	134	150	187
Williams	35,294	9,399	3,013	612	2,311	1,163	21	1,474	1,843	2,713
Totals	**331,212**	**76,777**	**39,495**	**4,995**	**22,774**	**12,215**	**192**	**16,451**	**19,775**	**31,082**

STATE TABLES

NORTH DAKOTA

American Lung Association in North Dakota

www.lung.org/northdakota

	HIGH OZONE DAYS 2013–2015					HIGH PARTICLE POLLUTION DAYS 2013–2015						
						24-Hour					Annual	
County	Orange	Red	Purple	Wgt. Avg.	Grade	Orange	Red	Purple	Wgt. Avg.	Grade	Design Value	Pass/ Fail
Billings	0	0	0	0.0	A	3	1	0	1.5	C	4.9	PASS
Burke	0	0	0	0.0	A	5	4	0	3.7	F	5.5	PASS
Burleigh	0	0	0	0.0	A	6	1	0	2.5	D	5.3	PASS
Cass	0	0	0	0.0	A	4	0	0	1.3	C	6.4	PASS
Dunn	1	0	0	0.3	B	10	1	0	3.8	F	5.1	PASS
McKenzie	0	0	0	0.0	A	4	2	0	2.3	D	3.4	PASS
Mercer	0	0	0	0.0	A	5	2	0	2.7	D	5.5	PASS
Oliver	1	0	0	0.3	B	6	1	0	2.5	D	4.9	PASS
Williams	0	0	0	0.0	A	7	2	0	3.3	F	6.9	PASS

STATE TABLES

OHIO

American Lung Association in Ohio

www.lung.org/ohio

		AT-RISK GROUPS								
				Lung Diseases						
County	Total Population	Under 18	65 & Over	Pediatric Asthma	Adult Asthma	COPD	Lung Cancer	Cardiovascular Disease	Diabetes	Poverty
Allen	104,425	24,346	17,055	1,753	8,035	6,376	72	7,507	8,857	15,229
Ashtabula	98,632	22,120	17,501	1,592	7,671	6,382	68	7,634	9,028	17,636
Athens	65,886	9,882	7,559	711	5,658	3,636	45	3,860	4,586	17,573
Belmont	69,154	13,189	13,339	949	5,601	4,681	48	5,645	6,629	9,524
Butler	376,353	90,328	51,037	6,503	28,834	21,736	259	24,687	29,593	52,356
Clark	135,959	30,897	24,918	2,224	10,513	8,720	93	10,504	12,315	20,019
Clermont	201,973	48,113	29,391	3,464	15,505	12,247	139	14,130	16,999	19,052
Clinton	41,917	9,921	6,529	714	3,217	2,554	29	2,983	3,551	5,513
Cuyahoga	1,255,921	268,170	210,832	19,306	99,147	79,368	861	93,526	110,646	224,256
Delaware	193,013	52,718	23,146	3,795	14,185	10,754	133	12,061	14,687	8,353
Fayette	28,679	6,849	4,866	493	2,189	1,783	20	2,121	2,502	4,575
Franklin	1,251,722	295,725	138,531	21,290	96,685	67,131	861	72,955	88,119	208,972
Geauga	94,102	22,331	17,501	1,608	7,188	6,237	65	7,563	8,957	6,298
Greene	164,427	34,044	26,323	2,451	13,098	10,146	113	11,809	13,961	19,772
Hamilton	807,598	187,937	116,074	13,530	62,391	47,619	554	54,606	65,154	130,935
Jefferson	67,347	13,199	13,329	950	5,414	4,584	46	5,566	6,523	11,547
Knox	61,061	14,158	10,223	1,019	4,704	3,770	42	4,461	5,257	8,510
Lake	229,245	47,536	42,296	3,422	18,209	15,263	158	18,324	21,649	18,884
Lawrence	61,109	13,547	10,753	975	4,767	3,907	42	4,660	5,495	12,680
Licking	170,570	40,213	26,543	2,895	13,109	10,454	117	12,208	14,558	20,933
Lorain	305,147	68,903	51,233	4,960	23,715	19,284	210	22,810	27,050	39,833
Lucas	433,689	100,612	65,018	7,243	33,505	25,953	298	30,017	35,721	82,814
Madison	44,094	9,215	6,244	663	3,518	2,685	31	3,055	3,676	3,614
Mahoning	231,900	47,425	45,088	3,414	18,446	15,530	159	18,829	22,053	37,640
Medina	176,395	40,862	28,428	2,942	13,627	11,121	122	13,076	15,628	12,287
Miami	104,224	24,089	18,432	1,734	8,029	6,632	72	7,939	9,354	10,992
Montgomery	532,258	119,127	90,442	8,576	41,422	33,149	365	39,253	46,195	91,879
Noble	14,326	2,646	3,478	190	1,162	1,086	10	1,372	1,597	1,741
Portage	162,275	31,122	24,393	2,241	13,204	9,990	112	11,433	13,617	20,927
Preble	41,329	9,520	7,350	685	3,187	2,653	28	3,180	3,754	5,160
Scioto	76,825	16,922	13,094	1,218	6,006	4,801	53	5,683	6,687	16,881
Stark	375,165	81,870	67,972	5,894	29,375	24,258	258	29,084	34,211	48,889
Summit	541,968	116,666	89,731	8,399	42,718	34,297	372	40,333	47,877	76,554
Trumbull	203,751	42,580	40,561	3,065	16,103	13,752	140	16,777	19,626	35,069
Warren	224,469	57,543	30,240	4,143	16,843	13,101	155	14,960	18,078	11,375
Washington	61,112	12,223	12,007	880	4,888	4,128	42	5,010	5,868	8,906
Wood	129,730	26,801	18,693	1,929	10,356	7,572	89	8,603	10,167	14,385
Totals	**9,137,750**	**2,053,349**	**1,420,150**	**147,824**	**712,220**	**557,341**	**6,285**	**648,226**	**770,225**	**1,351,563**

STATE TABLES

OHIO

American Lung Association in Ohio

www.lung.org/ohio

	HIGH OZONE DAYS 2013–2015					HIGH PARTICLE POLLUTION DAYS 2013–2015						
						24-Hour					Annual	
County	Orange	Red	Purple	Wgt. Avg.	Grade	Orange	Red	Purple	Wgt. Avg.	Grade	Design Value	Pass/ Fail
Allen	4	0	0	1.3	C	0	0	0	0.0	A	INC	INC
Ashtabula	7	0	0	2.3	D	DNC	DNC	DNC	DNC	DNC	DNC	DNC
Athens	DNC	DNC	DNC	DNC	DNC	0	0	0	0.0	A	7.8	PASS
Belmont	DNC	DNC	DNC	DNC	DNC	INC	INC	INC	INC	INC	INC	INC
Butler	11	0	0	3.7	F	0	0	0	0.0	A	10.9	PASS
Clark	11	0	0	3.7	F	0	0	0	0.0	A	9.7	PASS
Clermont	4	0	0	1.3	C	DNC	DNC	DNC	DNC	DNC	DNC	DNC
Clinton	6	0	0	2.0	C	DNC	DNC	DNC	DNC	DNC	DNC	DNC
Cuyahoga	9	1	0	3.5	F	3	0	0	1.0	C	12.4	FAIL
Delaware	6	0	0	2.0	C	DNC	DNC	DNC	DNC	DNC	DNC	DNC
Fayette	7	0	0	2.3	D	DNC	DNC	DNC	DNC	DNC	DNC	DNC
Franklin	16	0	0	5.3	F	0	0	0	0.0	A	10.1	PASS
Geauga	9	0	0	3.0	D	DNC	DNC	DNC	DNC	DNC	DNC	DNC
Greene	6	0	0	2.0	C	0	0	0	0.0	A	9.3	PASS
Hamilton	16	1	0	5.8	F	1	0	0	0.3	B	11.2	PASS
Jefferson	3	0	0	1.0	C	4	0	0	1.3	C	10.8	PASS
Knox	6	0	0	2.0	C	DNC	DNC	DNC	DNC	DNC	DNC	DNC
Lake	16	0	0	5.3	F	0	0	0	0.0	A	8.5	PASS
Lawrence	4	0	0	1.3	C	0	0	0	0.0	A	8.0	PASS
Licking	3	0	0	1.0	C	DNC	DNC	DNC	DNC	DNC	DNC	DNC
Lorain	0	0	0	0.0	A	0	0	0	0.0	A	8.7	PASS
Lucas	5	0	0	1.7	C	1	0	0	0.3	B	10.1	PASS
Madison	4	0	0	1.3	C	DNC	DNC	DNC	DNC	DNC	DNC	DNC
Mahoning	1	0	0	0.3	B	0	0	0	0.0	A	10.6	PASS
Medina	1	0	0	0.3	B	0	0	0	0.0	A	9.3	PASS
Miami	5	0	0	1.7	C	DNC	DNC	DNC	DNC	DNC	DNC	DNC
Montgomery	5	0	0	1.7	C	1	0	0	0.3	B	INC	INC
Noble	3	0	0	1.0	C	DNC	DNC	DNC	DNC	DNC	DNC	DNC
Portage	0	0	0	0.0	A	0	0	0	0.0	A	INC	INC
Preble	2	0	0	0.7	B	0	0	0	0.0	A	9.1	PASS
Scioto	DNC	DNC	DNC	DNC	DNC	0	0	0	0.0	A	8.6	PASS
Stark	11	0	0	3.7	F	1	0	0	0.3	B	11.6	PASS
Summit	0	0	0	0.0	A	1	0	0	0.3	B	11.2	PASS
Trumbull	5	0	0	1.7	C	0	0	0	0.0	A	INC	INC
Warren	11	0	0	3.7	F	DNC	DNC	DNC	DNC	DNC	DNC	DNC
Washington	4	0	0	1.3	C	DNC	DNC	DNC	DNC	DNC	DNC	DNC
Wood	1	0	0	0.3	B	DNC	DNC	DNC	DNC	DNC	DNC	DNC

STATE TABLES

OKLAHOMA

American Lung Association in Oklahoma

www.lung.org/oklahoma

				AT-RISK GROUPS						
				Lung Diseases						
County	Total Population	Under 18	65 & Over	Pediatric Asthma	Adult Asthma	COPD	Lung Cancer	Cardiovascular Disease	Diabetes	Poverty
Adair	22,004	5,835	3,271	594	1,556	1,443	15	1,787	1,962	6,197
Bryan	44,884	10,515	7,768	1,070	3,274	3,053	31	3,842	4,138	7,924
Caddo	29,343	7,495	4,653	762	2,096	1,958	21	2,446	2,664	5,828
Canadian	133,378	35,367	16,305	3,598	9,419	8,213	94	9,750	10,969	12,844
Cherokee	48,447	11,088	7,479	1,128	3,559	3,184	34	3,896	4,265	10,023
Cleveland	274,458	60,824	33,816	6,188	20,371	17,047	193	19,823	22,387	30,190
Comanche	124,648	30,129	14,223	3,065	9,013	7,439	88	8,556	9,727	17,201
Cotton	5,996	1,418	1,115	144	441	435	4	561	602	995
Creek	70,892	17,030	12,230	1,732	5,181	4,988	50	6,332	6,850	10,927
Dewey	4,995	1,336	952	136	350	349	3	455	482	640
Jefferson	6,276	1,506	1,247	153	458	461	4	603	640	1,216
Johnston	10,980	2,552	2,029	260	807	784	8	1,004	1,076	2,276
Kay	45,366	11,477	8,310	1,168	3,238	3,140	32	4,034	4,306	8,261
Lincoln	35,042	8,681	6,031	883	2,542	2,473	25	3,151	3,409	5,097
Love	9,870	2,477	1,834	252	706	688	7	887	945	1,213
Mayes	40,887	9,954	7,040	1,013	2,976	2,867	29	3,641	3,938	7,471
McClain	38,066	9,807	5,679	998	2,723	2,530	27	3,133	3,445	4,040
Oklahoma	776,864	199,953	98,327	20,341	55,262	47,978	544	57,019	63,883	123,515
Ottawa	31,981	7,992	5,750	813	2,289	2,193	22	2,800	2,996	7,103
Pittsburg	44,610	10,011	8,213	1,018	3,313	3,195	31	4,082	4,381	7,163
Pottawatomie	71,875	17,434	11,470	1,774	5,213	4,824	50	6,002	6,541	11,672
Sequoyah	41,153	9,726	7,162	989	3,021	2,905	29	3,689	3,987	9,934
Tulsa	639,242	163,049	84,306	16,587	45,693	40,342	447	48,432	54,032	99,650
Totals	**2,551,257**	**635,656**	**349,210**	**64,665**	**183,501**	**162,489**	**1,789**	**195,925**	**217,626**	**391,380**

STATE TABLES

OKLAHOMA

American Lung Association in Oklahoma

www.lung.org/oklahoma

	HIGH OZONE DAYS 2013–2015					HIGH PARTICLE POLLUTION DAYS 2013–2015						
						24-Hour					Annual	
County	Orange	Red	Purple	Wgt. Avg.	Grade	Orange	Red	Purple	Wgt. Avg.	Grade	Design Value	Pass/ Fail
Adair	3	0	0	1.0	C	DNC	DNC	DNC	DNC	DNC	DNC	DNC
Bryan	INC	INC	INC	INC	INC	DNC	DNC	DNC	DNC	DNC	DNC	DNC
Caddo	0	0	0	0.0	A	DNC	DNC	DNC	DNC	DNC	DNC	DNC
Canadian	4	0	0	1.3	C	DNC	DNC	DNC	DNC	DNC	DNC	DNC
Cherokee	1	0	0	0.3	B	DNC	DNC	DNC	DNC	DNC	DNC	DNC
Cleveland	4	0	0	1.3	C	INC	INC	INC	INC	INC	INC	INC
Comanche	7	0	0	2.3	D	INC	INC	INC	INC	INC	INC	INC
Cotton	INC	INC	INC	INC	INC	DNC	DNC	DNC	DNC	DNC	DNC	DNC
Creek	2	0	0	0.7	B	DNC	DNC	DNC	DNC	DNC	DNC	DNC
Dewey	4	0	0	1.3	C	INC	INC	INC	INC	INC	INC	INC
Jefferson	INC	INC	INC	INC	INC	DNC	DNC	DNC	DNC	DNC	DNC	DNC
Johnston	INC	INC	INC	INC	INC	DNC	DNC	DNC	DNC	DNC	DNC	DNC
Kay	5	0	0	1.7	C	3	0	0	1.0	C	INC	INC
Lincoln	INC	INC	INC	INC	INC	DNC	DNC	DNC	DNC	DNC	DNC	DNC
Love	INC	INC	INC	INC	INC	1	1	0	0.8	B	INC	INC
Mayes	3	0	0	1.0	C	DNC	DNC	DNC	DNC	DNC	DNC	DNC
McClain	3	0	0	1.0	C	DNC	DNC	DNC	DNC	DNC	DNC	DNC
Oklahoma	15	0	0	5.0	F	0	0	0	0.0	A	8.6	PASS
Ottawa	1	0	0	0.3	B	DNC	DNC	DNC	DNC	DNC	DNC	DNC
Pittsburg	5	0	0	1.7	C	2	0	0	0.7	B	8.8	PASS
Pottawatomie	INC	INC	INC	INC	INC	DNC	DNC	DNC	DNC	DNC	DNC	DNC
Sequoyah	1	0	0	0.3	B	0	0	0	0.0	A	8.9	PASS
Tulsa	12	0	0	4.0	F	0	0	0	0.0	A	8.8	PASS

STATE TABLES

OREGON

American Lung Association in Oregon

www.lung.org/oregon

		AT-RISK GROUPS								
				Lung Diseases						
County	Total Population	Under 18	65 & Over	Pediatric Asthma	Adult Asthma	COPD	Lung Cancer	Cardiovascular Disease	Diabetes	Poverty
Clackamas	401,515	88,343	67,006	8,291	35,479	18,252	226	25,041	34,780	37,507
Columbia	49,600	10,906	8,810	1,023	4,368	2,336	28	3,237	4,469	6,595
Crook	21,630	4,183	5,347	393	1,935	1,143	12	1,719	2,217	3,423
Deschutes	175,268	36,927	33,117	3,465	15,586	8,234	99	11,673	15,765	23,298
Harney	7,200	1,476	1,642	139	638	366	4	541	708	1,147
Jackson	212,567	44,332	44,244	4,160	18,855	10,252	119	14,926	19,715	40,427
Josephine	84,745	16,554	21,343	1,554	7,553	4,474	48	6,783	8,687	18,268
Klamath	66,016	14,286	13,086	1,341	5,811	3,122	37	4,495	5,994	12,966
Lake	7,829	1,456	1,844	137	709	412	4	609	798	1,374
Lane	362,895	68,799	64,973	6,456	33,296	16,555	204	23,240	31,518	69,999
Marion	330,700	83,148	48,905	7,803	28,173	13,540	186	18,453	25,643	53,817
Multnomah	790,294	154,609	96,666	14,509	73,114	31,912	444	41,027	59,635	121,528
Umatilla	76,531	19,800	11,009	1,858	6,461	3,107	43	4,207	5,881	13,860
Washington	574,326	137,564	70,107	12,910	50,119	22,712	323	29,388	42,614	59,471
Totals	**3,161,116**	**682,383**	**488,099**	**64,038**	**282,096**	**136,418**	**1,778**	**185,339**	**258,424**	**463,680**

STATE TABLES

OREGON

American Lung Association in Oregon

www.lung.org/oregon

	HIGH OZONE DAYS 2013–2015					HIGH PARTICLE POLLUTION DAYS 2013–2015						
						24-Hour					Annual	
County	Orange	Red	Purple	Wgt. Avg.	Grade	Orange	Red	Purple	Wgt. Avg.	Grade	Design Value	Pass/ Fail
Clackamas	3	0	0	1.0	C	DNC	DNC	DNC	DNC	DNC	DNC	DNC
Columbia	0	0	0	0.0	A	DNC	DNC	DNC	DNC	DNC	DNC	DNC
Crook	DNC	DNC	DNC	DNC	DNC	8	3	0	4.2	F	9.9	PASS
Deschutes	1	0	0	0.3	B	DNC	DNC	DNC	DNC	DNC	DNC	DNC
Harney	DNC	DNC	DNC	DNC	DNC	7	1	0	2.8	D	9.1	PASS
Jackson	1	1	0	0.8	B	11	3	1	5.8	F	11.8	PASS
Josephine	DNC	DNC	DNC	DNC	DNC	2	1	0	1.2	C	9.2	PASS
Klamath	DNC	DNC	DNC	DNC	DNC	10	3	0	4.8	F	10.3	PASS
Lake	DNC	DNC	DNC	DNC	DNC	13	9	0	8.8	F	10.6	PASS
Lane	4	0	0	1.3	C	14	1	0	5.2	F	9.6	PASS
Marion	2	0	0	0.7	B	DNC	DNC	DNC	DNC	DNC	DNC	DNC
Multnomah	1	0	0	0.3	B	3	1	0	1.5	C	7.4	PASS
Umatilla	3	0	0	1.0	C	5	2	0	2.7	D	INC	INC
Washington	1	0	0	0.3	B	6	1	0	2.5	D	8.0	PASS

STATE TABLES

PENNSYLVANIA

American Lung Association in Pennsylvania

www.lung.org/pennsylvania

				AT-RISK GROUPS						
				Lung Diseases						
County	Total Population	Under 18	65 & Over	Pediatric Asthma	Adult Asthma	COPD	Lung Cancer	Cardiovascular Disease	Diabetes	Poverty
Adams	102,295	21,070	19,261	2,355	8,250	5,971	67	8,193	8,914	8,365
Allegheny	1,230,459	233,675	217,210	26,121	102,088	69,398	807	93,646	102,520	145,454
Armstrong	67,052	13,037	13,867	1,457	5,448	4,137	44	5,751	6,223	8,334
Beaver	168,871	33,153	33,941	3,706	13,729	10,208	111	14,116	15,302	21,668
Berks	415,271	94,450	67,198	10,558	32,891	22,274	273	29,968	32,895	50,814
Blair	125,593	25,939	24,852	2,900	10,102	7,381	82	10,174	11,031	18,616
Bradford	61,281	13,427	12,190	1,501	4,832	3,639	40	5,048	5,465	7,881
Bucks	627,367	132,377	107,816	14,798	50,440	35,909	412	48,892	53,504	39,001
Cambria	136,411	26,377	28,534	2,949	11,114	8,324	90	11,550	12,488	19,450
Centre	160,580	24,411	20,365	2,729	14,328	7,762	107	9,715	10,961	22,716
Chester	515,939	120,162	77,227	13,432	40,664	27,246	339	36,441	40,187	30,147
Clearfield	80,994	14,976	15,660	1,674	6,708	4,835	54	6,630	7,213	12,487
Cumberland	246,338	50,023	42,941	5,592	20,103	13,677	162	18,463	20,208	17,149
Dauphin	272,983	61,299	42,684	6,852	21,743	14,543	179	19,477	21,436	36,332
Delaware	563,894	125,524	86,401	14,032	45,114	29,719	369	39,628	43,687	56,493
Elk	30,872	6,030	6,463	674	2,499	1,936	20	2,702	2,921	2,821
Erie	278,045	60,598	44,847	6,774	22,329	14,928	183	20,015	21,996	45,339
Franklin	153,638	34,945	28,517	3,906	12,067	8,644	101	11,848	12,880	14,258
Greene	37,519	7,221	6,584	807	3,100	2,129	25	2,878	3,151	5,200
Indiana	86,966	15,860	15,277	1,773	7,302	4,848	57	6,505	7,130	14,789
Lackawanna	211,917	42,598	40,519	4,762	17,222	12,291	139	16,831	18,302	31,144
Lancaster	536,624	128,793	89,727	14,397	41,751	28,456	353	38,439	42,053	55,725
Lawrence	88,082	17,798	17,902	1,990	7,102	5,314	58	7,365	7,973	15,015
Lebanon	137,067	31,439	25,574	3,514	10,736	7,699	90	10,559	11,473	15,464
Lehigh	360,685	82,249	58,165	9,194	28,575	19,173	237	25,744	28,267	42,456
Luzerne	318,449	62,459	61,036	6,982	26,033	18,616	209	25,496	27,732	46,457
Lycoming	116,048	23,833	20,789	2,664	9,415	6,552	76	8,898	9,717	16,377
Mercer	114,234	22,901	23,137	2,560	9,243	6,836	75	9,451	10,236	15,242
Monroe	166,397	34,257	25,870	3,829	13,551	9,240	109	12,406	13,675	20,559
Montgomery	819,264	178,455	137,266	19,949	65,556	45,144	538	61,016	66,866	52,939
Northampton	300,813	61,413	53,683	6,865	24,435	17,070	198	23,194	25,338	25,559
Perry	45,685	9,948	7,509	1,112	3,651	2,553	30	3,457	3,792	4,322
Philadelphia	1,567,442	346,932	198,475	38,782	127,499	74,034	1,024	94,862	106,183	385,781
Somerset	75,522	13,718	15,829	1,533	6,244	4,675	50	6,482	7,015	10,165
Tioga	41,877	8,324	8,398	930	3,401	2,486	28	3,428	3,716	5,233
Washington	208,261	41,143	40,169	4,599	16,954	12,373	137	17,016	18,497	20,501
Westmoreland	357,956	67,000	75,735	7,490	29,318	22,397	235	31,186	33,713	39,587
York	442,867	99,147	71,845	11,083	35,199	24,097	291	32,488	35,662	45,255
Totals	**11,271,558**	**2,386,961**	**1,883,463**	**266,826**	**910,734**	**616,511**	**7,400**	**829,957**	**910,319**	**1,425,095**

STATE TABLES

PENNSYLVANIA

American Lung Association in Pennsylvania

www.lung.org/pennsylvania

	HIGH OZONE DAYS 2013–2015					HIGH PARTICLE POLLUTION DAYS 2013–2015						
						24-Hour					Annual	
County	Orange	Red	Purple	Wgt. Avg.	Grade	Orange	Red	Purple	Wgt. Avg.	Grade	Design Value	Pass/ Fail
Adams	3	0	0	1.0	C	3	0	0	1.0	C	9.6	PASS
Allegheny	20	1	0	7.2	F	15	2	0	6.0	F	12.6	FAIL
Armstrong	11	1	0	4.2	F	0	0	0	0.0	A	11.1	PASS
Beaver	14	1	0	5.2	F	1	0	0	0.3	B	10.8	PASS
Berks	8	0	0	2.7	D	17	0	0	5.7	F	10.2	PASS
Blair	4	0	0	1.3	C	3	0	0	1.0	C	11.4	PASS
Bradford	0	0	0	0.0	A	DNC	DNC	DNC	DNC	DNC	DNC	DNC
Bucks	24	2	0	9.0	F	13	0	0	4.3	F	10.2	PASS
Cambria	3	0	0	1.0	C	2	0	0	0.7	B	11.7	PASS
Centre	2	0	0	0.7	B	2	0	0	0.7	B	8.6	PASS
Chester	6	1	0	2.5	D	2	0	0	0.7	B	10.0	PASS
Clearfield	0	0	0	0.0	A	DNC	DNC	DNC	DNC	DNC	DNC	DNC
Cumberland	DNC	DNC	DNC	DNC	DNC	12	0	0	4.0	F	10.1	PASS
Dauphin	6	0	0	2.0	C	15	0	0	5.0	F	11.0	PASS
Delaware	15	0	0	5.0	F	3	0	0	1.0	C	11.6	PASS
Elk	3	0	0	1.0	C	DNC	DNC	DNC	DNC	DNC	DNC	DNC
Erie	3	0	0	1.0	C	0	0	0	0.0	A	10.8	PASS
Franklin	3	0	0	1.0	C	DNC	DNC	DNC	DNC	DNC	DNC	DNC
Greene	8	0	0	2.7	D	DNC	DNC	DNC	DNC	DNC	DNC	DNC
Indiana	10	1	0	3.8	F	DNC	DNC	DNC	DNC	DNC	DNC	DNC
Lackawanna	4	0	0	1.3	C	0	0	0	0.0	A	INC	INC
Lancaster	5	0	0	1.7	C	26	1	0	9.2	F	11.2	PASS
Lawrence	6	0	0	2.0	C	DNC	DNC	DNC	DNC	DNC	DNC	DNC
Lebanon	15	0	0	5.0	F	16	0	0	5.3	F	INC	INC
Lehigh	6	0	0	2.0	C	DNC	DNC	DNC	DNC	DNC	DNC	DNC
Luzerne	2	0	0	0.7	B	DNC	DNC	DNC	DNC	DNC	DNC	DNC
Lycoming	0	0	0	0.0	A	DNC	DNC	DNC	DNC	DNC	DNC	DNC
Mercer	9	0	0	3.0	D	0	1	0	0.5	B	9.7	PASS
Monroe	2	0	0	0.7	B	0	0	0	0.0	A	8.7	PASS
Montgomery	14	0	0	4.7	F	4	0	0	1.3	C	9.0	PASS
Northampton	4	0	0	1.3	C	11	0	0	3.7	F	10.0	PASS
Perry	INC	INC	INC	INC	INC	DNC	DNC	DNC	DNC	DNC	DNC	DNC
Philadelphia	21	3	0	8.5	F	9	0	0	3.0	D	11.8	PASS
Somerset	1	0	0	0.3	B	DNC	DNC	DNC	DNC	DNC	DNC	DNC
Tioga	1	0	0	0.3	B	INC	INC	INC	INC	INC	INC	INC
Washington	11	0	0	3.7	F	1	0	0	0.3	B	11.7	PASS
Westmoreland	7	0	0	2.3	D	0	0	0	0.0	A	9.8	PASS
York	9	0	0	3.0	D	6	0	0	2.0	C	10.1	PASS

STATE TABLES

RHODE ISLAND

American Lung Association in Rhode Island

www.lung.org/rhodeisland

				AT-RISK GROUPS						
				Lung Diseases						
County	Total Population	Under 18	65 & Over	Pediatric Asthma	Adult Asthma	COPD	Lung Cancer	Cardiovascular Disease	Diabetes	Poverty
Kent	164,801	31,665	29,398	3,101	14,638	8,784	117	10,569	12,804	14,250
Providence	633,473	132,542	91,356	12,982	55,645	29,827	449	35,158	42,350	104,385
Washington	126,517	22,283	23,507	2,183	11,447	6,849	90	8,290	9,985	11,912
Totals	**924,791**	**186,490**	**144,261**	**18,266**	**81,730**	**45,460**	**655**	**54,017**	**65,138**	**130,547**

STATE TABLES

RHODE ISLAND

American Lung Association in Rhode Island

www.lung.org/rhodeisland

HIGH OZONE DAYS 2013–2015

County	Orange	Red	Purple	Wgt. Avg.	Grade
Kent	8	1	0	3.2	D
Providence	10	1	0	3.8	F
Washington	16	1	0	5.8	F

HIGH PARTICLE POLLUTION DAYS 2013–2015

	24-Hour					Annual	
	Orange	Red	Purple	Wgt. Avg.	Grade	Design Value	Pass/ Fail
Kent	0	0	0	0.0	A	4.9	PASS
Providence	1	1	0	0.8	B	8.1	PASS
Washington	0	0	0	0.0	A	5.1	PASS

STATE TABLES

SOUTH CAROLINA

American Lung Association in South Carolina

www.lung.org/southcarolina

				AT-RISK GROUPS						
				Lung Diseases						
County	Total Population	Under 18	65 & Over	Pediatric Asthma	Adult Asthma	COPD	Lung Cancer	Cardiovascular Disease	Diabetes	Poverty
Abbeville	24,932	5,332	4,973	452	1,621	1,530	16	2,100	2,554	4,617
Aiken	165,829	36,383	29,985	3,085	10,685	9,783	109	13,223	16,185	29,497
Anderson	194,692	45,054	33,829	3,820	12,344	11,213	128	15,093	18,504	32,807
Berkeley	202,786	49,143	25,819	4,167	12,568	10,415	134	13,345	16,679	25,852
Charleston	389,262	78,207	57,844	6,631	25,386	21,392	255	27,842	34,524	56,459
Cherokee	56,194	13,378	8,734	1,134	3,526	3,110	37	4,114	5,081	11,195
Chesterfield	46,017	10,586	7,528	898	2,937	2,656	30	3,540	4,366	10,653
Colleton	37,731	8,550	7,241	725	2,418	2,277	25	3,114	3,796	8,601
Darlington	67,548	15,405	11,535	1,306	4,310	3,911	44	5,246	6,446	14,194
Edgefield	26,514	5,036	4,394	427	1,777	1,585	18	2,099	2,595	4,459
Florence	138,900	33,464	21,513	2,837	8,670	7,614	90	10,074	12,433	27,558
Greenville	491,863	115,082	71,724	9,758	30,913	26,554	323	34,724	43,049	66,299
Lexington	281,833	66,209	41,223	5,614	17,775	15,468	185	20,257	25,138	36,805
Oconee	75,713	15,209	16,645	1,290	5,009	4,846	50	6,745	8,156	13,493
Pickens	121,691	23,855	18,905	2,023	7,956	6,702	80	8,773	10,836	20,751
Richland	407,051	88,453	47,511	7,500	25,787	20,235	267	25,368	31,886	59,495
Spartanburg	297,302	69,835	45,633	5,921	18,703	16,355	195	21,578	26,665	43,326
York	251,195	61,836	33,653	5,243	15,602	13,338	165	17,268	21,538	30,789
Totals	**3,277,053**	**741,017**	**488,689**	**62,830**	**207,986**	**178,985**	**2,150**	**234,503**	**290,433**	**496,850**

STATE TABLES

SOUTH CAROLINA

American Lung Association in South Carolina

www.lung.org/southcarolina

	HIGH OZONE DAYS 2013–2015					HIGH PARTICLE POLLUTION DAYS 2013–2015						
						24-Hour					Annual	
County	Orange	Red	Purple	Wgt. Avg.	Grade	Orange	Red	Purple	Wgt. Avg.	Grade	Design Value	Pass/ Fail
Abbeville	0	0	0	0.0	A	DNC	DNC	DNC	DNC	DNC	DNC	DNC
Aiken	0	0	0	0.0	A	DNC	DNC	DNC	DNC	DNC	DNC	DNC
Anderson	0	0	0	0.0	A	DNC	DNC	DNC	DNC	DNC	DNC	DNC
Berkeley	0	0	0	0.0	A	DNC	DNC	DNC	DNC	DNC	DNC	DNC
Charleston	0	0	0	0.0	A	1	0	0	0.3	B	7.9	PASS
Cherokee	2	0	0	0.7	B	DNC	DNC	DNC	DNC	DNC	DNC	DNC
Chesterfield	0	0	0	0.0	A	0	0	0	0.0	A	7.9	PASS
Colleton	0	0	0	0.0	A	DNC	DNC	DNC	DNC	DNC	DNC	DNC
Darlington	0	0	0	0.0	A	DNC	DNC	DNC	DNC	DNC	DNC	DNC
Edgefield	1	0	0	0.3	B	0	0	0	0.0	A	8.4	PASS
Florence	DNC	DNC	DNC	DNC	DNC	0	0	0	0.0	A	8.7	PASS
Greenville	1	0	0	0.3	B	2	0	0	0.7	B	9.2	PASS
Lexington	DNC	DNC	DNC	DNC	DNC	0	0	0	0.0	A	9.3	PASS
Oconee	0	0	0	0.0	A	INC	INC	INC	INC	INC	INC	INC
Pickens	0	0	0	0.0	A	DNC	DNC	DNC	DNC	DNC	DNC	DNC
Richland	0	0	0	0.0	A	0	0	0	0.0	A	9.0	PASS
Spartanburg	1	0	0	0.3	B	0	0	0	0.0	A	8.8	PASS
York	0	0	0	0.0	A	DNC	DNC	DNC	DNC	DNC	DNC	DNC

STATE TABLES

SOUTH DAKOTA

American Lung Association in South Dakota

www.lung.org/southdakota

		AT-RISK GROUPS								
				Lung Diseases						
County	Total Population	Under 18	65 & Over	Pediatric Asthma	Adult Asthma	COPD	Lung Cancer	Cardiovascular Disease	Diabetes	Poverty
Brookings	33,897	6,856	3,643	581	2,312	1,215	21	1,707	1,964	4,419
Brown	38,785	9,206	6,242	781	2,477	1,671	24	2,579	2,772	3,846
Codington	27,939	6,862	4,415	582	1,761	1,199	17	1,850	1,994	2,976
Custer	8,446	1,380	2,234	117	581	497	5	826	837	873
Hughes	17,555	4,206	2,734	357	1,113	759	11	1,168	1,265	1,821
Jackson	3,321	1,116	452	95	185	123	2	188	203	1,067
Meade	26,986	6,396	3,833	542	1,729	1,105	17	1,667	1,829	2,598
Minnehaha	185,197	46,279	23,258	3,924	11,663	7,218	113	10,689	11,947	21,865
Pennington	108,702	25,681	17,633	2,177	6,946	4,719	67	7,295	7,836	12,946
Union	14,909	3,644	2,394	309	936	657	9	1,017	1,097	942
Totals	**465,737**	**111,626**	**66,838**	**9,465**	**29,703**	**19,163**	**285**	**28,987**	**31,745**	**53,353**

STATE TABLES

SOUTH DAKOTA

American Lung Association in South Dakota

www.lung.org/southdakota

	HIGH OZONE DAYS 2013–2015					HIGH PARTICLE POLLUTION DAYS 2013–2015						
						24-Hour					Annual	
County	Orange	Red	Purple	Wgt. Avg.	Grade	Orange	Red	Purple	Wgt. Avg.	Grade	Design Value	Pass/ Fail
Brookings	0	0	0	0.0	A	2	0	0	0.7	B	INC	INC
Brown	DNC	DNC	DNC	DNC	DNC	0	0	0	0.0	A	6.6	PASS
Codington	DNC	DNC	DNC	DNC	DNC	1	0	0	0.3	B	7.1	PASS
Custer	0	0	0	0.0	A	2	0	0	0.7	B	3.2	PASS
Hughes	DNC	DNC	DNC	DNC	DNC	INC	INC	INC	INC	INC	INC	INC
Jackson	0	0	0	0.0	A	2	0	0	0.7	B	4.7	PASS
Meade	0	0	0	0.0	A	DNC	DNC	DNC	DNC	DNC	DNC	DNC
Minnehaha	0	0	0	0.0	A	3	0	0	1.0	C	8.3	PASS
Pennington	DNC	DNC	DNC	DNC	DNC	2	0	0	0.7	B	7.8	PASS
Union	0	0	0	0.0	A	3	0	0	1.0	C	8.5	PASS

STATE TABLES

TENNESSEE

American Lung Association in Tennessee

www.lung.org/tennessee

				AT-RISK GROUPS						
				Lung Diseases						
County	Total Population	Under 18	65 & Over	Pediatric Asthma	Adult Asthma	COPD	Lung Cancer	Cardiovascular Disease	Diabetes	Poverty
Anderson	75,749	15,904	14,578	1,549	5,382	6,163	57	7,382	8,189	14,721
Blount	127,253	26,593	24,050	2,590	9,052	10,324	97	12,324	13,704	16,388
Claiborne	31,709	6,219	6,001	606	2,285	2,576	24	3,069	3,415	6,575
Davidson	678,889	145,277	76,326	14,149	46,887	45,604	514	50,248	58,858	111,678
DeKalb	19,182	4,223	3,473	411	1,343	1,518	15	1,803	2,011	3,814
Dyer	37,893	9,170	6,385	893	2,572	2,856	29	3,371	3,776	8,374
Hamilton	354,098	74,599	57,953	7,265	24,920	26,989	268	31,502	35,529	52,287
Jefferson	53,240	10,896	10,271	1,061	3,801	4,330	40	5,184	5,750	8,627
Knox	451,324	96,191	66,821	9,368	31,513	33,063	343	38,002	43,287	68,679
Lawrence	42,564	10,676	7,487	1,040	2,858	3,222	32	3,837	4,270	7,931
Loudon	51,130	10,141	12,833	988	3,693	4,513	39	5,653	6,075	6,804
Madison	97,610	22,374	15,115	2,179	6,713	7,242	74	8,408	9,521	16,874
Maury	87,757	20,627	13,377	2,009	6,004	6,508	67	7,544	8,558	11,432
McMinn	52,639	11,338	10,008	1,104	3,714	4,249	40	5,085	5,644	11,864
Meigs	11,830	2,461	2,407	240	846	988	9	1,194	1,317	2,351
Montgomery	193,479	52,142	16,996	5,078	12,300	11,310	148	12,142	14,451	25,378
Putnam	74,553	15,787	12,232	1,538	5,194	5,498	57	6,430	7,225	14,166
Roane	52,753	10,283	11,475	1,001	3,845	4,582	40	5,579	6,125	9,180
Sevier	95,946	20,280	17,553	1,975	6,800	7,694	73	9,139	10,197	13,806
Shelby	938,069	237,852	113,176	23,165	62,228	63,837	709	71,647	83,069	186,186
Sullivan	156,791	30,977	32,448	3,017	11,325	13,169	119	15,927	17,548	25,241
Sumner	175,989	42,434	26,488	4,133	11,963	13,003	134	15,057	17,099	17,557
Williamson	211,672	59,107	25,560	5,757	13,764	14,807	161	16,702	19,368	10,548
Wilson	128,911	30,931	19,198	3,012	8,798	9,604	98	11,097	12,629	10,676
Totals	**4,201,030**	**966,482**	**602,211**	**94,128**	**287,800**	**303,651**	**3,187**	**348,325**	**397,614**	**661,137**

STATE TABLES

TENNESSEE

American Lung Association in Tennessee

www.lung.org/tennessee

	HIGH OZONE DAYS 2013–2015					HIGH PARTICLE POLLUTION DAYS 2013–2015						
						24-Hour					Annual	
County	Orange	Red	Purple	Wgt. Avg.	Grade	Orange	Red	Purple	Wgt. Avg.	Grade	Design Value	Pass/ Fail
Anderson	0	0	0	0.0	A	DNC	DNC	DNC	DNC	DNC	DNC	DNC
Blount	2	0	0	0.7	B	INC	INC	INC	INC	INC	INC	INC
Claiborne	0	0	0	0.0	A	DNC	DNC	DNC	DNC	DNC	DNC	DNC
Davidson	4	0	0	1.3	C	INC	INC	INC	INC	INC	INC	INC
DeKalb	0	0	0	0.0	A	DNC	DNC	DNC	DNC	DNC	DNC	DNC
Dyer	DNC	DNC	DNC	DNC	DNC	INC	INC	INC	INC	INC	INC	INC
Hamilton	5	0	0	1.7	C	0	0	0	0.0	A	9.0	PASS
Jefferson	3	0	0	1.0	C	DNC	DNC	DNC	DNC	DNC	DNC	DNC
Knox	1	0	0	0.3	B	INC	INC	INC	INC	INC	INC	INC
Lawrence	DNC	DNC	DNC	DNC	DNC	INC	INC	INC	INC	INC	INC	INC
Loudon	2	0	0	0.7	B	INC	INC	INC	INC	INC	INC	INC
Madison	DNC	DNC	DNC	DNC	DNC	INC	INC	INC	INC	INC	INC	INC
Maury	DNC	DNC	DNC	DNC	DNC	INC	INC	INC	INC	INC	INC	INC
McMinn	INC	INC	INC	INC	INC	0	0	0	0.0	A	8.6	PASS
Meigs	INC	INC	INC	INC	INC	DNC	DNC	DNC	DNC	DNC	DNC	DNC
Montgomery	DNC	DNC	DNC	DNC	DNC	INC	INC	INC	INC	INC	INC	INC
Putnam	DNC	DNC	DNC	DNC	DNC	INC	INC	INC	INC	INC	INC	INC
Roane	DNC	DNC	DNC	DNC	DNC	INC	INC	INC	INC	INC	INC	INC
Sevier	0	0	0	0.0	A	DNC	DNC	DNC	DNC	DNC	DNC	DNC
Shelby	8	0	0	2.7	D	INC	INC	INC	INC	INC	INC	INC
Sullivan	0	0	0	0.0	A	INC	INC	INC	INC	INC	INC	INC
Sumner	2	0	0	0.7	B	INC	INC	INC	INC	INC	INC	INC
Williamson	1	0	0	0.3	B	DNC	DNC	DNC	DNC	DNC	DNC	DNC
Wilson	0	0	0	0.0	A	DNC	DNC	DNC	DNC	DNC	DNC	DNC

STATE TABLES

TEXAS

American Lung Association in Texas

www.lung.org/texas

		AT-RISK GROUPS								
				Lung Diseases						
County	Total Population	Under 18	65 & Over	Pediatric Asthma	Adult Asthma	COPD	Lung Cancer	Cardiovascular Disease	Diabetes	Poverty
Bell	334,941	93,147	33,942	7,371	18,436	11,419	181	17,333	24,804	51,728
Bexar	1,897,753	494,269	218,139	39,112	106,843	70,076	1,023	108,644	154,343	288,976
Bowie	93,389	22,169	14,727	1,754	5,411	3,976	51	6,461	8,867	16,170
Brazoria	346,312	92,721	38,491	7,337	19,276	12,985	188	20,194	29,003	35,519
Brewster	9,145	1,752	1,878	139	561	448	5	752	1,004	1,349
Cameron	422,156	132,069	54,064	10,451	22,076	15,253	227	24,295	33,605	133,508
Collin	914,127	246,271	92,102	19,488	50,752	33,687	493	51,814	75,532	59,993
Dallas	2,553,385	682,485	252,270	54,006	142,402	90,900	1,377	138,406	200,959	451,795
Denton	780,612	201,646	70,965	15,957	44,046	27,885	421	42,057	62,008	61,186
El Paso	835,593	233,304	97,233	18,462	45,852	30,316	450	47,241	66,708	165,987
Ellis	163,632	44,077	19,927	3,488	9,080	6,354	88	10,033	14,265	17,580
Galveston	322,225	79,179	42,148	6,266	18,452	13,130	174	20,870	29,546	44,355
Gregg	124,108	32,020	17,698	2,534	6,999	4,996	67	8,024	11,115	20,438
Harris	4,538,028	1,224,413	428,697	96,889	252,264	158,961	2,452	240,522	350,940	744,712
Harrison	66,746	16,910	10,327	1,338	3,783	2,825	36	4,602	6,340	12,036
Hidalgo	842,304	281,203	90,076	22,252	42,759	27,637	453	42,854	60,247	259,506
Hood	55,423	11,607	13,395	918	3,319	2,893	30	5,004	6,519	5,364
Hunt	89,844	21,419	13,951	1,695	5,194	3,868	48	6,290	8,692	14,418
Jefferson	254,308	60,384	34,403	4,778	14,740	10,306	138	16,368	22,964	40,306
Johnson	159,990	41,857	21,591	3,312	8,971	6,439	87	10,300	14,450	17,955
Kaufman	114,690	31,704	13,801	2,509	6,304	4,385	62	6,917	9,825	14,824
McLennan	245,671	60,939	33,372	4,822	14,060	9,608	132	15,226	21,150	46,949
Montgomery	537,559	143,545	66,131	11,359	29,920	21,043	290	33,281	47,307	53,837
Navarro	48,323	12,673	7,978	1,003	2,706	2,070	26	3,411	4,643	9,312
Nueces	359,715	90,534	47,578	7,164	20,468	14,191	194	22,497	31,521	70,336
Orange	84,260	20,854	12,913	1,650	4,813	3,582	45	5,824	8,049	13,443
Parker	126,042	30,860	19,085	2,442	7,217	5,459	68	8,882	12,369	11,680
Polk	46,972	9,604	9,187	760	2,833	2,277	26	3,813	5,142	7,304
Randall	130,269	31,609	17,919	2,501	7,503	5,223	70	8,308	11,583	10,887
Rockwall	90,861	24,947	11,026	1,974	5,004	3,533	49	5,590	7,958	5,403
Smith	222,936	55,137	35,076	4,363	12,754	9,316	120	15,144	20,694	34,786
Tarrant	1,982,498	533,475	208,355	42,215	110,194	72,657	1,068	111,992	161,771	255,993
Travis	1,176,558	267,942	102,528	21,203	69,258	41,330	638	61,060	90,267	152,195
Victoria	92,382	23,834	13,673	1,886	5,210	3,756	50	6,064	8,350	12,329
Webb	269,721	91,421	23,938	7,234	13,588	8,425	145	12,741	18,399	81,276
Totals	**20,332,478**	**5,441,980**	**2,188,584**	**430,631**	**1,133,050**	**741,209**	**10,973**	**1,142,813**	**1,640,941**	**3,223,435**

STATE TABLES

TEXAS

American Lung Association in Texas

www.lung.org/texas

	HIGH OZONE DAYS 2013–2015					HIGH PARTICLE POLLUTION DAYS 2013–2015						
						24-Hour					Annual	
County	Orange	Red	Purple	Wgt. Avg.	Grade	Orange	Red	Purple	Wgt. Avg.	Grade	Design Value	Pass/ Fail
Bell	11	0	0	3.7	F	DNC	DNC	DNC	DNC	DNC	DNC	DNC
Bexar	31	5	0	12.8	F	0	0	0	0.0	A	8.5	PASS
Bowie	DNC	DNC	DNC	DNC	DNC	0	0	0	0.0	A	9.8	PASS
Brazoria	19	8	0	10.3	F	DNC	DNC	DNC	DNC	DNC	DNC	DNC
Brewster	0	0	0	0.0	A	DNC	DNC	DNC	DNC	DNC	DNC	DNC
Cameron	0	0	0	0.0	A	INC	INC	INC	INC	INC	INC	INC
Collin	28	0	0	9.3	F	DNC	DNC	DNC	DNC	DNC	DNC	DNC
Dallas	32	1	0	11.2	F	1	0	0	0.3	B	10.2	PASS
Denton	59	7	0	23.2	F	DNC	DNC	DNC	DNC	DNC	DNC	DNC
El Paso	18	0	0	6.0	F	8	2	0	3.7	F	9.9	PASS
Ellis	11	0	0	3.7	F	0	0	0	0.0	A	9.3	PASS
Galveston	20	3	0	8.2	F	0	0	0	0.0	A	INC	INC
Gregg	8	0	0	2.7	D	DNC	DNC	DNC	DNC	DNC	DNC	DNC
Harris	47	14	1	23.3	F	3	0	0	1.0	C	11.6	PASS
Harrison	4	0	0	1.3	C	0	0	0	0.0	A	9.0	PASS
Hidalgo	0	0	0	0.0	A	0	0	0	0.0	A	INC	INC
Hood	13	4	0	6.3	F	DNC	DNC	DNC	DNC	DNC	DNC	DNC
Hunt	3	0	0	1.0	C	DNC	DNC	DNC	DNC	DNC	DNC	DNC
Jefferson	18	1	0	6.5	F	DNC	DNC	DNC	DNC	DNC	DNC	DNC
Johnson	20	1	0	7.2	F	DNC	DNC	DNC	DNC	DNC	DNC	DNC
Kaufman	5	0	0	1.7	C	DNC	DNC	DNC	DNC	DNC	DNC	DNC
McLennan	8	0	0	2.7	D	DNC	DNC	DNC	DNC	DNC	DNC	DNC
Montgomery	15	0	0	5.0	F	DNC	DNC	DNC	DNC	DNC	DNC	DNC
Navarro	6	0	0	2.0	C	DNC	DNC	DNC	DNC	DNC	DNC	DNC
Nueces	3	0	0	1.0	C	0	0	0	0.0	A	10.1	PASS
Orange	4	0	0	1.3	C	DNC	DNC	DNC	DNC	DNC	DNC	DNC
Parker	34	0	0	11.3	F	DNC	DNC	DNC	DNC	DNC	DNC	DNC
Polk	3	0	0	1.0	C	DNC	DNC	DNC	DNC	DNC	DNC	DNC
Randall	2	0	0	0.7	B	DNC	DNC	DNC	DNC	DNC	DNC	DNC
Rockwall	17	0	0	5.7	F	DNC	DNC	DNC	DNC	DNC	DNC	DNC
Smith	5	0	0	1.7	C	DNC	DNC	DNC	DNC	DNC	DNC	DNC
Tarrant	59	7	0	23.2	F	1	0	0	0.3	B	10.0	PASS
Travis	14	0	0	4.7	F	0	0	0	0.0	A	9.2	PASS
Victoria	1	0	0	0.3	B	DNC	DNC	DNC	DNC	DNC	DNC	DNC
Webb	1	0	0	0.3	B	DNC	DNC	DNC	DNC	DNC	DNC	DNC

STATE TABLES

UTAH

American Lung Association in Utah

www.lung.org/utah

				AT-RISK GROUPS						
				Lung Diseases						
County	Total Population	Under 18	65 & Over	Pediatric Asthma	Adult Asthma	COPD	Lung Cancer	Cardiovascular Disease	Diabetes	Poverty
Box Elder	52,097	16,873	6,463	1,198	3,204	1,406	14	2,220	2,804	4,345
Cache	120,783	37,123	10,685	2,636	7,531	2,768	32	4,057	5,140	18,657
Carbon	20,479	5,456	3,241	387	1,370	637	5	1,040	1,297	3,247
Daggett	1,109	254	235	18	78	40	0	69	84	84
Davis	336,043	111,031	31,398	7,885	20,377	8,120	89	12,138	15,590	23,138
Duchesne	20,862	7,230	2,283	513	1,236	517	6	802	1,014	2,247
Garfield	5,009	1,233	1,025	88	346	178	1	304	374	543
Salt Lake	1,107,314	311,386	109,258	22,113	72,084	28,671	293	42,720	54,993	117,311
San Juan	15,772	5,071	1,853	360	974	425	4	662	844	4,397
Tooele	62,952	21,418	5,557	1,521	3,763	1,497	17	2,220	2,871	4,493
Uintah	37,928	12,923	3,410	918	2,262	889	10	1,322	1,697	3,733
Utah	575,205	198,953	42,066	14,129	33,832	12,002	152	17,123	21,908	70,537
Washington	155,602	43,096	31,425	3,061	10,259	5,108	41	8,826	10,649	20,252
Weber	243,645	70,325	27,606	4,994	15,725	6,546	64	10,045	12,791	29,768
Totals	**2,754,800**	**842,372**	**276,505**	**59,822**	**173,040**	**68,805**	**729**	**103,548**	**132,056**	**302,752**

STATE TABLES

UTAH

American Lung Association in Utah

www.lung.org/utah

	HIGH OZONE DAYS 2013–2015					HIGH PARTICLE POLLUTION DAYS 2013–2015						
						24-Hour					Annual	
County	Orange	Red	Purple	Wgt. Avg.	Grade	Orange	Red	Purple	Wgt. Avg.	Grade	Design Value	Pass/ Fail
Box Elder	8	0	0	2.7	D	7	1	0	2.8	D	7.5	PASS
Cache	3	0	0	1.0	C	38	15	0	20.2	F	9.1	PASS
Carbon	4	0	0	1.3	C	DNC	DNC	DNC	DNC	DNC	DNC	DNC
Daggett	INC	INC	INC	INC	INC	DNC	DNC	DNC	DNC	DNC	DNC	DNC
Davis	14	0	0	4.7	F	16	0	0	5.3	F	7.8	PASS
Duchesne	21	22	5	21.3	F	INC	INC	INC	INC	INC	INC	INC
Garfield	4	0	0	1.3	C	DNC	DNC	DNC	DNC	DNC	DNC	DNC
Salt Lake	38	0	0	12.7	F	47	12	0	21.7	F	9.0	PASS
San Juan	1	0	0	0.3	B	DNC	DNC	DNC	DNC	DNC	DNC	DNC
Tooele	9	0	0	3.0	D	INC	INC	INC	INC	INC	INC	INC
Uintah	30	24	18	34.0	F	INC	INC	INC	INC	INC	INC	INC
Utah	27	0	0	9.0	F	24	15	0	15.5	F	9.0	PASS
Washington	6	0	0	2.0	C	0	0	0	0.0	A	INC	INC
Weber	18	1	0	6.5	F	24	6	0	11.0	F	INC	INC

STATE TABLES

VERMONT

American Lung Association in Vermont

www.lung.org/vermont

		AT-RISK GROUPS								
				Lung Diseases						
County	Total Population	Under 18	65 & Over	Pediatric Asthma	Adult Asthma	COPD	Lung Cancer	Cardiovascular Disease	Diabetes	Poverty
Bennington	36,317	6,999	7,896	725	3,205	1,980	22	2,673	2,666	4,102
Chittenden	161,382	29,797	22,049	3,086	14,815	7,330	96	8,926	9,526	15,695
Rutland	59,736	10,817	12,005	1,120	5,377	3,204	36	4,247	4,301	6,560
Totals	**257,435**	**47,613**	**41,950**	**4,930**	**23,397**	**12,514**	**153**	**15,846**	**16,493**	**26,357**

STATE TABLES

VERMONT

American Lung Association in Vermont

www.lung.org/vermont

	HIGH OZONE DAYS 2013–2015					HIGH PARTICLE POLLUTION DAYS 2013–2015						
						24-Hour					Annual	
County	Orange	Red	Purple	Wgt. Avg.	Grade	Orange	Red	Purple	Wgt. Avg.	Grade	Design Value	Pass/ Fail
Bennington	1	0	0	0.3	B	0	0	0	0.0	A	6.2	PASS
Chittenden	0	0	0	0.0	A	0	0	0	0.0	A	6.3	PASS
Rutland	DNC	DNC	DNC	DNC	DNC	6	0	0	2.0	C	8.7	PASS

STATE TABLES

VIRGINIA

American Lung Association in Virginia

www.lung.org/virginia

		AT-RISK GROUPS								
				Lung Diseases						
County	Total Population	Under 18	65 & Over	Pediatric Asthma	Adult Asthma	COPD	Lung Cancer	Cardiovascular Disease	Diabetes	Poverty
Albemarle	105,703	21,846	18,063	1,852	6,674	5,025	63	6,684	9,069	9,462
Alexandria City	153,511	27,554	15,874	2,336	10,006	6,410	91	7,896	10,885	13,832
Arlington	229,164	40,006	21,698	3,392	15,031	9,204	137	11,139	15,335	16,031
Bristol City	17,141	3,408	3,413	289	1,094	868	10	1,179	1,593	3,260
Caroline	29,984	7,130	4,670	605	1,817	1,373	18	1,818	2,480	3,531
Charles City	7,040	1,100	1,557	93	473	402	4	554	754	814
Chesterfield	335,687	81,561	44,925	6,915	20,191	14,765	199	19,183	26,357	22,942
Fairfax	1,142,234	271,539	136,327	23,023	69,150	48,796	680	62,353	85,991	69,985
Fauquier	68,782	16,340	10,588	1,385	4,167	3,231	41	4,286	5,880	4,646
Frederick	83,199	19,427	13,087	1,647	5,070	3,865	50	5,124	7,000	6,342
Giles	16,708	3,416	3,426	290	1,058	865	10	1,185	1,603	1,751
Hampton City	136,454	29,445	19,217	2,497	8,509	6,064	81	7,858	10,733	20,072
Hanover	103,227	23,125	16,704	1,961	6,367	4,957	61	6,601	9,037	6,268
Henrico	325,155	75,430	46,015	6,396	19,852	14,479	192	18,876	25,832	30,037
Loudoun	375,629	109,247	31,044	9,263	21,135	13,961	224	17,211	23,976	13,953
Lynchburg City	79,812	15,534	11,277	1,317	5,119	3,390	47	4,330	5,846	15,975
Madison	13,134	2,726	2,759	231	829	690	8	950	1,286	1,351
Norfolk City	246,393	49,439	25,062	4,192	15,658	9,727	148	11,908	16,313	45,756
Page	23,726	4,791	4,822	406	1,507	1,232	14	1,684	2,282	3,532
Prince Edward	22,952	3,702	3,609	314	1,533	1,054	14	1,364	1,843	4,172
Prince William	451,721	125,637	39,298	10,653	25,879	17,061	269	21,074	29,283	29,925
Richmond City	220,289	40,012	25,506	3,393	14,329	9,365	130	11,694	16,040	50,763
Roanoke	94,409	19,582	19,014	1,660	5,958	4,834	56	6,603	8,935	6,744
Roanoke City	99,897	22,184	15,144	1,881	6,180	4,558	59	5,985	8,166	20,913
Rockbridge	22,354	3,881	5,538	329	1,472	1,274	13	1,784	2,400	2,834
Rockingham	78,593	17,492	14,401	1,483	4,863	3,831	47	5,173	7,016	8,422
Salem City	25,432	4,918	4,476	417	1,633	1,240	15	1,653	2,244	2,391
Stafford	142,003	37,700	13,452	3,197	8,277	5,610	85	7,005	9,733	7,448
Suffolk City	88,161	21,858	11,713	1,853	5,268	3,833	52	4,976	6,831	11,370
Virginia Beach City	452,745	102,144	57,630	8,661	27,869	19,333	269	24,736	33,881	36,451
Wythe	29,119	5,837	5,864	495	1,853	1,507	17	2,056	2,786	4,163
Totals	**5,220,358**	**1,208,011**	**646,173**	**102,425**	**318,821**	**222,804**	**3,102**	**284,920**	**391,408**	**475,136**

STATE TABLES

VIRGINIA

American Lung Association in Virginia

www.lung.org/virginia

	HIGH OZONE DAYS 2013–2015					HIGH PARTICLE POLLUTION DAYS 2013–2015						
						24-Hour					Annual	
County	Orange	Red	Purple	Wgt. Avg.	Grade	Orange	Red	Purple	Wgt. Avg.	Grade	Design Value	Pass/ Fail
Albemarle	0	0	0	0.0	A	0	0	0	0.0	A	7.4	PASS
Alexandria City	INC	INC	INC	INC	INC	DNC	DNC	DNC	DNC	DNC	DNC	DNC
Arlington	11	1	0	4.2	F	0	0	0	0.0	A	8.9	PASS
Bristol City	DNC	DNC	DNC	DNC	DNC	0	0	0	0.0	A	8.2	PASS
Caroline	0	0	0	0.0	A	DNC	DNC	DNC	DNC	DNC	DNC	DNC
Charles City	4	0	0	1.3	C	0	0	0	0.0	A	7.7	PASS
Chesterfield	0	0	0	0.0	A	0	0	0	0.0	A	INC	INC
Fairfax	6	0	0	2.0	C	0	0	0	0.0	A	8.2	PASS
Fauquier	0	0	0	0.0	A	DNC	DNC	DNC	DNC	DNC	DNC	DNC
Frederick	0	0	0	0.0	A	1	0	0	0.3	B	9.0	PASS
Giles	0	0	0	0.0	A	DNC	DNC	DNC	DNC	DNC	DNC	DNC
Hampton City	2	0	0	0.7	B	0	0	0	0.0	A	7.3	PASS
Hanover	1	0	0	0.3	B	DNC	DNC	DNC	DNC	DNC	DNC	DNC
Henrico	3	0	0	1.0	C	0	0	0	0.0	A	8.0	PASS
Loudoun	7	0	0	2.3	D	0	0	0	0.0	A	8.7	PASS
Lynchburg City	DNC	DNC	DNC	DNC	DNC	0	0	0	0.0	A	7.4	PASS
Madison	0	0	0	0.0	A	DNC	DNC	DNC	DNC	DNC	DNC	DNC
Norfolk City	DNC	DNC	DNC	DNC	DNC	0	0	0	0.0	A	7.7	PASS
Page	0	0	0	0.0	A	0	0	0	0.0	A	INC	INC
Prince Edward	1	0	0	0.3	B	DNC	DNC	DNC	DNC	DNC	DNC	DNC
Prince William	1	0	0	0.3	B	DNC	DNC	DNC	DNC	DNC	DNC	DNC
Richmond City	DNC	DNC	DNC	DNC	DNC	INC	INC	INC	INC	INC	INC	INC
Roanoke	0	0	0	0.0	A	1	0	0	0.3	B	INC	INC
Roanoke City	DNC	DNC	DNC	DNC	DNC	INC	INC	INC	INC	INC	INC	INC
Rockbridge	0	0	0	0.0	A	DNC	DNC	DNC	DNC	DNC	DNC	DNC
Rockingham	0	0	0	0.0	A	0	0	0	0.0	A	8.5	PASS
Salem City	DNC	DNC	DNC	DNC	DNC	0	0	0	0.0	A	8.5	PASS
Stafford	2	0	0	0.7	B	DNC	DNC	DNC	DNC	DNC	DNC	DNC
Suffolk City	1	0	0	0.3	B	DNC	DNC	DNC	DNC	DNC	DNC	DNC
Virginia Beach City	DNC	DNC	DNC	DNC	DNC	0	0	0	0.0	A	7.9	PASS
Wythe	0	0	0	0.0	A	DNC	DNC	DNC	DNC	DNC	DNC	DNC

STATE TABLES

WASHINGTON

American Lung Association in Washington

www.lung.org/washington

				AT-RISK GROUPS						
				Lung Diseases						
County	Total Population	Under 18	65 & Over	Pediatric Asthma	Adult Asthma	COPD	Lung Cancer	Cardiovascular Disease	Diabetes	Poverty
Benton	190,309	50,899	26,210	3,325	13,172	8,583	106	10,631	11,734	26,824
Chelan	75,644	18,190	13,547	1,188	5,459	3,797	42	4,953	5,333	9,458
Clallam	73,486	12,880	20,298	841	5,803	4,522	41	6,419	6,630	11,195
Clark	459,495	114,536	65,323	7,481	32,661	21,440	255	26,573	29,368	48,401
King	2,117,125	438,574	263,386	28,646	157,724	97,651	1,176	116,316	130,619	205,336
Kitsap	260,131	53,941	42,954	3,523	19,521	13,074	145	16,577	18,085	24,950
Kittitas	43,269	7,689	6,540	502	3,314	2,060	24	2,556	2,781	8,190
Pierce	843,954	201,220	110,163	13,143	60,558	38,426	469	46,643	51,946	102,917
Skagit	121,846	27,143	23,517	1,773	9,000	6,344	68	8,382	8,962	17,965
Snohomish	772,501	177,236	96,213	11,577	56,362	35,894	429	42,913	48,418	71,017
Spokane	490,945	109,896	74,486	7,178	35,959	23,541	273	29,445	32,284	74,144
Thurston	269,536	58,760	42,752	3,838	19,931	13,225	150	16,672	18,229	32,458
Whatcom	212,284	42,086	33,919	2,749	15,982	10,360	118	13,054	14,194	29,802
Yakima	248,830	74,063	32,662	4,838	16,416	10,504	138	13,029	14,296	46,794
Totals	**6,179,355**	**1,387,113**	**851,970**	**90,602**	**451,863**	**289,421**	**3,432**	**354,163**	**392,878**	**709,451**

STATE TABLES

WASHINGTON

American Lung Association in Washington

www.lung.org/washington

	HIGH OZONE DAYS 2013–2015					HIGH PARTICLE POLLUTION DAYS 2013–2015						
						24-Hour					Annual	
County	Orange	Red	Purple	Wgt. Avg.	Grade	Orange	Red	Purple	Wgt. Avg.	Grade	Design Value	Pass/ Fail
Benton	INC	INC	INC	INC	INC	DNC	DNC	DNC	DNC	DNC	DNC	DNC
Chelan	DNC	DNC	DNC	DNC	DNC	2	2	0	1.7	C	INC	INC
Clallam	0	0	0	0.0	A	DNC	DNC	DNC	DNC	DNC	DNC	DNC
Clark	1	0	0	0.3	B	4	2	0	2.3	D	INC	INC
King	8	0	0	2.7	D	7	0	0	2.3	D	6.7	PASS
Kitsap	DNC	DNC	DNC	DNC	DNC	0	0	0	0.0	A	INC	INC
Kittitas	DNC	DNC	DNC	DNC	DNC	INC	INC	INC	INC	INC	INC	INC
Pierce	0	0	0	0.0	A	13	1	0	4.8	F	7.5	PASS
Skagit	0	0	0	0.0	A	0	0	0	0.0	A	INC	INC
Snohomish	DNC	DNC	DNC	DNC	DNC	15	2	0	6.0	F	8.1	PASS
Spokane	1	0	0	0.3	B	5	0	0	1.7	C	INC	INC
Thurston	0	0	0	0.0	A	INC	INC	INC	INC	INC	INC	INC
Whatcom	0	0	0	0.0	A	0	0	0	0.0	A	7.0	PASS
Yakima	DNC	DNC	DNC	DNC	DNC	17	1	0	6.2	F	9.1	PASS

STATE TABLES

WEST VIRGINIA

American Lung Association in West Virginia

www.lung.org/westvirginia

				AT-RISK GROUPS						
				Lung Diseases						
County	Total Population	Under 18	65 & Over	Pediatric Asthma	Adult Asthma	COPD	Lung Cancer	Cardiovascular Disease	Diabetes	Poverty
Berkeley	111,901	26,911	15,243	2,534	9,221	10,805	91	10,968	11,588	13,823
Brooke	23,350	4,124	5,158	388	2,096	2,682	19	2,901	2,960	3,338
Cabell	96,844	19,614	16,756	1,847	8,326	9,800	78	10,149	10,561	18,776
Gilmer	8,518	1,193	1,310	112	786	877	7	877	929	1,650
Greenbrier	35,516	6,979	7,789	657	3,114	4,013	29	4,354	4,437	6,629
Hancock	29,815	5,781	6,177	544	2,628	3,371	24	3,629	3,718	4,032
Harrison	68,714	14,900	12,499	1,403	5,855	7,237	56	7,643	7,901	10,861
Kanawha	188,332	38,490	35,175	3,624	16,307	20,209	152	21,378	22,079	30,529
Marion	56,925	11,532	10,481	1,086	4,917	5,964	46	6,266	6,482	8,899
Marshall	31,978	6,368	6,457	600	2,796	3,555	26	3,813	3,913	3,965
Monongalia	104,236	16,820	11,513	1,584	9,288	9,493	85	8,956	9,755	19,051
Ohio	43,066	8,330	8,520	784	3,775	4,692	35	4,991	5,135	5,711
Raleigh	77,510	16,482	14,532	1,552	6,623	8,139	63	8,606	8,878	14,676
Tucker	6,966	1,219	1,620	115	628	821	6	897	911	1,165
Wood	86,452	18,498	16,258	1,742	7,401	9,235	70	9,804	10,108	14,793
Totals	**970,123**	**197,241**	**169,488**	**18,570**	**83,761**	**100,893**	**785**	**105,231**	**109,355**	**157,898**

STATE TABLES

WEST VIRGINIA

American Lung Association in West Virginia

www.lung.org/westvirginia

	HIGH OZONE DAYS 2013–2015					HIGH PARTICLE POLLUTION DAYS 2013–2015						
						24-Hour					Annual	
County	Orange	Red	Purple	Wgt. Avg.	Grade	Orange	Red	Purple	Wgt. Avg.	Grade	Design Value	Pass/ Fail
Berkeley	0	0	0	0.0	A	1	0	0	0.3	B	10.3	PASS
Brooke	DNC	DNC	DNC	DNC	DNC	0	0	0	0.0	A	11.2	PASS
Cabell	2	0	0	0.7	B	0	0	0	0.0	A	9.2	PASS
Gilmer	0	0	0	0.0	A	DNC	DNC	DNC	DNC	DNC	DNC	DNC
Greenbrier	0	0	0	0.0	A	DNC	DNC	DNC	DNC	DNC	DNC	DNC
Hancock	6	0	0	2.0	C	0	0	0	0.0	A	INC	INC
Harrison	DNC	DNC	DNC	DNC	DNC	0	0	0	0.0	A	8.8	PASS
Kanawha	3	0	0	1.0	C	0	0	0	0.0	A	9.6	PASS
Marion	DNC	DNC	DNC	DNC	DNC	0	0	0	0.0	A	9.4	PASS
Marshall	DNC	DNC	DNC	DNC	DNC	0	0	0	0.0	A	10.7	PASS
Monongalia	3	0	0	1.0	C	0	0	0	0.0	A	8.6	PASS
Ohio	4	0	0	1.3	C	1	0	0	0.3	B	10.3	PASS
Raleigh	DNC	DNC	DNC	DNC	DNC	0	0	0	0.0	A	INC	INC
Tucker	1	0	0	0.3	B	DNC	DNC	DNC	DNC	DNC	DNC	DNC
Wood	6	0	0	2.0	C	0	0	0	0.0	A	9.4	PASS

STATE TABLES

WISCONSIN

American Lung Association in Wisconsin

www.lung.org/wisconsin

				AT-RISK GROUPS						
				Lung Diseases						
County	Total Population	Under 18	65 & Over	Pediatric Asthma	Adult Asthma	COPD	Lung Cancer	Cardiovascular Disease	Diabetes	Poverty
Ashland	15,843	3,542	2,833	260	1,157	621	10	996	1,100	2,616
Brown	258,718	62,681	34,930	4,606	18,884	8,819	155	13,713	15,620	27,979
Columbia	56,743	12,579	9,524	924	4,170	2,190	34	3,470	3,876	4,908
Dane	523,643	109,975	64,580	8,081	40,551	16,979	314	26,290	30,144	57,411
Dodge	88,502	18,187	14,761	1,336	6,664	3,427	53	5,421	6,066	7,157
Door	27,554	4,529	7,601	333	2,084	1,370	16	2,313	2,427	2,317
Eau Claire	102,105	20,961	14,721	1,540	7,907	3,459	61	5,497	6,148	13,260
Fond du Lac	101,973	22,331	17,318	1,641	7,537	3,913	61	6,233	6,928	9,248
Forest	9,057	1,823	2,016	134	670	394	5	651	698	1,284
Grant	52,250	10,640	8,626	782	4,010	1,884	31	3,043	3,347	6,622
Jefferson	84,559	18,608	13,050	1,367	6,291	3,118	51	4,903	5,520	7,534
Kenosha	168,437	40,321	21,512	2,963	12,345	5,738	101	8,805	10,154	20,812
Kewaunee	20,366	4,483	3,922	329	1,482	833	12	1,346	1,474	1,652
La Crosse	118,212	23,826	17,986	1,751	9,144	4,151	71	6,615	7,372	16,248
Manitowoc	79,806	16,743	15,197	1,230	5,887	3,292	48	5,289	5,825	8,466
Marathon	135,868	31,458	22,337	2,312	9,891	5,104	81	8,108	9,037	12,675
Milwaukee	957,735	233,159	118,711	17,132	70,675	30,571	572	47,491	54,244	189,827
Outagamie	183,245	43,882	24,843	3,224	13,390	6,343	110	9,829	11,229	16,225
Ozaukee	87,850	19,169	15,833	1,409	6,435	3,525	53	5,625	6,236	4,488
Racine	195,080	46,202	29,573	3,395	14,155	7,136	117	11,184	12,626	23,505
Rock	161,448	38,325	24,969	2,816	11,732	5,853	97	9,248	10,366	21,946
Sauk	63,642	14,520	11,094	1,067	4,639	2,441	38	3,914	4,323	7,340
Sheboygan	115,569	26,084	19,254	1,917	8,460	4,412	69	7,000	7,810	10,167
Taylor	20,455	4,832	3,821	355	1,456	822	12	1,323	1,454	2,491
Vilas	21,387	3,623	6,283	266	1,590	1,100	13	1,872	1,949	2,829
Walworth	102,804	22,330	16,304	1,641	7,679	3,802	62	6,018	6,736	12,374
Waukesha	396,488	87,705	67,598	6,444	29,037	15,576	237	24,644	27,546	18,401
Totals	**4,149,339**	**942,518**	**609,197**	**69,255**	**307,919**	**146,872**	**2,484**	**230,839**	**260,254**	**509,782**

STATE TABLES

WISCONSIN

American Lung Association in Wisconsin

www.lung.org/wisconsin

	HIGH OZONE DAYS 2013–2015					HIGH PARTICLE POLLUTION DAYS 2013–2015						
						24-Hour					Annual	
County	Orange	Red	Purple	Wgt. Avg.	Grade	Orange	Red	Purple	Wgt. Avg.	Grade	Design Value	Pass/ Fail
Ashland	0	0	0	0.0	A	0	0	0	0.0	A	5.1	PASS
Brown	3	0	0	1.0	C	1	0	0	0.3	B	8.2	PASS
Columbia	3	0	0	1.0	C	DNC	DNC	DNC	DNC	DNC	DNC	DNC
Dane	1	0	0	0.3	B	1	0	0	0.3	B	9.0	PASS
Dodge	7	0	0	2.3	D	0	0	0	0.0	A	8.0	PASS
Door	9	0	0	3.0	D	DNC	DNC	DNC	DNC	DNC	DNC	DNC
Eau Claire	0	0	0	0.0	A	0	0	0	0.0	A	7.5	PASS
Fond du Lac	2	0	0	0.7	B	DNC	DNC	DNC	DNC	DNC	DNC	DNC
Forest	0	0	0	0.0	A	0	0	0	0.0	A	INC	INC
Grant	DNC	DNC	DNC	DNC	DNC	0	0	0	0.0	A	8.3	PASS
Jefferson	7	0	0	2.3	D	DNC	DNC	DNC	DNC	DNC	DNC	DNC
Kenosha	24	0	0	8.0	F	0	1	0	0.5	B	8.5	PASS
Kewaunee	5	0	0	1.7	C	DNC	DNC	DNC	DNC	DNC	DNC	DNC
La Crosse	0	0	0	0.0	A	0	0	0	0.0	A	8.0	PASS
Manitowoc	12	0	0	4.0	F	DNC	DNC	DNC	DNC	DNC	DNC	DNC
Marathon	1	0	0	0.3	B	DNC	DNC	DNC	DNC	DNC	DNC	DNC
Milwaukee	10	0	0	3.3	F	0	0	0	0.0	A	9.7	PASS
Outagamie	3	0	0	1.0	C	1	0	0	0.3	B	8.0	PASS
Ozaukee	15	0	0	5.0	F	0	0	0	0.0	A	7.6	PASS
Racine	INC	INC	INC	INC	INC	DNC	DNC	DNC	DNC	DNC	DNC	DNC
Rock	6	0	0	2.0	C	DNC	DNC	DNC	DNC	DNC	DNC	DNC
Sauk	3	0	0	1.0	C	0	0	0	0.0	A	7.2	PASS
Sheboygan	25	1	0	8.8	F	DNC	DNC	DNC	DNC	DNC	DNC	DNC
Taylor	0	0	0	0.0	A	0	0	0	0.0	A	6.5	PASS
Vilas	1	0	0	0.3	B	0	0	0	0.0	A	5.0	PASS
Walworth	6	0	0	2.0	C	DNC	DNC	DNC	DNC	DNC	DNC	DNC
Waukesha	3	0	0	1.0	C	0	0	0	0.0	A	9.8	PASS

WYOMING

American Lung Association in Wyoming

www.lung.org/wyoming

		AT-RISK GROUPS								
				Lung Diseases						
County	Total Population	Under 18	65 & Over	Pediatric Asthma	Adult Asthma	COPD	Lung Cancer	Cardiovascular Disease	Diabetes	Poverty
Albany	37,956	6,264	3,881	538	2,526	1,852	15	1,790	1,902	7,181
Big Horn	12,022	3,083	2,363	265	715	740	5	837	876	1,437
Campbell	49,220	13,816	3,674	1,187	2,812	2,173	19	2,132	2,473	3,668
Carbon	15,559	3,677	2,241	316	947	865	6	927	1,010	1,682
Converse	14,236	3,652	2,020	314	844	781	6	840	920	1,205
Fremont	40,315	10,278	6,773	883	2,399	2,335	16	2,573	2,747	5,071
Goshen	13,383	2,695	2,823	232	856	878	5	990	1,031	1,852
Laramie	97,121	22,812	14,266	1,960	5,929	5,384	38	5,765	6,216	10,084
Natrona	82,178	19,800	10,804	1,701	4,972	4,371	32	4,607	5,031	8,827
Park	29,228	5,898	6,063	507	1,867	1,924	11	2,170	2,282	2,739
Sheridan	30,009	6,456	5,731	555	1,883	1,893	12	2,113	2,242	2,777
Sublette	9,899	2,383	1,348	205	599	547	4	584	647	605
Sweetwater	44,626	11,984	4,474	1,030	2,597	2,140	18	2,180	2,451	3,744
Teton	23,125	4,349	3,001	374	1,496	1,280	9	1,331	1,464	1,516
Uinta	20,822	6,141	2,432	528	1,169	1,029	8	1,082	1,201	2,030
Weston	7,234	1,570	1,331	135	453	451	3	501	536	675
Totals	**526,933**	**124,858**	**73,225**	**10,727**	**32,063**	**28,641**	**208**	**30,421**	**33,029**	**55,093**

STATE TABLES

WYOMING

American Lung Association in Wyoming

www.lung.org/wyoming

	HIGH OZONE DAYS 2013–2015					HIGH PARTICLE POLLUTION DAYS 2013–2015						
						24-Hour					Annual	
County	Orange	Red	Purple	Wgt. Avg.	Grade	Orange	Red	Purple	Wgt. Avg.	Grade	Design Value	Pass/ Fail
Albany	2	0	0	0.7	B	0	0	0	0.0	A	4.3	PASS
Big Horn	0	0	0	0.0	A	INC	INC	INC	INC	INC	INC	INC
Campbell	0	0	0	0.0	A	1	0	0	0.3	B	4.2	PASS
Carbon	1	0	0	0.3	B	0	0	0	0.0	A	INC	INC
Converse	2	0	0	0.7	B	3	0	0	1.0	C	INC	INC
Fremont	0	0	0	0.0	A	1	0	0	0.3	B	6.9	PASS
Goshen	INC	INC	INC	INC	INC	INC	INC	INC	INC	INC	INC	INC
Laramie	3	0	0	1.0	C	0	1	0	0.5	B	4.1	PASS
Natrona	2	0	0	0.7	B	0	0	0	0.0	A	4.6	PASS
Park	DNC	DNC	DNC	DNC	DNC	0	0	0	0.0	A	4.1	PASS
Sheridan	DNC	DNC	DNC	DNC	DNC	2	0	0	0.7	B	6.9	PASS
Sublette	1	0	0	0.3	B	0	0	0	0.0	A	5.0	PASS
Sweetwater	4	0	0	1.3	C	0	0	0	0.0	A	4.8	PASS
Teton	0	0	0	0.0	A	0	0	0	0.0	A	4.7	PASS
Uinta	2	0	0	0.7	B	DNC	DNC	DNC	DNC	DNC	DNC	DNC
Weston	0	0	0	0.0	A	INC	INC	INC	INC	INC	INC	INC

AMERICAN LUNG ASSOCIATION. STATE OF THE AIR 2017

We will breathe easier when the air in every American community is clean and healthy.

We will breathe easier when people are free from the addictive grip of tobacco and the debilitating effects of lung disease.

We will breathe easier when the air in our public spaces and workplaces is clear of secondhand smoke.

We will breathe easier when children no longer battle airborne poisons or fear an asthma attack.

Until then, we are fighting for air.

About the American Lung Association

The American Lung Association is the leading organization working to save lives by improving lung health and preventing lung disease, through research, education and advocacy. The work of the American Lung Association is focused on four strategic imperatives: to defeat lung cancer; to improve the air we breathe; to reduce the burden of lung disease on individuals and their families; and to eliminate tobacco use and tobacco-related diseases. For more information about the American Lung Association, a holder of the Better Business Bureau Wise Giving Guide Seal, or to support the work it does, call 1-800-LUNGUSA (1-800-586-4872) or visit: www.Lung.org.

AMERICAN LUNG ASSOCIATION.

THESIS FOR THE DEGREE OF LICENTIATE OF ENGINEERING

Application of solar FTIR spectroscopy for quantifying gas emissions

Manne Kihlman

Department of Radio and Space Science
Chalmers University of Technology
Göteborg, Sweden 2005

Application of solar FTIR spectroscopy for quantifying gas emissions
MANNE KIHLMAN

MANNE KIHLMAN, 2005.
ISSN 1652-9103

Technical report No. 4L
Department of Radio and Space Science

Chalmers University of Technology
SE-412 96 Göteborg, Sweden
Telephone +46 (0) 31-772 1000

Cover:
The cover picture shows a 3D representation of a measurement done with the Solar Occultation Flux method to determine the total emission from a refinery. The red vertical lines correspond to solar lines. The colors in between the solar lines (blue to red) correspond to the integrated concentration of alkane (blue is low concentration while green and red are higher). The wind vectors are shown as green horizontal lines pointing into the measurement-surface. *(Aerial photo: Copyright Lantmäteriet 2004-11-09. Ur Din Karta och SverigeBilden)*

Printed by Chalmers reproservice
Göteborg, Sweden 2005

Application of solar FTIR spectroscopy for quantifying gas emissions
MANNE KIHLMAN
Department of Radio and Space Science
Chalmers University of Technology

Abstract

In environmental science there is an interest in quantifying gas emission rates to the lower atmosphere from anthropogenic and biogenic sources since there are many gases that constitute a potential short or long-term threat for human health.

Optical remote sensing methods give the possibility to get real time measurements

of gases in the lower atmosphere where the instrument need not be located at the place where the gas is located. These methods also have the possibility to measure the concentration integrated along a line or a surface. This may be of more relevance for risk assessment than a measurement in one point. IR, visible or UV light is detected with a spectrometer and the molecules cause a fingerprint on the measured spectra by absorption of light on the molecules.

The Solar Occultation Flux (SOF) method is a relatively new method to measure gas emission rates. The method is based on recording broadband infrared spectra of the sun with a FTIR spectrometer that is connected to a solar-tracker. The latter is a mirror device that tracks the sun and reflects the light into the spectrometer independent of its position. From the solar spectra it is possible to retrieve the line-integrated concentration (molecules/cm_2) between the sun and the spectrometer. To obtain the gas emission from a source, the instrument is placed in a car and is driven in such way that the detected solar light cuts through the emission plume. To calculate the gas emission, the wind direction and speed is also required.

In the years 2002 to 2005, a project (KORUS) was run in cooperation with four industries to explore the possibilities to measure gas emissions of volatile organic compounds (VOC) with the SOF method. The four industries were three refineries, Preemraff-Göteborg, Preemraff-Lysekil and Shellraff-Göteborg, and the Oil harbour of Göteborg. All industries are located on the west coast of Sweden. The project aimed at lifting the usability of the method to commercially competitive performance, by increasing reliability and automatization. Simultaneously with the work to improve the method, an extensive measurement-program was run to put the method into a full-scale test to demonstrate its capacity for routine measurements.

This thesis gives an overview of the SOF method. It describes the technical challenges that have been solved to make the method more operative. General conclusions from the measurements are presented. A special report not appended in this thesis has been published that contain detailed results of all measurements. A detailed error analysis of the method is presented.

Keywords: Remote sensing, VOC, refinery, emission, solar occultation, FTIR

List of publications

Appended papers

Paper A

Kihlman M., Mellqvist J., Samuelsson J., Tang L., Chen D., **Monitoring of VOC emissions from refineries in Sweden using the SOF method**. *Manuscript in preparation for Environmental Science & Technology.*

Paper B

Mellqvist J., Kihlman M., Galle B., Fransson K., Samuelsson J., **The Solar Occultation Flux method, a nouvelle technique for quantifying fugitive gas emissions.** *Manuscript in preparation for Environmental Science & Technology.*

Related paper

Kihlman M., Mellqvist J., Samuelsson J., **Monitoring of VOC emissions from three refineries in Sweden and the Oil harbour of Göteborg using the Solar Occultation Flux method**, *Technical Report,* Optical Remote Sensing Group, Department of Radio and Space Science, Chalmers University of Technology, 2005.

Acknowledgments

I thank:

my supervisors Dr. Johan Mellqvist and Bo Galle,

Jerker Samuelsson,

Lin Tang and Deliang Chen at Gothenburg University for providing the TAPM data,

Karin Fransson for having performed the SF_6 measurements presented in chapter 6,

Anders Strandberg, Andreas Nilsson, Elisabeth Undén, Gunner Hanehöj, Karin Fransson Samuel Brohede, Åke Fält that have participated in the field measurements,

the personnel involved at the different industries,

Klas Folkesson for showing how an Acknowledgment chapter can be written,

all the people at the Department of Radio and Space Science,

my family and friends.

Table of contents

1 Introduction

This chapter argues that gas measurements are needed to assess the impact of biogenic and anthropogenic gas emissions. It then focuses on the formation of ozone in the lower troposphere where anthropogenic emission of VOC plays an important role. This motivates why VOC emissions from industries should be controlled.

1.1 General introduction

Emission of gases to the lower atmosphere from anthropogenic and biogenic activities constitute a potential hazard for human health and the environment. Some gases constitute a direct threat for human health, for example H_2S, that may lead to direct death in high concentration. Other gases constitute a long-term threat for example carcinogenic benzene. There are also long-term threats to the environment. One example is the global warming that is possibly an effect of emissions of green-house gases, for example carbon-dioxide and methane. Another example is the annual ozone losses at the south pole discovered in the mid eighties by Farman et al. [1], that is driven by human emissions of chlorofluorocarbons (CFC). Furthermore, acid rain, which causes forest decline, is the result of emissions of sulfur dioxide occurring both from anthropogenic sources by burning fossil fuels, and from biogenic sources by emissions from volcanoes.

Gas measurements are essential when determining what actions should be taken to lower the anthropogenic emissions of hazardous gases and to verify that the actions had the desired effect. Measurements on biogenic sources are of importance to warn the population if concentrations reach dangerous levels. Geophysical activity may also change the composition of gases as is the case with volcanic gases before an eruption. Gas detections can thus be used to alarm the population and in that way prevent a catastrophe.

The emission of volatile organic compounds (VOC) to air is a potential hazard for human health and the environment. The formation of ozone in the lower troposphere takes place through a photochemical reaction driven by VOC and nitrogen oxides. The formed ozone is a powerful oxidant that causes inflammation of the respiratory tract and exacerbates existing lung disease [2]. There are also indications that ozone in the lower troposphere may contribute to forest decline [3]. Furthermore, VOC can react with ozone and form secondary organic aerosols [4] that are also a threat to human health. Furthermore, some of the anthropogenic emissions of VOC are in the form of carcinogenic benzene. It is therefore of importance that the anthropogenic emissions of VOC should be minimized. This thesis is focused on measurements of VOC and a closer study of how the ozone is formed will therefore be presented.

1.2 The process of ozone formation

In the lower troposphere, ozone is formed in the presence of VOC and NO_x and sunlight. However, the chemistry behind the ozone formation is complex. Ozone is

actually formed by the photolysis of nitrogen dioxide (NO_2). Instead of actually playing a role in the formation of ozone, the presence of VOC affect the efficiency with which NO_x forms ozone. The reaction scheme will here be presented as is given

1

in the report by SMHI [5]. A steady state between the following four reactions determines the concentration of O_3:

$$NO_2 + h\nu \rightarrow NO + O \quad (1.$$
$$NO + O_3 \rightarrow NO_2 + O_2 \quad (1.$$
$$O_3 + h\nu \rightarrow O_2 + O \quad (1.$$
$$O_2 + O \rightarrow O_3 \quad (1.$$

A steady state is typically settled between these reactions within a few minutes during daytime. The stable concentration of O_3 is then dependent of the sun radiation and temperature. If NO_2 is added to the air by emissions, there is no net production of O_3 since as much O_3 is consumed by reaction 1.2 as is produced by reaction 1.1 followed by 1.4. However, if new reactions are added that also consumes NO without consuming O_3, this balance is not stable anymore and the presence of NO_x will then produce additional O_3. One such reaction that consumes NO is the reaction with peroxy-radicals:

$$RO_2 + NO \rightarrow NO_2 + RO \quad (1.$$

where R can be either a hydrogen atom or a hydrocarbon. Peroxy-radicals are produced from the atmospheric decomposition of hydrocarbons. An example is the reaction between ethane (C_2H_6) and OH:

$$HC_2 \quad _6 + OH \rightarrow HC_2 \quad _5 + OH_2 \quad (1.$$
$$HC_2 \quad _5 + O_2 \rightarrow OHC_2 \quad _5 \quad _2 \quad (1.$$

If NO is present it will then be converted to NO_2 by the following reaction system:

$$OHC_2 \quad _5 \quad _2 + NO \rightarrow OHC_2 \quad _5 \quad + NO_2 \quad (1.$$
$$OCOHC_2 \quad + \quad _2 \rightarrow CH_3CHO + HO_2 \quad (1.$$
$$HO_2 + NO \rightarrow OH + NO_2 \quad (1.$$

The scheme will thus not consume any OH-radicals if it goes all the way from reaction 1.6 to reaction 1.10. The presence of an ethane molecule will thus convert two NO molecules to NO_2 without consuming any O_3 and will thus disturb the

balance that was settled by reactions 1.1 to 1.4. The potential of a specific hydrocarbon to increase the O_3 concentration is to first order dependent on its reaction rate with OH. A study based on this approach was presented by Darnall 1976 [6]. A more complete study based on the reaction scheme called the Master Chemical Mechanism (MCM) was presented in a paper by Derwent et al. [7]. The ozone creation potential presented there describes the increase in ozone concentration compared to the increase in ozone caused by ethylene if an additional term of 4.7 kg/km^2 of the hydrocarbon is employed in the MCM. This thesis will concentrate on alkanes which is the dominant hydrocarbon emitted from refineries. The ozone creation potential for some alkanes is presented in Table 1 together with some other hydrocarbons for comparison. Since the ozone creation potential of methane is low it is most often excluded in environmental VOC measurements and is then called

NMVOC (Non-Methane-VOC). Isoprene is emitted by biogenic emissions, for example tropical forests, and can cause high O_3 increase due to its high ozone creation potential if it resides together with high NO_x concentrations.

Table 1. Ozone creation potentials derived by Derwent et al. [7].

Organic compound	Ozone creation potential
Methane	0.6
Ethane	12.3
Propane	17.6
n-Butane	35.2
n-Pentane	39.5
n-Hexane	48.2
n-Heptane	49.4
n-Octane	45.3
n-Nonane	41.4
n-Decane	38.4
Isoprene	109.2
Benzene	21.8
Toluene	63.7
o-Xylene	105.3
m-Xylene	110.8
p-Xylene	101.0
Acetylene	8.5
Ethylene	100.0 (reference)

Since the ozone is produced in a photochemical reaction, the concentration is highest in the summer. The concentration limits recommended by WHO (from year 2000) are

relatively often exceeded during sunny summer days in Sweden according to a study by SMHI [5]. Because of the complexity of the O_3 production, the relationship between VOC and NO_x emissions and O_3 concentration is not linear. A computer simulation by SMHI [5] based on emission estimates from 1999, showed that if the NO_x emissions were reduced with 45% in western Sweden, it would actually increase O_3 in areas with high NO_x emissions, for example in the neighborhood of Gothenburg but would reduce O_3 concentrations outside Gothenburg. Reducing VOC emissions would decrease the O_3 emissions on all places, but the reduction in O_3 outside Gothenburg were 7 times smaller than the reduction in O_3 caused by reducing the NO_x emissions. The isopleth diagram shown in Figure 1 is commonly used to show the complex relationship between O_3 concentration and the concentrations of VOC and NO_x. In regions with high VOC concentrations, the O_3 production will be NO_x limited and not sensitive to variations in VOC concentration. In high NO_x concentrations, it will be VOC limited. At a VOC concentration of around 0.3 ppmC, the isopleth diagram shows that the O_3 concentration will decrease if the NO_x concentration were increased. This is what was observed for the neighborhood of Gothenburg in the study by SMHI. The ratio $VOC/NO_x=8/1$ that defines the rim of maximum O_3 in the figure, is actually dependent on the kind of VOC in the mixture and many times a much higher ratio is observed for the rim.

3

Page 14

Figure 1. The isopleth diagram describing the relationship between O_3 concentration and its precursors. Picture is taken from Finlaysson-Pitts [8].

1.3 Sources for VOC emissions

Both anthropogenic and biogenic emissions from the European countries were compiled in the Corinair 94 inventory [9]. The total emission of NMVOC from Sweden was reported to 787 Kton/y and the anthropogenic emissions to 381 Kton/y. The emissions from 11 categories are shown in Table 2. Category 4 is represented by petroleum industries (12 Kton/y), organic chemical industries (3 Kton/y) and wood, paper pulp, food, drink and other industries (19 Kton/y). Thus petroleum industries are responsible for 3% of the anthropogenic emissions in Sweden.

Table 2. The emissions of NMVOC from Sweden in the Corinair 94 inventory.

Source	NMVOC (Kton/year)
1. Combustion in energy and transformation industries	4
2. Non-industrial combustion plants	0
3. Combustion in manufacturing industry	4
4. Production processes	34
5. Extraction and distribution of fossil fuels/geothermal energy	6
6. Solvent and other product use	152
7. Road transport	45
8. Other mobile sources and machinery	36
9. Waste treatment and disposal	0
10. Agriculture and forestry, land use and wood stock changes	*388*
11. Nature	*17*
Total:	***787***

2 Optical remote sensing

This chapter introduces the methods of optical remote sensing to measure gases and then concentrates on methods where the sun is used as the light source. This gives a preparation for the discussion of the SOF method that has been extensively used to monitor VOC emissions from industries.

2.1 Optical remote sensing for gas measurements

Historically, measurements of gases have been done by collecting gas in a point with some kind of absorber or a container. The samples are later analyzed with a gas chromatograph (GC) and mass spectrometry (MS). However, these methods fall short when used for real-time process monitoring and control. Historically, gas chromatographs produce useful data only a small fraction of their working time because of the sample collection requirements and in some cases the sample preparation. The sensitivity and selectivity of these method are however superior to most other methods.

Optical remote sensing methods gives the capability to get results in real time without the need to first collect a sample. Typically, repetitive measurements can be retrieved with a time resolution faster than 1 minute. These methods also have the possibility to measure the concentration integrated along a line or a surface and this may be of more relevance for risk assessment than a measurement in one point.

The methods are based on that IR, visible or UV light is detected with a spectrometer and the molecules cause a fingerprint on the measured spectra either by thermal emission of light from the molecules or by absorption of light on the molecules. Thermal emission from molecules is generally weak and measurements using emission spectroscopy are therefore considered more troublesome. It is therefore more common to use absorption spectroscopy to measure gases in the lower atmosphere. However, the analyzed gas must then be located between a light source and the spectrometer. The light source can either be a lamp or a natural object. The sun and the moon can be used as natural object when measuring with IR, visible and UV light. When measuring with visible and UV light the “blue sky” can also be used as a natural light source. Depending on what compounds that one wants to measure, the wavelength interval must be chosen so that the compounds have absorption structures in that region. With visible and UV light, three categories of compounds can be measured [10]:

- NO_x, O_3, HNO_2, CH_2O, SO_2
- Some aromatic hydrocarbons
- Radicals: BrO, OClO, IO, and OH

In the IR region, nearly all volatile compounds can be measured except atomic species. For a gas to have strong absorption structures in the IR region, the molecules must have a permanent magnetic dipole moment. Therefore, homonuclear diatomic species (e.g. Cl_2, N_2, O_2, H_2, etc.) should in theory not be detectable in IR. Similarly symmetrical linear polyatomic molecules (having a center of inversion) such as S=C=S and H-C≡C-H should not be detectable in IR. However, these molecules are still detectable if the concentrations are high due to much weaker magnetic dipole

moment caused by fine structures in these molecules [11]. For instance, it is possible to measure the total column of N_2 and O_2 in the atmosphere [12].

2.2 Light absorption on gas and particles

In absorption spectroscopy, the attenuation of light on molecules and particles is determined by Beer-Lambert's law:

$$\nu I_m(\ ) = \nu I_L(\ ) \cdot \exp\ -\nu^4 \cdot \alpha_R \cdot L_R - \alpha_{Mie} \cdot L_{Mie} - \sum_i \sigma_i(\nu) \cdot conc_i \cdot L_i \quad (2.$$

$\nu I_m(\ )$ is the light intensity at each wave number ν after it has passed through the gas.

$\nu I_L(\ )$ is the light intensity at each wave number ν for the light source.

$\sigma_i(\ )\nu$ is the absorption cross section (cm^2/molecule) of the gas with index i.

L_i is the path length where the gas with index i is present.

$conc_i$ is the concentration of the gas with index i. (molecules/m^3)

$\alpha_R L_R$, represents the Rayleight scattering which occurs on particles and molecules with a size smaller than the wavelength of the light. The strength of the scattering depends on ν^4 and is therefore much higher at higher wave numbers.

$\alpha_{Mie} L_{Mie}$, represents the Mie scattering which occurs on particles and molecules with a size larger than the wavelength of the light. For large particles, the strength of scattering is independent on the wave number. Scattering on particles of a size that lies in the intermediate region between Rayleigh scattering and Mie scattering will show a more complicated dependence on the wave number and particles size.

When measuring at high wave numbers and when high concentrations of scattering particles is present, it is also required to include a term in the equation that represents the light scattered into the light path by multiple scattering from particles and molecules located outside the observed light path. Using the sun as light source has the benefit that the shape of the light source as seen on earth is relatively small and has a huge contrast compared to other light sources. This makes the light path well defined and scattering has to occur at least two times instead of just one time for the light to be scattered into the observed light path. Using infrared light in comparison to UV/visible light also has the benefit that Rayleigh scattering is much weaker due to the ν^4 dependence. However, cloud droplets have a particle size distribution with a maximum between 1 and 2,5 µm [13] and thus falls between the Rayleigh and Mie scattering regions when using infrared light at 3 µm. The dependence of the scattering strength on the wave number will therefore vary between independent and ν^4 dependent.

In this thesis, there has been no effort to further determine Rayleigh and Mie scattering. However, particle loads in the atmosphere is varying and the varying scattering imposes changes in the measured spectra. Typically, when the sun is used as the light source and when faint clouds block the light path, a tilt in the measured spectra with a wave number dependence of approximately $\nu^{5.1}$ is observed. This must be compensated for when evaluating the spectra and is done by including a polynomial in the spectral fitting algorithm.

2.3 The solar occultation method

Retrieving the contents of trace gases in the atmosphere has been done with solar occultation techniques both with instruments onboard aeroplanes (already 1952 [14]) on satellites (in 1977 [15]) and from ground [16] . The systems consist of a solar tracker and an infrared spectrometer. 50 years ago, infrared grating spectrometers with low resolutions were used but the resolution of the spectrometers has been constantly improving since then. Today, very high-resolution FTIR spectrometers are commonly used for these studies.

From the solar spectra it is possible to retrieve the path-integrated concentration (molecules/cm_2) between the sun and the spectrometer. The concentrations of the gases of interest is determined by looking at how the solar light is absorbed in the atmosphere and to synthesize a spectra from guessed concentration profiles that fits the measured spectra in the best possible way. From high-resolution spectra (<0.125 cm_{-1}) it is also possible to derive height information by considering the temperature and pressure broadening of the spectral absorption lines. When synthesizing spectra, the atmosphere is usually divided in many layers stacked in altitude and the concentration, pressure and temperature broadening in each layer is taken into account to synthetically calculate how solar spectra in the infrared region would be observed by the instrument after it has passed through the atmosphere. The gas concentration in each layer is calculated with an optimum estimation method [17]. Usually, one measurement takes up to 10 minutes due to the high resolution required, and also requires a very stable optical system.

Another application of the solar-occultation technique is to study emission sources at ground level. When measuring localized emissions, the background atmosphere is no longer of interest but instead low concentrations of emitted compounds at low altitudes are of interest. Local wind situations will be of primary concern in such studies since it decides how the emission is transported and diluted. Therefore, pure concentration measurements are of little interest in such measurements. However, concentration ratios between different compounds can be of relevance. For example, volcanoes have been extensively studied by monitoring the ratios between SO_2, HCl and HF [18]. This can also be combined with controlled releases of trace gases at the same location as the emission source to determine the gas emission rate from localized sources by simultaneously measuring the trace gas and the gas of interest.

2.4 The HITRAN database

To calculate how a gas in the atmosphere absorbs light, the HITRAN database [12] can be used. It contains parameters for each absorption line for the 63 most common gases in the atmosphere, including parameters for the pressure and temperature broadening effects. From this it is possible to calculate how a specific gas at a specific temperature and pressure absorbs light. The absorption cross section for a single absorption line can be described by:

$$\sigma(\nu) = \nu\nu g(TS \cdot (- _{\eta\eta} -)\delta \quad (2.$$

7

Page 18

where g is a function describing the broadening of the line. Figure 2 describes the different parameters in this equation. $\nu_{\eta\eta}$, is the center frequency for the absorption line. $S_{\eta\eta}$, is the line strength i.e. the total shaded area in the figure. δ is a shift in frequency caused by air-broadened pressure shift.

Figure 2. The figure show fundamental spectroscopic parameters of a line transition in HITRAN. The dotted line refers to a perturbed transition (with a negative δ). Picture is from the HITRAN paper [12].

The line strength S(T) used in equation 2.2 is dependent on the temperature since the temperature determines how strongly the upper and lower energy levels are populated:

(2.

$$1 - \exp \quad - c \quad \nu_{\eta\eta},$$

$$TS(\quad = S_{\eta\eta,} \cdot \exp\quad - E_{\eta} c \cdot \cdot \frac{1}{T} - \frac{1}{296} \cdot \frac{296}{T}^{m} \cdot \frac{1 - \exp\quad - c_{1} \frac{T}{v_{\eta\eta,}}}{1 - \exp\quad - c_{1} \frac{296}{v_{\eta\eta,}}}$$

This equation is based on the Blotzmann equation for the distribution on the rotational and vibrational levels. Here $c_1=hc/k=1.4388$ cm·K. η E is the energy (cm^{-1}) of the lower energy level. The parameter m represents the temperature dependence of the rotational partition function and has the value 1 for linear molecules and 1.5 otherwise.

There are two effects that contribute to the line broadening represented by function g in equation 2.2. The first is the doppler broadening due to random molecular motion and lead to a Gaussian line shape [19]:

8

Page 19

$$f_{G}(\Delta)v = \frac{1}{\alpha_{G} \pi} \cdot \exp\quad - \frac{(\Delta)v^{2}}{\alpha_{G}^{2}} \qquad (2.$$

where $_G\alpha$ is the Gaussian half-width at half-height:

$$\alpha = \frac{v_{\eta\eta,}}{c} \cdot \frac{2kT}{m} \qquad (2.$$

where m is the molecular mass. This is commonly called the temperature broadening effect and increases with increasing temperature. Pressure broadening is due to collisions perturbing the molecular energy levels and leads to a Lorentzian line shape:

$$vf_{L}(\Delta) = \frac{\alpha_{L} / \pi}{(\Delta)v^{2} + \alpha_{L}^{2}} \qquad (2.$$

where $_L\alpha$ is the Lorentzian half-width at half-height and is calculated by:

$$\alpha_{L} = \frac{296}{T}^{n} (\gamma_{air} \cdot (pp - {}_{s}) + \gamma_{self} \cdot (p))_{s} \qquad (2.$$

where $_{air}\gamma$ represents the broadening due to collisions with other molecules and $_{self}$ the brodening due to collisions of molecules of the same kind. p is the pressure of the air and p_s is the pressure if the specific gas were the only present gas. The coefficient

n is transition dependent.

Typical values are around 0.07 cm-1 for α_L and 0.003 cm-1 for α_G medium-sized molecules at room temperature and 1 atmosphere pressure [19]. If couplings between these broadening effects are neglected, the combined broadening can be calculated by the convolution between them. This is commonly called the voigt line profile:

$$g_{voigt}(\nu) = \int \nu_{yf}(\nu') \left(_{G} - ' \right) \cdot d\nu' \quad (2.$$

This is the commonly used line broadening function used in equation 2.2 above. All parameters are individually given for each absorption line in the HITRAN database. By calculating the line profiles for all absorption lines and summing up, an absorption spectrum can be calculated based on these parameters.

9

Page 20

2.5 Methods to retrieve gas emission rates

In environmental and geological work there is often need to quantify the amount of gas emitted from biogenic or anthropogenic sources. There is a method for this where the gas concentration is measured and integrated over a surface that is selected in air. The mass-flow of gas through that surface is then determined by multiplying the surface integrated concentration with the wind transport through that surface. If the ambient concentrations of the studied gases are zero, the flux through the surface is equal to the emission on the leeward side of the surface.

One way to cut out this surface is to use a scanning system that measures the line integrated concentration in different directions as is commonly done with DIAL [20-22] and scanning DOAS [23]. Another method is to look in one direction but to move the platform the system resides on, commonly a car, an aeroplane or a ship. This was for example done from a ship to quantify the SO_2 emission from volcanoes both with DIAL, DOAS and COSPEC by Weibring et al. [24]. All three gas-monitoring instruments were then configured to look in the vertical direction and measured the total line integrated column of molecules through the whole atmosphere.

The DIAL also has the added capability to resolve the variation in concentration along the line where the instrument is looking.

2.6 The SOF method

When scanning the surface by moving the platform, it is also possible to use solar-occultation spectroscopy. This is the Solar Occultation Flux method (SOF). The Optical Remote Sensing group at Chalmers has been working with this method since 1997. From the beginning the focus of the work was to develop a method to estimate VOC gas emission rates [25, 26]. However, the group has also demonstrated other applications with the method such as volcanic and agricultural measurements.

There is limited publication on studies where the solar-occultation method has been used to quantify gas emission rates. Duffel et al. measured volcanic gas emission rates with solar occultation and FTIR [27]. Weibring et al. [28] used solar occultation and DOAS for the same purpose. Appended **paper A** reports a monitoring project where the method was extensively used during three years to monitor the emissions of alkanes from four industries. Furthermore, appended **paper B** gives more examples where the method has been used to quantify the emissions of various gases from various sources.

The surface integrated concentration of gas is determined by cutting the surface into many parallelograms by continuously measuring spectrum after spectrum while moving the instrument. Each spectrum is evaluated separately to derive the line-integrated concentration represented by each spectrum. The position of the instrument during the traverse is measured with a GPS at the beginning and at the end of each measured spectrum and determines the base of each parallelogram. The surface integration is done by multiplying each line-integrated concentration with this base and summing up. The flow of gas through the surface is determined by a scalar-multiplication in vector representation between the wind-vector and the normal to each parallelogram. A look at Figure 3 gives an intuitive feeling for the surface where the measurement is done. The solar rays detected by the SOF instrument are shown as vertical lines. The area between these lines corresponds to the surface integrated

concentration observed, which if multiplied by the local wind-speed, corresponds to the mass-flux through the area.

Figure 3. A 3D plot of a SOF measurement conducted at the oil harbour.

Here follows a more rigorous derivation of the equations that has been implemented in a real time software (QESOF) to calculate the flux. The position of the system is at the beginning and at the end of the collection of a spectrum defines a vector of movement $\vec{m} = \vec{V}_{stop} - \vec{V}_{start}$. This vector defines the short side of a parallelogram. The long side of the parallelogram is determined by the vector pointing towards the sun from the instrument. This can be calculated if the time, date and the position of the instrument are known. There are many algorithms for doing this, some more exact than others. In the QESOF software the following simplified equations has been used:

$$
\begin{aligned}
d &= 2\pi \cdot \text{daynr} \; 0.365/ \\
\text{DEC} &= \frac{\pi}{180} \cdot .0\,322003 - 9711.22 \cdot \cos(d .0) + 357898 \cdot .0)2\cos(2 - 14398 \cdot)3\cos(d \\
&\quad + .3\,94638 \cdot \sin(d .0) + 019334 \cdot .0)2\sin(2 + 05928 \cdot)3\sin(d \\
\text{eqTime} &= 9.87 \cdot \sin(4\pi \cdot (\text{daynr} - 81)/365.0) \; 7.53 - \cdot \cos(2\pi \cdot (\text{daynr} - 81)/365.0) \\
&\quad 1.50 - \cdot \sin(2\pi \cdot (\text{daynr} - 81)/365.0) \\
\text{LHA} &= \frac{\pi}{180^\circ} \cdot (\text{second}_{GMT} / 3600 + \text{eqTime} \; 60/ - 12) \cdot 15^\circ + \text{Longitude} \\
\text{solar\_zenith} &= \arccos[\sin(\text{DEC}) \cdot \sin(\text{Latitude}) + \cos(\text{DEC}) \cdot \cos(\text{Latitude}) \cdot \cos(\text{LHA}) \\
\text{ca} &= \frac{\cos(\text{solar\_zenith}) \cdot \sin(\text{Latitude}) - \sin(\text{DEC})}{\sin(\text{solar\_zenith}) \cdot \cos(\text{Latitude})} \\
&\textit{if } \text{LHA}(<)0 \rightarrow \text{solar\_azim} = \pi - \arccos( )\text{ca} \\
&\textit{else} \rightarrow \text{solar\_azim} = \pi + \arccos( )\text{ca}
\end{aligned}
\qquad (2.
$$

The input parameters are the time in seconds from mindnight according to Greenwich-Mean-Time ($second_{GMT}$), the day number of the year (daynr) and the position in degrees (Latitude, Longitude). The results are given as zenith and azimuth angles to the sun in radians where solar_zenith=0 corresponds to that the sun is straight up and solar_azim=π corresponds to that the sun is at its southmost position in

the day (assuming northern hemisphere). The direction to the sun can also be represented with a vector:

$$\vec{S} = \begin{matrix} \hat{x}\cdot\sin(solar\_zen)\cdot\sin(solar\_azim) \\ \hat{y}\cdot\sin(solar\_zen)\cdot\cos(solar\_azim) \\ \hat{z}\cdot\cos(solar\_zen) \end{matrix} \quad (2.$$

The cross multiplication between the vector of movement $\vec{m}$ and the vector to the su $\vec{S}$ determines the normal of the parallelogram and its length is equal to the area of the parallelogram. The results of the spectral evaluation is a line integrated concentration that will here be represented by $[conc\cdot]L$ where L is supposed to represent a fiction height of the side of the parallelogram. The following formula calculates the normal to the parallelogram area and the normal vector has a length that is equal to the concentration integrated over the area of the parallelogram:

$$\vec{S}\vec{m} = \vec{v}\times\vec{n}\cdot[conc\cdot]L \quad (2.$$

The length of $\vec{n}$ has unit mass/length. It is then assumed that the flow of the gases is following the wind. By a scalar multiplication of the vector $\vec{n}$ with the wind vect $\vec{v}$, the flow of the gas through the parallelogram is calculated:

$$vS\vec{m}vn\vec{F}\cdot\vec{n} = \vec{v}\times\vec{n}\cdot\vec{n}\cdot[conc\cdot]L \quad (2.$$

The flux F has unit mass/time, typically kg/h. In most circumstances it can be assumed that the z component of $\vec{m}$ and $\vec{v}$ are zero and this simplifies the calculation of the flux to:

$$F = (S_{vy}m S_{vx}m\cdot_z - {}_x\cdot{}_y\cdot{}_z)\cdot[conc\cdot]L \quad (2.$$

Rewriting this in polar coordinates it becomes:

$$F = \cos(solar\_zen)\cdot(\sin v_\alpha - m_\alpha)\cdot m_y\cdot{}_L\cdot[conc\cdot]L \quad (2.$$

where $_\alpha v$ and $_\alpha m$ are the wind and driving directions, $_s v$ the wind speed and $_L$ length of movement.

If there exists a strong difference in the wind on different heights, then a mass weighted wind must be used. This can be calculated by splitting equation 2.14 into smaller segments stacked in height and considering the wind in each segment:

$$F = \cos(solar\_zen)\cdot m_L\cdot\sum_j \sin(v_{\alpha,j} - m_\alpha)\cdot v_{jS,}\cdot[conc_j\cdot L_j] \quad (2.$$

$$[conc\cdot L] = \sum_j [conc_j\cdot L_j] \quad (2.$$

Only the total column $[conc\cdot]L$ is measured with SOF. The concentration in each height segment must be determined by other methods.

3 FTIR spectroscopy

This chapter gives an introduction to the FTIR (Fourier Transform Infrared) spectrometer and how the data collected from a FTIR is handled to retrieve a spectrum and how this should be done to get good quality in the spectra. In particular, resampling spectra to different wavelengths and the imposed side-lobes for different apodization functions are considered. This is presented here to give a preparation to the discussions in chapter 6 about the algorithm that have been implemented in the real time evaluation software (QESOF) that was developed to make the SOF method more operative.

3.1 The FTIR spectrometer

A FTIR spectrometer is an interferometer for IR light. The incoming light beam in the interferometer is divided into two separate light paths in a beam-splitter where half of the radiation is reflected and the rest is transmitted. The transmitted light travels to a movable mirror and the reflected light to a fixed mirror. The reflected light from the fixed mirror and the transmitted light from the moving mirror recombine at the beamsplitter, and hit the detector. The components of the interferometer are shown in Figure 4. All mirrors must be reflective in the infrared region. The beamsplitter is typically made of KBr or ZnSe to be able to handle infrared light. The detector must be sensitive to infrared radiation and is therefore made of HgCdTe, InSb, InAs, InGaAs, PbS or PbSe. The first four versions must be cooled by liquid nitrogen to work. The last two works at room temperature but has lower sensitivity.

Figure 4. A common construction of a FTIR spectrometer (a Michelson interferometer).

The electrical signal from the detector represents the light intensity on the detector for different positions of the movable mirror and is called an interferogram. Figure 5

shows a typical interferogram. The spectrum is calculated in a computer by Fourier-transforming the interferogram. Figure 6 shows an example of a solar spectrum measured with a FTIR equipped with an InSb detector. This type of detector is not sensitive to wavelengths longer than 1700 cm-1.

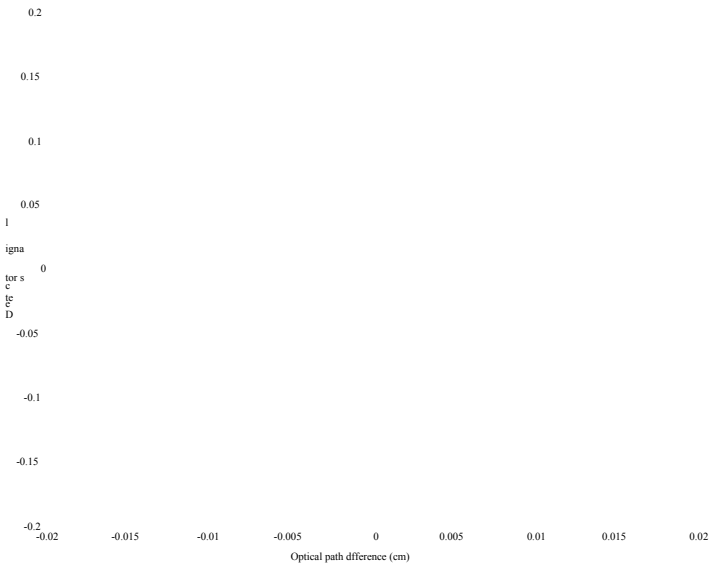

Figure 5. The figure shows the center of a typical interferogram.

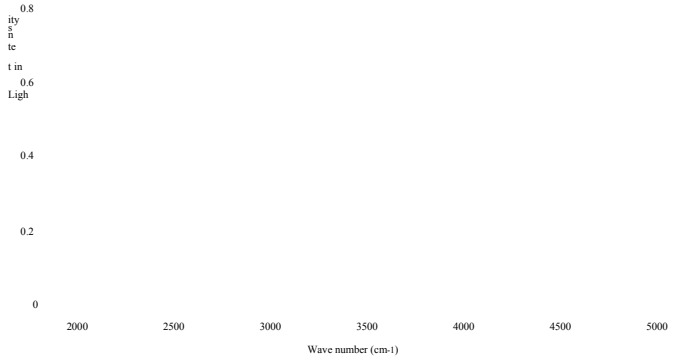

Figure 6. A solar spectrum measured on ground. The absence of light between 3000 to 4000 cm^{-1} is due to strong absorption on atmospheric H_2O and CO_2.

Page 25

3.2 FTIR theory

The resolution of a spectrum is first of all restricted by the maximum optical path difference (OPD) in the movement of the movable mirror. The optical path difference is always measured in relation to the zero point where there is equal distance for the light to travel along the two paths to the two mirrors. If an interferogram is measured both at positive and negative path differences it is called a double sided interferogram. If it is only measured on one side of the zero point it is called single sided. If the interferometer is perfect then the interferogram is symmetric. A single sided interferrogram will therefore give the same resolution as a double sided interferogram but with only half the amount of movement of the mirror. Therefore, to get the highest resolution, single sided interferograms are commonly used. However, if the mirrors are misaligned, the interferogram will not be perfectly symmetric. Therefore, if these effects are strong, double sided interferograms should be used. If a single sided interferogram is measured, one side is mirrored around the zero point and copied to the other side to create a symmetric double sided interferogram.

From a direct discrete Fourier transform of the double sided interferogram, the spectral points will be separated with a wave number of $v_1 = 2/(1 \cdot OPD)$. A d discrete Fourier transform is here defined to be the Fourier transform that contains as many output parameters as the number of sampling points in the interferogram and therefore defines a linear equation system:

$$A_n = \sum_{k=0}^{N} I_k \cdot \cos \frac{v_n}{v_1} \cdot \frac{2\pi k}{N} \quad (3.$$

$$B_n = \sum_{k=0}^{N} I_k \cdot \sin\left(\frac{v_n}{v_1} \cdot \frac{2\pi k}{N}\right) \quad (3.$$

$$v_n = n\nu \cdot = \frac{n}{2 \cdot OPD} \quad (3$$

where N is the number of sampling points in the interferogram. The vector I with indexes k represents the interferogram. The vector A represents the cosine term and the B vector represents the sine terms. Each index n represents the signal strength at the wave-number ν_n. If the interferogram is perfectly symmetric then all B components in equation 3.2 will become zero, and the components A_n alone represents the light intensity at different wave numbers. However if the interferogram is unsymmetric, the light intensity must be calculated by:

$$S_n = A_n^2 + B_n^2 \quad (3$$

Component number zero of A represents the bias component of the interferogram and component number N/2 represents the highest wave number that can be represented by the interferogram. The corresponding two numbers in the B vector will always be zero and can therefore be omitted. The spectrum S_n will contain light intensities at equal number of equidistant wave numbers (ν_n) as there are equidistant sampling points in the interferogram on one side of the zero point.

15

Page 26

The discrete Fourier transform can be calculated by fast algorithms if the number of points in the interferogram (N) can be represented by $N=2_m$ where m is an integer. Even faster algorithms can be applied if N can be represented by $N=4_m$. The algorithms take advantage of the periodicity of the sine and cosine functions that occurs at these specific choices of N and thereby reduces the number of multiplications required.

The resolution of a spectrum is usually defined as the full width at half maximum of an individual peak in the spectrum and according to this definition, the resolution will be lower than the wave-number separation between each point in the direct Fourier-transform. The spectrum can be evaluated at different wave numbers than what is represented by the direct Fourier-transform by assuming the interferogram to be larger than what is actually measured and forcing the interferogram to be zero outside the limits of the measured interferogram. This is called zero-fill and has the effect of interpolating the spectrum based on the assumption that the original interferogram can be constructed by a sum of the cosine and sine functions that is represented by the non-zerofilled Fourier-transform. The

zerofilling has the same effect as convoluting the spectrum with a *sinc* function. Thus, each peak S_n of the spectrum will have the following shape:

$$vS( ) = S_n \frac{\sin(\pi \cdot (v\nu - n)/ 1)}{\pi \cdot (v\nu - n)/1} \quad (3$$

In this way, the complete spectrum defined by all spectral points can be interpolated to any wave-number ν of interest:

$$vS( ) = \sum_n S_n \frac{\sin(\pi \cdot (v\nu - n)/ 1)}{\pi \cdot (v\nu - n)/1} \quad (3$$

An individual peak will have the shape of the function *sinc(x)=sin(x)/x* shown in Figure 7. Solving *sinc(x)=0.5* gives *x=0.6034* which corresponds to a full width at half maximum (FWHM) of 0.6034/OPD.

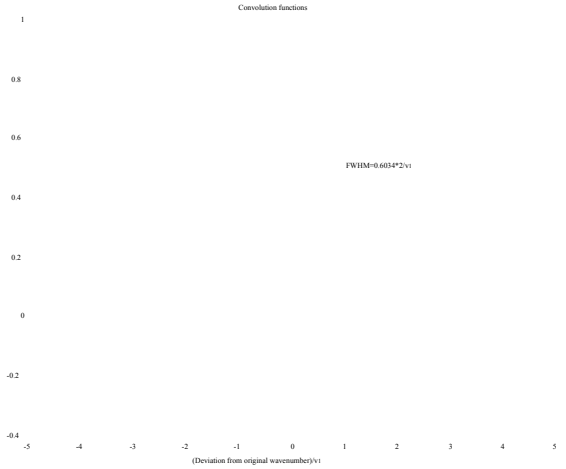

Figure 7. The figure shows the sinc function and the full width at half maximum.

16

Page 27

Figure 7 shows the side-lobes that will occur if the wave-number of the incoming light does not exactly match one of those wave-numbers that is represented by the direct discrete Fourier transform. In a real measurement, a perfect match will never occur and there will therefore always be side-lobes. The side-lobes are strongest if the incoming light has a wave number that falls just in the middle between two of the wave-numbers in the direct discrete Fourier-transform. This coincides with that the wave-number causes maximum difference in signal strength between the end-points

in the interferogram. For high quality evaluations of spectra, these side-lobes must be considered and there are two ways to do this. The two methods can also be used simultaneously. In the first method, a high-resolution spectrum is synthesized from guessed concentration profiles at typically around 16 times higher resolution than the actual measurement. The resolution is then degraded to the same resolution as the measurement in such a way that the side-lobes are synthesized as well. This can be done directly from equation 3.6. The best fit for the guessed concentration profiles is then searched for by a non-linear method. Thus, this method requires high-resolution absorption profiles for all the gases that has prominent absorption features in the measured spectra. It also requires a non-linear search algorithm. Another method to deal with the side-lobes is to multiply the interferogram with a function to force the signal strength to approach zero at the ends of the interferogram. This method, called apodization, has the disadvantage of reducing the resolution since the information contained at the ends of the interferogram is suppressed. A set of apodization functions that are commonly used is the Norton-Beer functions in its three versions: weak, medium and strong. These functions has been selected to minimize the effect of side lobes on discrete line spectra, see paper [29] by Norton and Beer from 1976. Another function commonly used is the triangular apodization, which however does not result in optimal suppression of side-lobes of a discrete line. Equation 3.7-3.9 shows the Norton-Beer functions and equation 3.10 the triangular function. The variable L represents the length of the interferogram. Figure 8 shows the apodization functions.

$$xF_1.0)(= \quad 384093 \quad - .0\,087577 \cdot 1 - \frac{x^2}{L^2} \quad + 0.703484 \cdot 1 - \frac{x^2}{L^2}^2 \qquad (3$$

$$xF_2.0)(= \quad 152442 \quad - .0\,136176 \cdot 1 - \frac{x^2}{L^2} \quad + 0.983734 \cdot 1 - \frac{x^2}{L^2}^2 \qquad (3.$$

$$xF_3.0)(= \quad 045335 \quad - .0\,554883 \cdot 1 - \frac{x^2}{L^2}^2 \quad + 0.399782 \cdot 1 - \frac{x^2}{L^2}^3 \qquad (3.$$

$$xF_4=1)(\quad - \frac{x}{L} \qquad (3.$$

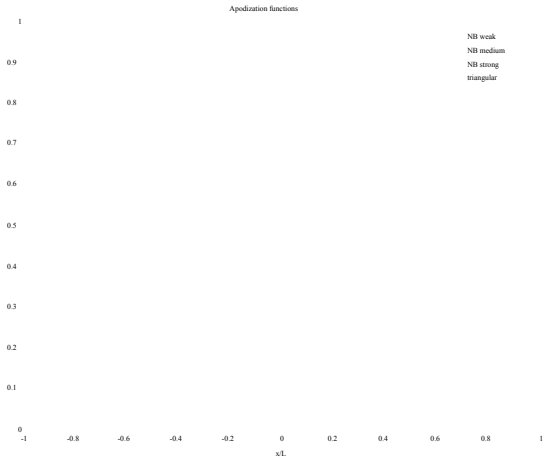

Figure 8. The Norton-Beer apodization functions and the triangular apodization function.

Multiplicating the interferogram with an apodization function has the same effect as convoluting the spectrum with the Fourier transform of the apodization-function. Figure 9 shows the convolution functions corresponding to the apodizations given in Figure 8. The FWHM for the convolution functions then becomes 0.715/OPD, 0.838/OPD, 0.941/OPD for Norton-Beer weak, medium and strong and 0.886/OPD for triangular apodization.

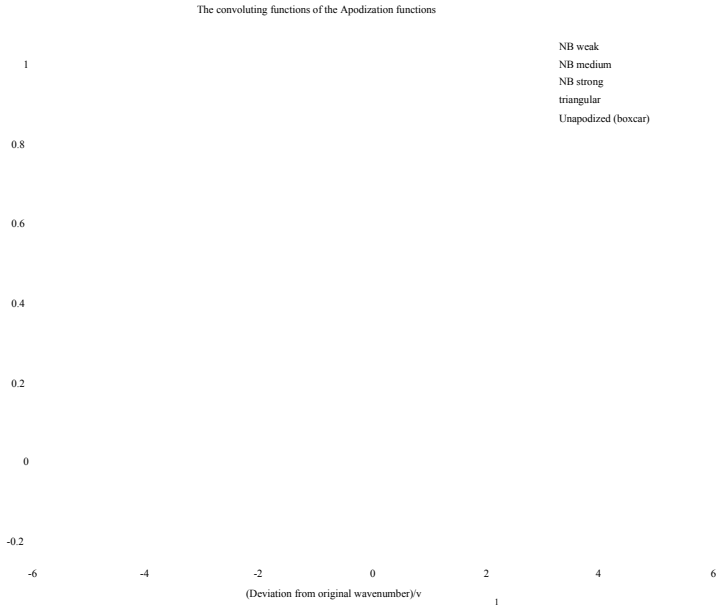

Figure 9. The Fourier transform of the apodization functions i.e. the functions that convolutes the spectra.

When measuring spectra with the OPUS software, the resolution is defined as the FWHM when using triangular apodization. For example, when measuring at 8 cm^{-1} an optical path difference of OPD=0.886/8 cm^{-1}=0.1108 cm is required. For the FTIR-spectrometers it is common to trigger the sampling of the interferogram by detecting the zero-crossings of the interferrogram from a Helium-Neon laser with a wavelength of 15798.84 cm^{-1} (632nm). The interferogram will consist of 15798.84 cm^{-1} × 0.1108 cm=1751 discretization points if it is single sided, or 3502 points if it is double sided. The shortest wavelength represented in such a spectra is twice the laser wavelength i.e. 7900 cm^{-1} (1.26 µm). However, the commonly used detectors do not work at such short wavelengths.

3.3 The effect of nonzero incidence angle

If it is assumed that the incoming light is perfectly parallel but the direction is tilted compared to the optical axis of the FTIR-spectrometer, it will cause a squeezing effect of the measured spectra in such a way that emission lines will show up at lower wave-numbers than the true wave-numbers. Figure 10 describes the principle behind this. The upper part shows the traditional way to picture an interferometer. An observer at the position of the detector will see both mirrors simultaneously. In the lower picture, the interferometer has been redrawn as if the elements were in a straight line. Assume that mirror 1 is fixed and that mirror 2 moves a distance *dx*. If the incoming light is tilted with an angle α, the movement of the mirror 2 with a distance *dx* will then cause the path difference between path 1 and 2 to change with a factor cos(α) lower than if the light were not tilted. This will produce less interference points in the recorded interferogram and this corresponds to that a monochromatic light source of wave number ν will cause a peak at wave number ·νos(α) in the spectrum.

Figure 10. The figure shows the principle behind the squeezing effect when the incoming light is tilted with an angle α in comparison with the optical axis.

Page 30

This reasoning can be extended to consider the case when the incoming light is coming from a distribution of angles. This will cause a broadening of the lines towards lower wave-numbers since the incoming light has a distribution inside a maximum angle Ω. If R(α) is the normalized distribution of light intensity over the different angles of incidence, then the spectra F will be distorted according to the following equation:

$$vG)(= \int_{0}^{\Omega} 3 \cdot \alpha^{2} \cdot R(\alpha) \left(vF \cdot \cos(\alpha) \right) \cdot \Omega^{2} \quad (3.$$

The dependence of α^2 is a result of that the light is entering through a bigger area at high angles. If there is an even distribution of light over all angles then $R(\alpha) = ( )$ for $0<\alpha<\Omega$.

The optical set up used for the measurements presented in this thesis includes an aperture before the spectrometer to limit the field of view of the spectrometer to force a well defined incidence angle that optimally should be zero. When using a large aperture, a larger squeeze factor is many times observed. However, even at the highest resolution used, 0.5cm^{-1}, it is difficult to observe a broadening of the lines when a large aperture is chosen.

4 This thesis

In the years 2002 to 2005, a project (KORUS) was run in cooperation with four industries to explore the possibilities to measure gas emissions of volatile organic compounds (VOC) with the SOF method. The four industries were three refineries, Preemraff-Göteborg, Preemraff-Lysekil and Shellraff-Göteborg, and the Oil harbour of Göteborg. All industries are located on the west coast of Sweden. The project aimed at lifting the usability of the method to commercially competitive performance, by increasing reliability and automatization. Simultaneously with the work to improve the method, an extensive measurement-program was run to put the method into a full-scale test to demonstrate its capacity for routine measurements. The success of the project is a result of the combined effort from many people in the Optical Remote Sensing group and many years of preparations.

Detailed results of the measurements on the industries are presented in the report: **Monitoring of VOC emissions from three refineries in Sweden and the Oil harbour of Göteborg using the Solar Occultation Flux method** [30]. This report is not appended to this thesis because it is too long. A summary of the results and general conclusions from the measurements are presented in the appended **paper A**. Some additional information that did not fit in **paper A** is given in chapter 7. A detailed error analysis of the measurements on the industries is presented in chapter 8 and a much shorter version is also included in appended **paper A**.

The SOF method and some examples of applications are described in the

appended **paper B**.

To validate and test what precision that could be expected with the SOF method, two experiments were done where known amount of SF_6 trace gas was released and then measured with the SOF method. This is presented in chapter 5.

To make the SOF method more operative, development of the hardware and software of the measurement system was done. A new software for real time evaluation of the measurement was developed which made the measurements more efficient since it was possible to directly see if a measurement was successful or not. Also, the real time information has shown to be beneficial since it is possible to quickly scan through an industry and in real time detect leaks. This has resulted in that unexpected emission sources inside the industries have been discovered.

The newly developed QESOF software is described in chapter 6. Also, new post processing software was required to be able to handle and compile the results from the large number of measurements done on the industries. These are however not presented further in this thesis.

A new active solar tracker-was built that allowed 540° rotation. The old solar tracker only allowed 30° rotation and the heavy instrument must be moved by hand each time the measurement car made a turn. With the new solar tracker, this is not required anymore. The new solar tracker is described in chapter 9.

Page 32

5 Validation of the SOF method with SF_6

The method to retrieve fluxes from traverses with a mobile solar-occultation system was tested on two experiments, carried out in year 2002 by Karin Fransson and Johan Mellqvist. In the first experiment, a trace gas (SF_6) was emitted from the top of a 17 m tall mast in the middle of an open field at Åby in Göteborg. Traverses were then done downwind with the measurement system at varying distances from the emission source. The wind was measured with a wind-meter located in the top of the same mast. The true amount of emitted trace gas was estimated by weighting the gas tube before and after the experiment and also measuring the time when the gas was emitted. The emitted gas was always approximately 2 kg/h. The measured peak concentrations were about 10 mg/m_2 for most scans.

The spectral evaluation was done in the region 925-975 cm_{-1} and included

H_2O, CO_2, SF_6 and a fitted sky-reference spectra. Spectra for H_2O and CO_2 were created from the HITRAN database at a temperature of 288K and a pressure of 1 atm. SF_6 spectra was taken from the NIST database [31]. Figure 11 shows the transmission spectra for 1 mg/m2 of SF_6. As can be seen, SF_6 is absorbing about 1% of the light in its peak at this concentration and this should be easily detected in the measured spectra. There is however a strong absorption-line of H_2O at wave number 948 cm^{-1} that is causing some trouble in the SF_6 retrieval. For the results presented here, non-linear spectral evaluation was used, Norton-Beer strong apodization [29] was used and a polynomial of 4th order was also fitted.

Figure 11. The transmission spectra of H_2O, CO_2 and the reference spectrum for SF_6.

Table 3 shows the results from the four days when the field experiment was done. The standard deviations for the calculated averages indicates that the result of just one traverse is uncertain and that averaging of many traverses are required to get reasonable results. As can be seen, each traverse has a low reliability but the average over many traverses comes close to the true value. Figure 12 shows a plot of the emissions derived from all the traverses for each day plotted towards the average wind speed during the traverse.

Page 33

Table 3. Summary for each day in year 2002, when measurements on the Åby field were done.

Day	Emitted SF_6 (kg/h)	Calculated average (kg/h)	Number of accepted traverses	Average wind speed (m/s)	Average wind direction	Err
May-22	1.92	2.3±1.3	4	4.9-8.6	152°-169°	20%
May-23	1.97	2.2±0.6	15	3.9-5.6	120°-142°	10%

June-03	1.97	1.6±0.9	16	2.7-5.3	235°-273°	-20
Jun-04	1.89	2.0±1.4	9	5.9-7.8	152°-191°	5%

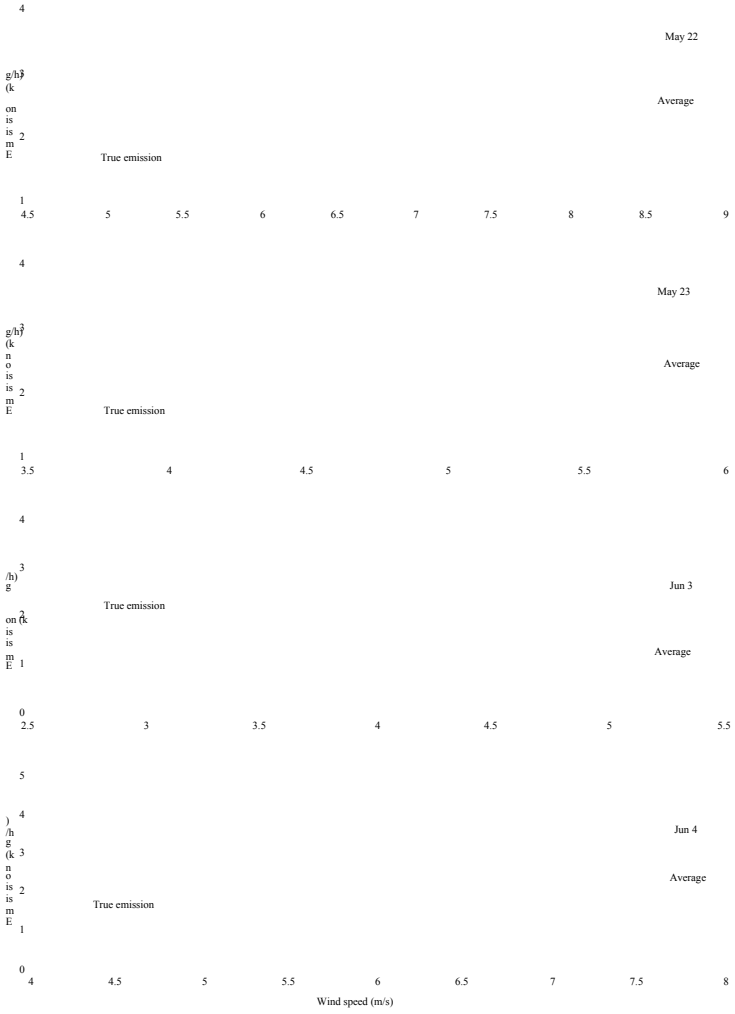

Figure 12. The figure shows the calculated SF_6 emission versus wind speed on all traverses.

Page 34

Another experiment was done where SF_6 was emitted from the roof of a crude oil tank. The tank (Tank 105 at Preemraff-Göteborg) is located in a tank-park where nine tanks are standing close together, see Figure 13. It can be expected that the wind field is irregular close to the ground inside the tank-park. Traverses were done on a road along the side of the tank park, approximately 150 m away from the emission point. Figure 13 shows the location of a typical traverse on a map. During day 24-June 2002, eight traverses were successfully retrieved. Table 4 shows all the traverses done during that day. The true released amount of SF_6 was estimated to 2.0 kg/h by weighting the gas-tube before and after the experiment and the retrieved average emission was 3.0±1.1 kg/h which corresponds to an error of 50%.

Table 4. The traverses done on day 24-June 2002. True emitted amount of SF_6 has been determined to 2.0 kg/h.

Time (24 h)	**Emission SF_6 (kg/h)**	**Average wind speed (m/s)**	**Average wind direction**
12:45	3.1	6.5	252°
12:54	1.8	7.2	252°
13:05	1.3	6.0	259°
13:17	2.7	7.5	253°
13:29	3.1	5.4	255°
13:56	5.2	7.4	264°
14:05	3.7	7.2	251°
14:24	2.6	7.3	262°
14:31	3.4	6.5	260°
Average	**3.0±1.1**		

Figure 13. A typical traverse done when the SF_6 gas was emitted on top of tank 105. The broad lines along the traverse points towards the wind direction. *(Aerial photo: Copyright Lantmäteriet 2004-11-*

09. Ur Din Karta och SverigeBilden)

24

Page 35

6 The QESOF program

To render the SOF method more effective, an on line software was developed to allow real time evaluation when measuring gas emissions. The program waits for interferograms to be ready for evaluation, loads them, Fourier transform them and retrieves the line-integrated concentrations of the gases of interest from the spectra with a nonlinear algorithm. It combines this with the position of the vehicle retrieved by GPS, and wind information from wind-meters and calculates the flux of gas through the surface that is sliced out along the path the vehicle is driving. Linear interpolation is used both for the position, wind speed and wind-direction. It gives a graphical representation of the measured flux on a map while the measurement is running. The software was tailored to work with the Bruker OPAG and the Bruker IrCube spectrometers, and to do spectral evaluation with a resolution between 0.5 and 12 cm^{-1}. Two separate measurement systems were built with these two spectrometers.

6.1 The user interface

In Figure 14 the screen of the measurement-computer is shown. The upper left window shows a map of the measurement, with lines pointing toward the wind along the driving route. The measured and fitted absorption spectra are shown in the lower left window, and the retrieved data on the right side. All parameters are given to the program by text-files and results for post processing are saved as text files.

Figure 14. The figure shows the screen of the measurement computer with the presentation by the automatic retrieval software that has been developed, allowing online evaluation of the measured spectra. In the upper left is shown a map of the measurement with lines pointing toward the wind, the measured and fitted absorption spectra in the lower left, and the retrieved data on the right side.

6.2 Spectral evaluation in QESOF

Figure 15 shows a schematic view of the internal functions of the retrieval of the line-integrated concentrations in the QESOF-software. Each part will be described in this section. Each part has been numbered in the figure to simplify the discussion.

Figure 15. The internal functions of the spectral evaluation code in the QESOF software.

6.2.1 Hitran spectral line parameters - Part 1

The HITRAN database is probably the most exact and useful database for calculating cross sections of the most abundant compounds in the atmosphere at the date when this report was written. It is constantly updated when new and better information is available. Current version contains 63 compounds including most compounds that are of importance for studying the chemical properties of the atmosphere. The strength and wavelength of each absorption line is given as well as parameters that describe the pressure and temperature broadening of each line.

6.2.2 Synthesize spectrum - Part 2

The user chooses what compounds to be included in the spectral fit and the temperature and pressure for each compound (part 3). High-resolution spectra are then calculated for each compound based on the line parameters from the HITRAN database. For molecules with many absorption lines, this may require lots of computation. Therefore a buffert of the synthesized spectra is stored in a file the first time the program is run with new parameters. An old existing file is read in if it exists

and parameters are unchanged to reduce start-up time of the program. The resolution is set to 16 times higher than the distance between each discrete point in the measured spectrum that is entering in part 13. This determines what resolution is used in all parts that are working with high resolution.

6.2.3 External Reference Spectra - Part 4

QESOF was primarily developed to measure emission of alkanes from refineries. Unfortunately, data for the important alkanes are not present in the HITRAN database and therefore has to be retrieved from other database in the form of measured absorbance spectra. Spectra for propane and butane with 0.25 cm^{-1} resolution from the Pacific North West database and octane spectra with 0.5 cm^{-1} resolution from the QASoft database was used. External spectra can be provided to the program in either Galactic SPC format or in OPUS format. The spectra is converted to the same resolution as the synthetisized HITRAN spectra in part 5. To reduce calculations at start-up, buffers containing spectra with already converted resolution is maintained in a file and is used as long as parameters are not changed. The resolution of the absorbance spectra is converted with a linear interpolation that only considers the two points on each side of a wave number to calculate the absorbance at the new wave number. There is a possibility that this conversion can induce distortion if dealing with narrow absorption lines. For measurements at 0.5 cm^{-1} the internal high

resolution will be 0.03 cm^{-1} and anticipating a safety factor of 4, spectral lines sharper than 0.12 cm^{-1} is possibly distorted. This can be neglected when dealing with compounds with broad spectral features, for example the alkanes.

6.2.4 Mixing of reference spectra - Part 6

The weight for each high-resolution reference spectra is provided by the non-linear fitting algorithm (part 17) and represents the guessed line integrated concentration of each compound. All absorbance spectra are then summed (part 7) to give the guessed synthesized high-resolution spectrum.

6.2.5 Squeezing of synthesized spectra - Part 8

When evaluating high-resolution spectra (0.5 cm^{-1}) it is most times required to compensate for nonzero incidence angle in the spectrometer. As described in section 3.3, this causes a squeeze of the spectra so that spectral lines will show up at lower wave numbers. This is anticipated by also squeezing the synthesized spectra by either forcing the squeeze factor to a value chosen by the user or letting the non-linear algorithm find the best squeeze to get the best fit between the final low-resolution synthesized spectra and the measured spectra.

The algorithm used for squeezing the high-resolution absorbance spectra rearranges the vector that is representing the individual intensity values in the spectra and uses linear interpolation that only considers the two points on each side of a wave number to calculate the absorbance at the new wave number. Just like mentioned with part 5, this can cause some errors when dealing with spectra with narrow absorption lines.

6.2.6 Conversion to transmission of synthesized spectra - Part 9

The synthesized absorbance spectra is converted to transmission:

$$Transmission = \exp(-Absorbance) = \exp\left(-\sum_i conc_i \cdot L_i \cdot \sigma_i\right) \quad (6.$$

This is the same as equation 2.1 except that scattering has not been considered. The effect of scattering will be removed by including a polynomial with part 14.

6.2.7 Resolution conversion with side lobe simulation - Part 10

When the concentrations of all compounds, and pressure, temperature and squeeze parameters is close to a perfect match to the conditions imposed on the measured spectra, the high resolution synthesized spectra reaching part 10 is hopefully a high resolution representation of the light that is actually reaching the spectrometer. As previously shown in Figure 7, each wavelength will induce side-lobes in the spectra especially if the wavelength causes high light intensities at the edge of the sampled interferogram. This is simulated by convoluting with the modified *sinc* functions that was previously shown in Figure 9 when converting from the high resolution to the low resolution. The convolution functions representing the different apodization functions are calculated in advance and the desired one is read by the code depending on what apodization function the user has chosen. The conversion to low resolution is done to the same set of wave numbers as in the measured spectra. Then, a direct comparison between synthesized spectra and measured spectra is possible, point for point. When the user has chosen no apodization, then the convolution with the sinc function is done in the following way:

$$vG(\ )_L = \frac{\sum_j vS(\ )_j \cdot Sinc\ \left(\pi \cdot (v_j - v_L) \cdot \frac{zf}{\Delta v}\right)}{\sum_j Sinc\ \left(\pi \cdot (v_j - v_L) \cdot \frac{zf}{\Delta v}\right)} \quad (6.$$

$$Sinc\ (x) = \frac{\sin(x)}{x} \quad (6.$$

$vG(\ )_L$ is the resulting low resolution transmission at one data point with wave number v_L. The data points in the vector G have a wave number separation of Δv. *zf* is the zero-filling factor chosen by the user. Thus, the combination $\frac{zf}{\Delta v}$ repre the wave number separation as if no zero-filling was chosen. If the user has chosen to use apodization then the *sinc* function shown in equation 6.3 is replaced with the functions shown in Figure 9. These must however be calculated numerically by Fourier-transforming the apodization functions. $vS(\ )_j$ is the high resolution spectra that has data points at the wave numbers v_j, not necessarily coinciding with v_L. The summation over j is done at all data points on the high resolution spectra that lies inside the spectral interval where the spectral evaluation is done plus 320 extra points on each side of that interval. The extra 320 points is included to avoid side-lobe

Page 39

effects at the edges of the chosen interval. It is required that $vS(\ )_j$ has valid spectral-information these extra 320 spectral points. The resulting low-resolution spectrum has spectral information at the same wave numbers as the measured spectra and a direct

comparison point by point is therefore possible. Before a comparison is done, the multiplicator marked 11 will incorporate optional components in the synthesized spectra.

6.2.8 Calculation of residual – Part 12

The residual is calculated i.e. the discrepancies between the measured and the synthesized spectra by the following formula:

$$\vec{R} = \log \frac{\vec{T}_{measured}}{\vec{T}_{synthesized}} \quad (6.$$

The letter T has been chosen to represent the spectra to indicate that they represent transmission. Equation 6.4 is the residual in represented as absorbance and this representation has been chosen since it will make the search for the next guess more linear in the non-linear algorithm (part 17).

6.2.9 Measured spectrum – Part 13

The software will automatically wait for new measurements to be evaluated. It can either be set up to load files generated by the Bruker OPUS software in a continuous way. The OPUS software is then set up to take spectra with the spectrometer, store it in a file and unloading them in a repetitive way. When the file is valid for reading, QESOF will automatically load it and evaluate it. QESOF can also be set up to directly communicate with the IrCube spectrometer by its web-server interface, without using OPUS, and request new spectra in a repetitive way.

The user has the choice to prefer interferogram information or already Fourier transformed spectra in the retrieved files. If the user prefer interferogram and an interferogram is present in the file, then a Fourier transform is done inside the QESOF software with the zero-filling and apodization parameters that the user has chosen even if a spectra is also present in the file. If an interferogram is not present then a spectrum will be read if it is present in the file. If the user prefers already existing transformed spectra and a spectra is present in the file, then the spectra will be read from the file. Otherwise an interferogram will be read and Fourier-transformed if it is present in the file.

When Fourier-transforming in the software, the user can choose to perform a slow discrete Fourier transform with the same number of data points as the interferogram or optionally cut the interferogram before its actual ends. This is useful if one wants to study the consequences of lowering the resolution. This is also useful if the interferogram is noisy close to its edges and therefore should be omitted. The user also has the choice to zero-fill the interferogram to the closest higher exponential of 4. The software will then use a much faster Radix-4 algorithm for the Fourier-transform.

6.2.10 Polynomial – Part 14

An optional polynomial can be multiplied to the low-resolution spectra. Fitting of a bias term is always required to take care of varying light intensities in the measurement. Fitting of a linear term takes care of most variations caused by scattering. Even the Rayleigh scattering that has ν^4 dependence can be approximated with a line if the wave-number interval for the evaluation is small. Fitting of higher polynomials is possible but may lead to errors due to that compounds with broad absorption structures is partly fitted with a polynomial instead. This has been observed when using polynomials with four terms when evaluating measurements containing alkanes of low concentrations.

6.2.11 Optical filter – Part 15

With both the Bruker OPAG and the IrCube spectrometer, optical filters has been placed just before the entrance to the spectrometer to test if it will result in better signal to noise ratio. The benefit of using optical filters is that more light at the interesting wavelength interval can be used without saturating the infrared detector. Unfortunately, the use of optical filters has shown to cause problems if the filter function has structures in the neighborhood of the evaluation interval. Even faint structures in the filter function can be huge in comparison to the absorption on the molecules of interest. The effects of these are difficult to compensate for due to the rough and varying situation imposed by the environment in a field measurement, where vibrations are strong and where temperature and the incidence angle into the spectrometer is varying.

The spectral shape of the filter function of the optical filter can be measured in lab. One or many filter functions can then be incorporated into the synthesizing if needed. The optimal strength for each filter function is then found by the non-linear algorithm. It has been observed that the strength of the filter function is dependent on if the filter is slightly tilted, which is many times the case when doing field measurements. This is taken care of by fitting the strength of the filter function. It has also been observed that the shape of the filter function is temperature dependent. This has been taken care of to a first degree by heating the filter in the lab to 30K above room temperature and dividing the measured filter function with the filter function measured at room temperature. This deviation is then also included as a filter function where the strength is decided by the non-linear algorithm. This temperature dependence is quite severe since the filter is usually exposed and thereby heated by concentrated sunlight. Due to the mentioned problems, it has most times been decided that optical filters should not be used.

The filter functions should be given as transmittance and can be provided to the program as Galactic SPC files or OPUS files in any desired resolution. The resolution of each filter function is converted to the same resolution as the measured spectra with linear interpolation. The weight of each filter function is decided by the non-linear algorithm and is then multiplied by the synthesized low-resolution spectra.

6.2.12 Measured references – Part 16

When the study of localized emission sources at ground level is the prime focus, the upper atmosphere is of no interest. However, with the SOF method the influence of

30

Page 41

the upper atmosphere will always be present. This can be a problem if there are strong absorption structures overlapping with the absorption structures of the molecules of interest. One approach that is sometimes used to solve this is to find a match for all the spectral properties, by simulating an atmosphere with many layers and determining concentrations in each layer. This is difficult to do when working at low resolution due to the limited amount of information in the measured spectra. Another approach is to measure a spectrum at a place where one can assume that the concentrations are zero of the compounds that one wants to study. This spectral measurement then represents the sky and is included in the spectral evaluation where the weighting of the spectrum representing the sky is decided by the spectral evaluation. The fitting of the weight makes the measurement of the sky usable even if the path length through the atmosphere varies. If the sky spectrum is evaluating itself in the spectral evaluation, all other compounds will evaluate to zero since it represents a perfect fit. This method is not limited to one measurement of the sky but any number of measured spectra throughout a day can be used as sky references. These points are thereby forced to give zero alkane concentration. By choosing a few sky references throughout a day where it can be assumed that the alkane concentration is zero, it has been observed that an efficient removal of the influence of the upper atmosphere can be done. However, this method will cause errors in the retrieval if any of the chosen references have nonzero alkane concentration and should therefore be used with care. A strategy that has shown to give reasonable results is to start the measurements at a clean place and then drive into the contaminated area. The scan should if possible also be ended at a clean place. The first measured spectrum is then taken as the sky. If this is not enough to remove the influence of the upper atmosphere, the last measured spectrum is also taken as a reference. This also has the benefit that time variations occurring in the atmosphere during the traverse can to a first order be simulated by the weighted superposition of the first and last spectra.

6.2.13 Non-linear search algorithm – Part 17

The input to the non-linear search algorithm is the residual from the last guess. The outputs are the weights to all the selected compounds and polynomial in part 6, 14, 15 and 16. The guessed squeeze factor is also output to part 8 if fitting of the squeeze is selected. The step taken in the next iteration is given by finding the best least square solution of the vector x r to the following equation system:

r

$$\mathbf{A}\mathbf{x} = \mathbf{r} = \log \frac{T_{measured}}{T_{synthesized}} \quad (6.$$

The last identity is the same as equation 6.4. The equation is solved in the code by an implementation of the Householder algorithm. The equation requires some further explanations:

$$\mathbf{A} = \begin{bmatrix} | & | & & | \\ \mathbf{a}_1 & \mathbf{a}_2 & \dots & \mathbf{a}_n \\ | & | & & | \end{bmatrix} \quad (6.$$

Page 42

$$\mathbf{a}_i = \log \frac{\mathbf{T}d_{synthesized}}{dx_i} \quad (6.$$

$\mathbf{T}_{synthesized}$ is the synthesized spectra from last iteration. $\mathbf{T}_{measured}$ is the measured spectr

$\frac{\mathbf{T}d_{synthesized}}{dx_i}$ represents the change in the total synthesized spectra if the weight x_i is changed.

Equation 6.5 is then solved so that the values of x_i are determined. The solved values of x_i are then multiplied by 0.9 and added to the weights that were used in the last iteration. An approximate solution is often found after just two iterations. The iterations are forced to stop after 100 iterations or if the last solution caused a higher RMS error than the previous guess.

To make the algorithm more stable and to speed up evaluation, a linear solution is always first calculated and is used as the first guess in the non-linear search. The non-linear search can also be completely skipped if the concentrations of the studied compounds as retrieved by the linear method are lower than a threshold defined by the user. In this way, the results from the faster linear method will be used if the concentrations are low, and the results from the non-linear method will be used if the concentrations are high. This is motivated by that non-linear effects typically become important when absorptions are strong.

The linear method is based on a variation of the non-linear code. The columns of the A matrix in equation 6.6 is instead built one at at time by simulating a spectra with the same code but only with one weight set to nonzero and the others set to zero. The synthesized spectrum is not converted to transmission in part 9 but takes another route through a linear resolution converter that does not simulate side lobes. The

production of side lobes is a non-linear effect and cannot be considered when doing a linear fit. The polynomial, filter function and measured references from part 14, 15 and 16 are instead treated as absorbance. Equation is then replaced with the corresponding equation:

$$\vec{xA} \cdot \vec{r} = -\log\left(\vec{r}_{T_{measured}}\right) \quad (6.$$

The vector $\vec{x}$ representing the weights of the compounds is found by finding the best least square solution. The values of $\vec{x}$ are taken as the first guess for the non-linear search algorithm. The fitting of the squeeze factor is highly non linear and the squeeze-factor must therefore be forced to a default value chosen by the user when finding the linear solution. The default value will also be the first guess for the squeeze factor in the non-linear search algorithm.

6.2.14 Non-linear fit of the squeeze factor

The search for the best squeeze factor is slightly different. First guess for the squeeze factor is given by the default value chosen by the user. A perfect, undistorted spectra, corresponds to a squeeze factor of 1. The result is highly dependent on the choice of the first guess since there is a risk that the algorithm finds a local minimum instead of

Page 43

the best solution. The diagram in Figure 16 describes the search algorithm. It first makes two iterations for the non-linear fitting to get a good first guess for the concentrations. It then tests if lowering or increasing the squeeze will cause a better fit to the measurement. After it has found the optimum squeeze for the current set of guessed concentrations it retrieves new guesses for the concentrations by making just one iterative step in the non-linear algorithm. This continues until no better solution is found.

Figure 16. The diagram describes the algorithm used for finding the best squeeze.

6.3 Mathematical presentation of the algorithm

In section 6.2 all the blocks of the spectral evaluation algorithm was presented in detail. The algorithm implements some new ideas that are more clearly presented with equations, which here will follow. The linear solver can be described with the following method:

$$\ln\left(\vec{T}_{measured}(\nu)\right) - DC + BA + \quad + \quad = residual \qquad (6.$$

$$A = \sum_i w_{sky,i} \cdot \ln\left(\vec{T}_{sky,i}(\nu)\right)$$

$$B = \sum_j w_{filter,j} \cdot \ln\left(\vec{T}_{filter,j}(\nu)\right)$$

$$C = \sum_k w_{ref,k} \cdot \sigma_{ref,k}(\nu)$$

$$D = \sum_{l=0} w_{polynomial,l} \cdot \nu^l$$

$\vec{T}_{measured}$ is the measured spectra.

$\vec{T}_{sky,i}$ are the selected reference measurements that are used to eliminate the atmosphere.

$\vec{T}_{filter,j}$ are the transmission functions of the optical filters (optional).

$\sigma_{ref,k}$ is the cross sections for the molecules that one wants to quantify.

The linear system is then solved by selecting the weights $w_{sky,i}$ $w_{filter,j}$, $w_{ref,k}$ $w_{polynomial,l}$ so that the length of the residual vector is minimized.

Page 44

The non-linear algorithm can also be represented by equation 6.9 but with factor C replaced with the factor F here described:

$$\ln\left(\vec{T}_{measured}(\nu)\right) - DF + BA + \quad + \quad = residual \qquad (6.$$

$$F = -\ln\left[Distort\left[\exp(-)C\right]\right]$$

where *Distort* is an operator that represents the distortion in the spectra due to instrument line-shape factors, the incidence angle of the light, and the side lobes. These effects should be simulated in the software and applied to the synthesized spectra. These effects are weak for spectra with smooth properties, and has therefore

little importance for the smooth structures in the filter function and the polynomial.

6.4 Validation of the spectral algorithm in QESOF

The results of the spectral fitting algorithm has been compared and verified with the results retrieved from other software, a Classical Least Square (CLS) method in the Grams software [32] and the non-linear NLM4 software developed by Griffith [19]. Comparisons were also done with a software used for FTIR measurements of volcanic gases by INGV (Istituto Nationale di Geofisica e Vulcanologia) [18], where the spectral evaluation of QESOF showed a very good agreement with the INGV results.

Figure 17 shows a comparison between the QESOF, NLM4 and CLS. The comparison was done on the total alkane concentration in a traverse done with a mobile solar occultation system outside a refinery. At the point of maximum concentration, the figure indicates that the values from QESOF are very similar to the NLM4 code and 10% higher than for the CLS code. The discrepancy towards the CLS algorithm is understandable for two reasons. First, since the CLS is a linear algorithm it underestimates the concentrations at high values. Second, close examination at the points of maximum concentrations shows that evaluating a mixture of propane and butane gives a much better spectral fitting to the measured spectra and this should therefore also give a higher total alkane mass.

The parameters used in the evaluation are the same as the standard parameters in the refinery application but with the addition that an optical filter was used in the set up. This was compensated for in the evaluation by adding two filter functions representing the filter to the evaluation in the QESOF and NLM4 evaluation. In the NLM4 evaluation, the filter functions were treated as external absorption spectra to be included in the evaluation. For the CLS evaluation, no filter function for the filter was provided to the evaluation. For NLM4, and CLS, Fourier-transforming was done with OPUS. For QESOF, Fourier-transform was done with the internal code. In all cases were no zero-fill and Norton-Beer strong apodization chosen. For the QESOF and NLM4 evaluation the evaluated alkanes were propane, butane and octane while butane was the only alkane included in the CLS evaluation.

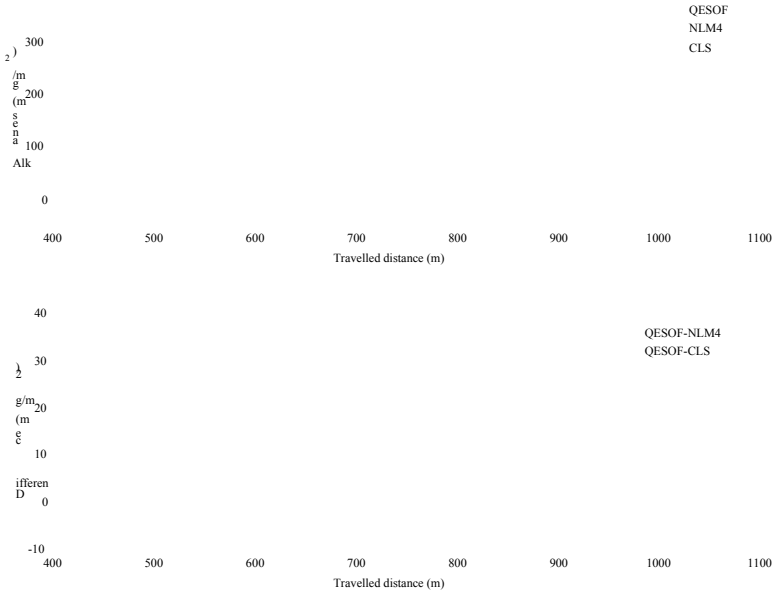

Figure 17. Comparison between three spectral algorithms when evaluating total alkane concentration in a traverse done with a mobile solar-occultation system outside a refinery. The results from QESOF and NLM4 are coinciding over almost the whole scan in the upper picture.

Figure 18 shows comparisons between the QESOF code and the INGV code when evaluating SO_2 and HCl from emissions from the Etna volcano. For the INGV data presented in the figure, a bias of 6 mg/m2 in the HCl concentrations and 118 mg/m2 has been subtracted to force the baseline to zero. There is no bias present in the QESOF results. This indicates that the inclusion of a "sky" reference is able to eliminate the influence of the atmosphere without distorting the measurements of SO_2 and HCl. For the QESOF results, the two isotopes ^{35}HCl and ^{37}HCl were retrieved separately and then added to get the total concentration of HCl. For the QESOF code, fitting of the stretch parameter was used and no zero-fill was used. Apart from the sky reference, H_2O, CH_4, O_3 and N_2O were also fitted.

Page 46

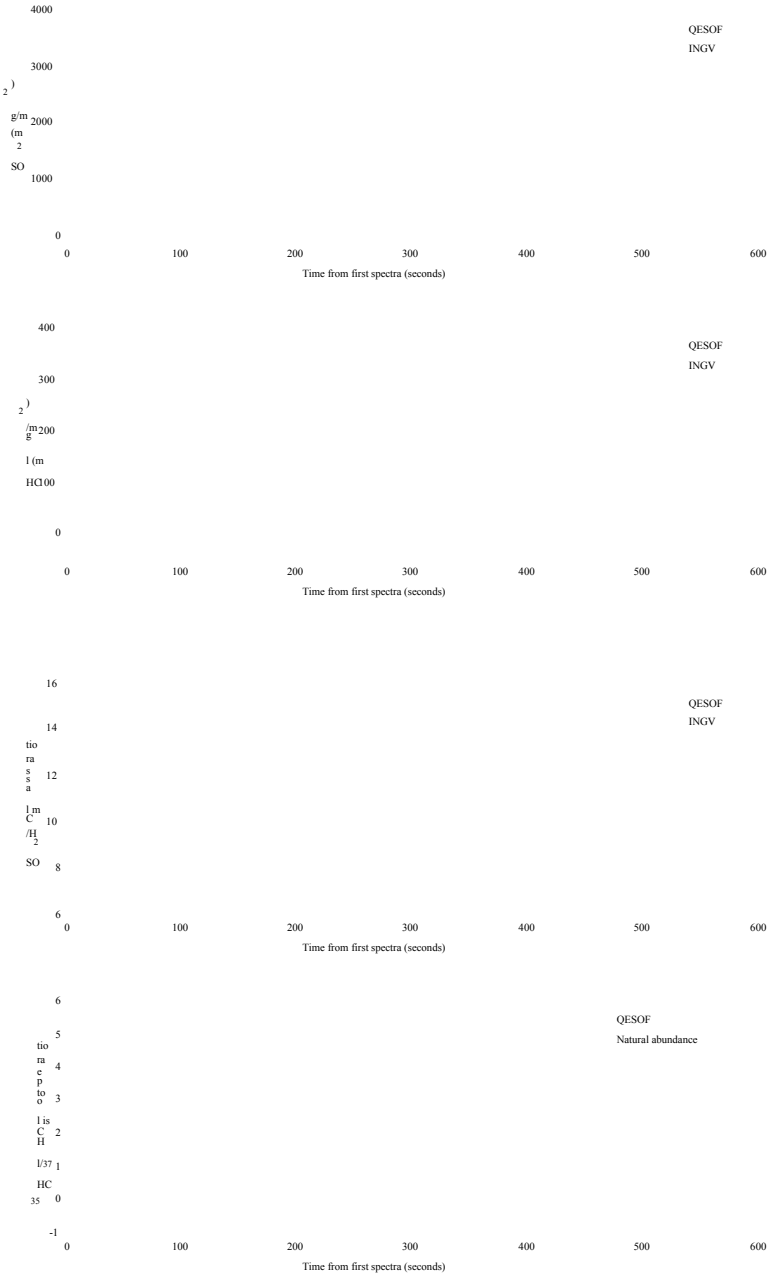
QESOF
INGV
Time from first spectra (seconds)
QESOF
Natural abundance

Figure 18. Comparison between the QESOF code and the INGV code for a traverse done with a mobile solar-occultation system 17 km away from the Etna Volcano on Sicily. The selected "sky" reference for QESOF is taken 570 seconds after first spectra and is indicated with a star.

7 Measurement of VOC from refineries

In the appended **Paper A** the method and the essential results from the monitoring project on the refineries are presented. Some additional information and some more examples of interesting measurements that did not fit in the paper are given in this chapter.

7.1 More on spectral evaluation of alkanes

In **Paper A** it is concluded that most of the VOC emitted from refineries is in the form of alkanes. A spectroscopic approach was therefore chosen for the refinery measurements that measure the emission of total mass of alkanes in the emitted gas. Measuring the total mass of alkanes independent on the exact alkane compound is possible with low resolution FTIR in the 3.3 μm region since the absorption occurring in this region is specific for the vibration/rotation occurring in a bond between a hydrogen atom and a carbon atom. The SOF instrument is sensitive to the alkanes shown in Figure 19. The figure shows the transmission structures for these alkanes. A transmission below one indicates that absorption has occurred. When measuring at a spectral resolution of 8 cm^{-1} it is difficult to resolve the individual types of alkanes from each other since their spectral shapes are overlapping and similar in shape to each other. However, the absorption strength is approximately proportional to the number of C-H bonds in the molecule. In addition, the molecular mass of an alkane is approximately proportional to the number of C-H bonds in the molecule. Absorption strength will therefore be approximately proportional to the mass of alkanes.

The time it takes to retrieve a spectrum with the FTIR-spectrometer grows with the square of the resolution. Measurements can therefore be performed much faster if performed at low spectral resolution. Alkanes have wide absorption structures and this makes it possible to use low spectral resolution for the quantification. For the measurements on the refineries, it is important that measurements are taken with a high repetitive speed because it is advisable that a traverse is done within a short time so that the local wind direction is kept the same during the whole traverse. Therefore a relatively low resolution of 8 cm^{-1} has been chosen since it has shown to give the highest repetitive speed in the measurements without loosing the capability to identify the average number of carbon atoms in the measured alkane. Spectra are measured

with a repetition of 3.2 seconds. When doing leakage search inside the industry area the distance between measurements need to be short in order to be able to identify the source of a registered emission. Therefore the car is then driven at approximately 10 km/h. When measuring total emissions from a whole industry at a far away distance of approximately 1 km, the car is driven at approximately 40 km/h. The car should not be driven slower than this in order to avoid that the local wind direction changes during the traverse.

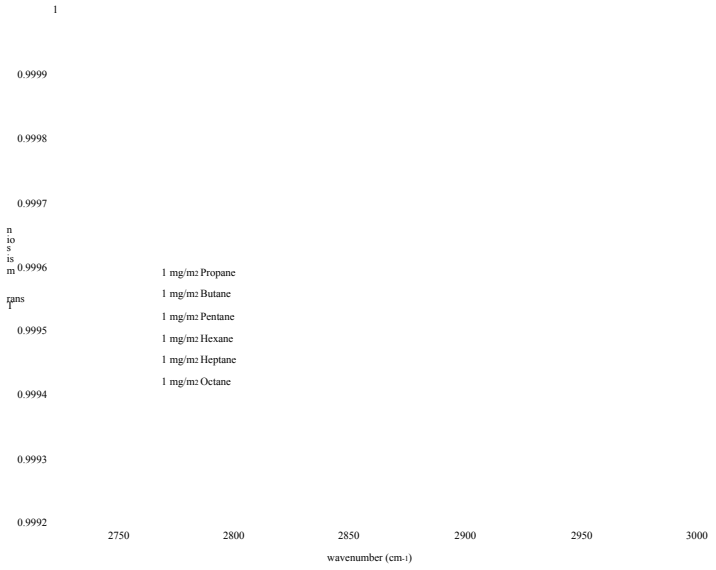

Figure 19. The picture shows the transmission for 1 mg/m$_2$ of the alkanes. The shown spectral region is the same as the region where the spectral fitting is performed. The spectral resolution shown has been degraded to the same resolution as for the measurements.

7.2 More on determination of carbon count number

It was realized that the kind of alkane observed in the SOF-measurements is an indication of the origin of the gas. If propane, butane and octane (with respectively 3, 4 and 8 carbon atoms in the molecule) are simultaneously included in the spectral fitting, the average number of carbon atoms in the measured alkane can be calculated by the following equation:

$$C_{avg} = \frac{3 \cdot m_{propane} + 4 \cdot m_{butane} + 8 \cdot m_{octane}}{m_{propane} + m_{butane} + m_{octane}} \quad (7.$$

where m stands for the line integrated mass concentration of each compound. Typical observed carbon count numbers were 3.7 for crude-oil tanks, 4 for gasoline tanks, 6 for kerosene tanks, 5 for process and 6.5 for the water treatment facility. An example of how this was determined is shown in Figure 20 where the measured alkane plume and the calculated average carbon count for a water treatment facility is shown.

To evaluate propane, butane and octane simultaneously thus give valuable information but is done at the expense of more noise in the baseline i.e. registered alkane concentration even though no alkanes can be expected. A more sophisticated method has therefore been used that first evaluates the spectrum as butane only. If the evaluated butane concentration is higher than 12 mg/m2, a new spectral evaluation is done with propane butane and octane. The sum of the three is taken as the total concentration of alkanes and is sensitive to the presence of all alkanes since other alkanes have spectral absorption structures similar to these three.

Page 49

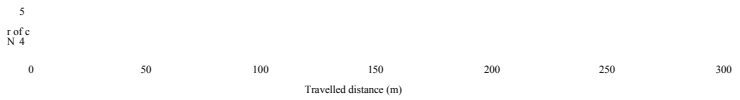

Figure 20. The figure shows the measured concentration of alkanes in a traverse of the plume from a water treatment facility (Preemraff-Göteborg, day 040910, time 15:13). When located in the plume, the average number of carbon atoms can be calculated and used for determining the source of the gas emission. Observe that only butane is evaluated when the alkane concentration is below 12 mg/m$_2$ and the average carbon count is then 4.

7.3 More on the parameters for spectral evaluation

Table 5 and Table 6 show the parameters that have been used with the QESOF software to retrieve the total alkane concentration in the measurements on the refineries. Is has been observed that some of the nonlinear effects due to the strong absorption lines of atmospheric H_2O, CH_4 and HDO can be removed if the square-root of the absorption spectra of compounds are also fitted. The square-root of the absorption spectra have been created by changing the line-strengths in the HITRAN database to the square root of its original value. This approach is valid since the aim is to remove the spectral structures of the species and not to evaluate the column values.

Table 5. The following table summarizes the standard parameters used for the spectral fitting of the alkanes in the KORUS-project.

Wavenumber interval	2725-3005 cm^{-1}
Resolution	8 cm^{-1}
Nr of averaged interferograms per sample 16	
Apodization	Norton-Beer Strong
Fitting of a linear polynomial.	
No fitting of the spectrum stretch.	

Table 6. The gases included in the spectral fitting for the standard parameters in the KORUS-project.

Gas	**Temperature (K)**	**Pressure (atm)**	**Database**
H_2O	283	1	HITRAN ([12])
H_2O	253	0.5	HITRAN
Square root of H_2O	273	1	HITRAN
CH_4	253	0.5	HITRAN
Square root of CH_4	273	1	HITRAN
HDO	253	0.5	HITRAN

Square root of HDO	273	1	HITRAN
Propane	298	1	PNW ([33])
Butane	298	1	PNW
Octane	298	1	QAsoft ([34])
Reference	-	-	Typically first measured spectrum in a traverse. See section 6.2.12.

7.4 More on calculation of the yearly averages

Paper A describes how total measurements and sub-sector measurements are done. Daily averages of emission are calculated for all total measurements and sub-sector measurements done on the same day. During one year, total measurements on an industry were typically collected on four days and close measurements on each sub-sector were done at least on two days. Low variation in the measured emissions over a day is an indication of high quality in the measurements that day and that no exceptional activity was taking place at the industry on that day. A day with low variation of the total emission over the traverses during the day should therefore be more important when determining the total emission during that year. The main purpose of the measurements in the KORUS project was to determine emissions when the refinery was running under normal conditions. Therefore, the daily averages of the emissions for all days during a year are averaged in such a way that the weight of the average of a day is inversely proportional to the standard deviation among the traverses during that day. This will lead to that a day with low variation of the emission over the traverses will be more important when determining the total emission during that year.

7.5 Examples of unexpected emission sources

When a traverse was done to the north-most corner of Preemraff-Lysekil one day in 2004 a new emission source was by coincidence discovered that was identified to be the rock cavern exhaust. When this was discovered, the old measurements from 2003 were reevaluated to try to find signs of emissions source at the same place but no emissions was then found. However, it is possible that the source was completely missed in 2003.

Another unexpected source was found while measuring on the same refinery in summer 2004. It was discovered that the preskimmer was a significant point source. The preskimmer is a part of the waste water treatment system. It is constructed as a sewer with a filter where large debris is removed from the water before it gets to the waste water facility. From old measurements from year 2003, a few measurements could be retrieved but these measurements do not have as high quality as from year

2004. However they indicates clearly that the preskimmer had lower emissions year 2003. In year 2003 another unexpected emission source was found in the corner of the crude-oil tank park on Preemraff-Göteborg and were identified to be a sewer. However, in year 2004 almost no emissions were found from the sewer. There were no measurements found from year 2002 that indicated emissions from the sewer. However, emissions from the sewer were not anticipated then and may therefore have been missed.

7.6 Examples of observed changes in the emissions

Shellraff had a routine total maintenance stop in year 2003 and the refinery was restarted two weeks before the measurements started. Figure 21 shows the change of emissions from the hysomer[1] and process during year 2003 and 2004. The reason for the reductions in emissions is believed to be that process-equipment was leaking after the total maintenance stop and the leaking equipments were later found and repaired. In August-2003 there is a drop in the hysomer emission that can be explained by three documented repairs that have been done because leaks were detected. Between August-2003 and May-2004 there is a drop in the emission from the process that can be explained by seven documented repairs that have been done because leaks were detected or because of equipment breakdown. These measurements gave new insight of the emission picture after a total maintenance stop. The measurements showed that the emission picture returned to normal within less than a year. This would not have been detected if measurements were only done every third year, as was the routine before on the refinery. Thus, measuring every year has shown to give new valuable information. The relatively low cost of the method motivates that routine measurements should be done every year on the refineries in order to quickly detect changes in the emission picture.

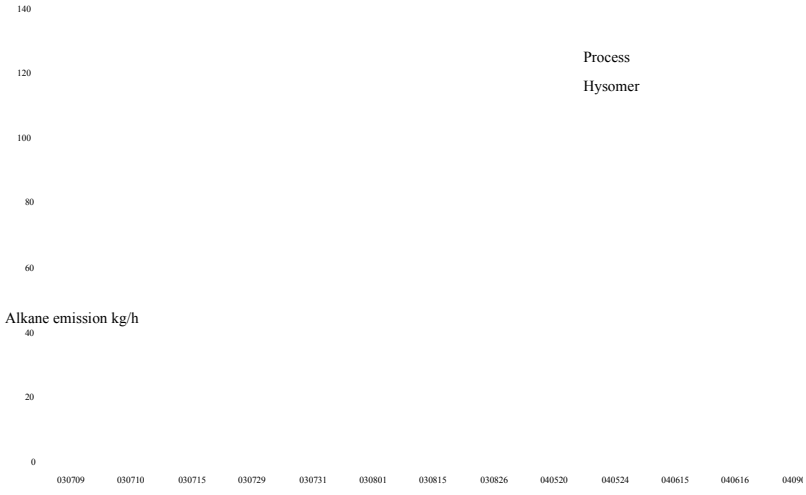

Figure 21. The figure shows the change of emissions from process and hysomer. Notice the drop in hysomer emission after 1-August-2003 and the drop in process emission after 26-August-2003.

[1] Hysomer is an abbreviation for hydro-isomerisation and is a part of the process where normal and mono-branched paraffins are converted into higher branched (high octane) components.

Measurements on the flare were done on day 14-July-2003 during 1.5 hours by driving back and forth about 50 meters in such way that the sun-ray traversed the flare. This resulted in 73 traverses and the average of all traverses were 15 kg/h. Figure 22 shows the variation over the whole set of traverses. The emission is higher than what has been observed on other measurements. After the total maintenance stop earlier year 2003, there was an error in the control of the flare that caused it to pulsate. This can probably explain the high measured emission. The problem with the flare was fixed later in year 2003.

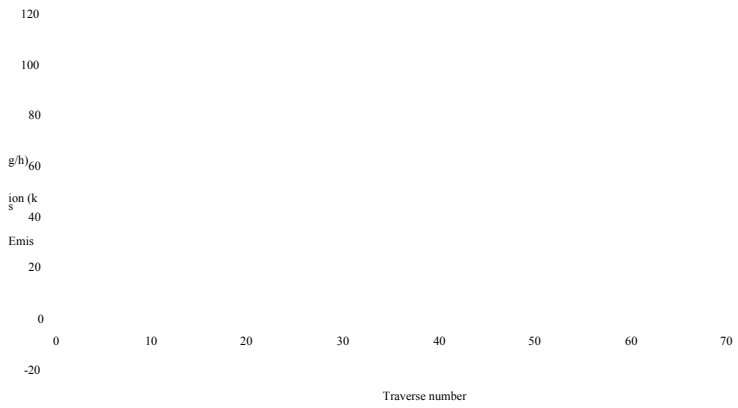

Figure 22. Results of individual traverses to measure the emission from the flare.

During day 8-June-2004, traverses for measuring total emissions were done along Oljevägen. It was quickly observed that emissions were much higher than normal. The measurements indicated a strong emission source inside the west tank-park. Measurements were then done inside the west tank-park and the point source was identified to be tank 105 containing residues of water mixed with oil. This was immediately reported to the personnel-in-charge. After investigations, it was found out that the tank-roof was tilting. This was fixed just a few hours later. Table 7 shows the total measurements done along Oljevägen before the roof was fixed. Total emissions should be compared to the average emission for 2004 that were 122.1 kg/h.

Table 7. Results of individual traverses on day 8-June-2004 when the roof of tank 105 was tilting.

Time	Total emission Shellraff (kg/h)	Tank 105 (kg/h)	Wind speed (m/s)	Wind direction
12:45	1490		5.0	36°
12:55	541		4.6	59°
13:15	691	126	4.7	44°

13:25	830	186	4.5	39°
13:40	199		3.3	55°
13:50	714		3.9	39°
14:10	633		3.1	42°

Crude oil tank 1406 on Preemraff-Lysekil was of special interest since earlier measurements with the DIAL method had shown high emissions from this tank and it was known that the floating roof on the tank was not tight. Before year 2003 a second

seal was built around the tank-roof in hope that it would decrease the emissions. Figure 23 shows how the emissions were still high in 2003 after the second seal was fitted but much lower in 2004. No construction changes or maintenance work was done with the tank between 2003 and 2004. However, the type of crude oil in the tank changed from 2003 to 2004. It is possible that this is the cause for the reduction in the emissions.

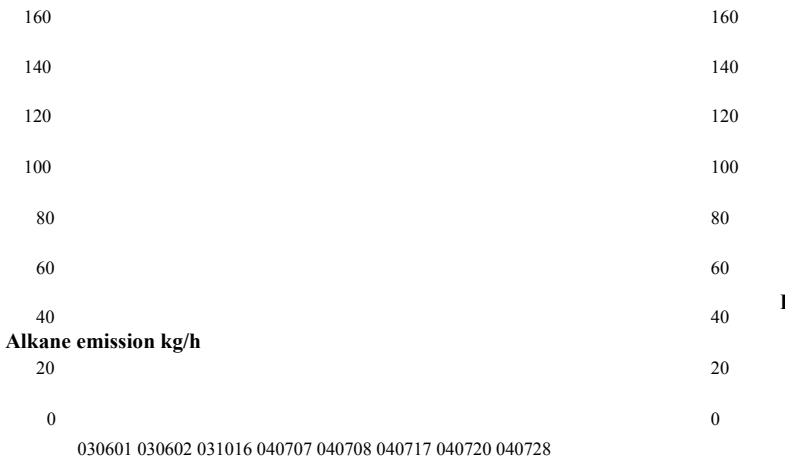

Figure 23. The figure shows the change of emission from crude-oil tank 1406. The crude-oil type changed from a mixture of Gullfaks A&C and DUC in 2003 to 100% DUC in 2004. The tank-roof level was at top on all days except 8-July when it was at 70% and 20-July when it was low.

7.7 The mobile wind meter

A new method was tested to measure the local wind speed at ground level where an ultrasonic wind meter was mounted in the front of the measurement car, see Figure 24.

The true wind was then calculated by subtracting the velocity vector for the car from the measured wind vector. The resulting wind vector is then averaged over 60 seconds to get an average wind. The speed of the vehicle was either measured by a speedometer mounted on one wheel on the car, or by differentiating the GPS positions. The driving direction of the car was determined by differentiating the GPS positions. According to the manufacturer of the wind-meter (Waisala), the WAS425 has an error of ±0.135 m/s (0.3 mph) or 3% whichever is greater, up to 144 mph. This is a very good precision for a wind meter.

An experiment was conducted by Jerker Samuelsson in our group, in order to

Figure 24. The ultrasonic wind meter.

validate the method. This was done by driving at different speeds on a straight road and simultaneously measuring the wind-speed and wind direction with a traditional wind-meter located 3 m above the surface. Figure 25 shows a comparison where the wind speed was varying and shows good agreement with the fixed wind-meter at high wind speeds.

It was found that this method was not usable at wind speed below 3 m/s or at driving speeds above 5 m/s. However, at strong winds or low driving speed, the method was giving useful information. When measuring the emissions from the water treatments on the refineries, where the plume is located close to ground, the wind information from this method was commonly used.

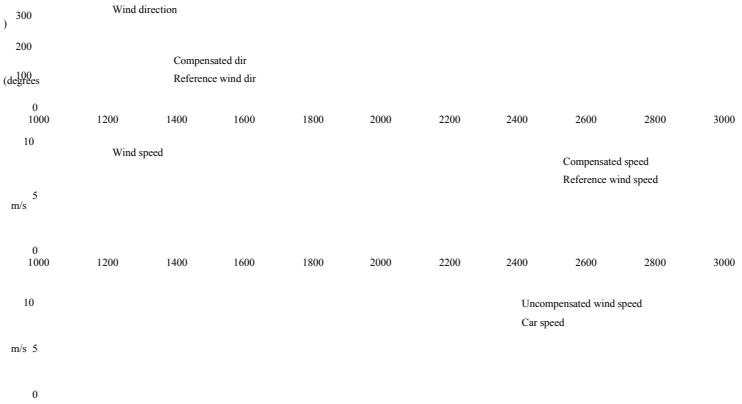

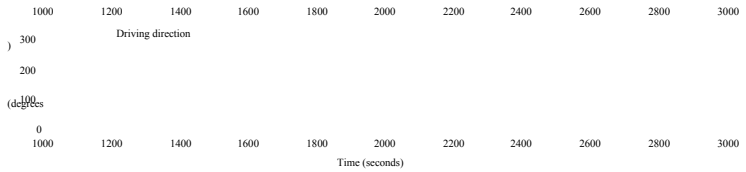

Figure 25. The two top figures shows the compensated wind speed and wind direction and the wind measured with the fixed wind meter.

Page 55

7.8 Conclusions on VOC measurements

This chapter and **paper A** makes some general statements on the alkane emissions from the four industries based on the collected data. The alkane emission was divided into five groups and compared between the industries. Table 8 shows the emission from these five groups and also the total emissions of alkanes measured on the four industries. The annual throughput of refined crude oil is 10 Mton/y for Preemraff-Lysekil, 5 Mton/y for Shellraff and 3 Mton/y for Preemraff-Göteborg. Reflecting this, the emissions have been normalized to annual throughput in Table 9 to give the emission in each sector as ton alkanes per Mton refined crude oil.

Table 8. Summary of the measured emissions of alkanes from the four industries. First number in parenthesis indicates number of measurement days. Second number indicates total number of traverses.

Emission each year (ton/y)	Preemraff-Lysekil	Shellraff-Göteborg	Preemraff-Göteborg	Oil Harbour

Total 2002	4818 *(2, 22)*	3051 *(4, 19)*	3464 *(3, 13)*	1771 *(2, 11)*
Total 2003	4818 *(2, 22)*	3051 *(4, 19)*	2014 *(3, 27)*	1771 *(2, 11)*
Total 2004	4704 *(5, 42)*	1070 *(3, 18)*	2683 *(6, 38)*	1788 *(4, 15)*
Averages all years (ton/y)				
Total	4760 *(7, 64)*	2060 *(7, 37)*	2720 *(14, 78)*	1780 *(6, 26)*
Process	760 *(6, 23)*	930 *(12, 140)*	610 *(7, 54)*	0
Crude-oil tanks	1470 *(8, 93)*	410 *(9, 61)*	1000 *(10, 66)*	0
Product-tanks	2080 *(16, 115)*	260 *(7, 39)*	940 *(14, 78)*	1115 *(6, 26)*
Water treatment Facility	140 *(6, 32)*	390 *(7, 37)*	160 *(7, 91)*	0
Transport related activity	240 *(2, 17)*	80 *(3,11)*	0 (1)	665 *(12, 60)*

(1) Transport to/from Preemraff-Göteborg is only done through pipelines to the oil harbour.

Table 9. Normalized alkane emission in ton per megaton refined crude oil.

	Preemraff-Lysekil	Shellraff-Göteborg	Preemraff-Göteborg	Average
Process	76	186	203	155 (26%)
Crude-oil tanks	147	82	333	187 (31%)
Product tanks	208	52	310	190 (32%)
Water treatment facility	14	78	53	48 (8%)
Transport related activity	24	16	0	13 (2%)
Total (ton/Mton)	476	412	907	598

Thus for a typical refinery, about 0.06% (598 ton/Mton) of the mass of the crude oil is lost due to vaporization to the atmosphere. Of the emitted gas, 26% originates from the process, 31% from crude-oil tanks, 32% from product tanks, 8% from the water treatment facility and 2% from transport related activities. As transport related activity was counted loading/unloading to/from ships and trucks inside the industry areas. Transport related activities are typically intermittent and are therefore difficult to quantify. Therefore, this value has a high uncertainty.

8 Error estimation

This chapter gives a detailed error estimation of the calculated yearly average emissions for the industry measurements due to the limitation in measurement time, spectral errors and wind properties. A much shorter and less detailed version of this chapter is presented in the end of **paper A.**

8.1 Errors due to limitation in measurement time

One aim of the measurements is to make an estimation of the total emission from a refinery during a whole year. Since total measurements have only been done on two to six days within a time-span of a month, it must be assumed that the emissions on those days can represent the average emission the whole year.

Since year 1972, the U.S. Environmental Protection Agency (EPA) has contracted an extensive study to determine the parameters that decides the emissions from organic liquid storage tanks [35]. The results show that emissions from tanks with external floating roofs are increasing with the wind speed [35]. It also shows that emissions from fixed roof tanks are dependent on the level of the liquid surface in the tank. For floating roof tanks, it has also been observed that emissions increase when a tank is emptying i.e. when the roof is on the way down. Emission from all tanks is also dependent on vapor pressure of the stored liquid and is therefore also dependent on the liquid temperature. Emission is also dependent on outer temperature and therefore varies slightly with the seasonal variation. Equations to calculate the dependence from all these factors are presented in [35] but reliable results are dependent on that correct parameters for each tank is determined.

Thus, this dependence is complicated and the parameters for the EPA equations must more or less be determined for each tank individually. It has been outside the scope of this project to try to compensate the measured emissions to the winds, tank-roof heights and liquid temperature that was present during the days when the measurements were performed. All calculated emissions are therefore presented without compensations to these variations over the year.

If using the strategy of measuring each tank individually during a short time, and then summing the measured emissions from all tanks to determine the total emission from a tank-park, each tank must be compensated for the factors mentioned above individually, to give a reliable total emission estimate. This approach has previously been used with the DIAL method. However in the KORUS project, the whole tank-park is measured at once and the measurements are repeated on different days. It can then be expected that there is a variation in the activity between the tanks in the tank-park and also variations between days that will cancel out each other. This situation causes an average that is relevant for the emission of the whole tank park. The activity on each individual tank can then be neglected.

The variation of the emission from tanks due to changes in outer temperature has not been taken into account. For the DIAL measurements by Shell Global Solutions [36], correction factors for the tank emissions were applied that represented the changes of emission due to temperature variations over the year as calculated by the EPA model. Comparing this to the DIAL measurements and the temperature when the DIAL measurements took place, the correction factors for the tanks were determined to values between 0.91 and 0.99 depending on the tank-roof construction

and the content. Since the error is low compared to the total expected error, it has not been further considered.

VOC emission from a refinery can be divided into continuous emissions and intermittent emissions caused by short-term activities. On many occasions when higher emissions than normal was observed, it could be explained by short-term activities taking place inside the industries. If higher emissions than normal were found during a day and could be explained by short-term activity, then the measurements from that day were discarded. It is therefore believed that the average emission from all days will represent the continuous emission of the industry. For the cases where short term emissions were discovered, some sporadic tests were done afterwards to try to identify how big the emissions are in comparison to the continuous emissions. It has however become clear that a thorough study of this issue requires much more time and effort than what was available within this project. An example of one such study was done when an increased emission of 70 kg/h was measured a few hours after opening a tank for maintenance at Shellraff. Shellraff has reported that opening of a tank for maintenance work was done in the eastern tank park at 11 times during the period from summer 2003 to summer 2004. If assuming that the increased emission is maintained during 12 hours after opening the tank, then this will cause an increased emission of 9 ton/year. This should be compared to the average measured emission from the east-tank park of 146 ton/year for 2004. If the assumptions are correct then this indicates that the emission increase related to maintenance of tanks cause a 6% increase in the yearly emissions.

The impression gained during the project indicates that intermittent emissions correspond to 1-10% of the continuous emissions. To simplify the picture, the values presented later in this report correspond to the continuous emissions and do not include intermittent emissions on the industries. There is however a potential error source in that one may fail to detect a situation as intermittent, and the emission estimations will then be too high. Representatives from the industries with knowledge of the activities have been participating in the interpretation of the measurements in order to avoid this.

Since there are just a few measurement days each year, the situation is heavily under-sampled and there will be an error in the estimated annual emission due to this. The best dataset produced from the KORUS-project to estimate the variation of the continuous emission is probably five days of total measurements from Preemraff-Lysekil during July-September 2004. This dataset gives an average emission of 509.6 kg/h with a variance of 85.3 kg/h between the average emissions of the five days thus giving a standard deviation of 17% between days. It is possible that some of this variation is due to errors in the measurements but it is still safe to assume that the true variation in the total emission has a standard deviation of less than 17% between days for this case.

8.2 Spectral evaluation errors

Three different studies are presented to further describe the errors done with the chosen spectroscopy method. The first simulates the error in the spectral evaluation if the gas contains just one kind of alkane. The second simulates the errors on the gas-mixture of VOC that were measured with bag-samples in a crude-oil tank-park. The third investigates the baseline error due to imperfect incidence angle of the light into the spectrometer.

8.2.1 Error simulation of pure alkanes

Table 10 shows the total alkanes reported by the method if 1 mg/m2 of each alkane is present in the sample. A sample consisting of 1000 mg/m2 of water was also analyzed to check the sensitivity to changes in water concentration. The study has been performed by synthetically applying the transmission of each alkane/water to a measured sky spectrum and then evaluating the resulting spectrum. The standard parameters for the alkane evaluation were used including fitting of methane and water. The original sky spectrum were taken as the reference and included in the fitting. Spectra for ethane, pentane, hexane, heptane, octane and water were taken from the PNW database [33]. Spectra for methane, propane, butane and water were taken from the QASoft database [34]. The results show that the largest error (30%) for the non-linear method can be expected if the sample contains hexane. No cross-sensitivity to methane is observed. Methane is included in the fitting in both methods but the evaluated concentration is not included in the sum of the alkanes.

The non-linear method is more disturbed by water than the linear method. The total atmospheric water vapor column is typically in the range 1200 to 3600 g/m2 [37]. Therefore the change in water vapor concentration during a traverse is probably more than 1 g/m2. It is surprising to see a disturbance due to water since spectra for water at two different temperatures (283K and 253K) are included in the fitting. However, the water spectrum applied in the test was measured at room temperature. The spectral properties of water have strong temperature dependence in the used wavelength interval, and this is possibly the reason for the disturbance. This issue needs some further investigation.

Table 10. The table shows the interpreted concentration of total alkanes for a synthetically calculated spectrum that contains 1 mg/m2 of a single alkane or 1 g/m2 of water superimposed on a measured sky spectrum.

	Linear method Interpreted concentration of Butane (mg/m2)	**Non-linear method** Interpreted concentration of Propane, Butane and Octane and the sum of the three (mg/m2)
1 mg/m2 Methane	0.000	0+0+0=**0.00**
1 mg/m2 Ethane	0.195	0.032+0.087+0.157=**0.28**
1 mg/m2 Propane	0.825	1.027-0.007+0.020=**1.04**
1 mg/m2 Butane	1.004	0.101+0.847+0.065=**1.01**
1 mg/m2 Pentane	1.133	-0.006+0.801+0.431=**1.23**
1 mg/m2 Hexane	1.086	0.104+0.472+0.725=**1.30**
1 mg/m2 Heptane	0.861	-0.07928+0.187+1.0383=**1.16**
1 mg/m2 Octane	0.700	0.004-0.004+0.999=**1.00**
1 g/m2 Water	-0.106	0.041-0.118-0.107=**-0.18**

8.2.2 Error simulation of a typical gas mixture from a crude-oil tank

A field measurement was done where approximately 2 liters of gas were collected into two aluminum-coated bags from the west side of the crude-oil tank-park at Preemraff-Göteborg. The gas in the two bags was analyzed with a GC system by IVL (Swedish Environmental Research Institute) within two hours to determine the mix of different hydrocarbons in the sampled gas mixture. Table 11 shows the average retrieved fraction by molecules and the fraction by mass for each compound. The total fraction by mass was 98.5% for the alkanes, 1.1% for aromatic hydrocarbons and 0.5% for alkenes/alkynes.

Cross sensitivity calculations for the measured compounds has been carried out by Jerker Samuelsson in our group. Table 11 shows the cross sensitivity of each compound in a spectral evaluation of butane. For example 1 mg/m2 of pure ethylbenzene will be interpreted as 0.27 mg/m2 of butane by the SOF evaluation. The emissions presented in the KORUS-project are the estimation of emitted alkanes. However, it is possible that other compounds than the alkanes are interpreted as alkanes and therefore causes an error. To determine this, the cross sensitivity was multiplied with the mass ratios given in Table 11. It was found out that the cross sensitivity of the most abundant alkenes/alkynes and aromatics are low and therefore result in very low errors. In the sample gas-mixture, the alkenes/alkynes only causes an error of 0.07% and the aromatics an error of 0.06% in the spectral evaluation of alkanes. These errors are therefore neglected in the following discussions.

Table 11. Gas mixture of the emissions from a crude-oil tank-park obtained by collecting air in bags followed by GC-analysis.

Compound	Mixing ratio by molecules (%)	Mass ratio (%)	Cross sensitivity as mass of Butane
Alkanes			
Propane	38.78	32.50	0.98
n-Butane	20.28	22.41	1.00
Ethane	14.48	8.28	0.26
Iso-Butane	8.69	9.59	1.60
n-Pentane	6.20	8.49	1.01
Iso-Pentane	5.66	7.76	1.29
Decane	1.44	3.88	0.74
Hexane	1.12	1.82	0.94
2-Methylpentane 0.98		1.60	1.05
3-Methylpentane 0.47		0.76	1.02
Cyclohexane	0.45	0.72	0.21
n-Heptane	0.27	0.51	0.76
Octane	0.05	0.11	0.55
Nonane	0.01	0.03	0.42
Aromatics			

Benzene	0.09	0.13	0.00
Toluene	0.21	0.37	0.04
Ethylbenzene	0.06	0.12	0.27
1,2,4-TMB	0.11	0.24	0.00
1,3,5-TMB	0.01	0.02	0.00
M+p-xylene	0.07	0.14	0.03
o-xylene	0.03	0.05	0.10
Alkenes/alkynes			
Etene	0.10	0.05	0.02
Etyne	0.05	0.02	0.24
Propene	0.23	0.18	0.11
Iso-Butene	0.11	0.12	0.19
c-2-Butene	0.01	0.01	0.34
1,3-Butadiene	0.01	0.01	0.09
t-2-Pentene	0.01	0.02	0.00
c-2-Pentene	0.01	0.02	0.42
1-Butene	0.01	0.01	0.28
t-2-Butene	0.01	0.01	0.75
Propyne	0.01	0.01	0.27
Total:	100	100	

(TMB=Trimethylbenzene)

Page 60

The error in the spectral evaluation of a typical VOC gas-mixture was determined by a simulation, by creating a spectrum where absorption on the concentrations of the alkanes shown in Table 12 were applied. These have been set to the same concentrations that were measured with bag-samples in the crude-oil tank-park on Preemraff-Göteborg presented in Table 11. Reference spectrum for Propane and n-Butane were taken from the QASoft database [33] and the other spectra were taken from the PNW database [34]. The absorption was then applied to a measured solar spectrum and the resolution degraded to the same resolution as the measured spectrum ($8cm^{-1}$).

The spectral fitting of n-Butane represents compounds with similar absorption structures as n-Butane (iso-Butane, n-Pentane, iso-Pentane and to some degree n-Hexane). The spectral fitting of n-Octane represents compounds having similar broad absorption structures as n-Octane (n-Heptane, Cyclohexane, 2-Methylpentane, 3-Methylpentane and to some degree n-Hexane)

As can be seen in Table 12, the spectral evaluation overestimates the total simulated alkane-concentration with a factor 1.10 (231.1/210.4). Thus, the conclusion is that for a typical gas-mixture of hydrocarbons emitted from a crude-oil tank-park, the total mass of alkane in the gas-mixture will be determined with an error of **10%**. There is also an uncertainty in the spectral cross sections used that also contributes with an error of %10 .

Table 12. Concentration of alkanes in the error simulation.

Alkane compund	Simulated concentration (mg/m2)	Evaluated concentration (mg/m2)
Ethane	18.4	
Propane	72.3	97.1
n-Butane	49.9	114.6
Iso-Butane	21.3	
n-Pentane	18.9	
Iso-Pentane	17.3	
n-Hexane	4.0	
2-Methylpentane	3.6	
3-Methylpentane	1.7	
Cyclohexane	1.6	
n-Heptane	1.13	
n-Octane	0.24	19.4
Total:	**210.4**	**231.1**

8.2.3 Baseline error

When conducting SOF measurements, the flux is obtained by adding all columns above the baseline of the traverses. If the baseline drifts around, which was the case in many earlier measurements it will cause an error. The drift in the baseline occurs if the tilt of the path of the incoming light into the spectrometer is changed during a traverse. Changes in the tilt during a traverse is caused by imperfect aligning of the solar-tracker which causes the output angle to wobble around as the solar-tracker looks in different direction i.e. when the car is changing its direction or the sun moves over the sky. During the KORUS project, the solar-tracker has been under constant development. Therefore, this problem was big in the beginning but is almost not present at all with the latest version of the solar-tracker. Optical filter were also used

in earlier measurements but it was found that it also caused baseline drifts. The drift due to the filter could partially be compensated for in the software but it was later decided that optical filters should not be used so that baseline drifts were as much as possible avoided.

It was first believed that the broad structures of the alkanes would make the spectral evaluation almost insensitive to changes in the tilt of the incoming light. However, it was found out that since the stretch and smear effect also distorts the spectral lines of water and methane and since these have strong absorption lines overlapping with the alkanes in the spectral-evaluation range, it also disturbs the evaluation of the alkanes. It is difficult to completely compensate for this effect by fitting the stretch since the spectrum has a low resolution and single lines of water and methane are not resolved. The problem is not completely understood but is believed to be related to the big slant that is present in a solar spectrum around 2990 cm^{-1} due to that water in the atmosphere is absorbing strongly above this wave number, and that

this slant coincides with the slant in the spectral shape of the alkanes around this wave number.

Figure 26 represents a traverse with a high baseline error. The traverse in the figure was not used to determine the emission that day but the average from 9 other traverses gives an average emission of 170 kg/h. A baseline error of 10 mg/m2 over a traveled distance of 3000m and a wind speed of 5 m/s would have given an incorrect flux of about 150 kg/h and thus would have caused an error of 90% for that traverse. In the KORUS project, traverses with a baseline error of more than 3 mg/m2 have been manually rejected and this gives an upper limit for the error of 30%. The evaluation method relies on that the user selects a zero point on the traverse and the baseline error is thus dependent on the choice of the user. Especially for traverses with high noise, it is difficult to locate the zero-point with high certainty. It is however believed that the error will be Gaussian distributed and will thus decrease when taking average of many traverses in the same day. Typically, 10 traverses are averaged and the error for the average due to baseline errors will then reduce and become %5.9 = 10/%30 .

Figure 26. The figure shows the line-integrated concentration along a traverse. This shows a big baseline error since the concentration at the endpoint is evaluated to 10 mg/m2 in a location where no alkane concentration is expected.

8.3 Errors in the retrieved flux due to wind properties

Calculation of emission relies on information of how the wind varies over the whole surface where the gas is measured. Since this information is not possible to completely retrieve, errors in the calculated emission will be induced. In the

monitoring project, wind information was typically taken from a wind meter located 25 m above ground taking averages of wind speed and direction every 30 seconds. Since there are height variations both in wind speed and direction, there is a discrepancy between the wind at the position of the plume and the wind measured at 25 m. This error is difficult to determine since the height of the plume cannot be determined by the gas measurements.

A study of the errors due to the wind was made by looking at the variation in a dataset retrieved by a simulation of the micrometeorology model TAPM [38]. The data from the TAPM model simulations was provided by Lin Tang and Deliang Chen at Gothenburg University. Simulations were done for the time-span from 1st August to 30th September 2001 for three selected positions of relevance for the monitoring project. The used data from the simulation consists of wind speed and wind direction for every hour at 16 different altitudes between 10 and 1000 m and also the solar radiation at the surface.

For validation, the wind speed and wind direction retrieved for the TAPM model at an altitude of 100 m at the location of Oljehamnen was compared to the wind measured at Älvsborgsbron on an altitude of 100 m. The comparison is shown in Figure 27 and indicates a good correlation between measured wind and modelled wind.

Figure 27. Comparison between measured wind at 100m at Älvsborgsbron and modelled wind at Oljehamnen.

Page 63

Figure 28 shows the average solar radiation reaching the ground according to the model data between time 9:00 to 17:00 in the day. The days were grouped into three groups representing low, mid, and high average radiation during the day. The limits are shown by two tilting lines in the figure. Among the 61 days the distribution of the days in the different groups were according to Table 13.

Table 13. Number of days in each group. Sorted by average solar radiation.

Location	Low sun intensity	Middle sun intensity	High sun intensity
Oljehamnen	19	25	17
Risholmen	16	28	17
Preemraff-Lysekil	15	21	25

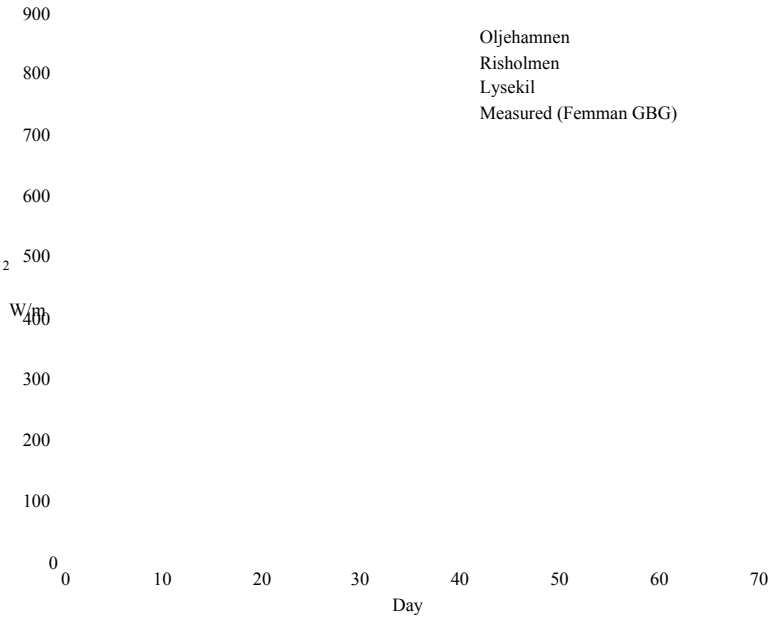

Figure 28. The average solar radiation reaching the ground between time 9:00 and 17:00 each day according to the TAPM simulations. Days are numbered with 1 starting on 1st August 2001. The vertical lines indicate days where SOF-measurements took place. The dashed line shows maximum intensity during a day measured at Femman in Gothenburg. The data from Femman was downloaded from Luftnet [39].

Usually, SOF measurements are only practically efficient during days with high sun radiation. The amount of turbulence in the lower troposphere is typically higher on such days, and this could potentially lead to stronger coupling between the wind speeds on different altitudes. Figure 29 shows as expected that the average difference in wind velocity with height is lower on days with high sun radiation. However the figure also shows that the variance in wind profile is stronger on sunny days.

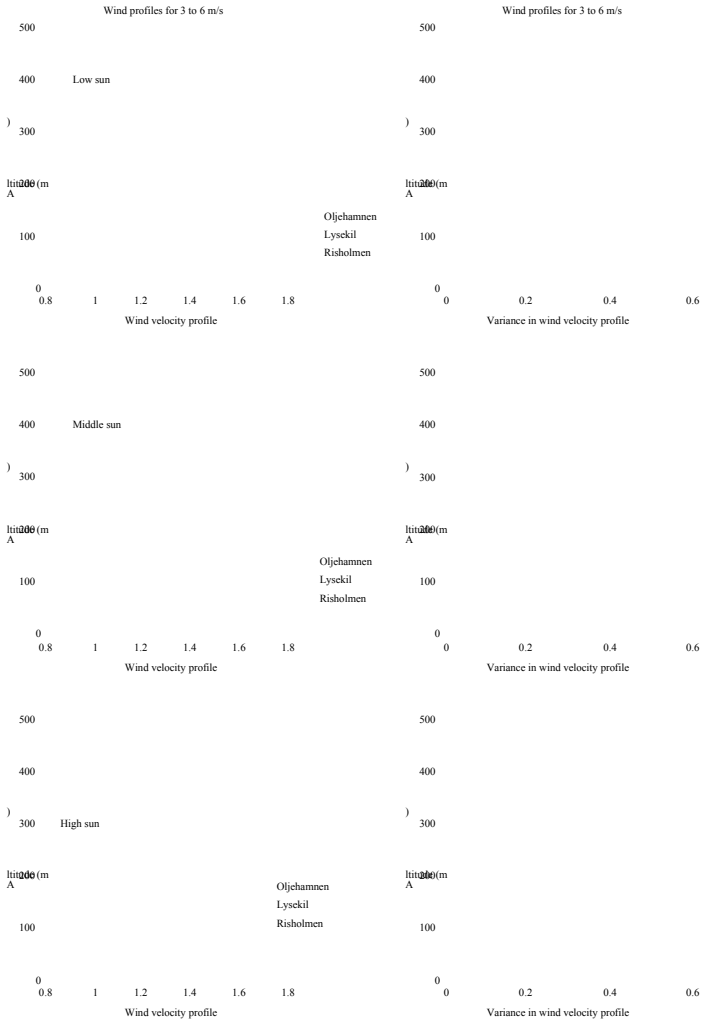
Wind profiles for 3 to 6 m/s
Low sun
Middle sun
High sun
Oljehamnen
Lysekil
Risholmen
Wind velocity profile
Variance in wind velocity profile
0.8
1
1.2
1.4
1.6
1.8
0.2
0.4
0.6
0
100
200
300
400
500

Figure 29. The averaged wind speed profile from all hours in a day between 9:00 and 17:00 when the wind speed at 10 meters were between 3 m/s and 6 m/s. Top figure shows average over days belonging to the low sun intensity group. Lowest figure shows average over days belonging to the high sun intensity group. Dotted lines shows log-profiles fitted to the lowest 7 data-points.

For simulating the error of a typical total measurement on a refinery, a case is simulated where a process and a tank-park is assumed to emit the same amount of VOC. It is assumed that the plume from the tank-park can be distributed anywhere between 0 and 100 m above ground with equal probability. It is further assumed that the plume from the process can be distributed anywhere between 100 and 300 m above ground. The wind data from all hours between 9:00 and 17:00 on days with

high sun-radiation and with a wind speed of 3-6 m/s at an altitude of 25 m are then selected. There are valid wind data on 25 days that fulfilled these criteria. Figure 30 shows the average wind profile retrieved by the selected data. The error bars show the standard deviation between daily averages.

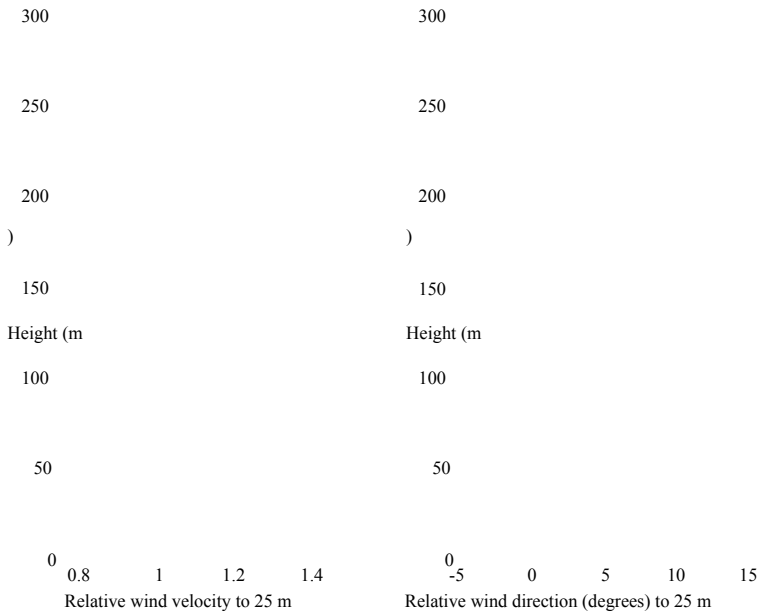

Figure 30. The figure shows the wind velocity and wind direction profile retrieved by simulation and averaged over daytime all sunny days with a wind-speed of 3-6 m/s at ground. The error bars indicate standard deviation between daily averages.

The selected data is then combined with the probability distributions of the process plume and the tank-park plume and a combined probability distribution curve is finally calculated. The average of the distributions and the variance is shown in Table 14 and corresponds to the overestimation done when calculating the emission. An overestimation below one tells that the calculated emission is lower than the true emission and is thus actually an underestimation. The error due to wind velocity and direction is individually presented as well as the combined error due to both. The probability function for the bolded case in Table 14 is shown in Figure 31. A slot-size of width 0.01 has been used for the distribution. Some examples might explain this figure. The figure shows that there is 5% chance to have a overestimation factor in the range 0.9±0.005 and 0,12% chance of having an overestimation in the range 1.2±0.005. For the error in wind direction, it is assumed that the car is driven at an angle of 45° to the wind direction and always in the direction that causes an underestimation and represents an upper limit on the expected error. The error factor for the tank-park and the process are given individually as well as the case where the two emission sources are both considered.

Table 14. Error factors in the retrieved flux due to wind variations with height.

	Factor due to wind velocity	Factor due to wind direction	Combined factor due to wind velocity and direction
Tank-park (0-100 m)	0.97±0.06	0.98±0.02	0.95±0.07
Process (100-300 m)	0.92±0.18	0.85±0.11	0.80±0.23
50% tank-park 50% process	0.95±0.13	0.91±0.07	**0.86±0.15**

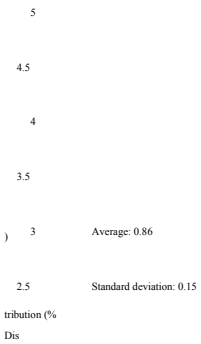

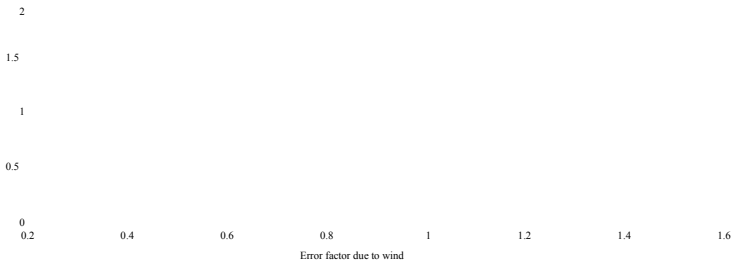

Figure 31. The distribution of the error factor for the simulated case when including all data-points between time 9:00 and 17:00 on days with high sun-radiation. The shaded area represents the standard deviation around the average value 0.86. Both the effect of wind-speed and wind-direction has been included.

For determining the total error in the yearly estimate from a refinery the case that is bolded in Table 14 is used. Thus the systematic error is expected to be $\sigma_{wind,sys} = -\%14$ and the standard deviation between days to $\sigma_{wind,day} = \%15$.

Errors in calculated flux due to variations of the wind with location is another consideration but this issue was not possible to study with the available dataset. There are also variations in the wind with a much shorter timescale than 1 hour. The induced errors in calculated flux from the short timescale variations in wind can however be expected to reduce by taking the average of many traverses in one day. About 10 traverses of the same kind are done on a good measurement-day and are averaged to represent the emission on that day. The errors due to short timescale variations are therefore expected to be much lower than the errors due to the altitude and wind profile variations and will therefore be ignored hereafter.

8.4 Conclusion about total error

The combined errors from all expected error sources for the total emission measurements can be calculated by:

$$\sigma_{total} = \sigma_{wind,sys} + \sigma_{alkane}^2 + \sigma_{cross}^2 + \frac{\sigma_{wind,day}^2 + \sigma_{BL}^2 + \sigma_{true}^2}{N} \quad (8.$$

As concluded in previous chapters, the error in the spectral evaluation is $\sigma_{alkane} = \%10$ (chapter 8.2.2). There is also an uncertainty in the spectral cross section used that contributes with an error $\sigma_{cross} = \%10$ (chapter 8.2.2) and the systematic

error due to wind is $\sigma_{wind,sys} = -\%14$ (chapter 8.3). These three errors are systematic and do not reduce by averaging the measurements over many days. The statistical error in the daily averages due to the wind is $\sigma_{wind,day} = \%15$ (chapter 8.3), tl variation between days induced by the baseline error is $\sigma_{BL} = \%5.9$ (chapter 8.2 and the true variation between days $\sigma_{true} < \%17$ (chapter 8.1). The true variation is possibly less than 17% but setting it to 17% will give an upper limit of the expected error. These three errors are not systematic and will reduce when averaging over the number of measurement days, here denoted by letter N. Measurements are typically done on four days (N=4) and the total error in the estimate of yearly emission will then be calculated by equation 8.1 to $\sigma_{total} = \%19$. Measurements will however on average be underestimated with a factor 14% due to the systematic error in the wind.

The errors associated with leakage-search measurements will here be handled with the same equation for a comparison. The measurements on subsections of the industry, for example on a crude oil tank are typically done on four days but a higher true variation between days is also expected from a single crude oil tank. Due to the complexity of the wind-situation close to ground, the errors in the measurements of both wind-direction and wind-speed are expected to be high. This was observed in the trace gas experiment in chapter 5 where the flux was determined with an error of 50%. Assuming no systematic error and a standard deviation of 50% due to the wind and a variation in the true emission of 40% between days, the error for a tank measurement is:

$$\sigma_{tank} = \frac{10.0^2 + 10.0^2 + 5.0^2 + 4.0^2 + 095.0^2}{4} = \%35 \quad (8.$$

Thus there will be more errors in the estimation from individual tanks than for the total emission-measurements.

For the measurement on the water treatment it is also expected that the error caused by the spectral evaluation is larger since the gas-mixture of alkanes have been observed to be quite different there than on the rest of the refinery. Since no bag-measurements have been done to determine this gas-mixture, it is unknown. However, the observed carbon count number (6.5) indicates that the plume contains hexane and Table 10 indicates that the spectral method makes an error of 30% when measuring hexane.

9 The solar tracker

To make the SOF-method more operative, a new active solar tracker was developed.

Figure 32 shows a schematic figure of the solar tracker. The solar light is first reflected on the tilt mirror that is mounted directly on a motor axis. With the motor, the tilt of the path of the incoming light is decided so that the reflection hits another mirror (upper mirror). The upper mirror is tilted with 15° so that the reflected light goes straight vertical down the tower of the solar tracker. In the bottom of the solar tracker, the light reflects on a mirror mounted at a 45° angle so that the light exits in the horizontal direction.

The upper part of the tower is mounted on a ball bearing and is free to rotate. The tower is turned by a timing belt driven by the rotation motor. The electronics in the upper part of the tower is connected by a spiral cable to the lower part and this limits the freedom in rotation to 540°.

In the upper mirror, there is a 5mm drilled hole and behind that there is a small aperture of ∅0.5 mm. A small part of the solar light enters a black box through the aperture and is imaged as a small spot on a photosensitive plate after having traveled 6 cm inside the box. In front of the photosensitive plate there is a thin black plastic tape to dampen the intensity of the light. The photosensitive plate is a so called XY-plate with an active surface of 10x10 mm. The active surface corresponds to a field of view of ±5°.

The XY plate has been purchased from the manufacturer Sitek located in Gothenburg. The XY-plate can be considered as a large photodiode located between two high-resistive plates. The bottom resistive plate has electrodes along two opposite sides of the plate and the top plate has electrodes along the other two sides. When a current is created in the photodiode, different amounts of current will go to each electrode depending on the distance from the light spot to the electrode. By taking the difference in currents between two opposite electrodes, the position of average light intensity can be determined in two dimensions. The total light intensity can also be determined by measuring the total current created between the bottom and top plate.

The solar tracker determines if it has found the sun by comparing the total light intensity to a threshold value. When the solar tracker has successfully found the sun, the positions derived from the XY plate is used to drive the two motors to compensate so that the tiny light spot is always in the middle of the XY plate. The solar tracker also has a manual mode where the position can be manually controlled. Furthermore, it has an automatic seek-mode where it scans the rotation ±60° in order to find the sun.

The rotation motor is a synchronous motor with a maximum power of 109 W and is powered by 12 V and driven by a digital motor controller. The motor and the controller are manufactured by Faulhaber. The motor controller is working in analog mode when the tracker has successfully found the sun. When in seek and manual mode, it is digitally controlled by the microprocessor (PIC16C84) in the solar tracker.

The tilt motor is also a synchronous motor manufactured by Faulhaber with three outer windings and a magnet as rotor. This motor is however not controlled in conventional ways. Only two of the windings are controlled and the third winding is connected by a resistor to ground, see Figure 33. By balancing the two active windings, the force on the magnet in the rotor can be controlled and this determines the angle of the tilt mirror.

Page 69

After the light exits the solar tracker it is focused on a 3 mm aperture with a mirror. After the aperture, optical filter can be mounted if needed. The light is then defocused into parallel light by a second mirror and then enters the spectrometer.

Figure 32. Schematic picture of the solar-tracker and the optics between the solar-tracker and spectrometer.

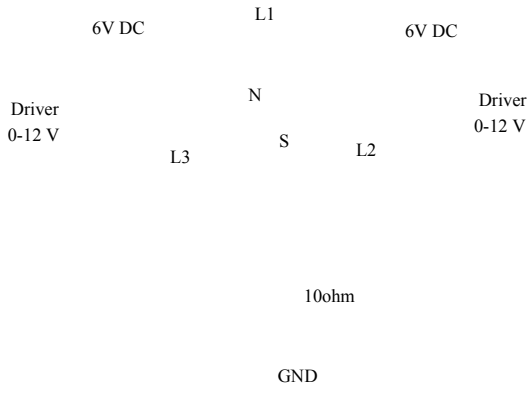

Figure 33. Schematic picture of the steering of the tilt motor. The two analog drivers can deliver a voltage between 0 and 12 V in reference to ground. The mirror obtains its center position when both

drivers outputs 6 V.

59

Page 70

Figure 34. Drawing 1 of the electronics of the solar tracker.

Figure 35. Drawing 2 of the electronics of the solar tracker.

Figure 36. Drawing 3 of the electronics of the solar tracker.

10 Conclusions and outlook

The results from the KORUS project have proven that it is possible to make routine monitoring with the SOF method on industries. However, the results from the measurements show that intermittent emissions from industries were more common than first anticipated. Therefore, more measurements dedicated to the study of the intermittent emissions should preferably be done in the future. Since the available time for this was very limited within the project, this issue was more or less put aside.

The use of the SOF method to quantify the alkane emissions on industries have shown to both have strengths and weaknesses. The strength can be summarized

into the following:

1 It is possible to quickly scan through an industry in the search for potential emission sources. As a result, new emission sources have been discovered that were not anticipated before.
2 Relatively inexpensive and not technically complicated.
3 Some capability to identify the kind of VOC in the measured gas.
4 Low noise in the measurement of gas concentration. This makes far-away measurements possible, where the concentrations are low.

The weakness can be summarized into the following:

1 No possibility to determine the height of the plume. This must therefore be assumed and can thus cause an error if done incorrectly.
2 Since only spatially resolved in one dimension, it gives limited possibility to separate emissions sources that are close to each other.

Paper A describes measurements of the concentration profile versus height and concludes that emissions from tank parks stay close to the ground. However, these measurements were not done high enough to be able to determine the typical plume height for the process emissions. This would have been relevant information since it affects what wind information that should be used and the estimation of the error that was determined in chapter 8.3. Therefore, similar measurements should be done again and then higher up to more accurately determine the plume height for a process plume.

In chapter 8.2.1 it was indicated that the current spectral evaluation of alkanes is sensitive to changes in water vapor. Typical changes in water vapor should be determined and the errors due to this should be determined and reduced if possible.

The measurements after the total maintenance stop at Shellraff-Göteborg gave new insight of the emission picture after a total stop. The measurements showed that the emission picture returned to normal within less than a year. This would not have been detected if measurements were only done every third year, as was the routine before on the refinery. Thus, measuring every year has shown to give new valuable information. The relatively low cost of the method motivates that routine measurements should be done every year on the refineries in order to quickly detect changes in the emission picture.

Experience has shown that much more work is required the first year measurements are done at a new industry. It takes time to learn which surrounding sources that can interfere, both from sources inside the same industry, or from

neighboring industries. The latter was the case with Shellraff-Göteborg and the Oil harbour in Göteborg that are located beside each other. It also takes time to see what

variability that can be expected from the different sources. With knowledge about these factors, it is much easier to repeat measurements the following years at the same industries.

The newly developed hardware reduces the amount of work required to make measurements with the SOF method. Also, the newly developed software for real time information and post processing makes the compilation of the results more efficient. However, current versions of the programs are not user friendly and require much training by the personnel in the beginning. There is a need for more user-friendly versions of the programs. This would make the method more available and useful for other people.

Measurements with the SOF method require a human to drive the car. This human must constantly make decisions since the optimal location for a measurement within an industry is determined by the position of the sun in the sky (i.e. the time and day of the year), the wind direction and the activity inside the industry. It is difficult to automate this task and measurements with the SOF-method are therefore labor intensive.

Bibliography

1. Farman J.C., Gardiner B.G., and Shanklin J.D., *Large Losses Of Total Ozone In Antarctica Reveal Seasonal Clox/Nox Interaction.* Nature, 1985. **315**(6016): p. 207-210.
2. Yang C.Y., et al., *Respiratory and irritant health effects of a population living in a petrochemical-polluted area in Taiwan.* Environmental Research, 1997. **74**(2): p. 145-149.
3. Pye J.M., *Impact Of Ozone On The Growth And Yield Of Trees - A Review.* Journal Of Environmental Quality, 1988. **17**(3): p. 347-360.
4. Odum J.R., et al., *Aromatics, Reformulated Gasoline, and Atmospheric Organic Aerosol Formation.* Environ. Sci. Technol., 1997. **31**(7): p. 1890 - 1897.
5. Langner J., et al., *Nuläge och scenarier för inverkan på marknära ozon av emissioner från Västra Götalands län*. 2004, SMHI.
6. Darnall K.R., et al., *Reactivity Scale For Atmospheric Hydrocarbons Based On Reaction With Hydroxyl Radical.* Environmental Science & Technology, 1976. **10**(7): p. 692-696.
7. Derwent R.G., et al., *Photochemical ozone creation potentials for organic compounds in northwest Europe calculated with a master chemical mechanism.* Atmospheric Environment, 1998. **32**(14-15): p. 2429-2441.
8. Finlaysson-Pitts B.J. and Finlaysson-Pitts J., *Chemistry of the upper and lower atmosphere*. 2000, San Diego: Academic Press Inc.
9. *Corinair 94: Summary report: Report to the European Environment Agency*. 1997: Copenhagen.
10. Galle B., *Developement and application of methods based on DOAS and FTIR absorption spectroscopy for atmospheric research, Ph.D. thesis*. 1999, Chalmers University of Technology: Gothenburg, Sweden.
11. Tinkham M. and Strandberg M.W.P., *Theory of fine structure of molecular oxygen ground state and measurement of its paramagnetic spectrum.* Physical Review, 1955. **97**(4): p. 937.
12. Rothman L.S., et al., *The HITRAN Molecular Database and HAWKS (HITRAN atmospheric workstation) 1996 Edition.* J Quant. Spectrosc. Radiat. Transfer, 1998. **60**: p. 665-710.
13. Benayahu Y., et al., *Cloud-droplet-size distribution from lidar multiple-scattering measurements.* Applied Optics, 1995. **34**(9): p. 1569.
14. Yarnell J. and Goody R.M., *Infra-red solar spectroscopy in high-altitude aircraft.* Journal of Scientific Instruments, 1952. **29**(11): p. 352.
15. Russell J.M., Park J.H., and Drayson S.R., *Global Monitoring Of Stratospheric Halogen Compounds From A Satellite Using Gas Filter Spectroscopy In Solar Occultation Mode.* Applied Optics, 1977. **16**(3): p. 607-612.
16. Goldberg L., et al., *Carbon Dioxide In The Infra-Red Solar Spectrum.* Physical Review, 1949. **76**(12): p. 1848-1858.

17. Rodgers C.D., *Inverse methods for atmospheric sounding: Theory and practice, 1 ed.* 2000: World Scientific Publishing.
18. Burton M.R., et al., *Diurnal changes in volcanic plume chemistry observed by lunar and solar occultation spectroscopy.* Geophysical Research Letters, 2001. **28**: p. 843-846.

Page 76

19. Griffith D.W.T., *Synthetic calibration and quantitative analysis of gas-phase FT-IR spectra.* Applied Spectroscopy, 1996. **50**(1): p. 59-70.
20. Milton M.J.T., et al. *Measurements of fugitive hydrocarbon emissions with a tunable infrared dial*. 1992. Cambridge, MA, USA: Publ by NASA, Washington, DC, USA.
21. Robinson R.A., Woods P.T., and Milton M.J. *DIAL measurements for air pollution and fugitive-loss monitoring*. 1995. Munich, Ger: Society of Photo-Optical Instrumentation Engineers, Bellingham, WA, USA.
22. Walmsley H.L. and O'Connor S.J. *The measurement of atmospheric emissions from process units using differential absorption LIDAR*. 1997. Munich, Germany: The International Society for Optical Engineering.
23. McGonigle A., et al., *Walking traverse and scanning DOAS measurements of volcanic gas emission rates.* Geophysical Research Letters, 2002. **29**(20): p. 46.
24. Weibring P., et al., *Monitoring of volcanic sulphur dioxide emissions using differntial absorption lidar (DIAL), differential optical absorption spectroscopy (DOAS), and correlation spectroscopy (COSPEC).* Applied Physics B Lasers and Optics, 1998(67): p. 419-426.
25. Fransson K. and Mellqvist J., *Measurements of VOCs at Refineries Using the Solar Occultation Flux Technique*. 2002, Chalmers report: Gothenburg.
26. Mellqvist J., *Fackelmätning med SOF vid Borealis Polyeten sommaren 2000*. 2001, Chalmers report: Gothenburg.
27. Duffell H., Oppenheimer C., and Burton M., *Volcanic gas emission rates measured by solar occultation spectroscopy.* Geophysical Research Letters, 2001. **28**(16): p. 3131.
28. Weibring P., et al., *Optical monitoring of volcanic sulphur dioxide emissions - comparison between four different remote-sensing spectroscopic techniques*. Optics and Lasers in Engineering, 2002. **37**: p. 267-284.
29. Norton R.H. and Beer R., *New Apodizing Functions For Fourier Spectrometry.* Journal Of The Optical Society Of America, 1976. **66**(3): p. 259-264.
30. Kihlman M., Mellqvist J., and Samuelsson J., *Monitoring of VOC emissions from three refineries in Sweden and the Oil harbour of Göteborg using the Solar Occultation Flux method*. 2005, Chalmers: Gothenburg.
31. Chu P.M., et al., *The NIST Quantitative Infrared Database.* J. Res. Natl. Inst. Stand. Technol., 1999. **104**(59).

32. *GRAMS/AI*. 2004, Galactic Industries Corporation.
33. *Pacific Northwest National Laboratory*. 2004 [cited; Available from: https://secure.pnl.gov/nsd/nsd.nsf/Welcome.
34. Hanst P.L., *QASoft '96, Database and quantitative analysis program for measurements of gases.* Infrared Analysis Inc., 1996.
35. EPA. *AP42, Fifth Edition. Organic Liquid Storage Tanks*. 1997 [cited; Available from: http://www.epa.gov/ttn/chief/ap42/].
36. *Measurement of the VOC emissions from Shell Raffinaderi, Göteborg, Autumn 1999*. 2000, Shell Global Solutions.
37. Tomasi C., et al., *Mean vertical profiles of temperature and absolute humidity from a 12-year radiosounding data set at Terra Nova Bay (Antarctica)*. Atmospheric Research, 2004. **71**(3): p. 139.

Page 77

38. Hurley P.J., Physick W.L., and Luhar A.K., *TAPM: A practical approach to prognostic meteorological and air pollution modelling.* Environmental Modelling and Software, 2005. **20**(6): p. 737.
39. *Väder och luftkvalitet i Göteborg*. 2001 [cited 2005; Available from: http://www.miljo.goteborg.se/luftnet/].

Page 79

Pap

Monitoring of VOC emissions from refineries in Sweden using the SOF method

Kihlman M., Mellqvist J., Samuelsson J., Tang L., Chen D.

Manus

Page 80

Monitoring of VOC emissions from refineries in Sweden using the Solar Occultation Flux method

Manne Kihlman[1], Johan Mellqvist*[1], Jerker Samuelsson[1], Lin Tang[2], Deliang Chen[2]

[1] Chalmers University of Technology, Göteborg, Sweden
[2] Gothenburg University, Sweden

* Corresponding author Johan.mellqvist@rss.chalmers.se, +46317724855

Short title: Mon. of VOCs from refineries using SOF

Abstract

A new spectroscopic technique for mobile gas flux measurements of VOCs, the Solar Occultation Flux method, has been further developed and successfully tested for its capability of conducting large scale monitoring of fugitive gas emissions from industries. During 2002-2004 three refineries and an oil harbour in Sweden were monitored. The measurement errors were, at good conditions, estimated to be around 25%, caused mainly by uncertainties of the wind field. The SOF instrument was tuned to detect alkanes, which contributes to the dominant fraction of the VOCs emitted from a refinery. Complimentary measurements were conducted to assess the emissions also of the aromatic species, typically 5-10% by mass of the alkanes. Each industry was divided into smaller sectors and the emission from each sector was determined as well as the total emission. With this method, it is possible to quickly scan through an industry and in real time detect leaks. For a typical refinery 0.06% of the mass of the crude oil is lost due to vaporization. Of the emitted gas 26% originates from the process, 31% from crude-oil tanks, 32% from product tanks, 8% from the water treatment facility and 2% from transport related activities.

Keywords: VOC, refinery, emission, SOF, solar occultation, FTIR

1

Page 82

Introduction

Emission of volatile organic compounds (VOC) to air is a potential hazard for human health and the environment. The formation of ozone in the lower troposphere takes place through a photochemical reaction driven by VOCs and nitrogen oxides. The formed ozone is a powerful oxidant that causes inflammation of the respiratory tract and exacerbates existing lung disease [1], a serious health problem in many large cities of the world. Ozone in the lower troposphere also has negative impact on the vegetation [2] and contributes to global warming. In Europe, and other parts of the world, the levels of ozone exceed critical levels. Therefore a European protocol exists for abatement of ground level ozone by reducing VOCs and other compounds. (Convention on Long range transboundary pollution, UNECE).

The refineries are the single largest point sources of VOCs, and may contribute significantly to ozone formation on a regional scale. For instance, recent studies [3] have shown that the refineries in Houston may have a major impact on the ozone formation in Texas, although car traffic is the largest emission source of VOCs. In the Corinair 94 inventory [4], the emission of NMVOC from Swedish refineries and petrochemical industries was reported to 12 Kton/year, representing 3% of the anthropogenic emissions in Sweden. In Europe the emission from refineries and petrochemical industries are regulated by the authorities and control programs are required for reporting the VOC leakages.

A commonly used method to estimate the annual emissions from a refinery-process is the EPA method 21 [5]. The concentration of VOC is measured in a point close to valves, pumps and flanges etc. and the measured concentrations are used as screening values. These values are then incorporated into calculations that are based on the typical emission picture for that specific kind of equipment. The calculated emissions from all valves, pumps and flanges etc. on the whole refinery are then summed to estimate the total emission. The most widely used methods for estimations of the emissions of storage tanks and loading and unloading is the EPA AP42 model [6]. This method is completely based on calculations with equations derived from previous measurements on typical tanks where parameters related to the design of the tank, the product in the tank and the meteorological conditions at the site are considered. There are also examples [7,8] where concentration measurements have been done with GC combined with FID or MS. The prime interests in these studies were to identify what concentrations of VOC is expected in the neighborhood of a

refinery and to identify the gas mixture of VOC that is emitted. Measurements on refineries have also been done with long-path systems, with FTIR [9,10] and UV-DOAS [8,11]. However, if the emitted amount of gas should be estimated with these methods, they must be complemented with a plume model.

Measurements with the DIAL method [12-14] provide a direct measure of the gas emission when combined with wind measurements. DIAL measurements have been performed both for the estimation of total emissions and to identify the emission from each sector inside a refinery. The measurements conducted in the past has shown that the emissions estimated by calculations were commonly underestimated with a factor 3 to 18 [15], hence indicating the need for more measurements. The DIAL method is however rather complex and expensive which has lead to little usage of this method during the more than 15 years it has been available for VOC flux measurements. In 1997 the development of a new method called SOF (Solar Occultation Flux) was started at Chalmers University, as described in a parallel paper [16]. The SOF equipment can be placed inside a small car, making it possible to quickly scan through an industry and in real time detect leaks. Compared to DIAL the

SOF method has better mobility and cost effectiveness, lower technical complexity, higher specificity and higher signal-to-noise making remote (far away) measurements possible. The weakness of the SOF-method is that the plume height is not determined and there is less possibility to separate emissions sources that are close to each other.

In this study the aim was to investigate whether the SOF method could be employed for large scale monitoring, and to understand the uncertainties involved in the measurements. This has included dedicated technical work building a new solar tracker and automation software for real time analysis that has proven vital for the ability to conduct measurements on larger scale. Results from an extensive monitoring project, denoted KORUS, are presented where the SOF method was applied during 3 years at three refineries and an oil harbour in Sweden. The results have contributed with information that is guiding when determining what actions should be taken to further reduce the emissions on the industries. A report with more details of the conducted measurements in the monitoring program has been published [17].

Methodology

The SOF method is thoroughly described in a separate paper [16]. It is based on recording broadband infrared spectra of the sun with a FTIR spectrometer that is connected to a solar-tracker, Figure 1. The latter is a mirror device that tracks the sun and reflects the light into the spectrometer independent of its position. From the solar spectra it is possible to retrieve the path-integrated concentration (molecules/cm^2) between the sun and the spectrometer. To obtain the gas emission from a source, the instrument is placed in a car and is driven in such way that the detected solar light cuts through the emission plume. To calculate the gas emission, the wind direction and speed is also required. The wind was measured from high masts and towers but

also using an ultrasonic wind meter positioned on the car.

An additional point measuring FTIR has been utilized in order to obtain information about the plume height and to extend the number of compounds measured. This system has also been used for flux measurements using tracer gas [18].

Figure 1. Schematic picture of the mobile measurement-system.

Page 84

Spectroscopy

The VOCs leaking from refineries correspond mostly to alkanes. These compounds can be measured in the infrared region around 2950 cm^{-1}, using the vibration transition in the carbon and hydrogen bond (CH stretch). The absorption features of the alkanes are similar and interfere with each other. A study of the cross sensitivity of various compounds to butane was conducted by fitting absorbance spectra of butane to other compounds [17]. The results showed that alkanes (C3-C9), had cross sensitivities around one (0.7-1.6), while other compounds had considerably smaller cross sensitivities, around 0.03-0.27 for aromatics and 0.02-0.11 for olefines, respectively. The concentrations of these interfering compounds were then determined by sampling the hydrocarbon mixture in the plume from a crude oil tank. This was conducted by bag sampling followed by quantitative analysis by gas chromatography within 2 hours by an accredited laboratory. The mass fractions in the samples were 98.5% alkanes, 1.1% aromatic hydrocarbons and 0.5 % alkenes/alkynes. Taking the cross sensitivities and gas composition into account shows that interference from non-alkanes is of little importance when measuring on a refinery. It is also clear that the

measurements in the CH stretch region within certain error bars, corresponds to the sum of the number of C-H bonds, independently of the assumption of alkanes in the mixture. Both these issues are further discussed in the error analysis section.

Even though the alkane spectra are similar, they are still significantly different so that molecular specificity can be partly obtained. If propane, butane and octane are simultaneously included in the spectral fitting, the average number of carbon atoms in the measured alkane can be calculated. In this study typical observed number of carbon atoms was 3.7 for crude-oil tanks, 4 for gasoline tanks, 6 for kerosene tanks, 5 for process and 6.5 for the water treatment facility. The simultaneous fitting of multiple reference spectra yields valuable information but it is done at the expense of more noise in the baseline. A two-step method has therefore been used that first evaluates the spectrum as butane only. If the evaluated butane concentration is higher than 12 mg/m$_2$, a new spectral evaluation is done with propane, butane and octane. The sum of the three is taken as the total concentration of alkanes and is sensitive to the presence of all alkanes since other alkanes have spectral absorption structures similar to these three. In addition to the alkanes, for which reference spectra from PNW database were used [19], synthesized spectra of H_2O, HDO and CH_4 were also included in the spectral fitting obtained by using line parameters in the HITRAN database [20]. The spectral retrieval was conducted in the interval 2725-3005 cm^{-1} at 8 cm^{-1} resolution.

To render the SOF method more effective, an on line software was developed to allow real time evaluation of alkanes when measuring gas emissions from the refineries. The program retrieves the line-integrated concentrations of the gases of interest from the spectra with a nonlinear algorithm [21]. It combines this with the position of the vehicle retrieved by GPS, and wind information from wind-meters and calculates the flux of gas through the surface that is sliced out along the path the vehicle is driving. It gives a graphical representation of the measured flux on a map while the measurement is running. The software was tailored to work with the Bruker OPAG and the Bruker IrCube spectrometers, and to do spectral evaluation with a resolution between 0.5 and 12 cm^{-1}. Two separate measurement systems were built with these two spectrometers.

Aromatic emissions

It is difficult to measure aromatic compounds using the SOF method. In order to be able to estimate emissions of the latter compounds an approach was adapted in which the ratios of aromatic hydrocarbons to alkanes was measured in different parts of the refinery such as in the plumes from the waste water treatment area, process area, and crude oil tanks. The aromatic compounds were sampled with TENAX absorption tubes that were later analyzed with GC. The alkanes were measured by the point FTIR

shown in Figure 1. The results showed that the average mass fraction of aromatic hydrocarbons were 3% in a crude-oil tank-park, 11% from a process, 14% from a product tank-park and 15% from a water treatment facility Thus, most of the VOC emission on a refinery is in the form of alkanes. Aromatic emissions were later obtained by multiplying the aromatic/alkane ratios with the emission values of alkanes obtained from the SOF method.

Flux measurements of sub-sectors and total industry

The wind field inside an industry area is expected to be very complex since there are many large buildings that cause disturbances in the wind-field. It is therefore difficult to determine the wind field inside the industry area. When determining the total emission from a refinery it has therefore been done with measurements approximately 1 km away from the industry, where it is expected that the plume has risen to altitudes where the turbulence imposed by the structures and the ground has decreased. When measuring the emission far away, the errors induced by the variation in height of the wind-speed and direction will however be present. Total industry measurements are typically done over 3 hours and about 10 traverses can then be collected during good conditions. All traverses done in one day are averaged and are taken to represent the average emission that day. Figure 2 shows an example of how the measurement car was driven to measure the total emission from Refinery A. When conducting far away measurements the speed of the car was 40 km/h, to minimize wind changes, and 10 km/h for close by measurements. Typically 16 spectra were coadded, yielding a sampling time of 3 s.

5

Figure 2. The figure shows how the measurement car was driven to do a total measurement on Refinery A. The car was driven along the road to the product harbour. The position of the car when the measurement of a new spectrum was started is indicated with dots with attached lines. The lines indicate the wind direction (they point towards a possible emission source). Dark dots indicates points where high line integrated concentrations have been measured. *(Aerial photo: Copyright Lantmäteriet 2004-11-09. Ur Din Karta och SverigeBilden)*

It is also of interest to know the emission of each sub-sector inside the industry and measurements inside the industry area are done to get the proportions of the emissions from each area. It is preferred that many sectors are measured within a limited time-period so that the meteorological conditions remain the same for the measurements on all sectors. The calculated emissions for the sub-sectors will typically be too high since the wind-speed just behind a tank is lower than the average wind-field. However, the size proportions between the sub-sectors can be decided. The estimated emission for all sub-sectors are summed and a normalization factor is determined by dividing this sum with the total emission measured approximately 1 km away. The errors in the absolute emission on each sub-sector are then compensated by dividing the value with the normalization factor. With this approach, much less labor is required for the meteorological measurements since a few single wind-meters

representing the average wind field can be used. These are typically permanently mounted in existing towers in the industry area or mobile masts.

The subsectors correspond to areas with similar products or processes and these were usually chosen by the industries themselves. However, there are limitations in how the sub-sectors can be chosen since it must be possible to drive between each sub sector in order to separate them and there must not be strong emission sources behind a weak source.

For Refinery A, the emissions were divided into nine sectors and the emission from each sector is shown in Table 1. Figure 3 shows how a measurement was done on a sub-sector, in this case the crude oil tank-park on Refinery A. The emissions have been further divided into individual tanks, when this was possible and of interest to the industries.

Table 1. Emissions of alkanes (kg/h) from the different sectors on Refinery A. First number in parenthesis indicates number of measurement days. Second number indicates total number of traverses the whole year.

Source	**Year 2003**		**Year 2004**	
Process	88	*(1, 6)*	85	*(5, 17)*
Crude-oil tank-park	209	*(2, 25)*	126	*(6, 68)*
Black components tank-park	124	*(2, 8)*	108	*(2, 14)*
White components tank-park	49	*(3, 21)*	36	*(2,19)*
Gasoline components tank-park 27		*(2, 24)*	37	*(5, 29)*
Water treatment facility	12	*(4, 22)*	19	*(2, 10)*
Preskimmer	3.5	*(2, 17)*	14	*(5, 32)*
Rock cavern exhaust	8.0	*(1, 4)*	85	*(3, 12)*
Product harbour	27	*(2, 17)*	27*	
Total	**550**	*(2, 22)*	**537**	*(5, 42)*

* The product harbour was not measured 2004 and the same emission as 2003 was assumed.

Figure 3. The figure shows how the measurement car was driven to measure the emission from the crude-oil tank-park on Refinery A.

Results

Continuous emissions

One aim of the measurements is to make an estimation of the total emission from a refinery during a whole year. Since total measurements have only been done on a few days within a time-span of a month, it must be assumed that the emissions on those days can represent the average emission for the whole year.

VOC emission from a refinery can be divided into continuous emissions and intermittent emissions caused by short-term activities. On many occasions when higher emissions than normal were observed it could be explained by short-term activities taking place and the measurements from that day were then discarded. The best data produced from the industry monitoring project to estimate the variation of the continuous emission is five days of total measurements from Refinery A during July-September 2004. This data gives an average emission of 509.6 kg/h with a variance of 85.3 kg/h between the five days thus giving a standard deviation of 17% between days. It is possible that some of this variation is due to errors in the measurements but it is still safe to assume that the true variation in the total emission has a standard deviation of less than 17% between days for this case. With this approach, variations in the wind were partly captured which may have an impact on the emissions. However, the effect of the annual variation in the temperature was not captured.

Intermittent emissions

Intermittent emissions were more frequently observed at the oil harbour than at the refineries. The reason is that more than ten different companies are working independently with activities in the area that temporarily causes emissions, such as loading of trucks and ships, filling of caverns, and cleaning of tanks and pipes. An example of measurements during an intermittent emission in the oil harbour is shown in Figure 4, illustrating both a strong short-term emission and how the emission returns to the average emission. On several occasions high emissions were found which originated from loading of ships. When ships are loading low volatile products (class II and III) in the harbour this is generally done without vapor recovery unit.

High emissions from such loading were found on cases where the ships had previous loads with high volatile products (class I). The reason is probably that the old volatile load was pushed out when the ship was refilled with a low volatile product. Emissions were varying between 10-300 kg/h. Measurements over a full loading cycle are needed to more accurately determine the average emission. There is a potential error source in that one may fail to detect a situation as intermittent, and the estimation of continuous emission will then be too high.

8

Page 89

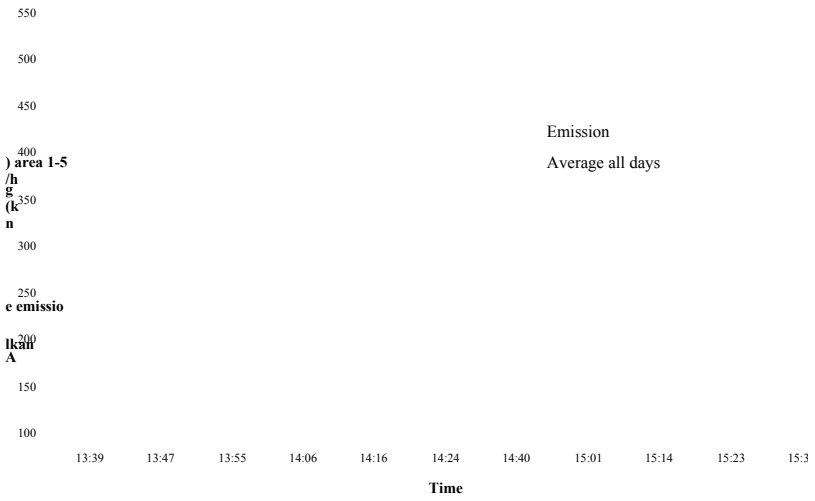

Figure 4. Measured emission of alkanes from an oil harbour. The emission values gradually increased with a peak around 14:10 and then stabilized close to the continuous emission average of 143 kg/h. The reason for the peak in the emission is either loading of a ship with gas-oil or filling of a tank, both finishing at around 14:00.

When short-term emissions were discovered, some sporadic tests were done

afterwards to try to identify how big the emissions are in comparison to the continuous emissions. It has however become clear that a thorough study of this issue requires much more time and effort than what was available. Some calculations of the contribution of short-term activity are shown in Table 2. All examples are based on measured emissions, the frequency of each short-term activity has been based on statistics but the duration of the short-term emissions have been guessed.

Table 2. Calculated examples of the relevance of intermittent emissions compared to the continuous emission, based on the measurements and the here given assumptions.

Assumptions	Intermittent emission compared to continuous emission
Cleaning activities causing emissions of 100 kg/h during 2 h every day at the oil harbour.	(73 ton of total 1600) 5%
Loading of ships in the oil harbour causing emissions of 100 kg/h for 12 h every third day.	(146 ton of total 1600) 10%
Rock cavity in the oil harbour is filled causing emission of 149 kg/h and is done 3 times a year during 48 hours.	(21 ton of total 1600) 1%
Cleaning a tank at Refinery B causing emission of 70 kg/h for 12 h and is done 11 times during a year.	(9 ton of total 146) 6%

General results from 3 years of monitoring

From the collected data some general statements of the VOC emissions from the four studied industries can be done. The alkane emission was divided into five groups and compared between the industries. Table 3 shows the emission from these five groups and also the total emissions of alkanes measured on the four industries. The annual throughput of refined crude oil is 10 Mton/y for Refinery A, 5 Mton/y for Refinery B and 3 Mton/y for Refinery C. Reflecting this, the emissions have been normalized to

annual throughput in Table 4 to give the emission in each sector as ton alkanes per Mton refined crude oil.

Table 3. Summary of the measured emissions of alkanes from the four industries. First number in parenthesis indicates number of measurement days. Second number indicates total number of traverses.

Emission each year (ton/y)	Refinery A	Refinery B	Refinery C	Oil Harbour
Total 2002	-	-	3464 *(3, 13)*	-
Total 2003	4818 *(2, 22)*	3051 *(4, 19)*	2014 *(5, 27)*	1771 *(2, 11)*
Total 2004	4704 *(5, 42)*	1070 *(3, 18)*	2683 *(6, 38)*	1788 *(4, 15)*
Averages all years (ton/y)				
Total	4760 *(7, 64)*	2060 *(7, 37)*	2720 *(14, 78)*	1780 *(6, 26)*
Process	760 *(6, 23)*	930 *(12, 140)*	610 *(7, 54)*	0
Crude-oil tanks	1470 *(8, 93)*	410 *(9, 61)*	1000 *(10, 66)*	0

Product-tanks	2080 *(16, 115)*	260 *(7, 39)*	940 *(14, 78)*	1115 *(6, 26)*
Water treatment Facility	140 *(6, 32)*	390 *(7, 37)*	160 *(7, 91)*	0
Transport related activity	240 *(2, 17)*	80 *(3,11)*	0 (1)	665 *(12, 60)*

(1) Transport to/from Refinery C is only done through pipelines to the oil harbour

Table 4. Normalized alkane emission in ton per megaton refined crude oil.

	Refinery A	Refinery B	Refinery C	Average
Process	76	186	203	155 (26%)
Crude-oil tanks	147	82	333	187 (31%)
Product tanks	208	52	310	190 (32%)
Water treatment facility	14	78	53	48 (8%)
Transport related activity	24	16	0	13 (2%)
Total (ton/Mton)	476	412	907	598

Thus for a typical refinery, about 0.06% (598 ton/Mton) of the mass of the crude oil is lost due to vaporization to the atmosphere. Of the emitted gas, 26% originates from the process, 31% from crude-oil tanks, 32% from product tanks, 8% from the water treatment facility and 2% from transport related activities. As transport related activity was counted loading/unloading to/from ships and trucks inside the industry areas. Transport related activities are typically intermittent and are therefore difficult to quantify. Therefore, this value has a high uncertainty.

Figure 5 shows the measured daily averaged total emission from each industry. The emissions from Refinery B were substantial during the early part of 2003, probably caused by leaks that emerged in an isomerisation process area during a complete maintance stop conducted 2 weeks prior to the first SOF measurements. The emissions were reduced after having conducted several documented repairs of the process equipment. In 2004 the emission decreased even more, probably caused by a tenfold of documented repairs in the main process area. The measurements showed that the emission picture returned to normal within less than a year and that measuring every year yields valuable information. The relatively low cost of the method motivates annual routine measurements in order for rapid assessment of new leaks and better control of the plant. The apparent low variability in the Oil harbour is a result of that days with unusually high emissions has been discarded and treated as intermittent activity.

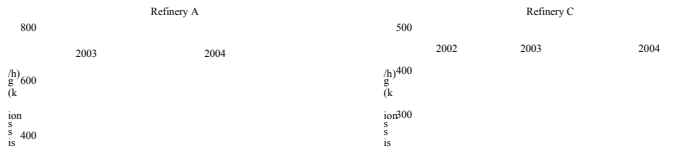

Figure 5. The figure shows the measured daily averaged total emission on each industry.

Discussion

The SOF method is based on two parts, mobile spectroscopic measurements and measurements of the wind at the plume height. Both parts cause uncertainties in the flux values and this will be further discussed here.

Plume height determination

The plume height cannot be determined by the SOF method. Since the wind should be measured at the plume height to determine the gas emission rate, this must therefore be assumed and can thus cause errors if done incorrectly. In order to get more height information the point measuring system shown in Figure 1 was applied. With this system it was possible to obtain the ratio between the alkane concentration on the ground and the alkane column measured in the solar beam with the SOF. In general the plume from the process areas seems to raise very quickly, since little gas was found at ground level, while the plumes from a tank park seems to be well mixed from tank height (25 m) to the ground. In order to quantify this better an experiment was done to determine the plume height from a refinery process and a product tank park. Air was sucked in through a long teflon tube connected to a point measurement system located in the car and the tube end was lifted between the ground and 50 m height. The expected center of emission was located 250 m from the measurement point both for the process and product tank park. The local wind direction determined if a measurement was done on the process or the tank park. Figure 6 shows the distribution of all measurements and the average profile. This indicates that the tank park plume is located close to ground and the concentration decreases at 50 m. The center of the plume is located at approximately 25 m. From the process there is zero concentration on ground and the plume starts at 25 m. The center of the plume is probably located well above 50 m but measurements higher up is required to actually tell.

Page 92

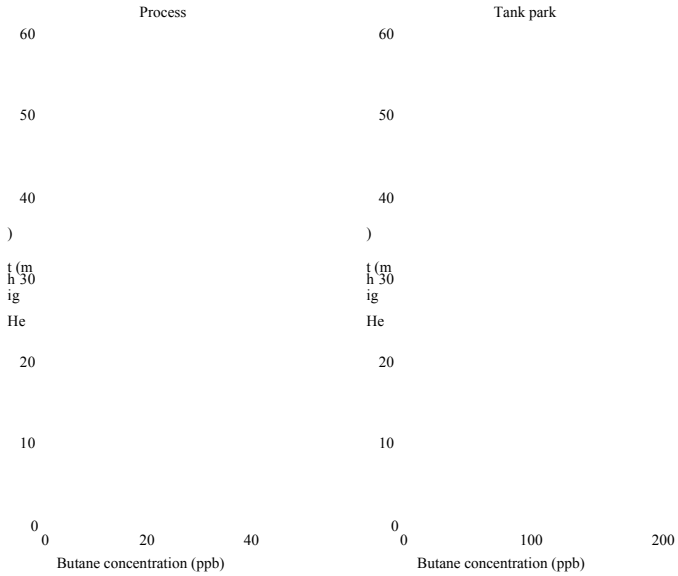

Figure 6. The dots indicate the concentration measurements. The lines indicate the average concentration profile.

In Figure 7 results from a plume height experiment is shown in which simultaneous measurements with the SOF and the point measuring system were conducted downwind a crude oil tank. The points with maximum concentrations were measured to 370 mg/m$_2$ and 3 mg/m$_3$ in the SOF and point measurement respectively. Assuming a constant concentration from ground and up, this gives a path-length of around 120 m. By taking into account the slant column to the sun, the height of the column is halved to 60 m. Note that the positions do not coincide due to the slant angle of the SOF measurements and a time delay in the point measuring system.

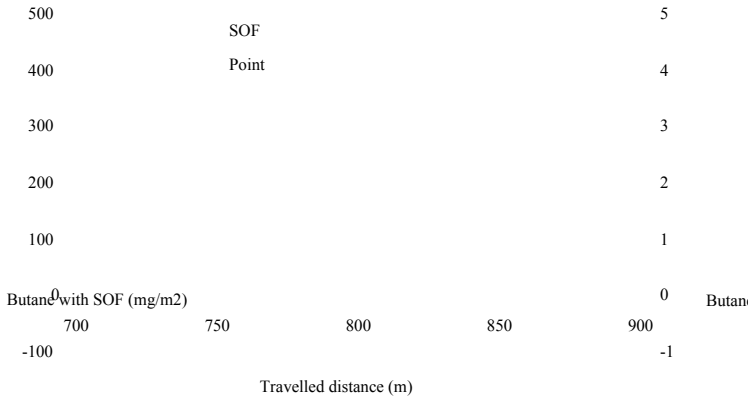

Figure 7. Simultaneous measurement with the SOF (left peak) and the point measurement at the surface (right peak) close to a crude oil tank.

Spectral evaluation errors

The error in the spectral evaluation of a typical VOC gas-mixture was determined by a simulation, by creating a synthetic spectrum at 8 cm^{-1} resolution that included absorption of the alkanes given in Table 6, superimposed on a real measured solar spectrum. The concentrations of the alkanes correspond to the ones measured by bag-samples in the crude-oil tank-park on Refinery C. Reference spectrum for Propane and n-Butane were taken from the QASoft database [22] and the other spectra were taken from the PNW database [19]. The total amout of alkanes in the synthetic spectrum was then obtained by simultaneous fitting of 3 compounds: propane, n-butane and octane.

The spectral fitting of n-Butane represents compounds with similar absorption structures as n-Butane (iso-Butane, n-Pentane, iso-Pentane and to some degree n-Hexane). The spectral fitting of n-Octane represents compounds having similar broad absorption structures as n-Octane (n-Heptane, Cyclohexane, 2-Methylpentane, 3-Methylpentane and to some degree n-Hexane).

As can be seen in Table 5, the spectral evaluation overestimates the total simulated alkane-concentration with 10%, for this typical crude oil gas-mixture. We assume that the overall uncertainty in the total alkane estimation at a refinery is of the same size. There is also an uncertainty in the spectral cross sections used that contributes with an error of %10 .

Table 5. Concentration of alkanes in the error simulation. Here 3 compounds, propane, n-butane and octane were fitted simultaneously to a synthetic spectrum corresponding to the concentration in the left column.

Alkane compund Simulated concentration (mg/m_2)	**Evaluated concentration (mg/m_2)**
Ethane 18	
Propane 72	97
n-Butane 50	115
Iso-Butane 21	
n-Pentane 19	
Iso-Pentane 17	
n-Hexane 4.0	
2-Methylpentane 3.6	
3-Methylpentane 1.7	
Cyclohexane 1.6	
n-Heptane 1.1	
n-Octane 0.24	19
Total: 210	**231**

When conducting SOF measurements, the flux is obtained by adding all columns above the baseline of the traverses. The baseline is the registered concentration at a

position with zero alkane concentration. If the baseline drifts around, which was the case in many earlier measurements, it will cause an error. The drift in the baseline occurs if the tilt of the incoming light into the spectrometer is changed during a traverse. This will occur if the solar-tracker is misaligned causing the output angle to wobble around at different viewing directions. Baseline drift is also caused by temperature variations in the transmittance properties of the optical filters if this is used. The size of this effect is dependent on the spectral characteristics of the filter and can be partly compensated for in the software.

Page 94

In the monitoring project, traverses with a baseline error of more than 3 mg/m$_2$ were manually rejected and this gives an upper limit for the error of 30%. It is here assumed that the error is Gaussian distributed and will thus decrease when taking average of many traverses in the same day. Typically, 10 traverses are averaged and the error for the average due to baseline errors will then reduce to $10/\%3 = \%5.9$ The uncertainties caused by baseline drift are applicable for the results here, but today this problem has been minimized.

Errors in the retrieved flux due to wind properties

Calculation of emission relies on information of how the wind varies over the whole surface where the gas is measured. Since this information is not possible to completely retrieve, errors in the calculated emission will be induced. In the monitoring project, wind information was typically taken from a wind meter located 25 m above ground recording averages of wind speed and direction every 30 seconds. Since there are variations both in wind speed and direction with height, there is a discrepancy between the wind at the position of the plume and the wind measured at 25 m. This error is difficult to determine since the height of the plume cannot be determined by the gas measurements.

A study of the errors due to the wind was made by looking at the variation in a dataset retrieved by a simulation of the micrometeorology model TAPM [23]. Simulations were done for the time-span from 1$_{st}$ August to 30$_{th}$ September 2001 for three selected positions of relevance for the monitoring project. The used data from the simulation consists of wind speed and wind direction for every hour at 16 different altitudes between 10 and 1000 m and also the solar radiation at the surface.

For simulating the error of a typical total measurement of an industry, a case is simulated where a process and a tank-park is assumed to emit the same amount of VOC. It is assumed that the plume from the tank-park is equally distributed from the ground to 100 m above. It is further assumed that the plume from the process is equally distributed between 100 and 300 m above ground. The wind data from all hours between 9 and 17 on days with high-sun radiation and with a wind speed of 3-6

m/s at an altitude of 25 m are then selected. There are valid wind data on 25 days that fulfilled these criteria. Figure 8 shows the average wind profile retrieved by the filtered data. The error bars show the standard deviation between daily averages.

The selected wind data is then combined with the height distributions of the VOCs in the process plume and the tank-park plume and a combined height distribution curve is finally calculated. The average of the distributions and the variance is shown in Table 6 and corresponds to the overestimation done when calculating the emission. The error due to wind velocity and direction is individually presented as well as the combined error due to both. For the error in wind direction, it is assumed that the car is driven at an angle of 45° to the wind direction and always in the direction that causes an underestimation and this represents an upper limit on the expected error. The overestimation for the tank-park and the process are given individually as well as the case where the two emission sources are both considered.

14

Page 95

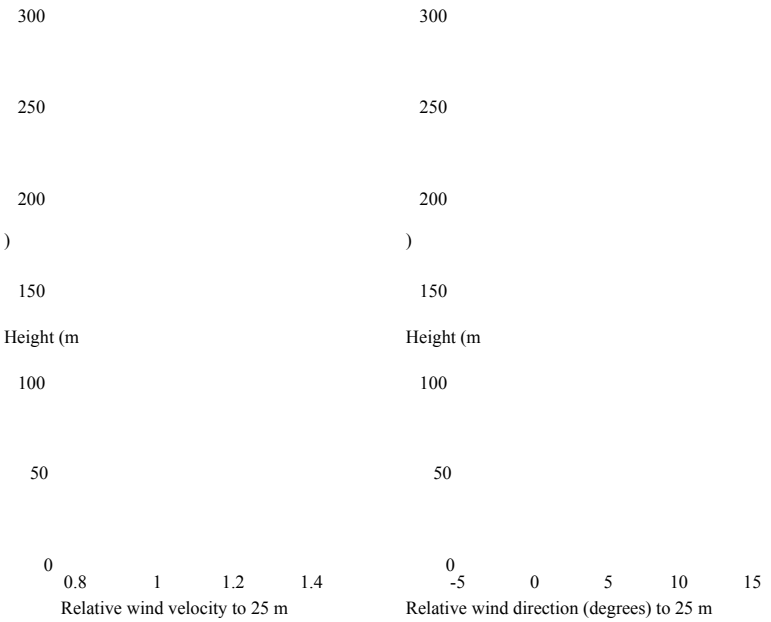

Figure 8. The figure shows the wind velocity and wind direction profile retrieved by simulation and averaged over daytime all sunny days with a wind-speed of 3-6 m/s at ground. The error bars indicate standard deviation between daily averages.

Table 6. Error factors in the retrieved flux due to wind variations with height.

	Factor due to wind velocity	Factor due to wind direction	Combined factor due to wind velocity and direction
Tank-park (0-100 m)	0.97±0.06	0.98±0.02	0.95±0.07
Process (100-300 m)	0.92±0.18	0.85±0.11	0.80±0.23
50% tank-park 50% process	0.95±0.13	0.91±0.07	**0.86±0.15**

For determining the total error in the yearly estimate from a refinery, the case that is bolded in Table 6 is used. Thus the systematic error is expected to be -14% and the standard deviation between days 15%.

Conclusion on total error

The total error is calculated by taking into account the three systematic errors: the error in the spectral evaluation of alkane, the error in spectral cross section and error due to the wind, and the three temporarily errors that occur due to variation between days: true variation, baseline error and variation due to wind. Measurements are typically done on four days and the total error in the estimate of yearly emission will then be 19%, obtained as the square root sum of the quadratic errors. Measurements will however on average be underestimated with a factor 14% due to the systematic error in the wind.

The measurements on sub-sectors of the industry, for example on a crude oil tank are typically conducted over four individual days but a higher true variation between days is also expected from a single crude oil tank. Due to the complexity of the wind-situation close to the ground, the errors in the measurements of the wind are expected to be high. Assuming a systematic error of 25% and a standard deviation of 50% due to the wind and a variation in the true emission of 40% between days, the error for a tank measurement will be 35%. For close by measurements of tanks this uncertainty is probably low, as has been shown elsewhere by tracer experiments [16, 21].

Acknowledgment

The authors would like to thank Anders Strandberg, Andreas Nilsson, Bo Galle, Elisabeth Undén, Gunner Hanehöj, Karin Fransson, Samuel Brohede and Åke Fält

that have participated in the field measurements.

References

1. Yang C.Y., et al., Respiratory and irritant health effects of a population living in a petrochemical-polluted area in Taiwan. Environmental Research, 1997. **74**(2): p. 145-149.
2. Pye J.M., *Impact Of Ozone On The Growth And Yield Of Trees - A Review.* Journal Of Environmental Quality, 1988. **17**(3): p. 347-360.
3. Ryerson T.B., et al., *Effect of petrochemical industrial emissions of reactive alkenes and NOx on tropospheric ozone formation in Houston, Texas.* Journal Of Geophysical Research-Atmospheres, 2003. **108**(D8).
4. *Corinair 94: Summary report: Report to the European Environment Agency*. 1997: Copenhagen.
5. EPA, *EIIP-Volume II, chapter 4 – Preferred and alternative methods for estimating emissions from equipment leaks*. 1996.
6. EPA. *AP42, Fifth Edition. Organic Liquid Storage Tanks*. 1997 Available from: http://www.epa.gov/ttn/chief/ap42/.
7. Domeno C., et al., *Sampling and analysis of volatile organic pollutants emitted by an industrial stack.* Analytica Chimica Acta, 2004. **524**(1-2): p. 51-62.
8. Lin T.Y., et al., *Volatile organic compound concentrations in ambient air of Kaohsiung petroleum refinery in Taiwan.* Atmospheric Environment, 2004. **38**(25): p. 4111-4122.
9. Wu R.T., et al., *FTIR remote sensor measurements of air pollutants in the petrochemical industrial park*. 1995. San Diego, CA, USA: Society of Photo-Optical Instrumentation Engineers, Bellingham, WA, USA.
10. Yan Li H.X., et al., *Path Concentration Distribution of Toluene using Remote Sensing FTIR and One-Dimensional Reconstruction Method.* Journal of Environmental Science and Health, Part A, 2005. **40**: p. 183 - 191.
11. Lee C., et al., *Measurement of atmospheric monoaromatic hydrocarbons using differential optical absorption spectroscopy: Comparison with on-line gas chromatography measurements in urban air.* Atmospheric Environment, 2005. **39**(12): p. 2225-2234.
12. Milton M.J.T., et al. *Measurements of fugitive hydrocarbon emissions with a tunable infrared dial*. 1992. Cambridge, MA, USA: Publ by NASA, Washington, DC, USA.

13. Robinson R.A., Woods P.T., and Milton M.J. *DIAL measurements for air pollution and fugitive-loss monitoring*. 1995. Munich, Ger: Society of Photo-Optical Instrumentation Engineers, Bellingham, WA, USA.
14. Walmsley H.L. and O'Connor S.J. *The measurement of atmospheric emissions*

from process units using differential absorption LIDAR. 1997. Munich, Germany: The International Society for Optical Engineering.

15. IMPEL, *Diffuse VOC emissions*. 2000: Brussels.
16. Mellqvist J., et al., *The Solar Occultation Flux method, a nouvelle technique for quantifying fugitive gas emissions*. To be published.
17. Kihlman M., Mellqvist J., and Samuelsson J., *Monitoring of VOC emissions from three refineries in Sweden and the Oil harbour of Göteborg using the Solar Occultation Flux method. 2005*, Chalmers, Göteborg.
18. Galle B., et al., *Measurements of methane emissions from landfills using a time correlation tracer method based on FTIR absorption spectroscopy*. Environmental Science & Technology, 2001. **35**(1): p. 21-25.
19. *Pacific Northwest National Laboratory*. 2004 Available from: https://secure.pnl.gov/nsd/nsd.nsf/Welcome.
20. Benner D.C., et al., *The HITRAN molecular spectroscopic database: Edition of 2000 including updates through 2001*. Journal of Quantitative Spectroscopy and Radiative Transfer, 2003. **82**(1-4): p. 5.
21. Kihlman M., *Application of solar FTIR spectroscopy for quantifying gas emissions*. 2005, Licentiate thesis at Chalmers University of Technology: Gothenburg.
22. Hanst P.L., *QASoft '96, Database and quantitative analysis program for measurements of gases.* Infrared Analysis Inc., 1996.
23. Hurley P.J., Physick W.L., and Luhar A.K., *TAPM: A practical approach to prognostic meteorological and air pollution modelling.* Environmental Modelling and Software, 2005. **20**(6): p. 737.

Page 98

technique for quantifying fugitive gas emissions

Mellqvist J., Kihlman M., Galle B., Fransson K., Samuelsson J.

Manus

Page 100

The Solar Occultation Flux method, a nouvelle technique for quantifying fugitive gas emissions

Johan Mellqvist*, Manne Kihlman, Bo Galle, Karin Fransson and Jerker Samuelsson

[1] Chalmers University of Technology, Göteborg, Sweden
* Corresponding author Johan.mellqvist@rss.chalmers.se, +46317724855

Short title: The SOF method, a new technique for quantifying gas emissions

Abstract

A new remote sensing method named SOF (Solar Occultation Flux) has been developed since 1997 and applied to locate and quantify fugitive hydrocarbon emissions from industry. The method is based on measuring infrared (2.5-15 μm) intensity spectra of the sun from a moving platform, vehicle or ship. In order to obtain

the flux from a particular emission source, the vehicle is driven in such as way that the detected solar light traverses across the actual emission plume. The flux is then obtained as the integrated sum of the retrieved path averaged concentrations, multiplied by the wind speed. The main uncertainty for the method is in the assessment of the wind field. The retrieval code has been tested and compared to other published codes for alkanes, HCl and SO_2, with generally good agreement. Results from a validation experiment utilizing SF_6 trace gas shows that if averaging enough data, 10 traverses, accuracies of 10-20% are obtained from simple emissions sources. Another tracer experiment, simulating emission from a crude oil tank showed an error of 50% when measuring in the *near field* where meteorological disturbances are caused by the tanks. The good performance of the method for estimation of ammonia emissions from fertilized land is demonstrated, with fluxes of 6 kg ammonia per hour, 24 hours after fertilization. A ship traverse in the Göteborg harbor in 2001, passing one refinery and the oil harbor showed an emission of 900 kg/h of alkanes, with average carbon number of 4.5.

Keywords: gas, emission, fugitive, solar, occultation, flux, FTIR, ammonia, fertilized land, VOC, alkanes

Introduction

In environmental work there is a need to quantify the amount of gas emitted from biogenic or anthropogenic sources. Often the emissions occur over a certain area from multiple emissions points, such as a process area in a refinery, where releases occur from leaking valves and vents (*fugitive emissions*), a crude oil tank with a floating roof or a fertilized field from which ammonia is leaking. To quantify such emissions is often very difficult and requires combining the measurements with a dispersion model [1] or simulation of the leakage by using a tracer gas in combination with measurements of the ratio between the tracer and the leaking gas [2-4]. There is a family of methods where the gas concentration is measured and integrated over a surface corresponding to the cross section of the emission plume. The mass-flow of

gas through that surface is then determined by multiplying the integrated concentration with the wind transport through that surface. One way to determine the gas concentration over the cross section of the plume is to actively look in different angles with a scanning system based on reflected solar light [5] or DIAL [6-8], a technique sending out laser pulses and receiving them after reflection and absorption on the molecules of interest. Another method is to look in one direction but to move the platform the system resides on, commonly a car or a boat. For example, this has been done from a boat to quantify the SO_2 emission from the volcano MtEtna both with DIAL and passive UV/visible methods such as DOAS and COSPEC [9].

Since 1997 a measurement approach, denoted the Solar Occultation Flux method (SOF), has been developed in our group based on measuring infrared solar light in occultation mode. The aim was to develop a method for the estimation of fugitive emissions of volatile hydrocarbons which only are measurable in the infrared region, but also other applications have been demonstrated such as volcanic and agricultural ones. The method is based on experience gained working with high resolution solar FTIR [10, 11] and industrial measurements using long path FTIR [4]. In the recent years other groups have also used solar occultation measurements both in the UV and infrared spectral region to quantify emissions from volcanoes of SO_2 [12] and HCl [13].

Here the SOF method and several examples, as applied in our group for industrial measurements, are for the first time presented in a scientific paper. In two parallel papers a more detailed description of VOC measurements from refineries together with an error analysis is given [14-16].

Methodology

Flux measurement

The Solar Occultation Flux method (SOF) is based on recording broadband infrared spectra of the sun with a FTIR spectrometer that is connected to a solar-tracker. The latter is a mirror device that tracks the sun and reflects the light into the spectrometer independent of its position. From the solar spectra it is possible to retrieve the path-integrated concentration (molecules/cm_2) between the sun and the spectrometer. To obtain the gas emission from a source, the instrument is placed in a car and is driven in such way that the detected solar light cuts through the emission plume. In this way, the solar-ray going between the sun and the mobile instrument is cutting out an area in the sky. The surface integrated concentration of alkanes on this surface is determined. This is done by cutting the surface into many parallelograms by continuously measuring spectrum after spectrum while driving. Each spectrum is evaluated separately to derive the line-integrated concentration represented by each spectrum

[conc·L]. The position of the car during the traverse is measured with a GPS at the beginning and at the end of each measured spectrum and determines the base of each

parallelogram, x. The surface integration is done by multiplying each line-integrated concentration with this base and summing up. The flow of gas through the surface is determined by a scalar-multiplication in vector representation between the wind-vector, and the normal to each parallelogram, as shown in Eq. 1. A more thorough description can be found elsewhere [15].

$$F = \cos(SZA) \cdot \sin(u_a - x_a) \cdot u \cdot x_L \cdot [conc] \cdot L$$

Where u_a and x_a are the wind and driving directions, u the wind speed, x_L the length of movement and SZA corresponds to the solar zenith angle. Thus, the calculation of flux also requires information about the wind on the surface. A look at Figure 1 gives an intuitive feeling for the surface where the measurement is done. The solar rays detected by the SOF instrument are shown as vertical lines. The area between these lines corresponds to the surface integrated concentration observed. If these values are multiplied by the local wind-speed the mass-flux through the area is obtained.

Figure 1. A 3D plot of a SOF measurement conducted at the oil harbor. The lines correspond to the solar light, which together with the movement defines the area cut out through the atmosphere.

The wind through the surface is not straightforward to obtain, since the wind is usually complex and varies with the height. The situation is simpler for a plume without extension in height (flue gas plume) but for a complex one the appropriate wind value to use corresponds to the mass weighted wind over the plume. This in turn requires knowledge about the concentration height profile of the plume and of the wind profile, neither of which are measured by the SOF technique. In applications we have often used complimentary measurements by a point measuring system [3] to obtain more height information. The SOF method can only be applied in sunny conditions. This is advantageous since this corresponds to *unstable meteorological conditions* for which wind gradients due to convection are smoothed out. For flat conditions the wind on average, varies less than 20% between 20 and 100 m height, using standard calculations of logarithmic wind. The best approach to minimize the problem with wind gradients for complex gas plumes, is to measure at distances far away, i.e. 0.5-2 km downwind the releases, so that most of the plume have had time to rise to heights above the first 20-40 m, where the wind is usually disturbed due to various structures (building, trees, tanks). In the SOF method the direction of

movement through the plume is seldom horizontal due to the slant observation angle of the sun, in contrast to vertically observing techniques, such as UV/DOAS [5]. For instance at 45_0 SZA the movement through the plume will be equally upwards and sidewards. This fact makes it difficult to resolve plumes from different emission sources late in the day. On the other hand for steady wind conditions, it can also be of advantage, since it might provide height information.

Equipment

Three different SOF systems were built around a commercial Fourier Transform spectrometer (Bruker-OPAG 22) having a spectral resolution of 0.5 cm^{-1}, a field of view of 30 mrad and an entrance aperture of 38 mm, Figure 2. With this instrument two cryogenically cooled detectors InSb and MCT are used, with 1 mm^2 detector area. The first system (top left) utilizes a 10 cm diameter solar tracker, from the National Physics Laboratory (NPL) in UK, and uses focusing and defocusing optics to obtain 5 times higher light intensity, which is valuable in the 10 μm region. With this system the detector views only half the sun diameter. The light is focused on an aperture and optical filters can be placed after the aperture. This system is relatively large and the solar tracker allows only a 30° rotation wherefore the whole instrument has to be rotated for each turn of the car. A more mobile system is shown in the top right panel in Figure 2, as applied on a refinery measurement at Tula near Mexico city. This system uses the same solar tracker and spectrometer as above but only flat front optics. The throughput is considerably smaller than the previous system and it detects 4 sun diameters, and the latter may introduce spectral shifts in the spectra due to possible variations of the incidence angle into the spectrometer. This system has recently been rebuilt and instead uses a smaller spectrometer (Bruker IrCube) with the same resolution. This spectrometer is conveniently interfaced through an Ethernet connection and has its own web interface. It has a smaller entrance aperture of 25 mm but the direct solar light is strong enough to saturate the detector in the 3 μm region. A metal grating has been placed in front of the opening to reduce the light if no optical filters are used. Figure 2 (lower panel) shows the most recent system that has been developed during the last years [15]. A new active solar tracker with 540° freedom in rotation has been developed. The light is first focused with a 90° off axis parabolic mirror with 110 mm focal length onto a 3 mm aperture. Optical filters can be inserted after the aperture. The light is then defocused by a 69 mm off-axis mirror into the spectrometer OPAG-22 spectrometer. The detector views 2 sun diameters and the instrument is susceptible to variations in the incidence angle, putting considerable requirements on the solar tracker.

4

Page 105

Figure 2. Several SOF systems are shown that have been utilized during the last years. The top left panel shows the oldest system, including a schematic of the light path. The top right panel shows a mobile system with flat entrance optics. The bottom left and right panels show the new system with 540_o rotating solar tracker positioned inside a VW bus.

The benefit of introducing optical filters in the solar light beam, is that more light at the interesting wavelength-interval can be used without saturating the infrared detector. When tested in the alkane measurement application, the filters cause problems if they have spectral structures in the neighborhood of the evaluation interval. Even faint structures in the filter function can be large in comparison to the absorption on the molecules of interest. This was the case with one of our filters for which the strength of the filter function was varying with the incident angle and the shape varied with temperature. This dependence is severe since the filter is usually

exposed to concentrated sunlight. These two effects could only be partly compensated for by the software, but fortunately the measurements worked well without. A second filter with less structure has been working well, however. Filters are more essential for the 10 μm region, since the solar light is weak. A filter with a cutoff at 10.2 μm has successfully been used when measuring SF_6 and ethylene in this region.

5

Page 106

Spectroscopy

The spectral lines of the gas will cause a fingerprint on the measured spectra according to Beer-Lambert's law, as shown below:

$$A(\nu) = -\ln\left[I(\nu)/I_0(\nu)\right] = \sum_i \sigma_i(\nu) \cdot \int conc_i(x)\,dx$$

here we define A as absorbance, I is the measured light intensity at wave number ν, I_0 is the light intensity before the light enters the gas and σ_i are the absorption spectra of the gas. By fitting known fingerprints of the gases to the measured absorbance spectrum, in a linear least squares fit, the line-integrated concentration of the gas is retrieved. Reference spectra are possible to simulate for the atmospheric species using the HITRAN database [17]. Additional spectra such as volatile hydrocarbons can be found in other databases, such as PNW [18] or Hanst [19]. When studying localized emission sources one approach is to measure a reference spectrum at ground on a place with zero concentration of the gases of interest and use that spectrum as I_0. This is the method we have applied in several of the measurements shown in this paper, i.e. for alkanes and ammonia. Linear evaluation of spectra was performed with the Classical Least Square (CLS) algorithm in the GRAMS software [20]. Later, non-linear evaluation was also used with the help of the NLM4 and MALT software [21]. One disadvantage with this approach is that the reference measurement of I_0 will only be useful as long as the path length through the atmosphere is constant, which is the case only for a limited time due to the movement of the sun. One way to solve this is to let the spectral evaluation determine the change of path length by representing I_0 as an absorbance. This also makes it possible to use more than one measured references $I_{0,j}$, to include filter functions in the fit and to shift the wavenumber scale of the

reference spectrum.

$$\ln\left[I(\nu)\right] = \sum_j F_j \cdot \ln\left[I_{0,j}(\nu)\right] - \sum_i \sigma_i(\nu) \cdot \int conc_i(x)\,dx$$

where the factors F_j are determined in the same way as the concentrations. If the spectra $I_{0,j}$ are evaluated they are forced to give zero gas concentrations since they represent a perfect fit. By choosing a few sky references throughout a day, such as in the beginning and end of the traverses, where it can be assumed that the gas concentration is zero, it has been observed that an efficient removal of the influence of the upper atmosphere can be done. However, this method will cause errors in the retrieval if any of the chosen references have nonzero gas concentration and should therefore be used with care.

The SOF measurements are presently evaluated with a new software (QESOF) based on Eq. 3. Non-linear effects will be present, however, as a result of the fact that the spectrometer broadens and distorts the spectral absorption lines. This can be simulated by a broadening operator *D* that is applied to the synthetic spectra, according to Eq. 4. Since this problem is non-linear it must be solved in an iterative way.

$$\ln\left[I(\nu)\right] = \sum_j F_j \cdot \ln\left[I_{0,j}(\nu)\right] + \ln\left[D\left(\exp\left(-\sum_i \sigma_i(\nu) \cdot \int conc_i(x)\,dx\right)\right)\right]$$

Page 107

Results

Validation

The method to retrieve fluxes from traverses with a mobile solar-occultation system was tested on two tracer experiments. In the first one, a trace gas (SF_6) was emitted from the top of a 17 m tall mast in the middle of a large open parking lot in Göteborg, Figure 3. Traverses were done downwind with the measurement system at varying distances from the emission source. The wind was measured with a Yong wind-meter located in the top of the same mast, averaging the wind for 1 minute. The true amount of emitted trace gas was estimated by weighing the gas tube before and after the experiment and also measuring the duration time of the gas release. The emitted gas was always around 1.9 kg/h. The measured peak concentrations were slightly less than 10 mg/m$_2$ for most scans. The spectral evaluation was done using the non-linear algorithm QESOF in the region 925-975 cm^{-1} and included H_2O, CO_2, SF_6 and a fitted sky-reference spectra [15]. Spectra for H_2O and CO_2 were created from the HITRAN database at a temperature of 288K and a pressure of 1 atm. SF_6 spectra were taken from the NIST database [22]. A polynomial of 4th order was also fitted.

Table 1 shows the results from the four days when the field experiment was

done and the individual data points for May 23 is shown in Figure 3. There is considerable scatter in the individual data but for May 23 the average lies within 10% from the real release rate. Most of this scatter is not caused by the spectroscopic measurements, but rather by short term turbulence in the wind field, not captured by the 1 minute averages of the wind that was used. This turbulence can be seen in the plume measurements. For this type of measurements with a narrow plume such turbulence may cause more effect than on a broader one. The average error varied over the days, as can be seen in Table 1. This is not well understood but may be caused by variations in the atmospheric conditions.

Table 1. Summary for each day in year 2002, for which tracer release experiments measurements were conducted at the Åby field.

Day	Emitted SF_6 (kg/h)	Calculated average (kg/h)	Number of accepted traverses	Average wind speed (m/s)	Average wind direction	Err
May-22	1.9	2.3±1.3	4	4.9-8.6	152°-169°	21%
May-23	2.0	2.2±0.6	15	3.9-5.6	120°-142°	10%
June-03	2.0	1.6±0.9	16	2.7-5.3	235°-273°	-20%
June-04	1.9	2.0±1.4	9	5.9-7.8	152°-191°	5%

Page 108

3.5

3

2.5

2

/m 2

mg

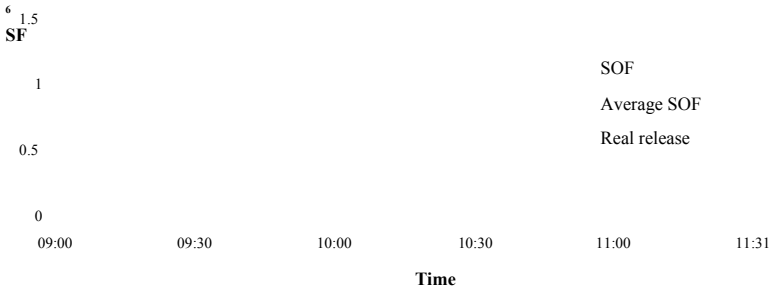

Figure 3. Results from a validation experiment in which SF_6 was emitted from a 17 m mast on May 23 2002 at an open field. The average of the measured emissions was 11% higher than the real release rate.

Another experiment was conducted in which SF_6 was emitted from the roof of a crude oil tank, in June 2002. The tank is located in a tank-park where nine tanks are standing close together, see Figure 4. It can be expected that the wind field is irregular close to the ground inside the tank-park. Traverses were done on a road along the side of the tank park, approximately 150 m away from the emission point, but close to the other tanks. The wind was measured from a Yong windmeter on a 5 m mast on the top of a small mountain just west of the tanks, as indicated by the arrow in the picture.

Table 2 shows all the traverses done during that day. The released amount of SF_6 was estimated to 2.0 kg/h by weighing the gas-tube before and after the experiment and the retrieved average emission was 3±1 kg/h, i.e. 50% overestimation of the flux. Figure 4 shows an example of a typical traverse. The plumes were in many cases broad, as shown in Table 2, indicating a downwash of the plume into the wake of the tanks. This reduces the retrieved flux because the plume will reside leeward of the tanks were the wind is much weaker. The narrow plumes on the other hand had flux values much closer to the true value, probably corresponding to occasions when little downwash occurred. The windmeter used here was noisy and probably causes a certain amount of the scatter. Nevertheless, even though this measurement was conducted in the near field, where we anticipate great difficulties in conducting the measurements, the value were *only* 50% off. Usually the measurements are conducted further away from the sources.

Table 2. Trace gas experiment in which SF_6 was emitted from tank 105, on June 24, 2002. SOF measurements were conducted in the near field. The release rate of SF_6 has been determined to 2.0 kg/h.

Time	Emission SF_6 (kg/h)	Average wind speed (m/s)	Average wind direction	Plume width	Error
12:45	3.1	6.5	252°	80	55%
12:54	1.8	7.2	252°	70	-10%
13:05	1.3	6	257o	30	-35%
13:17	2.7	7.5	253°	72	35%
13:29	3.1	5.4	255°	80	55%
14:05	5.2	7.4	264°	70	160%
14:10	3.7	7.2	251°	100	85%
14:24	2.6	7.3	262°	75	30%
14:31	3.4	6.5	260°	40	70%
Average 3 ±1.0					**50%**

Figure 4. A traverse conducted during a tracer release of SF_6 on top of tank 105. The lines point towards the wind, towards a potential emission source. The position of the wind meter is indicated by an arrow. *(Aerial photo: Copyright Lantmäteriet 2004-11-09. Ur Din Karta och SverigeBilden)*

Results from intercomparison exercises with other flux measuring techniques are not available. An indication, however, of the validity of the SOF technique is the following: During 1995 and 1999 the DIAL technique, operated by a commercial company, was applied to estimate emission from a certain refinery in Sweden. According to official reports to the provincial government they estimated fugitive emission from the whole process area corresponding to 64 and 87 kg/h of alkanes during 1995 and 1999, respectively, with reported error bars of 15-20%. The SOF

method was applied two years later, in 2001, to our knowledge measuring in a similar geometry along the main refinery road. Measurements of the process area during two days yielded a total flux of 74±20 kg/h. This falls surprisingly close to the values spanned by the DIAL measurements. The measurements were not conducted at the same occasion, but the process area seems quite constant since the values for 2002, 2003 and 2004 were 57, 75 and 76 kg/h, respectively [15, 16]. Also, the process area is a good test case since it shows less intermittent emissions and it is less susceptible to variations in wind and temperature, which may the case for emissions from storage tanks.

Another type of validation test is to compare the retrieval algorithms used. The results of the spectral fitting algorithm for alkanes in our software QESOF [15] has been compared and verified with the results retrieved from other software, a Classical Least Square (CLS) method in the Grams software [32] and the non-linear NLM4 software developed by Griffith [19]. The agreement between NLM4 and QESOF was very good, within a few percent. The CLS code agreed less well with the other codes, with discrepancies of 30% in the plume, but this can be explained by several reasons. Verification of the software has also been conducted for the volcanic species HCl and SO_2. Solar spectra measured in the plume of Mt Etna in Sicily in October 2000 were analyzed by two independent retrieval algorithms, i.e. QESOF and a code developed by Mike Burton at INGV [23] for spectral evaluation on measurements of volcanic gases. This comparison shows very good agreement, with differences of a few percent, both for SO_2 and HCl, if the column amount above the baseline is considered.

Ammonia emissions from fertilized fields

A field test was conducted using SOF in the summer of 1998 measuring the amount of ammonia released when fertilizing fields with manure. A first prototype of a SOF system was used similar to the old system in Figure 2, but with a 1 cm^{-1} FTIR spectrometer (Bomem MB100) having an MCT detector, and an optical interference filter. Emissions of ammonia from agriculture cause eutrophication, decrease in the biological variety and acidification on local and regional scale. Ammonia emissions also represent a loss of nitrogen otherwise available as fertilizer. To find methods to reduce ammonia emissions from agriculture is therefore of high concern. In order to evaluate the effects of such methods quantitative measurements of the emissions needs to be done. Ammonia is difficult to measure by point sampling techniques, since it is relatively reactive compound. In addition, will the spreading of manure cause emissions over a whole area and there are few techniques for estimating such emissions.

Measurements were done during the summer of 1998, approximately 24 hours after spreading fertilizer on a field corresponding to 1.5 ha. In Figure 5 an absorbance spectrum of ammonia is shown, measured downwind the field. In addition, a spectral fit of ammonia, and H_2O is shown using the codes MALT [21] combined with CLS [20], and the retrieval yields a column of ammonia of around 5 mg/m^2.

The detection limit of the ammonia is here estimated to 0.3 mg/m^2. In Figure 6

the retrieved total column of ammonia along the measurements path is shown, as well as the accumulated mass flux. The wind was measured with a single wind meter to 5.4 m/s, but considering the open field situation, this is ideal for the SOF method. The total massflux corresponds to 6 kg/h. This application is suitable for the SOF method, and rather straightforward.

10

Page 111

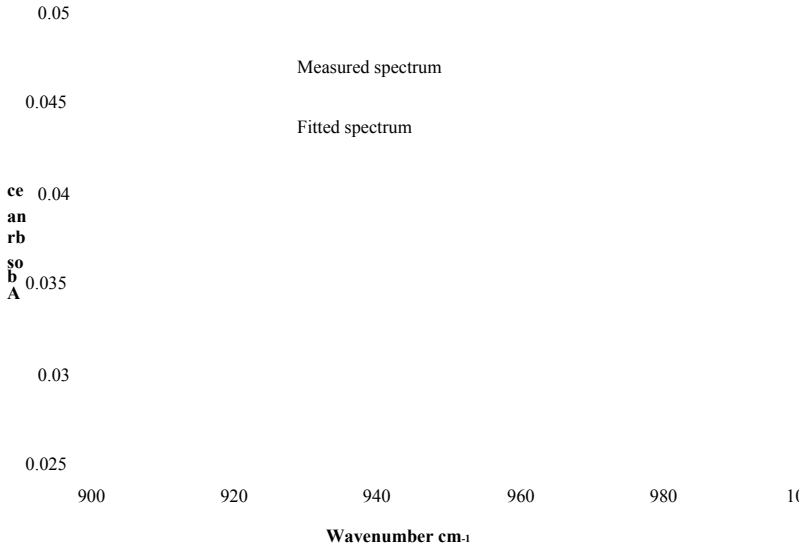

Figure 5. An absorbance spectrum of ammonia (-log(I/I$_0$), corresponding to 5 mg/m$_2$, measured downwind a fertilized field of 5 ha, together with a spectral fit of ammonia and water.

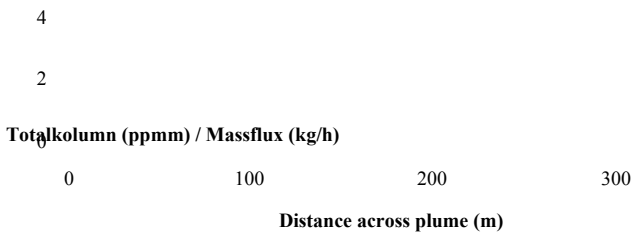

Figur 6 . Total column and mass flux of ammonia from a fertilized field, measured using the SOF method, 24 h after fertilization.

Total flux estimate of VOCs from Göteborg harbour

The combination of volatile organic compounds (VOC), nitrogen oxides and sunlight causes secondary production of ground level ozone, a species that has negative effect on both the health and the environment. The largest point sources for VOCs are refineries and petrochemical industries and the emissions from these occur from a number of points such as: process equipment, crude oil tanks, storage tanks, dockside loading operation, water treatment facilities and flaring. The SOF method is suitable, and has been demonstrated for quite a few VOC compounds, both olefins measured around 10 µm (ethylene and propylene) and straight chained alkanes measured around 3.3. µm. In a separate paper results from an extensive study of VOC measurements is given [16]. In Figure 7 is shown a SOF traverse conducted from a ship, R/V Arne Tiselius, in the Göteborg harbor on June 19, 2001. The measurements were conducted using the instrument shown in the top left panel in Figure 2. A measurement was carried out beginning east of Älvsborgsbron and ending at Skandiahamnen, passing by the Port of Göteborg and a refinery. The wind was northerly with a velocity of 2.8 m/s. It can be seen in Figure 7, that a plume was traversed south of the oil harbour, situated in the middle of picture. Figure 8 shows the total column of alkanes and the accumulated total flux. The emission, originating from the whole industrial complex including the oil harbour and a refinery, was estimated to 900 kg/h. There are however uncertainties in the wind speed. The spectral analysis was conducted using CLS [20] and a composition of alkanes with a mean carbon number of 4.5 was retrieved by fitting several species (propane, butane, 2-methylbutane and 3-metylpentane), as shown in Figure 9 for the spectrum with the highest column in Figure 8.

Figure 7. SOF measurement from R/V Arne Tiselius on June 19, 2001, at 10:30. The arrows point towards the wind, which was northerly. The colorscale corresponds to the column of alkanes.

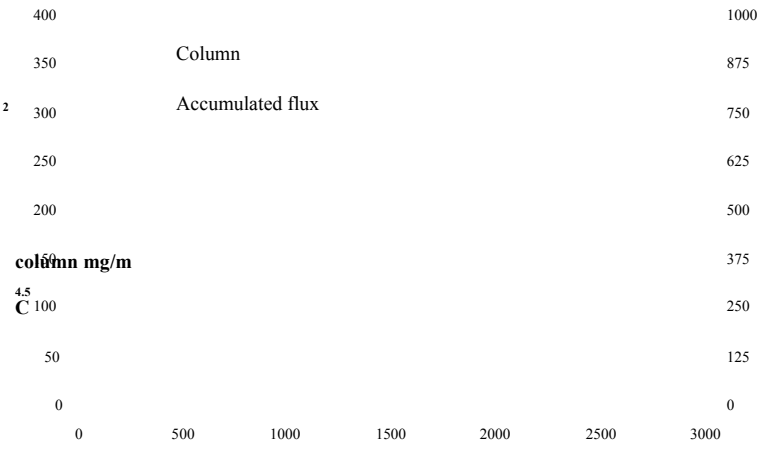

Distance across the wind (m)

Figure 8. The column and accumulated mass flux across the Göteborg harbour is shown here. The data corresponds to the one in Figure. 7.

Figure 9. A spectrum measured with a resolution of 2 cm^{-1} together with a fitted spectrum consisting of four different alkanes (propane, butane, 2-methylbutane and 3-metylpentane) with a mean carbon number of 4.5. The difference between the two absorption spectra (the residual) is also shown.

Acknowledgement

Financial support from Vinnova research council and Preem environmental foundation is acknowledged. We also thank Elisabeth Unden and Gunner Hanehoj for participating in the measurements.

References

1. Sommer, S.G., Mikkelsen, H. and Mellqvist, J., *Evaluation of meteorological Techniques for Measurements of Ammonia Loss from Pig Slurry*. Agric. For. Meteorol., 1994(74), p 169-179
2. Siversten, B., *Estimation of Diffuse Hydrocarbon Leakages from Petrochemical Factories*. J. of Air. Poll. Cont. Assoc, 1983. 33(4)
3. Galle B., et al., *Measurements of methane emissions from landfills using a*

time correlation tracer method based on FTIR absorption spectroscopy. Environmental Science & Technology, 2001. **35**(1): p. 21-25.

4 Mellqvist., Johan, *Application of infrared and UV-visible remote sensing techniques for studying the stratosphere and for estimating anthropogenic emissions*, Chalmers Dissertation, ISBN 91-7197-765-I, Göteborg, 1999

5. Galle B., Oppenheimer C., Geyer A., McGonigle A. and Edmonds M., *A miniaturised ultravioletspectrometer for remote sensing of SO2 fluxes: a new tool for volcano surveillance*. Journal of Volcanology, 2002. 119: p. 241-254

6 Milton M.J.T., et al. *Measurements of fugitive hydrocarbon emissions with a tunable infrared dial*. 1992. Cambridge, MA, USA: Publ by NASA, Washington, DC, USA.

7. Robinson R.A., Woods P.T., and Milton M.J. *DIAL measurements for air pollution and fugitive-loss monitoring*. 1995. Munich, Ger: Society of Photo-Optical Instrumentation Engineers, Bellingham, WA, USA.

8. Walmsley H.L. and O'Connor S.J. *The measurement of atmospheric emissions from process units using differential absorption LIDAR*. 1997. Munich,

9. Weibring P., et al., *Monitoring of volcanic sulphur dioxide emissions using differential absorption lidar (DIAL), differential optical absorption spectroscopy (DOAS), and correlation spectroscopy (COSPEC)*. Applied Physics B Lasers and Optics, 1998. 67: p. 419-426.

10. Mellqvist, J., et al., *Ground-based FTIR observations of chlorine activation and ozone depletion inside the Arctic vortex during the winter of 1999/2000*, JGR, 2002. 107(D20)

11. Galle, B.; Mellqvist, J., et al., *Ground Based FTIR Measurements of Stratospheric Trace Species from Harestua, Norway during Sesame and Comparison with a 3-D Model*, JAC, **1999**. 32(1): p147-164.

12. Weibring P., et al., *Optical monitoring of volcanic sulphur dioxide emissions - comparison between four different remote-sensing spectroscopic techniques. Optics and Lasers in Engineering*, 2002. 37: p. 267-284.

13. Duffell H., Oppenheimer C., and Burton M., *Volcanic gas emission rates measured by solar occultation spectroscopy*. Geophysical Research Letters, 2001. 28(16): p. 3131.

14. Kihlman M., Mellqvist J., and Samuelsson J., *Monitoring of VOC emissions from three refineries in Sweden and the Oil harbour of Göteborg using the Solar Occultation Flux method*. 2005. Chalmers: Gothenburg.

15. Kihlman, M., *Application of solar FTIR spectroscopy for quantifying gas emissions*, Technical report No. 4L, ISSN 1652-9103 Department of Radio and Space Science, Chalmers University of Technology, 2005

16. Kihlman M ., Mellqvist J., Samuelsson J., Tang L., Chen D., *Monitoring of VOC emissions from refineries in Sweden using the SOF method*, in manuscript, 2005

17. Benner D.C., et al., *The HITRAN molecular spectroscopic database: Edition of 2000 including updates through 2001*. Journal of Quantitative Spectroscopy and Radiative Transfer, 2003. 82(1-4): p. 5

18. *Pacific Northwest National Laboratory*. 2004 Available from: https://secure.pnl.gov/nsd/nsd.nsf/Welcome.

19. Hanst P.L., *QASoft '96, Database and quantitative analysis program for measurements of gases.* Infrared Analysis Inc., 1996.

20. GRAMS/AI. 2004, Galactic Industries Corporation.

21. Griffith D.W.T., *Synthetic calibration and quantitative analysis of gas-phase FT-IR spectra.* Applied Spectroscopy, 1996. **50**(1): p. 59-70.

22. Chu P.M., et al., *The NIST Quantitative Infrared Database.* J. Res. Natl. Inst. Stand. Technol., 1999. **104**(59).

23 Burton M.R., et al., *Diurnal changes in volcanic plume chemistry observed by lunar and solar occultation spectroscopy.* Geophysical Research Letters, 2001. **28**: p. 843-846.